Follow the book : ' aircraft material and processes – by Titterton G F'

In the notes, I have covered up the part of syllabus which is not mentioned in the aforesaid book

I have collected the information for notes from various books and research journals

- Dr Upasana Panigrahi

Smart and nano materials

Introduction

In the industrial word, the rush for adopting creative and innovative solutions is accelerating. Considered by many as the main engine of any economic growth, innovation is the basic factor to achieve prosperity. Smart and nano materials, structures and systems are at the forefront of this innovation process, and the NDE field will certainly be one of the winners of this race.

After defining the features of a smart system and its advantages, the emerging smart and nano materials are introduced as well as their benefits and applications. Finally, the perspective of their use is exposed, particularly in aerospace.

Smart Systems

Smart entities trace their origin to a field of research that envisioned materials, devices and systems that mimic human muscular and nervous systems. The idea is to produce non-biological entities that will achieve the optimum functionality observed in biological systems through emulation of their adaptive capabilities and integrated design.

By definition, the concept consists of combining sensors and actuators as well as a command and control units to be incorporated as an integral part of a structure or system. This entity will react in a predicted manner and in a pattern that emulates a biological function: first by sensing any internal and/or external stimuli and then by responding to those stimuli in some appropriate and predicted way in real or near real time

Figure 1 presents the basic components of a smart system as defined previously by the author [1-4]. They are listed below and *(their equivalents in the human body appear in parentheses)*
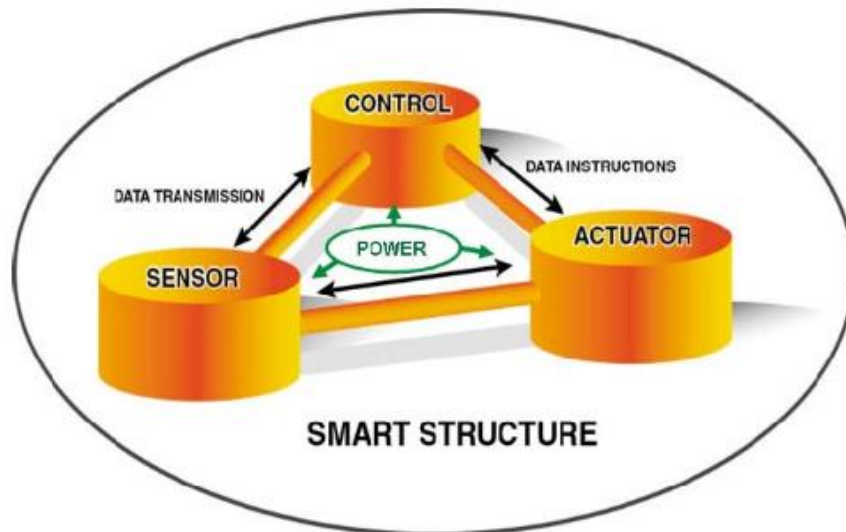

Fig. 1 Components of a smart system

1. Data acquisition (*tactile sensing*): collect the required raw data needed for an appropriate control and monitoring of the structure.
2. Data transmission (*sensing nerves*): forward the raw data to the local and central control units.
3. Command and control center (*brain*): analyse the data, reach the appropriate conclusion and determine the specific actions.
4. Data instructions (*motion nerves*): transmit the decisions and the associated instructions back to the members, and
5. Controlling devices (*muscles*): take action by triggering the controlling devices/units

Since its beginning, materials science has undergone a clear and distinctive evolution: from inert materials to functional materials to nano materials. These new materials are used for active, adaptive and/or smart system with more acute recognition, discrimination and reaction capabilities.

Emerging Smart Materials

- *Piezoelectric:* Undergo mechanical change when subjected to electric charge/voltage and vice versa (direct and converse effects).
- *Electrostrictive:* Same as piezoelectric but proportional to the square of the field.
- *Magnetostrictive:* Undergo mechanical strain when subjected to a magnetic field and vice versa (direct and converse effects) i.e. Terfenol and Galfenol.
- *Magnetorheological fluid:* Change from fluid to viscous solid when subjected to a magnetic field.
- *Electrorheological fluid:* Change from fluid to viscous solid when subjected to an electrical field.

- *Shape Memory Alloys (SMA):* Undergo shape changes due to phase transformations when subjected to a thermal field. It deforms to its martensitic condition, and regains its original shape to its austenite condition when heated i.e. Nitinol.
- *Shape Memory Polymers (SMP):* Same as SMA but with polymers instead of Alloys (Fig 2).
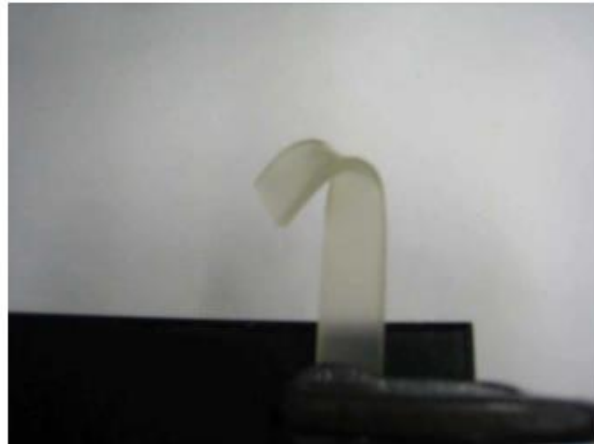

Fig. 2 Shape memory polymer (SMP)

Combining two or more materials in an attempt to utilise *synergistically* the best properties of their individual constituents is the ultimate objective of any smart composite material. Their advantages and adaptability to the above design requirements have led to a profusion of new products.

Nano Materials

Nanomaterials are materials with dimensions ranging between 1 to 100 nm with better properties than steel (up to 5 times the elastic modulus and 50 times the tensile strength), silver (100 times electrical conductivity) and copper (10 times thermal conductivity). These features provide a lot of potential for multifunction such as reinforcement, sensing, SHM, etc. However, these remarkable characteristics have their disadvantages: difficulty of manufacturing, manipulation and mixing with the host material.

Nanomaterials specifically Carbon nanotubes can be used in many applications but particularly for NDT applications including SHM. Being very conductive, they are used as strain gages for sensing purposes: any change in the resistance will produce a variation of conductivity and hence, sensing functions. Because of their very small size increasing their ability to penetrate the cracks/openings when incorporated in any matrix, they are perfect candidates to detect fracture and hence for structural health monitoring.

Nano materials and NDE

Nanotechnology as well as smart materials can and will improve NDE and SHM for better health monitoring of the following applications:

1. *Welding Verification*

    Instead of using the conventional well-known NDE techniques such as radiography, CT scanning, ultrasonic, liquid penetrant, acoustic emission or Eddy current, emerging

materials particularly nano materials, could be used advantageously to find, define and locate cracks in welding.

2. *Structural Mechanics*

   Instead of using hammer, impulse or vibration, smart nano materials will provide continuously the desired characteristics such as displacements, accelerations, movements, etc. at different points of the structure. This continuous and planned monitoring could enhance the performance of the system or increase its capabilities or both.

3. *Medical or other applications*

   A wide array of possible improvement and application of NDE can be envisioned using new emerging smart and nano materials.

The very small size and continuously diminishing cost of nano materials will allow building and implementing hundreds if not thousands of sensors which will be attached or incorporated in any system to be monitored. The continuous gathering of data for NDE purposes will become an integral part of any system. The analysis in real-time of all the collected data and the possibility to act, with or without human interaction, will certainly replace any conventional NDE whether for quality inspection, verification or property depiction and characterization.

Advantages of smart and nano materials

Using smart and nano materials in systems could have the following advantages:

1. Optimizing the response of complex systems. This is done by establishing early warning systems, enhancing the range of survivability conditions and/or providing adaptive response to cope with unforeseen conditions and situations.
2. Enhancements otherwise not possible; such as minimizing the distortion of the responses, increasing the precision as well as providing better control of the system. This could lead to improving the design and performance of new geometries for special applications.
3. Improving the functionality of the system by a proper preventive maintenance and performance optimization.
4. Significant impact on manufacturing and processing techniques.
5. Improving the health monitoring of the system and better control of its active, adaptive or smart functions.

All these added values open the door to use more nano and smart materials for monitoring, SHM and NDE of all types of applications.

Applications of smart and nano materials

- *Made-up smart nano composite*:

  In recent years, reducing healthcare costs while maintaining a high quality of care have been the focus of government and healthcare providers. They shift the expenditure of wellness programs from treatment to prevention. This is basically done among other things by monitoring vital health signs such as heart and respiratory rate, ECG, blood pressure, skin temperature, etc. The monitoring is performed by smart clothing which incorporates technologies and disciplines such as nano and microtechnologies as well as sensors, actuators, processing and communication, energy sources within clothes and

wearable systems; or by smart patches. Figure 3 shows an ultrathin skin-like patch that mounts directly onto the skin with the ease, flexibility and comfort of a temporary tattoo. This patch produced in 2010 by John A. Rogers, the Lee J. Flory-Founder professor of engineering at the University of Illinois [5] is used for monitoring purposes. The same technology, materials and techniques can be adapted and duplicated for the aerospace industry.

Fig. 3 Ultrathin path that mounts directly onto the skin with
the flexibility and comfort of a temporary tattoo

● *Structural health monitoring (SHM) and assessment of structural components* [6]: Composites are used more and more in the aerospace industries due to their light weight, better stiffness and corrosion properties. Boeing and Airbus are trying very hard to increase the ratio of composites in their fleet. On the other hand, the response of composites to solicitations and vibrations require better checkup and inspection techniques. Smart nano composites can handle favourably this problem by incorporating sensors and actuators in the layers of composites with a minimum incidence to the integrity of the structural components.

Monitoring composite materials can also be done with layered composition and printed circuit board techniques. This makes it possible to embedded low-cost sensors into composite structures, with minimal impact on the overall integrity of the structure. Ihn and Chang [7] invented an example of this monitoring technique in the form of the SMART Layers [8], shown in figure 4. This method uses a combination of actuators and sensors to detect modifications in the composite material. The actuators excite the composite material and generate waves that are sensed. When a crack appears, or an existing crack grows, it modifies the pattern of propagation of the waves that is detected by the sensors. This approach has been demonstrated in experiments in 2006 and showed that embedded piezoelectric sensors could detect cracks as small as 0.1mm [9].
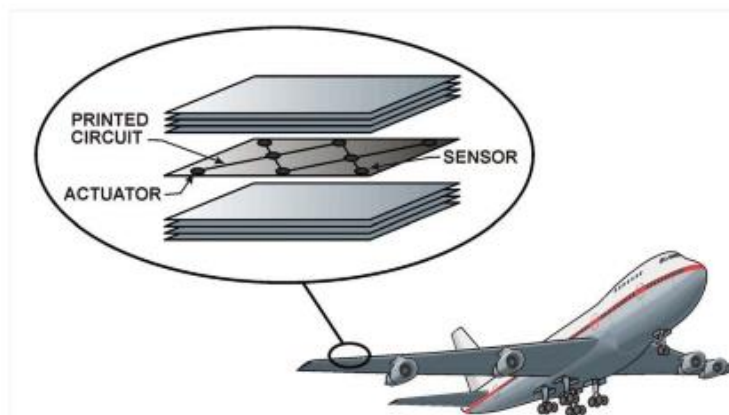

Fig 4: Embedding of smart nano materials in composite structure
using printed circuit technology

- *Reduction of structural vibration*: Reducing or eliminating the noise and vibration of helicopters is a complicated task and smart and nano composites could be the answer. The Smart Material Actuated Rotor Technology (SMART) of Boeing (Fig 5) aims to reduce the vibrations by up to 80% and by the same token improve the flight performance [10-13]. Eurocopter is developing similar systems [14, 15]

A GE-115B engine with "smart" metals installed is shown during preparations for flight tests on the Boeing 777-300ER Quiet Technology Demonstrator 2 airplane.

Fig. 5: Boeing-Noise Control system using SMA

- *Control surface morphing for aerospace structures*: These smart structures deal with the optimizing control or lifting of surfaces with the use of smart structures. Projects are looking at concept to use smart and nano materials, such as shape memory alloys (SMA) to change the shape of wings for flapping in manners similar to those of birds or bats. This area is not likely to see applications in commercial aircraft in the short term, but research projects are underway, particularly focusing on applications with high potential such as UAVs. [16, 17]
- *Multiple thin sheets*: for moulded shapes Terfenol-D/PZT/polymer composites to produce products with greatly improved mechanical properties [18]
- *Electroactive polymers*: for many electromechanical actuator, transducer and active vibration damping applications [19-20]
- *SHM for civil engineering applications* Fig 6 shows a schematic representation of a smart bridge [1-4]. Nanosensors and nanoactuators could enhance tremendously the monitoring and SHM.
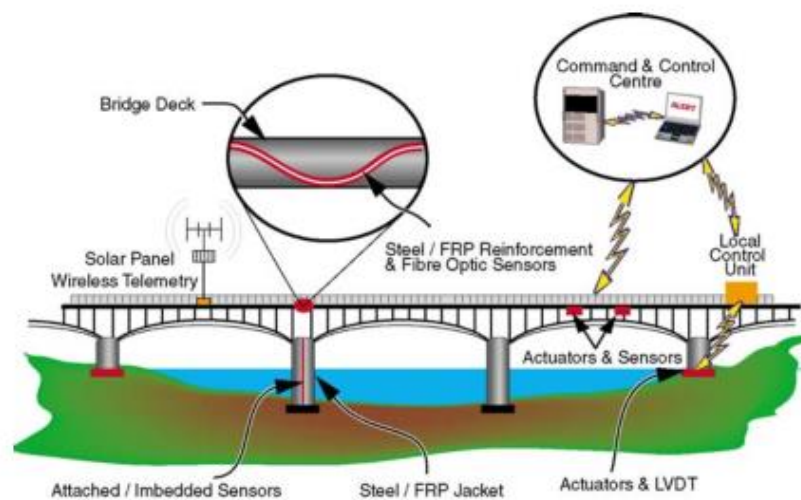

Fig. 6 Schematic representation of a smart bridge

Aluminium alloys for aircraft structures

8.1 Introduction

Aluminium has been an important aerospace structural material in the development of weight-efficient airframes for aircraft since the 1930s. The development of aircraft capable of flying at high speeds and high altitudes would have been difficult without the use of high-strength aluminium alloys in major airframe components such as the fuselage and wings. Compared with other major aerospace materials, such as magnesium, titanium, steel and fibre-reinforced polymer composite, aluminium is used in greater quantities in the majority of aircraft. Aluminium accounts for 60–80% of the airframe weight of most modern aircraft, helicopters and space vehicles. Aluminium is likely to remain an important structural material despite the growing use of composites in large passenger airliners such as the Airbus 380 and 350XWB and the Boeing 787. Around 400 000 tonne of aluminium is used each year in building military and civil aircraft. Many types of airliners continue to be constructed mostly of aluminium, including aircraft built in large numbers such as the Boeing 737, 747 and 757 and the Airbus A320 and A340. Competition between aluminium and composite as the dominant structural material is likely to intensify over the coming years, although aluminium remains central to weight-efficient airframe construction.

Figure 8.1 shows examples of the present day use of aluminium alloys in passenger and military aircraft: the Boeing 747 and *Hornet* F/A-18. The weight percentages of structural materials used in the Boeing 747 is typical of passenger aircraft built between 1960 and 2000. Most of the airframe is constructed using high-strength aluminium alloys, and only small percentages of other metals and composites are used. Aluminium is used in the main structural sections of the B747, including the wings, fuselage and empennage. The only major components not built almost entirely from aluminium are the landing gear (which is made using high-strength steel and titanium) and turbine engines (which are made using various heat-resistant materials including nickel-based superalloys and titanium).
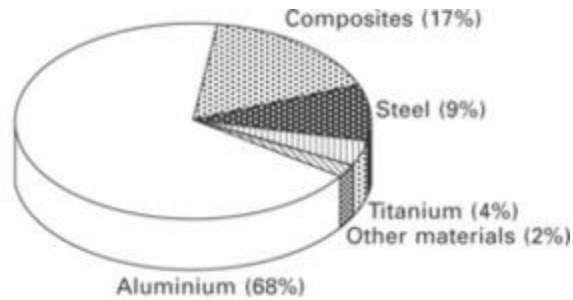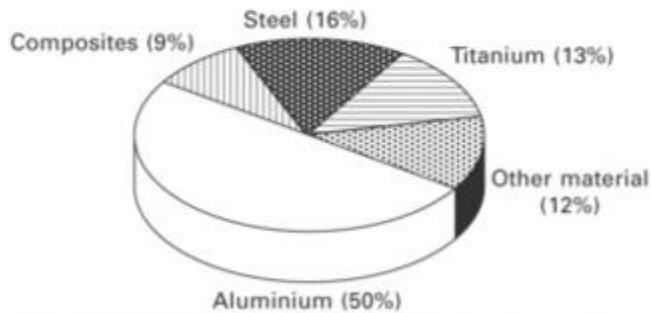
8.1 Use of aluminium alloys and other structural materials in (a) the Boeing 747 and (b) *Hornet* F/A-18. (a) Photograph supplied courtesy of M. Tian. (b) Photograph supplied courtesy of M. Nowicki.

The amount of aluminium alloy used in modern fighters varies considerably between aircraft types, although many are built almost entirely using aluminium. In general, the percentage of the airframe made

using aluminium is lower for military attack aircraft than for civil aircraft. The airframe of most modern military aircraft consists of 40–60% aluminium, which is less than the 60–80% used in commercial airliners. The *Hornet* is typical of military aircraft built over the past thirty years in that aluminium is the most common structural material.

Aluminium is a popular aerospace structural material for many important reasons, including:
- moderate cost;
- ease of fabrication, including casting, forging and heat-treatment;
- light weight (density of only 2.7 g cm^{-3});
- high specific stiffness and specific strength;
- ductility, fracture toughness and fatigue resistance; and
- good control of properties by mechanical and thermal treatments.

As with any other aerospace material, there are several disadvantages of using aluminium alloys in aircraft structures including:
- low mechanical properties at elevated temperature (softening occurs above ~ 150 °C);
- susceptibility to stress corrosion cracking;
- corrosion when in contact with carbon-fibre composites; and
- age-hardenable alloys cannot be easily welded.

This chapter describes aluminium alloys, with special attention given to those alloys that are used in aircraft, helicopters, spacecraft and other aerial vehicles. The following aspects of aluminium alloys are covered: the benefits and problems of using aluminium alloys in aircraft; the different grades of aluminium alloys and the types used in aircraft; and engineering properties of aerospace aluminium alloys and their heat treatment.

8.2 Aluminium alloy types

8.2.1 CASTING AND WROUGHT ALLOYS

Aluminium alloys are classified as casting alloys, wrought non-heat-treatable alloys or wrought heat-treatable alloys. Casting alloys are used in their as-cast condition without any mechanical or heat treatment after being cast. The mechanical properties of casting alloys are generally inferior to wrought alloys, and are not used in aircraft structures. Casting alloys are sometimes used in small, non-load-bearing components on aircraft, such as parts for control systems. However, the use of casting alloys in aircraft is rare and, therefore, these materials are not discussed.

Nearly all the aluminium used in aircraft structures is in the form of wrought heat-treatable alloys. The strength properties of wrought alloys can be improved by plastic forming (e.g. extrusion, drawing, rolling) and heat treatment. Heat treatment, in its broadest sense, refers to any heating and cooling operation used to alter the metallurgical structure (e.g. crystal structure, grain size, dislocation density, precipitates), mechanical properties (e.g. yield strength, fatigue resistance, fracture toughness), environmental durability (e.g. corrosion resistance, oxidation resistance) or the internal residual stress state. However, when the term 'heat treatment' is applied to wrought aluminium alloys it usually implies that heating and cooling operations are used to increase the strength via the process called age (or precipitation) hardening.

There are two major groups of wrought aluminium alloys: non-age-hardenable and age-hardenable alloys. The distinguishing characteristic of non-age-hardenable alloys is that when heat treated they cannot be strengthened by precipitation hardening. These alloys derive their strength from solution solid strengthening, work hardening and refinement of the grain structure. The yield strength of most non-age-hardenable alloys is below about 300 MPa, which is inadequate for aircraft structures. Age-hardenable alloys are characterised by their ability to be strengthened by precipitation hardening when heat treated. These alloys achieve high strength from the combined strengthening mechanisms of solid solution hardening, strain hardening, grain size control and, most importantly, precipitation hardening. The yield strength of age-hardenable alloys is typically in the range of 450 to 600 MPa. The combination of low cost, light weight, ductility, high strength and toughness makes age-hardenable alloys suitable for use in a wide variety of structural and semistructural parts on aircraft.

8.2.2 INTERNATIONAL ALLOY DESIGNATION SYSTEM

There are over 500 different aluminium alloys, and for convenience these are separated into categories called alloy series. The International Alloy Designation System (IADS) is a classification scheme that is used in most countries to categorise aluminium alloys according to their chemical composition. This system is used by the aerospace industry to classify the alloys used in aircraft. All aluminium alloys are allocated into one of eight series that are given in Table 8.1. The main alloying element(s) is used to determine into which one of the eight series an alloy is allocated. The main alloying element(s) for the different series are given in Table 8.1. The 8000 series is used for those alloys that cannot be allocated to the other series, although the principal alloying element is usually lithium.

Table 8.1

Wrought aluminium alloy series

Alloy series	Main alloying element(s)	
1000	Commercially pure Al (>99% Al)	Not age-hardenable
2000	Copper	Age-hardenable
3000	Manganese	Not age-hardenable
4000	Silicon	Age-hardenable (if magnesium present)
5000	Magnesium	Not age-hardenable
6000	Magnesium and silicon	Age-hardenable
7000	Zinc	Age-hardenable
8000	Other (including lithium)	Mostly age-hardenable

Each alloy within a series has a four-digit number: XXXX. The first digit indicates the series number. For example, 1XXX indicates it is in the 1000 series, 2XXX is a 2000 series alloy, and so forth. The second digit indicates the number of modifications to the alloy type. For example, with the alloy 5352 Al the second digit (3) indicates that the alloy has been modified three times, but has a similar composition to earlier versions 5052 Al, 5152 Al and 5252 Al. The last two numbers in the four-digit system only have meaning for the 1000 series alloys. In this series, the last two digits specify the minimum purity level of the aluminium. As examples, 1200 Al has a minimum purity of 99.00% and 1145 Al is at least 99.45% pure. The last two digits in the 2000 to 8000 series has no meaningful relationship to the alloy content and serves no purpose other than to identify the different alloys in a series.

When an alloy is being developed it is prefixed with an X to signify it has not yet been fully evaluated and classified by the IADS. For example, the alloy X6785 indicates it is a new 6000 series alloy that is being tested and evaluated. When the evaluation process is complete, the prefix is dropped and the alloy is known as 6785 Al.

Most countries use the IADS to classify aluminium alloys. However, some nations use a different classification system or use the IADS together with their own system. For example, in the UK the IADS is used by the aerospace industry, although sometimes the British Standards (BS) system is also used to classify aluminium alloys. There are three principal types of specifications used in the UK: (i) BS specifications for general engineering use, (ii) BS specifications for aeronautical use (designated as the L series), and (iii) DTD (Directorate of Technical Development) specifications for specialist aeronautical applications.

8.2.3 TEMPER DESIGNATION SYSTEM

A system of letters and numbers known as the temper designation system is used to indicate the type of temper performed on an aluminium alloy. Temper is defined as the forging treatment (e.g. cold working, hot working) and thermal treatment (e.g. annealing, age-hardening) performed on an aluminium product to

achieve the desired level of metallurgical properties. The temper designation system has been approved by the American Standards Association, and is used in the USA and most other countries. The system is applied for all wrought and cast forms of aluminium (except ingots).

Basic temper designations consist of individual capital letters, such as 'F' for as-fabricated and 'T' for age-hardened. Major subdivisions of basic tempers, when required, are indicated by one or more numbers. The letters and numbers commonly used to describe the temper of aluminium alloys are given in Table 8.2. The temper designation follows the alloy designation, and is separated from it by a hyphen. As examples, 1100 Al-O means the aluminium has been heat treated by annealing and 2024 Al-T6, shown in Table 8.3, means that the alloy has been tempered to the T6 condition, which involves solution treatment followed by artificial ageing as given in Table 8.2.

Table 8.2

Temper designations for aluminium alloys

|	
F	As-fabricated (eg. hot-worked, forged, cast, etc.)
O	Annealed (wrought products only)
H	Cold-worked (strain hardened) H1x – cold-worked only (x refers to amount of cold working and strengthening) H2x – cold-worked and partially annealed H3x – cold-worked and stabilised at a low temperature to prevent age-hardening
W	Solution-treated
T	Age-hardened T1 – cooled from fabrication temperature and naturally aged T2 – cooled from fabrication temperature, cold-worked and naturally aged T3 – solution treated, cold-worked and naturally aged T4 – solution treated and naturally aged T5 – cooled from fabrication temperature and artificially aged T6 – solution-treated and artificially aged T7 – solution-treated and stabilised by over-ageing T8 – solution-treated, cold-worked and artificially aged T9 – solution-treated, artificially aged and cold-worked T10 – cooled from fabrication temperature, cold-worked and artificially aged

Table 8.3

Composition of 2000 alloys used in aircraft

| Alloy	Cu	Mg	Zn	Mn	Cr (max)	Si (max)	Fe (max)
2017	3.5–4.5	0.4–0.8	0.25	0.4–1.0	0.1	0.8	0.7
2018	3.5–4.5	0.45–0.9	0.25	0.2	0.1	0.9	1.0
2024	3.8–4.9	1.2–1.8	0.3	0.3–0.9	0.1	0.5	0.5
2025	3.9–5.0	0.05	0.3	0.4–1.2	0.1	1.0	1.0
2048	2.8–3.8	1.2–1.8	0.25	0.2–0.6		0.15	0.2
2117	2.2–3.0	0.2–0.5	0.25	0.2	0.1	0.8	0.7
2124	3.8–4.0	1.2–1.8	0.3	0.3–0.9	0.1	0.2	0.3

8.3 Non-age-hardenable aluminium alloys

The use of non-age-hardenable wrought alloys in aircraft is limited because they lack the strength, fatigue resistance and ductility needed for structural components such as skin panels, stiffeners, ribs and spars. The proof strength of most tempered non-age-hardenable alloys is below 225 MPa, which is inadequate for highly stressed aircraft structures. However, these alloys are used in some nonstructural aircraft parts and therefore it is worthwhile to briefly examine these materials.

The 1000, 3000, 5000 and most of the 4000 alloys cannot be age-hardened via heat-treatment processing. Solid solution strengthening, strain hardening and grain size control determine the strength of non-age-hardenable alloys. The improvement in strength achieved by solid solution strengthening is modest because most of the alloying elements have low solubility limits in aluminium at room temperature. The inability to dissolve large amounts of alloying elements into either interstitial or substitutional sites within the aluminium crystal structure means that very little strengthening can be achieved. Figure 8.2 shows the increase to the yield strength of high-purity aluminium from solid solution strengthening with several important alloying elements. Only a small improvement in strength is achieved. Strain hardening and grain size control are more effective mechanisms for strengthening non-age-hardenable alloys. For example, Fig. 8.3 shows the improvement in yield and ultimate tensile strengths of pure aluminium with percentage cold-working.
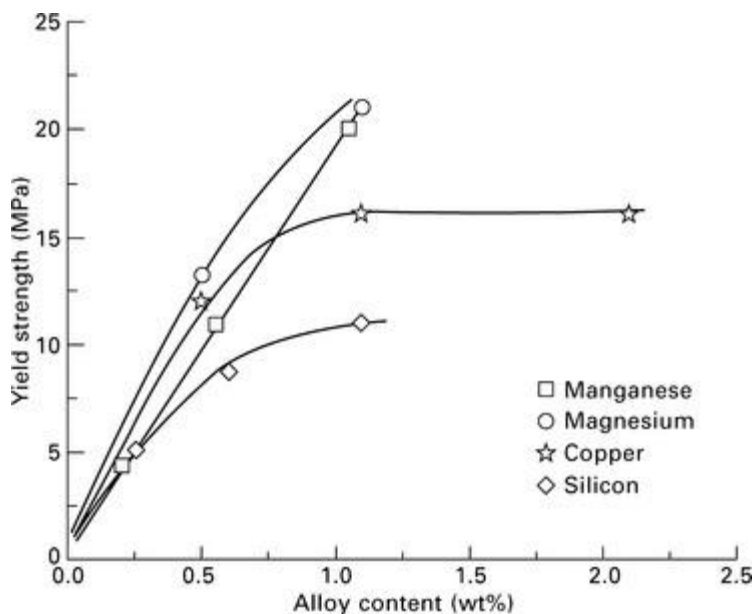
8.2 Effect of different alloying elements on the solid solution strengthening of pure aluminium in the annealed condition.
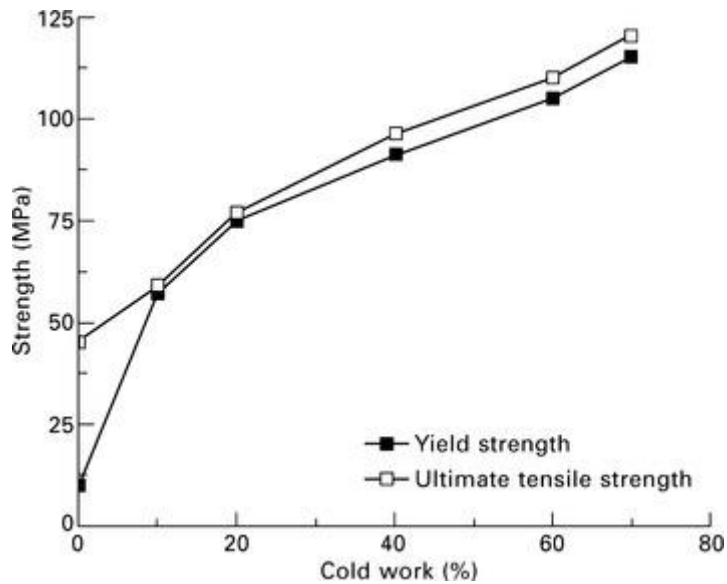
8.3 Effect of amount of cold working (strain hardening) on the yield and ultimate tensile strengths of pure aluminium.

8.3.1 1000 SERIES ALUMINIUM ALLOYS

The 1000 series is the highest purity form of aluminium alloys. An alloy is classified in the 1000 series when its aluminium content is greater than 99%. Only rarely are very small amounts of alloying elements deliberately added to 1000 metals. Instead, the trace amounts of impurity elements (e.g. Cu, Fe) are inadvertently extracted from the ore (bauxite) in the production of aluminium metal after extraction, refinement and processing. It is difficult and expensive to completely remove impurities, and so small amounts are left in the metal. Despite their low concentration, impurities can have a marked effect on the mechanical properties. For example, impurities such as copper, silicon and iron in amounts of less than 1% can increase the yield strength and ultimate tensile strength by as much as 300 and 40%, respectively. These improvements in strength are caused by solid solution strengthening and refinement of the grain structure. The 1000 series alloys are characterised by low yield strength, poor fatigue resistance and high ductility. The yield strength of most annealed 1000 series alloys is below 40 MPa. The low strength of 1000 alloys makes them unsuitable as structural materials on aircraft. However, occasionally these alloys are used in nonstructural aircraft parts where high strength is not required but weight and cost are important. Examples of the use of 1000 alloys include cowl bumps and scoops on small civil aircraft. Alloy 1100 is sometimes used for aircraft fuel tanks, fairings, oil tanks, and in the repair of wing tips and tanks.

8.3.2 3000 SERIES ALUMINIUM ALLOYS (AL–MN)

The main alloying element in this series is manganese, which provides some improvement in strength by solid solution hardening. It is not possible to age-harden 3000 alloys because manganese does not form precipitates in aluminium upon heat treatment. The yield strength of most 3000 alloys is below 200 MPa and, for this reason, they are rarely used in aircraft. The alloy 3003 Al, which contains 1.2% Mn, is used as a nonstructural material in fairing, fillets, tanks, wheel pants, nose bowls and cowlings in some aircraft. 3000 alloys are mostly used in non-aerospace components, such as automotive components (e.g. radiators, interior panels and trim).

8.3.3 4000 SERIES ALUMINIUM ALLOYS (AL–SI)

The 4000 alloys contain significant amounts of silicon. These alloys cannot be strengthened by heat treatment, unless magnesium is present to form high-strength precipitates (Mg_2Si). The use of 4000 alloys

in aircraft is limited because a brittle silicon phase can form in the aluminium matrix which reduces the ductility and fracture toughness. 4000 alloys are used in non-aerospace applications, in particular as brazing and welding filler materials.

8.3.4 5000 SERIES ALUMINIUM ALLOYS (AL–MG)

The main alloying element in these alloys is magnesium, which is usually present in concentrations of a few percent. Magnesium forms hard intermetallic precipitates in aluminium (Mg_2Al_3) that increase the strength of the alloy. However, the formation and growth of these precipitates cannot be controlled by heat treatment, and therefore the 5000 series alloys are not age-hardenable. As with the other non-age-hardenable alloys, 5000 alloys are used occasionally in nonstructural aircraft parts. For example, the alloy 5052 Al, which contains 2.5% Mg and 0.25% Cr, is one of the highest strength non-age-hardenable alloys that is available, and is used in wing ribs, wing tips, stiffeners, tanks, ducting and framework.

8.4 Age-hardenable aluminium alloys

The 2000, 6000, 7000 and many 8000 alloys can be strengthened by age-hardening. It is only by age-hardening that aluminium alloys obtain the strength needed for use in highly loaded structures and, therefore, this process is critical in the construction of aircraft. We first examine the composition and uses of the age-hardenable alloys used in aircraft, and then examine the age-hardening process.

8.4.1 2000 SERIES ALUMINIUM ALLOYS (AL–CU)

The 2000 alloys are used in many structural and semistructural components in aircraft. The main alloying element is copper, which readily forms high-strength precipitates when aluminium is age-hardened by heat treatment. 2000 alloys are characterised by high strength, fatigue resistance and toughness. These properties make the alloys well suited for fuselage skins, lower wing panels and control surfaces.

There are many types of 2000 alloys, but only a few are used in aircraft structures. One of the most common is 2024 Al (Al–4.4Cu–1.5Mg), which has been used for many years in aircraft structures such as stringers, longerons, spars, bulkheads, carry-throughs, stressed skins and trusses. 2000 alloys are used in damage-tolerant applications, such as lower wing skins and the fuselage structure of commercial aircraft which require high fatigue resistance. The alloy is also used in nonstructural parts such as fairings, cowlings, wheel pants and wing tips. Newer alloys are being introduced with superior properties to 2024 Al. For instance, 2054 Al is 15–20% higher in fracture toughness and twice the fatigue resistance of 2024 Al. Other 2000 series used in aircraft include 2018 Al, 2025 Al, 2048 Al, 2117 Al and 2124 Al. Reducing impurities, in particular iron and silicon, has resulted in higher fracture toughness and better resistance to fatigue crack initiation and crack growth. The composition and mechanical properties of 2000 alloys used in aircraft are given in Tables 8.3 and 8.4.

Table 8.4

Tensile properties of 2000 alloys used in aircraft

Alloy	Temper	Yield strength (MPa)	Tensile strength (MPa)	Elongation (%)
2017	T4	275	425	22
2018	T61	320	420	12
2024	T4	325	470	20
2024	T6	385	475	10
2024	T8	450	480	6
2025	T6	255	400	19
2048	T85	440	480	10
2117	T4	165	300	27
2124	T8	440	480	6

The alloying elements provide important properties that aid in the processing or strengthening of aluminium. Cu, Mg and Zn provide high strength through solid solution strengthening and precipitation hardening. These elements react with aluminium during heat treatment to create intermetallic precipitates (e.g. $CuAl_2$, Al_2CuMg, $ZnAl$) that increase the strength and fatigue resistance. Mn and Cr are present in small amounts to produce dispersoid particles (e.g. $Al_{20}Cu_2Mn_3$, $Al_{18}Mg_3Cr_2$) that restrict grain growth and thereby increase the yield strength by grain boundary hardening. The addition of trace amounts (0.1–0.2%) of Ti also reduces the grain size. Si is added to reduce the viscosity of molten aluminium, thus making it easier to cast into thick and complex shapes that are free of voids. Fe is used to reduce hot cracking in the casting. However, Si and Fe form coarse intermetallic particles (Al_7Cu_2Fe, Mg_2Si) which lower the fracture toughness, and, therefore, the amount of these elements is kept to a low concentration.

8.4.2 6000 SERIES ALUMINIUM ALLOYS (AL–MG–SI)

The principal alloying elements in the 6000 series are magnesium and silicon. 6000 alloys can be age-hardened with the formation of Mg_2Al_3 and Mg_2Si precipitates. 6000 alloys are used in a wide range of non-aerospace components, such as buildings, rail cars, boat hulls, ship superstructures and, increasingly, in automotive components. However, these alloys are rarely used in aircraft because of their low fracture toughness. 6061 Al (Al–1%Mg–0.6Si) is used occasionally in wing ribs, ducting, tanks, fairing and framework, although this alloy is one of very few used in aircraft.

8.4.3 7000 SERIES ALUMINIUM ALLOYS (AL–CU–ZN)

The 7000 alloys together with the 2000 alloys represent by far the most common aluminium alloys used in aircraft. The main alloying elements in 7000 alloys are copper and zinc, with the zinc content being three to four times higher than the copper. Magnesium is also an important alloying element. These elements form high-strength precipitates [$CuAl_2$, Mg_2Al_3, $Al_{32}(Mg, Zn)_{49}$] when aluminium is age-hardened.
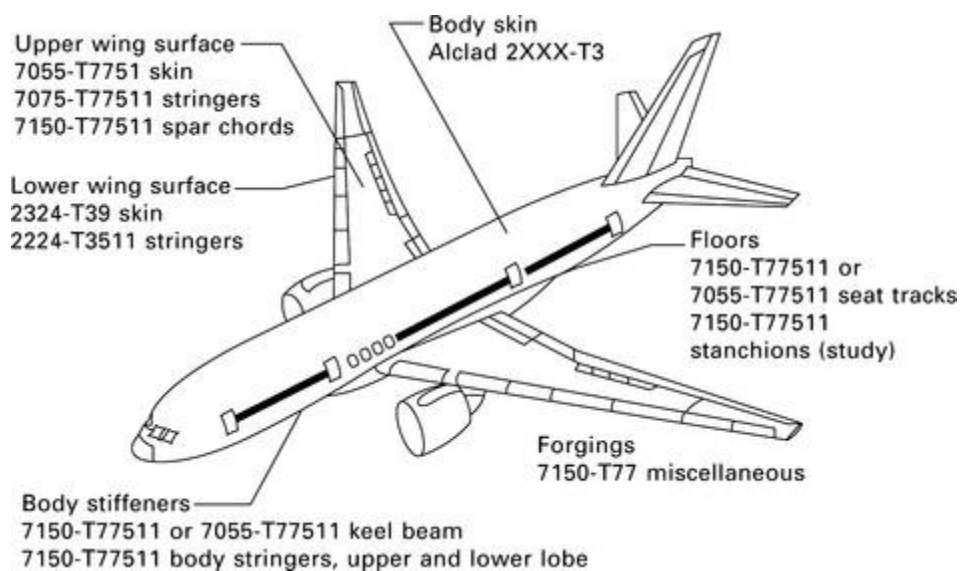7000 alloys generally have higher strength than 2000 alloys. The yield strength of the 7000 alloys used in aircraft is typically in the range 470 to 600 MPa as opposed to the 2000 alloys, which are between about 300 and 450 MPa. 7000 alloys are therefore used in aircraft structures required to carry higher stresses than 2000 alloy components, such as upper wing surfaces, spars, stringers, framework, pressure bulkheads and carry-throughs. The 7000 alloy most often used in aircraft is 7075 Al. Other 7000 alloys used in aircraft structures include 7049 Al, 7050 Al, 7079 Al, 7090 Al, 7091 Al, 7178 Al and 7475 Al. The composition and properties of these aluminium alloys are given in Tables 8.5 and 8.6. Figure 8.4 shows the new types of aluminium alloys and tempers used in the fuselage and wings of the Boeing 777. New high-toughness aluminium alloys for fuselage skins have enabled significant weight reductions through removal of some circumferential frames. The B777 is typical of most modern aircraft in that it uses both conventional and new aluminium alloys. The new alloy is usually superior in one or two properties over the conventional alloy. For example, the fuselage skin material is an alclad 2XXX-T3 alloy which has higher toughness and resistance to fatigue crack growth than 2024-T3.

Table 8.5

Composition of 7000 alloys used in aircraft

Alloy	Cu	Zn	Mg	Mn	Cr (max)	Si (max)	Fe (max)
7049	1.2–1.9	7.2–8.2	2.0–2.9	0.2	0.22	0.25	0.35
7050	2.0–2.6	5.7–6.7	1.9–2.6	0.1	0.04	0.12	0.15
7075	1.2–2.0	5.1–6.1	2.1–2.9	0.3	0.28	0.4	0.5
7079	0.4–0.8	3.4–4.8	2.9–3.7	0.3	0.25	0.3	0.4
7090	0.6–1.3	7.3–8.7	2.0–3.0			0.12	0.15
7091	1.1–1.8	5.8–7.1	2.0–3.0			0.12	0.15
7178	1.6–2.4	6.3–7.3	2.4–3.1	0.3	0.35	0.4	0.5
7475	1.2–1.9	5.2–6.2	1.9–2.6	0.6	0.25	0.1	0.12

Table 8.6

Tensile properties of 7000 alloys used in aircraft

Alloy	Temper	Yield strength (MPa)	Tensile strength (MPa)	Elongation (%)
7049	T73	470	530	11
7050	T736	510	550	11
7075	T6	500	570	11
7075	T73	430	550	13
7075	T76	470	540	12
7079	T6	470	540	14
7090	T7E71	580	620	9
7091	T7E69	545	590	11
7178	T6	540	610	10
7475	T651	560	590	12

Upper wing surface
7055-T7751 skin
7075-T77511 stringers
7150-T77511 spar chords

Lower wing surface
2324-T39 skin
2224-T3511 stringers

Body skin
Alclad 2XXX-T3

Floors
7150-T77511 or
7055-T77511 seat tracks
7150-T77511
stanchions (study)

Forgings
7150-T77 miscellaneous

Body stiffeners
7150-T77511 or 7055-T77511 keel beam
7150-T77511 body stringers, upper and lower lobe

8.4 New aluminium alloys and tempers used on the Boeing 777 (adapted from E. A. Starke and J. T. Staley, Application of modern aluminium alloys to aircraft, *Progress in Aerospace Science,* Vol 32, pp. 131–172, 1996).

8.4.4 8000 SERIES ALUMINIUM ALLOYS (AL–LI)

Aluminium alloys that cannot be classified according to their chemical composition into any one of the 1000 to 7000 series are allocated to the 8000 series. Several 8000 alloys contain lithium, which is unique amongst the alloying elements used in aluminium because it reduces density while simultaneously increasing elastic modulus and tensile strength. (Lithium is also an important, but not the principal, alloying element in a number of 2000 alloys, such as 2020 Al, 2090 Al and 2091 Al, which are used in some aircraft). Figure 8.5 shows the effect of lithium content on the density and Young's modulus of aluminium. The density decreases by 3% whereas the modulus increases by 5% for every 1% addition of lithium. This shows that lithium in low concentrations can provide significant weight savings to large aluminium structures. In addition, Al–Li alloys generally have better fatigue properties than 2000 and 7000 alloys.
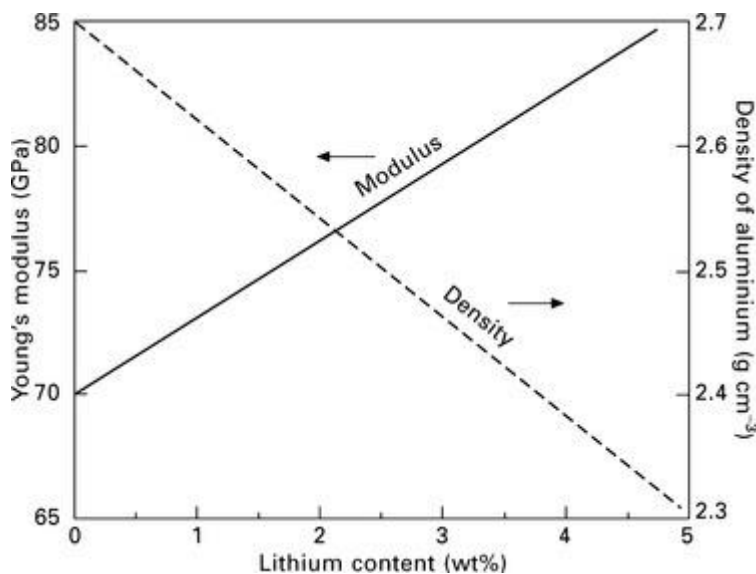
8.5 Effect of lithium content on the Young's modulus and density of aluminium.

The three Al–Li alloys most often used in aircraft structures are 8090 Al (2.4%Li–1.3%Cu–0.9%Mg), 8091 Al (2.6%Li–1.9%Cu–0.9%Mg), and 8092 Al (2.4%Li–0.65%Cu–1.2%Mg). Despite the higher specific stiffness and strength gained by increasing the Li content, the alloys used in aircraft have a relatively low content (less than 3%Li). This is because Al–Li alloys can only be processed using conventional casting technology when the Li content is under 3%. Alloys containing higher amounts of Li must be processed using rapid solidification technology, whereby the molten alloy is solidified rapidly as tiny drops. The solid droplets are then compressed with a binding agent into a metal block using powder metallurgy methods. Rapid solidification processing of alloys for aircraft structures is very expensive, and therefore Li contents below 3% are used to avoid this processing route.

The aerospace industry has invested heavily in the development of Al–Li alloys since the 1980s to produce lighter, stiffer and stronger aircraft structures. However, these alloys have not lived up to their initial promise of widespread use in airframes, and have largely failed to replace conventional aluminium alloys (e.g. 2024 Al, 7075 Al) in most aerospace applications. The limited use of Al–Li alloys is the result of several problems, including the high cost of lithium metal and the high processing cost of Al–Li alloys

making them prohibitively expensive for many aircraft structures. Al–Li alloys also have low ductility and toughness in the short transverse direction, which can lead to cracking.

Al–Li alloys are mainly used in military fighter aircraft where cost is secondary to structural performance. For example, Al–Li–Cu alloys are used in the fuselage frames of the F16 (*Flying Falcon*) as a replacement for 2024 Al, resulting in a three-fold increase in fatigue life, a 5% reduction in weight and higher stiffness. 8090 Al is used in the fuselage and lift frame of the EH 101 helicopter, again for improved fatigue performance and lower weight (by 180 kg), as shown in Fig. 8.6.

(a)

(b)

8.6 Al–Li alloy used in the EH101 helicopter. The shaded region in the illustration shows the external structures made using Al–Li alloys.

Al–Li alloys are also used in the super lightweight tanks for the space shuttle, which provided a weight saving of over 3 tonne, which translates directly into a similar increase in shuttle payload. The improved hydrogen tank is 5% lighter and 30% stronger than the original tank made using an Al–Cu (2119) alloy.

8.5 Speciality aluminium alloys

Occasionally, existing aluminium alloys do not have all the properties required for an aerospace application, and so the aircraft industry develops a new alloy. The practice of developing new aluminium alloys was common in the era between the mid-1930s and 1970 to meet the needs of the rapid advances in the aerospace industry. For example, a complex Al–Cu–Mg–Ni–Fe alloy known as Hiduminium RR58 was specifically developed for the Concorde. This alloy was created to maintain high tensile strength, creep resistance and fatigue endurance at the high temperatures caused by frictional heating during supersonic flight. Conventional 2000 and 7000 alloys used in the external structures of supersonic aircraft soften above about Mach 2 and, therefore, aluminium alloys with superior heat-resistant properties are required.

Aluminium–beryllium (Al–Be) alloys were developed for use in communications satellites and in load-bearing rings and brackets for spacecraft. Al–Be alloys are better than conventional aluminium alloys in terms of mechanical stability over a wide temperature range, vibrational dampening, thermal management and reduced weight, which are desirable properties for spacecraft materials.

8.6 Heat treatment of age-hardenable aluminium alloys

8.6.1 BACKGROUND

The heat-treatment process of age-hardenable aluminium alloys called ageing is essential to achieve the high mechanical properties required for aerostructures. Without the ageing process, the heat-treatable alloys would not have the properties needed for highly loaded aircraft components. As mentioned, the ageing process is only effective in the 2000, 4000 (containing Mg), 6000, 7000 and 8000 alloys; the ageing of the other alloy series provides no significant improvement to their mechanical properties.

The heat-treatment process consists of three operations which are performed in the following sequence: solution treatment, quenching, artificial (or thermal) ageing. The process of age-hardening is described in underline chapter 4, and the explanation provided here is specific to aluminium. Solution treatment involves heating the aluminium to dissolve casting precipitates and disperse the alloying elements through the aluminium matrix. Quenching involves rapid cooling of the hot aluminium to a low temperature (usually room temperature) to avoid the formation of large, brittle precipitates. After quenching the aluminium matrix is supersaturated with solute (alloying) elements. The final operation of ageing involves reheating the alloy to a moderately high temperature (usually 150–200 °C) to allow the alloying elements to precipitate small particles that strengthen the alloy. The heat-treatment process can improve virtually every mechanical property that is important to an aircraft structure (except Young's modulus that remains unchanged). Properties that are improved include yield strength, ultimate strength, fracture toughness, fatigue endurance and hardness. The heat-treatment process is performed in a foundry using specialist furnaces and ovens, and then the alloy is delivered in the final condition to the aircraft manufacturer. Some large aerospace companies have their own foundry because of the large amount of aluminium alloys used in the production of their aircraft.

In this section, we examine the heat treatment of age-hardenable aluminium alloys. Special attention is given to the age-hardening of 2000, 7000 and 8000 alloys because of their use in aircraft. We focus on the effect of the heat treatment process on the chemical and microstructural changes to aluminium, and the affect of these changes on the mechanical properties. It is worth noting that changes caused by heat treatment are subtlely different between alloy types, and the description provided here is a general overview of the ageing process.

8.6.2 SOLUTION TREATMENT OF ALUMINIUM

Solution treatment is the first stage in the heat-treatment process, and is performed to dissolve any large precipitates present in the metal after casting. These precipitates can seriously reduce the strength, fracture

toughness and fatigue life of aluminium, and therefore it is essential they are removed before the metal is processed into an aircraft structure. The precipitates are formed during the casting process. As the metal cools inside the casting mould, the alloying elements react with the aluminium to form intermetallic precipitates. Depending on the cooling rate and alloy content, the precipitates may develop into coarse brittle particles. The particles can crack at a small plastic strain that effectively lowers the fracture toughness. The purpose of the solution treatment process is to dissolve the large precipitates, and thereby minimise the risk of fracture.

The solution treatment process involves heating the aluminium to a sufficiently high temperature to dissolve the precipitates without melting the metal. The rate at which the precipitates dissolve and the solubility of the alloying elements in solid aluminium both increase with temperature, and therefore it is desirable to solution treat the metal at the highest possible temperature that does not cause melting. The solution treatment temperature is determined by the alloy composition, and allowances are made for unintended temperature variations of the furnace. Control of the temperature during solution treatment is essential to ensure good mechanical properties. When the temperature is too low, the precipitates do not completely dissolve, and this may cause a loss in ductility and toughness. When the temperature is too high, local (or eutectic) melting can occur that also lowers ductility and other mechanical properties. The treatment temperature for most aluminium alloys is within the range of 450–600 °C. The alloy is held at the treatment temperature for a sufficient period, known as the 'soak time', to completely dissolve the precipitates and allow the alloying elements to disperse evenly through the aluminium matrix. The soak time may vary from a few minutes to one day, depending on the size and chemical composition of the part. After the alloy has been solution treated it is ready to be quenched.

8.6.3 QUENCHING OF SOLUTION-TREATED ALUMINIUM

Quenching involves rapid cooling from the solution-treatment temperature to room temperature to suppress the reformation of coarse intermetallic precipitates and to freeze-in the alloying elements as a supersaturated solid solution in the aluminium matrix. Quenching is performed by immersing the hot aluminium in cold water or spraying the metal with water, and this cools thin sections in less than a few seconds. However, with aluminium components with a complex shape it is often necessary to quench at a slower rate to avoid distortion and internal (residual) stress. Slow quenching is done using hot water or some other fluid (e.g. oil, brine). Ideally, the aluminium alloy should be in a supersaturated solid solution condition with the alloying elements uniformly spread through the aluminium matrix after quenching. However, when slow cooling rates are used some precipitation can occur, and this reduces the ability to strengthen the alloy by thermal ageing. Figure 8.7 shows the effect of quenching rate on the final yield strength of 2024 Al and 7075 Al, which are alloys used in aircraft structures. The final yield strength is determined after the alloys have been quenched and thermally aged. It is seen that increasing the quenching rate results in greater final yield strength. Therefore, it is important to quench at an optimum cooling rate that maximises the concentration of alloying elements dissolved into solid solution whilst minimising distortion and residual stress.
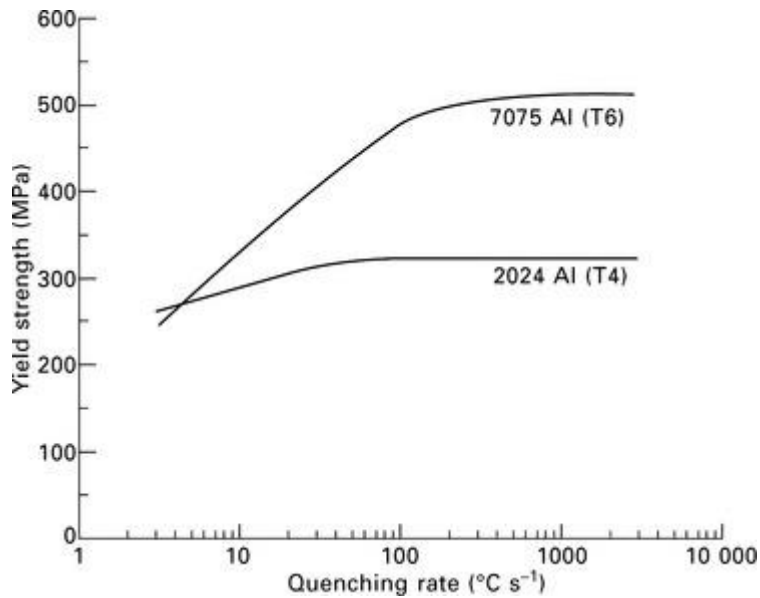
8.7 Effect of average quenching rate on the final yield strength of aerospace alloys 2024 Al and 7075 Al.

After quenching, the aluminium is soft and ductile, and this is the best condition to press, draw and shape the metal into the final product form. For example, when manufacturing aircraft parts using age-hardenable alloys it is easiest to plastically form the components when in the quenched condition. After forming, the aluminium is ready for ageing.

8.6.4 THERMAL AGEING OF ALUMINIUM

Ageing is the process that transforms the supersaturated solid solution to precipitate particles that can greatly enhance the strength properties. It is the formation of precipitates that provide aluminium alloys with the mechanical properties required for aerospace structures. Ageing can occur at room temperature, which is known as natural ageing, or at elevated temperature, which is called artificial ageing. Natural ageing is a slow process in most types of age-hardenable alloys, and the effects of the ageing process may only become significant after many months or years. Figure 8.8 shows the increase in yield strength of 2024 Al and 7075 Al alloys when naturally aged at room temperature for more than one year. The strength of 2024 Al alloy rises rapidly during the first few days following quenching, and then reaches a relatively stable condition. The strength of 7075 Al alloy, on the other hand, continues to rise over the entire period. Natural ageing can occur, albeit very slowly, at temperatures as low as − 20 °C. For this reason, it is sometimes necessary to chill aluminium below this temperature immediately after quenching to suppress or delay the ageing process. It is sometimes necessary to postpone ageing when manufacturing aircraft components and, therefore, the metal must be refrigerated immediately after quenching. For example, it is common practice to refrigerate 2024 Al rivets until they are ready to be driven into aircraft panels to maintain their softness which allows them to deform more easily in the rivet hole. More often, however, the alloy is artificially aged immediately or shortly after quenching.
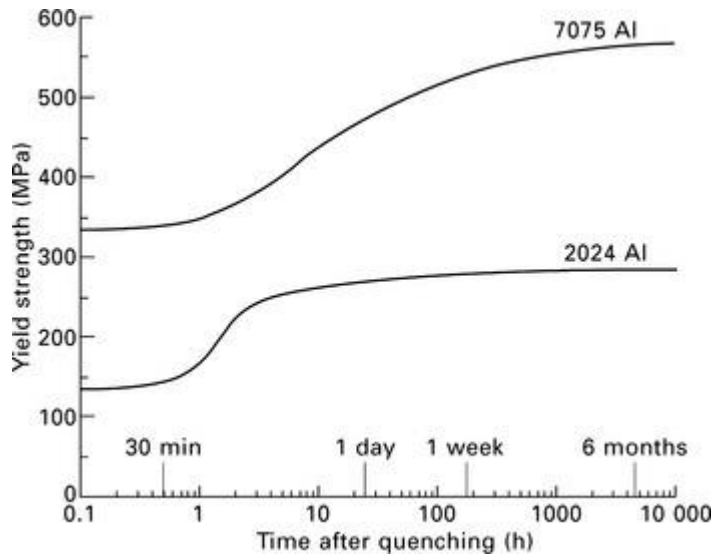
8.8 Effect of natural ageing time on the yield strength of 2024 Al and 7075 Al.

The artificial ageing process is performed at one or more elevated temperatures, which are usually in the range of 150 to 200 °C. The alloy is heated for times between several minutes and many hours, depending on the part size and the desired amount of hardening. During ageing, the alloy undergoes a series of chemical and microstructural transformations that have a profound impact on the mechanical and corrosion properties. The order of occurence of the transformations is:

○ supersaturated solid solution (α_{SS});
○ solute atom clusters (GP1 and GP2 zones);
○ intermediate (coherent) precipitates; and
○ equilibrium (incoherent) precipitates.

A summary of the transformations that occur to 2000, 7000 and 8000 aerospace alloys are provided in Table 8.7. It is seen that all the alloys undergo the transformation sequence: supersaturated solid solution → GP zones → intermediate precipitates → equilibrium precipitates. However, the changes that occur depend on the types and concentration of the alloying elements.

Table 8.7

Ageing transformations of 2000, 7000 and 8000 alloys

2000 Alloys
α_{ss} → GP zones → Coherent θ″ ($CuAl_2$) → Semicoherent θ′ ($CuAl_2$) → Incoherent θ ($CuAl_2$)
α_{ss} → GP zones → Coherent S′ (Al_2CuMg) → Incoherent S (Al_2CuMg) – high Mg content
7000 Alloys
α_{ss} → GP zones → Coherent θ″ ($CuAl_2$) → Semicoherent θ′ ($CuAl_2$) → Incoherent θ ($CuAl_2$)
α_{ss} → GP zones → Semicoherent η′ ($MgZn_2$) → Incoherent η ($MgZn_2$)
α_{ss} → GP zones → Semicoherent T′ [$Al_{32}(Mg,Zn)_{49}$] → Coherent T [$Al_{32}(Mg,Zn)_{49}$]
8000 Alloys
Al–Li: α_{ss} → Semicoherent δ′ (Al_3Li) → Incoherent δ (AlLi)
Al–Li–Mg: α_{ss} → Semicoherent δ′ (Al_3Li) → Incoherent Al_2MgLi
Al–Li–Cu (low Li:Cu): α_{ss} → GP zones → T_1 (Al_2CuLi) → Coherent θ″ ($CuAl_2$) → Semicoherent θ′ ($CuAl_2$) → Incoherent θ ($CuAl_2$)
Al–Li (high Li:Cu): α_{ss} → GP zones → Incoherent T_1 (Al_2CuLi)
Al–Li–Cu–Mg: α_{ss} → GP zones → Semicoherent S′ (Al_2CuMg) → Incoherent S (Al_2CuMg)

Figure 8.9 shows the different stages of the ageing process with time and the growth in the average size of the solute cluster and precipitate with time. The sizes shown are approximate and depend on the alloy composition and ageing temperature, although the trend shown is similar for most aged metals. We now examine each of the transformations in greater detail.
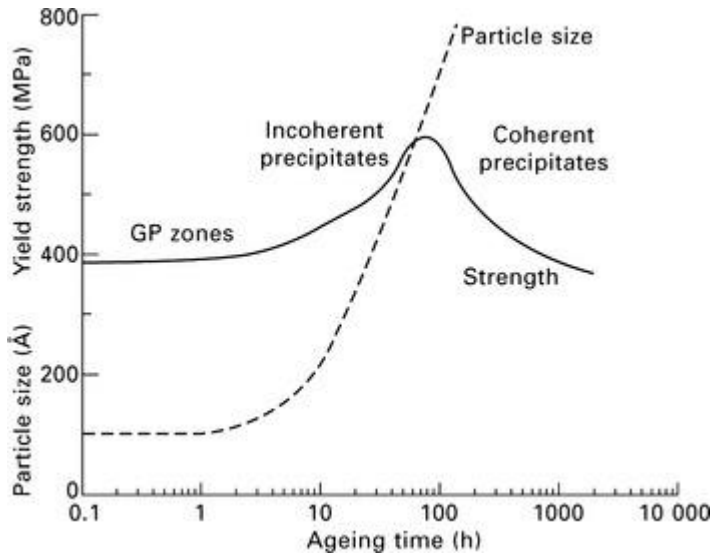
8.9 Effect of time on the ageing of an aluminium alloy.

When aluminium in the supersaturated solid solution condition is aged, the first significant change is the formation of solute atom clusters, known as Guinier–Preston (GP) zones. GP zones develop by the solute (alloying) atoms moving over relatively short distances to cluster into solute-rich regions. When the zones first develop, the atoms of the alloying elements are randomly arranged relative to the lattice structure of the aluminium matrix, and these are called GP1 zones. The composition of the GP zone is dependent on the alloy content. For example, GP zones formed in 2024 Al alloy are rich in copper and in 7075 Al are rich in copper and zinc. Minor alloying elements (e.g. Mn) can also be present in the zones.

With further ageing the solute atoms become arranged into an ordered pattern that is coherent with the aluminium lattice matrix, and these are known as GP2 zones. The number of GP zones is dependent on the temperature, time and alloy content, and their density can reach 10^{23} to 10^{24} m^{-3}. However, GP zones are very small, typically one or two atom planes in thickness and several tens of atom planes in length. Despite their small size, GP zones generate elastic strains in the surrounding matrix that raise the yield strength and hardness. The GP zones grow in size and decrease in number with ageing time until eventually they transform into intermediate precipitates.

During ageing the GP2 zones transform into metastable intermediate precipitates. These precipitates are coherent or semicoherent with the lattice structure of the aluminium matrix. The precipitates are often plate- or needle-shaped and grow along the crystal planes of the matrix. The precipitates nucleate at the sites of GP2 zones and this is known as homogeneous nucleation. Precipitates also grow in regions rich in solute atoms, such as dislocations and grain boundaries, and this is called heterogenous nucleation. Both homogeneous and heterogenous processes are important in the nucleation of precipitates. Following nucleation, the precipitates grow with ageing time as they scavenge solute atoms from the surrounding matrix, and they can reach 0.1 μm or more in size.

In many aluminium alloys, the intermediate precipitates undergo a number of transformations before developing into the final stable condition. For example, in aluminium containing copper, a number of intermediate $CuAl_2$ precipitates (θ', θ'') having different degrees of coherency with the matrix lattice develop before the final formation of stable $CuAl_2$ (θ) precipitates. During the nucleation and growth of

intermediate particles many of the mechanical properties, such as yield strength, fatigue endurance and hardness, are improved. Eventually, the intermediate precipitates transform into stable, equilibrium particles and, at this point, the mechanical properties are maximised.

Equilibrium of the precipitates occurs when the particles reach a final chemical composition and crystal structure that does not change with further ageing. The type of equilibrium precipitates produced by ageing is determined by the composition of the aluminium alloy. The main equilibrium precipitates found in aerospace 2000, 7000 and 8000 alloys are given in Table 8.7. The single most important precipitate in 2000 alloys (Al–Cu) is θ ($CuAl_2$). Various precipitates occur in 7000 alloys (Al–Cu–Zn) including θ, η ($MgZn_2$) and T [$Al_{32}(Mg,Zn)_{49}$]. Many types of precipitates are also found in 8000 alloys (Al–Li). In Al–Li–Mg alloys, the other main precipitate is Al_2MgLi; in Al–Li–Cu alloys, the other precipitates are θ ($CuAl_2$) and T1 (Al_2CuLi); and in Al–Li–Cu–Mg alloys the other precipitate is S (Al_2CuMg). Examples of precipitates are shown in Fig. 8.10.


(a)

(b)

(c)
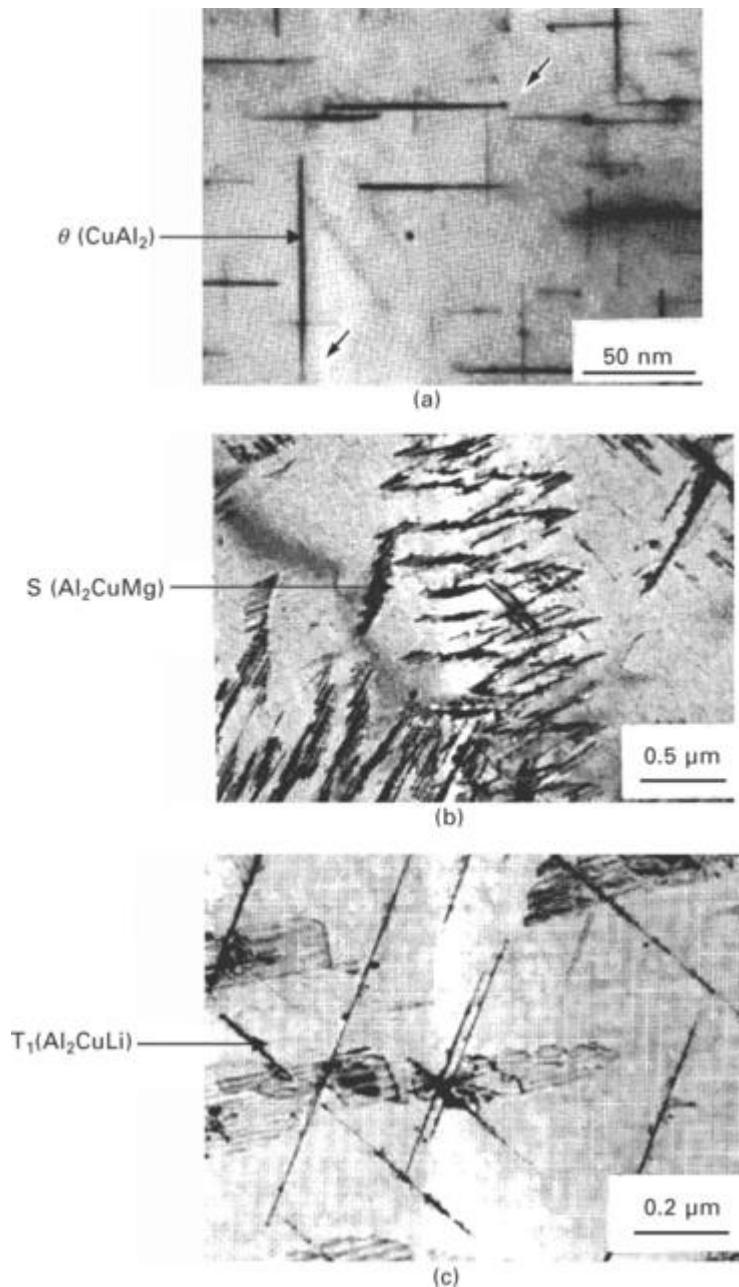
8.10 Precipitates in an age-hardenable aluminium alloy (from I. J. Polmear, *Light alloys,* Butterworth–Heinemann, 1995).

The mechanical properties reach their highest value at the stage when the precipitates transform from coherent to incoherent particles. Continued ageing at too high a temperature for too long a time degrades properties such as strength and hardness as the equilibrium particles grow in size. The largest precipitates continue to grow whereas the smaller particles disappear, resulting in an increase in the average particle size and a reduction in the number of particles. The softening of an alloy as a result of particle coarsening is called over-ageing, and it must be avoided if optimum properties are required.

The optimum ageing condition is achieved by heat treating the aluminium alloy in a foundry at the correct temperature and time. The optimum heat-treatment condition is governed by the composition of the alloy and geometry of the part. However, it is possible that natural ageing of the alloy occurs after the part has been put into service on an aircraft, which may cause over-ageing. Although this is not a significant issue for subsonic aircraft, it may be problem with supersonic aircraft when frictional heating of the aluminium skins at high flight speeds may cause over-ageing. Surface temperatures in excess of 150 °C occur at the leading edges of aircraft during supersonic flight, and this has the potential to weaken the skins. However, structural failures of aluminium alloys on supersonic aircraft caused by over-ageing do not occur because of the design safety margins.

8.6.5 PROPERTIES OF AGE-HARDENED ALUMINIUM

The mechanical properties of age-hardenable alloys are dependent on the temperature and time of the ageing operation. Figure 8.11 shows the typical effect of ageing temperature on the tensile strength of an aluminium alloy. The strength increases as the metal undergoes the transformations from a supersaturated solid solution to GP zones to intermediate (coherent) precipitates. At the stage when the precipitates transform from coherent to incoherent particles the maximum strength is reached. Over-ageing causes a deterioration in strength owing to coarsening of the incoherent particles.
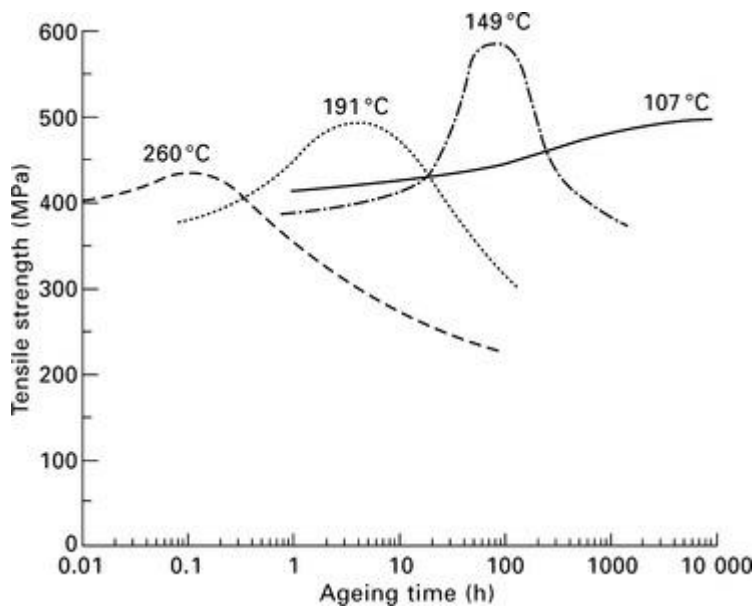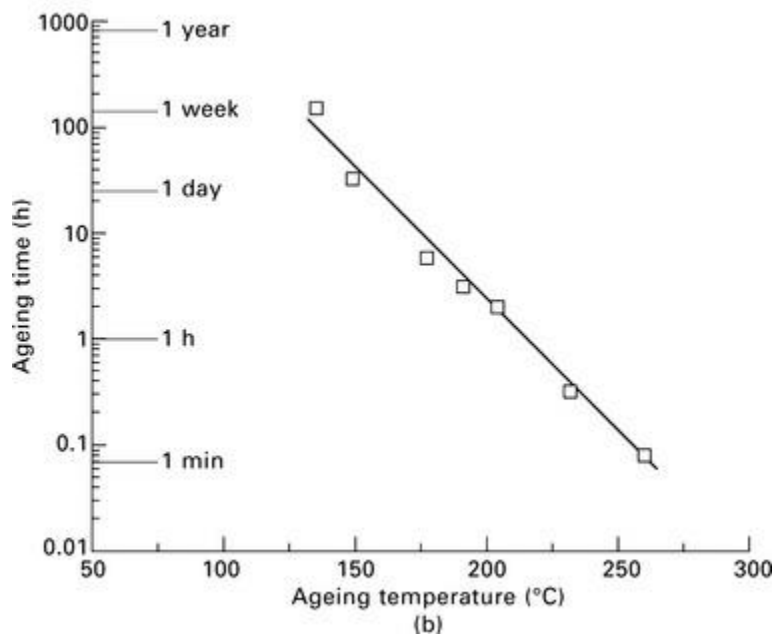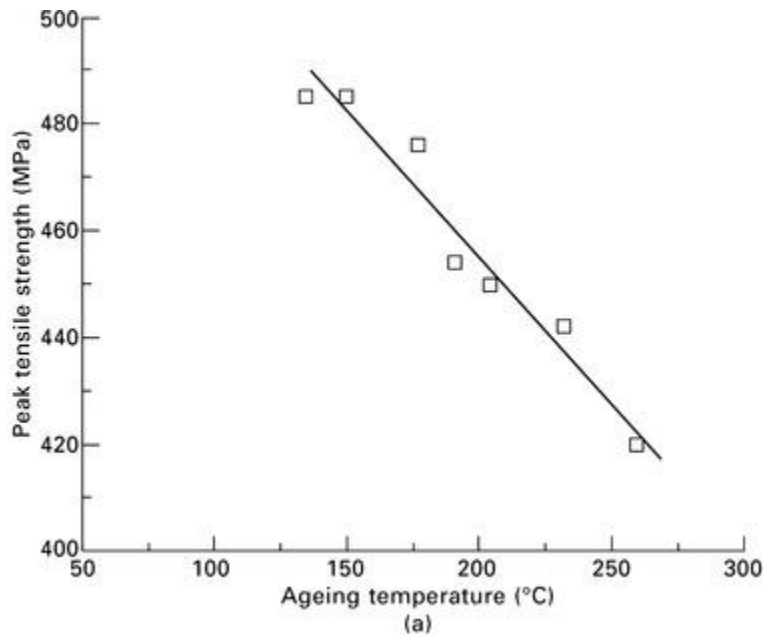

8.11 Effect of ageing temperature on the tensile strength of an aluminium alloy.

Aluminium alloys are strengthened by a combination of mechanisms involving solid solution hardening, work hardening and grain boundary hardening, although the dominant mechanism is precipitation hardening. Without the extra strength provided by the precipitates many alloys would not have sufficient

strength and toughness for use in lightweight aircraft structures. The initial improvement in strength shown in Fig. 8.11 results from GP zones resisting the movement of dislocations. GP zones generate an elastic strain in the surrounding matrix lattice that resists dislocation slip. Each GP zone provides only a small amount of resistance, but the very high density of GP zones (up to 10^{23} to 10^{24} m^{-3}) generates a sufficiently high internal strain to impede dislocation movement. It is the restriction of dislocation movement that causes the yield strength of aluminium to increase during the early stage of ageing. However, GP zones cannot completely stop the movement of dislocations. Dislocations can cut through the zones and continue to move through the aluminium matrix. The coherent precipitates cause a further improvement in strength because they generate a higher internal strain in the matrix lattice than GP zones. As the coherent particles grow in size they provide greater resistance to dislocation slip. As with GP zones, when a dislocation reaches a coherent precipitate it cuts through and then continues to move through the matrix. Maximum strength is achieved at the stage when the precipitates transform from coherent to incoherent particles. Dislocations are unable to cut through incoherent particles, and instead must move around them by the Orowan mechanism. The Orowan strengthening mechanism is described in chapter 4. This mechanism is very resistant to dislocation movement and, thereby, is extremely effective in raising the yield strength. High resistance to dislocation slip occurs when the precipitates are small and closely spaced, that is the situation when the particles are initially transformed into incoherent particles. Over-ageing beyond this stage causes the incoherent precipitates to coarsen and become more widely spaced, and this reduces the efficacy of the strengthening process.

The maximum strength that can be achieved by ageing is dependent on the temperature. Figure 8.12 shows the maximum strength and the heat-treatment time taken to reach the maximum strength for a range of ageing temperatures. The peak strength decreases with increasing temperature, although the time required to reach maximum strength increases rapidly with decreasing temperature. It is often not practical to heat treat a metal product over many days or weeks. A temperature should be selected that provides a compromise between high strength and short ageing time. In the production of aluminium aircraft structures, the ageing temperature is usually in the range of 150–200 °C, which provides a good balance between strength and process time.

18.12 Effect of ageing temperature on (a) maximum tensile strength and (b) time to reach maximum strength of an age-hardenable aluminium alloy.

Although ageing improves mechanical properties such as strength and fatigue resistance, the ageing process may degrade some other properties. Ageing lowers the ductility of aluminium, although the elongation-to-failure of many fully-aged alloys is above 5–10%. The resistance of aluminium alloys to stress corrosion cracking (SCC) may also be affected by age-hardening. The SCC process is described in chapter 21 and involves the growth of cracks under the combined effects of tension loads and corrosive fluids that lowers the fracture stress of the material. Figure 8.13 shows the effect of ageing time on the SCC resistance of an aluminium alloy, and it reaches a minimum level when the alloy is fully hardened. It is therefore necessary to protect age-hardened alloys against SCC when used in aircraft by using corrosion-resistant protective

coatings. Several types of coatings are used for aircraft, including cladding and anodised films, and these are described in chapter 21.
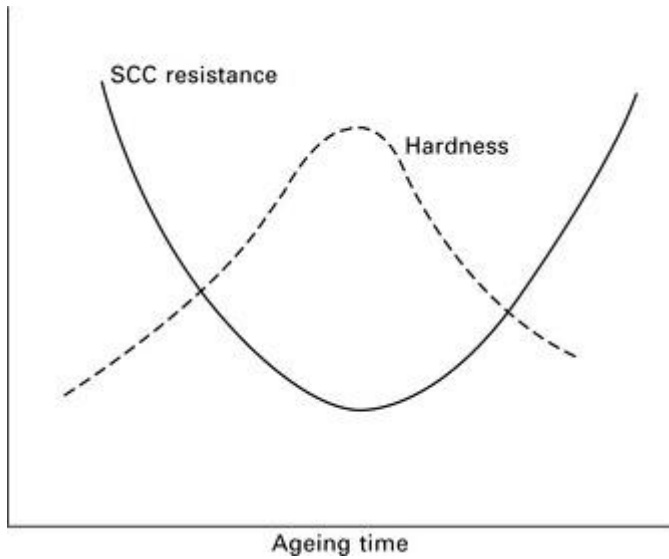
8.13 Effect of ageing time on the resistance of aluminium to stress corrosion cracking (SCC).

8.7 High-temperature strength of aluminium

An important consideration when using aluminium alloys (and other materials) in aircraft structures is softening that occurs at elevated temperature. Care must be taken when selecting materials for supersonic aircraft to ensure structural weakening does not occur owing to excessive heating. Material properties such as stiffness, strength, fatigue resistance and toughness are degraded at high temperature. The loss in stiffness and strength of an aluminium alloy with increasing temperature is shown in Fig. 8.14. The sensitivity of the engineering properties to temperature differs between alloy types, but they all experience a large reduction in their mechanical properties when heated above 100–150 °C.
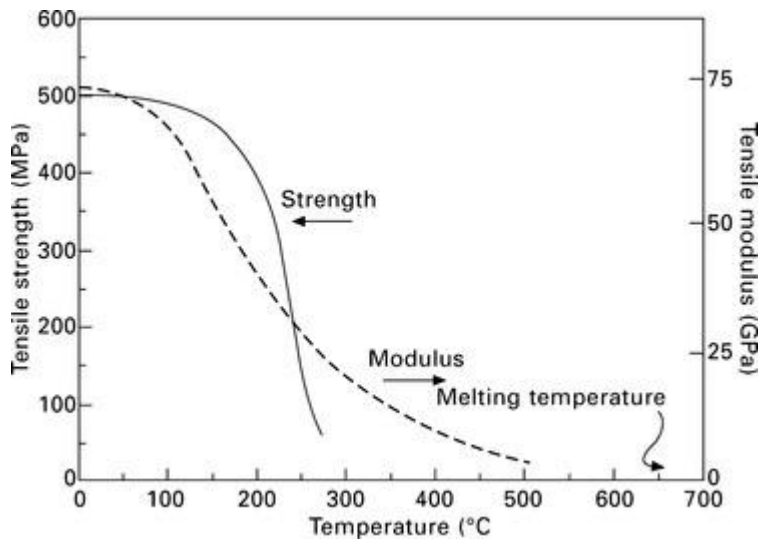
8.14 Effect of temperature on the tensile properties of an aluminium alloy.

Thermal softening is a key factor in the selection of aluminium alloys for aircraft structures that experience a large temperature rise as a result of frictional skin heating. The nose section, leading edges and skins of aircraft are heated owing to friction caused by molecules in the atmosphere moving across the aircraft surfaces at high speed. Frictional heating is generally not a problem when flying at subsonic speeds because the surface temperature does not rise much above 80–90 °C, which is below the temperature at which aircraft materials experience significant softening. However, higher temperatures are generated when flying at supersonic speeds. The hottest parts of the aircraft are the nose cone and leading edges of the wings and tail sections, with temperatures in excess of 150 °C being reached at Mach 2. As Fig. 8.14 shows, at 150 °C the modulus and strength is 10–20% below room temperature. Temperatures exceeding 1000 °C are experienced during re-entry of spacecraft such as the space shuttle and temperatures above 500 °C can occur in ultra-high speed aircraft. At these temperatures, the aluminium must be thermally protected by a heat shield, such as ceramic tiles.

Titanium alloys for aerospace structures and engines

9.1 Introduction

Titanium alloys are used in airframe structures, landing gear components and jet engine parts for their unique combination of properties: moderate density, high strength, long fatigue life, fracture toughness, creep strength, and excellent resistance to corrosion and oxidation. Titanium alloys also have good mechanical performance at high temperature (up to 500–600 °C), which is well above the operating temperature limit of lightweight aerospace materials such as aluminium alloys, magnesium alloys and fibre–polymer composites. For this reason, when titanium alloys were originally used in aircraft in the early 1950s it was for high-temperature applications. The earliest use of titanium was in compressor discs and fan blades for gas turbine engines, which require excellent creep resistance at high operating temperature. The use of titanium was important in the early development of jet engines, which were originally built using heat-resistant steels and nickel alloys. Both steels and nickel alloys are 'heavy materials', and their replacement with titanium in discs and blades reduced the weight of early jet engines by more than 200 kg. Titanium has been an important engineering material in gas turbine engines for more than fifty years, and currently it accounts for 25–30% of the weight of most modern engines. Titanium can be used in engine components required to operate at temperatures up to 500–600 °C. The engine components made using titanium are fan blades, shafts and casings in the inlet region; low-pressure compressors; and plug and nozzle assemblies in the exhaust section. Titanium is also used in the engine frames, casings, manifolds, ducts and tubes. It is not possible to use titanium in all parts of the engine, and it is unsuitable within the combustion chamber and other sections where the temperature exceeds 600 °C. Above this temperature, titanium rapidly softens, creeps and oxidises, and more heat-resistant materials such as nickel alloys are required. The application and metallurgical properties of nickel alloys for jet engines is covered in chapter 12.

Titanium is also an important material for heavily-loaded airframe structures. Titanium is used in a wide variety of structures on commercial aircraft, including wing boxes, wings and undercarriage parts. Titanium is used when its high strength (compared with aluminium) allows the same load to be carried by a physically smaller structural part, even though there is no weight advantage because of the higher density. Forged titanium is used in airframes requiring high strength and high toughness or when there is too little airframe space for aluminium alloys. For many years, steel has been used in aircraft landing gear because of its high stiffness, strength, fatigue resistance and toughness. However, high-strength steels are susceptible to corrosion and hydrogen embrittlement, which is the phenomenon whereby steel becomes very brittle owing to the absorption of hydrogen. Titanium is used as a replacement material for steel in landing gear to eliminate the problems of corrosion and hydrogen embrittlement as well as to achieve a significant weight saving. The use of titanium in large passenger aircraft designed before 1980 was relatively modest at 3–5% of the structural weight, but more recent aircraft use a greater percentage (Fig. 2.9). For example, titanium accounts for 9% of the structural weight of the A380 and 10% of the B777.

Aerospace is the single largest market for titanium products; with the industry consuming about 80% of the global production of the metal. The aerospace applications of titanium in the USA are approximately:

∞ jet engines for commercial aircraft: 37%;
∞ jet engines for military aircraft: 24%;
∞ airframes for commercial aircraft: 18%;
∞ airframes for military aircraft: 12%;
∞ rockets and spacecraft: 8%; and
∞ helicopters and armaments: 1%.

Titanium accounts for a higher percentage of the structural mass of military aircraft compared with commercial airliners in order to withstand the higher airframe loads generated by extreme manoeuvres during combat operations. The structural mass of fighter aircraft made using titanium is often in the range of 10–30%. For example, Fig. 9.1 shows that titanium alloys account for 26% (or 7000 kg) of the structural

weight of the F-14 *Tomcat* fighter aircraft. The components made using titanium range in size from highly stressed wing structures, landing gear parts and tail sections down to small fasteners, springs and hydraulic tubing. Other examples of the use of titanium in fighter aircraft are the F/A-18 *Hornet* and F-15 *Eagle*. About 26% of the airframe of the F-15 is made of titanium, including the fuselage skin, wing torque box, wing spars and bulkheads, engine pod frames, and firewalls that separate the engines from the main frame. Titanium is also used in helicopters for the main rotor hub, tail rotor hub, pivots, clamps, and blade tips which require high strength and fracture toughness. Titanium alloys are also used in solid-fuel and liquid-fuel engines, high-pressure gas and fuel storage tanks and, in some cases, the skin of rockets.
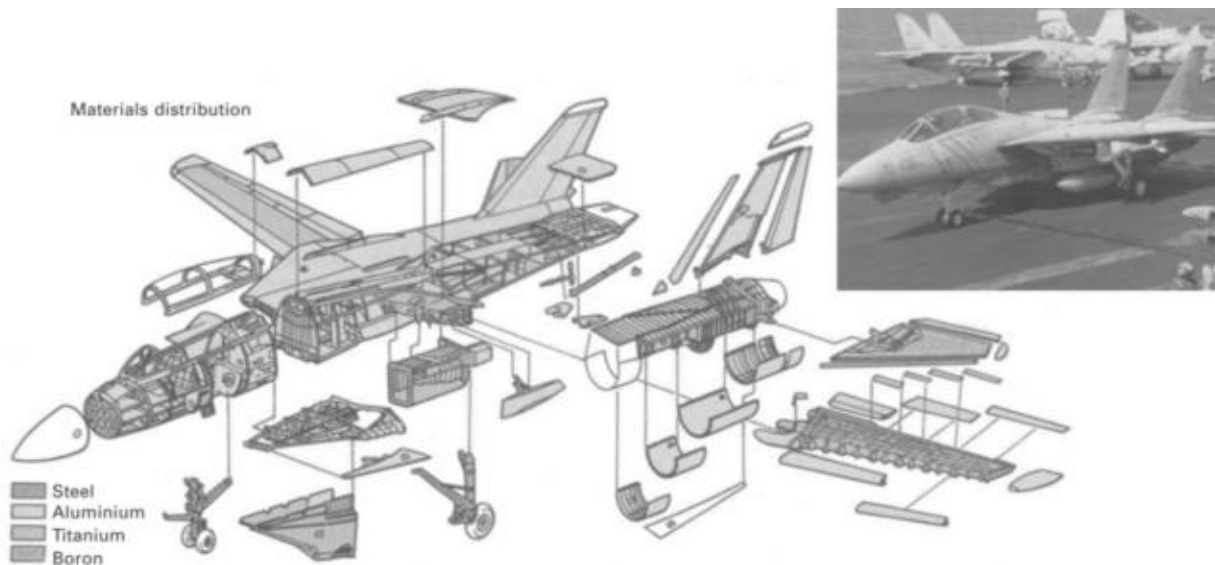
9.1 Use of titanium alloys in the F-14 *Tomcat*. (reproduced with permission from M. Spick, *The great book of modern warplanes*, Salamander Books Ltd, 2000)

In this chapter, we discuss the metallurgical and structural properties of titanium alloys and their applications in aerospace structures and engines. The benefits and drawbacks of using titanium in aircraft are examined and the different types of titanium alloys, and how their properties are controlled by alloying, forging and heat-treatment are studied. New types of titanium-based materials with potential aerospace applications are also reviewed. The metallurgical and mechanical properties of titanium aluminides and titanium shape-memory alloys are described, together with their potential applications in future aircraft.

9.2 Titanium alloys: advantages and disadvantages for aerospace applications

9.2.1 ADVANTAGES

There are many benefits to using titanium in aircraft structures and engines, although (as with any material) there are also disadvantages. Table 9.1 compares the stiffness and strength of several types of titanium with that of other aerospace structural materials. There are different classes of titanium which are called commercially pure titanium, α-titanium, β-titanium and α+β-titanium. The specific stiffness of titanium alloys is slightly lower than that of other aerospace materials, so there is no benefit in using them in aircraft structures designed for high stiffness. The strength of the titanium alloys varies over a wide range. This is because the properties are dependent on the alloy composition and heat treatment. However, the specific strength properties of titanium alloys are superior to the other materials (except carbon–epoxy composite), and for this reason they are good materials to use in aircraft structures required to carry high loads, such as airframe components, undercarriage parts, and wing boxes.

Materials	Average specific gravity (g cm^{-3})	Young's modulus (GPa)	Specific modulus (MPa m^3 kg^{-1})	Yield strength (MPa)	Specific strength (kPa m^3 kg^{-1})
Pure titanium	4.6	103	22.4	170–480	37–104
α-Ti alloys	4.6	100–115	21.7–25.1	800–1000	174–217
β-Ti alloys	4.6	100–115	21.7–25.1	1150–1300	180–282
α+β-Ti alloys	4.6	100–115	21.7–25.1	830–1300	180–282
Aluminium (2024-T6)	2.7	70	25.9	385	142
Aluminium (7075-T76)	2.7	70	25.9	470	174
Magnesium	1.7	45	26.5	200	115
High-strength low-alloy steel	7.8	210	26.9	1000	128
Carbon–epoxy composite*	1.7	50	29.4	760	450

*[0/± 45/90] Carbon–epoxy; fibre volume content = 60%.

Other benefits of using titanium include high strength, good fatigue resistance, creep resistance at high temperature, and excellent oxidation resistance up to 600 °C. Certain types of titanium alloys can be joined by welding or diffusion bonding; thereby reducing the need for mechanical fasteners (bolts, screws, rivets) and adhesive bonding that is a requirement for age-hardened aluminium assemblies. Titanium has better resistance to corrosion than high-strength aluminium alloys, including the most damaging forms such as stress corrosion cracking and exfoliation. Titanium has the ability to form a thin oxide surface layer, which is resistant and impervious to most corrosive agents and which provides the material with excellent corrosion resistance. Titanium is used as a replacement material for aluminium in aircraft structures when corrosion resistance is the prime consideration.

An important advantage of titanium alloys over many other aerospace materials, particularly aluminium alloys and fibre–polymer composites, is high strength at elevated temperature. Titanium is often selected for use at temperatures too high for aluminium or composite material but where the temperatures/loads do not dictate the use of steel or nickel superalloys if weight is a key consideration. Figure 9.2 shows the effect of temperature on the yield strength of two titanium alloys used in gas turbine engines. The loss in strength with increasing temperature for an aluminium alloy (7075 Al-T6) is shown for comparison. The strength of titanium drops gradually with increasing temperature, and adequate strength is retained to 500–600 °C. It is for this reason, together with excellent resistance to creep and oxidation, that titanium is used in gas turbine engines and other high-temperature applications.
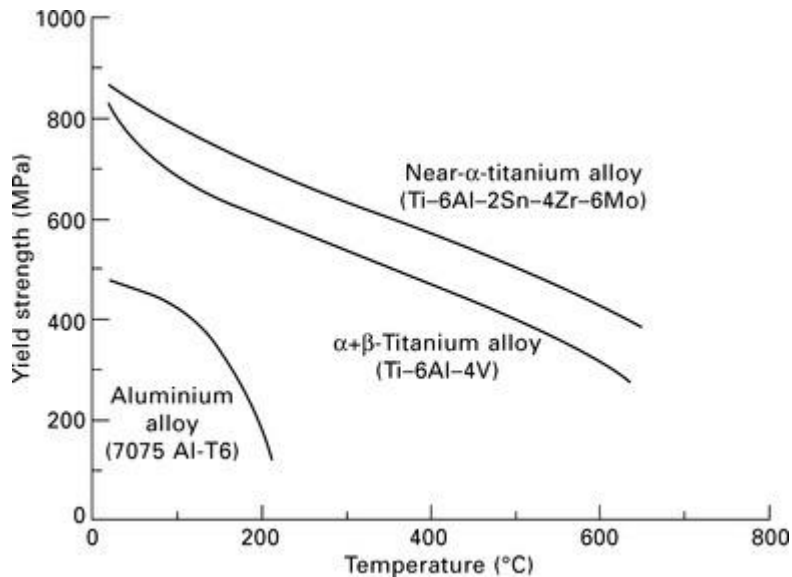
9.2 Effect of temperature on the yield strength of titanium and aluminium alloys.
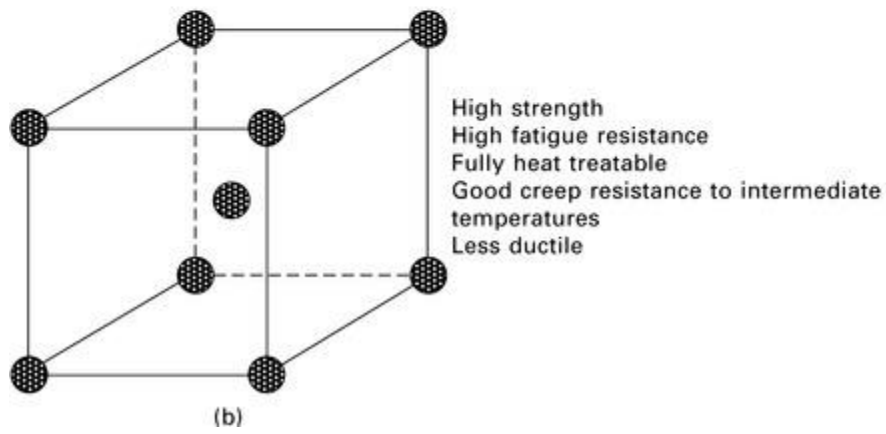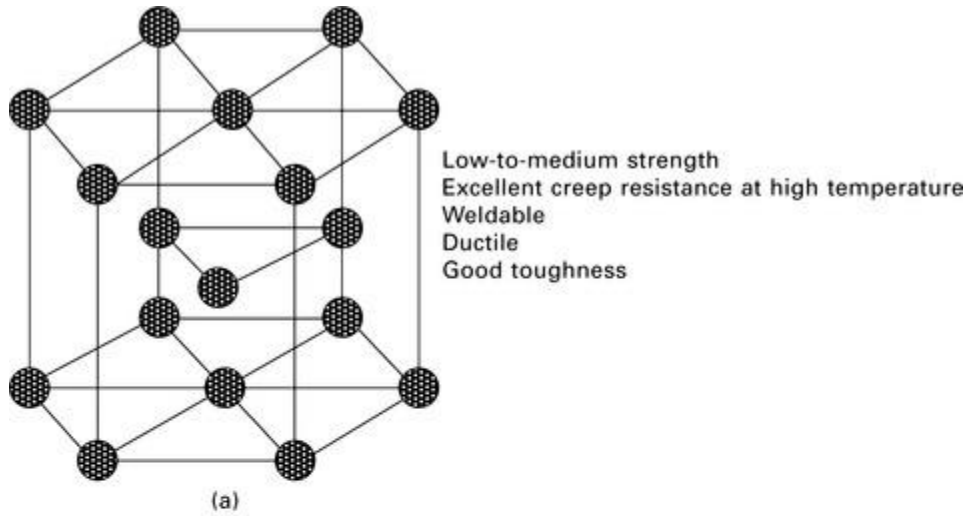
9.2.2 DISADVANTAGES

Disadvantages of using titanium include relatively high density (4.5 g cm^{-3}) compared with aluminium alloys (2.7 g cm^{-3}) and carbon–epoxy composites (1.5–2.0 g cm^{-3}). However, it is lighter than nickel superalloys (8.7 g cm^{-3}) when used in jet engines. A major disadvantage of titanium is the high cost, which varies with the usual price fluctuations in the global metals commodity market; the raw material cost is typically $10 000–12 000 per tonne (June 2010). The high cost is the result of the expensive process used to extract titanium from its ore together with the costly processes used in fabricating and shaping the metal into an aerospace component. Titanium is difficult to machine and requires specialist material removal processes (such as laser-assisted machining) to produce aircraft components free of machining damage.
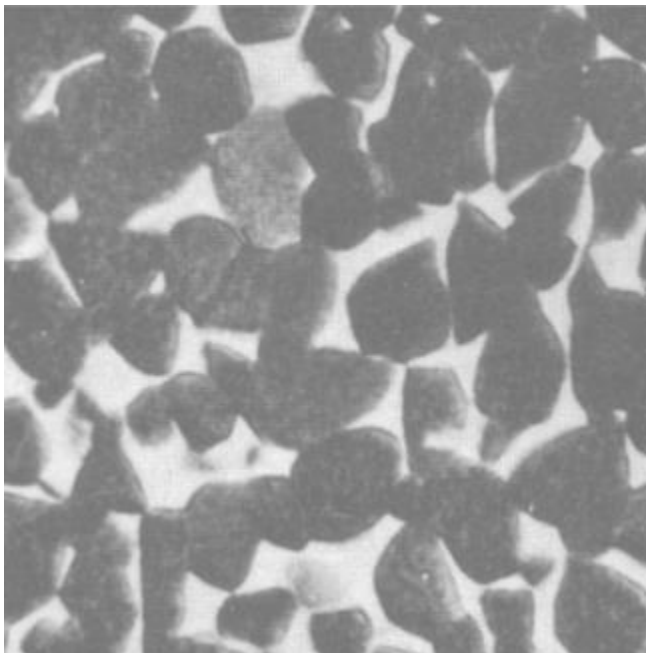
9.3 Types of titanium alloy

9.3.1 PHASES OF TITANIUM

A metallurgical property of titanium alloys that is important in their use in aircraft is allotropy, which is defined as different physical forms of the same material that are chemically very similar. Many metals, including the aluminium, magnesium and nickel alloys used in aircraft, can only occur in one crystalline phase at 20 °C. For instance, aluminium can only have a face-centred-cubic crystal structure at room temperature, and no other. As another example, the crystal structure of magnesium is always hexagonal close packed at 20 °C. Titanium alloys, on the other hand, can have a hexagonal-close-packed (hcp) crystal structure, which is known as α-Ti, and a body-centred-cubic (bcc) structure, which is called β-Ti, at room temperature.

The crystal structure and properties of the α-Ti and β-Ti phases are given in Fig. 9.3. The chemical composition of both phases is virtually identical, but their properties are different because of the different crystal structures. From a practical viewpoint, this means that α-Ti and β-Ti have different uses on aircraft: α-Ti has better creep resistance and ductility at high temperature than β-Ti, which makes it more suited for aeroengine applications. ß-Ti has higher tensile strength and fatigue resistance than α-Ti owing to fewer slip systems in the bcc crystal, which makes it better suited for highly-loaded aircraft structures. It is also possible for titanium alloys to consist of a mixture of the α and β phases. α+β-Ti occurs when the metal contains both α-Ti and β-Ti grains, as shown in Fig. 9.4. The properties of α+β-Ti is somewhere between pure α-Ti and pure β-Ti. The α+β-Ti alloys generally have better strength than α-Ti alloys and higher creep strength and ductility than β-Ti alloys, which makes them useful for both aircraft engines and structures.

Low-to-medium strength
Excellent creep resistance at high temperature
Weldable
Ductile
Good toughness

(a)

High strength
High fatigue resistance
Fully heat treatable
Good creep resistance to intermediate
temperatures
Less ductile

(b)

9.3 Crystal structure and properties of (a) α-titanium and (b) β-titanium.

9.4 Microstructure of α+β-Ti alloy. The α-phase is the dark region and the β-phase the light region. (reproduced with permission from R. M. Brick, A. W. Pense and R. B. Gordon, *Structure and properties of engineering materials*, McGraw-Hill Book Company, 1977)

Pure titanium metal undergoes an allotropic transformation that changes the crystal structure from the α-phase to the β-phase at about 885 °C. An allotropic transformation simply means the crystal structure changes when the material is heated above or cooled below a critical temperature called the transus temperature. In pure titanium, the β-phase can only exist above the transus temperature, and the α-phase only occurs below the transus temperature. However, it is possible for β-Ti to be stable at room temperature by the addition of certain alloying elements. The ability of alloying elements to stabilise the formation of the α or β phases is determined by their electron valence number. This number describes the number of electrons in the outer orbital shell of an atom. Titanium has an electron valence number of two, three or four, and any element with a different valence number can promote the formation of the α- or β-phases. Elements with a lower valence number than titanium promote the formation of α-Ti, and these are called alpha-stabilisers. The most common α-stabilising element is aluminium, although tin is also regularly used. Elements with a higher electron valence number promote the formation of the β-phase. The elements stabilise the β-phase when the metal is cooled rapidly from the transus temperature to room temperature. These elements are the so-called beta-stabilisers, and include vanadium, molybdenum, chromium and copper. Alloying elements with the same valence number as titanium are called neutral elements because they do not stabilise either the α- or β-phases. Neutral elements are used to increase strength or improve some other property.

9.3.2 COMMERCIALLY PURE TITANIUM

Commercially pure titanium (> 99% Ti) is a low-to-moderate strength metal that is not well suited for aircraft structures or engines. The yield strength of high-purity titanium is within the range of 170–480 MPa, which is too low for heavily loaded aerostructures. The composition and properties of several commercially pure titanium alloys are given in Table 9.2. In the USA, the commercially pure forms of titanium are classified according to the ASTM standard, although not all countries have adopted this system. The standard simply classifies the metal types according to a numbering system, e.g. Grade 1, Grade 2 and so on.

Table 9.2

Composition and tensile properties of commercially pure titanium alloys

Type	Maximum impurity limits (wt%)					Young's modulus (GPa)	0.2% Yield strength (MPa)	Tensile strength (MPa)	Elongation (%)
	N	C	H	Fe	O				
ASTM Grade 1	0.03	0.10	0.015	0.20	0.18	103	170	240	25
ASTM Grade 2	0.03	0.10	0.015	0.30	0.25	103	280	340	20
ASTM Grade 3	0.05	0.10	0.015	0.30	0.35	103	380	450	18
ASTM Grade 4	0.05	0.10	0.015	0.50	0.40	103	480	550	15

Table 9.2 shows that some grades of pure titanium have a tensile strength of more than 450 MPa, which is similar to the 2000 aluminium alloys used in aircraft structures. However, the specific strength of pure titanium is not as high as the aluminium alloys because of its higher density. Commercially pure titanium contains a low concentration of impurities which remain in the metal after refining and processing from the rutile ore. Titanium contains trace amounts of impurities such as iron and atomic oxygen, and they have the beneficial effect of increasing strength and hardness by solid solution hardening. For example, ultra-high purity titanium (with an oxygen content of under 0.01%) has an ultimate tensile strength of about 250 MPa. In comparison, the ultimate strength of titanium with a small amount of oxygen (0.2–0.4%) is 300–

450 MPa. However, it is not advantageous to strengthen titanium using impurity elements because there is a large loss in ductility, thermal stability and creep resistance.

Pure titanium is rarely, if ever, used in aircraft. However, one important engineering property of titanium is the ability to retain strength and ductility at very low temperatures, and therefore is useful for cryogenic applications. An aerospace application of commercially pure titanium is in fuel storage tanks containing liquid hydrogen for space vehicles. Liquid hydrogen must be stored below − 210 °C under normal atmospheric conditions, at which temperature commercially pure titanium has good strength and toughness.

9.3.3 ALPHA TITANIUM ALLOYS

There are two major groups of alpha titanium alloys known as super-alpha and near-alpha. Super-alpha alloys contain a large amount of α-stabilising alloying elements (> 5 wt%) and are composed entirely of α-Ti grains. Near-alpha alloys contain a large amount of α-stabilisers with a smaller quantity of β-stabilising elements (< 2 wt%). The microstructure of near-alpha alloys consists of a small volume fraction of β-Ti grains dispersed between the much greater volume fraction of α-Ti grains.

Near-alpha alloys have higher strength properties than super-alpha alloys (owing to the small amount of the hard β-Ti phase) and also have excellent creep resistance at high temperature. For this reason, near-alpha alloys are preferred over super-alpha alloys in components for gas turbine engines and rocket propulsion systems required to operate for long times at 500–600 °C. Above this temperature, the alloys soften and creep, and other materials with better thermal stability (such as nickel superalloys) are required. The composition and properties of several super-alpha and near-alpha alloys are given in Table 9.3. There is no standardised system for classifying titanium alloys based on their composition. The designation system that is most often used simply lists the weight percentages of the principal alloying additions. As examples, Ti–8Al–1Mo–1 V contains 8% aluminium, 1% molybdenum and 1% vanadium and Ti–6Al–4 V means 6% aluminium and 4% vanadium. In addition, the IMI numbering system is used for some, but not all, titanium alloys. For example, the alloy Ti–5Al–2.5Sn is known as IMI317 whereas Ti–2.25Al–11Sn–5Zr–1Mo is known as IMI679. Although commonly used, the IMI number gives no clue to the types and amounts of alloying elements.

Table 9.3

Composition and properties of alpha alloys used in gas turbine engines

Alloy type	Composition	Young's modulus (GPa)	0.2% Yield strength (MPa)	Tensile strength (MPa)
Super-α	Ti–5Al–2.5Sn (IMI317)	103	760	790
Near-α	Ti–6Al–2Sn–4Zr–6Mo	114	862	930
	Ti–5.5Al–3.5Sn–3Zr–1Nb (IMI829)	120	860	960
	Ti–5.8Al–4Sn–3.5Zr–0.7Nb (IMI834)	120	910	1030
	Ti–2.25Al–11Sn–5Zr–1Mo (IMI679)	115	900	1000
	Ti–6Al–4Zr–2Mo (IMI685)	115	960	1030

Near-alpha alloys are used more often than super-alpha alloys in aircraft because of their superior high-temperature properties, particularly strength and creep resistance. In fact, only one super-alpha alloy is used in significant amounts. Ti–5Al–2.5Sn (IMI317) is used in cryogenic applications for its ability to retain high ductility and fracture toughness at very low temperatures. Of the α-Ti alloys listed in Table 9.3, the near-alpha alloys IMI 685, IMI 829 and IMI 834 are used in jet engines. The yield strength of these alloys is within 800 to 1000 MPa, which is nearly twice that that for age-hardened aluminium alloys.

Strengthening of α-Ti alloys is achieved by work hardening, solid solution hardening and grain-size refinement. Work hardening by plastic forming processes such as rolling or extrusion can more than double the tensile strength from about 350 to 800 MPa. Solid solution hardening increases the tensile strength between 35 and 70 MPa for every 1% of alloying element. Aluminium is the main alloying element and is used to stabilise the α-phase and to increase the creep and tensile strengths. Figure 9.5 shows the effect of aluminium content on the yield strength and ductility of α-Ti, and the strength increases rapidly owing to solid solution hardening whereas the ductility drops owing to embrittlement. Adding more than about 9% Al promotes the formation of brittle titanium aluminide (Ti$_3$Al) precipitates that reduce the fracture toughness and ductility, and for this reason most α-Ti alloys have an aluminium content under 6–7%. A class of aerospace titanium alloys known as titanium aluminides are produced by the addition of a high concentration of aluminium. Titanium aluminides are composed entirely of Ti$_3$Al, and are described later in this chapter. The strength of α-Ti alloys cannot be raised by heat treatment, which is one reason for their use in high-temperature applications. The thermal stability and resistance to thermal ageing of near-alpha alloys ensures that their mechanical properties are not changed appreciably when operating at high temperatures for long periods.
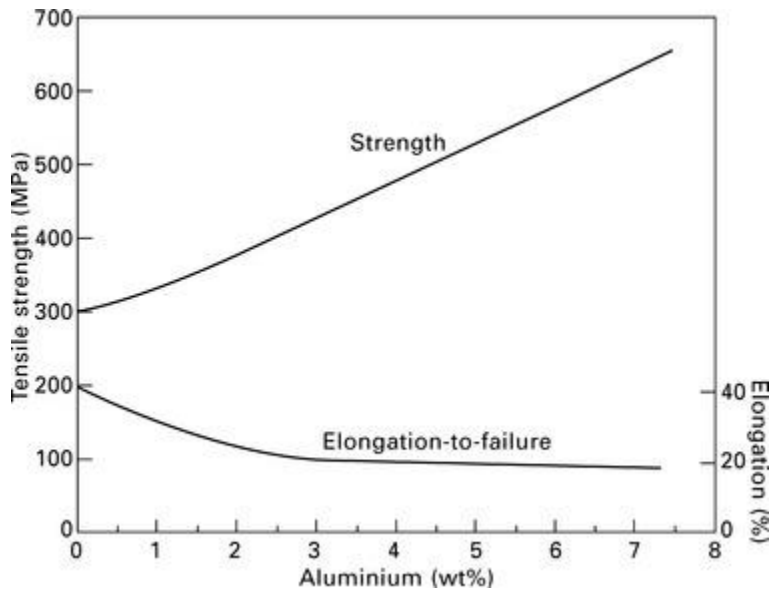
9.5 Effect of aluminium content on the tensile properties of α-Ti.

9.3.4 BETA TITANIUM ALLOYS

Beta-titanium alloys are produced by the addition of β-stabilising elements that retain the β-phase when the metal is cooled rapidly from the transus temperature. A large number of alloying elements can be used as β-stabilisers, although only V, Mo, Nb, Fe and Cr are used in significant amounts (typically 10–20 wt%). The composition, tensile properties and aircraft applications of several β-Ti alloys are given in Table 9.4. The strength and fatigue resistance of β-Ti alloys is generally higher than the α-Ti alloys. However, the use of β-Ti alloys is very low; accounting for less than a few percent of all the titanium used by the aerospace industry owing to their low creep resistance at high temperature.

Table 9.4

Composition, properties and application of β-Ti alloys in aircraft structures

Composition	Young's modulus (GPa)	0.2% Yield strength (MPa)	Tensile strength (MPa)	Application
Ti–13V–11Cr–3Al	103	1200	1280	SR-71 *Blackbird*
Ti–8V–6Cr–4Mo–4Zr–3Al (Beta C)	103	1130	1225	Aircraft fasteners
Ti–11.5Mo–6Zr–4Sn (Beta III)	103	1315	1390	Aircraft fasteners
Ti–10V–2Fe–3Al	103	1250	1320	Airframes, landing gear, helicopter rotor blades
Ti–15V–3Al–3Cr–3Sn	103	966	1000	Airframes
Ti–15Mo–2.7Nb–3Al–0.2Si (Timetal 21S)	103	1170	1240	Jet engine nacelles

The first β-Ti alloy to be used in commercial quantities was Ti–13 V–11Cr–3Al, which was used in the airframe of the SR-71 *Blackbird* military aircraft. The alloy was used in the fuselage frame, wing and body skins, longerons, bulkheads, ribs and landing gear. *Blackbird* was designed to fly at Mach 2.5 (3200 km h^{-1}) and, at this speed, the skins are heated to nearly 300 °C by frictional aerodynamic drag. Aluminium alloys soften at these temperatures, and therefore titanium alloy was used because of its superior strength at high temperature. The Boeing 777 uses β-Ti alloys in many components, including landing gear, exhaust plugs, nozzles, and sections of the nacelle. The β-Ti alloy used in the B777 landing gear is Ti–10 V–2Fe–3Al, which is used as a replacement to high strength steel. β-Ti alloy is used to eliminate the risk of hydrogen embrittlement experienced with steel as well as providing a weight saving of 270 kg. β-alloys are also used in the fan disc of gas turbine engines to save weight. The two most common β-Ti alloys for fan discs are Ti–5Al–2Zr–2Sn–4Cr–4Mo and Ti–6Al–2Sn–4Zr–6Mo, and they provide weight reductions of more than 25% compared with the use of high-temperature steel or superalloy.

The yield strength of most β-Ti alloys is between 1150 and 1300 MPa, which is greater than the strength of α-Ti alloys (750–1000 MPa). The higher strength is the result of greater solid solution hardening together with precipitation hardening. Solution treatment and thermal ageing can increase the strength by 30–50% or more over the annealed condition. The heat treatment conditions used to strengthen β-Ti alloys are more extreme than the age-hardening of aluminium alloys described in chapter 8. A typical treatment for β-Ti alloys involves solution treatment at about 750 °C, rapid quench to room temperature, and then thermal ageing at 450–650 °C for several hours. The ageing causes some of the β-phase to transform into α-Ti particles. These particles are finely dispersed through the β-matrix, and are often found at grain boundaries and dislocations. The particles increase the yield strength of β-Ti by the precipitation hardening mechanism. In addition, the ageing process produces ω-phase precipitate particles that also strengthen the β-Ti alloy. The tensile strength of β-Ti alloys increases with the volume fraction of α- and ω-particles to 1400 MPa. The strength of β-Ti alloys can also be increased by work-hardening. Sheets of β-Ti alloy can be strengthened up to 1500 MPa by cold deformation by 50–70%. However, the increase in strength by cold working is accompanied by losses in ductility and toughness and, therefore, cold deformation is not widely used for raising the strength of aircraft titanium alloys.

9.3.5 ALPHA+BETA TITANIUM ALLOYS

α+β-Ti alloys are by far the most important group of titanium alloys used in aircraft. These alloys are produced by the addition of α-stabilisers and β-stabilisers to promote the formation of both α-Ti and β-Ti grains at room temperature. The popularity of α+β-Ti alloys stems from their excellent high temperature creep strength, ductility and toughness (from the α-Ti phase) and high tensile strength and fatigue resistance (from the β-Ti phase). The composition and tensile properties of several α+β-Ti alloys are given in Table 9.5, and the amounts of α-stabilisers and β-stabilisers are typically in the range of 2–6% and 6–10%, respectively.

Table 9.5

Composition and tensile properties of α+β alloys

Composition	Young's modulus (GPa)	0.2% Proof strength (MPa)	Tensile strength (MPa)	Elongation (%)
Ti–6Al–4V (IMI318)	114	830	900	10
Ti–6Al–2Sn–4Zr–6Mo	114	1100	1170	10
Ti–5Al–2Sn–2Zr–4Mo–4Cr	114	1055	1125	–
Ti–10V–2Fe–3Al	103	1100	1170	–
Ti–2Al–2Sn–4Mo–0.5Si	114	1000	1100	13
Ti–6Al–6V–2Sn	114	1170	1275	10

Of the many types of α+β-Ti alloys, the most important is Ti–6Al–4 V (IMI318), which makes up more than one-half the sales of titanium in the United States and Europe, and is the most used titanium alloy in aircraft. Ti–6Al–4 V is used in both jet engines and airframes; it accounts for about 60% of the titanium used in jet engines and up to 80–90% for airframes. Figure 9.6 shows a Ti–6Al–4 V engine blisk for the F-35 *Lightning II* fighter. The maximum operating temperature limit of Ti–6Al–4 V under creep conditions is 300–450 °C and, therefore, this alloy is used for the fan and cooler parts of the engine compressor, whereas α-Ti alloys are used in hotter engine components where higher temperature creep strength is required. Ti–6Al–4 V is the most commonly used titanium alloy in airframes, and is found in highly-loaded structures such as wing boxes, stiffeners, spars and skin panels. For example, most of the titanium structures in the F-14 *Tomcat* shown in Fig. 9.1 are made using Ti–6Al–4 V.

9.6 Ti–6Al–4 V blisk for a jet engine in the Joint Strike Fighter project. This photograph is reproduced with the permission of Rolls-Royce plc, copyright © Rolls-Royce plc 2010
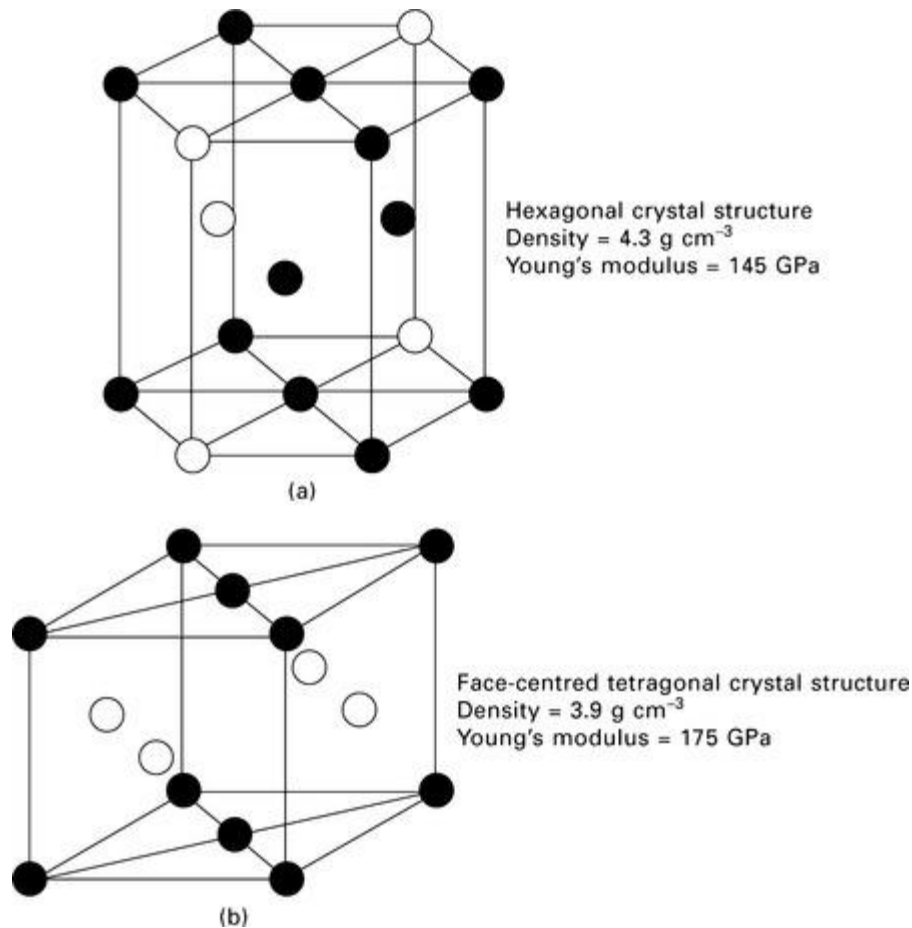
The mechanical properties of α+β-Ti alloys are often between those of α-Ti and β-Ti alloys. For example, the yield strength of annealed Ti–6Al–4 V is about 925 MPa, which is higher than most near-alpha Ti alloys (~ 800 MPa) but lower than many β-Ti alloys (1150–1400 MPa). Similar comparisons can be made for other properties, including creep strength, fatigue resistance, fracture toughness, ductility and ultimate

tensile strength. The strength of α+β-Ti alloys is derived from several hardening processes, including solid solution hardening, grain boundary strengthening and work hardening, although the most important is precipitation hardening of the β-Ti grains. As with β-Ti alloys, the thermal ageing of α+β-Ti alloys causes some of the β-phase to transform into α-Ti particles and ω precipitates which raise the strength. α+β-Ti alloys are strengthened following thermal ageing, normally at 480–650 °C, which increases the proof strength by 30–50% over the annealed alloy. Fully age-hardened α+β-Ti alloys have tensile strengths exceeding 1400 MPa.

9.4 Titanium aluminides

Titanium aluminides are a special class of titanium alloy emerging as an important high-temperature material for next-generation aeroengines. These materials have a similar or lower density and higher Young's modulus than conventional titanium alloys. The density of titanium aluminides is between 3.9 and 4.3 g cm^{-3} against 4.4 to 4.8 g cm^{-3} for titanium alloys. The Young's modulus of titanium alumimides is 145–175 GPa versus 90–120 GPa for titanium. Titanium aluminides also have higher oxidation resistance and strength retention at high temperature, which makes them better suited for use in gas turbine engines and rocket propulsion systems. Several types of titanium aluminide alloys retain strength to 750 °C, which is at least 150 °C higher than the operating temperature limit of conventional titanium alloys.

Titanium aluminides are classified as ordered intermetallic compounds, which means they form when atoms of two or more metals combine in a fixed ratio to produce a crystalline material different in structure from the individual metals. For titanium aluminides, the two metals are titanium (with a body-centred-cubic crystal structure) and aluminium (face-centred-cubic structure). The metals combine to produce Ti_3Al (hexagonal) and $TiAl$ (face-centred tetragonal) compounds (Fig. 9.7). Ti_3Al is called α$_2$-aluminide and forms when the aluminium content of the alloy is about 25%. The composition of common α$_2$-aluminide alloys are Ti–25Al–5Nb, Ti–24Al–11Nb, Ti–25Al–10Nb–3 V–1Mo and Ti–24.5Al–12.5Nb–1.5Mo. Niobium (Nb) is added to produce Ti_2Nb precipitates, which contribute to strength retention at high temperature and increased ductility at room temperature. The TiAl compound is known as γ-aluminide, and is formed when there are approximately equal amounts of Ti and Al. γ-aluminide alloys include Ti–48Al–1 V, Ti–48Al–2Mn, Ti–48Al–2Cr–2Nb and Ti–47Al–2Cr–2Ni.

Hexagonal crystal structure
Density = 4.3 g cm^{-3}
Young's modulus = 145 GPa

(a)

Face-centred tetragonal crystal structure
Density = 3.9 g cm^{-3}
Young's modulus = 175 GPa

(b)

9.7 Crystal structure and properties of (a) Ti$_3$Al and (b) TiAl; the black and white circles represent titanium and aluminium atoms, respectively.

A benefit of using titanium aluminide as a structural material is high-temperature strength. Titanium aluminides have a small number of slip systems in their crystal structure which limits the movement of dislocations at high temperature, thereby retaining the strength. Figure 9.8 shows the effect of increasing temperature on the specific proof strengths of α_2- and γ-aluminides against a near-alpha titanium alloy (IMI834) that is currently used in jet engines. The α_2-alloy has superior specific strength compared with the near-alpha alloy up to 800 °C, and therefore Ti$_3$Al could be used as a lightweight replacement for conventional titanium alloys in jet engines. The γ-aluminide has a lower specific yield strength than the near-alpha alloy, but is able to retain its strength to higher temperatures. The maximum operating temperature of γ-aluminides is similar to nickel superalloys used in the hottest sections of jet engines. Titanium aluminides have potential application in high-pressure compressor and turbine blades. However, γ-aluminides have more than one-half the density (3.9 g cm^{-3}) of nickel alloys (8.7–8.9 g cm^{-3}) and therefore can be used as a lighter-weight engine material.
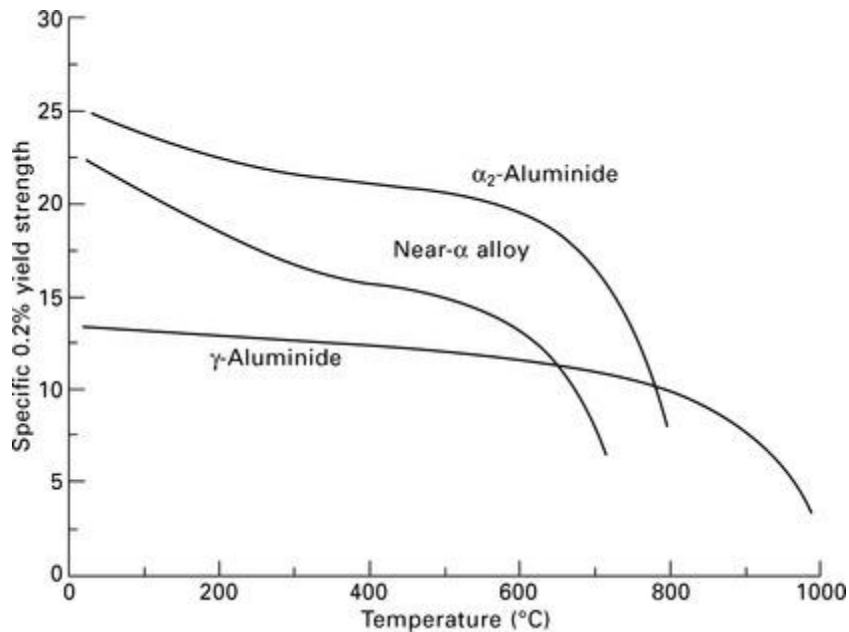
9.8 Effect of temperature on the average specific yield strengths of α_2-aluminide, γ-aluminide and a near-alpha alloy (data from J. Kumpfert and C. H. Ward, in *Advanced aerospace materials*, ed. H. Buhl, Springer Verlag, Berlin, 1992).

The outstanding high-temperature strength of titanium aluminides offers the possibility of increasing the maximum temperature limit of titanium-based alloys as well as being a lighter-weight substitute for nickel alloys in jet engines. However, titanium aluminides are susceptible to brittle fracture owing to their low ductility and poor fracture toughness, and this is a key factor stopping their use in aircraft engines. Typically, titanium aluminides have a room temperature ductility of 1–2% and a fracture toughness of about 15 MPa m$^{-0.5}$, which is lower than the ductility and toughness of conventional titanium alloys. Another problem is the high cost of processing engine components from titanium aluminides, being more expensive than for conventional titanium and nickel alloys. Aerospace companies are seeking ways to reduce the manufacturing costs and increase the ductility so titanium aluminides may eventually find use in jet engines.
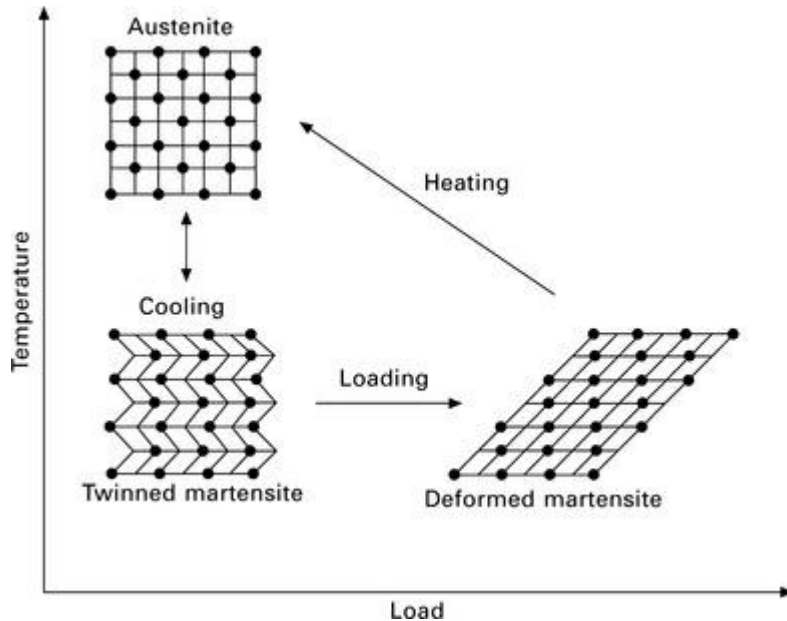
9.5 Shape-memory titanium alloys

Shape-memory alloys are a unique class of material with the ability to 'remember' their shape after being plastically deformed. Shape-memory alloys revert back to their original shape by heating or some other external stimulus, provided the deformation they experience is within a recoverable range. The process of deformation and shape recovery can be repeated many times, and this offers the possibility of using shape-memory alloys in flight control systems. These alloys are being evaluated for a number of aircraft systems that would benefit from the shape-memory effect, such as control surfaces and hydraulic systems. Shape-memory alloys are not presently used in aircraft, although it is still worthwhile studying these materials because of their possible use in the future.

The most effective and common shape-memory alloy is nickel-titanium, where the titanium content is 45–50%. Nickel–titanium alloys that are commercially available are traded under the brand-name 'Nitinol'. Several non-titanium alloys also have shape-memory properties, most notably copper–zinc–aluminium and copper–aluminium–nickel alloys, but their shape-memory performance and mechanical properties are not as good as nickel–titanium.

The shape-memory effect is possible because a phase change or, in other words, a change to the crystal structure occurs in the material with the application of stress and heat, as shown schematically in Fig. 9.9. Nickel–titanium alloys being considered for use in aircraft exist as two phases: martensite and austenite. A

shape-memory alloy in the undeformed (original) condition exists as twinned martensite. The microstructure of twinned martensite consists of grains separated by twin boundaries. These boundaries can be considered as planes of symmetry with a mirror-image of identical bonding and atomic configuration in both directions. When twinned martensite is deformed under an externally applied load the twin boundaries move to produce deformed martensite. This change is called a displacive transformation, which involves the co-operative rearrangement of atoms into a different, more stable crystal structure without a corresponding change in volume.


9.9 Effect of load and temperature on the shape-memory effect in nickel–titanium alloys.

The shape-memory effect occurs because deformed martensite converts back to twinned martensite by heating the nickel–titanium alloy to a moderate temperature. Heat provides the energy needed to transform deformed martensite into austenite, which has a cubic crystal structure, which then transforms to twinned martensite upon cooling. When deformed martensite converts back into twinned martensite via the austenite phase the alloy recovers its original shape. This process of shape change under applied loading and then shape recovery by heating can be repeated many times. The temperature that shape-memory alloys must be heated to in order to induce the shape-memory effect is determined by their chemical composition, and for nickel–titanium alloys this is within the range of − 100 and + 100 °C.

It is worth noting that there is a strain limit to which shape-memory alloys can be deformed. Full shape recovery cannot be achieved when the material is deformed above this limit. The strain limit for nickel–titanium alloys is about 8.5%, which is high enough for many aerospace applications. There is a special class of material, known as ferromagnetic shape-memory alloys, which recover their shape under a strong magnetic field rather than heat.

Nickel–titanium alloys are being evaluated for a variety of aircraft components for their shape-memory properties. One of the most promising applications is control surfaces, such as flaps, rudders and ailerons. The movement of control surfaces on most modern aircraft is performed using hydraulic actuator systems, which are heavy, expensive and difficult to maintain. It is considered possible to replace hydraulic systems with shape-memory alloys embedded in the control surface. <u>Figure 9.10</u> illustrates the design concept for a 'smart wing' that contains shape-memory alloy to control and manipulate a flexible surface. The wing contains wires of shape-memory alloy along the top and bottom surfaces. When the wing flexes down, the top wire is stretched thus transforming the alloy from twinned martensite to deformed martensite. Likewise,

when the wing is bent upwards the bottom wire is stretched and thereby transformed to deformed martensite. The shape-memory effect in the wires is simply induced by heating them using an electric current, which causes the wing to recover its original shape. In this way, shape-memory alloys can be used to operate control surfaces without the need for conventional hydraulic systems.
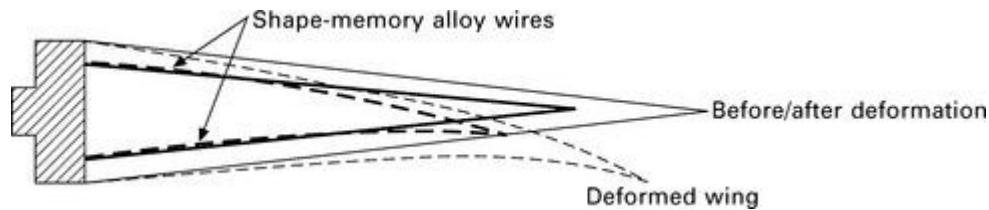
9.10 Schematic of a flexible smart aircraft wing containing shape-memory alloy.

9.6 Summary

Titanium alloys are used in heavily-loaded airframe sections, undercarriage parts, skins to high Mach speed aircraft, jet engines, and many other aircraft components requiring high strength, fracture toughness and resistance to fatigue, creep and corrosion. These mechanical properties are generally superior to lightweight structural materials, including aluminium alloys and magnesium alloys.

Titanium alloys occur in two allotropic forms at room temperature: α-Ti and β-Ti. α-Ti occurs when titanium contains a sufficient quantity of α-stabilising alloy elements, such as Al and Sn. β-Ti exists with the use of β-stabilising elements, such as V, Cr and Mo.

Near α-Ti is characterised by high creep resistance and, therefore, is used in jet engine and rocket propulsion components operating up to 500–600 °C. α-Ti also has good fracture toughness and ductility.

β-Ti is characterised by high strength and fatigue resistance which makes it suitable for heavily loaded aircraft components.

Titanium alloys comprising both α-Ti and β-Ti are most often used in aircraft. Ti–6Al–4 V is the most common α+β-Ti alloy, which possesses high creep resistance and toughness (from the α-Ti) and high strength and fatigue resistance (from the β-Ti). Ti–6Al–4 V is used in airframes and jet engines.

Titanium aluminides (Ti$_3$Al, TiAl) may emerge as an important aerospace material in future jet engines because of their lower density, higher stiffness and superior high-temperature strength compared with titanium alloys. However, titanium aluminides are susceptible to brittle fracture owing to their low fracture toughness as well as being expensive to process and manufacture.

Shape-memory alloys based on nickel–titanium alloys possess the unique property of recovering their original shape following plastic deformation. These alloys undergo displacive transformation processes during deformation and then heating which allows the material to return to its original shape. Shape-memory alloys have potential aerospace applications where this property is useful, such as aircraft control surfaces.

Magnesium alloys for aerospace structures

10.1 Introduction

Magnesium is the lightest of all the metals used in aircraft. The density of magnesium is only 1.7 g cm^{-3}, which is much lower than the specific gravity of the other aerospace structural metals: aluminium (2.7 g cm^{-3}), titanium (4.6 g cm^{-3}), steel (7.8 g cm^{-3}). Only carbon-fibre composite material has a density (~ 1.7 g/cm^3) that is similar to magnesium. Magnesium alloys have lower stiffness and strength properties than the aerospace structural materials, but because of its low density the specific properties are similar. However, there are several problems with using magnesium alloys, including higher cost and lower strength, fatigue life, ductility, toughness and creep resistant properties compared with aluminium alloys. Poor resistance against corrosion is one of the greatest problems with magnesium. Magnesium and its alloys are one of the least corrosion-resistant metals, with its corrosion performance being vastly inferior to the other aerospace metals. There is a widespread belief that a serious safety concern with using magnesium is flammability. Magnesium burns when exposed to high temperature, and therefore may pose a major fire risk. However, there have been no cases of aircraft accidents caused by the ignition of magnesium. Magnesium meets all the aerospace standards for material flammability resistance. The main reason why magnesium is used sparingly in modern aircraft, typically less than 1% of the structural mass of large passenger aircraft, is poor corrosion resistance.

Although the use of magnesium in aerospace structures is now extremely limited, for many years it was used extensively in structural components in aircraft, helicopters and spacecraft because of its light weight. Magnesium was originally used in aircraft during the 1940s and for the next thirty years was a common structural material. Magnesium passed through a boom period between the 1950s and early 1970s when military and civilian aircraft were built using hundreds of kilograms of the material. Magnesium was used extensively in airframes, aviation instruments and low-temperature engine components for aircraft, especially fighters and military helicopters, and semistructural parts for spacecraft and missiles. Since the 1970s, however, the use of magnesium has declined owing to high cost, poor corrosion resistance and other factors, and it is now rarely used in aircraft, spacecraft and missiles. The use of magnesium alloys is now largely confined to engine parts, and common applications are gearboxes and gearbox housings for aircraft and the main transmission housing for helicopters (Fig. 10.1). Magnesium has good damping capacity and therefore is often the material of choice in harsh vibration environments, such as helicopter gearboxes.

10.1 Helicopter gearbox casing made of magnesium alloy.

Despite the general decline in the use of magnesium, it remains an important material for specific aerospace applications. In this chapter, we study the metallurgy, mechanical properties and aerospace applications of magnesium. The following aspects of magnesium alloys are discussed: advantages and drawbacks of using magnesium in aircraft and helicopters; classification system for magnesium alloys; types of magnesium alloys used in aircraft and helicopters; and the engineering properties of magnesium alloys.

10.2 Metallurgy of magnesium alloys

10.2.1 CLASSIFICATION SYSTEM FOR MAGNESIUM ALLOYS

An international standardised system for classifying magnesium alloys, similar to the International Alloy Designation System for aluminium, does not exist. However the American Society for Testing and Materials (ASTM) has developed a coding system that is widely used by the magnesium industry. The system is a 'letter-letter-number-number' code. The letters indicate the two principal alloy elements listed in order of decreasing content. When the two alloying elements are present in an equal amount, then they are listed alphabetically. The code letters used to identify the alloying elements are given in Table 10.1. The two numbers specify the weight percent of the two principal alloying elements, rounded off to the nearest whole number and listed in the order of the two elements. For instance, the alloy AZ91 signifies that aluminium (A) and zinc (Z) are the two main alloy elements, and these are present in weight percentages of about 9 and 1%, respectively. As another example, WE43 identifies the alloy as containing 4% yttrium and 3% rare earth elements. In addition to the alloying elements specified in the code, magnesium alloys often contain other elements in lesser amounts. However, the coding system provides no information about these elements. In exceptional circumstances when an alloy contains three main alloying elements, then a 'three letter–three number' code system is used. For example, ZMC711 contains about 7% zinc, 1% manganese and 1% copper.

Table 10.1

ASTM lettering system for magnesium alloys

A: Aluminium	B: Bismuth	C: Copper	D: Cadmium
E: Rare earths	F: Iron	H: Thorium	K: Zirconium
L: Lithium	M: Manganese	N: Nickel	P: Lead
Q: Silver	R: Chromium	S: Silicon	T: Tin
W: Yttrium	Z: Zinc		

Magnesium alloys are classified as wrought or casting alloys. Wrought alloys account for only a small percentage (under 15%) of the total consumption of magnesium, and these alloys are not used in aircraft. A problem with wrought alloys is their low yield strength (typically less than 170 MPa). Most magnesium alloys that are used commercially, including those in aircraft and helicopters, are casting alloys. The casting alloys are often used in the tempered condition; that is heat-treated and work hardened, under conditions similar to the tempering of aluminium alloys. For this reason, the system used to describe the temper of aluminium alloys is also used for magnesium alloys (see Table 8.2). The temper conditions most often applied to magnesium are T5 (alloy is artificially aged after casting), T6 (alloy is solution treated, quenched and artificially aged), and T7 (alloy is solution treated only).

The major groups of magnesium alloys are based on the following compositions:
• magnesium–aluminium–manganese (Mg–Al–Mn)
• magnesium–aluminium–zinc (Mg–Al–Zn)
• magnesium–zinc–zirconium (Mg–Zn–Zr)
• magnesium–rare earth metal–zirconium (Mg–E–Zr)
• magnesium–rare earth metal–silver–zinc (with or without thorium) (Mg–E–Ag–Zn)
• magnesium–thorium–zirconium (with or without zinc) (Mg–Th–Zr)

10.2.2 COMPOSITION AND PROPERTIES OF MAGNESIUM ALLOYS

The composition and tensile properties of pure magnesium and several alloys used in aircraft are given in Table 10.2. Most of the magnesium alloys used in aircraft are from the Mg–Al–Zn, Mg–Al–Zr and Mg–E–Zr systems. The aerospace applications for magnesium alloys are listed in Table 10.3. As mentioned, the most common application is the transmission casings and main rotor gearbox of helicopters which utilise the low weight and good vibration damping properties of magnesium. Magnesium alloys are also used in aircraft engine and gearbox components.

Table 10.2

Composition and properties of pure magnesium and its alloys used in aircraft and helicopters

Alloy	Composition	Yield strength (MPa)	Tensile strength (MPa)	Elongation (%)
Pure Mg (annealed)	>99.9% Mg	90	160	15
Pure Mg (cold-worked)	>99.9% Mg	115	180	10
WE43 (T6)	Mg–5.1Y–3.25Nb–0.5Zr	200	285	4
ZE41 (T5)	Mg–4.2Zn–1.3E–0.7Zr	135	180	2
QE21 (T6)	Mg–2.5Ag–1Th–1Nb–0.7Zr	185	240	2
AZ63 (T6)	Mg–6Al–3Zn–0.3Mn	110	230	3
AK61 (T6)	Mg–6Zn–0.7Zr	175	275	5

Table 10.3

Aerospace applications for magnesium alloys

Alloy	Application
RZ5	Helicopter transmission; aircraft gearbox casings; aircraft generator housing (e.g. A320, *Tornado, Concorde*)
WE43	Helicopter transmission (e.g. *Eurocopter* EC120, NH90; *Sikorsky* S92)
ZE41	Helicopter transmission
QE21	Aircraft gearbox casing; auxiliary gearbox (e.g. F-16, *Eurofighter, Tornado*)
ZW3	Aircraft wheels; helicopter gearbox (e.g. Westland *Sea King*)

10.2.3 STRENGTHENING OF MAGNESIUM ALLOYS

Pure magnesium does not have sufficient strength or corrosion resistance to be suitable for use in aircraft. Magnesium has a hexagonal close packed (hcp) crystal structure. As mentioned in chapter 4, hcp crystals have few slip systems (three) along which dislocations can move during plastic deformation. As a result, it is not possible to greatly increase the strength of hcp metals by work-hardening. For example, annealed magnesium has a yield strength of about 90 MPa, and heavy cold-working of the metal only increases the strength to about 115 MPa. Another consequence of the hcp structure is the mechanical properties of wrought magnesium alloys are anisotropic and are different dependent on the loading direction. Owing to the anisotropy, the compressive yield strength of wrought magnesium alloys can be 30–60% lower than the tensile yield strength.

There are two broad classes of magnesium alloys that are strengthened by cold working or solid solution hardening combined with precipitation hardening. As mentioned, it is difficult to greatly increase the strength of magnesium by cold working owing to the hcp crystal structure, and therefore the majority of magnesium alloys used in aerospace applications are strengthened by the combination of solid solution and precipitation hardening. The strength properties of magnesium are improved by a large number of different alloying elements, and the main ones are aluminium and zinc. Other important alloying elements are zirconium and the rare earths. Rare earths are the thirty elements within the lanthanide and actinide series of the Periodic Table, with thorium (Th) and neodymium (Nd) being the most commonly used as alloying elements.

A problem with magnesium, however, is that the addition of alloying elements provides only a relatively small improvement to the strength properties. Compared with the annealed pure metal, the increase in yield strength of magnesium owing to alloying is typically in the range of 20 to 200%. In comparison, the alloying of annealed aluminium increases the yield strength by more than 1000% and the strength of annealed titanium is improved by up to 700%. The low response of magnesium to strengthening by alloying and

work-hardening, together with low elastic modulus, ductility and corrosion resistance, are important reasons for the low use of this material in modern aircraft.

The majority of alloying elements used in magnesium increase the strength by solid-solution hardening and dispersion hardening. The alloying elements react with the magnesium to form fine intermetallic particles that increase the strength by dispersion hardening. The three most common intermetallic particles have the chemical composition: MgX (e.g. MgTl, MgCe, MgSn); MgX_2 (e.g. $MgCu_2$, $MgZn_2$); and Mg_2X (e.g. Mg_2Si, Mg_2Sn). These compounds are effective at increasing the strength by dispersion hardening, but they reduce the fracture toughness and ductility of magnesium. For example, the Mg–Al–Mn and Mg–Al–Zn alloys used in aircraft form particles ($Mg_{17}Al_{12}$) at the grain boundaries which lower the toughness and ductility.

Magnesium alloys must be heat treated before being used in aircraft to minimise the adverse effects of the intermetallic particles on toughness. This involves solution treating the magnesium at high temperature to dissolve the intermetallic particles in order to release the alloying elements into solid solution. The material is then thermally aged to maximise the tensile strength by precipitation hardening. A typical heat-treatment cycle involves solution treating at about 440 °C, quenching, and then thermally ageing at 180–200 °C for 16–20 h. These heat-treatment conditions are similar to those used to strengthen age-hardenable aluminium alloys. However, the response of magnesium to precipitation hardening is much less effective than aluminium. Only relatively small improvements to the tensile strength of magnesium alloys are gained by precipitation hardening. This is because the density and mobility of dislocations in magnesium is relatively low owing to the small number of slip systems in the hexagonal crystal structure.

The precipitation processes that occur in most magnesium alloys during thermal ageing are complex. In chapter 8, it is mentioned that aluminium alloys undergo the following transformation sequence in the age-hardening process: supersaturated solid solution → GP1 zones → GP2 zones → coherent intermetallic precipitates → incoherent intermetallic precipitates. Some magnesium alloys also undergo this sequence of transformations during ageing whereas other alloys form precipitates without the prior formation of GP zones. The types of precipitates that develop are obviously dependent on the composition and heat-treatment conditions. Precipitates in Mg–E–Zr alloys, such as WE43 used in helicopter transmissions, are $Mg_{11}NdY$ and/or $Mg_{12}NdY$ compounds. Precipitates in Mg–Zn alloys, such as ZE41 that is also used in helicopter transmissions, are coherent $MgZn_2$, semicoherent $MgZn_2$, and incoherent Mg_2Zn_3 particles. Several magnesium alloys used in aircraft contain aluminium, such as QE21 that is used in aircraft gearboxes. The main precipitate formed in Mg–Al alloys is $Mg_{17}Al_{12}$, which is effective at increasing strength. Figure 10.2 shows the effect of aluminium content on the tensile properties of a fully heat-treated Mg–Al–Zn alloy. The yield and ultimate tensile strengths increase with the aluminium content owing to solid solution hardening and precipitation hardening. When the aluminium content exceeds 6–8%, the ductility is reduced owing to embrittlement of the grain boundaries by $Mg_{17}Al_{12}$ particles and, for this reason, the aluminium concentration is kept below this limit.
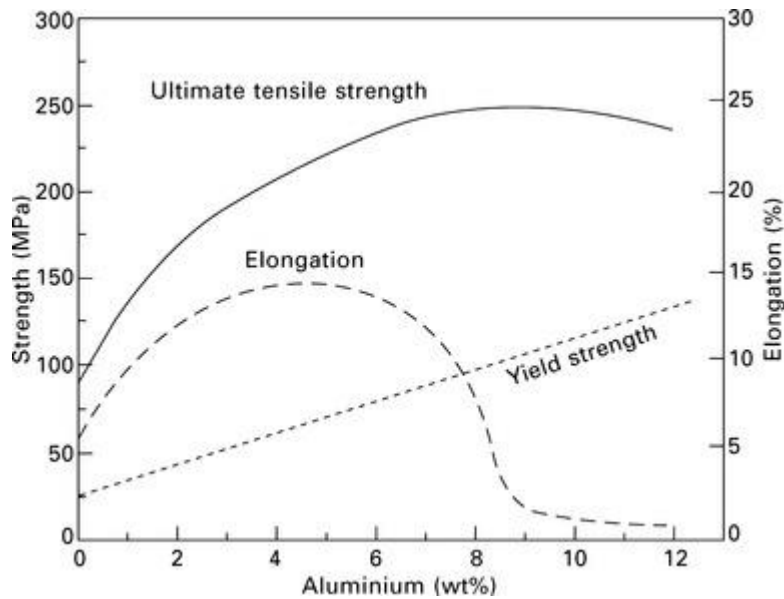
10.2 Effect of aluminium content on the tensile properties of a heat treated magnesium alloy.

Two important alloying elements used in magnesium are zirconium and thorium. Zirconium is used for its ability to reduce the grain size. Cast magnesium has a coarse grain structure which results in low strength owing to the weak grain boundary hardening effect. Zirconium is used in small amounts (0.5% to 0.7%) to refine the grain structure and thereby increase the yield strength. In the past, thorium was often used to reduce the grain size and, for many years, magnesium–thorium alloys were used in components for missiles and spacecraft. However, thorium is a radioactive element that poses a health and environment hazard and, therefore, its use has been phased out over the past twenty years and it is now obsolete as an alloying element.

10.2.4 CORROSION PROPERTIES OF MAGNESIUM ALLOYS

The biggest obstacle to the use of magnesium alloys is their poor corrosion resistance. Magnesium occupies one of the highest anodic positions in the galvanic series, and for this reason has a high potential for corrosion. There are many types of corrosion (as explained in chapter 21), and the most damaging forms to magnesium and its alloys are pitting corrosion and stress corrosion. Pitting corrosion, as the name implies, involves the formation of small pits over the metal surface where small amounts of material are dissolved by corrosion processes. These pits are sites for the formation of cracks within aircraft structures. Stress corrosion involves the formation and growth of cracks within the material under the combined effects of stress and a corrosive medium, such as salt water. Magnesium is much more susceptible to corrosion than other aerospace metals, and must be protected to avoid rapid and severe damage.

The corrosion resistance of magnesium generally decreases with alloying and impurities. The addition of alloying elements to increase the strength properties comes at the expense of reduced corrosion resistance. The most practical methods of minimising the damaging effects of corrosion are careful control of impurities and surface protection. The corrosion resistance of magnesium can be improved by ensuring a very low level of cathodic impurities. Iron, copper and nickel, which are not completely removed from magnesium during processing from the ore, act as impurities that accelerate the corrosion rate. The amount of iron, copper and nickel must be kept to very low levels to ensure good corrosion resistance. The maximum concentrations are only 1300 ppm (parts per million) for copper, 170 ppm for iron and and 5 ppm for nickel. In some aerospace magnesium alloys (e.g. AZ63), a small amount of manganese (< 0.3%) is used to improve corrosion resistance. The manganese reacts with the impurities to form relatively harmless

intermetallic compounds, some of which separate out during melting. The other way of protecting magnesium alloys from corrosion is surface treatments and coatings.

Steels for aircraft structures

11.1 Introduction

Steel is an alloy of iron containing carbon and one or more other alloying elements. Carbon steel is the most common material used in structural engineering, with applications in virtually every industry sector including automotive, marine, rail and infrastructure. The world-wide consumption of steel is around 100 times greater than aluminium, which is the second most-used structural metal. Figure 11.1 shows the production of steel, aluminium, magnesium and composites over the course of the 20th century, and the usage of steel amounts to more than 90% of all metal consumed. Although steel is used extensively in many sectors, its usage in aerospace is small in comparison to aluminium and composite material. The use of steel in aircraft and helicopters is often limited to just 5–8% of the total airframe weight (or 3–5% by volume).
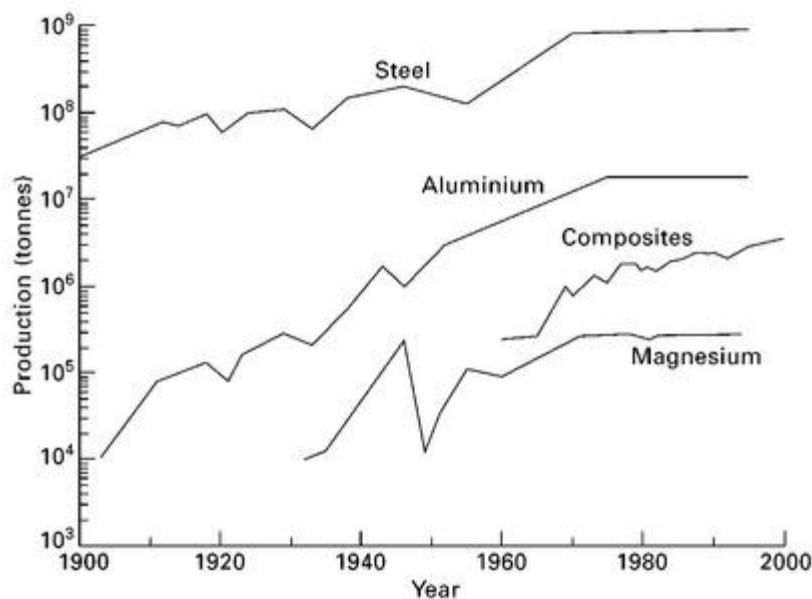
11.1 Production figures (approximate) for aluminium, magnesium, steel and composites.

The use of steel in aircraft is usually confined to safety-critical structural components that require very high strength and where space is limited. In other words, steel is used when high specific strength is the most important criterion in materials selection. Steels used in aircraft have yield strengths above 1500–2000 MPa, which is higher than high-strength aluminium (500650 MPa), α/β titanium (830–1300 MPa) or quasi-isotropic carbon-epoxy composite (750–1000 MPa). In addition to high strength, steels used in aircraft have high elastic modulus, fatigue resistance and fracture toughness, and retain their mechanical performance at high temperature (up to 300–450 °C). This combination of properties makes steel a material of choice for heavily-loaded aircraft structures. However, steel is not used in large quantities for several reasons, with the most important being its weight. The density of steel ($\rho = 7.2$ g cm^{-3}) is over 2.5 times higher than aluminium, 1.5 times greater than titanium, and more than 3.5 times heavier than carbon–epoxy composite. In addition to weight problems, most steels are susceptible to corrosion which causes surface pitting, stress corrosion cracking and other damage. High-strength steels are prone to damage by hydrogen embrittlement, which is a weakening process caused by the absorption of hydrogen. A very low concentration of hydrogen (as little as 0.0001%) within steel can cause cracking which may lead to brittle-type fracture at a stress level below the yield strength.

Aircraft structural components made using high-strength steel include undercarriage landing gear, wing-root attachments, engine pylons and slat track components ([Fig. 11.2](#)). The greatest usage of steel is in landing gear where it is important to minimise the volume of the undercarriage while having high load capacity. The main advantage of using steel in landing gear is high stiffness, strength and fatigue resistance, which provide the landing gear with the mechanical performance to withstand high impact loads on landing and support the aircraft weight during taxi and take-off. Owing to the high mechanical properties of steel, the load-bearing section of the landing gear can be made relatively small which allows storage within minimum space in the belly of an aircraft. Steel is also used in wing root attachments and, in some older aircraft, wing carry-through boxes owing to their high stiffness, strength, toughness and fatigue resistance. For similar reasons, steel is used in slat tracks which form part of the leading edge of aircraft wings.
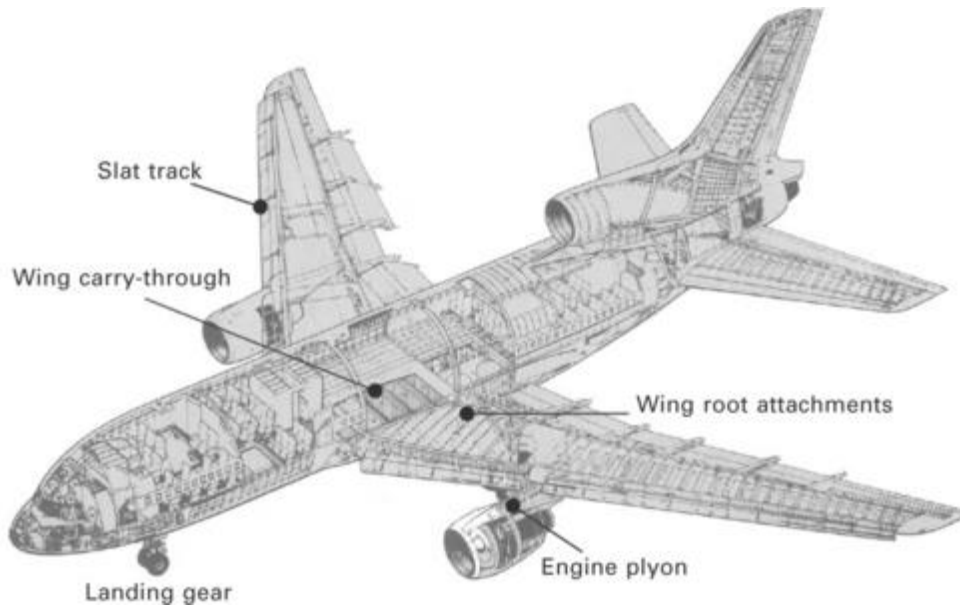
11.2 Aircraft applications of steel.

This chapter presents an overview of the metallurgical and mechanical properties of steels for aircraft structural applications. The field of steel metallurgy is large and complex, although this chapter gives a short, simplified description of the basic metallurgy of steel. The chapter describes the steels used in landing gear and other high-strength components, namely, the maraging steels, medium-carbon low-alloy steels, and stainless steels.

11.2 Basic principles of steel metallurgy

11.2.1 GRADES OF STEEL

Iron is alloyed with carbon and other elements, forged and then heat-treated to produce high-strength steel. Pure iron is a soft metal having a yield strength under 100 MPa, but a tenfold or more increase in strength is achieved by the addition of carbon and other alloying elements followed by work hardening and heat treatment. By control of the alloy composition and thermomechanical processing, it is possible to produce steels with yield strengths ranging from 200 MPa to above 2000 MPa. Other important structural properties such as toughness, fatigue resistance and creep strength are also controlled by alloying and thermomechanical treatment.

There are many hundreds of grades of steel, although only a small number have the high strength and toughness required by aircraft structures. Steels contain less than about 1.5% carbon (together with other

alloying elements), and are categorised, rather imprecisely, on the basis of their carbon and alloying element contents. Some of the most important groups of steels are:

Mild steels

Mild steels (also called low-carbon steels) contain less than about 0.2% carbon and are hardened mainly by cold working. Mild steels have moderate yield strength (200–300 MPa) and are therefore too soft for aircraft structural applications.

High-strength low-alloy steels

High-strength low-alloy (HSLA) steels contain a small amount of carbon (under 0.2%) like mild steels, and also contain small amounts of alloying elements such as copper, nickel, niobium, vanadium, chromium, molybdenum and zirconium. HSLA steels are referred to as micro-alloyed steels because they are alloyed at low concentrations compared with other types of steels. The yield strength of HSLA steels is 250–600 MPa and they are used in automobiles, trucks and bridges amongst other applications. The use of HSLA steels in aircraft is rare because of low specific strength and poor corrosion resistance.

Medium-carbon steels

Medium-carbon steels contain somewhere between 0.25 and 0.5% carbon and are hardened by thermomechanical treatment processes to strengths of 300–1000 MPa. This group of steels is used in the greatest quantities for structural applications, and they are found in motor cars, rail carriages, structural members of buildings and bridges, ships and offshore structures and, in small amounts, aircraft.

Medium-carbon low-alloy steels

Medium-carbon low-alloy steels also contain somewhere between 0.25 and 0.5% carbon but have a higher concentration of alloying elements to increase hardness and high-temperature strength. They contain elements such as nickel, chromium, molybdenum, vanadium and cobalt. Examples are given in Table 11.1 At the higher alloy contents these steels are used as tool steels (e.g. tool bits, drills, blades and machine parts) which require hardness and wear resistance at high temperature. Strength levels up to 2000 MPa can be achieved. These steels are used in aircraft, typically for undercarriage parts.

Table 11.1

Composition and properties of selected steels used in aircraft

Steel	Average composition	Yield strength (MPa)	Ultimate strength (MPa)	Elongation (%)
Maraging steels				
18Ni (200)	0.03 max C, 18 Ni, 8.5 Co, 3.3 Mo, 0.2 Ti, 0.1 Al	660	970	17
18Ni (250)	0.03 max C, 18 Ni, 8.5 Co, 5 Mo, 0.4 Ti, 0.1 Al	1700	1790	11
18Ni (300)	0.03 max C, 18 Ni, 9 Co, 5 Mo, 0.7 Ti, 0.1 Al	1950	2000	9
18Ni (350)	0.03 max C, 18 Ni, 12.5 Co, 4.2 Mo, 1.6 Ti, 0.1 Al	2300	2370	6
Medium-carbon low-alloy steels				
4130	0.3 C, 1.0 Cr, 0.5 Mn, 0.25 Si, 0.2 Mo	540	700	25
4340	0.4 C, 1.8 Ni, 0.8 Cr, 0.7 Mn, 0.25 Si, 0.25 Mo	410	750	22
300M	0.38 C, 1.8 Ni, 1.6 Si, 0.8 Cr, 0.8 Mn, 0.4 Mo, 0.05 min V	1590	1930	7
Aermet 100	0.25 C, 13.5 Co, 11 Ni, 3 Cr, 1.2 Mo	1720	1960	14
H11	0.35 C, 5.0 Cr, 1.5 Mo, 1.0 Si, 0.45 V, 0.4 Mn,0. 0.3 Ni	1650	2000	9
Precipitation-hardening stainless steels				
15-5 PH	0.07 C, 15 Cr, 4.5 Ni, 3.5 Cu, 1 Mn, 1 Si, 0.3 Nb	1400	1470	10
17-4 PH	0.07 C, 16 Cr, 4 Ni, 4 Cu, 1 Mn, 1 Si, 0.3 Nb	1150	1330	10

Maraging steels

Maraging steels also have a high alloy content, but with virtually no carbon (less than 0.03%). Alloying together with heat treatment (which, unlike that for the other steels described above, includes age-hardening) produces maraging steels with the unusual combination of high strength, ductility and fracture toughness. The strength of maraging steels is within the range of 1500–2300 MPa, which puts them amongst the strongest metallic materials. Maraging steel is used in heavily loaded aerospace components.

Stainless steels

Stainless steels are corrosion resistant materials that contain a small amount of carbon (usually 0.08–0.25%) and a high concentration of chromium (12–26%) and sometimes nickel (up to about 22%). There are several classes of stainless steels with various mechanical properties, and their yield strength covers a wide range (200–2000 MPa). Precipitation-hardening (PH) stainless steels are used increasingly in aerospace applications, particularly where both high strength and excellent corrosion resistance is required.

Of the many steels available, it is the medium carbon low-alloy steels, maraging steels and PH stainless steels that are most used in aircraft. The alloy composition and mechanical properties of several steels (but not all the grades) used in aircraft are given in Table 11.1.

11.2.2 MICROSTRUCTURAL PHASES OF STEELS

Steel is an allotropic material that can occur as several microstructural phases at room temperature depending on the alloy composition and heat treatment. The main phases of steel are called austenite, ferrite, pearlite, cementite, bainite and martensite. These phases have their own crystal structure and can all exist at room temperature. The high strength steels used in aircraft usually have a martensite microstructure, and steels with another microstructure are rarely used in highly-loaded aircraft components due to their lower strength. Although martensitic steels are the steel of choice for aircraft structural applications, it is still worth examining the other microstructural phases of steel to understand the reasons for selecting martensitic steels for aircraft.

The microstructural phases of steel can be understood from the phase diagram for iron–carbon, which is shown in Fig. 11.3. This diagram shows the equilibrium phases of iron that exist at various carbon contents and temperatures. This iron–carbon diagram is only valid when changes in temperature occur gradually (i.e. the steel is cooled or heated slowly) to allow sufficient time for the formation of stable (equilibrium) phases. The diagram is not valid when steel is cooled rapidly, which is a condition when metastable phases develop that are not represented in the diagram. Also, the phase diagram is only valid for the binary system of iron–carbon, and significant changes to the diagram may occur with the addition of alloying elements.
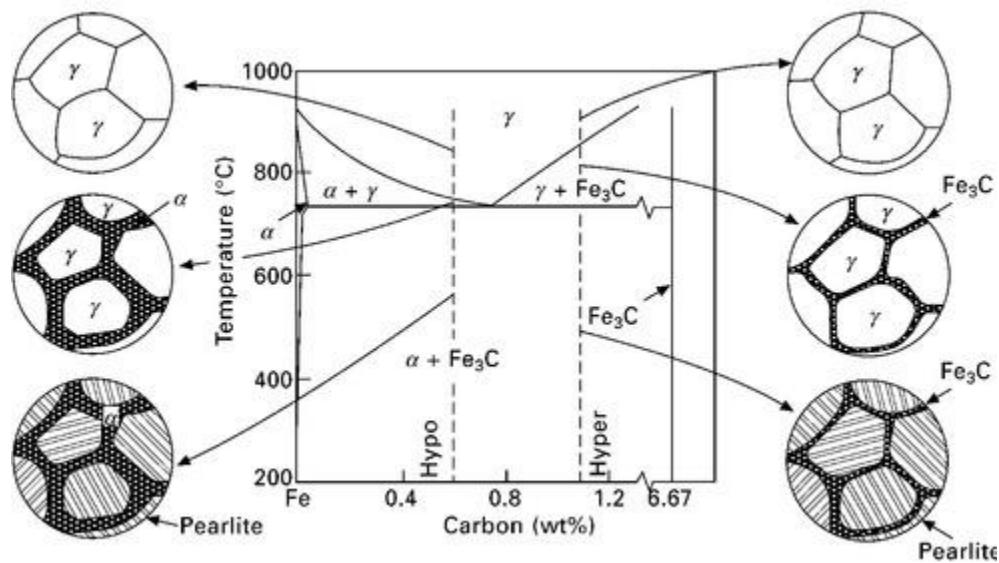
11.3 Iron–carbon phase diagram showing the microstructural phases during slow cooling (equilibrium conditions) of hypoeutectic and hypereutectic steels. reproduced with permission (from D. R. Askeland, *The science and engineering of materials*, Stanley Thornes (Publishers) Ltd., 1996)

The phase diagram for iron–carbon is complex, although there are just a few simple things we need to understand from this diagram. The different phase regions of the diagram indicate different stable microstructures that exist for the range of temperatures and carbon contents bounded by the phase lines. The main phases in Fig. 11.3 are austenite (also called γ-iron), ferrite (α-iron) and cementite (Fe_3C).

Austenite

Austenite is a materials science term for iron with a face-centred-cubic (fcc) crystal structure, and this phase occurs in the Fe–C system above the eutectoid temperature of 723 °C. The eutectoid temperature is the minimum temperature at which a material exists as a single solid solution phase or, in other words, when the alloying elements are completely soluble in the matrix phase. Alloying elements present in austenite are located at interstitial or substitutional sites in the iron fcc crystal structure, depending on their atomic size and valence number. Austenite becomes unstable when Fe–C is cooled below 723 °C, when it undergoes an allotropic transformation to ferrite and cementite (α-Fe + Fe_3C) during slow cooling. However, the addition of certain alloying elements, such as nickel and manganese, can stabilise the austenite phase at room temperature. On the other hand, elements such as silicon, molybdenum and chromium can make austenite unstable and raise the eutectoid temperature.

Ferrite

One phase formed during slow cooling of steel from the austenite phase is ferrite, which is a solid solution of body-centred-cubic (bcc) iron containing interstitial elements such as carbon and substitutional elements such as manganese and nickel. Carbon has a powerful hardening effect on ferrite by solid solution strengthening, but only a very small concentration can be dissolved into the interstitial lattice sites. The maximum solubility of carbon is about 0.02% at 723 °C, and the soluble concentration drops with the temperature to 0.005% at room temperature. Despite the low solubility of carbon, its presence in iron increases the strength at room temperature by more than five times. This is because the carbon atoms, which are about twice the diameter of the interstitial gaps in the ferrite crystal, induce a high elastic lattice strain which causes solid solution hardening. However, ferrite is soft and ductile compared with other phases of steel (i.e. cementite, bainite, martensite).

Cementite and pearlite

When the carbon content of steel exceeds the solubility limit of ferrite, then the excess carbon reacts with the iron to form cementite (or iron carbide) during slow cooling from the austenite phase region. Cementite is a hard, brittle compound with an orthorhombic crystal structure having the composition Fe_3C (Fig. 11.4). Upon slow cooling from the austenite phase, cementite and ferrite form as parallel plates into a two-phase microstructure called pearlite. The microstructure of pearlite is shown in Fig. 11.5, and it consists of thin plates of alternating phases of cementite and ferrite. The plates are very narrow and long, which gives pearlite its characteristic lamellae structure. Pearlite is essentially a composite microstructure consisting of cementite layers (which are hard and brittle) sandwiched between ferrite layers (which are soft and ductile).
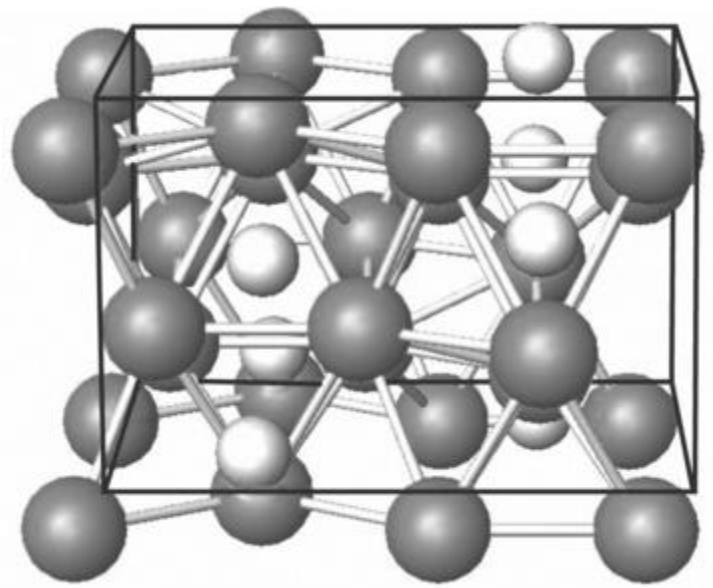
11.4 Orthorhombic Fe$_3$C; iron is shown as the dark atoms and carbon as the lighter atoms.
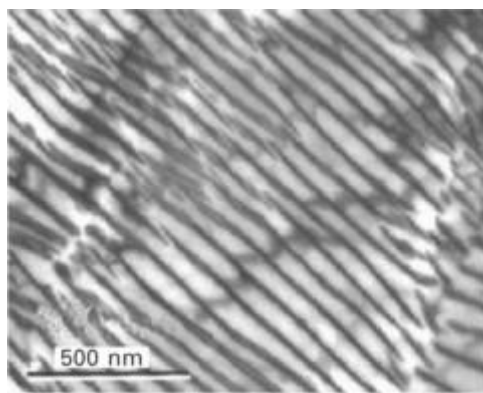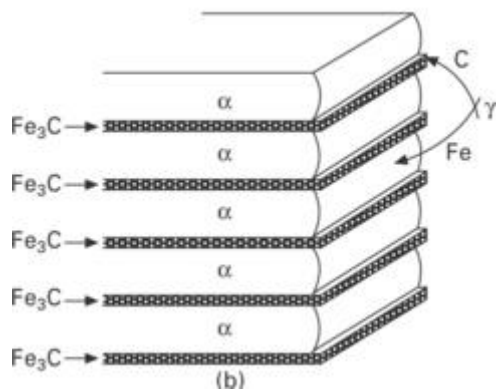

11.5 (a) Photograph and (b) schematic representation of pearlite. (the photograph is from msm.cam.ac.uk)

Hypo- and hypereutectic steels

The microstructure of steel at room temperature is controlled by the carbon content. Steel containing less than 0.005% C is composed entirely of ferrite, whereas above 6.67% C it is completely cementite. The Fe–

C phase diagram shows that ferrite co-exists with cementite at room temperature over the carbon content range of 0.005 to 6.67%. However, the microstructure of the steel changes over this composition range even though both ferrite and cementite are always present. At a carbon content of about 0.8% the steel is eutectic, which means the microstructure consists of an equal amount of ferrite and cementite (i.e. 100% pearlite). A eutectic material has equal amounts of two (or more) phases and, for steel, it is composed of 50% ferrite and 50% cementite.

Steel containing more than 0.8% carbon is hypereutectic, which means the carbon content is greater than the eutectic composition. Hypereutectic steel contains grains of cementite and pearlite, with the volume fraction of cementite grains increasing with the carbon content above 0.8%. Steel is hypoeutectic when the carbon content is below 0.8%, and the microstructure consists of ferrite grains and pearlite grains (i.e. lamellae of ferrite and cementite within a single grain), as shown in Fig. 11.6. The volume fraction of pearlite grains increases, with a corresponding reduction in ferrite grains, when the carbon content is increased to the eutectic composition.
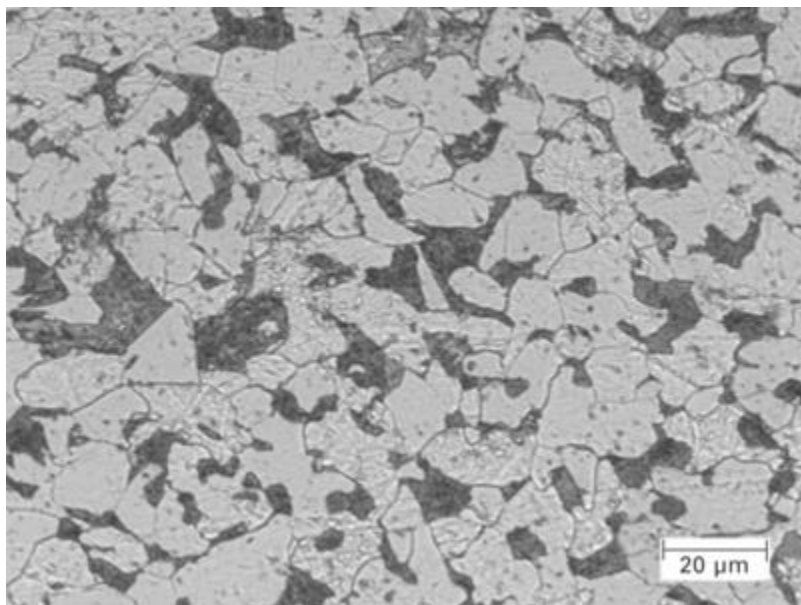
11.6 Hypoeutectic steel containing ferrite (light grey) and pearlite (dark grey) grains (from tms.org).

The majority of steels used in engineering structures, including aerospace, are hypoeutectic. Eutectic and hypereutectic steels lack sufficient ductility and toughness for most structural applications owing to the high volume fraction of brittle cementite. The mechanical properties of hypoeutectic steels are controlled by their carbon content. Figure 11.7 shows that raising the carbon content increases the strength properties and lowers the ductility and toughness. This is because the volume fraction of pearlite, which is hard and brittle, increases with the carbon content.
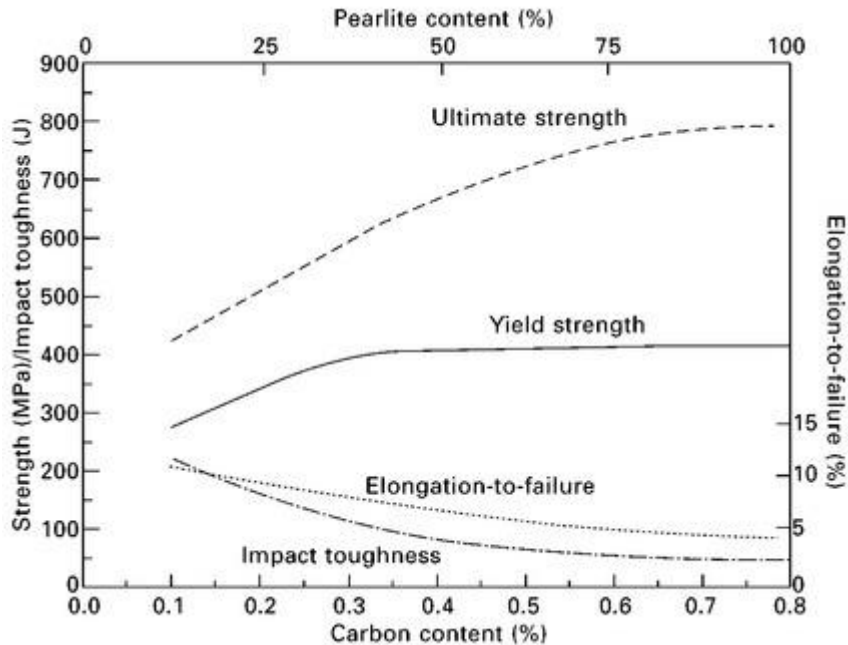
11.7 Effect of carbon content on the volume fraction of pearlite and mechanical properties for a hypoeutectic steel.

Martensite

The microstructure and mechanical properties of the hypoeutectic steels used in aircraft structures is controlled by heat-treatment as well as the carbon and alloy contents. Ferrite and cementite form when hypoeutectic steel is cooled slowly from the austenite phase. Heat treatment processes that involve different cooling conditions can suppress the formation of ferrite and cementite and promote the formation of other phases which provide the steel with different mechanical properties such as higher hardness and strength. The principal transformational phases are bainite and martensite. Bainite is a metastable phase that exists in steel after controlled heat treatment. Bainite can form when steel is cooled from the austenite phase at an intermediate rate which is too rapid to allow the formation of ferrite and cementite but too slow to promote the formation of martensite. Bainite is generally harder and less ductile than ferrite and is tougher than martensite. Steels with a bainite microstructure are used in engineering structures, but not in aerospace applications.

When hot steel in the austenite-phase region is cooled rapidly it does not change into ferrite and cementite, but instead transforms to a metastable phase called martensite. Ferrite and cementite can only form from austenite when there is sufficient time for the iron and carbon atoms to move into the bcc crystal structure of α-iron and the orthorhombic structure of Fe$_3$C. When the cooling rate is rapid then the iron and carbon atoms in austenite do not have time to form these phases, and instead the material undergoes a diffusionless transformation to martensite, which has the body centred tetragonal structure (bct) of iron as shown in Fig. 11.8. The bct martensite structure is essentially the bcc austenite structure distorted by interstitial carbon atoms into a tetragonal lattice. The carbon atoms remain dissolved in the crystal structure because there is insufficient time during quenching to form a carbon-rich second phase (Fe$_3$C). As a result, martensite is supersaturated with interstitial carbon atoms, which cause severe distortion and induce high strains in the crystalline lattice. Other alloying elements are dissolved in interstitial or substitutional sites and this also increases distortion of the lattice. This distortion increases the strength of martensite steel, with the yield stress being as high as 1800–2300 MPa. This is much higher than the strength of a steel with the same composition but consisting of ferrite and cementite (250–600 MPa). Unfortunately, the distortion

of the crystal lattice makes martensite brittle and prone to cracking at low strain, and therefore as-quenched martensitic steel is not suitable for aircraft structures that require high toughness and damage tolerance.
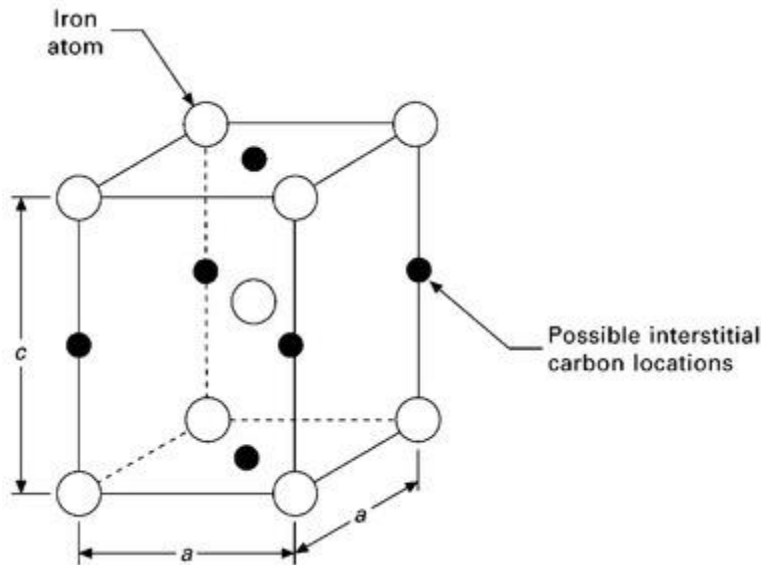
11.8 Body-centred-tetragonal structure of martensite.

Martensitic steels are tempered after quenching to increase ductility and toughness. Tempering involves heating the steel to a temperature below 650 °C to release some of the carbon trapped at the interstitial sites of the bct crystal and thereby relax the lattice strain. The freed carbon atoms react with the iron to produce iron carbides within the tempered martensite microstructure. However, tempering at too high a temperature causes the martensite to transform into ferrite and pearlite, and produces a large loss in strength. Figure 11.9 shows the effect of tempering temperature on the mechanical properties of a medium-carbon steel. The strength decreases whereas the ductility improves with increasing temperature owing to the lattice strain relaxation of the martensite. Tempered martensitic steels are used extensively in high hardness engineering structures, including many aircraft components.
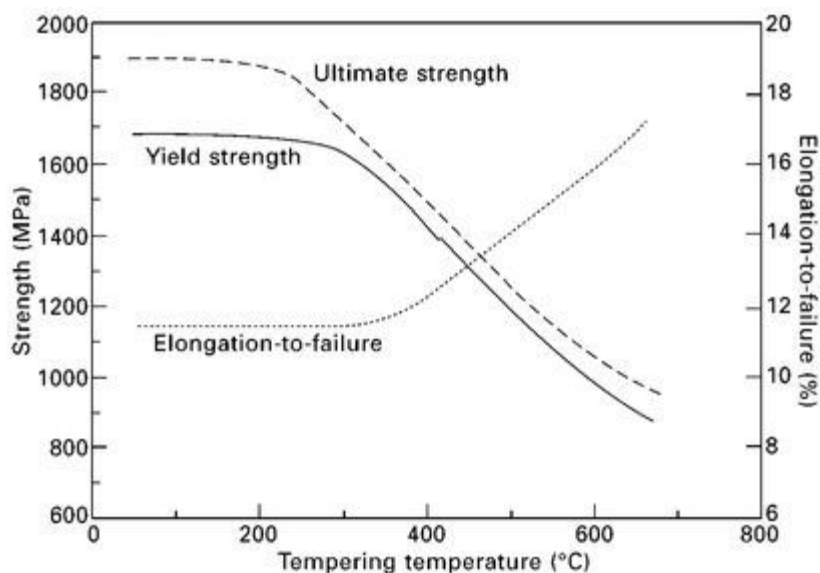
11.9 Effect of tempering temperature on the properties of 4340 medium-carbon low-alloy steel.
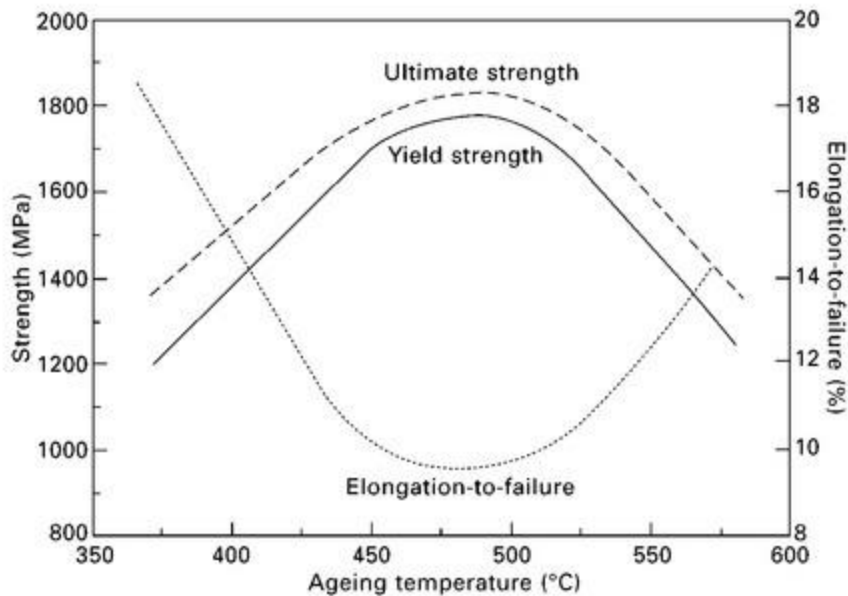
11.3 Maraging steel

Maraging steel is used in aircraft, with applications including landing gear, helicopter undercarriages, slat tracks and rocket motor cases – applications which require high strength-to-weight material. Maraging steel offers an unusual combination of high tensile strength and high fracture toughness. Most high-strength steels have low toughness, and the higher their strength the lower their toughness. The rare combination of high strength and toughness found with maraging steel makes it well suited for safety-critical aircraft structures that require high strength and damage tolerance. Maraging steel is strong, tough, low-carbon martensitic steel which contains hard precipitate particles formed by thermal ageing. The term 'maraging' is derived from the combination of the words martensite and age-hardening.

Maraging steel contains an extremely low amount of carbon (0.03% maximum) and a large amount of nickel (17–19%) together with lesser amounts of cobalt (8–12%), molybdenum (3–5%), titanium (0.2–1.8%) and aluminium (0.1–0.15%). Maraging steel is essentially free of carbon, which distinguishes it from other types of steel. The carbon content is kept very low to avoid the formation of titanium carbide (TiC) precipitates, which severely reduce the impact strength, ductility and toughness when present in high concentration. Because of the high alloy content, especially the cobalt addition, maraging steel is expensive. Maraging steel is produced by heating the steel in the austenite phase region (at about 850 °C), called austenitising, followed by slow cooling in air to form a martensitic microstructure. The slow cooling of hypoeutectic steel from the austenite phase usually results in the formation of ferrite and pearlite; rapid cooling by quenching in water or oil is often necessary to form martensite. However, martensite forms in maraging steel upon slow cooling owing to the high nickel content which suppresses the formation of ferrite and pearlite. The martensitic microstructure in as-cooled maraging steel is soft compared with the martensite formed in plain carbon steels by quenching. However, this softness is an advantage because it results in high ductility and toughness without the need for tempering. The softness also allows maraging steel to be machined into structural components, unlike hard martensitic steels that must be tempered before machining to avoid cracking.

After quenching, maraging steel undergoes a final stage of strengthening involving thermal ageing before being used in aircraft components. Maraging steel is heat-treated at 480–500 °C for several hours to form a fine dispersion of hard precipitates within the soft martensite matrix. The main types of precipitates are Ni_3Mo, Ni_3Ti, Ni_3Al and Fe_2Mo, which occur in a high volume fraction because of the high alloy content. Carbide precipitation is practically eliminated owing to the low carbon composition. Cobalt is an important alloying element in maraging steel and serves several functions. Cobalt is used to reduce the solubility limit of molybdenum and thereby increase the volume fraction of Mo-rich precipitates (e.g. Ni_3Mo, Fe_2Mo). Cobalt also assists in the uniform dispersion of precipitates through the martensite matrix. Cobalt accelerates the precipitation process and thereby shortens the ageing time to reach maximum hardness. Newer grades of maraging steel contain complex $Ni_{50}(X,Y,Z)_{50}$ precipitates, where X, Y and Z are solute elements such as Mo, Ti and Al.

The precipitates in maraging steel are effective at restricting the movement of dislocations, and thereby promote strengthening by the precipitation hardening process. <u>Figure 11.10</u> shows the effect of ageing temperature on the tensile strength and ductility of maraging steel. As with other age-hardening aerospace alloys such as the 2XXX Al, 7XXX Al, β-Ti and α/β-Ti alloys, there is an optimum temperature and heating time to achieve maximum strength in maraging steel. When age-hardened in the optimum temperature range of 480–500 °C for several hours it is possible to achieve a yield strength of around 2000 MPa while retaining good ductility and toughness. Over-ageing causes a loss in strength owing to precipitate coarsening and decomposition of the martensite with a reversion back to austenite. The strength of maraging steels is much greater than that found with most other aerospace structural materials, which combined with ductility and toughness, makes them the material of choice for heavily loaded structures that require high levels of damage tolerance and which must occupy a small space on aircraft.

11.10 Effect of ageing temperature on the strength and ductility (percentage elongation to failure) of a maraging steel.

11.4 Medium-carbon low-alloy steel

Medium-carbon low-alloy steel contains 0.25–0.5% carbon and moderate concentrations of other alloying elements such as manganese, nickel, chromium, vanadium and boron. These steels are quenched from singlephase austenite condition, and then tempered to the desired strength level. Aircraft applications for this steel include landing gear components, shafts and other parts. There are numerous grades of medium-carbon low-alloy steel, and the most important for aerospace are Type 4340, 300 M and H11 which cover the range from moderate-to-high strength, and provide impact toughness, creep strength and fatigue resistance.

11.5 Stainless steel

Aircraft components are made using stainless steel when both high strength and corrosion resistance are equally important. Stainless steel contains a large amount of chromium (12–26%) which forms a corrosion-resistant oxide layer. Chromium at the steel surface reacts with oxygen in the air to form a thin layer of chromium oxide (Cr_2O_3) which protects the underlying material from corrosive gases and liquids. The Cr_2O_3 layer is a very thin and impervious barrier which protects the underlying steel substrate.

There are several types of stainless steel: ferritic, austenitic, martensitic, duplex and precipitation-hardened stainless steels; although only the latter is used for structural aerospace applications because of its high tensile strength and toughness. Precipitation-hardened stainless steel used in aircraft has a tempered martensitic microstructure for high strength with a chromium oxide surface layer for corrosion protection. Like maraging steel, precipitation-hardened stainless steel is age-hardened by solution treatment, quenching and then thermal ageing at 425–550 °C. The most well known precipitation-hardened stainless steel is 17–4 PH (ASTM Grade A693), which contains a trace amount of carbon (0.07% max) and large quantity of chromium (15–17.5%) with lesser amounts of nickel (3–5%), copper (3–5%) and other alloying elements (Mo, V, Nb). The nickel is used to improve toughness and the other alloying elements promote strengthening by the formation of precipitate particles.

An early application of stainless steel was in the skins of super- and hypersonic aircraft, where temperature effects are considerable. Stainless steel was used in the skin of the Bristol 188, which was a Mach 1.6 experimental aircraft built in the 1950s to investigate kinetic heating effects. Stainless steel was also used

in the American X-15 rocket aircraft capable of speeds in excess of Mach 6 (Fig. 11.11). The skin of these aircraft reaches high temperature owing to frictional heating, and this would cause softening of aluminium if it were used. Steel is heat resistant to 400–450 °C without any significant reduction in mechanical performance. Stainless steel is no longer used in super- and hypersonic aircraft owing to the development of other heat-resistant structural materials which are much lighter, such as titanium. Stainless steel is currently used in engine pylons and several other structural components which are prone to stress corrosion damage, although its use is limited.

(a)

(b)

11.11 Stainless steel was used in the (a) Bristol 188 and (b) X-15. (a) Photograph reproduced with permission from Aviation Archives. (b) Photograph reproduced with permission from NASA

11.6 Summary

There are many types of steels used in structural engineering, but only maraging steel, medium-carbon low-alloy steel and precipitation-hardened stainless steel are used in aircraft structures. Steel is used in structures requiring high strength and toughness but where space is limited, such as landing gear, track slats, wing carry-through boxes, and wing root attachments. The percentage of the airframe mass that is constructed of steel is typically 5–8%.

Advantages of using steel in highly-loaded aircraft structures include high stiffness, strength, fatigue resistance and fracture toughness. Stainless steel provides the added advantage of corrosion resistance. Problems encountered with steels include high weight, potential hydrogen embrittlement, and (when stainless steel is not used) stress corrosion cracking and other forms of corrosion.

Maraging steel is used in aircraft components because it combines very high strength (about 2000 MPa) with good toughness, thereby providing high levels of damage tolerance. These properties are achieved by the microstructure consisting of a ductile martensite matrix strengthened by hard precipitate particles formed by thermal ageing.

Medium-carbon low-alloy steel also combines high strength and toughness owing to a microstructure of tempered martensite containing hard carbide precipitates. This type of steel has similar mechanical properties to maraging steel, but is more susceptible to stress corrosion cracking. It is used widely in aerospace structural components.

Precipitation-hardened stainless steel is characterised by high strength and excellent corrosion resistance, and is used in aircraft structures prone to stress corrosion. The microstructure consists of martensite and precipitation particles. High corrosion resistance occurs by the formation of a chromium oxide surface layer which is impervious to corrosive gases and fluids.
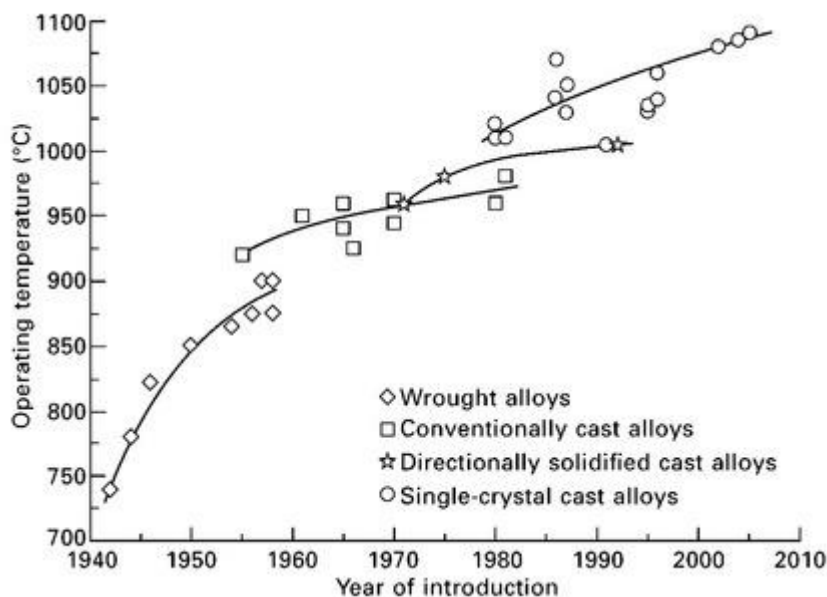
Superalloys for gas turbine engines

12.1 Introduction

Superalloys are a group of nickel, iron–nickel and cobalt alloys used in aircraft turbine engines for their exceptional heat-resistant properties. Materials used in jet engines must perform for long periods of time in a demanding environment involving high temperature, high stress and hot corrosive gas. Many materials simply cannot survive the severe conditions in the hottest sections of engines, where the temperatures reach ~ 1300 °C. Superalloys, on the other hand, possess many properties required by a jet-engine material such as high strength, long fatigue life, fracture toughness, creep resistance and stress-rupture resistance at high temperature. In addition, superalloys resist corrosion and oxidation at high temperatures, which cause the rapid deterioration of many other metallic materials. Superalloys can operate at temperatures up to 950–1300 °C for long periods, making them suitable materials for use in modern jet engines.

Superalloys have played a key role in the development of high thrust engines since the 1950s when the era of jet-powered civil aviation and rocketry began. Jet aircraft would fly at slower speeds and with less power without superalloys in their engines. The most effective way of increasing the thrust of jet engines is by increasing their operating temperature. This temperature is limited by the heat resistance of the engine materials, which must not distort, soften, creep, oxidise or corrode. Superalloys with their outstanding high-temperature properties are essential in the development of jet engines.

The important role of superalloys in raising the maximum operating temperature of jet engines is shown in Fig. 12.1. This figure shows the improvement in creep resistance using an industry benchmark of the maximum temperature that materials can withstand without failing when loaded at 137 MPa (20 ksi) for 1000 h. Over the era of jet aircraft, the maximum temperature has risen over 50%. The benefits that the increased operating temperature has provided in engine power have been enormous. Over the past 20 years the thrust of the gas turbine engine has increased by some 60% while over the same period the fuel consumption has fallen by 15–20%. The impressive achievements in engine power and fuel efficiency have been accomplished in part by improvements in the material durability in the hottest sections of the engine, and in particular the high-pressure turbine blades.


12.1 Improvement in the temperature limit of superalloys for aircraft turbine engines. The operating temperature is defined as the creep life of the material when loaded to 137 MPa (20 ksi) for 1000 h.

Engine durability has also improved dramatically owing to advances in engine design, propulsion technology and materials. Improved durability allows the operator to better utilise the aircraft by increasing engine life and reducing maintenance inspections and overhauls. When the Boeing 707 first entered service in 1957 the engines were removed for maintenance after about 500 h of operation. Today, a modern Boeing 747 engine can operate for more than 20 000 hours between maintenance operations. This remarkable improvement is the result of several factors, including the use of materials with improved high-temperature properties and durability.

The development of superalloys together with other advances in engine technology has pushed the operating limit to ~ 1300 °C, resulting in powerful engines for large civil aircraft and high thrust engines for supersonic military fighters. The processing methods used to fabricate engine components have been essential in raising the operating temperatures of engines. The development of advanced metal casting and processing methods has been important in increasing properties such as creep resistance at high-temperature.

Figure 12.2 shows the materials used in the main components of a modern jet engine. Superalloys account for over 50% of the total weight. Superalloys are used in the hottest components such as the turbine blades, discs, vanes and combustion chamber where the temperatures are 900–1300 °C. Superalloys are also used in the low-pressure turbine case, shafts, burner cans, afterburners and thrust reversers. In general, nickel-based superalloys are used in engine components that operate above 550 °C. A problem with superalloys is their high density of 8–9 g cm^{-3}, which is about twice as dense as titanium and three times denser than aluminium. Lighter materials are used whenever possible to reduce the engine weight. Titanium alloys are used to reduce the engine weight, but their use is restricted to components in the fan and compressor sections where the temperature is less than 550 °C. Titanium is used on the leading edges of carbon-fibre fan blades. Aircraft engines also contain aluminium alloys and fibre–polymer composites to reduce weight, although these materials can only be used in the coolest regions of the engine such as the fan blades and inlet casing, where the temperatures are less than 150 °C.
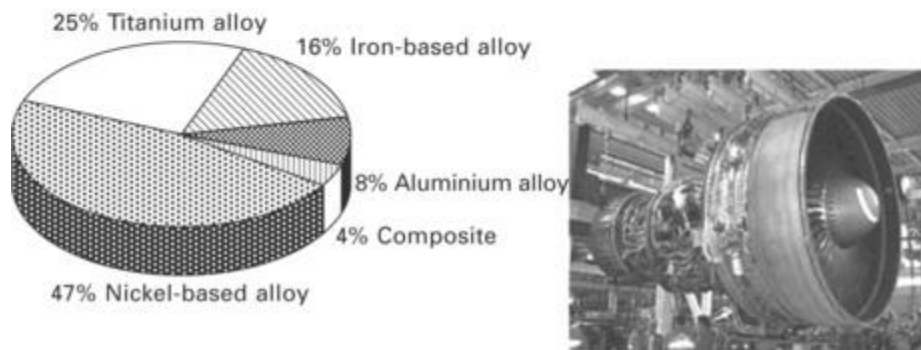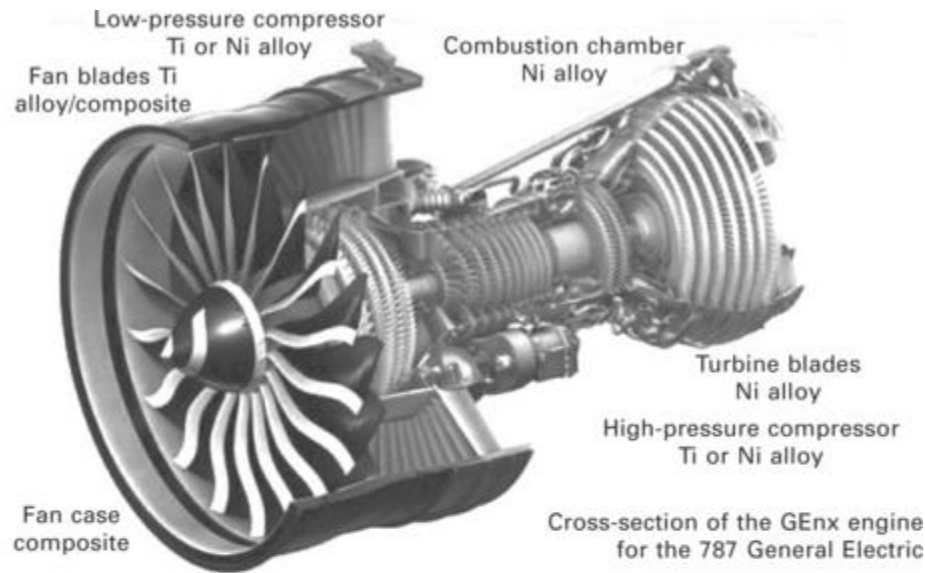
12.2 Material distribution in an aircraft turbine engine. The engine is the General Electric (CF6) used in the Boeing 787.

The use of superalloys in jet engines is explored in this chapter. The properties needed by materials used in engines are examined, such as high creep resistance and long fatigue life. The types of nickel, iron–nickel and cobalt superalloys are investigated, including their metallurgical properties that make them important engine materials. We also examine the advanced processing methods used to maximise the high-temperature properties of superalloys. The surface coating materials used to protect superalloys in the hottest regions of engines are also investigated.

12.2 A simple guide to jet engine technology

Since the introduction of commercial jet engines in the 1950s, the aerospace industry has made on-going advances in engine technology to improve performance, power, fuel efficiency and safety. Figure 12.3 shows the improvements in the performance parameters of jet engines used in passenger aircraft. The maximum thrust at take-off has increased by 300% whereas the specific fuel consumption and engine weight per unit thrust has more than halved since the introduction of jet-powered airliners. In addition, modern jet engines are more durable, reliable, quieter and less polluting. These improvements in engine performance are the result of many factors, but without a doubt the development of nickel-based superalloys has been essential to the success.
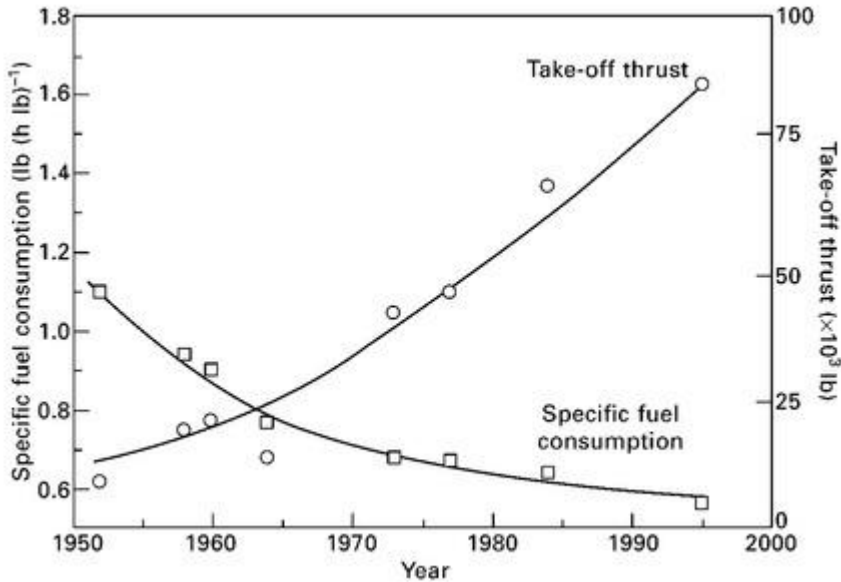
12.3 Performance improvements in jet engines. adapted from R. C. Reed, *The superalloys: fundamentals and applications*, Cambridge University Press, 2006

The materials used in jet engines must survive arduous temperatures and withstand high stress for long periods. For example, turbine blades are designed to last at least 10 000 h of flying, which is equivalent to 8 million km of flight, at temperatures up to ~ 1200 °C. At this temperature the blades rotate at more 10 000 rpm which generates a speed of 1200 km h^{-1} at the blade tip and stress of about 180 MPa (or 20 tonne per square inch) at the blade root. To perform under such extreme conditions, materials used in the hot sections of jet engines must have some outstanding high temperature properties, which include:
• high yield stress and ultimate strength to prevent yield and failure;
• high ductility and fracture toughness to provide impact resistance and damage tolerance;
• high resistance to the initiation and growth of fatigue cracks to provide long operating life;
• high creep resistance and stress rupture strength;
• resistance against hot corrosive gases and oxidation;
• low thermal expansion to maintain close tolerances between rotating parts.
Jet engines are complex engineering systems made using various types of metals, ceramics and composites, although superalloys are the key material to their high thrust and long operating life. There are many types of jet engines, with the most common on large passenger aircraft and military fighter aircraft being turbojets or turbofans. The basic difference between turbojets and turbofans is the way air passes through the engine to generate thrust. Turbojets operate by drawing all the air into the core of the engine. With turbofans the air passes through the engine core as well as by-passing the core. Most modern jet engines are turbofans, which are more fuel efficient than turbojets during flights at subsonic speeds and, for this reason, their operation is described.
Figure 12.4 shows the main sections of a turbofan engine. The first inlet section is the fan, which consists of a large spinning fan system that draws air into the engine. Air flowing through the fan section is split into two streams: one stream continues through the main core of the engine whereas the second stream by-passes the engine core. The by-passed air flows through a duct system that surrounds the core to the back of the engine where it produces much of the thrust that propels the aircraft forward. The temperatures within the fan section are not high, which allows titanium or composite materials to be used for their high specific stiffness, strength and fatigue life. Other considerations in the selection of materials in the fan region include resistance to corrosion, erosion and impact damage (from bird strike), making titanium alloys and composites suitable.
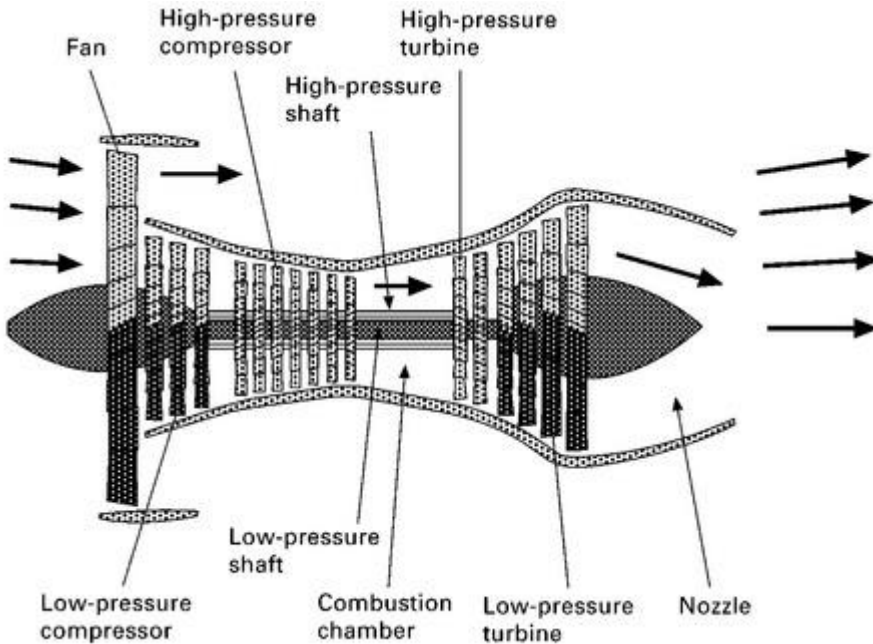
12.4 Main sections of a turbofan engine.

The air in turbofan engines passes through the engine core and enters the compressor section where it is compressed to high pressure. The compressor is made up of stages, with each stage consisting of compressor blades and discs, which squeeze the air into progressively smaller regions. As air is forced through the compressor section its pressure and temperature rapidly increase, thus requiring the use of heat-resistant materials. Hot compressed air then flows into the combustion chamber where it is mixed with jet fuel and ignited. This produces high-pressure gases that may reach a velocity of 1400 km h^{-1} and temperatures between 850 and 1500 °C. The combustion temperatures can exceed the melting point of the superalloys used in the combustion chamber. To survive, the superalloy engine components are protected with an insulating layer of ceramic material called a thermal barrier coating. The hot, high-pressure gases flow from the combustion chamber into the turbine section, which consists of bladed discs attached to shafts which run almost the entire length of the engine. The gases are allowed to expand through the turbine section which spins the blades. Power is extracted from the spinning turbine to drive the compressor and fan via the shafts. The turbine blades and discs are made using superalloys to withstand the hot gases coming from the combustion chamber. The gases that pass through the turbine are combined in the mixer section with the colder air that by-passed the engine core. The hot gases then flow into the rear-most section called the nozzle where high thrust is generated to propel the aircraft forward.

12.3 Nickel-based superalloys

12.3.1 BACKGROUND

Nickel-based superalloy is the most used material in turbine engines because of its high strength and long fatigue life combined with good resistance to oxidation and corrosion at high temperature. Nickel-based superalloy is the material of choice for the hottest engine components that are required to operate above 800 °C. Without doubt, one of the most remarkable properties of nickel superalloys that is utilised in jet engines is their outstanding resistance against creep and stress rupture at high temperature. (The creep and stress rupture properties of materials are explained in chapter 22). Creep is an important material property in order to avoid seizure and failure of engine parts. Creep involves the plastic yielding and permanent distortion of materials when subjected to elastic loads. Most materials experience rapid creep at temperatures of 30–40% of their melting temperature. For example, aluminium and titanium alloys, which

are used in the cooler regions of jet engines, creep rapidly above 150 and 350 °C, respectively. Nickel superalloys resist creep so well they can be used at 850 °C, which is over 70% of their melting temperature (T_m = 1280 °C). Very few other metallic materials possess excellent creep resistance at such high temperatures. The exceptional creep and stress rupture resistance of nickel superalloys means that engines can operate at higher temperatures to produce greater thrust. The outstanding creep and stress rupture resistance of nickel-based superalloys is shown in Fig. 12.5. Compared with the materials used in aircraft structures, aluminium, titanium and magnesium alloys, the stress rupture strength of nickel-based alloys is outstanding.
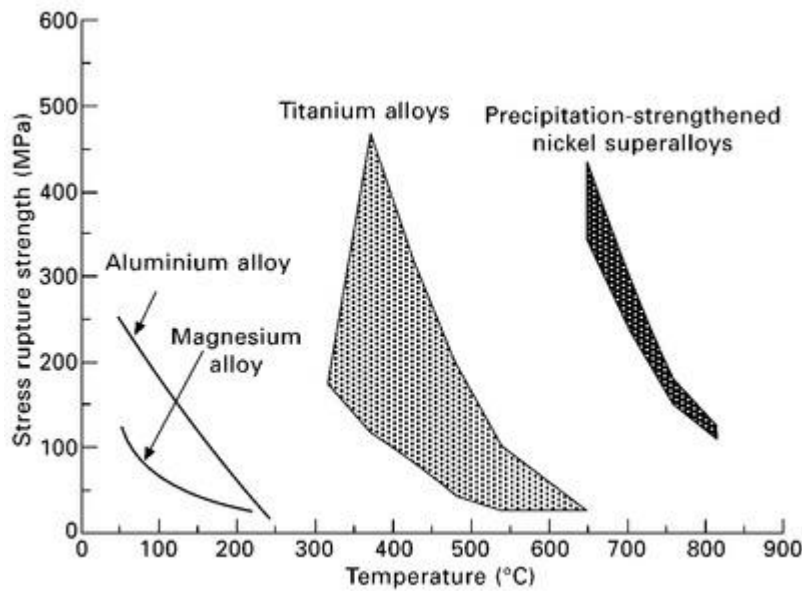
12.5 Stress rupture curves for aerospace materials.

12.3.2 COMPOSITION OF NICKEL SUPERALLOYS

Nickel superalloys contain at least 50% by weight of nickel. Many of the superalloys contain more than ten types of alloying elements, including high amounts of chromium (10–20%), aluminium and titanium (up to 8% combined), and cobalt (5–15%) together with small amounts of molybdenum, tungsten and carbon. Table 12.1 gives the composition of several nickelbased superalloys used in jet engines.

Table 12.1

Average composition of nickel superalloys

Alloy	Ni	Fe	Cr	Mo	W	Co	Nb	Al	C	Other
						Composition				
Astroloy	55.0	–	15.0	5.3		17.0	–	4.0	0.06	
Hastelloy X	49.0	18.5	22.0	9.0	0.6	1.5	3.6	2.0	0.1	
Inconel 625	61.0	2.5	21.5	9.0	–	–	–	0.2	0.15	<0.25 Cu
Nimonic 75	75.0	2.5	19.5	–	–	–	–	0.15	<0.08	1 V
Inconel 100	60.0	<0.6	10.0	3.0	–	15.0	–	5.5	<0.08	2.9 (Nb+Ta)
Inconel 706	41.5	37.5	16.0	–	–	–	5.1	0.2	0.12	<0.15 Cu
Inconel 716	52.5	18.5	19.0	3.0	–	–	5.2	0.5	0.05	0.1 Zr
Inconel 792	61.0	3.5	12.4	1.9	3.8	9.0	–	3.5	0.04	
Inconel 901	42.7	34	13.5	6.2	–	–	–	0.2	0.16	0.3 V
Discaloy	26.0	55	13.5	2.9	–	–	3.5	0.2	0.15	0.5 Zr
Rene 95	61.0	<0.3	14.0	3.5	3.5	8.0	–	3.5	0.14	
Rene 104	52.0	–	13.1	3.8	1.9	182	1.4	3.5	0.03	2.7 Ta
SX PWA1480	64.0	–	10.0	–	4.0	5.0	–	5.0		2 Hf
DS PWA1422	60.0	–	10.0	–	12.5	10.0		5.0		

The functions of the alloying elements are summarised in Table 12.2. The elements serve several important functions, which are to:

Table 12.2

Functions of alloying elements in nickel superalloys

Alloying element	Function
Chromium	Solid solution strengthening; corrosion resistance
Molybdenum	Solid solution strengthening; creep resistance
Tungsten	Solid solution strengthening; creep resistance
Cobalt	Solid solution strengthening
Niobium	Precipitation hardening; creep resistance

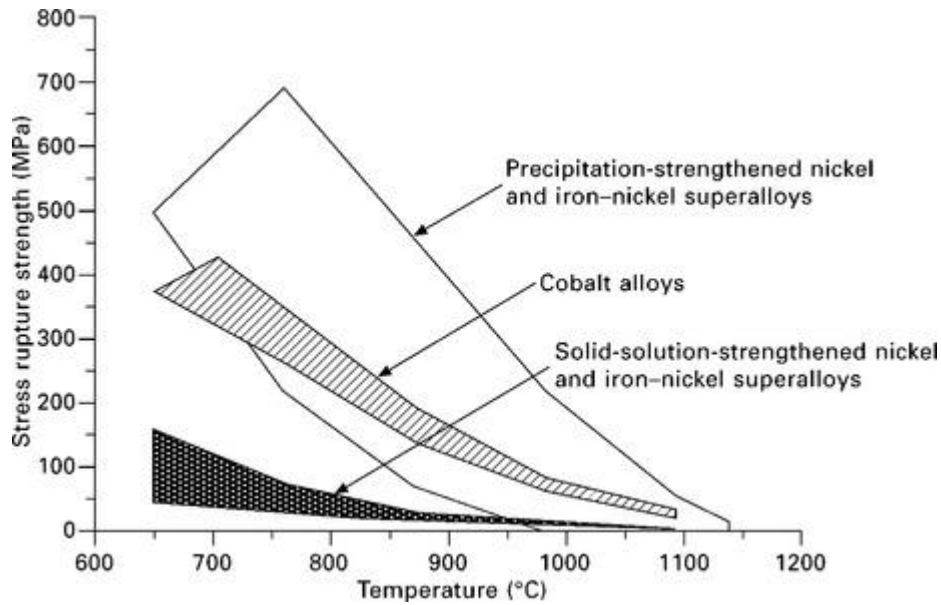| Aluminium	Precipitation hardening; creep resistance
Carbon	Carbide hardening; creep resistance

• strengthen the nickel by solid solution hardening with the addition of elements such as molybdenum, chromium, cobalt and tungsten;

• strengthen the nickel by hard intermetallic precipitates and carbides with the addition of aluminium, titanium, carbon; and

• create a surface film of chromium oxide (Cr_2O_3) to protect the nickel from oxidation and hot corrosion.

Superalloys are not named or numbered according to any system; they are usually given their name by the company that developed or commercialised the alloy. Of the many alloys, the most important for aerospace is Inconel 718 which accounts for most of the nickel superalloy used in jet engines. For example, superalloy 718 accounts for 34% of the material in the General Electric CF6 engine (shown in Fig. 12.2) used on the Boeing 787. Alloy 718 is a high-strength, corrosion-resistant alloy that is used at temperatures up to about 750 °C. Hastelloy X and Inconel 625 are often used in combustion cans and Inconel 901, Rene 95 and Discaloy are used in turbine discs. Nickel-based superalloys are available in extruded, forged and rolled forms. The higher strength forms are generally only found in the cast condition, such as directional and single crystal castings. The alloys PWA1480 and PWA1422 are special types of superalloys used in turbine blades that are produced by single crystal (SX) and directional solidification (DS) methods, respectively. These casting methods for producing blades are explained in chapter 6.

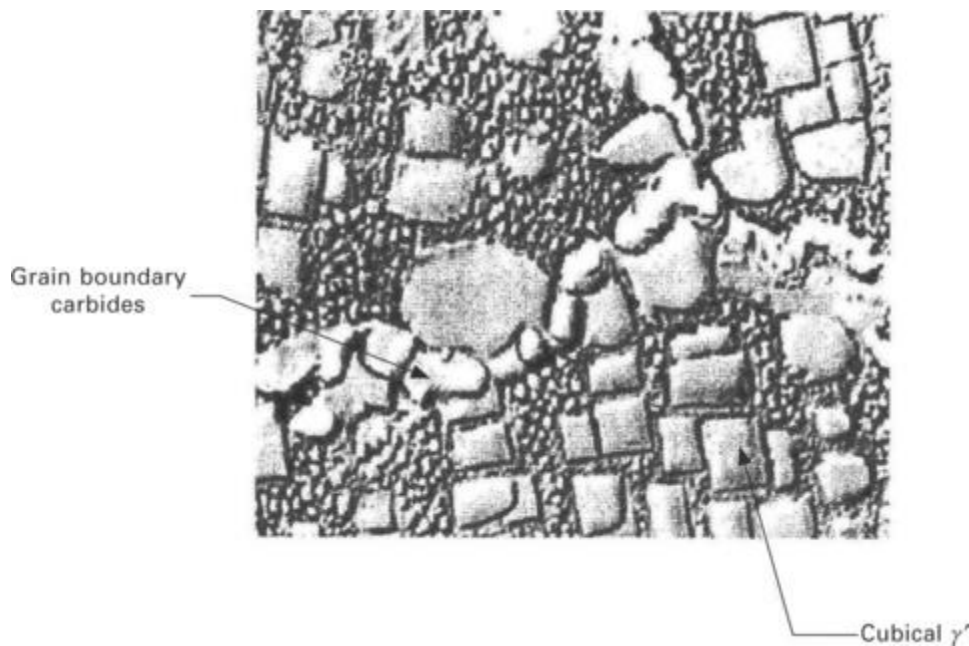### 12.3.3 PROPERTIES OF NICKEL SUPERALLOYS

Nickel superalloys derive their strength by solid solution hardening or the combination of solid solution and precipitation hardening. Superalloys that harden predominantly by solid solution strengthening contain potent substitutional strengthening elements, such as molybdenum and tungsten. These two alloying elements have the added benefit of having low atomic diffusion rates in nickel, and move very slowly through the lattice structure at high temperatures. Creep is controlled by atomic diffusion processes, with the creep rate increasing with the diffusion rate of the alloying elements. Therefore the slow movement of alloying elements impedes the creep of nickel.

Solid solution-hardened nickel alloys have good corrosion resistance, although their high-temperature properties are inferior to precipitation hardened alloys. Figure 12.6 shows the creep-rupture strength of nickel-based superalloys hardened by means of solid solution strengthening or precipitation strengthening. Here, the stress necessary to cause tensile rupture in 100 h is given over a range of temperatures. Nickel superalloys hardened by precipitation strengthening provide the best high-temperature performance and, for this reason, are used in jet-engine parts such as blades, discs, rings, shafts, and various compressor components. Precipitation-hardened nickel alloys are also used in rocket motor engines.

12.6 Stress rupture properties of nickel superalloys hardened by solid solution strengthening or precipitation strengthening.

Precipitation-hardened nickel alloys contain aluminium, titanium, tantalum and/or niobium that react with the nickel during heat treatment to form a fine dispersion of hard intermetallic precipitates. The most important precipitate is the so-called gamma prime phase (γ') which occurs as Ni_3Al, Ni_3Ti, or $Ni_3(Al,Ti)$ compounds. These precipitates have excellent long-term thermal stability and thereby provide strength and creep resistance at high temperature (<u>Fig. 12.7</u>). A high volume fraction of γ' precipitates is needed for high strength, fatigue resistance and creep properties (typically above 50%).

12.7 Microstructure of precipitation-hardened nickel superalloy showing γ' precipitates and carbides which provide high-temperature creep properties.

The γ′ precipitates are formed by a heat-treatment process that involves solution treatment followed by thermal ageing to dissolve the alloying elements into solid solution. Solution treatment is performed at 980–1230 °C. Single-crystal nickel alloys are solution treated at higher temperatures (up to 1320 °C). Following solution treatment and quenching, the nickel alloy is aged at 800–1000 °C for 4–32 h to form the γ′ precipitates. The ageing temperature and time is determined by the application of the superalloy. Lower ageing temperatures and shorter times produce fine γ′ precipitates for engine parts requiring strength and fatigue resistance, such as discs. Higher temperatures produce coarse γ′ precipitates desirable for creep and stress rupture applications, such as turbine blades.

Precipitation-hardened nickel alloys contain other thermally stable compounds (in addition to γ′) which also contribute to the high-temperature properties. Titanium, tantalum, niobium and tungsten react with carbon to form several types of hard carbide precipitates: MC, $M_{23}C_6$, M_6C and M_7C_3 where M stands for the alloying element. These carbides perform three important functions:

• prevent or slow grain boundary sliding that causes creep;
• increase tensile strength; and
• react with other elements that would otherwise promote thermal instability during service.

Small amounts of boron, hafnium and zirconium are often used as alloying elements in nickel. These elements combine with other elements to pin grain boundaries, thereby reducing their tendency to slide under load and thereby increasing the creep strength. Niobium is an important alloying element for the precipitation hardening of nickel alloys. The most commercially important superalloy is Inconel 718, and it is strengthened mainly by niobium precipitates (Ni_3Nb).

The newest types of superalloys contain rare earth elements (such as yttrium or cerium) at concentrations of 2.5 to 6% to increase the high-temperature creep strength by precipitation and solid solution hardening. However, rare earth elements are expensive to use, they increase the density of the superalloy, and they can produce casting defects. Ruthenium is increasingly being used instead of, or in combination with, the rare earth elements to achieve similar improvements in high-temperature mechanical performance without the problem of casting defects. The platinum group of elements (platinum, iridium, rhodium, palladium) are also being used to increase the operating temperature limit to 1100–1150 °C, but these are expensive.

Some grades of nickel superalloys contain submicrometre-sized oxide particles, such as ThO_2 or Y_2O_3, to promote higher elevated temperature tensile and stress rupture properties. For example, superalloy MA754 is produced by powder metallurgy involving mechanical alloying to introduce about 1% by volume of a fine dispersion of nano-sized oxide particles.

A problem with using metals at high temperature is rapid oxidation which quickly breaks down and degrades the material. Nickel alloys also contain 10–20% chromium to provide oxidation resistance through the formation of a protective surface oxide film composed of Cr_2O_3 or $NiCr_2O_4$. Nickel alloys rapidly degrade by oxidation without this surface film, which must be stable at the high operating temperatures of gas turbine engines.

12.4 Iron–nickel superalloys

Iron–nickel superalloys are used in gas turbine engines for their structural properties and low thermal expansion at high temperature. Iron–nickel alloys expand less than nickel or cobalt superalloys at high temperature, which is an important material property for engine components requiring closely controlled clearances between rotating parts. Iron–nickel alloys are generally less expensive than nickel- and cobalt-based superalloys, which is another advantage. The main uses for Iron–nickel alloys in jet engines are blades, discs and casings.

The composition of several Iron–nickel alloys used in jet engines is given in Table 12.3, and most contain 15–60% iron and 25–45% nickel. Iron–nickel superalloys are hardened by solid solution strengthening and precipitation strengthening. Aluminium, niobium and carbon are used as alloying elements to promote the formation of hard intermetallic precipitates or carbides that are stable at high temperature. The precipitates are similar to those present in nickel-based superalloys, and include γ′ $Ni_3(Al,Ti)$, γ″(Ni_3Nb) and various types of carbides. The precipitates provide Iron–nickel alloys with good resistance against creep and stress

rupture at elevated temperature. Chromium is used to form an oxide surface layer to protect the metal from hot corrosive gases and oxidation.

Table 12.3

Composition of iron–nickel superalloys

Alloy	Composition (%)									
	Fe	Ni	Cr	Mo	W	Co	Nb	Al	C	Other
Solid solution-hardened alloys										
Haynes 556	29.0	21.0	22.0	3.0	2.5	20.0	0.1	0.3	0.1	0.5 Ta
Incoloy	44.8	32.5	21.0	–	–	–	–	0.6	0.36	
Precipitation-hardened alloys										
A-286	55.2	26.0	15.0	1.25	–	–	–	0.2	0.04	0.3 V
Incoloy 903	41.0	38.0	<0.1	0.1	–	15.0	3.0	0.7	0.04	

12.5 Cobalt superalloys

Cobalt superalloys possess several properties which make them useful materials for gas turbine engines, although they are more expensive than nickel superalloys. Cobalt alloys generally have better hot-corrosion resistance than nickel-based and iron–nickel alloys in hot atmospheres containing lead oxides, sulfur and other compounds produced from the combustion of jet fuel. Cobalt alloys have good resistance against attack from hot corrosive gases, which increases the operating life and reduces the maintenance of engine parts. However, comparison between nickel and cobalt alloys must be treated with some caution because there are wide differences in hot corrosion resistance within each group of superalloys. That is, certain nickel superalloys also have excellent resistance against hot corrosion. Cobalt alloys also have good stress rupture properties, although not as good as precipitation-hardened nickel-based alloys (Fig. 12.6).
Cobalt superalloys contain about 30–60% cobalt, 10–35% nickel, 20–30% chromium, 5–10% tungsten, and less than 1% carbon. The composition of some cobalt alloys used in jet engine components is given in Table 12.4. The main functions of the alloying elements are to harden the cobalt by solid solution or precipitation strengthening. The precipitates that form in cobalt alloys do not provide the same large improvement in high-temperature strength as nickel alloys and, for this reason, the resistance of cobalt alloys against creep and stress rupture is inferior to precipitation-hardened nickel-based and Iron–nickel alloys. Cobalt alloys are generally used in components that operate under low stresses and need excellent hot-corrosion resistance.

Table 12.4

Composition of cobalt-based superalloys

Alloy	Composition (%)									
	Co	Fe	Ni	Cr	Mo	W	Nb	Al	C	Other
Haynes 25	50.0	3.0	10.0	20.0	–	15.0	–	–	0.1	1.5 Mn
Haynes 188	37.0	<3.0	22.0	22.0	–	14.5	–	–	0.1	0.9 La
MP35-N	35.0	–	35.0	20.0	10.0	–	–	–	–	

12.6 Thermal barrier coatings for jet engine alloys

Turbine blades contain rows of hollow aerofoils for cooling to increase the engine operating temperature. Cool air flows through the holes, which are located just below the surface, to remove heat from the superalloy. The aerofoils are remarkably effective at cooling, which allows increased operating temperature and associated improvements in engine efficiency. To increase the operating temperature even further, the hottest engine parts are coated with a thin ceramic film to reduce heat flow into the superalloy. The film is called a thermal barrier coating, which has higher thermal stability and lower thermal conductivity (1 W m^{-1} K^{-1}) than nickel superalloy (50 W m^{-1} K^{-1}). The use of the coating allows higher operating temperatures (typically at least 170 °C) in the turbine section. The coating provides heat insulation and this lowers the temperature of the superalloy engine component. Thermal barrier coatings can survive temperatures well in excess of the melting temperature of the superalloy itself, and also provide protection from the effects of thermal fatigue and creep and the oxidising effect of sulfates and other oxygen-containing compounds in the combustion gases.

Thermal barrier coatings are complex multilayered structures, as shown in Fig. 12.8. The coating can be applied using various deposition methods, with the most common being electron-beam physical vapour deposition (EBPVD). In this process, a target anode material consisting of zirconium oxide (ZrO_2) and yttrium oxide (Y_2O_3) is bombarded with a high-energy electron beam under vacuum. The electron beam heats the anode material to high temperature which causes atoms and oxide molecules from the target to transform from the solid into gas phase. The gaseous atoms and molecules then precipitate as a thin solid layer of the anode material onto a substrate, such as a nickel superalloy component. The coating is deposited on the surface to a thickness of about 0.1–0.3 mm, which is sufficient to provide heat protection to the underlying metal.

High temperature

Metal substrate

$ZrO_2(Y_2O_3)$
Ceramic overcoat

MCrAlY
Bond coat
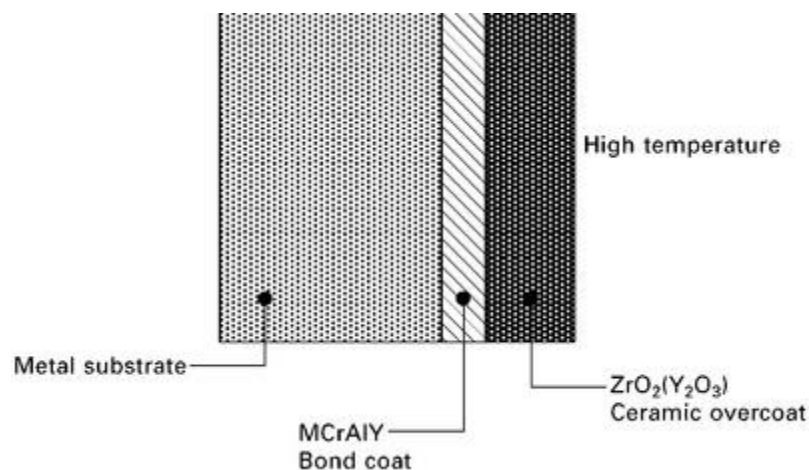
12.8 Through-thickness composition of a typical thermal barrier coating system.

The most common coating material is yttria-stabilised zirconia (YSZ), which is based on zirconia doped with 7% yttria. The YSZ is bonded to the surface via intermediate layers which improve the adhesion strength properties. An intermediate bond coat with a chemical composition MCrAlY (where M = Co, Ni or Co + Ni) or NiAl–Pt are often used. The bond coat also provides oxidation and corrosion resistance to the underlying superalloy component. Thermal barrier coatings are used on engine components in the combustion chamber and turbine sections, including high-pressure blades and nozzle guide vanes. However, YSZ TBCs are unsuitable for use on loaded rotating components because their low tensile strength and toughness causes them to crack and spall.

12.7 Advanced materials for jet engines

The aerospace industry is continually developing new materials to increase the operating temperature limit of gas turbine engines. As mentioned in <u>chapter 9</u>, titanium aluminides are being developed for engine applications. A group of refractory intermetallics based on metal silicides (Mo_5Si_3, Nb_5Si_3, Ti_5Si_3) retain high strength to about 1300 °C, which is 200 °C higher than single-crystal nickel superalloys. Nb_5Si_3 is attracting the greatest interest of the silicides, although it is prone to oxidation at high temperature. Other types of advanced materials such as eutectic solidified ceramics, ceramic matrix composites (e.g. carbon/carbon), and silicon nitride are also being evaluated as high-temperature engine materials. For the foreseeable future, however, nickel-based superalloys are likely to be the dominant structural material for high-temperature components in jet engines.

12.8 Summary

Superalloys have played a central role in the development of jet engine technology. The development of superalloys with better high-temperature and hot-corrosion properties together with advances in engine design and propulsion technology has resulted in great improvements in engine performance. Over the past 20 years, the thrust of jet engines has increased by more than 60% whereas the fuel consumption has fallen by 15–20%, and these improvements are, in part, the result of improvements in the high-temperature properties of superalloys.

A variety of high-performance materials is used in modern jet engines. Aluminium and carbon-fibre composites are used in the coolest sections of engines (operating at temperatures below about 150 °C), such as the fan and inlet casing, to minimise weight. Titanium ($\alpha + \beta$ and β) alloys are used in engine components with operating temperatures below about 550 °C, which includes parts in the fan and compressor sections. Superalloys are used for components that operate above 550 °C, such as the blades, discs, vanes and other parts found in the combustion chamber and other high-temperature engine sections.

Materials used in the hottest engine components, such as high-pressure turbine blades and discs, must have high strength, fatigue life, fracture toughness, creep resistance, hot-corrosion resistance and low thermal expansion properties. Nickel-based superalloys are the material of choice of these engine components because of their capability to operate at temperatures up to 950–1200 °C for long periods of time.

Nickel-based superalloys used in jet engines have a high concentration of alloying elements (up to about 50% by weight) to provide strength, creep resistance, fatigue endurance and corrosion resistance at high temperature. The types and concentration of alloying elements determines whether the superalloy is a solid solution-hardened or precipitation-hardened material. Precipitation-hardened superalloys are used in the hottest engine components, with their high-temperature strength and creep resistance improved by the presence of γ' [Ni_3Al, Ni_3Ti, $Ni_3(Al,Ti)$] and other precipitates that have high thermal stability.

The casting process is important in the production of heat-resistant superalloy engine components. The creep resistance of materials is improved by minimising or eliminating the presence of grain boundaries that are aligned transverse to the load direction. Superalloys are cast using directional solidification which produces a columnar grain structure with few transverse grain boundaries or single crystal casting which eliminates all grain boundaries.

Iron–nickel superalloys are used in jet engines for their high-temperature properties and low thermal expansion. These superalloys, which contain 15–60% iron and 25–45% nickel, are used in blades, discs and engine casings that require low thermal expansion properties.

Cobalt superalloys are used in jet engine components that require excellent corrosion resistance against hot combustion gases. The alloys contain 30–60% cobalt and high concentrations of nickel, chromium and tungsten which provide good resistance against lead oxides, sulfur oxides and other corrosive compounds in the combustion gas.

Thermal barrier coatings are a ceramic multilayer film applied to the superalloy surface to increase the operating temperature of the engine. The coating is an insulating layer that reduces the heat conducted into the superalloy. Yttria-stabilised zirconia (YSZ) is the most common coating material, and is used on engine components in the combustor chamber and turbine sections, including high-pressure blades and nozzle guide vanes.

AIRCRAFT METALS

An overview of some major metals commonly found in aircraft is given in the following paragraphs. For more complete coverage of aircraft metals, see *Metallic Materials and Elements for Aerospace Vehicle Structures, MIL-HDBK-5*, published by the U.S. Government Printing Office.

Aluminum (Al)

Aluminum is the principal structural metal for aircraft. A unique combination of properties makes aluminum a very versatile engineering and construction material. Light weight is perhaps aluminum's best known characteristic. With a specific gravity of 2.7, the metal weighs only about 0.1 lb/in^3 [2.8 g/cm^3], as compared with 0.28 lb/in^3 [7.8 g/cm^3] for iron and 0.32 lb/in^3 [8.86 g/cm^3] for copper. Commercially pure aluminum has a tensile strength of about 13 000 psi [89.6 MPa]. Its usefulness as a structural metal in this form is somewhat limited, although its strength can be approximately doubled by cold working. Much greater increases in strength can be obtained by alloying with other metals. Aluminum alloys having tensile strengths approaching 100 000 psi [689.6 MPa] are available. Aluminum and its alloys lose strength at elevated temperatures, although some retain good strength at temperatures as high as 400°F [204°C]. At subzero temperatures, aluminum's strength increases without loss of ductility. Aluminum in general is considered as having good corrosion resistance. The ease and versatility with which aluminum is made surpasses that of virtually any other material.

Aluminum products are made in two forms, east and wrought. **Cast aluminum** is formed into a shape by pouring molten aluminum into a mold of the required shape. **Wrought aluminum** is mechanically worked into the form desired by rolling, drawing, and extruding.

Wrought Aluminum Code

Wrought aluminum and aluminum alloys are designated by a four-digit system, with the first digit of the number indicating the principal alloying element:

1000 Series. When the first digit is 1, the material is 99% or higher pure aluminum.

2000 Series. Copper is the principal alloying element in this group. The addition of copper allows aluminum to be heat-treated to high strengths, but also reduces its corrosion resistance.

3000 Series. Manganese is the principal element in this series. It is added to increase hardness and strength. Alloys of this series are non-heat treatable.

4000 Series. The major alloying element of this group is silicon, which can be added in sufficient quantities to cause substantial lowering of the melting point without producing brittleness. The principal use of 4000-series alloys is for welding wire.

5000 Series. Magnesium is one of the most effective and widely used alloys for aluminum. When it is used as the major alloying element, the result is a moderate- to high-strength, non-heat-treatable alloy. Alloys in this series have good welding characteristics and high corrosion resistance.

6000 Series. Alloys in this group contain silicon and magnesium in proportions to form magnesium-silicide, thus making them heat-treatable. Though not as strong as the 2000 and 7000 alloys, the magnesium-silicon alloys possess good formability and corrosion resistance with moderate strength.

7000 Series. Zinc is the major alloying element of this group and, when coupled with a small percentage of magnesium, results in a heat-treatable alloy of very high strength. Usually, other elements, such as copper and chromium, are added in small quantities.

8000 Series. This series is a category mainly used for lithium alloys.

The second digit of the code number identifies any modifications made to the original alloy. In the 2000 to the 8000 numbers, the last two digits have little significance other than to identify the alloys and the sequence of development. In the 1000 series, the last two digits indicate the amount of pure aluminum

above 99% in hundredths of 1%. For example, aluminum identified with the number 1240 would be 99.40% pure aluminum. In the 1000 series a modification is for the purpose of controlling one or more of the impurities. Examples of the alloy code are shown in
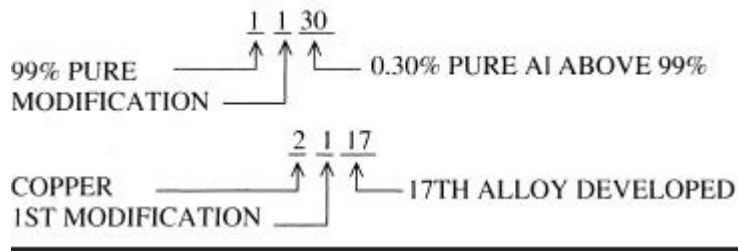

FIGURE 8-19 Aluminum alloy identification.

Cast Aluminum Code

Cast aluminum also uses a four-digit identification system with the first digit indicating the alloy group. The numbers used are not the same as for wrought alloys. Cast alloy groups are
1—aluminum, 99% or more
2—copper
3—silicon, with copper and/or magnesium
4—silicon
5—magnesium
6—not used
7—zinc
8—lithium
9—other elements

The second two digits identify the aluminum alloy or indicate the aluminum purity. The last digit is separated from the other three by a decimal point and indicates the product form, that is, castings or ingots. A modification of the original alloy is indicated by a serial letter before the numerical designation. Alloy A514.0, for example, indicates an aluminum alloy casting with magnesium as the principal alloy. One modification to the original alloy has been made, as indicated by the letter A.

Hardness and Temper Designation

An important factor for aluminum alloy identification is the **temper**, or **hardness** value. A letter and number combination is placed after the alloy code to indicate the processes that have taken place and the degree of hardness. Basic designations are as follows:
F—as fabricated (no treatment)
O—annealed
H—cold worked or strain hardened (wrought products)
W—unstable condition (temporary condition while the material ages after solution heat treatment)
T—solution heat treated

The H designations are used only for the non-heat-treatable alloys. These are generally the alloys in the 1000, 3000, and 5000 series. These materials can only be hardened through the effects of cold working. The T designations are used after alloys capable of being hardened by thermal treatment. Heat-treatable alloys contain elements such as copper, magnesium, silicon, and zinc. Alloys from the 2000, 6000, and 7000 series use T designations. The W designation applies only to those alloys capable of heat treatment. The annealed designation, O, and the as-fabricated designation, F, can apply to any of the alloys.
The H tempers are further subdivided to indicate the specific combination of basic operations. For example,
H1—strain hardened only
H2—strain hardened and partially annealed

H3—strain hardened and stabilized

A number following the H1, H2, or H3 indicates the degree of strain hardening of the alloy. The number 8 indicates that the maximum degree of strain hardening has occurred. The number 2 indicates that the metal is one-quarter hard, 4 indicates one-half hard, and 6 indicates three-quarters hard.
The T designation is followed by a number that indicates specific sequences of basic treatments. Frequently used numbers are
T3—solution heat-treated, cold-worked
T4—solution heat-treated
T6—solution heat-treated and artificially aged

The term **cold working**, or **strain hardening** describes any process applied at room temperature that stretches, compresses, bends, draws, or otherwise changes the shape of the metal to any appreciable degree. **Solution heat treating** is a thermal process for hardening aluminum. It involves heating the material to a specified temperature, causing the chemical structure of the material to change. The material is then quickly cooled or quenched. Upon quenching, the material is soft and unstable. Chemical changes continue within the metal at room temperature until a stable condition is reached. This is known as **aging**. Acceleration of the aging process by additional thermal treatment is known as **artificial aging**

Corrosion

Aluminum is considered to be highly corrosion resistant under the majority of service conditions. When aluminum surfaces are exposed to the atmosphere, a thin, invisible oxide (Al_2O_3) skin forms, which protects the metal from further oxidation. Unless this coating is destroyed, the material remains fully protected against corrosion. Aluminum is highly resistant to weathering and is corrosion resistant to many acids. Alkalis are among the few substances that attack the oxide skin and are therefore corrosive to aluminum.
High-strength alloys containing copper are less resistant to corrosion than the other alloys. Alloys of this type often have a thin layer of pure aluminum rolled on each side. The pure aluminum acts as a barrier between the environment and the less resistant alloy. Aluminum of this type is known as **clad aluminum**. (Alclad is a trade name used by ALCOA for this product.)
While highly corrosion resistant by itself, aluminum is susceptible to galvanic corrosion resulting from contact with other materials. Among the structural metals, aluminum is second only to magnesium on the electromotive series. Galvanic corrosion with any structural metal other than magnesium results in aluminum being the material corroded or decomposed.

Workability

Aluminum can be cast by any method known. It can be rolled to any desired thickness, including a foil thinner than paper. It can be stamped, drawn, spun, or roll formed. The metal can be hammered or forged, and there is almost no limit to the different shapes into which it may be extruded. Aluminum can be turned, milled, bored, or machined in other manners at the maximum speed at which the majority of the machines are capable. Almost any method of joining is applicable to aluminum; riveting, welding, brazing, soldering, or adhesive bonding.

Alloys Used for Aircraft

The majority of the aluminum products that the technician encounters will consist of the following alloys:

Non-Heat-Treatable Alloys

1100. Pure aluminum that is soft, ductile, and low strength. Its use on aircraft is limited to nonstructural application. It is also used for making low-strength rivets.

3003. This alloy is similar to 1100 but has about 20% greater strength. It is used on aircraft for fluid lines, with limited application for fairings or cowlings.

5052. The highest strength of the non-heat-treatable alloys, 5052 has high corrosion resistance and high fatigue strength. Having excellent workability, it is widely used for aircraft cowlings, fairings, and other nonstructural parts requiring forming. Fluid lines are frequently made of this alloy.

5056. This alloy is used to make rivets for riveting magnesium sheet.

Heat-Treatable Alloys

2017. Used more frequently on older aircraft, 2017 alloy is seen today, if at all, only in aluminum rivets.

2117. A modification of alloy 2017, this alloy is used exclusively for the manufacture of aluminum rivets. The 2117 rivet is not as strong as a 2024 rivet but can be driven with no special treatment.

2024. Alloy 2024 is probably the "standard" structural metal as well as the most-used metal for aircraft. It is found in virtually every form available, including sheet, extrusion, bar stock, standard hardware, and tubing. Heat treatable to high strengths, its ability to be cold-worked is good to excellent for everything except rivets. Like most heat-treatable alloys, 2024 is not recommended for welding. To improve corrosion resistance, 2024 sheet stock is available as a clad material. Alloy 2024 ages rapidly after heat treatment, and most forms will be in the T3 condition. Alloy 2024 is highly susceptible to **intergranular corrosion** if heat treatment is done improperly.

6061. An easily worked metal, 6061 has a strength only two-thirds that of 2024. A good general-purpose material, it can be welded, offers high corrosion resistance, and can be worked by almost any means. To develop full strength after heat treatment normally requires artificial aging; such metal will have a T6 designation.

7075. This is one of the highest strength aluminum alloys available and also one of the more difficult aluminum alloys to work. Parts should be formed in the annealed state or at an elevated temperature. Arc and gas welding is not recommended. Alloy 7075 is available in a clad form to improve corrosion resistance. This alloy is normally artificially aged and carries the T6 designation.

AEROSPACE APPLICATIONS OF SHAPE MEMORY ALLOYS

Darren Hartl
Dimitris C. Lagoudas *

Aerospace Engineering Department
Texas A&M University
College Station, Texas 77843-3141

ABSTRACT

With the increased emphasis on both reliability and multifunctionality in the aerospace industry, active materials are fast becoming an enabling technology capturing the attention of an increasing number of engineers and scientists worldwide. This article reviews the class of active materials known as Shape Memory Alloys (SMAs), especially as implemented in aerospace applications. To begin, a general overview of shape memory alloys is provided. The useful properties and engineering effects of SMAs are described and the methods in which these may be utilized are discussed. A review of past and present aerospace applications is presented. The discussion addresses applications for both atmospheric earth flight as well as space flight. To complete the discussion, SMA design challenges and methodologies are addressed and the future of the field is examined.

1 Introduction to SMAs

Shape memory alloys (SMAs) are metallic alloys which undergo solid-to-solid phase transformations induced by appropriate temperature and/or stress changes and during which they can recover seemingly permanent strains. Such alloys include NiTi, NiTiCu, CuAlNi, and many other metallic alloy systems [1]. The phase transformation of an SMA is unique because such transformation is accompanied by large recoverable strains which have the potential to result in significant stresses when the material element is sufficiently constrained. Such strains are referred to as transformation strains and are in addition to standard thermoelastic strains. Because of their ability to recover strain in the presence of stress, SMAs are included in the class of materials known as active materials, which also includes piezoelectrics, magnetorestrictive materials, and shape memory polymers, among others [2]. SMAs provide high actuation forces and displacements compared to other active materials, though at relatively low frequencies.

Although they have been around for over half a century, new applications continue to be developed for shape memory alloys [3]. Many of these applications are intended to serve the needs of the biomedical industry while others are intended for use in consumer products. However, the aerospace industry is actively pursuing the development of new SMA technologies as well as assimilation of SMAs into existing systems. An SMA component, being both structural and active, can effectively reduce the complexity of a system when compared to the same system utilizing standard technology (i.e. an electromechanical or hydraulic actuator). This increased simplicity gained by trading multiple moving parts for a single active element can lead to a higher overall reliability, especially at low cycles. Such an integration of structure and actuator can also be accomplished in a compact arrangement. This compact integration is possible due to the high actuation stresses and strains generated, leading to a high energy density. These beneficial attributes make shape memory alloys an attractive active material candidate as the aerospace industry continues to push for so-called "smart" structures and "intelligent" systems [2]. This is a natural evolution within the aerospace field as these systems are often the only viable solution to very complex engineering problems. Furthermore, the technological requirements of the industry, especially in the area of defense, often reduce the importance of cost as a design driver. However, as more SMA applications are designed, produced, and used, the affordability of SMA utilization will continue to increase.

---

*Address all correspondence to this author: lagoudas@aero.tamu.edu

The remainder of the introduction will present a brief survey of SMA properties (Section 1.1) and their exhibited effects (Section 1.2). Section 2 provides a summary of the many current aerospace applications of shape memory alloys, including not only commercially available systems but also those in development. Finally, in Section 3, design methods and challenges are briefly reviewed and the future of SMA research and continued application is discussed.

1.1 Properties of SMA Behavior

As previously mentioned, it is a phase transformation which plays the key role in the SMA's unique behavior. The *martensitic* transformation converts the material between two particular phases, namely *austenite* and *martensite*. Austenite is the high temperature or "parent" phase and exhibits a cubic crystalline structure while martensite is the low temperature phase that exhibits a tetragonal or monoclinic crystalline structure [1, 4, 5]. The martensitic transformation is a shear-dominant, diffusionless transformation which occurs via the nucleation and growth of the martensitic phase from the parent austenitic phase. The transformation from austenite to martensite may lead to *twinned* martensite in the absence of internal and external stresses or *detwinned* martensite if such stresses exist at a sufficient level. Because the transformation from austenite to twinned martensite results in negligible macroscopic shape change, twinned martensite is often referred to as *self-accommodated* martensite. The reorientation of twinned martensite into detwinned martensite can take place under the application of sufficient stress.

Although SMAs can be fabricated in a single crystal form, the vast majority of SMA applications utilize polycrystalline components. In polycrystals, the crystallographic effects described above are observed in each individual grain and the total macroscopic response of the material is based on the combined response of all grains. This micromechanical "averaging" leads to a smoother material response as different grains experience transformation at different points in the thermomechanical loading path due to variation in orientation and local stress concentrations. In polycrystalline materials, the effects of plasticity are also apparent and must be considered. For the reminder of this work, polycrystalline SMA components will be assumed.

The transformation from austenite to martensite begins, in the absence of stress, at a temperature known as the *martensitic start temperature* (M_s). The transformation continues to evolve as the temperature is lowered until the *martensitic finish temperature* (M_f) is reached. When the SMA is heated from the martensitic phase in the absence of stress, the reverse transformation (martensite to austenite) begins at the *austenitic start temperature* (A_s), and upon reaching the *austenitic finish temperature* (A_f), the material is purely austenite. There is often a hysteresis between the transformation regions A_s to A_f and M_s to M_f as can be seen on the temperature axis in Figure 1. The transforma-

tion into austenite will always complete at a higher temperature than the transformation into martensite ($A_f > M_f$). An important characteristic of SMAs is that the temperatures at which the martensitic transformation begins and ends vary with stress and this is schematically represented in Figure 1. Though they are not strictly linear, the overall slope of the transformation lines in stress-temperature space is often referred to as the *stress rate* [3] or the *stress influence coefficient* [6, 7].

To help an analyst or designer identify which phase is present at a given thermomechanical state, a *phase diagram* is constructed [8–10] which illustrates the stress dependence of the martensitic transformation temperatures. This is schematically represented in Figure 1. Some distinct partitions of the phase diagram indicate where phases are expected to exist in pure form while other regions indicate where transformation from one phase to another will occur and where two or more phases can coexist. Recall once more that these transformation boundaries are not necessarily linear and are only represented as such for this schematic illustration. A more descriptive presentation of these transformation regions and their optional representations can be found in the literature [10]. Note that in the phase diagram presented in Figure 1, the stress axis represents a uniaxial component of stress or, in general, some scalar measure of stress (e.g. Von Mises stress). Note also that polycrystalline SMA materials often show significantly different transformation behavior in compression as opposed to tension. This tension/compression asymmetry is not accounted for in this description but a complete discussion has been provided in [11]. In many practical cases, particular regions of SMA components are generally known to be under either tension or compression, and thus this behavior can easily be considered by using different material properties for these different regions.
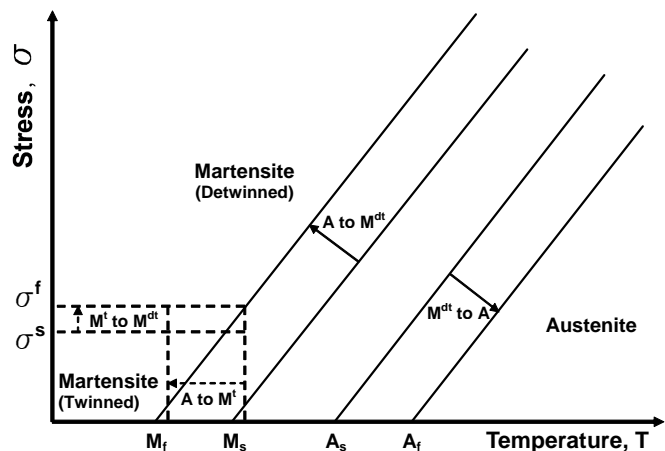

Figure 1. SMA stress-temperature phase diagram (schematic) [10].

The detwinning of martensite can also be represented on the phase diagram which is schematically shown in Figure 1. The application of stress to pure martensite above a certain stress threshold, σ^s, causes the twinned martensite to begin to deform in shear into detwinned martensite. Detwinning completes at the detwinning finish stress, σ^f. The process of stressing twinned martensite into detwinned martensite is not reversible by mechanical means. Upon removal of the detwinning load, the material will remain detwinned and thus deformed. A detwinning loading path is schematically demonstrated on the phase diagram in Figure 2, where it is represented by the mechanical loading/unloading path **B–C–D**. Figure 3 also illustrates detwinning by showing actual experimental results obtained during the loading nitinol SMA wire in the martensitic state (**B–C–D**). The recovery of this seemingly permanent deformation will be discussed in the following section.

1.2 Engineering Effects of SMAs

Having introduced the key properties of a shape memory alloy, it is now possible to review two important behaviors exhibited by such materials. These are the *shape memory effect* (SME) and the *pseudoelastic effect*. The usefulness of SMAs is most commonly found in the application of one of these two engineering effects, with SME used for actuation and pseudoelasticity employed for applications such as vibration isolation and dampening. These two behaviors will now be discussed in more detail. The stability of the material response when considering both effects will also be reviewed.

1.2.1 The Shape Memory Effect
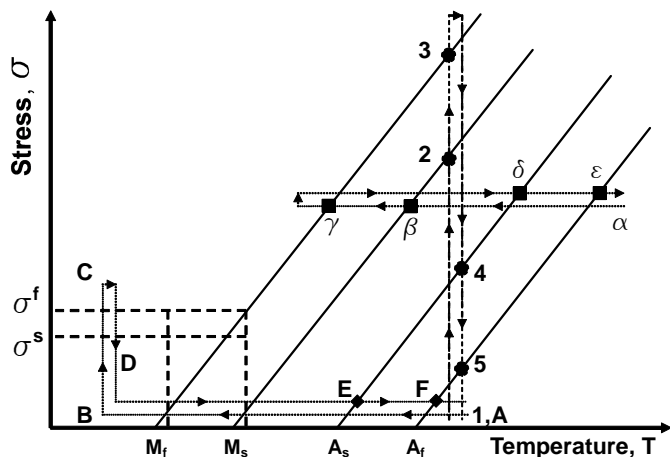Recovery of the seemingly permanent deformation observed during detwinning is associated with the phenomenon known as the stress-free shape memory effect. The nature of the SME can be better understood by following the process depicted in the stress-temperature phase diagram, schematically shown in Figure 2. This loading path is experimentally exemplified in $\sigma - \varepsilon - T$ space in Figure 3, which shows an actual loading path for a NiTi wire actuator captured during experimentation at Texas A&M University. At the start of the loading path (indicated by **A** in Figures 2 and 3) the SMA is in its parent austenitic phase. In the absence of applied stress, the SMA will transform upon cooling into martensite in the twinned or self accommodated configuration (indicated by **B** in Figures 2 and 3). As stress is applied causing the martensitic phase to be reoriented into a fully detwinned state, deformation takes place and large macroscopic strains are observed (indicated by **C** in Figures 2 and 3). The magnitude of this strain is on the order of 8% for some NiTi alloys [12]. Upon unloading, the elastic portion of the total strain is recovered while the inelastic strain due to the detwinning process remains due to the stability of detwinned martensite. This point is indicated by **D** in Figures 2 and 3. Upon heating the SMA at zero stress, the reverse transformation to the austenitic parent phase begins when the temperature reaches A_s (point **E**), and is completed at temperature A_f (point **F** Figures 2 and 3). The inelastic strain due to reorientation is recovered, and thus the original shape (before deformation **B–C**) is regained. Note that, in this case, the formation of any non-recoverable plastic strain has been neglected. Therefore, point **A** is equivalent to point **F** in terms of the state of the material. It is this reversion to an original or "remembered" shape that inspired the names "shape memory alloy." Note that subsequent cooling in the absence of stress will again result in twinned martensite with no substantial shape change in a manner identical to loading path **A–B** previously described.

Figure 2. Phase diagram schematic highlighting stress-free SME, isobaric SME, and isothermal pseudoelastic loading paths.
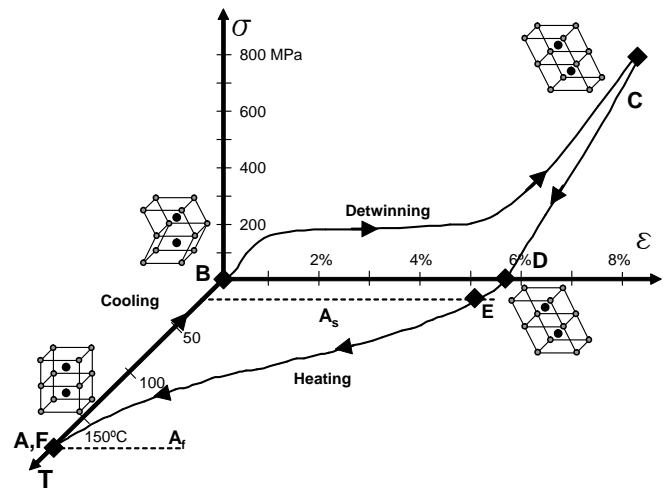

Figure 3. Experimental stress–strain–temperature curve of a NiTi SMA illustrating the shape memory effect (NiTiCu, Texas A&M University).

Now consider another loading path denoted by $\alpha - \beta - \gamma - \delta - \varepsilon$ in Figure 2 and also shown experimentally in Figure 4 [13]. Such a path is similar to the one previously described, though in this particular case a constant stress is maintained throughout the thermal cycle. This is exemplified by hanging a weight on an SMA component such as a wire or spring. If the SMA material begins in austenite (α) and is cooled through transformation into martensite ($\beta - \gamma$), it will exhibit large strains associated with the phase transformation. Such strains are the result of both the alteration of the crystal structure from austenite to detwinned martensite as well as the change in the elastic modulus during phase change. However, this elastic contribution is minor. Heating the material through the reverse transformation region ($\delta - \varepsilon$) leads to reversion to austenite and subsequent recovery of the large macroscopic strains, with the exception of any non-recoverable plastic strains. Such plastic strains can be observed at the end of heating in Figure 4. Because the recovered strain is used to provide displacement under a some force, it is also sometimes referred to as the *actuation strain* (ε^{act}). Note that this shape recovery will cease to occur if the applied stress exceeds some maximum level. This characteristic maximum actuation stress is often referred to as the blocking stress and can be easily experimentally determined.

1.2.2 The Pseudoelastic Effect A second commonly utilized phenomenon observed in SMAs is the *pseudoelastic effect*. This behavior is associated with stress-induced detwinned martensite (SIM) and subsequent reversal to austenite upon unloading. The transformation from austenite to detwinned martensite during pseudoelastic loading is analogous to the reorientation of twinned martensite into detwinned martensite during detwinning from the point of view that, in both cases, recover-
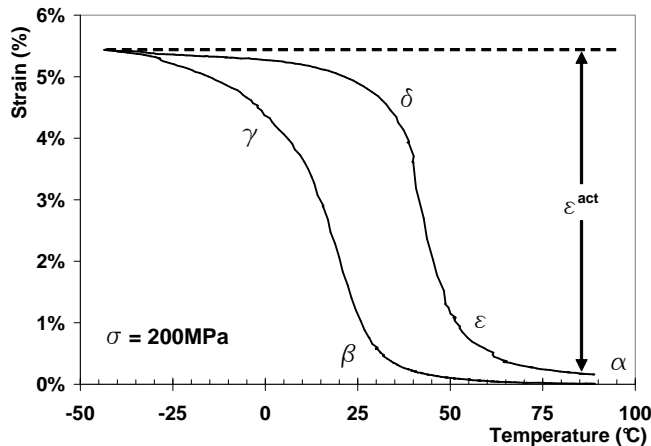
able inelastic strains are created. However, in the case of the pseudoelastic effect, the starting phase is austenite, and there is an actual phase transformation that takes place under the influence of stress. An isothermal pseudoelastic loading path in the stress-temperature space is schematically shown in Figure 2. Note that any load path which includes formation of SIM and begins and ends in the austenitic region results in the pseudoelastic effect. Initially, the material is in the austenitic phase (point **1** in Figures 2 and 5). The simultaneous transformation and detwinning of the martensite starts at point **2** and results in fully transformed and detwinned martensite (point **3**). Continued loading will lead to elastic deformation of the detwinned martensite. Upon unloading, the reverse transformation starts when point **4** is reached. By the end of the unloading plateau (point **5**), the material is again in the austenitic phase and upon unloading to zero stress all elastic strain (ε^{el}) and transformation strain (ε^{t}) is recovered. Only plastic strain (ε^{p}), if generated, remains.

A typical experimental result generated at Texas A&M and showing the pseudoelastic response of a NiTi SMA is presented in Figure 5. Here the temperature was maintained at a constant 80°C. For stresses below σ^{Ms} the SMA responds elastically. When the polycrystalline SMA critical stress (σ^{Ms}) is reached, (A→M^{dt}) transformation initiates and SIM begins to form. During the transformation into SIM, large inelastic strains are generated (upper plateau of stress-strain curve in Figure 5). This transformation completes when the applied stress reaches a critical value, σ^{Mf}. The material is now in a detwinned martensitic state. For further loading above σ^{Mf} the material responds nearly elastically. Upon unloading, which is initially elastic, the reverse transformation initiates at a critical stress, σ^{As}, and completes at a stress σ^{Af} because the mechanical load is applied at a temperature above A_f. Note that, due to the positive slopes of the four transformation lines in the phase diagram (Figure 1), increasing the test temperature results in an increase in the value of each critical transformation stress.

A hysteretic loop is obtained in the loading/unloading stress-strain diagram. If the applied stress exceeds the critical value σ^{Mf}, then the width of the hysteresis loop, less any accumulated non-recoverable plastic strain, is representative of the maximum amount of recoverable strain which can be produced due to stress-induced phase transformation from austenite to martensite (ε^{t}). Another important material characteristic observed in Figure 5 is the residual plastic strain (ε^{pl}) of $\sim 0.6\%$ seen remaining at the end of the loading cycle.

1.2.3 Stabilization of Material Response For polycrystalline SMA materials, the exact strain vs. temperature and stress vs. strain responses are heavily dependent on the loading history of the material. *Transformation-induced plasticity* (TRIP) is a phenomenon by which plastic strains are generated during a transformation cycle. Such permanent irrecoverable
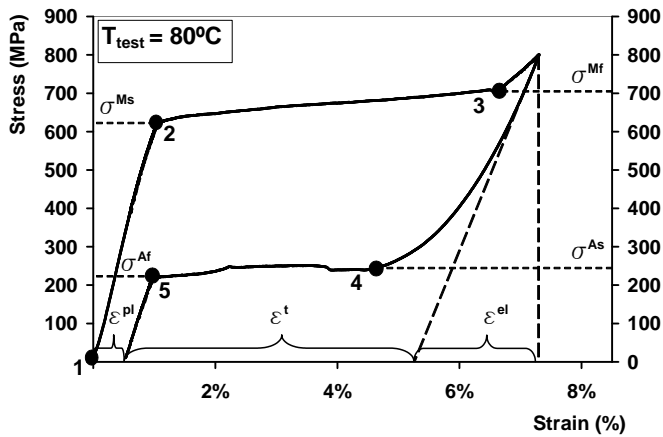

Figure 4. Experimental results illustrating the SME under a constant 200MPa stress (NiTi, [13]).

Figure 5. Experimental results for a single isothermal pseudoelastic loading cycle (NiTi, Texas A&M University).
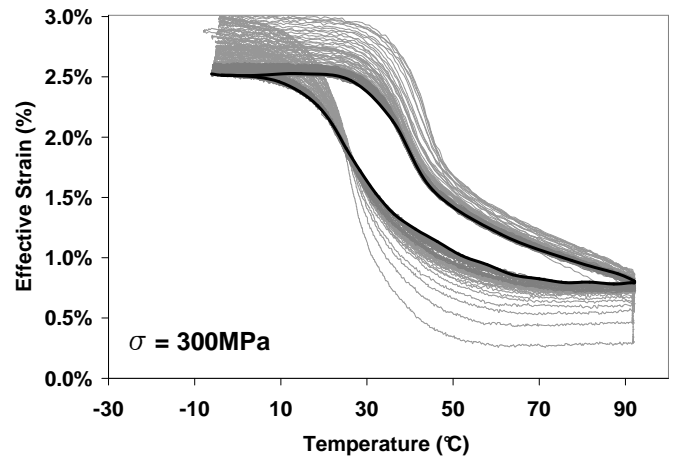

Figure 6. Experimental results for training via isobaric thermal cycling (Ni60Ti, [16]).

Figure 7. Experimental results for training via isothermal cycling of stress (NiTi, Texas A&M University).

strain will often be generated more quickly during initial material cycles and will then stabilize as the number of applied cycles increases. The topic of TRIP in SMAs has been discussed in more detail in [14, 15]. Many SMAs will cease to generate plastic strain after sufficient cycling, and this stabilizes the overall material response. Such repetition until stabilization is often referred to as *training* [1]. Aside from producing a stable material, sufficient training can also effectively eliminate the A→M^t transformation, thereby driving the minimum stress for shape recovery during (A↔M$^d t$) transformation to zero. This ability to recover shape at zero stress is known as *two-way shape memory effect* (TWSME). The phase diagram for a material exhibiting such behavior would therefore not require A↔M^t regions (see Figures 1 and 2).

For SMA material which will be used as an actuator via utilization of SME, such training often occurs by applying constant stress to an element and then cycling the temperature until the response has stabilized. An example of this can be seen in Figure 6, where the final cycle has been darkened. For material intended for pseudoelastic application, training is often performed by applying many stress cycles while maintaining a constant temperature. Figure 7 illustrates an example of such pseudoelastic training. The first of the grey cycles is equivalent to the loading cycle shown in Figure 5 while the 18th cycle is bolded. In agreement with previous discussion, it can be seen that several cycles are required before the stress/strain response becomes repeatable, and this is common in all SMAs.

2 Aerospace Applications of SMAs

From the early "thermal engines" [17], engineers and other designers in many fields have been developing ways to convert thermal energy into mechanical work via the crystallographic phase change of SMAs, which have now been used in real-world
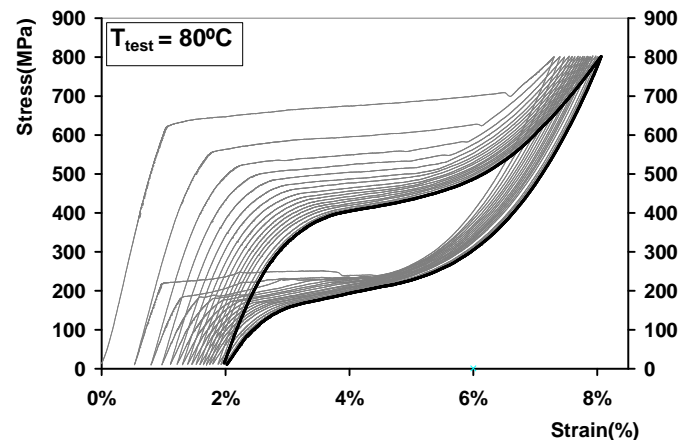
applications for several decades. As previously mentioned, one of the most well-known of these early applications was the hydraulic tubing coupling used on the F-14 in 1971 [18]. Since that time, designers have continued to utilize both the shape memory and pseudoelastic effects of SMAs in solving engineering problems in the aerospace industry. Such implementations of SMA technology have spanned the areas of fixed wing aircraft, rotorcraft, and spacecraft; work continues in all three of these areas. The following section describes some of the more recently explored aerospace applications of SMAs and then briefly summarizes the challenges facing the designers of such systems.

2.1 Fixed-Wing Aircraft and Rotorcraft Applications

Applications which apply specifically to the propulsion systems and structural configurations of fixed-wing aircraft will first

be considered. Perhaps two of the most well-known fixed-wing projects of the past are the Smart Wing program and the Smart Aircraft and Marine Propulsion System demonstration (SAMPSON) [19,20]. The Smart Wing program was intended to develop and demonstrate the use of active materials, including SMAs, to optimize performance of lifting bodies [21–24]. The project was split into two phases with the first being the most SMA-intensive. Here, SMA wire tendons were used to actuate hingeless ailerons while an SMA torque tube was used to initiate spanwise wing twisting of a scaled-down F-18. In each of these applications, the shape memory effect is used to provide actuation via shape recovery, and the recovery occurs at a non-zero stress as described in Section 1.2. Unlike the previous discussion, however, the stress state during actuation is variable and is a function of the elastic response of the actuated structure, in this case the wing. While the SMA was able to provide satisfactory actuation at 16% scale, it was found that the SMA torque tube in particular was not of sufficient strength to actuate a full-scale wing. As SMA material providers continue to increase their output, however, fabrication of larger SMA components for stronger actuation is now practical. The as-tested torque tube installation can be seen in Figure 8. This work was performed as part of a Defense Advanced Research Projects Agency (DARPA) contract to Northrop Grumman and monitored by the Air Force Research Lab (AFRL).

The SAMPSON program [25] was designed to demonstrate the usefulness of active materials in tailoring the inlet geometry and orientation of various propulsion systems. An experimental validation was performed on a full-scale F-15 inlet. The first series of wind tunnel tests performed at NASA Langley's high speed facility tested an antagonistic system in which one SMA cable is set in opposition to another. Here the SMAs employing the shape memory effect were used to rotate the inlet cowl in order to change its cross-sectional area. Two opposing SMA bundles were used to actuate in two directions, with the heating of one bundle causing shape recovery and thereby detwinning the unheated bundle. After the heated bundle was allowed to cool, the previously detwinned bundle was then heated, and reverse actuation occurred. SMA bundles consisting of 34 wires/rods were used to provide up to a 26700N force and rotated the inlet cowl 9°. Further tests demonstrated more complex SMA actuation, including inlet lip shaping [25]. This experimental setup can be seen in Figure 9. This work was performed as part of a DARPA contract to Boeing and monitored by the NASA Langley Research Center and the Office of Naval Research.

Portions of the SAMPSON project also studied the use of SMA "cables" wrapped circumferentially around the aft portion of the fan cowling of a high-bypass jet engine in order to increase/decrease fan nozzle area in different regions of the flight regime [26]. In the design, high exhaust temperature produced during takeoff and landing (slow speed flight) was used to cause SMA structural elements to transform into austenite, thus provid-
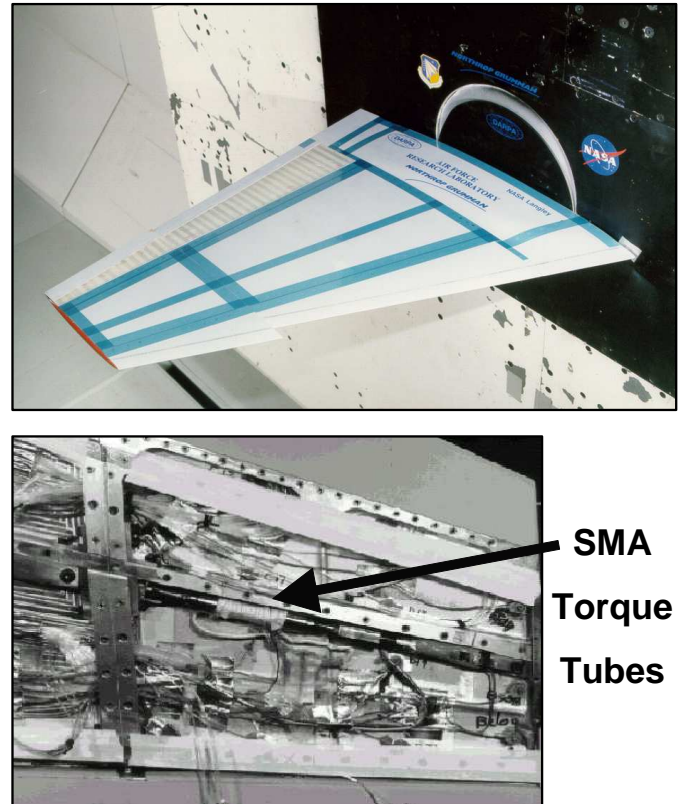

Figure 8. Total and cut-away view of the SMA torque tube as installed in the model wing during Phase I of the SMART Wing project [20].

ing recovery strain and opening the nozzle to its maximum cross-sectional area. At cruise, however, lower temperatures would allow the nozzle to close, optimizing performance at high altitudes. The experiment, which utilized SMA cable bundles for both opening and closing of the nozzle, proved the technology to be practical.

Research into a similar principle utilizing bending actuation of SMAs is also being performed. In this case the goal is to optimize the trade-off between noise mitigation at takeoff and landing and performance at altitude [16, 27–29]. Such engine noise levels are often highly regulated by various civil agencies. Often, flow mixing devices known as "chevrons" are statically installed along the trailing edges of the exhaust nozzles. Here the composite chevrons were designed to be reconfigurable with SMA beam components embedded inside. Again, actuation was based on the principle of changing flow temperature with altitude. The SMA beam elements are formed such that they force the chevron inward and mix the flow of gases (reducing noise) at low altitudes and low speeds where the engine temperature is high. They then relax and straighten at high altitude and high speeds, increasing engine performance. In the work cited [27], results are presented for both autonomous operation as well as controlled operation

Figure 9. The SAMPSON F-15 inlet cowl as installed in the NASA Langley Transonic Wind Tunnel [20].

environment. Experimental results were consistent with those of the model, and actuator performance was shown to meet the design goals. Each of these chevron research efforts demonstrate the capability of SMAs to be fabricated in the form required and then to be completely embedded within a structure, providing truly integrated actuation.

Figure 10. Boeing variable geometry chevron, flight testing [28].

via installed heaters. Tests demonstrated that the device works as expected, and development continues. Figure 10 illustrates the current Boeing design for the variable geometry chevron. Note that the composite layer has been removed from the chevron for exposition of the active SMA elements. Figure 11 illustrates the results of current efforts to model the Boeing chevron system. Here, complex behaviors such as elastic laminate response of the composite substrate, sliding contact, and 3-D non-homogeneous SMA loading have all been considered [16, 29].

NASA has approached the same chevron problem with a different design. In this case the active chevron is induced to bend by the incorporation of tensile SMA strips during chevron laminate fabrication. The strips are installed on each side of the chevron centroid [30]. Upon sufficient heating, the SMA elements contract and this leads to asymmetric stresses within the beam and thus an effective internal bending moment. Modeling was performed by considering both the SMA transformation and thermal strains as being caused by one "effective coefficient of thermal expansion" and implementing a model which predicted the nonlinear evolution of this strain in a finite element design
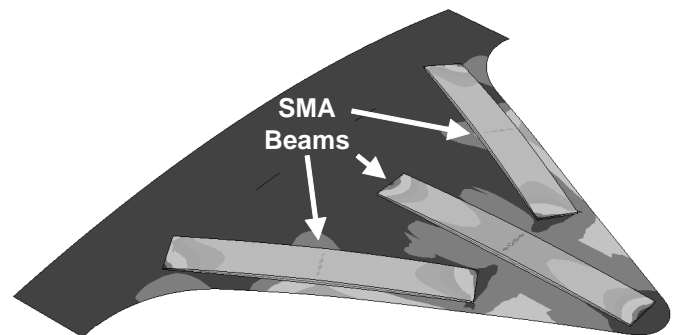

Figure 11. Stress contour results; FEA analysis of Boeing VGC, actuated position [16, 29].

In addition to propulsion system applications, shape memory effect actuation is also commonly applied to the problem of adaptable lifting bodies, including the morphing of the wing structure. The concept of integrating SMA elements into an aerostructure has been the topic of a number of studies [31]. One such research effort led to an airfoil which could effectively change its configuration from symmetric to cambered via actuation of SMA wires [32]. It was shown that the wing configuration could be changed during flight to optimize performance.

The shape memory behavior of the SMA wires was exploited and they were arranged in a spanwise configuration to increase actuation displacement. A series of pulleys transferred the load, now acting in a chordwise direction, to chosen points on the airfoil skin inner surface. During the design process, a genetic algorithm was used to determine the placement of these attachment points in order to achieve a predetermined final airfoil configuration. This modeling effort considered the full thermomechanical problem of SMA actuation and the coupled aerodynamic/structural response. A 9% increase in lift at constant 5° angle of attack was measured in the wind tunnel experiments. These results demonstrated the usefulness of an integrated design/analysis environment that accounts for both the constitutive response of the SMA actuator behavior and other external system effects (i.e. aeroelastic loads).

A different and interesting structural implementation of SMA actuation is found in a patent pertaining to actuation of the wing main spar [33]. Here the active elements are placed inside tubular spars which would be used to extend and/or retract a telescoping portion of the wing in the spanwise direction, again using SME. Another example of lifting body morphing is the "macro-scale morphing" which involves alterations in geometry with dimensional changes of the same order as the wing span [34]. Although the final morphed configuration chosen in this case was not explicitly intended to provide any type of aerodynamic enhancement, it demonstrated the feasibility of designing the mechanism required, should such morphing prove to be advantageous. Finally, in another application, researchers studied both the theoretical and experimental responses of morphing entire structures utilizing an antagonistic flexural unit cell, in which two opposing one-way SMA linear elements (ribbons or wires) are installed on either side of a simple hinging mechanism [35, 36]. This subsystem (the unit cell) is then repeated lengthwise to form a morphing truss-like structure. This idea was shown to be experimentally feasible and generally can apply to both aircraft as well as spacecraft as the structural unit cells can be arranged to fit the needs of the designer.

While morphing entire structures such as wings is one possibility, SMAs are also commonly used to actuate other smaller aerodynamic elements. This is possible because the behaviors which are unique to SMAs are exhibited across a large range of sizes. One recent example of small scale actuation is an extension of an earlier study into actuating wing surface vortex generators using shape memory wires [37]. Another proposed application pairs SMAs and Micro-Electromechanical Systems (MEMS). This MEMS-activated active skin [38] would include many devices incorporating thin-film SMA elements which could be microfabricated and placed under the skin of an aerodynamic surface. Activated spanwise in a sinusoidal sense, such devices would create a traveling wave in the skin which would help to energize the boundary layer and thus decrease turbulent drag. Although it is a problem that SMA components of

standard size provide low actuation frequencies, sufficiently thin SMA films have exhibited actuation frequencies of 30 Hz [39].

In addition to developing actuation applications, research is being performed into optimizing the dynamic properties of aircraft structural panels using SMA elements. Such applications often take advantage of the simple fact that a shape memory alloy will exhibit a change in elastic stiffness as it undergoes transformation. This behavior is often secondary in other applications but can be very important in manipulating the dynamic response of a structure. In one study [40], it was shown that thermally-induced post buckling deflection could be decreased by increasing the volume fraction of SMA fibers or the pre-strain (detwinned strain) of the SMA. It also happened that the natural frequencies for each mode of vibration were decreased due to the added weight and reduced stiffness of the added SMA, thus changing the structural flutter response. Modeling was performed by simply considering only the known non-linear stress/strain behavior of SMA elements during loading with the hysteresis being neglected. Such a model was implemented in a finite element environment. In a similar attempt to alter dynamic properties, the concept of a tunable SMA "Smart Spar" has also been introduced [41]. It should be noted that while the fabrication of SMA panels has been proven to be difficult, especially due to the curing step [42], investigations of alternative fabrication methods have been performed [43] which utilize thinner wire configurations.

There has also been significant research into applying the capabilities of SMAs to rotorcraft, especially for use in the main rotor [44]. An early preliminary study used SMA torque tubes to vary the twist of a rotor blade as used on a tiltrotor aircraft [45]. It was proposed that such onboard actuation provided by shape recovery of the torque tube would allow for the significantly different blade configurations required to optimize tiltrotor performance in both the hover and forward flight regimes. An experiment including the torque tube in opposition with a restoring force (to simulate the elastic rotor) as well as the proposed heating and cooling thermoelectric elements was performed. The system was simulated by considering a simple 1-D SMA model which accounted for both detwinning and transformation. Experimental results matched those predicted and it was shown that such a system was feasible. Today, research in this area of SMA blade twist actuation continues to move forward [46, 47]. The SMA solution is ideal for such an application because of the high energy density and force requirements on an actuator embedded in the small volume of a rotor blade. Aside from actuating the entire blade, recent work on developing SMA-actuated tabs for installation on the trailing edge of rotor blades to improve tracking has been performed [48,49]. To accomplish in-flight tracking adjustment, SMA wires actuating a trailing edge tab were built into an airfoil section. One attractive feature in this design is the inclusion of a passive friction brake, which allows electrical current to be removed from the SMA wires once the tracking tab is

set at a given angle. The SMA wires were modeled with a simple 1-D model which was coupled to the inputs and constraints of the overall system. The results of the initial benchtop testing were promising and matched the modeled behavior. Both open-loop and closed-loop responses showed improvement over that of earlier generation tracking tab actuators. In another phase of the study, operation under aerodynamic loading was attempted. While optimal control laws were not utilized in this test, it was shown that the tab deflection could be set from -5° to 5° to within less than 0.05° in airspeeds ranging from 0–37 m/s.

Another research team, working on the Smart Material Actuated Rotor Technology (SMART) Rotor project, approached this same application in a different manner [50]. Instead of utilizing antagonistic wires to provide tracking tab actuation, an SMA torque tube was linked to the tracking tab. Here active SMA braking was also employed, which allowed the brake to be released when the actuator was heated, thus allowing for freer motion of the tab. While no modeling of the SMA components was performed, benchtop tests showed that 7.5° actuation was possible with an error of 0.5°. Both tracking studies predict that dynamic testing (i.e. high-G rotational testing of the rotor blades) should produce similar satisfactory results. However, the low duty cycle was mentioned as a negative aspect of this design, and such a problem can only be overcome with creative heating/cooling configurations and sufficient power.

Rotorcraft applications which do not include tracking tab manipulation include the use of SMA wires for the collective control [51] or in a more recent study into providing rotor blade tip anhedral via SMA actuation [52]. This idea of minimizing Blade Vortex Interaction (BVI) noise by displacing the blade tip vortex from the rotor plane via SMA interaction may hold promise for future research.

2.2 Spacecraft Applications

Space applications are those which seek to address the unique problems of release, actuation, and vibration mitigation during either the launch of a spacecraft or its subsequent operation in a micro-gravity and zero-atmosphere environment. While actuated structures in space are subject to low gravitational forces which reduce required actuator power, heat transfer can quickly become problematic due to the lack of a convective medium. It should be noted that for most designs described below, little or no modeling of the SMA behavior was performed. Systems were designed through careful experimentation.

Perhaps the most prolific use of shape memory alloys in space is in solving the problem of low-shock release. These devices are quite popular in the design of spacecraft, and have been in development for some time [53]. It has been estimated that, up to 1984, 14% of space missions experienced some type of shock failures, half of these causing the mission to be aborted [54]. Pyrotechnic release mechanisms were often found to be the root

cause. Because they can be actuated slowly by gradual heating, SMA components are suited for use in low-shock release mechanisms and have been introduced for use on both average-sized and smaller "micro"-sized satellites [55]. The advent of these smaller satellites has created a need for more compact release devices which are an order of magnitude smaller than their off-the-shelf counterparts. Investigation into this unique problem has led to devices which are currently available, including the popular Qwknut [56]. Other, much smaller devices which use SMA elements for actuation have also been proposed, such as the Micro Sep-Nut [55]. In both of these devices, the simple shape memory effect is used. The active component is deformed and detwinned before installation. In orbit, the element is then heated, shape is recovered, and release occurs. Repeated use mechanisms such as the Rotary Latch have also been introduced, and this example can been seen in Figure 12. Even smaller rotary actuators are being developed through microfabrication methods such as shape deposition manufacturing and electroplating [57]. Using these methods, it was demonstrated that rotary actuators could be constructed with a maximum dimension of 5 mm, yet provide an actuation angle of 90°. Each of these small release devices demonstrates the scalability of designing with SMA components. To provide the same compact actuation with conventional methods (e.g. electric motors) would require that very small moving parts be fabricated. Active SMA components, on the other hand, are on the same size scale as the actuator housing itself.
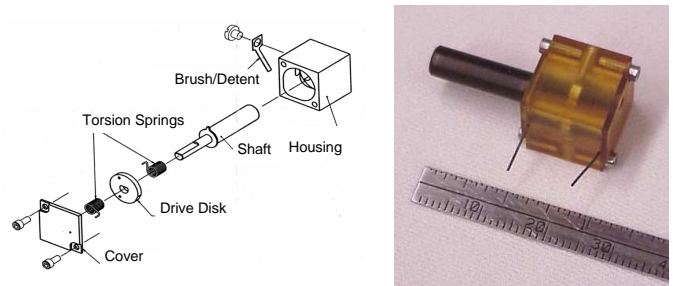

Figure 12. The Rotary Latch as design and tested at the Applied Physics Laboratory [55].

Another SMA application is the actuation of various spacecraft components via SME. One early example includes an SMA-actuated solar collector utilizing torsional elements which can modify its shape to optimize performance [44]. In a variation on this idea, another satellite utilized an SMA wire-actuated stepper motor for orientation of its solar flaps [54]. For a similar purpose, the Lightweight Flexible Solar Array (LFSA) and the Shape Memory Alloy Thermal Tailoring Experiment (SMATTE) were developed [54, 58]. The LFSA incorporated a thin SMA strip at the hinge location which, when heated and actuated, opened

a previously folded solar array. Deployment has been shown to take approximately 30 seconds. An illustration of this design is shown in Figure 13. This work was a collaborative effort between Lockheed Martin and NASA-Goddard. The SMATTE is a proof-of-concept experiment showing that a panel could be deformed from one stable shape to another via actuation of an SMA foil attached to only one surface of the panel. Such a design could be used to tailor the shape of spacecraft antennae. Another example of potential structural morphing is the antagonistic flexural unit cell discussed earlier in reference to fixed-wing aircraft [36].
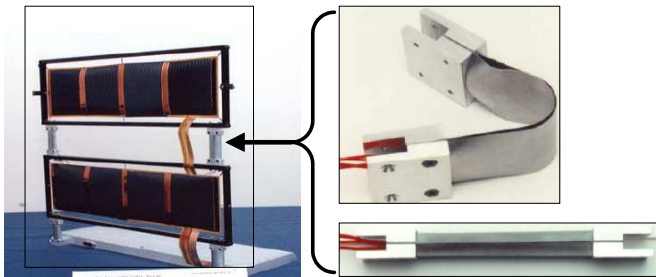
Figure 13. LFSA and detail of hinges, folded and deployed configurations [58].

A different and well-known SMA space actuation application of SMAs is the Mars Pathfinder mission in 1997. The mission included an SMA actuator which served to rotate a dust cover from a specific region of a solar cell so that the power output of this protected and clean region could be compared to the power output of non-protected regions, thereby quantifying the negative effects of dust settling on the solar panels [54]. Finally, researchers have investigated using SMA strips to support inflatable structures for use in space [59]. This interesting application can utilize both the shape memory and pseudoelastic effects as described in Section 1.2. The actuation of SME is used to help deploy the structure, while the large yet fully recoverable deformations provided during pseudoelastic loading help preserve its shape. Finite element implementation of a 3-D SMA constitutive model [6] was used to model this system and it was shown that such activated strips are able to maintain a given surface configuration of an inflatable structure. However, problems exist in using a relatively thick SMA strip attached to a thin inflatable membrane; it is expected that a thin film SMA may yield even better results.

SMAs have also been used as sensors. In the case of sensing, SMAs are used to acquire information from a thermomechanical system. This is possible due to the material property changes which occur during the phase transformation induced during heating or loading. For example, each phase has its own distinct electrical resistivity [1], which can be monitored to in-

dicate when an SMA element is experiencing a phase transformation induced by stress which is itself induced by deformation. An early example of a space application concept utilized ability of an SMA to act as a sensor in monitoring the deflection of large span space structures [44].

Finally, the large hysteresis and strong nonlinearity exhibited during the pseudoelastic effect make shape memory alloys suitable for use as vibration dampers and isolators [54, 60]. The hysteresis present in the pseudoelastic stress-strain response is indicative of some amount of mechanical energy being dissipated as thermal energy for every loading cycle. In addition, the initial stiffness and subsequent transformation plateau lend themselves to effective vibration isolation. Several U.S. patents have been filed employing this idea [61–63]. Such properties may prove to be useful in mitigating the high vibration loads placed on payloads during launch. Research is also being performed which takes into account the tunable nature of SMA vibration isolators. This concept was introduced around the beginning of the decade [64] and continues today. Because of the large change in elastic as well as transformation properties with temperature, SMA elements properly placed in structural attenuators allow for attenuation across a range of frequencies. Also interesting is a MEMS implementation of such vibration isolation. Sputtering deposition of an NiTi layer onto a MEMS sensing device in order to mitigate damage caused by external vibration has been studied [65]. Although no dynamic testing was performed in the given reference, it was shown that such a device could be fabricated and that, in theory, vibration isolation was possible. Finally, new investigation is being performed into the detailed dynamic response of SMA vibration isolation systems. Both numerical studies, including full thermomechanical coupling, and experimental studies are being performed [66] to determine the operation regimes in which any adverse dynamical behavior (i.e. chaos) might exist in order to provide guidelines for avoiding such adverse behavior in any future applications.

3   Design Advantages, Challenges, and the Future of SMAs

To conclude this work, we now review the advantages and challenges of designing SMA applications, especially in the aerospace field, and provide some outline of developments to come.

3.1   Advantages and Challenges of SMA Design

As reviewed above, shape memory alloys are capable of providing unique and useful behaviors. The shape memory effect, especially when utilized under applied stress, provides actuation. The pseudoelastic effect provides two very useful advantages to the aerospace designer: a non-linearity which allows vibration isolation and large recoverable deformations as well as an ac-

companying hysteresis which can dissipate energy and therefore dampen vibration. Because of these, shape memory alloys can provide a highly innovative method of addressing a given design problem and are often the only viable option. When considering actuation, a single SMA component represents a significantly more simplified solution than a standard electromechanical or hydraulic actuator. Compared to other classes of active materials, SMAs are able to provide substantial actuation stress over large strains. The subsequent high energy density leads to compact designs. Finally, SMAs are capable of actuating in a fully three-dimensional manner, allowing the fabrication of actuation components which extend, bend, twist, or provide a combination of these and other deformations. Each of the actuation application examples listed above exploit one or more of these positive attributes of SMA behavior. Some require simplicity and resulting reliability (Mars Pathfinder [54], LFSA [58]). Others require compact actuation (active skin [38], micro space actuation [55]), and still others impose geometric challenges (active chevrons [28], rotor blade actuation [50]). Because of their unique properties, SMAs are able to provide solutions to each of these sets of problems.

The SMA design process is not without some challenges, however, and several material attributes must be carefully considered. One common design challenge is the difficulty in rapidly transferring heat into and especially out of an SMA component. This is a result of the fact that, as a metallic material, SMAs have a relatively high heat capacity and density. When considering repeated actuation of SMA elements, for example, this heat transfer difficulty leads to a limited frequency of system response. Although the material mechanisms involved in the diffusionless phase transformation can occur almost instantaneously, the time-dependent process of sufficiently changing temperature to drive that transformation can limit actuation speed. Moreover, while the supply of thermal energy can be quickly accomplished (e.g. by direct Joule heating via application of electricity), the speed of energy removal is limited by the mechanisms of heat conduction and convection. Several methods have been employed in the hopes of expediting heat transfer, including forced convection via flowing cooled water [67] and forced conduction through the use of thermoelectric cooling modules [68]. A second challenge is the low actuation efficiency. Efficiencies can reach levels in the range of 10%–15% [69] though in some studies they have fallen short of the idealistic Carnot predictions of $\sim 10\%$ [70,71]. This is often not important for commercial and military aircraft applications because engine power and waste heat are often in excess. However, this property can present a significant challenge to those proposing SMA use on spacecraft, where power is more limited.

Finally, there are challenges stemming from the response of an SMA material when subjected to multiple transformation cycles. If a low number of cycles is required, the issue is material stability. For consistent multi-cyclic actuation, SMA elements

which have developed a sufficiently stable thermomechanical response via repeated training cycles should be used, as discussed in Section 1.2.3. SMA components which are not completely trained yet are repeatedly transformed will lead to system responses which evolve with every cycle. However, if a device is intended for one-time operation, such as a micro-actuator for satellite use, then training is not necessary. Designers must also consider the possible degradation of material response due to the generation of TRIP, especially when considering many actuation cycles. The topic of SMA fatigue has been discussed in the literature [4,72,73]. For the first 10–100 cycles, the material will stabilize, as previously discussed. As with all other metals, however, repeated deformation of sufficient magnitude will eventually lead to failure. Experimental studies on NiTi or NiTiCu SMA wires undergoing up to 2% transformation strain have shown that such SMA components can survive for $\sim$10,000 cycles [4]. This implies a limitation on the number of cycles an SMA application can provide.

As a summary of the various advantageous and challenging traits exhibited by SMAs, Table 1 has been provided. Note that while some behaviors are clearly positive or negative, others will depend upon the details of a given utilization. These have also been summarized. While some of the challenges described above can be met by creative engineering solutions, others will only be mitigated by future improvement of the material itself.

3.2 The Future of SMAs

The enabling advantages of SMA utilization often outweigh the challenges, and because of this, the future of this field is promising. As more applications across all industry sectors are designed and put into use, the SMA market will continue to grow and the cost of the material will continue to fall. The medical industry seems to be a key driver of this trend. At the same time, the quality of material produced will increase while advances in SMA research will lead to new alloys and much improved design and analysis tools.

The "smart materials" market worldwide is growing at a strong pace, and will continue to grow into the foreseeable future [75]. In 2005, these materials represented a global market of $8.1 billion, with products that *use* these materials valued at $27.7 billion. By 2010, it is projected that these numbers will rise to $12.3 and $52.2 billion, respectively [75]. Shape memory alloys represent 15% of the smart materials market and will also continue to grow in production and utilization. They are widely used in the biomedical industry where the number of vascular stents made from NiTi has grown dramatically, for example. While such applications of SMAs are not directly related to aerospace, the overall growth in SMA production has lead to an increase in production quality and consistency. Major manufacturers such as Wah Chang, Johnson-Mattheys, Memory-Metalle GmbH, and Memry Corporation have continued to grow in both

size and knowledge base. As one example, the shape memory division of Memry Corporation reported revenue growth averaging 4.4% per year from 2000 to 2005 (adjusted for inflation) [76,77]. As these business units grow, their ability to produce consistent material which meets customer specifications should improve, and this benefits designers in all fields.

While the market for conventional SMAs continues to grow, new alloys are also being developed. As described above, conventional shape memory alloys are capable of providing motion and force as a result of manipulating a single field, namely temperature, over a reasonable range. However, new alloy systems are being designed which increase the utility of SMAs, and research on these classes of materials is currently very active. One class can be used to provide actuation as a result of applied *magnetic* fields, and these materials are known as Magnetic Shape Memory Alloys (MSMAs) [78]. Because they convert the energy of magnetic fields into actuation, MSMAs are not hindered by

the relatively slow mechanisms of heat transfer. Therefore, high frequency actuation is possible. While several such alloys have been discovered (NiMnGa, FePd, NiMnAl) and actuators based on these alloys are already commercially available, fundamental research will continue as the mechanics community seeks to understand the constitutive behavior of these novel alloys [79, 80]. Another new alloy type can actuate at high temperatures, and this class is therefore known as High Temperature Shape Memory Alloys (HTSMAs) [81, 82]. HTSMAs, include NiTiPd, NiTiPt, and TiPd, and are being widely studied. These alloys can actuate at temperatures ranging from 100–800°C, and potential applications include oil drilling support [83] and actuation of internal jet engine components [84]. Basic research on these materials will include experimental observation and theoretical modeling of any viscous behavior exhibited due to sometimes lengthy exposure times at elevated temperatures.

For all classes of SMAs, whether conventional, MSMA, or HTSMA, computational tools for the design and analysis of smart structures are being developed and will continue to improve. Perhaps the most useful of these are Finite Element Analysis (FEA) implementations of some of the many available SMA constitutive models [4, 5, 7, 14, 85–88]. This is a new and welcome development in the area of SMA application design. In reviewing the variety of applications discussed above, it is important to note that many of these devices were designed and built without the use of modern tools of design and analysis. Throughout all industrial sectors, most utilized SMA systems have been the result of repeated design/build/test cycles which are almost purely empirical. One reason for this fact is that reliable models which can accurately account for the complex thermomechanical behavior of SMA components under completely general loading conditions had not yet been fully implemented into commercial codes. In addition, the incorporation of new advances in material constitutive modeling into legacy numerical codes commonly used throughout the aerospace industry was not straightforward. Some nonlinear packages, including ABAQUS [89] and MSC.MARC [90], have begun including SMAs as material options. However, many of the constitutive models currently preinstalled are more accurate for loading cases such as pseudoelastic loading, while in most aerospace applications it is actuation, usually over multiple cycles, which is of interest. Fortunately, some commercial codes also allow for the implementation of custom material subroutines to account for unique constitutive behavior such as is found in SMAs [91, 92]. In this way, powerful, fully three-dimensional FEA implementations will continue to be developed, and these will account for an increasing number of material effects. Material degradation and failure due to plastic and viscous creep effects will be included, as well as the ability to model the response of MSMAs by including ever-improving constitutive models. One example of such full 3-D modeling of an SMA-based application was discussed above in Section 2.1 with an illustration provided in Figure 11.

Table 1. Summary of various SMA properties and their effects

SMA TRAITS	CONSEQUENCES
Shape Memory Effect	Material can be used as an actuator, providing force during shape recovery.
Pseudoelasticity	Material can be stressed to provide large, recoverable deformations at relatively constant stress levels.
Hysteresis	Allows for dissipation of energy during pseudoelastic response.
High Act. Stress (400-700MPa) [18,74]	Small component cross-sections can provide substantial forces
High Act. Strain (8%) [18,74]	Small component lengths can provide large displacements.
High Energy Density ($\sim$ 1200J/kg) [69]	Small amount of material required to provide substantial actuation work.
Three-Dimensional Actuation	Polycrystalline SMA components fabricated in a variety of shapes, providing a variety of useful geometric configurations
Actuation Frequency	Difficulty of quickly cooling components limits use in high frequency applications.
Energy Efficiency (10%−15%) [69]	Amount of thermal energy required for actuation is much larger than mechanical work output.
Transformation-Induced Plasticity	Plastic accumulation during cyclic response eventually degrades material and leads to failure.

Considering the variety of research and development currently being performed in the area of shape memory alloys, it is clear that new applications will continue to be developed and that this field will continue to grow. The needs of various defense agencies will continue to present greater challenges to engineers and designers. The complexity of space operations is ever increasing and more is demanded of aircraft, both commercial and military, thus more innovative technological solutions will be required. The fields of SMA research and application are providing the tools to meet these challenges. The ability to custom order SMA material with particular properties manufactured to prescribed specifications has improved. The design and analysis environments are becoming more powerful by becoming more comprehensive. At the same time, systems integration capabilities have grown. These developments will result in an increased prevalence of integrated multifunctional SMA systems for aerospace applications. Such systems will be highly beneficial to the design of new UAVs and micro- and nano-satellites. Other industries will also benefit from the advances made in the SMA field. The automotive and and oil exploration sectors, each of which has already shown increasing interest, will continue to employ the properties of SMAs in solving design problems where constraints are imposed by extreme environments and operating conditions. It is widely expected that medical applications will further increase in number. This overall growth in the utilization of shape memory alloys and other active materials will provide designers with more options, and those in the aerospace industry should continue to take advantage of the unique engineering solutions provided by shape memory alloys.

REFERENCES

[1] K. Otsuka, C. M. Wayman (Eds.), Shape Memory Materials, Cambridge University Press, Cambridge, 1999.

[2] A. V. Srinivasan, D. Michael McFarland, Smart Structures: Analysis and Design, Cambridge University Press, 2000.

[3] T. Duerig, K. Melton, D. Stockel, C. Wayman (Eds.), Engineering Aspects of Shape Memory Alloys, Butterworth-Heinemann, London, 1990.

[4] E. Patoor, D. C. Lagoudas, P. B. Entchev, L. C. Brinson, X. Gao, Shape memory alloys, Part I: General properties and modeling of single crystals, Mechanics of Materials 38 (5–6) (2006) 391–429.

[5] D. C. Lagoudas, P. B. Entchev, P. Popov, E. Patoor, L. C. Brinson, X. Gao, Shape memory alloys, Part II: Modeling of polycrystals, Mechanics of Materials 38 (5–6) (2006) 430–462.

[6] M. A. Qidwai, D. C. Lagoudas, Numerical impementation of a shape memory alloy thermomechanical constitutive model using return mapping algorithms, International Journal for Numerical Methods in Engineering 47 (2000) 1123–1168.

[7] D. C. Lagoudas, Z. Bo, M. A. Qidwai, A unified thermodynamic constitutive model for SMA and finite element analysis of active metal matrix composites, Mechanics of Composite Materials and Structures 3 (1996) 153–179.

[8] L. C. Brinson, One-dimensional constitutive behavior of shape memory alloys: Thermomechanical derivation with non-constant material functions and redefined martensite internal variable, Journal of Intelligent Material Systems and Structures 4 (1993) 229–242.

[9] S. Leclercq, C. Lexcellent, A general macroscopic description of the thermomechanical behavior of shape memory alloys, JMPS 44 (6) (1996) 953–980.

[10] P. Popov, D. C. Lagoudas, A 3-D constitutive model for shape memory alloys incorporating pseudoelasticity and detwinning of self-accommodated martensite, Submitted to the International Journal of Plasticity .

[11] M. A. Qidwai, D. C. Lagoudas, On the thermodynamics and transformation surfaces of polycrystalline NiTi shape memory alloy material, International Journal of Plasticity 16 (2000) 1309–1343.

[12] J. Perkins, Shape Memory Effects in Alloys, Plenum Press, 1975.

[13] D. A. Miller, D. C. Lagoudas, Thermo-mechanical characterization of NiTiCu and NiTi SMA actuators: Influence of plastic strains, Smart Materials and Structures 9 (5) (2000) 640–652.

[14] Z. Bo, D. C. Lagoudas, Thermomechanical modeling of polycrystalline SMAs under cyclic loading, Part III: Evolution of plastic strains and two-way shape memory effect, International Journal of Engineering Science 37 (1999) 1175–1203.

[15] D. Lagoudas, P. Entchev, Modeling of transformation-induced plasticity and its effect on the behavior of porous shape memory alloys: Part I: Constitutive model for fully dense SMAs, Mechanics of Materials 36 (2004) 865–892.

[16] D. Hartl, B. Volk, D. C. Lagoudas, F. T. Calkins, J. Mabe, Thermomechanical characterization and modeling

of Ni60Ti40 SMA for actuated chevrons, in: Proceedings of ASME, International Mechanical Engineering Congress and Exposition (IMECE), 5–10 November, Chicago, IL, 2006, pp. 1–10.

[17] E. Renner, Thermal engine, U.S. Patent 3,937,019 (1976).

[18] K. R. Melton, General applications of shape memory alloys and smart materials, in: K. Otsuka, C. M. Wayman (Eds.), Shape Memory Materials, Cambridge University Press, Cambridge, 1999, Ch. 10, pp. 220–239.

[19] E. Garcia, Smart structures and actuators: Past, present, and future, Proceedings of SPIE, Smart Structures and Materials, San Diego, CA, 17–21 March (2002) 1–12.

[20] B. Sanders, R. Crowe, E. Garcia, Defense advanced research projects agency – Smart materials and structures demonstration program overview, Journal of Intelligent Material Systems and Structures 15 (2004) 227–233.

[21] J. Kudva, Overview of the DARPA smart wing project, Journal of Intelligent Material Systems and Structures 15 (2004) 261–267.

[22] J. Kudva, K. Appa, C. Martin, A. Jardine, Design, fabrication, and testing of the DARPA/Wright lab 'smart wing' wind tunnel model, in: Proceedings of the 38th AIAA/ASME/ASCE/AHS/ASC Structures, Structural Dynamics, and Materials Conference and Exhibit, Kissimmee, FL, 1997, pp. 1–6.

[23] P. Jardine, J. Kudva, C. Martin, K. Appa, Shape memory alloy NiTi actuators for twist control of smart designs, in: Proceedings of SPIE Smart Materials and Structures, Vol. 2717, San Diego, CA, 1996, pp. 160–165.

[24] P. Jardine, J. Flanigan, C. Martin, Smart wing shape memory alloy actuator design and performance, in: Proceedings of SPIE, Smart Structures and Materials, Vol. 3044, San Diego, CA, 1997, pp. 48–55.

[25] D. Pitt, J. Dunne, E. White, E. Garcia, SAMPSON smart inlet SMA powered adaptive lip design and static test, Proceedings of the 42nd AIAA Structures, Structrual Dynamics, and Materials Conference, Seattle, WA, 16–20 April 2001 .

[26] N. Reya, G. Tillmana, R. Millera, T. Wynoskyb, M. Larkin, Shape memory alloy actuation for a variable area fan nozzle, in: Proceedings of SPIE, Smart Structures and Materials, Vol. 4332, Newport Beach, CA, 2001, pp. 371–382.

[27] J. Mabe, R. Cabell, G. Butler, Design and control of a morphing chevron for takeoff and cruise noise reduction, in: Proceedings of the 26th Annual AIAA Aeroacoustics Conference, Monterey, CA, 2005, pp. 1–15.

[28] J. H. Mabe, F. Calkins, G. Butler, Boeing's variable geometry chevron, morphing aerostructure for jet noise reduction, in: 47th AIAA/ ASME / ASCE / AHS / ASC Structures, Structural Dynamics and Materials Conference, Newport, Rhode Island, 2006, pp. 1–19.

[29] D. Hartl, D. C. Lagoudas, Characterization and 3–D model-

ing of Ni60Ti SMA for actuation of a variable geometry jet engine chevron, in: Proceedings of SPIE, Smart Structures and Materials, Vol. 6529, San Diego, CA, 2007.

[30] T. Turner, R. Buehrle, R. Cano, G. Fleming, Modeling, fabrication, and testing of a SMA hybrid composite jet engine chevron concept, Journal of Intelligent Material Systems and Structures 17 (2006) 483–497.

[31] J. Balta, J. Simpson, V. Michaud, J. Manson, J. Schrooten, Embedded shape memory alloys confer aerodynamic profile adaptivity, Smart Materials Bulletin (2001) 8–12.

[32] J. K. Strelec, D. C. Lagoudas, M. A. Khan, J. Yen, Design and implementation of a shape memory alloy actuated reconfigurable wing, Journal of Intelligent Material Systems and Structures 14 (2003) 257–273.

[33] Knowles, Gareth, Bird, W. Row, Telescopic wing system, U.S. Patent 6,834,835 (28 December 2004).

[34] J. Manzo, E. Garcia, A. Wickenheiser, G. Horner, Design of a shape memory alloy actuated macro–scale morphing aircraft mechanism, in: Proceedings of SPIE, Smart Structures and Materials, Vol. 5764, San Diego, CA, 2005, pp. 232–240.

[35] D. Elzey, A. Sofla, H. Wadley, Shape memory–based multifunctional structural actuator panels, in: Proceedings of SPIE, Smart Structures and Materials, Vol. 4698, San Diego, CA, 2002, pp. 192–200.

[36] A. Sofla, D. Elzey, H. Wadley, An antagonistic flexural unit cell for design of shape morphing structures, in: Proceedings of ASME International Mechanical Engineering Congress and Exposition, 2004, pp. 1–9.

[37] F. Geraci, J. Cooper, M. Amprikidis, Development of smart vortex generators, in: Proceedings of SPIE, Smart Structures and Materials, Vol. 5056, San Diego, CA, 2003, pp. 1–8.

[38] R. Mani, D. Lagoudas, O. Rediniotis, MEMS based active skin for turbulent drag reduction, in: Proceedings of SPIE, Smart Structures and Materials, Vol. 5056, San Diego, CA, 2003.

[39] J. Gill, K. Ho, G. Carman, Three-dimensional thin-film shape memory alloy microactuator with two-way effect, Journal of Microelectromechanical Systems 11 (11) (2002) 68–77.

[40] M. Tawfik, J. Ro, C. Mei, Thermal post-buckling and aeroelastic behaviour of shape memory alloy reinforced plates, Smart Materials and Structures 11 (2002) 297–307.

[41] C. Nam, A. Chattopadhyay, Y. Kim, Application of shape memory alloy (SMA) spars for aircraft maneuver enhancement, in: Proceedings of SPIE, Smart Structures and Materials, Vol. 4701, San Diego, CA, 2002, pp. 226–236.

[42] V. Birman, Stability of functionally graded shape memory alloy sandwich panels, Smart Materials and Structures 6 (1997) 278–286.

[43] X. Y., K. Otsuka, N. Toyama, H. Yoshida, H. Nagai,

T. Kishi, A novel technique for fabricating SMA/CFRP adaptive composites using ultrathin TiNi wires, Smart Materials and Structures 13 (2004) 196–202.

[44] V. Birman, Review of mechanics of shape memory alloy structures, Applied Mechanics Reviews 50 (11) (1997) 629–645.

[45] H. Prahlad, I. Chopra, Design of a variable twist tiltrotor blade using shape memmory alloy (SMA) actuators, in: Proceedings of SPIE, Smart Structures and Materials, Vol. 4327, Newport Beach, CA, 2001, pp. 46–59.

[46] N. Caldwell, A. Glaser, E. Gutmark, R. Ruggeri, Heat transfer model for blade twist actuator system, in: Proceedings of 44th AIAA Aerospace Sciences Meeting and Exhibit, 2006, pp. 1–22.

[47] A. Jacot, R. Ruggeri, D. Clingman, Shape memory alloy device and control method, U.S. Patent 7,037,076 (2 May 2006).

[48] K. Singh, I. Chopra, Design of an imporoved shape memory alloy actuator for rotor blade tracking, in: Proceedings of SPIE, Smart Structures and Materials, Vol. 4701, San Diego, CA, 2002, pp. 244–266.

[49] K. Singh, J. Sirohi, I. Chopra, An imporoved shape memory alloy actuator for rotor blade tracking, Journal of Intelligent Material Systems and Structures 14 (2003) 767–786.

[50] D. Kennedy, F. Straub, L. Schetky, Z. Chaudhry, R. Roznoy, Development of an SMA actuator for in-flight rotor blade tracking, Journal of Intelligent Material Systems and Structures 15 (2004) 235–248.

[51] R. Loewy, Recent developments in smart structures with aeronautical applications, Smart Materials and Structures 6 (1997) R11–R42.

[52] C. Test, S. Leone, S. Ameduri, A. Concilio, Feasibility study on rotorcraft blade morphing in hovering, in: Proceedings of SPIE, Smart Structures and Materials, Vol. 5764, San Diego, CA, 2005, pp. 171–182.

[53] A. Johnson, Non-explosive seperation device, U.S. Patent 5,119,555 (June 1992).

[54] O. Godard, M. Lagoudas, D. Lagoudas, Design of space systems using shape memory alloys, in: Proceedings of SPIE, Smart Structures and Materials, Vol. 5056, San Diego, CA, 2003, pp. 545–558.

[55] C. Willey, B. Huettl, S. Hill, Design and development of a miniature mechanisms tool-kit for micro spacecraft, in: Proceedings of the 35th Aerospace Mechanisms Symposium, Ames Research Center, 9–11 May, 2001, pp. 1–14.

[56] A. Peffer, K. Denoyer, E. Fossness, D. Sciulli, Development and transition of low-shock spacecraft release devices, in: Proceedings of IEEE Aerospace Conference, Vol. 4, 2000, pp. 277–284.

[57] B. Park, M. Shantz, F. Prinz, Scalable rotary actuators with embedded shape memory alloys, in: Proceedings of SPIE, Smart Structures and Materials, Vol. 4327, Newport Beach,

CA, 2001, pp. 79–87.

[58] B. Carpenter, J. Lyons, EO-1 technology validation report: Lightweight flexible solar array experiment, Tech. rep., NASA Godard Space Flight Center, Greenbelt, MD (8 August 2001).

[59] J. Roh, J. Han, I. Lee, Finite element analysis of adaptive inflatable structures with SMA strip actuator, in: Proceedings of SPIE, Smart Structures and Materials, Vol. 5764, San Diego, CA, 2005, pp. 460–471.

[60] S. Saadat, J. Salichs, M. Noori, Z. Hou, H. Davoodi, I. Baron, An overview of vibration and seismic applications of NiTi shape memory alloy, Smart Materials and Structures 11 (2002) 218–229.

[61] R. Renz, J. Kramer, Metallic damping body, U.S. Patent 5,687,958 (November 1997).

[62] D. Grosskruger, B. Carpenter, B. Easom, J. Draper, Apparatus and associated method for detuning from resonance a structure, U.S. Patent 6,024,347 (February 2000).

[63] Y. Sherwin, D. Ulmer, Method for vibration damping using superelastic alloys, U.S. Patent 6,796,408 (September 2004).

[64] K. Williams, G. Chiu, R. Bernhard, Controlled continuous tuning of an adaptively tunable vibration absorber incorporating shape memory alloys, in: Proceedings of SPIE, Smart Structures and Materials, Vol. 3984, Newport Beach, CA, 2000, pp. 564–575.

[65] E. Ngo, W. Nothwang, M. Cole, C. Hubbard, G. Hirsch, Fabrication of active thin films for vibration damping in MEMS devices for the next generation army munition systems, in: Proceedings of the 24th Army Science Conference, Orlando, FL, 2004.

[66] D. C. Lagoudas, L. G. Machado, M. Lagoudas, Nonlinear vibration of a one-degree of freedom shape memory alloy oscillator: A numerical-experimental investigation, in: 46th AIAA/ ASME / ASCE / AHS / ASC Structures, Structural Dynamics and Materials Conference, Austin, TX. USA, 2005, pp. 1–18.

[67] O. Rediniotis, L. Wilson, D. Lagoudas, M. Khan, Development of a shape memory alloy actuated biomimetic hydrofoil, Journal of Intelligent Material Systems and Structures 13 (2002) 35–49.

[68] A. Bhattacharyya, D. C. Lagoudas, Y. Wang, V. K. Kinra, On the role of thermoelectric heat transfer in the design of SMA actuators: Theoretical modeling and experiment, Smart Materials and Structures 4 (1995) 252–263.

[69] C. M. Jackson, H. J. Wagner, R. J. Wasilewski, 55-Nitinol—The alloy with a memory: Its physical metallurgy, properties and applications, Tech. Rep. NASA SP-5110, NASA Technology Utilization Office, Washington, D.C. (1972).

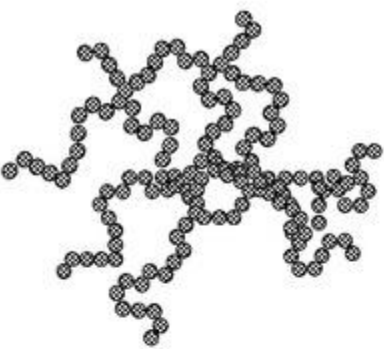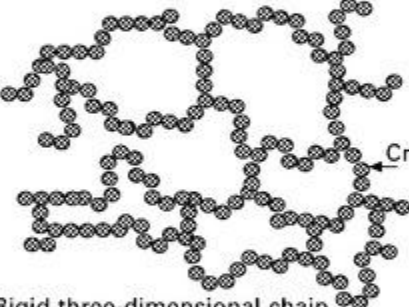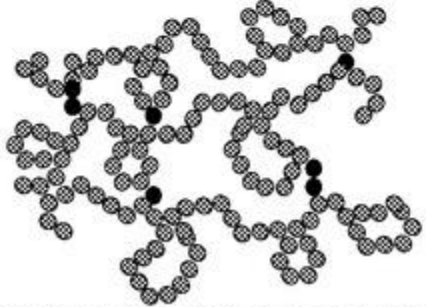[70] H. Jun, O. Rediniotis, D. Lagoudas, Devilopment of a fuel–powered shape memory alloy actuator system: II. Fabrica-

tion and testing, Smart Materials and Structures 16 (2007) S95–S107.

[71] M. Thrasher, A. Shahin, P. Meckl, Efficiency analysis of shape memory alloy actuators, Smart Materials and Structures 3 (1994) 226–234.

[72] D. C. Lagoudas, D. A. Miller, L. Rong, C. Li, Thermomechanical transformation fatigue of SMA actuators, in: Proceedings of SPIE, Smart Structures and Materials, Vol. 3992, 2000, pp. 420–429.

[73] O. Bertacchini, D. Lagoudas, E. Patoor, Fatigue life characterization of shape memory alloys undergoing thermomechanical cyclic loading, in: Proceedings of SPIE, Smart Structures and Materials, San Diego, CA, 2003.

[74] H. Funakubo (Ed.), Shape Memory Alloys, Gordon and Breach Science Publishers, 1987.

[75] RGB-154N smart materials: A technology and market assessment, Tech. Rep. Vol. 35, Issue 2, Business Communications Company, Norwalk, CT (2006).

[76] Form 10–K, Tech. rep., Memry Corporation, Bethel, CT (September 2004).

[77] Form 10–K, Tech. rep., Memry Corporation, Bethel, CT (September 2006).

[78] S. J. Murray, M. Marioni, S. M. Allen, R. C. O'Handley, 6% magnetic-field-induced strain by twin-boundary motion in ferromagnetic Ni-Mn-Ga, Applied Physics Letters 77 (6) (2000) 886–888.

[79] S. J. Murray, M. Marioni, P. G. Tello, S. M. Allen, R. C. O'Handley, Giant magnetic-field-induced strain in Ni-Mn-Ga crystals: Experimental results and modeling, Journal of Magnetism and Magnetic Materials 226–230 (1) (2001) 945–947.

[80] B. Kiefer, D. C. Lagoudas, Magnetic field-induced martensitic variant reorientation in magnetic shape memory alloys, Philosophical Magazine Special Issue: Recent Advances in Theoretical Mechanics, in Honor of SES 2003 A.C. Eringen Medalist G.A. Maugin 85 (33-35) (2005) 4289–4329.

[81] P. G. Lidquist, C. M. Wayman, Shape memory and transformation behavior of martensitic Ti-Pd-Ni and Ti-Pt-Ni alloys, in: T. W. Duerig, K. N. Melton, D. Stöckel, C. M. Wayman (Eds.), Engineering Aspects of Shape Memory Alloys, Butterworth-Heinemann, London, 1990, pp. 58–68.

[82] P. E. Thoma, J. J. Boehm, Effect of composition on the amount of second phase and transformation temperatures of NixTi90-xHf10 shape memory alloys, Materials Science and Engineering A 273–275 (1999) 385–389.

[83] P. Kumar, D. Lagoudas, K. Zanca, M. Lagoudas, Thermomechanical characterization of high temperature SMA actuators, in: Proceedings of SPIE, Smart Structures and Materials, Vol. 6170, San Diego, CA, 2006.

[84] R. Noebe, T. R. Quackenbush, I. Padula, S.A., Benchtop demonstration of an adaptive chevron completed using a new high-temperature shape-memory alloy, Tech. Rep.

20060054078, NASA, Glenn Research Center (May 2006).

[85] J. G. Boyd, D. C. Lagoudas, A thermodynamical constitutive model for shape memory materials. Part I. The monolithic shape memory alloy, International Journal of Plasticity 12 (6) (1996) 805–842.

[86] Z. Bo, D. C. Lagoudas, Thermomechanical modeling of polycrystalline SMAs under cyclic loading, Part I: Theoretical derivations, International Journal of Engineering Science 37 (1999) 1089–1140.

[87] D. C. Lagoudas, Z. Bo, Thermomechanical modeling of polycrystalline SMAs under cyclic loading, Part II: Material characterization and experimental results for a stable transformation cycle, International Journal of Engineering Science 37 (1999) 1141–1173.

[88] Z. Bo, D. C. Lagoudas, Thermomechanical modeling of polycrystalline SMAs under cyclic loading, Part IV: Modeling of minor hysteresis loops, International Journal of Engineering Science 37 (1999) 1205–1249.

[89] Hibbit, Karlsson, and Sorenson, Inc., Pawtucket, RI, ABAQUS/Standard User's Manual (2006).

[90] MSC Software Corporation, MSC MARC User's Manual (2006).

[91] J. Teresko, The new materials age, Industry Week 253 (6) (2004) 24–32.

[92] D. Lagoudas, Z. Bo, M. Qidwai, P. Entchev, SMA_UM: User Material Subroutine for Thermomechanical Constitutive Model of Shape Memory Alloys, Texas A&M University, College Station, TX (March 2003).

Polymers for aerospace structures

13.1 Introduction

Polymer is a generic term that covers a wide variety and large number of plastics, elastomers and adhesives. The three main groups of polymers are called thermoplastics, thermosetting polymers (or thermosets) and elastomers. The term 'plastic' is often used to describe both thermoplastics and thermosets, although there are important differences between the two. Elastomers are commonly called 'rubbers', although in the aerospace engineering community the former term is the correct one to use. Adhesives are an important sub-group of polymers, and can be thermoplastic, thermoset or elastomer.

The basic chemical properties used to distinguish between thermoplastics, thermosets and elastomers are shown in Fig. 13.1. Thermoplastics consist of long molecular chains made by joining together small organic molecules known as monomers. In effect, monomers are the basic building blocks that are joined end-to-end by chemical reactions to produce a long polymer chain. The property of thermoplastics that distinguishes them from other polymers is that strong covalent bonds join the atoms together along the length of the chain, but no covalent bonding occurs between the chains. Each thermoplastic chain is a discrete molecule. The molecular chains are entangled and intertwined in a thermoplastic, but the chains are not joined or connected. This structure provides thermoplastics with useful engineering properties, including high ductility, fracture toughness and impact resistance. The lack of bonding between the molecular chains causes thermoplastics to soften and melt when heated which allows them to be recycled.

Thermoplastic • moderate stiffness • moderate strength • high ductility • high impact resistance • poor creep resistance • recyclable	Flexible linear chains with no crosslinking
Thermoset polymer • high stiffness • high strength • high creep resistance • low/moderate ductility • poor impact resistance • cannot be recycled	Crosslinks Rigid three-dimensional chain structure with crosslinking
Elastomer • very low stiffness • low strength • very high elasticity • excellent impact resistance • not easily recycled	Linear coiled chains with some crosslinking

13.1 Basic properties of thermoplastics, thermoset polymers and elastomers.

Thermosetting polymers are also long molecular chains made by joining together smaller molecules, although the chemical reactions produce covalent bonds both along the chain and bridging across the chains. The bonding between the chains is known as crosslinking, and it produces a rigid three-dimensional molecular structure. It is the crosslinking of thermosets that distinguishes them from thermoplastics. The crosslinks generally provide thermosets with higher elastic modulus and tensile strength than thermoplastics, but they are more brittle and have lower toughness. Thermosets do not have a melting point because the crosslinks do not allow the chains to flow like a liquid at high temperature and, therefore, these polymers cannot be recycled.

Elastomers are natural and synthetic rubbers with a molecular structure that is somewhere between thermoplastics and thermosets. Some crosslinking occurs between elastomer chains, but to a lesser amount than with thermosets. The elastomer chains are coiled somewhat like a spring, and this allows them to be stretched over many times their original length without being permanently

deformed. Elastomers are characterised by low stiffness and low strength as well as good impact resistance and toughness.

In this chapter, the polymers, elastomers and structural adhesives used in aerospace structures are described. These materials lack the stiffness and strength to be used on their own in aircraft structures, but they are useful when used in combination with other materials such as fibre-polymer composites. The different types of polymers, viz. thermoplastics, thermosets, elastomers and adhesives, are examined. The polymerisation processes and chemical composition of polymers are studied. In addition, the mechanical and thermal properties of polymers, and their applications to aircraft, helicopters and spacecraft are discussed.

13.2 Aerospace applications of polymers

The most common use for polymers is the matrix phase of fibre composites. Polymers are the 'glue' used to hold together the high-stiffness, high-strength fibres in fibre–polymer composites, and these materials are described in chapters 14 and 15. Composites are used in the airframe and engine components of modern military and civilian aircraft, with polymers accounting for 40–45% of the total volume of the material. Moulded plastics and fibre-polymer composites are used extensively in the internal fittings and furniture of passenger aircraft.

Another important application of polymers is as an adhesive for joining aircraft components. It is possible to produce high strength, durable joints using polymer adhesives without the need for fasteners such as rivets and screws. Adhesives are used to join metal-to-metal, composite-to-composite and metal-to-composite components. For example, adhesives are used to bond ribs, spars and stringers to the skins of structural panels used throughout the airframe. Adhesives are also used to bond face sheets to the core of sandwich composite materials and to bond repairs to composite and metal components damaged during service. Thin layers of adhesive are used to bond together the aluminium and fibre–polymer composite sheets that produce the fibre–metal laminate called GLARE, which is used in the Airbus 380 fuselage. The use of elastomers is usually confined to nonstructural aircraft parts that require high flexibility and elasticity, such as seals and gaskets.

13.3 Advantages and disadvantages of polymers for aerospace applications

Polymers possess several properties that make them useful as aircraft materials, including low density (1.2–1.4 g cm^{-3}), moderate cost, excellent corrosion resistance, and high ductility (except thermosets). Some polymers are tough and transparent which makes them suitable for aircraft windows and canopies. However, polymers cannot be used on their own as structural materials because of their low stiffness, strength, creep properties and working temperature. Table 13.1 summarises the main advantages and disadvantages of thermoplastics, thermosets and elastomers whereas Table 13.2 gives the typical properties of polymers compared with several types of aerospace metals, and shows that the polymers are structurally inferior.

Table 13.1

Comparison of the advantages and disadvantages of polymers for aircraft structural applications

Thermoplastic	Thermoset	Elastomer
Advantages		
• Non-reacting; no cure required	• Low processing temperature	• Low processing temperature
• Rapid processing	• Low viscosity	• High ductility and flexibility
• High ductility	• Good compression properties	• High fracture toughness
• High fracture toughness	• Good fatigue resistance	• High impact resistance
• High impact resistance	• Good creep resistance	
• Absorbs little moisture	• Highly resistant to solvents	
• Can be recycled	• Good fibre wetting for composites	
Disadvantages		
• Very high viscosity	• Long processing time	• Long processing times
• High processing temperature (300–400 °C)	• Low ductility	• Poor creep resistance
• High processing pressures	• Low fracture toughness	• Low Young's modulus
• Poor creep resistance	• Low impact resistance	• Low tensile strength
	• Absorb moisture	
	• Limited shelf life	
	• Cannot be recycled	

Table 13.2

Comparison of the typical properties of a structural polymer (epoxy resin) against aerospace structural materials

| Materials	Average specific gravity (g cm^{-3})	Young's modulus (GPa)	Specific modulus (MPa m^3 kg^{-1})	Yield strength (MPa)	Specific strength (kPa m^3 kg^{-1})
Polymer (epoxy)	1.2	3	2.5	100	83
Aluminium (7075-T76)	2.7	70	25.9	470	174
Magnesium	1.7	45	26.5	200	115
α+β-Ti alloy	4.6	110	23.9	1000	217
Carbon/epoxy composite*	1.7	50	29.4	760	450

□[0/± 45/90] carbon/epoxy; fibre volume content = 60%.

13.4 Polymerisation

13.4.1 POLYMERISATION PROCESSES

Polymerisation is the chemical process by which polymers are made into long chain-like molecules from smaller molecules. Polymerisation is the process by which small molecules, known as monomers, are joined to create macromolecules. The polymerisation process is used to make thermoplastics, thermosets and elastomers, although the reaction processes are different. The chemistry of polymerisation is a complex topic, and only the basics are described here.

The polymerisation process can be divided into two types of chemical reaction: addition polymerisation and condensation polymerisation. Addition polymerisation involves the linking of monomers into the polymer chain by a chemical reaction that does not produce molecular by-products. For example, the major steps in the addition polymerisation reaction for polyethylene is shown in Fig. 13.2, which involves the joining of ethylene monomers (C_2H_4) into a long polyethylene chain $(CH_2)_{2n}$ where n is the number of ethylene monomers in the chain. A catalyst, also known as the 'initiator' because it starts the reaction, is added to the monomers. The catalyst splits the double covalent bond within the ethylene monomer to produce unpaired electrons. Each unpaired electron needs to immediately pair with another electron, so it joins with an unpaired electron at the neighbouring monomer. The pairing forms a single covalent bond that binds the two monomer units, and the process is repeated many, many times to produce a long molecular chain. A polymer chain is built-up from hundreds to many hundreds of thousands of monomer units, which are called mer units when joined into a chain. The addition of monomers to a chain continues until the supply of monomer units or catalyst is exhausted or a special chemical called a terminator is used to stop the reaction process, or there is self-termination when a chain end connects to the end of another chain growing independently. In addition to polyethylene, other examples of polymers produced by addition polymerisation are polyvinyl chloride (PVC), polystyrene and polytetrafluroethylene (Teflon).
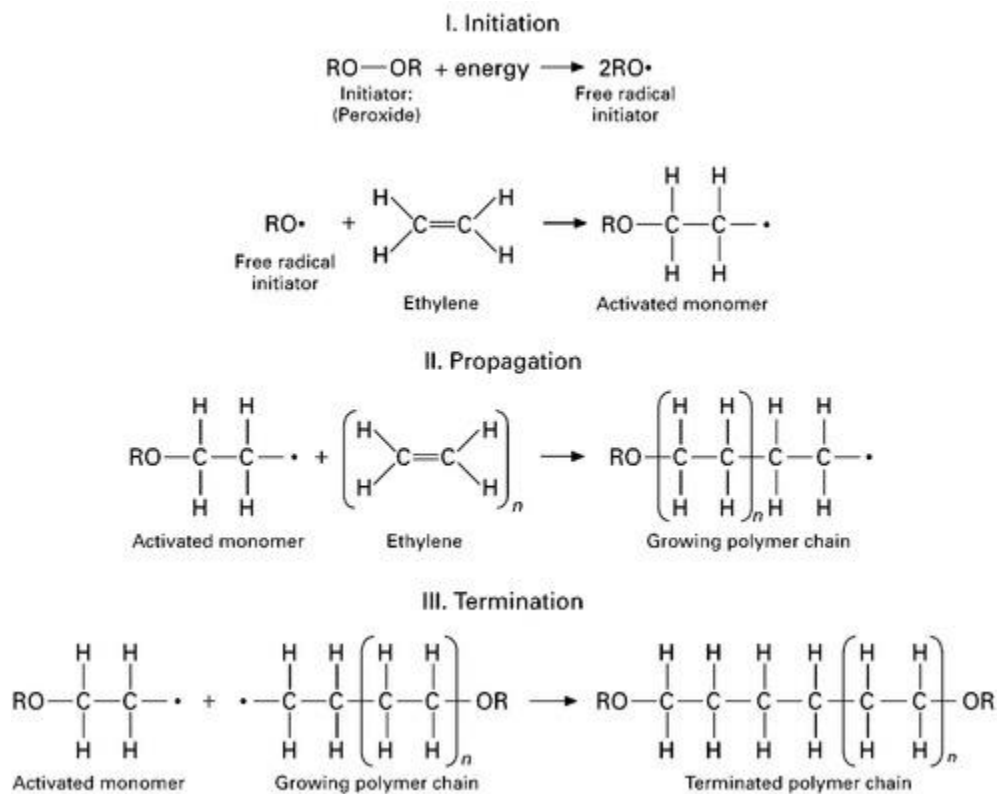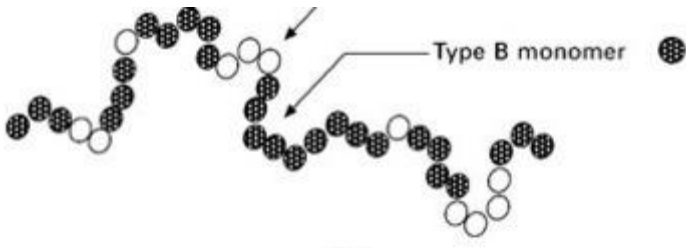

13.2 Addition polymerisation.

Condensation polymerisation is a process involving two or more different types of molecules that react to produce a molecular chain made of combinations of the starting molecules. Figure 13.3 shows a simple example of a condensation reaction between carboxylic acid and alcohol. A feature of the condensation reaction is that small molecules are produced as a byproduct. These by-product molecules do not form part of the polymer chain. Water is a by-product

of many condensation reactions and, when possible, it should be extracted from the polymer before use in aircraft. Examples of aerospace polymers produced by condensation reactions are epoxy resin, which is used as the matrix phase of carbon-fibre composite structures and as a structural adhesive, and phenolic resin which is used inside aircraft cabins for fire resistance.
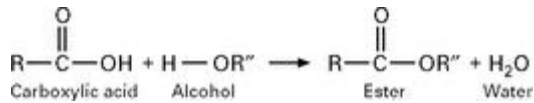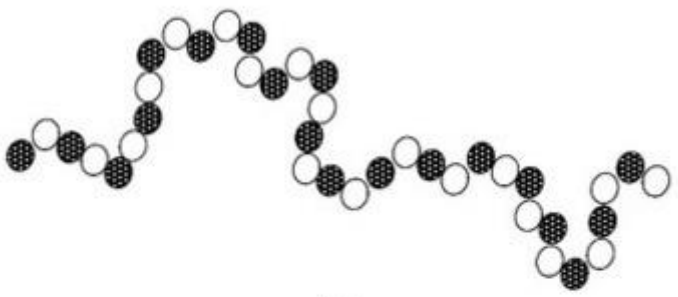

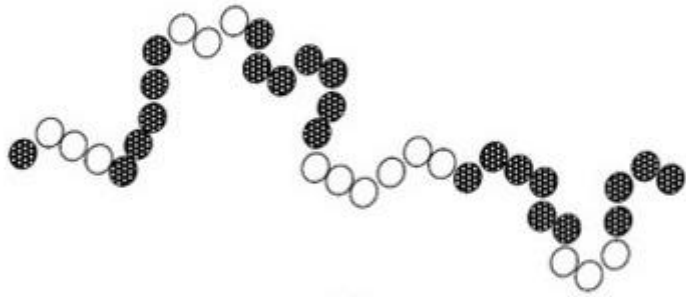**13.3** Condensation polymerisation.

Polymerisation reactions for most of the polymers used in aircraft involve just one type of monomer. When the polymer chain is made using just one monomer type it is known as a homopolymer. Polymers can also be produced by the polymerisation of two types of monomers, which is called a copolymer. Although copolymers are not used extensively in plastic aircraft parts, they are sometimes used as elastomers in seals. The two monomer types can be arranged in various ways along the chain, as illustrated in Fig. 13.4, thus resulting in different material properties. When the two different monomers are distributed randomly along the chain it is called a random copolymer. Under controlled processing conditions, the two monomer types may alternate as single mer units along the chain, and this is known as a regular copolymer. If, however, a long sequence of one type of mer units is followed by a long sequence of another type of mer units, it is termed a block copolymer. This latter type is called a graft copolymer when the chains produced from one type of monomer are attached (or grafted) to the chain created from the other monomer.
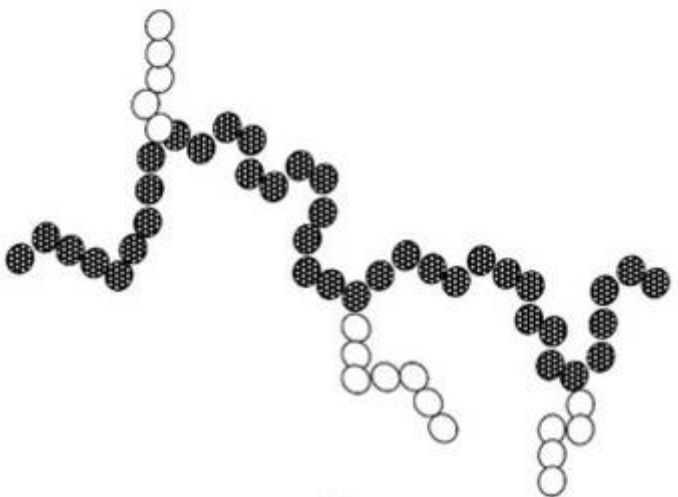
Type B monomer

(a)

(b)

(c)

(d)

**13.4** Structural types of copolymers: (a) random, (b) alternate, (c) block and (d) graft.

Addition and condensation reactions are started using a chemical catalyst, and the polymerisation rate is controlled by the amount of catalyst and the temperature. Increasing the catalyst content and temperature accelerates the reaction rate. However, other methods can be used to drive the

polymerisation process, most notably electrons (e-beam) and ultraviolet (UV) radiation. E-beam curing is a process that involves irradiating the polymer with an electron beam to split the double covalent bonds in the monomer to produce unpaired electrons. Irradiating the polymer with UV radiation is another method for producing unpaired electrons. The unpaired electrons then bond with unpaired electrons from other monomer units to produce long polymer chains. These methods are gaining importance in the aircraft industry because they eliminate the need to use corrosive and toxic catalysts, although at the moment the use of catalysts remains the most common way of curing most types of polymer.

13.4.2 POLYMER STRUCTURE

The structural arrangement of the chain-like molecules has a major impact on the mechanical properties of a polymer. Thermoplastics can be polymerised by both addition and condensation reactions, although the monomers that make up thermoplastics are always bifunctional. This means they have two sites in the molecule where pairing can occur with other molecules. As a result, the polymer can only grow as a linear chain. Thermosetting polymers are also produced by addition and condensation reactions, but are formed from trifunctional monomers which have three reaction sites, and this allows the polymer to grow with covalent bonds along the chain and covalent (crosslink) bonds bridging across the chains. Elastomers contain a mixture of bifunctional and trifunctional monomers, which produces long linear segments in the chain from the bifunctional units, and widely spaced crosslinks from the trifunctional units.

Structural variations can occur within the chain during the polymerisation process that may significantly alter the engineering properties. The three major types of polymer structures are called atactic, isotactic and syndiotactic, and they are shown in Fig. 13.5. The chemical composition of the three types of polymer structure is the same; with the only difference being the location of atoms and small compounds ('R' groups) attached as side groups to the chain. When the side groups are located randomly along the chain, this is called an atactic structure. When the side groups are placed on the chain in the same location in each mer, it is called an isotactic structure. Syndiotactic refers to a structure with the R groups placed on the chain in a more or less regular pattern, but having alternate positions on either side of the chain.
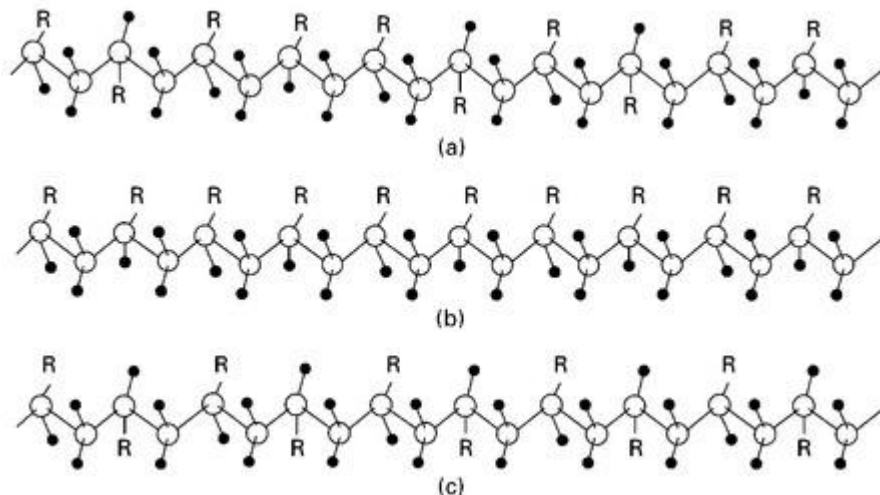

13.5 Models of polymer chains with (a) atactic, (b) isotactic and (c) syndiotactic structures.

The arrangement of the molecular chains at the end of the polymerisation process is complex, and simplified illustrations of the most common forms are shown in Fig. 13.6. The four most common structures are called linear, crosslinked, branched and ladder. Polymer chains are never straight, even over very short distances, and instead twist and turn along their length and become intertwined with other chains. Entanglement and intertwining of the chains is an important mechanism for providing stiffness and strength to polymers. This mechanism is particularly important for thermoplastics because they do not have crosslinking to resist sliding of the chains under an applied force. However, thermoplastics do have weak attraction forces between the chains. These are known as van der Waals bonds, also called 'secondary bonds', which is an electrostatic force between atoms owing to the nonsymmetric distribution of electrons around the atomic nucleus. These bonds are much weaker than the covalent bonds that form crosslinks between thermosets and, therefore, are less effective at resisting chain sliding.
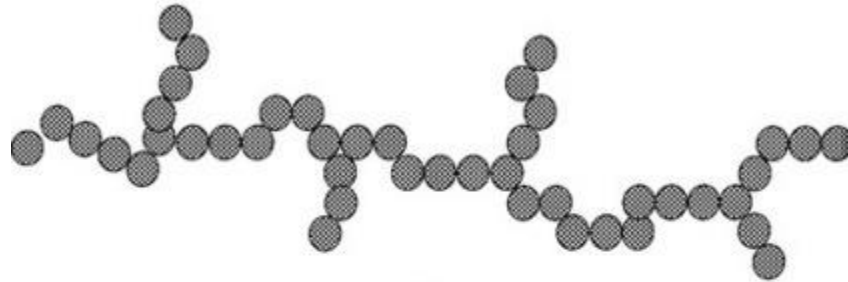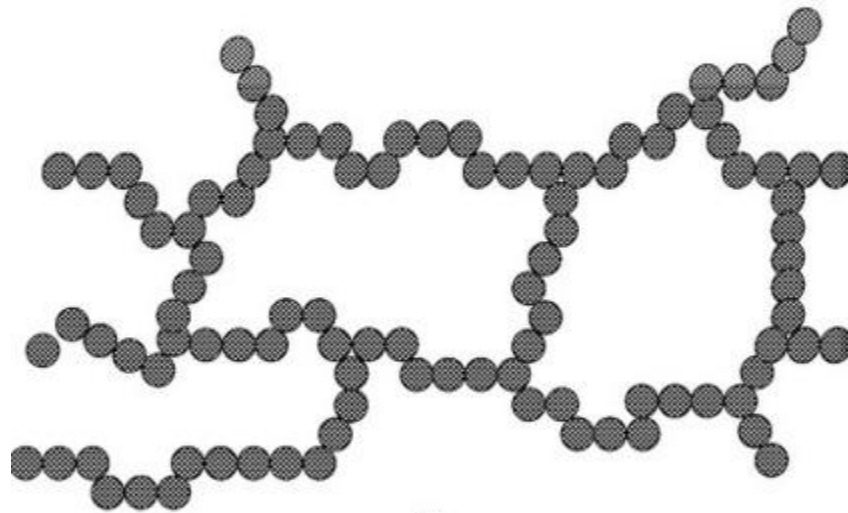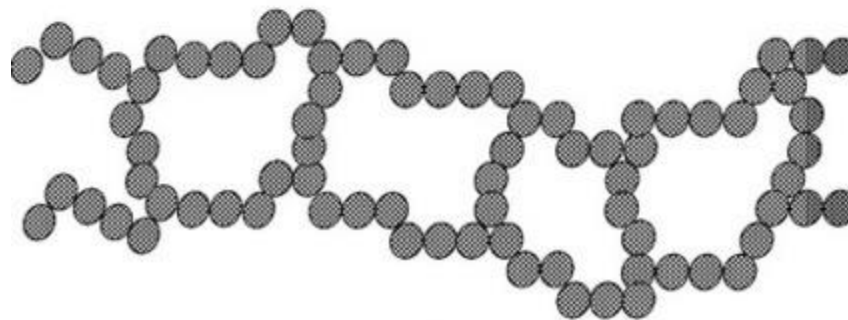
13.6 Schematic illustration of the molecular structure of (a) linear, (b) branched, (c) crosslinked, and (d) ladder polymers.

13.5 Thermosetting polymers

Thermosetting polymers are crosslinked polymers that have a three-dimensional network structure with covalent bonds linking the chains. Thermosets are produced by mixing a liquid resin consisting of monomers and oligomers (several monomer units joined together) with a liquid hardener, which can be another resin or catalyst. The resin and hardener react in a process that joins the monomers and oligomers into long polymer chains and forms crosslinks between the chains. Heat is often used to accelerate the reaction process and pressure is applied to squeeze out volatile by-products. When the crosslinks are formed they resist rotation and sliding of the chains under load, and this provides thermosets with better strength, stiffness and hardness than thermoplastics.

13.5.1 EPOXY RESIN

Epoxy resin is the most common thermosetting polymer used in aircraft structures. Epoxy resin is used as the matrix phase in carbon-fibre composites for aircraft structures and as an adhesive in aircraft structural joints and repairs. There are many types of epoxy resins, and the chemical structure of an epoxy resin often used in aerospace composite materials is shown in <u>Fig. 13.7</u>. Epoxy resin is a chemical compound containing two or more epoxide groups per monomer, and this molecule contains a tight C—O—C ring structure. During polymerisation, the hardener opens the C—O—C rings, and the bonds are rearranged to join the monomers into a three-dimensional network of crosslinked chain-like molecules. The cure reaction for certain types of epoxy resins occurs rapidly at room temperature, although many of the high-strength epoxies used in aircraft need to be cured at an elevated temperature (120–180 °C). Epoxy resins are the polymer of choice in many aircraft applications because of their low shrinkage and low release of volatiles during curing, high strength, and good durability in hot and moist environments.
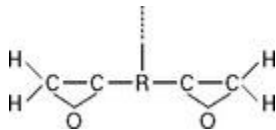
13.7 Functional unit of epoxy resins used in aircraft composite materials.

13.5.2 PHENOLIC RESIN

Epoxy resin is used extensively in aircraft composite structures, but cannot be safely used inside cabins because of its poor fire performance. Most epoxy resins easily ignite when exposed to fire, and release copious amounts of heat, smoke and fumes. Federal Aviation Administration (FAA) regulations specify the maximum limits on heat release and smoke produced by cabin materials in the event of fire, and most structural-grade epoxy resins fail to meet the specifications. Phenolic resins meet the fire regulations, and most of the internal fittings, components and furniture in passenger aircraft are made of fibreglass–phenolic composite and moulded phenolic resin.

13.5.3 POLYIMIDE, BISMALEIMIDE AND CYANATE

Thermosetting polymers that are also used in structural fibre composites are polyimides, bismaleimides and cyanate esters. These polymers are used in aircraft composite structures required to operate at temperatures above the performance limit of epoxy resin, which is usually in the upper range of 160–180 °C. Polyimides can operate continuously at temperatures up to 175 °C and have an operating limit of about 300 °C. The polyimide called PMR-15 is the most common, and is used as the matrix phase of carbon– fibre composites in high-speed military aircraft and jet engine components. The down-side of using polyimides is their high cost. Bismaleimide (BMI) is also used in fibre composites required to operate at temperature, with an upper service temperature of about 180 °C. Carbon–BMI composites are used in the F-35 *Lightning II* fighter along with carbon–epoxy materials.
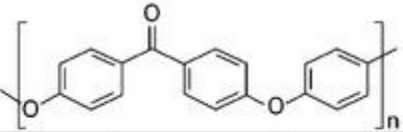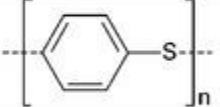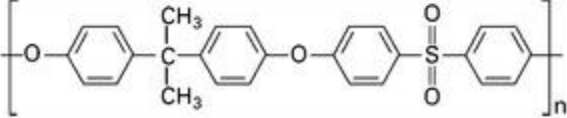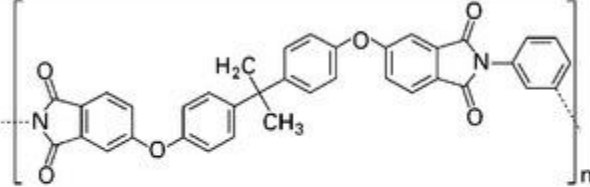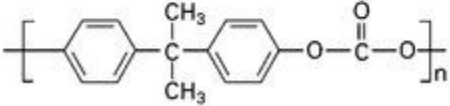
Cyanate resins, which are also known as cyanate esters, cyanic esters or triazine resins, have good strength and toughness at high temperature, and their maximum operating temperature is approximately 200 °C. However, cyanate resins pose a safety risk because they produce poisonous hydrogen cyanide during the cure reaction process.

13.6 Thermoplastics

13.6.1 AEROSPACE THERMOPLASTICS

The use of thermoplastics in aircraft, whether as the matrix phase of fibre–polymer composites or as a structural adhesive, is small compared with the much greater use of thermosets. Some sectors of the aerospace industry are keen to increase the use of thermoplastics in composite materials, and the number of applications is gradually increasing. Thermoplastics provide several important advantages over thermosets when used in composite materials, most notably better impact damage resistance, higher fracture toughness and higher operating temperatures. However, thermoplastics must be processed at high temperature that makes them expensive to manufacture into aircraft composite components.

The group of thermoplastics that are most used in aircraft composite structures are called polyketones, and include polyether ketone (PEK), polyether ketone ketone (PEKK) and, the most common, polyether ether ketone (PEEK). The main types of thermoplastics used in aircraft are given in Fig. 13.8.

Polyether ether ketone (PEEK)	
Polyphenylene sulfide (PPS)	
Polysulfone (PSU)	
Polyetherimide (PEI)	
Polycarbonate	

13.8 Thermoplastics used in aircraft.

Several types of thermoplastics are transparent, tough and impact resistant which makes them well suited for aircraft windows and canopies. The thermoplastics most often used in aircraft windows are acrylic plastics and polycarbonates. Acrylic plastics are any polymer or copolymer of acrylic acid or variants thereof. An example of acrylic plastic used in aircraft windows is polymethyl methacrylate

(PMMA), which is sold under commercial names such as Plexiglas and Perspex. Acrylic plastics are lighter, stronger and tougher than window glass. Polycarbonates get their name because they are polymers having functional groups linked together by carbonate groups (—O—(C==O)—O—) in the long molecular chain. Polycarbonates are stronger and tougher than acrylic plastics and are used when high-impact resistance is needed, such as cockpit windows and canopies. In these applications, the material must have high impact resistance because of the risk of collision with birds. Although bird strikes do not occur at cruise altitudes, they present a serious risk at low altitudes, particularly during take-off and landing. Polycarbonate windscreens are also resistant to damage by large hailstones. Figures 13.9 and 13.10 show examples of damage caused to aircraft windows by bird strike or hail, respectively. Although the polycarbonate windows are damaged, they were impacted under severe conditions that would have caused most other polymer materials to rupture leading to cabin depressurisation. A large bird hit the window shown in Fig. 13.9 when the aircraft was flying at several hundred kilometres per hour and hailstones larger than golf balls caused the damage shown in Fig. 13.10. Had these windows been made with glass the bird and hailstones would almost certainly have punctured through and entered the cockpit. Polycarbonate windows offer good safety to the flight crew against severe impact events.
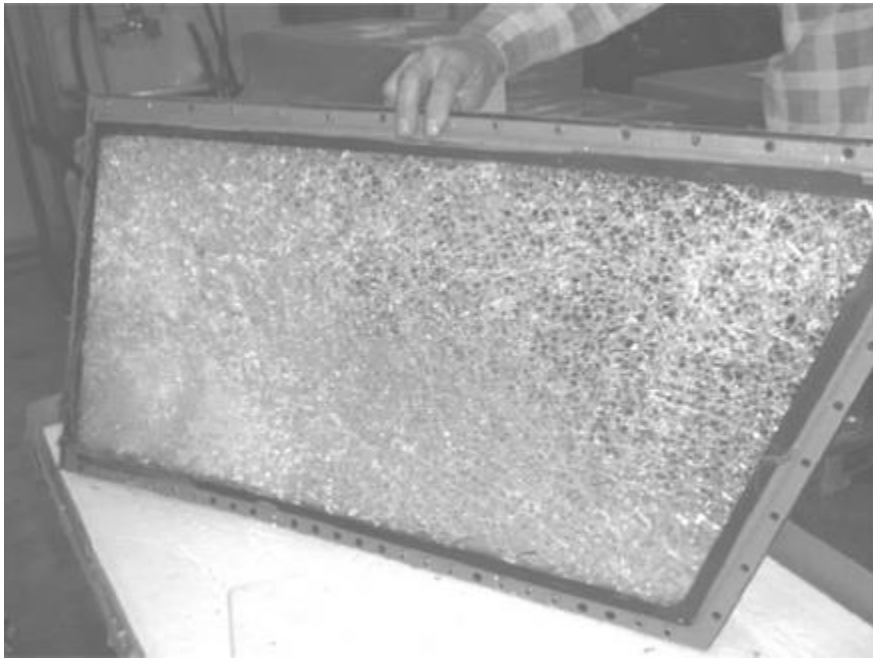
13.9 Bird strike damage to a cockpit window. Photograph reproduced with permission from AirSafe.com.

13.10 Hail damage to a cockpit window.

13.6.2 CRYSTALLISATION OF THERMOPLASTICS

A unique property of thermoplastics is the ability of their polymer chains to be amorphous or crystalline (Fig. 13.11). Amorphous polymers consist of long chains that are randomly shaped and disordered along their length. Each chain twists and turns along its length without order, and there is no pattern with the other chains. In comparison, crystalline polymers consist of chains with a well-ordered structure. Thermosets and elastomers always occur in the amorphous condition; crystallinity is a property unique to thermoplastics. The ability of thermoplastics to crystallise is important for their use in aircraft because crystalline polymers generally have better resistance to paint strippers, hydraulic fluids and aviation fuels, which can degrade amorphous polymers. A crystalline polymer also has higher elastic modulus and tensile strength than the same polymer in the amorphous condition.
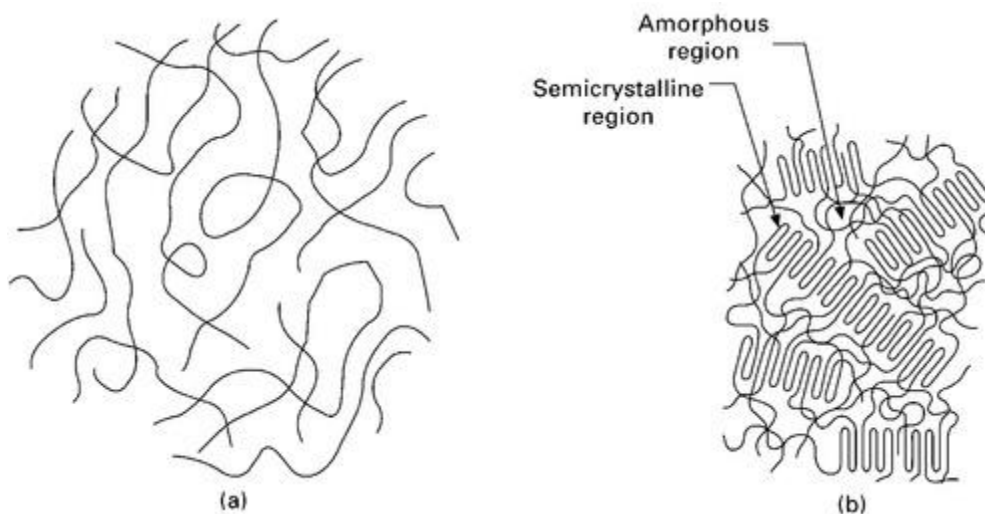
13.11 (a) Amorphous and (b) semicrystalline polymer structures.

Crystallisation occurs when a thermoplastic is cooled slowly from its melting temperature, which allows sufficient time for segments of the polymer chains to take an ordered structure. The folded chain model depicted in Fig. 13.11 is one representation of a crystallised polymer. A single chain folds back and forth over a distance of 50–200 carbon atoms, and the folded chains extend in three dimensions producing thin plates or lamellae. It is virtually impossible for thermoplastics to be completely crystalline because the entanglement and twisting of the chains stops them folding into an ordered pattern over large distances. Instead, thermoplastics can have both the amorphous and crystalline phases present together in the same material, and these are called semicrystalline thermoplastics. The crystalline phase occurs in tiny regions, typically only a few hundred angstroms wide, in which the chains are aligned. In some polymers these crystalline regions cluster into small groups known as spherulites. Surrounding these crystalline regions is the amorphous thermoplastic. The percentage volume fraction of crystallised material within a thermoplastic typically varies from 30% to 90%, with the actual amount being determined by several factors. Crystallisation occurs more easily for linear polymers that have small side groups attached to the main chain. Thermoplastics that have large side groups or have extensive chain branching are more difficult to crystallise. For example, linear polyethylene can be crystallised to 90% by volume, whereas branched polyethylene can be crystallised to only 65%. This occurs because the branches interfere with the chain-folding process, thereby limiting the growth of crystalline zones. The length of the polymer chain also controls the amount of crystallisation. Crystallisation occurs more easily with shorter chains because the entanglement, which hinders crystallisation, is less.

The most common method to control the amount of crystallinity is careful management of the polymer processing conditions. Cooling a thermoplastic slowly from its melting temperature increases the amount of crystallisation because more time is given for the chains to move into an ordered pattern. Slowly deforming a thermoplastic at high temperature (but below the melting temperature) also increases crystallinity by allowing the chains to straighten in the direction of the applied stress. Lastly, the process of annealing, which involves holding the polymer at high temperature for a period of time, increases crystallinity. Often two or more of these methods are used to control the amount of crystallisation to ensure the thermoplastic has the properties best suited for a specific application.
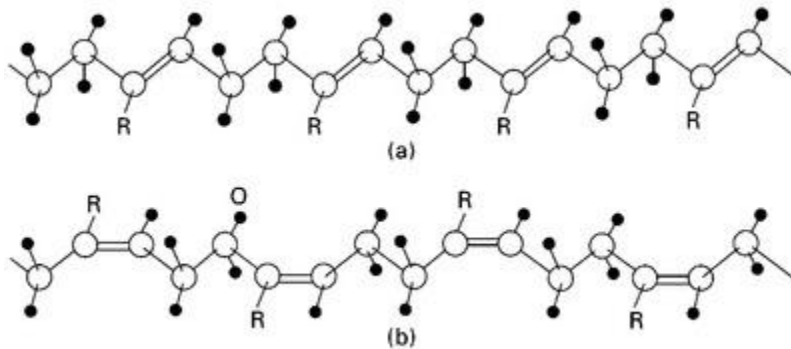
13.7 Elastomers

13.7.1 AEROSPACE APPLICATIONS OF ELASTOMERS

Elastomers are not suitable for use in aircraft structures because they lack stiffness and strength, but they do have exceptionally high elasticity with elongation values between one hundred and several thousand percent. This makes elastomers suitable when low stiffness and high elasticity is required, such as aircraft tyres, seals and gaskets. Many aircraft components that require a tight seal, such as window and door seals, use elastomers. These materials are used for their excellent elasticity; they can be easily compressed to make a tight seal without being damaged or permanently deformed. Although elastomers usually work well as seals and gaskets, they can gradually erode and degrade in harsh operating conditions, such as high temperatures. The most dramatic example of failure of an elastomer was the space shuttle *Challenger* accident. This accident is described in more detail in the case study in Section 13.15 at the end of the chapter.

13.7.2 STRUCTURE OF ELASTOMERS

The molecular structure of elastomers is characterised by coiling of their chains. The coiled structure occurs because the chain is not balanced along its length owing to the bonding pattern and the location of side groups along the chain. Curvature of the chain is produced by the arrangement of atoms and side groups along the chain. An atom or side group R can be placed in either the *cis* or *trans* position along the carbon chain, as shown in Fig. 13.12. The unsaturated segment of

the chain is where there are C==C double bonds. In the *trans* position, the unsaturated bonds are on opposite sides, whereas in the *cis* position the unsaturated bonds are on the same side of the chain and the R groups are on the opposite side. The location of the R groups on the same side of the chain causes it to become unbalanced, and this forces the chain to coil until it finds an equilibrium position. Elastomers usually have the unsaturated bonds in the *cis* position, which causes the chain to coil like a spring. It is the coiled structure of elastomers that distinguishes them from other polymers, and gives them their very high elasticity. Coiling allows the chains to stretch like a spring and, under an applied tensile force, they can elongate to many times their original length without permanently deforming. The chains spring back into their original coiled structure when the applied load is removed.

13.12 (a) *cis* and (b) *trans* structures of the polymer chain.

Elastomers have some crosslinking between the chains that provides a small amount of resistance to elastic stretching. The amount of crosslinking is much less than found in the heavily crosslinked thermosets. The crosslinks in elastomers are widely spaced along the coiled polymer chains. The crosslinks between the elastomer chains are created in a process called vulcanisation. The most common vulcanisation process involves heating rubber with sulfur to temperatures of about 120 to 180 °C. Without vulcanisation, elastomers behave like a very soft solid under load. When vulcanisation is carried too far, however, the chains are too tightly bound to one another by excessive crosslinking and the elastomer is very brittle. The crosslinks also improve the wear resistance and stiffness, which is important when elastomers are to be used in aircraft tyres. These properties improve with the amount of crosslinking, but the amount of sulfur present in the elastomer should not exceed about 5% otherwise the material becomes too brittle.

Not all elastomers are crosslinked; a special group known as thermoplastic elastomers are not crosslinked but still have the elasticity of a conventional elastomer. As mentioned, the chain in a block copolymer is made using two types of monomers, with a long sequence of one type of monomer followed by a sequence of the other monomer type. An elastomer copolymer is made with thermoplastic and elastomer monomers, and the chains consist of long coiled lengths of the elastomer joined to shorter sections of thermoplastic. A common thermoplastic elastomer is styrene–butadiene–styrene (SBS), where the styrene is the thermoplastic-based monomer and butadiene the elastomer monomer. The SBS chains are made of short linear segments of styrene bonded to longer coiled segments of butadiene. The styrene units from a number of chains clump together, and this stops chains from sliding freely pass each other when the material is under load. The rubbery butadiene units uncoil under load providing SBS with high elasticity.

13.8 Structural adhesives

13.8.1 AEROSPACE APPLICATIONS OF STRUCTURAL ADHESIVES

A structural adhesive can be simply described a 'high-strength glue' that bonds together components in a load-bearing structure. Structural adhesives are used extensively in aircraft for bonding metal-to-metal, metal-to-composite and composite-to-composite parts. Adhesives are most commonly used in joints of thin aerostructures with a well-defined load path. Adhesives are also used to join thick airframe structures with complex, multidirectional load paths, although the joint is usually reinforced with fasteners such as bolts, rivets or screws for added strength and safety. Adhesives are also used to bond repair patches to damaged aircraft structures.

13.8.2 PERFORMANCE OF STRUCTURAL ADHESIVES

Thermosets, thermoplastics and elastomers have adhesive properties, but specially formulated thermosets are used most often for bonding aircraft structures. There are many advantages of using adhesives for joining aircraft components, rather than relying solely on mechanical fasteners for strength. Adhesive bonding eliminates some, or all, of the cost and weight of fasteners in certain aircraft components. Another advantage of bonding is the reduced incidence of fatigue cracking in metal connections. Drilled holes for fasteners are potential sites for the start of fatigue cracks, and removing the need for holes by bonding reduces this particular problem. Adhesive bonding has the advantage of providing a more uniform stress distribution in the connection by eliminating the individual stress concentrations at fastener holes. Bonded joints are usually lighter than mechanically fastened joints and enable the design of smooth external surfaces. In addition to joining structural components, adhesives are used for bonding the skins and core in sandwich composites. Figure 13.13 shows the application of adhesively bonded sandwich composites in an aircraft.
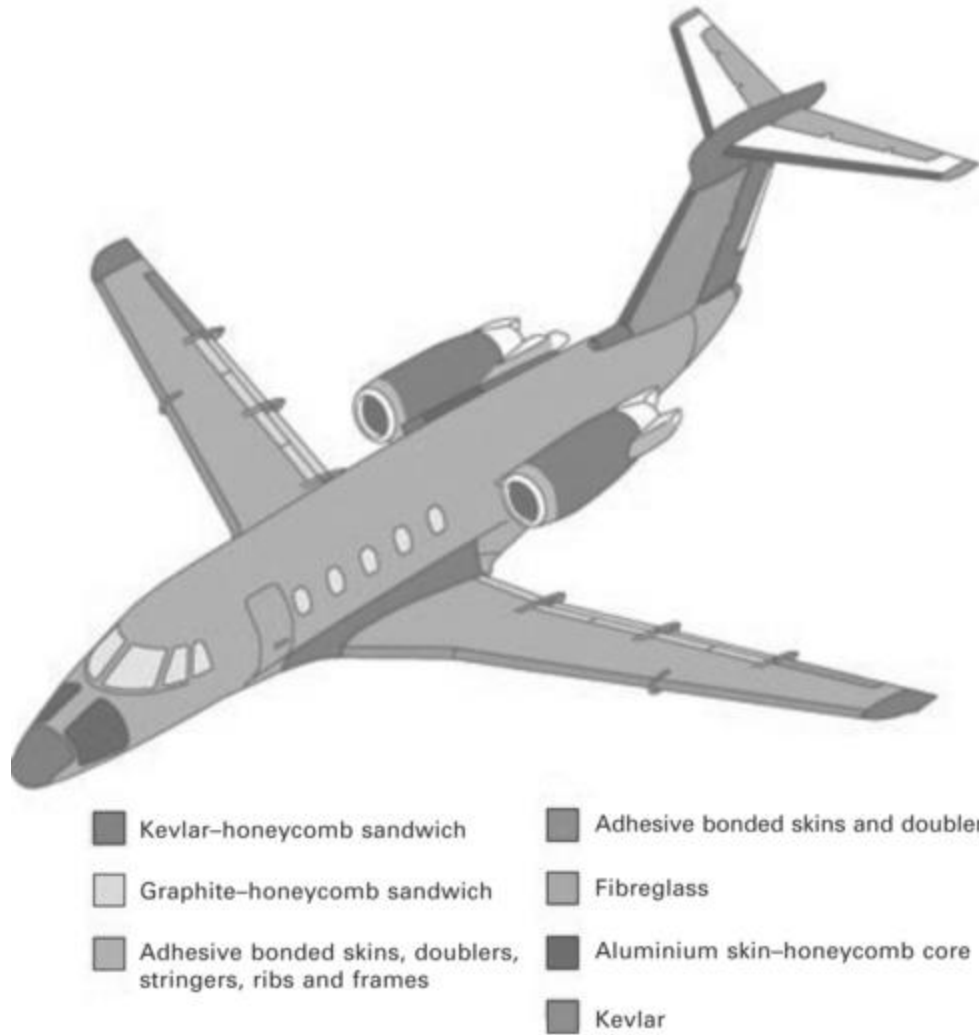
13.13 Application of adhesively bonded sandwich composites in the *Citation* III aircraft.

The adhesive must have high elastic modulus, strength and toughness. Toughening agents (such as tiny rubber particles) are often blended into the adhesive to increase fracture toughness. Structural adhesives must have low shrinkage properties when cured to avoid the development of residual stresses in the joint. Adhesives must also be resistant to attack or degradation in the operating environment. Water and liquids such as solvents (paint strippers), hydraulic fluids and aviation fuel can attack the bond between the adhesive and substrate, and therefore durable adhesive systems must be used.

Structural adhesives with the best mechanical properties and durability are useless unless they can bond strongly to the substrate. The type of adhesive used is critical to ensure strong adhesion. However, surface preparation of the substrate is the keystone upon which the adhesive bond is formed. The substrate must be grit blasted or lightly abraded, cleaned, dried, and then treated with a chemical coupling agent to ensure good adhesion. If the substrate surface is not suitably prepared, the adhesive fails owing to poor bonding.

13.8.3 TYPES OF STRUCTURAL ADHESIVES

The thermosetting adhesives used in aircraft structures are crosslinked polymers that are cured using heat, pressure or a combination of heat and pressure. Heat-curing adhesives are cured at temperatures close to (or preferably slightly over) the maximum-use temperature of the structure. Adhesives are available as films or pastes. Film adhesives are often used in bonding aircraft structures because they usually provide higher strength than paste adhesives. The film is simply placed between the substrates and then heated and pressurised to form a strong bond. Adhesive pastes can be a one-part system that is simply spread on the substrates and cured by heat and/or pressure. Alternatively, two-part systems consisting of resin and hardener are mixed together into an adhesive paste, which is then applied to the substrates.

The polymer most often used as a structural adhesive is epoxy resin because of its ability to adhere to most surfaces (including aircraft-grade aluminium alloys and fibre composites), high strength, and long-term durability over a wide range of temperatures and environments. Silicone is often used when a high toughness adhesive is needed, whereas bismaleimide and polyimide are used when a high-temperature adhesive is required. Other types of adhesives include urethanes, phenolic resins, acrylic resins and inorganic cements, although they are rarely used for bonding aircraft structures. Hot- melt adhesives are used occasionally, although not in highly-loaded aircraft structures. Hot-melt adhesives are thermoplastics or thermoplastic elastomers that melt when heated. On cooling the polymer solidifies and forms a bond with the substrate. Most commercial hot-melt adhesives soften at 80 to 110 °C, which makes them unsuitable as a high-temperature adhesive. Pressure sensitive adhesives (PSA) are usually elastomers or elastomer copolymers that are not crosslinked or are only slightly crosslinked and they bond strongly with a substrate. PSAs adhere simply by the application of pressure, and the most common (but obviously non-aerospace type) is Scotch® tape. Most PSAs are not suitable for joining aircraft structures because of their low strength at elevated temperature.

13.9 Mechanical properties of polymers

13.9.1 DEFORMATION AND FAILURE OF POLYMERS

Polymers deform elastically and plastically when under load, much like metals. However, the deformation processes for polymers are different to those for metals. The elastic deformation of metals involves elastic stretching of the bonds in the crystal structure and plastic deformation involves dislocation slip. Polymers do not have crystal structures as found in metals nor do they contain dislocations, and so the processes responsible for deformation are different from those for metals.

Tensile stress–strain curves for a thermoplastic, thermosetting polymer and elastomer are presented in Fig. 13.14. These curves are representative of the stress response of these different types of polymers, where the elongation-to-failure increases in the order: thermoset, thermoplastic, elastomer. The curves can be divided into three regimes that are controlled by different deformation processes: elastic, plastic and fracture regimes.
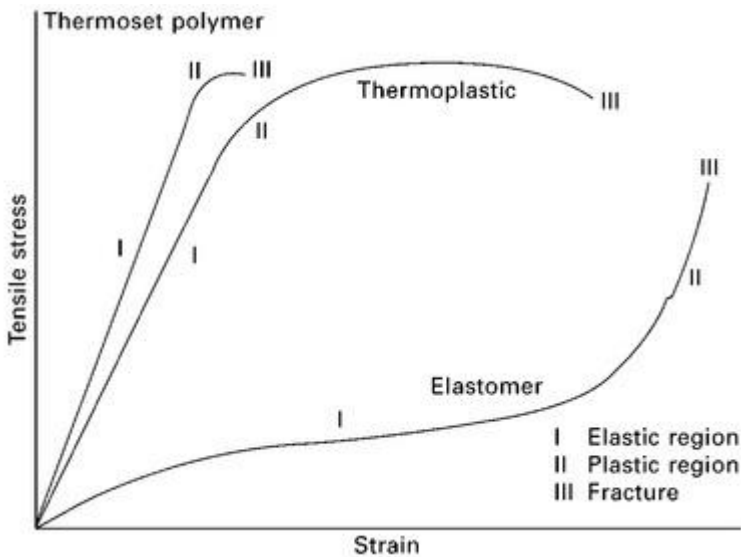
13.14 Typical stress–strain curves for a thermoplastic, thermoset polymer and elastomer.

Elastic deformation

When an elastic stress is applied to a polymer, the chains are stretched in the loading direction. Elastic stretching occurs in the covalent bonds between the atoms along the chain backbone. Stretching also involves some straightening of twisted segments of the chain. The stretching of the bonds and the twisted segments of the polymer chains increases with the applied stress. However, when the load is removed the chains relax back into their original position. The slope of the stress–strain curve in the elastic regime is rectilinear for thermoplastics and thermosets, and is used to calculate material stiffness, i.e. Young's modulus.

The situation is different for many elastomers, which do not have a rectilinear strain–stress response in the elastic regime. Instead, the apparent elastic modulus for elastomers decreases with increasing strain as the chains begin to uncoil and stretch in the load direction. The elastomer chains are so tightly coiled that they can be stretched many times their original length before there is any significant resistance to loading. As the chains start to straighten, the stiffness begins to increase owing to elastic stretching of the bonds within the chain and the crosslinking bonds between the chains. Because elastomers are not heavily crosslinked, the chains can stretch without a large amount of resistance from the crosslinking bonds. At any point in the elastic regime, the elastomer reverts back to its original shape (in the absence of creep) when the load is removed. Elastic recovery occurs by the bonds along the chains and the crosslinking bonds between the chains relaxing into their original state, allowing the chains to return to their original coiled position.

Plastic deformation

An amorphous polymer plastically deforms when the applied stress exceeds the yield strength. The yielding mechanisms are complicated and involve the stretching, rotation, sliding and disentanglement of the chains under load deformation. Eventually the chains become almost aligned parallel and close together and, at this point, the polymer reaches its ultimate strength. Plastic deformation of thermosets is resisted by the crosslinks and, therefore, the yield strength of these polymers is often higher than thermoplastics. The lack of crosslinks in amorphous thermoplastics allows the chains to stretch, slide and disentangle more readily than in thermosets, which results in greater ductility and toughness.

The yielding process in semicrystalline thermoplastics is a combination of the deformation processes just described for amorphous polymers together with different processes for the crystalline phase. When a tensile load is applied, the crystalline lamellae slide past one another and begin to separate as the chains are stretched. The folds in the lamellae tilt and become aligned in the load direction; at this stage the ultimate strength is reached.

Fracture

The process leading to fracture of polymers starts with the breaking of the weakest or most highly strained segments of the polymer chains. For thermoplastics, this occurs along the backbone of the chains, whereas in thermosets and elastomers it can start by the breaking of crosslinks. The breaking of the chains continues under increasing strain until micrometre- sized voids develop at the most damaged regions, as shown in Fig. 13.15. These voids grow in size and coalesce into cracks until the polymer eventually breaks.
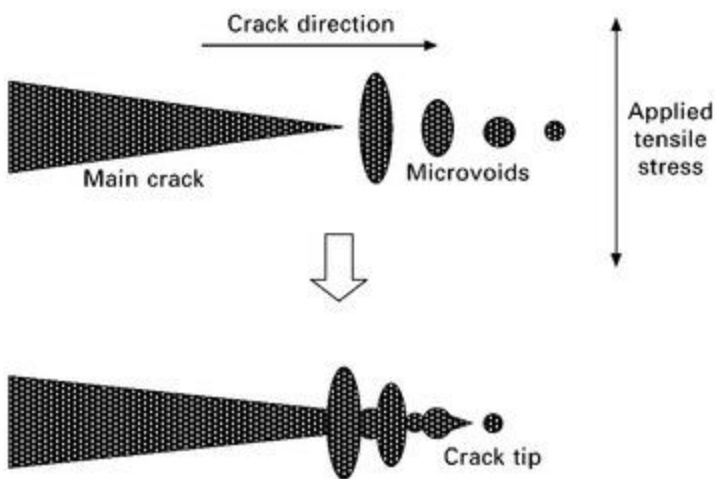
13.15 Schematic showing tensile failure of a polymer by the formation and coalescence of voids.

13.9.2 ENGINEERING PROPERTIES OF POLYMERS

Table 13.3 gives the mechanical properties of thermoplastics, thermosetting polymers and elastomers that have current or potential aerospace applications. The values are the average properties, which can vary owing to changes in the chemical state and processing conditions of the polymer. The Young's modulus of thermoplastics and thermosets is in the range of 2–6 GPa, which is much smaller than the elastic modulus of aluminium alloys (70 GPa), titanium alloys (110 GPa), steels (210 GPa) and other metals used in aircraft. Likewise, the tensile strength of most polymers is under 100 MPa, which is well below the strength of the aerospace alloys. It is because of the low mechanical properties that polymers are not used in heavily loaded aircraft structures.

Table 13.3

Tensile properties of polymers used in aircraft

	Young's modulus (GPa)	Tensile strength (MPa)	Elongation-to-failure (%)
Thermoplastic			
Polyether ether ketone (PEEK)	3.7	96	50
Polyether ketone (PEK)	4.6	110	12
Polyphenylene sulfide (PPS)	6.0	110	12
Polysulfone (PSU)	2.4	68	40
Polyether sulfone (PES)	2.3	81	80
Polyaryl sulfone (PAS)	2.7	75	8
Polyetherimide (PEI)	3.7	100	42
Polycarbonate (PC)	2.7	73	130
Thermoset			
Epoxy	4.5	85	3.0
Phenolic	6	55	1.7
Bismaleimide (524C)	3.3	50	2.9
Polyimide (PMR15)	4.0	65	6.0
Cyanate ester	3.0	80	3.2
Elastomer			
Polyisoprene		20	800
Polybutadiene		23	
Polyisobutylene		27	350
Polychloroprene (Neoprene)		23	800
Butadiene–styrene		30	2000
Thermoplastic elastomer		33	1300
Silicone		7	700

The tensile strength of polymers can be controlled in several ways:

• Increasing the degree of polymerisation. The strength properties of polymers increase with the length of the chains, which is controlled by the degree of polymerisation. For example, the tensile strength of polyethylene is directly related to the chain length, which is defined by the molecular weight (MW). Low-density polyethylene (MW ~ 200 000 monomer units) has a tensile strength of about 20 MPa, high-density polyethylene (MW ~ 500 000 monomer units) has the strength of 37 MPa, and ultra-high-density polyethylene (MW ~ 4 500 000 monomer units) the strength of 60 MPa. The strength increases with the chain length because they become more tangled and, therefore, a higher stress is needed to stretch and untangle them. The strength increases with the chain length up a limit beyond which further polymerisation does not add extra strength.

• Increasing the size of side groups attached to the main chain. Strength is increased by adding larger atoms or groups to the side of the chain backbone. This makes it more difficult for the chains to rotate, uncoil and disentangle when under load, thereby increasing strength. For example, polyetherimide (PEI) which has relatively large side groups has the tensile strength of about 100 MPa whereas polyphenylene sulfide (PPS) with no large side groups has the strength of only 60 MPa.

• Increasing the amount of chain branching. The strength is increased by extensive chain branching. A high density of branches along the main chain provides resistance against the stretching, sliding and disentanglement of neighbouring chains and, thereby, increases the strength. However, too much branching can prevent the close packing and crystallisation of the chains and, thereby, reduce the strength.

• Increasing the degree of crosslinking (for thermosets and elastomers). The strength increases with the number density of crosslinks between the chains.

• Increasing the degree of crystallisation (for thermoplastics). The strength increases with the volume percentage of thermoplastic that is crystallised. This is because a higher load is needed to permanently deform polymer chains when in a crystallised state rather than the amorphous condition.

Table 13.3 shows that thermosets have low ductility, with elongation- to-failure usually below 5%. This is because the high density of crosslinks between the chains resists extensive plastic deformation of the polymer. Many thermoplastics have high elongation-to-failure (above 50%), although their ductility decreases with increasing crystallinity. Elastomers have exceptionally high elongation-to-failure, in the range of several hundred to several thousand percent, because of their coiled chain structure.

13.9.3 THERMAL PROPERTIES OF POLYMERS

An important consideration in the use of polymers is softening that occurs owing to heating effects, such as the frictional heating of aircraft skins at fast flight speeds or the operating temperature of engine components. Polymers lose stiffness, strength and other properties at moderate temperature. Although other aerospace materials, including the metal alloys we have discussed, also lose mechanical performance when heated, the properties of polymers are reduced at much lower temperatures. The mechanical properties of most polymers drop sharply above 100–150 °C, and therefore their use in fibre composite airframe, bonded joints, engine components and other structural applications must be confined to lower temperatures. For high-temperature conditions, several polymer systems can be used, such as bismaleimides, polyimides and cyanates, but even here the maximum operating temperature is below 200–220 °C.

The effect of increasing temperature on the Young's modulus of polymers is shown in Fig. 13.16. At low temperature there is low internal energy within the polymer and, therefore, the chains are 'sluggish' and difficult to move under an applied force. In crystalline polymers, the sluggish behaviour makes it difficult for the chains to unfold and align themselves in the load direction. In amorphous polymers, the chains lack the energy to slide and move through the tangled network in order to align in the load direction. The ability of polymers to undergo large deformations is suppressed at low temperatures and they are more likely to resist the applied load, thus becoming stiff, strong and brittle. In this condition, polymers are often described as being glassy. When the temperature is raised more energy is available to the polymer chains to move under load. This is observed as a reduction in the elastic modulus and strength and an increase in the ductility (elongation- to-failure). When an amorphous polymer transforms from a rigid, brittle material to a soft, ductile material with increasing temperature it is described as converting from a glassy state to a rubbery state. Crystalline materials go through two stages of softening: a glassy-to-leathery transformation as the crystalline chains begin to unfold and assume an amorphous state, and a leathery-to-rubbery transformation as the chains are easily deformed under load.
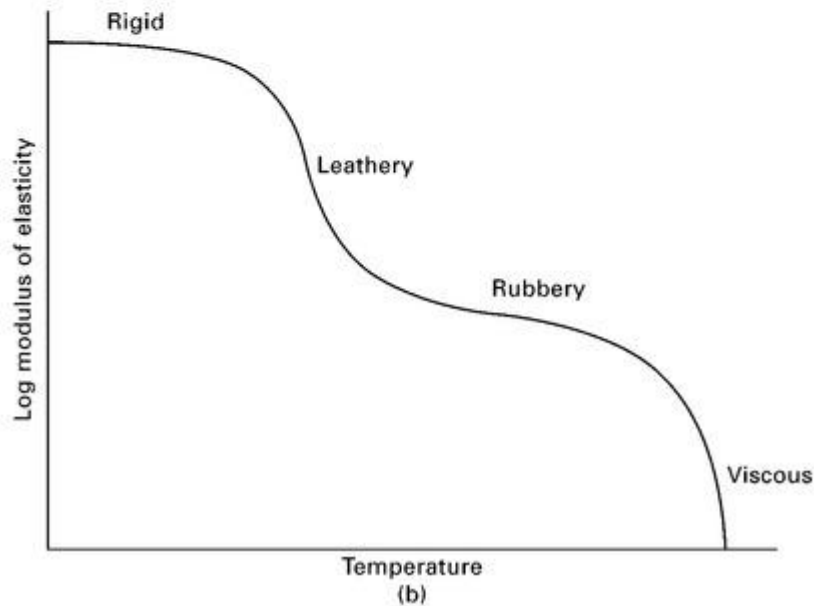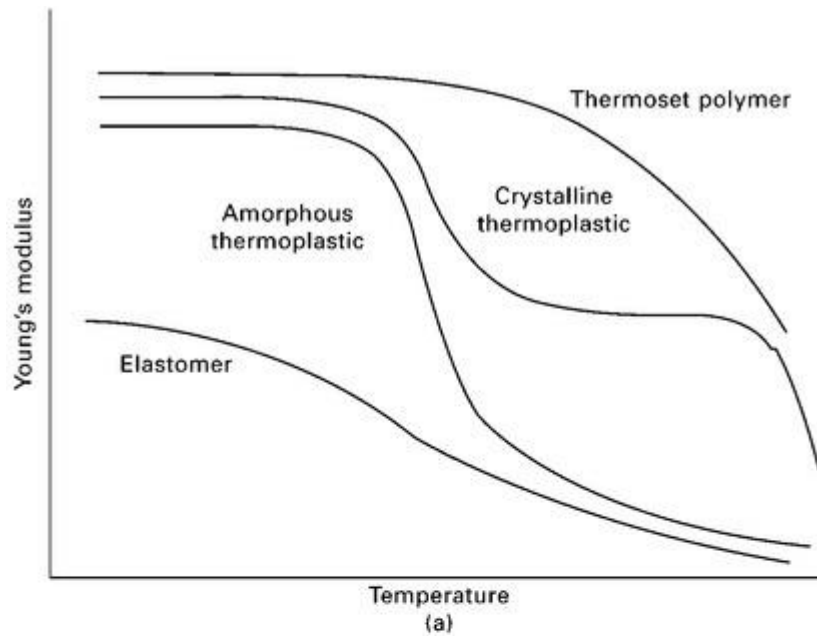
13.16 Variation of (a) Young's modulus with temperature and (b) deformability with temperature.

Two properties are used to define the softening temperature of polymers: heat deflection temperature (HDT) and glass transition temperature (T_g). The HDT is a measure of the ability of the polymer to resist deformation under load at elevated temperature. The definition of the HDT is simply the temperature required to deflect a polymer by a certain amount under heat and load. The stress applied to the polymer is usually 0.46 MPa (66 psi) or 1.8 MPa (264 psi). The higher the HDT then the greater is the temperature needed to deform a polymer when under load. The HDT is also sometimes called the 'deflection temperature under load' or 'heat deflection temperature'. A polymer used in an aircraft part should not exceed an operating temperature of about 80% of the HDT to avoid the likelihood of distortion.

The glass transition temperature T_g is used more often than the HDT to define the softening temperature of polymers. The T_g can be defined as the temperature when an amorphous polymer undergoes the glassy-to-rubbery transformation and there is a significant change in properties.

Below the T_g, the polymer is glassy and hard whereas above the T_g it is rubbery and soft. Many physical properties change suddenly around the T_g, including the viscosity, elastic modulus and strength and, therefore, it is considered an important property for defining the temperature operating limit of polymers. The T_g of various aerospace polymers are given in Table 13.4. It is common practice to set the maximum operating temperature of polymers as the glass transition temperature less a certain temperature interval such as 30 °C (i.e. $T_{max} = T_g - 30$ °C). This ensures that polymers do not suffer excessive softening during service. The T_g of elastomers is below room temperature, and therefore they respond as a rubbery and soft material under normal operating conditions. Elastomers with a low T_g are often used in seals because they are soft and compliant at most operating temperatures for aircraft.

Table 13.4

Temperature properties of aerospace polymers

	Glass transition temperature (°C)	Melting temperature (°C)
Thermoplastics		
Polyether ether ketone (PEEK)	140	245
Polyphenylene sulfide (PPS)	75	285
Polyetherimide (PEI)	218	220
Polycarbonate (PC)	150	155
Thermosets		
Polyester	110	–
Vinyl ester	120	–
Epoxy	110–220	–
Phenolic	100–180	–
Bismaleimide	220	–
Polyimide	340	–
Cyanate ester	250–290	–
Elastomers		
Polybutadiene	–90	120
Polychloroprene	–50	80
Polyisoprene	–73	30

Table 13.4 also gives the average melting temperatures for the thermoplastics, which is usually 1.5 to 2 times higher than the glass transition temperature. Thermosets do not have a melting temperature because the crosslinks stop the chains flowing like a liquid, and instead these polymers decompose at high temperature without melting.

13.10 Polymer additives

Additives are often blended into polymers during processing to improve one or more properties. Additives include chemical pigments to give colour; filler particles to reduce cost, increase mechanical performance and provide dimensional stability; toughening agents and plasticisers to increase fracture toughness and ductility; stabilisers to increase operating temperature or resistance

against ultraviolet radiation; and flame retardants. An important class of additives is fibrous fillers, such as glass, carbon, boron and aramid fibres, used as the reinforcement in fibre–polymer composites, which are described in chapters 14 and 15.

Additives are not always used in polymers for aircraft applications, and when they are used it is often for a specific purpose. Additives may be included in the polymer matrix phase of fibre composites to increase flame resistance and environmental durability. Additives are often used in structural adhesives to increase toughness and durability, particularly against hot–wet conditions. Elastomers used for aircraft tyres contain filler particles called carbon black to increase the tensile strength and wear resistance.

Toughening agents are used in thermosets to increase the fracture toughness, ductility and impact hardness. High-strength thermosets, such as epoxy resins, have low ductility with strain-to-failure values as low as a few percent. Adhesives used in aircraft structural joints require high ductility and fracture toughness and, therefore, toughening agents are used to improve fracture toughness. The most common toughening agent comprises small particles of rubber, usually carboxyl-terminated butadiene nitrile (CTBN) rubber. The rubber particles are only a few micrometres in size and are dispersed through the adhesive to impede crack growth. Fine thermoplastic fillers are also used as toughening agents.

Plasticisers are additives used to increase the toughness of crystalline thermoplastics, in which rubber toughening particles (such as CTBN) are usually ineffective. Plasticisers are low-molecular-weight polymers that increase the spacing between chains of crystalline polymer to make them more flexible and, thereby, tougher.

A safety concern with using polymers and polymer composites in aircraft is fire. Most polymers are flammable and release large amounts of heat, smoke and fumes when they burn. It is often necessary to use flame-retardant additives in polymers to achieve the fire resistant standards specified by safety regulators such as the FAA. Many types of additives are used to improve the flammability resistance of polymers, with the most common containing halogenated or phosphorus compounds. Flame-retardant additives are either discrete particles within the polymer or are chemically incorporated into the polymer chain structure. New and more effective flame retardant additives are being developed, with carbon nanotubes (see chapters 14) offering new possibilities for increased fire resistance combined with improved mechanical performance.

13.11 Polymers for radar-absorbing materials (RAMs)

Radar is the most common technique for the detection and tracking of aircraft. Although radar is an indispensable tool in aviation traffic management, it is a problem in offensive military operations which require aircraft to attack their target and then escape without being detected. Radar involves the transmission of electromagnetic waves into the atmosphere; they are then reflected off the aircraft back to a receiving antenna. Conventional aircraft, such as passenger airliners, are easily detected by radar because of their cylindrical shape together with bumps from the engines and tail plane. Metals used in the aircraft are also strong reflectors of electromagnetic waves, and can be easily detected using radar. Composites are also detected using radar, although usually not as easily as metals.

Radar-absorbing material (RAM) is a specialist class of polymer-based material applied to the surface of stealth military aircraft, such as the F-22 *Raptor* and F-35 *Lightning II* (Fig. 13.19), to reduce the radar cross-section and thereby make them harder to detect by radar. These materials are also applied in stealth versions of tactical unmanned aerial systems, such as the Boeing X-45. RAM is applied over the entire external skin or (more often) to regions of high radar reflection such as surface edges. RAM works on the principle of the aircraft absorbing the electromagnetic wave energy to minimise the intensity of the reflected signal. RAMs are used in combination with other stealth technologies, such as planar design and hidden engines, to make military aircraft difficult to detect.

It is possible to reduce the radar cross-section of a fighter aircraft to the size of a mid-sized bird through the optimum design and application of stealth technologies.

13.19 Explosion of the space shuttle *Challenger* (STS-51).

13.17 Examples of stealth aircraft that use radar-absorbing materials: (a) F-22 *Raptor* and (b) F-35 *Lightning* II. (a) Photograph supplied courtesy of S. Austen. (b) Photograph supplied courtesy of B. Lockett, Air-and-Space.com.

Information about the composition of RAMs is guarded by the military. Most RAMs consist of ferromagnetic particles embedded in a polymer matrix having a high dielectric constant. One of the most common RAMs is called iron ball paint, which contains tiny metal-coated spheres suspended in an epoxy-based paint. The spheres are coated with ferrite or carbonyl iron. When electromagnetic radiation enters iron ball paint it is absorbed by the ferrite or carbonyl iron molecules which causes them to oscillate. The molecular oscillations then decay with the release of heat, and this is an effective mechanism of damping electromagnetic waves. The small amount of heat generated by the oscillations is conducted into the airframe where it dissipates.

Another type of RAM consists of neoprene sheet containing ferrite or carbon black particles. This material, which was used on early versions of the F-117A *Nighthawk*, works on the same principle as iron ball paint by converting the radar waves to heat. The USAF has introduced radar-absorbent paints made from ferrofluidic and nonmagnetic materials to some of their stealth aircraft. Ferrofluids are colloidal mixtures composed of nano-sized ferromagnetic particles (under 10 nm) suspended in a carrier medium. Ferrofluids are superparamagnetic, which means they are strongly polarised by

electromagnetic radiation. When the fluid is subjected to a sufficiently strong electromagnetic field the polarisation causes corrugations to form on the surface. The electromagnetic energy used to form these corrugations weakens or eliminates the energy of the reflected radar signal. RAM cannot absorb radar at all frequencies. The composition and morphology of the material is carefully tailored to absorb radar waves over a specific frequency band.

13.12 Summary

There are three main classes of polymers: thermosets, thermoplastics and elastomers. The polymers most often used in aircraft are thermosets such as epoxy resins and bismaleimides, which are used as the matrix phase in fibre composites and as structural adhesives. The aerospace applications for thermoplastics and elastomers is much less.

The properties of polymers that make them useful aerospace materials are low weight, excellent corrosion resistance and good ductility. Some polymers are also transparent for use in window applications. However, polymers have low stiffness, strength, fatigue life and creep resistance and, therefore, should not be used on their own in structural applications.

Polymers are produced by polymerisation reactions called addition or condensation reactions, which join the monomer units together into long chainlike macromolecules. The chemical and physical structure of the molecular chains has a major influence on the mechanical properties. Thermosets have higher stiffness, strength and creep resistance compared with thermoplastics because the molecular chains are interconnected by crosslinks. These crosslinks resist the sliding of chains under stress and, thereby, increase the mechanical properties.

Epoxy resin is the most used polymer for aerospace, and finds applications in carbon-fibre composites and as a structural adhesive. Epoxy resin has good stiffness, strength and environmental durability and can be cured at moderate temperatures (under 180 °C) with little shrinkage. Other thermosets used in composite materials include bismaleimide and polyimide, which are suited for high-temperature applications. Phenolic resin has excellent flammability resistance and is used in moulded parts and composites for cabin interiors.

Thermoplastics have high toughness, ductility and impact resistance, but the high cost of processing and low creep resistance limits their use in aerospace. Thermoplastics such as PEEK are used as the matrix phase in fibre composites requiring impact toughness. Polycarbonate is used for aircraft windows because of its high transparency, scratch resistance and impact strength.

Elastomers lack the stiffness and strength needed for aerospace applications, although their high elasticity makes them useful as a sealing material. Elastomers have high elasticity owing to their coiled molecular structure which responds under load in a similar way to a spring.

Adhesives used for bonding aircraft components and sandwich composites are usually thermosets, such as epoxy resin. Adhesives must have low shrinkage during curing to avoid the formation of residual tensile stress in the bond. Correct surface preparation is essential to ensure a high strength and durable bond is achieved with a polymer adhesive.

The mechanical properties of polymers are inferior to aerospace structural metals, and their use is restricted to relatively low-temperature applications. Polymers transform from a hard and glassy condition to a soft and rubbery state during heating, and the maximum working temperature is defined by the heat-deflection temperature or glass transition temperature.

Polymers often contain additives for special functions such as colour, toughness or fire.

Radar–absorbing materials (RAMs) are a special class of polymer that convert radar (electromagnetic) energy to some other form of energy (e.g. heat) and thereby improve the stealth of military aircraft. RAM must be used with other stealth technologies such as design adaptations of the aircraft shape to minimise the radar cross-section.

Manufacturing of fibre–polymer composite materials

Fibre reinforcements for composites

14.2.1 CARBON FIBRES: PRODUCTION, STRUCTURE AND PROPERTIES

Carbon (graphite) fibres are very stiff, strong and light filaments used in polymer (usually epoxy) matrix composites for aircraft structures and jet engine parts. Polymer composites containing carbon fibres are up to five times stronger than mild steel for structural parts, yet are five times lighter. Carbon fibre composites have better fatigue properties and corrosion resistance than virtually every type of metal, including the high-strength alloys used in airframe and engine components. Carbon fibres do not soften or melt and, when used in reinforced carbon–carbon composites, have exceptional heat resistance for high-temperature applications such as thermal insulation tiles, aircraft brake pads and rocket nozzles (as described in chapter 16). Although carbon fibres do not soften/melt, they do ultimately lose strength at high temperature via oxidation.

Applications for carbon-fibre composites have expanded dramatically since their first use in the 1960s and, alongside aluminium, is the most used aircraft structural material. Important factors behind the greater use of composites have been improvement to the properties and reduction in the cost of carbon fibres. Figure 14.3 shows the large increase in the use and reduction in the average price of carbon fibres since their first application in aircraft. It is important to note that large variations exist in the price depending on the fibre properties, and therefore the figure provides an indicative trend.
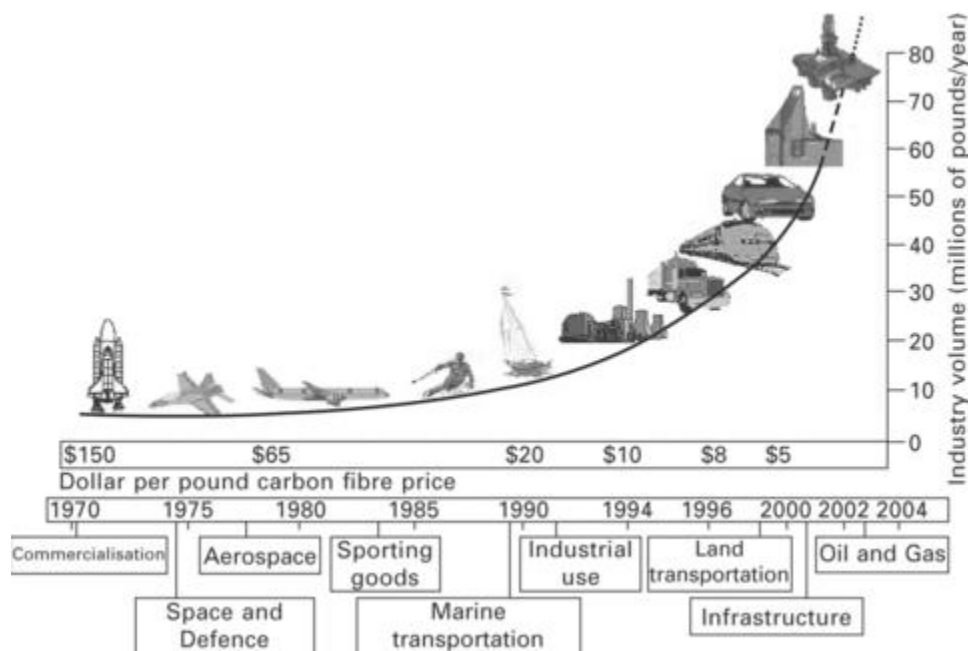
14.3 Changes to the consumption and average price of carbon fibre owing to increasing use in both aerospace and non-aerospace applications.

The properties of carbon fibre that make it an important aerospace material (stiffness, strength and fatigue resistance), are determined by the process methods used in its production. Carbon fibre is extracted via heat treatment from a carbon-rich precursor material, the most common of which are polyacrylonitrile (PAN), pitch and rayon. Carbon fibres produced for aerospace applications are made using PAN, which is an organic polymer. Other precursor materials such as pitch and rayon are rarely used in the production of

aircraft-grade carbon fibres because of their lower mechanical performance, but they are used to produce fibres for non-aerospace applications such as sporting equipment, civil infrastructure and marine craft.

Before the production of the carbon fibre, the PAN precursor material is stretched into long, thin filaments. This stretching causes the PAN molecules to align along the filament axis, which subsequently increases the stiffness of the carbon fibre after processing. The greater the stretch applied to the PAN, the higher the preferred orientation of the molecules along the filament, resulting in stiffer carbon fibre. PAN filaments are heat treated in a multistage process while under tension to produce carbon fibres. The process begins by stretching and heating the PAN filaments to 200–300 °C in air. This treatment oxidises and crosslinks the PAN into thermally stable carbon-rich fibres. The fibres are stretched during heating to prevent them contracting during oxidation. The PAN is then pyrolysed at 1500–2000 °C in a furnace having an inert atmosphere (e.g. argon gas), which stops further oxidation of the carbon. This heat treatment is called carbonisation because it removes non-carbon atoms from the PAN molecules (e.g. N, O, H) leaving a carbon-rich fibre with a purity content of 93–95%. The heat treatment changes the molecular bond structure into graphite. Carbon fibre consists of closely packed layers of graphite sheets in which the carbon atoms are arranged in a two-dimensional hexagonal ring pattern that looks like a sheet of chicken wire. The graphite sheets are stacked parallel to one another in a regular pattern (as represented in Fig. 14.4) and the sheets are aligned along the fibre axis.
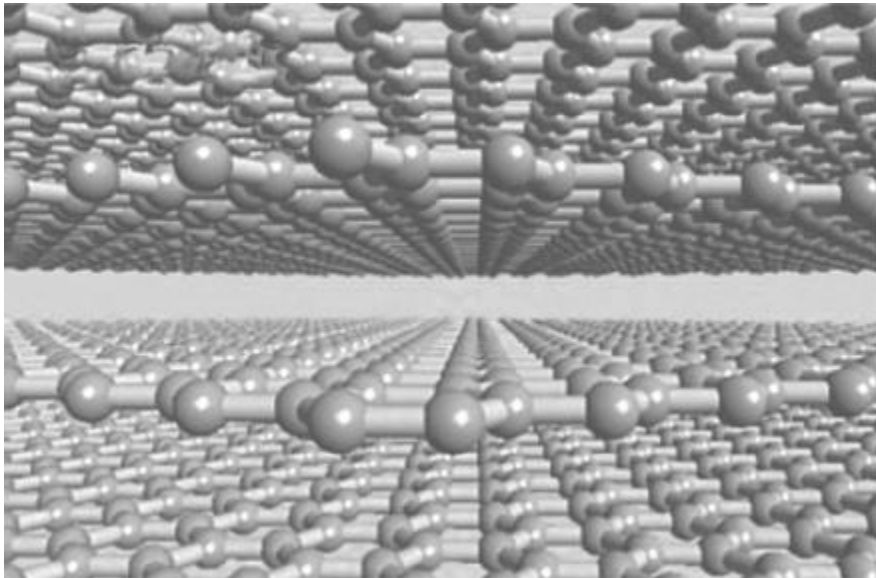

14.4 Sheet structure of graphite. Each sphere represents a carbon atom arranged in a hexagonal pattern in sheets.

The mechanical properties of carbon fibre vary over a large range depending on the temperature of the final heat treatment. There are two general categories of carbon fibre produced depending on the final temperature: high-modulus or high-strength (Table 14.1). The stiffness and strength of carbon fibre is determined by the pyrolysis temperature for the final processing stage, as shown in Fig. 14.5. Peak strength is reached by heating the fibre at 1500–1600 °C whereas the elastic modulus increases with temperature. The production of high-strength carbon fibres involves carbonisation of the PAN filaments at 1500–1600 °C. An additional heat treatment step called graphitisation is performed after carbonisation to produce high modulus fibres, which are heated in an inert atmosphere at 2000–3000 °C. The higher temperature used for graphitisation increases the preferred orientation of the graphite sheets along the fibre axis and thus raises the elastic modulus.

Table 14.1

Properties of PAN-based carbon fibres

| Property	High-modulus carbon fibres	High-strength carbon fibres
Density (g cm^{-3})	1.9	1.8
Carbon content (%)	+ 99	95
Tensile modulus (GPa)	350–450	220–300
Tensile strength (MPa)	3500–5500	3500–6200
Elongation-to-failure (%)	0.1–1.0	1.3–2.2
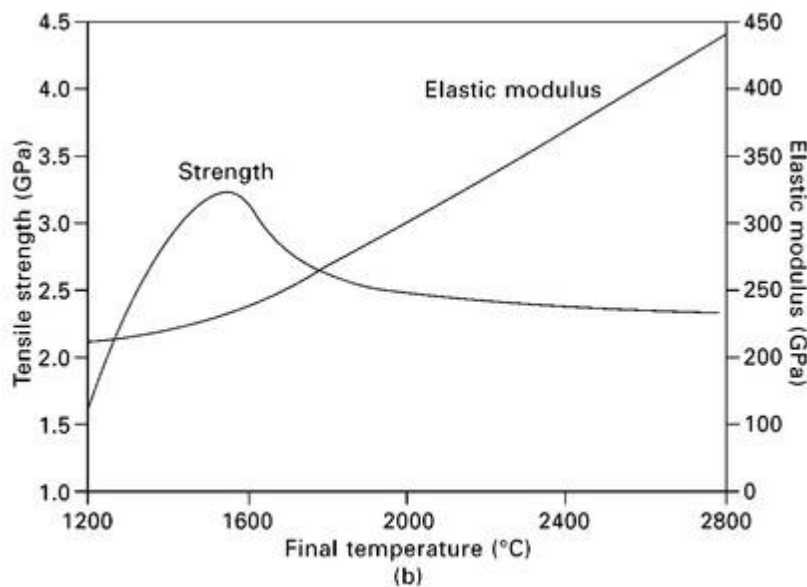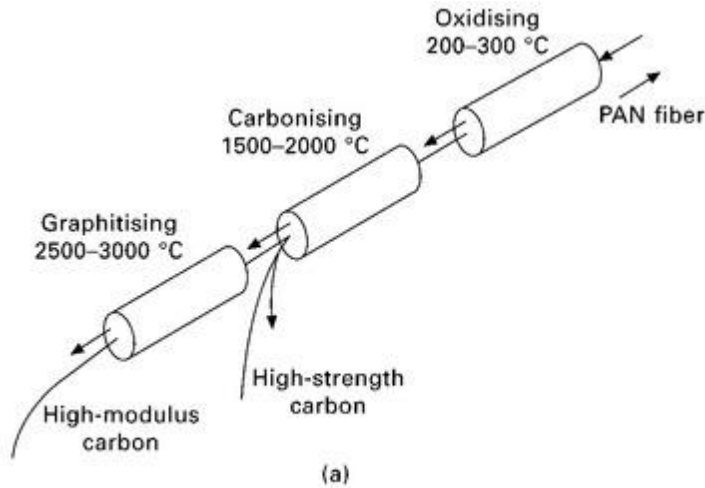
14.5 (a) Production process for carbon fibres; (b) effect of final processing temperature on the tensile modulus and strength of carbon fibre.

By appropriate choice of the final process temperature it is possible to control the elastic modulus and strength of carbon fibres for specific structural applications. For instance, carbon fibres used in composite structures which require a high strength-to-weight ratio, such as the wing box, are pyrolysed at 1500–1600 °C to yield high strengths of 3500–6000 MPa. Structures needing a high stiffness-to-weight ratio such as the control surfaces may contain high stiffness fibres heated at 2500–3000 °C which have an elastic modulus of 350–450 GPa. Structures that require both high stiffness and strength such as the fuselage and wings may contain intermediate modulus fibres.

The properties of carbon fibres are determined by the internal arrangement of the graphite sheets, which is controlled by the final temperature. A single carbon filament is a long rod with a diameter of 7–8 μm. Packed within PAN-based fibres are tiny ribbon-like carbon crystallites which are called turbostratic graphite. In turbostratic graphite, the graphite sheets are haphazardly folded or crumpled together as shown in <u>Fig. 14.6</u>. The intertwined sheets are orientated more or less parallel with the fibre axis, and this crystal alignment makes the fibres very strong along their axis. This arrangement also makes the fibres highly

anisotropic; the interatomic forces are much stronger along than between the sheets. For instance, the stiffness along the fibre axis is typically 15 to 30 times higher than across the fibre.
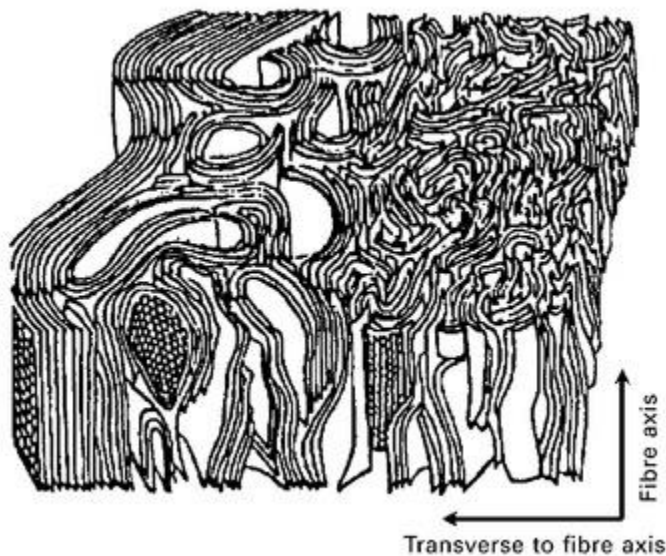
14.6 Three-dimensional representation of the turbostratic graphite structure of PAN-based carbon fibre (from S. C. Bennett and D. J. Johnston, *'Structural heterogeneity in carbon fibers'*, *Proceedings of the 5th London carbon and graphite conference,* Vol. 1, Society for Chemical Industries, London, 1978, pp. 377–386).

The stiffness of carbon fibre is dependent on the alignment of the crystalline ribbons and the degree of perfection of the graphite structure. The length and straightness of the graphite ribbons determines the fibre stiffness. The order between the ribbons becomes better with increasing temperature (up to 3000 °C), which is the reason for the steady improvement in elastic modulus with the final process temperature.

Fibre strength is determined by the number and size of flaws, which are usually tiny surface cracks. During processing, the fibres are damaged by fine-scale abrasion events when they slide against each other after leaving the furnace and during collimation into bundles. The rubbing action and other damaging events introduces surface cracks that are usually smaller than 100 nm. Although tiny, these cracks have a large impact on fibre strength.

After final heat treatment, carbon fibres are surface treated with various chemicals called the size which serves several functions. A thin film of chemicals is applied to the fibre surface to increase its bond strength to the polymer matrix. Carbon does not adhere strongly to most polymers, including epoxies, and it is necessary to coat the fibre surface with a thin sizing film to promote strong bonding. Size agents are also used to reduce friction damage between fibres. Shortly after the final heat treatment, the individual carbon fibres are collimated into bundles (which are also called tows) for ease of handling.

Section 14.11 at the end of this chapter presents a case study of carbon nanotubes in composites.

14.2.2 GLASS FIBRES: PRODUCTION, STRUCTURE AND PROPERTIES

Glass fibre composites are used sparingly in aircraft structures owing to their low stiffness. Glass fibre has a low elastic modulus (between 3 to 6 times lower than carbon fibre) which gives glass-reinforced composites a comparatively low stiffness-to-weight ratio. Glass fibre composites are only used in structures where specific stiffness is not a design factor, which is mainly secondary components such as aircraft fairings and helicopter structures such as the cabin shell. Glass fibre composites have low dielectric

properties and, therefore, are used when transparency to electromagnetic radiation (i.e. radar waves) is important, such as radomes and aerial covers.

Despite the restricted use of glass-reinforced composites in components where stiffness is a critical property, whenever possible they are used instead of carbon-fibre materials because of their lower cost. Glass fibres are anywhere from 10 to 100 times cheaper than carbon fibres. The greatest use of glass-reinforced composite is inside the aircraft cabin. The majority of cabin fittings, including overhead luggage storage containers and partitions, are fabricated using glass fibre-phenolic resin composite that is inexpensive and lightweight with good flammability resistance.

Glass fibre is a generic name similar to carbon fibre or steel, and as for these materials there are various types having different properties. Glass fibres are based on silica (SiO_2) with additions of oxides of calcium, boron, iron and aluminium. It is the different concentrations of metal oxides that allow different glass types to be produced. There are two types of glass fibres used for aircraft applications: E-glass (short for electrical grade) and S-glass (structural grade). E-glass is cheaper and lower in strength than S-glass and, therefore, is used mostly in composites for aircraft cabin fittings that do not require high structural properties. The higher strength S-glass composite is used in structural components. The composition and engineering properties of E- and S-glass fibres are given in Table 14.2.

Table 14.2

Composition and properties of E-glass and S-glass fibres

	E-glass	S-glass
Composition (%)		
SiO_2	52	64
CaO	17	
$Al_2O_3 + F_2O_3$	14	25
B_2O_3	11	
MgO	4.6	10
$Na_2O + K_2O$	0.8	0.3
Properties		
Density (g cm^{-3})	2.6	2.5
Young's modulus (GPa)	76	86
Tensile strength (MPa)	3500	4600

The internal structure of glass fibre is different from carbon fibre. Glass consists of a silica network structure containing metal oxides, as shown in Fig. 14.7. The network is a three-dimensional structure and, therefore, the fibre properties are isotropic, thus (unlike carbon) the elastic modulus is the same parallel and transverse to the fibre axis.
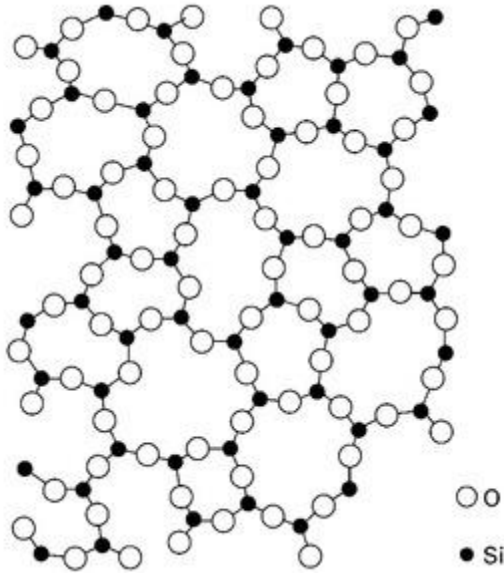
14.7 Internal molecular structure of glass fibre. The metal oxides in glass are not shown.

Glass fibre is manufactured using a viscous drawing process whereby silica and metal oxide powders are initially blended and melted together in a furnace at about 1400–1500 °C. The molten glass flows from the furnace via bushings or spinnerets containing a large number of tiny holes. The glass solidifies into thin continuous fibres as it passes through the holes. The fibre diameter is around 12 μm. Upon leaving the furnace the fibres are cooled using a water spray mist and then coated with a thin layer of size. The size consists of several functional components including chemicals to improve adhesion with the polymer matrix and lubricants to minimise surface abrasion during handling.

14.2.3 ARAMID (KEVLAR) FIBRES: PRODUCTION, STRUCTURE AND PROPERTIES

Synthetic organic fibres are used in polymer composites for specific aerospace applications. Organic fibres are crystalline polymers with their molecular chains aligned along the fibre axis for high strength. Examples of organic fibres are Dyneema® and Spectra®, which are both ultra-high-molecular-weight polyethylene filaments with high-strength properties. Of the many types of organic fibres, the most important for aerospace is aramid, whose name is a shortened form of aromatic polyamide (poly-p-phenylene terephthalamide). Aramid is also called Kevlar which is produced by the chemical company Du Pont.

The most common aerospace application for aramid fibre composites is for components that require impact resistance against high-speed projectiles. Aramid fibres absorb a large amount of energy during fracture, thus providing high perforation resistance when hit by a fast projectile. For this reason, aramid fibre composites are used for ballistic protection on military aircraft and helicopters. They are also used for containment rings in jet engines in the event of blade failure. Aramid composites, similarly to glass-reinforced composites, have good dielectric properties, making them suitable for radomes. Aramid composites also have good vibration damping properties, and therefore are used in components such as helicopter engine casings to prevent vibrations from the main rotor blades reaching the cabin. Figure 14.8 shows the vibration damping loss factor for several aerospace materials; aramid–epoxy has ten times the loss decrement of carbon–epoxy and nearly 200 times higher than aluminium.
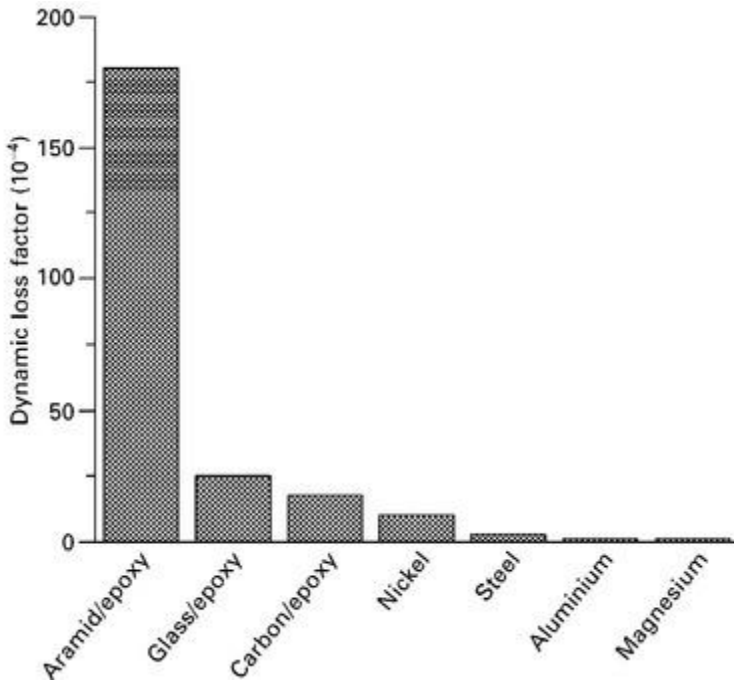
14.8 Vibration loss damping factor of aramid–epoxy composite compared with other aerospace materials.

The process of producing aramid fibres begins by dissolving the polymer in strong acid to produce a liquid chemical blend. The blend is extruded through a spinneret at about 100 °C which causes randomly oriented liquid crystal domains to develop and align in the flow direction. Fibres form during the extrusion process into highly crystalline, rod-like polymer chains with near perfect molecular orientation in the forming direction. The molecular chains are grouped into distinct domains called fibrils. The fibre essentially consists of bundles of fibrils that are stiff and strong along their axis but weakly bonded together, as shown in Fig. 14.9. As for carbon fibres, aramid fibres are highly anisotropic with their modulus and strength along the fibre axis being much greater than in the transverse direction. The properties of two common types of aramid fibre are given in Table 14.3, and they exceed the specific stiffness and strength of glass fibres. Aramid fibre composites are lightweight with high stiffness and strength in tension. However, these materials have poor compression strength (which is only about 10–20% the tensile strength) owing to low micro-buckling resistance of the aramid fibrils. Therefore, aramid composites should not be used in aircraft components subject to compression loads. Aramid fibres can absorb large amounts of water and are damaged by long-term exposure to ultraviolet radiation. Therefore, the surface of aramid composites must be protected to avoid environmental degradation.

Table 14.3

Comparison of average properties of aramid fibres against glass and carbon fibres

Property	Kevlar (Type 29)	Kevlar (Type 49)	E-glass	IM Carbon
Density (g cm^{-3})	1.44	1.44	2.6	1.8
Young's modulus (GPa)	70.5	112.4	76	230
Specific modulus (GPa m^3 kg^{-1})	49	78	29	128
Tensile strength (GPa)	2.9	3.0	3.5	4.2
Specific strength (GPa m^3 kg^{-1})	2	2.1	1.3	2.3
Elongation-to-failure (%)	3.6	2.4	4.8	1.9
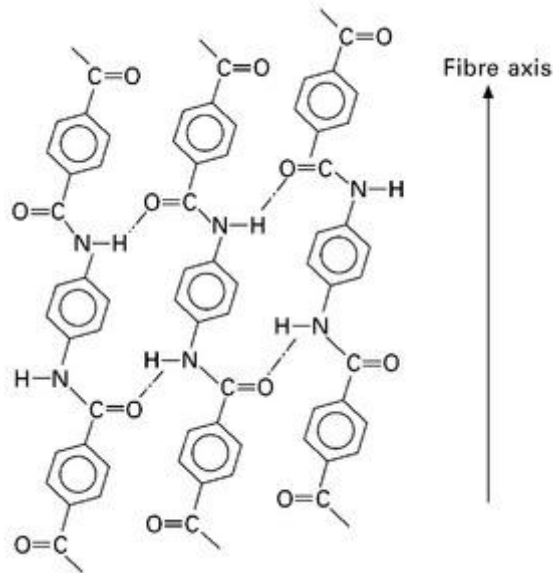
14.9 Polymer chains aligned in the fibre direction in aramid.

14.3 Production of prepregs and fabrics

Composite aircraft components contain anywhere from tens of thousands to many millions of fibres. For example, an average-sized wing panel made using carbon–epoxy composite comprises of the order of 20 000 million fibres. Fibres are too fine to easily handle and process into composite parts, with carbon fibres being only 1/10 to 1/20 the width of human hair (Fig. 14.10). Therefore, upon leaving the furnace the fibres are bundled together into tows or yarns. Aerospace fibres are collimated into tows that usually contain about 3 K (3000), 12 K (12 000) or 24 K (24 000) filaments (Fig. 14.11). These bundles are then used to make prepreg (resin pre-impregnated) material or dry fabric for the production of composite parts.
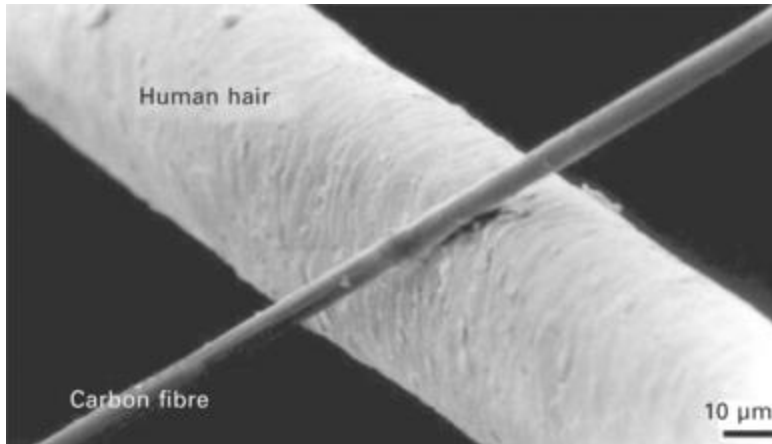
14.10 Comparison of the width of carbon fibre and human hair.
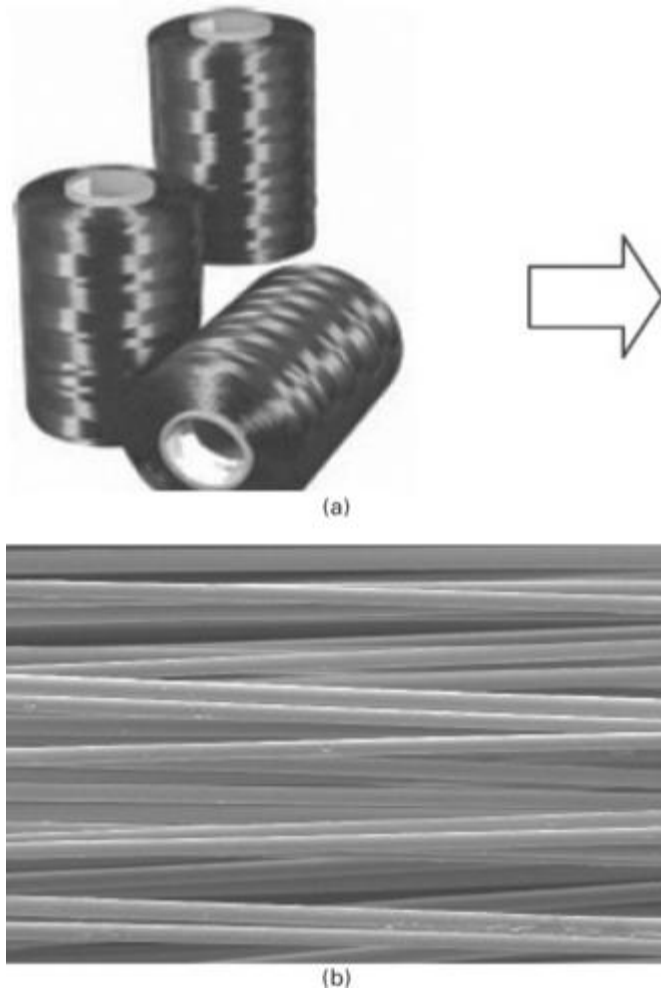
14.11 (a) Fibres bundled into a tow. (b) Internal view of a tow showing many individual fibres.

14.3.1 PREPREGS

Major aircraft manufacturers use prepreg tape in the production of composite structural components. The term prepreg is short form for pre-impregnated fibres. Prepreg is a two-part sheet material consisting of fibres (e.g. carbon) and partially cured resin (e.g. epoxy). The most common prepreg used in aircraft is carbon–epoxy, although many other types are used including carbon–bismaleimide, S-glass–epoxy and aramid-epoxy. The benefits of using prepreg include accurate control of the fibre volume content and the ability to achieve high fibre content, thus allowing high-quality composite components to be produced with high mechanical properties.

Several methods are used to produce prepreg, the most common being the solution dip, solution spray, and hot-melt techniques. The solution dip method involves dissolving the resin in solvent to a solids concentration of 40–50%. Fibres are then passed through the solution so that they pick up an amount of resin solids. The fibres leave the solution coated with a thin film of resin, and they are then pressed into thin sheets of prepreg. The solution spray method simply involves spraying liquid resin onto the fibres whereas the hot-melt technique involves direct coating of the fibres with a low viscosity resin.

After the prepreg is produced, the resin is partially cured to a condition where it is semisolid; it is too hard to flow like a liquid but soft enough to be pliable and flexible. The resin needs to be hard enough so it does not leak out from between the fibres during the cutting and laying of the prepreg plies. The resin also needs to be soft enough to allow the prepreg to be easily deformed to the shape of the composite component. The resin must be tacky enough (sticky to touch) in order to bond the prepreg layers together during the lay-up of the composite. Epoxy resin used in carbon-fibre prepreg is slightly cured to a semisolid condition, whereby the crosslinking between the polymer chains is about 15–30% complete. Prepreg in this condition is called B-stage cured. The prepreg must be stored at low temperature (about − 20 °C) inside a freezer to avoid further curing and crosslinking of the resin matrix which occurs at room temperature.

B-stage cure prepreg is produced as a thin sheet (usually 0.1–0.4 mm thick) with a fibre content of 58–64%. The prepreg is protected on both sides with easily removable separators called backing paper. Backing paper stops the prepreg sheets from sticking to each other before the lay-up of the composite part. Prepreg is used in the manufacture of composite parts by simply cutting to shape and size, removing the backing paper, laying the prepreg sheets in a stack in the preferred fibre orientation, and then consolidating and curing the final composite material using an autoclave as described in 14.5.1.

14.3.2 DRY FABRICS

The aerospace industry is increasingly using dry carbon fabric instead of carbon-fibre prepreg to manufacture aircraft structures. There are several advantages gained by using fabric rather than prepreg, including lower material cost, infinite storage life, no need for storage in a freezer, and better formability into complex shapes. The most common fabric is woven fabric produced on weaving looms, and the main styles are plain, twill and satin weaves as shown in Fig. 14.12. Woven fabrics contain fibre tows aligned in the warp direction (which is the weaving direction) and the weft direction, which is perpendicular to the warp. In plain woven fabric, each warp tow alternately crosses over and under each intersecting weft tow. Twill and satin fabrics are woven such that the tows go over and under multiple tows. When observed from the side, weaving causes periodic out-of-plane waviness of the fibres. The waviness results in significant loss in stiffness and strength of the composite because maximum structural performance is achieved when the fibres are absolutely straight and in-plane. Twill and satin weaves have lower degrees of fibre waviness than plain weave, and therefore their composites have higher in-plane mechanical properties. For this reason, twill and satin woven fabrics are preferred over plain woven fabric in the fabrication of aerospace composite components.
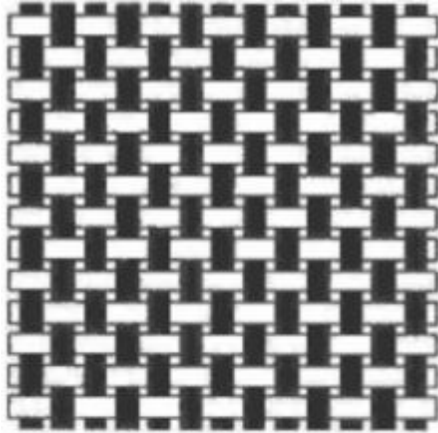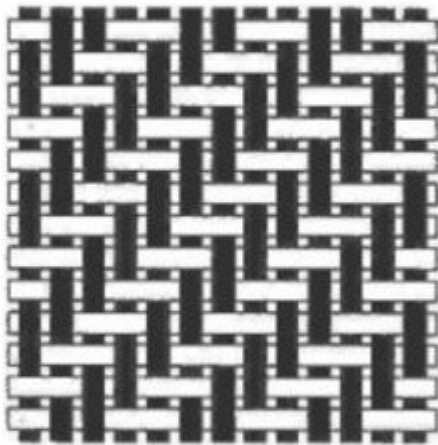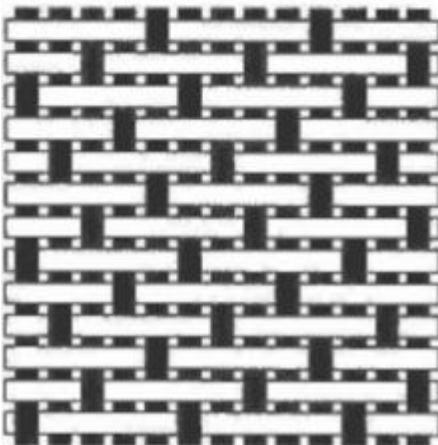
14.12 Common weave architectures: (a) plain, (b) twill and (c) satin.

Other types of fabric used in aircraft composite parts include non-crimp, braided and knitted fabrics. Non-crimp fabric consists of multiple layers of straight tows oriented at different angles, which are bound together by through-thickness stitches. The tows in non-crimp fabric are not forced to interlace with other

tows to produce a weave, and therefore the fibres are straight and in-plane for high structural performance. Braided and knitted fabrics are used when high impact collision resistance and high conformed shapes in composite components are required, respectively, although they have low in-plane mechanical properties. A family of fabrics containing fibre tows aligned in the in-plane direction together with tows running in the through-thickness direction are available for damage tolerant aircraft composite components. The fabrics have a three-dimensional array of fibres, as shown schematically in Fig. 14.13, which allows in-plane and through-thickness loads to be carried by the composite. Composite laminates made using woven fabrics (such as those shown in Fig. 14.13) do not have through-thickness fibres. Such composites have low through-thickness strength and damage resistance. Composites containing a three-dimensional fibre structure have superior damage tolerance because the through-thickness fibres can carry out-of-plane loads. There are various types of three-dimensional fabrics that are produced by orthogonal weaving, stitching, tufting and other specialist techniques. The application for these types of fabrics in aircraft structures is currently limited, although their use is expected to grow.

14.13 Three-dimensional fibre tow structure of fabrics.

14.4 Core materials for sandwich composites

Many aircraft structural components are required to carry only light or moderate loads. When a small load is applied on a composite laminate, the structure is designed with a thin skin and few ribs, frames and spars to reduce weight. When the skin becomes too thin and the stiffeners too few then the structure loses its resistance against buckling and, therefore, some additional form of stiffening is required. A common solution is to build the laminate skins as a sandwich by inserting a lightweight filler or core layer. Under bending, the skins carry in-plane tension and compression loads whereas the core is subjected to shear, as shown in Fig. 14.14. The skin-core construction greatly increases the bending stiffness and thereby makes sandwich structures more resistant to buckling, with only a small increase in weight. Examples of aircraft components made using sandwich composites are control surfaces (e.g. ailerons, flaps) and vertical tailplanes.
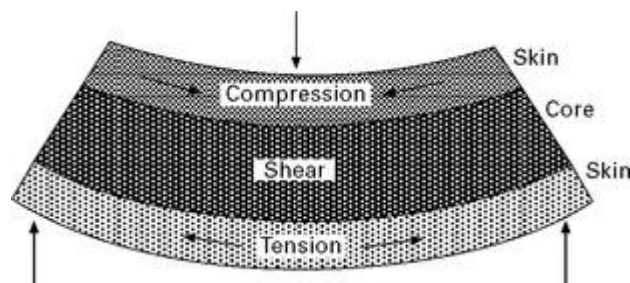
14.14 Basic loading of sandwich composite.

Various types of materials are used for the core, with aluminium honeycomb and Nomex being the most common in aircraft sandwich components. Nomex is the tradename for a honeycomb material based on aramid fibres in a phenolic-resin matrix. Aluminium and Nomex core materials have a lightweight cellular honeycomb structure, which provides high shear stiffness (Fig. 14.15). The aerospace industry is increasingly using polymer foams instead of aluminium honeycomb and Nomex because of their superior durability and high-temperature properties. Examples of polymer foams are polyetherimide (PEI) and polymethacrylimide (PMI), and these materials have a low density cellular structure which has high specific stiffness and strength (Fig. 14.16).
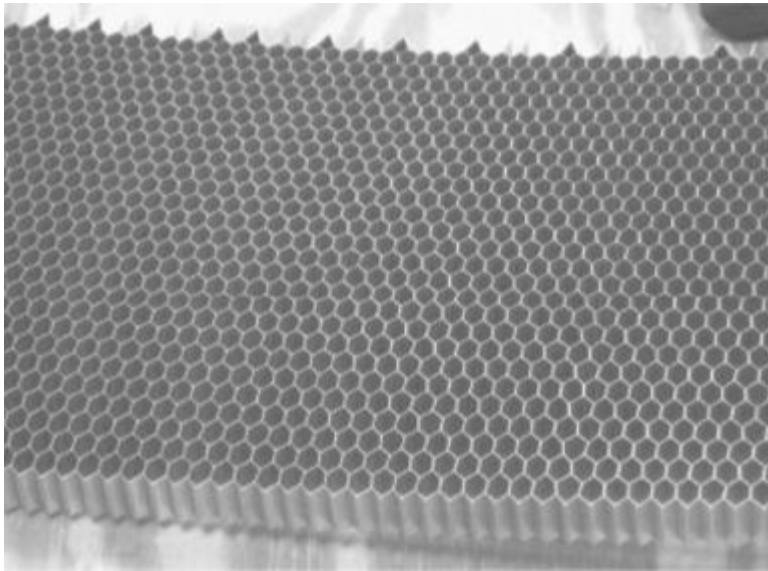
14.15 Honeycomb structure of aluminium.
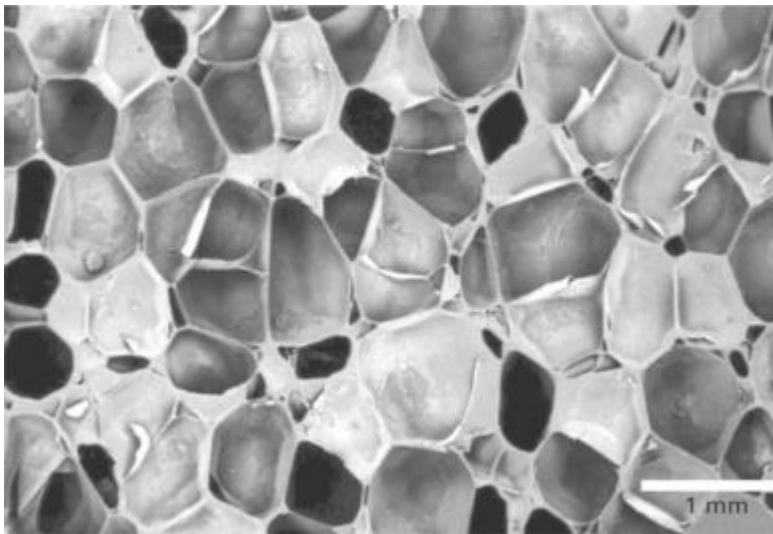
14.16 Cellular microstructure of polymer foams.

14.5 Composites manufacturing using prepreg

14.5.1 MANUAL LAY-UP

Composites have been fabricated using prepreg since the 1970s, and the original fabrication method involved the manual lay-up of the prepreg plies into the orientation and shape of the final component. Manual lay-up involves cutting the prepreg to size, removing the backing paper, and then stacking the prepreg plies by hand onto the tool surface. This process is slow, labour-intensive and inconsistent because of human error in the accurate positioning of the plies. For these reasons, manual hand-lay is rarely used in the construction of large composite components, although it is still used for making small numbers of parts when it is not economically viable to automate the process.

The prepreg is laid-up by hand directly onto the tool, which has the shape of the final component. The prepreg plies are oriented with their fibres aligned in the main loading directions acting on the component when used in service. The most common pattern used in the lay-up of plies for aircraft components is [0/+ 45/–45/90], which is shown in Fig. 14.17. A composite with this lay-up is called quasi-isotropic because the stiffness and strength properties are roughly equal when loaded along any in-plane direction. The 0° and 90° fibres carry the in-plane tension, compression and bending loa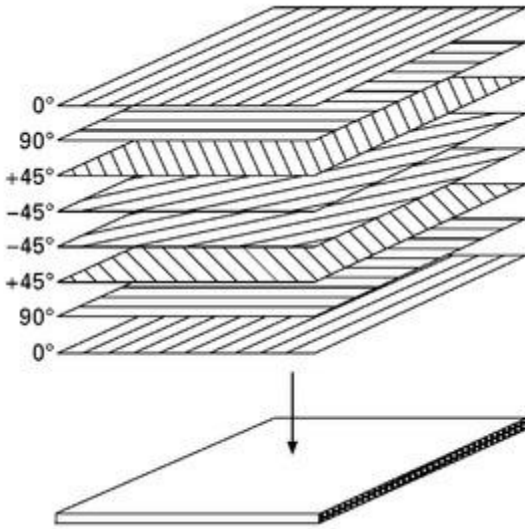ds whereas the 45° fibres support shear loads. Another common ply pattern is [0/90], known as cross-ply, which is used for composite components subject to in-plane tension or compression loads in service, but not shear loads.

14.17 Ply orientations for quasi-isotropic cross-ply composite reproduced with permission from D. R. Askeland, *The science and engineering of materials,* Stanley Thornes (Publishers) Ltd., 1998.

It is important that the orientation of the plies is symmetric around the mid-plane to ensure the material is balanced. That is, the plies in the upper half of the prepreg stack must be arranged as a mirror image of the plies in the lower half. If this does not occur, then the ply pattern is asymmetric and it is possible that the composite may distort or warp after the prepreg is cured. The symmetric lay-up of plies is required for all composite fabrication processes, and not just for prepreg.

After the prepreg is stacked to the correct ply orientation and thickness, it is then compacted by vacuum bagging to remove air from between the ply layers. The prepreg stack is sealed within a plastic bag from which air is removed using a vacuum pump, as shown in Fig. 14.18. The bag is a flexible membrane that conforms to the shape of the prepreg and the underlying tool to ensure good dimensional tolerance. Release film and bleeder layer cloth are placed over the prepreg stack within the vacuum bag. Release film, which is a nonstick flexible sheet containing tiny holes, is used to stop the prepreg from sticking to the bleeder cloth. This cloth is used to absorb excess resin, which is squeezed from the prepreg during consolidation.

The prepreg is consolidated and cured within an autoclave, and excess resin flows from the prepreg through the fine holes in the release film into the bleeder layer where it is absorbed.
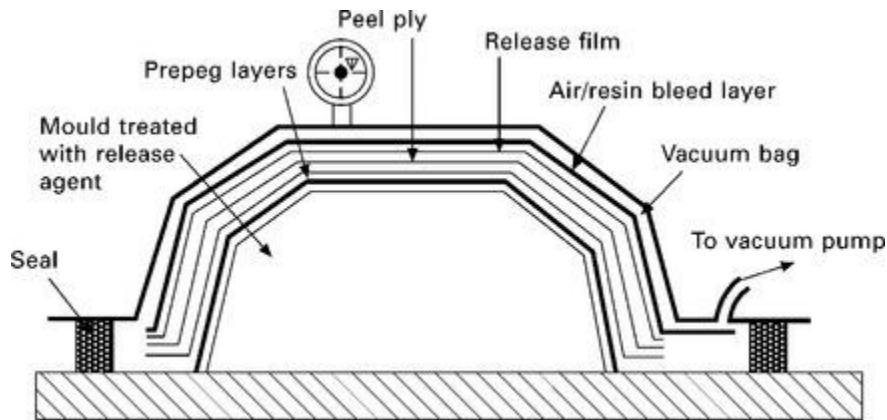
14.18 Schematic of vacuum bagging operation (from azom.com).

The final stage in the fabrication of prepreg composite involves consolidation and curing inside an autoclave (Fig. 14.19). The prepreg, which is resting on the tool and enclosed within the vacuum bag, is placed inside an autoclave, which is a closed pressure chamber in which consolidation and cure processes occur under the simultaneous application of pressure and high temperature. An autoclave is a large pressure cooker, in which the prepreg is compacted using pressurised nitrogen and carbon dioxide to over 700 kPa. At the same time, the autoclave is heated to cure the polymer matrix, which for a carbon–epoxy prepreg requires temperatures of 120–180 °C. The combined action of pressure and heat consolidates the composite, removes trapped air, and cures the polymer matrix. The autoclave process produces high-quality composites with high fibre contents (60–65% by volume) which are suitable for primary and secondary components for aircraft and helicopters.
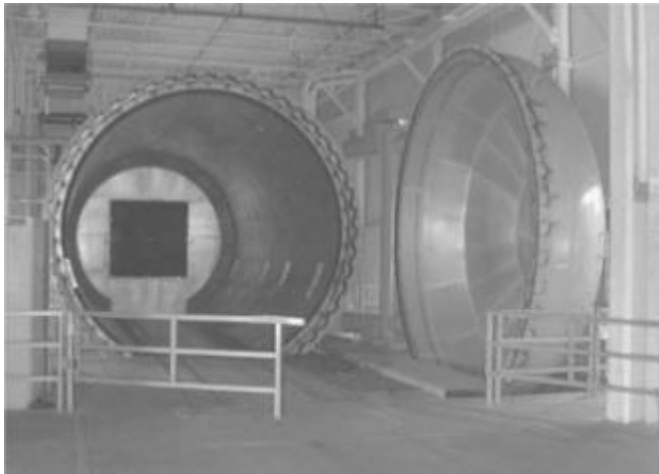
14.19 Autoclave used for consolidation and curing of prepreg composite.

The production of composite components using the autoclave process is practised throughout the aircraft industry. However, the industry is also using other manufacturing processes, as described in the following sections, that avoid the need for an autoclave. Autoclaves are expensive and can only produce components of limited size (less than about 15 m long and 4 m wide).

14.5.2 AUTOMATED TAPE LAY-UP

Automated tape lay-up (ATL) is an automated process used to lay-up prepreg tape in the fabrication of composite aircraft structures. The process is used in the manufacture of carbon–epoxy prepreg components for both military and commercial aircraft. Examples of military parts made using ATL are the wing skins of the F-22 *Raptor,* tilt rotor wing skins of the V-22 *Osprey,* and skins of the wing and stabiliser of the B-1 *Lancer* and B-2 *Spirit* bombers. ATL is used in the production of empennage parts (e.g. spars, ribs, I-beam stiffeners) for the B777, A340-500/600 and A380 airliners.

ATL is used instead of manual lay-up to reduce the time (by more than 70–85%) and cost spent in the lay-up of prepreg tape on the tool. For instance, the lay-up rate in the production of the primary wing spar to the Airbus A400M is increased from 1 to 1.5 kg h^{-1} of prepreg with manual lay-up to about 18 kg h^{-1} with ATL. The first wing spars to be produced using manual lay-up took about 180 h whereas the lay-up time using the ATL process is only 1.5 h. Other benefits of the ATL process include less material scrap and better repeatability and consistency of the manufactured parts.

The key component of the ATL process is a computer numerically controlled tape-laying head that deposits prepreg onto the tool at a fast rate with great accuracy (Fig. 14.20). The head device is suspended via a multi-axis gantry above the tool surface. A roll of prepreg (75–300 mm wide) in the tape-laying head is deposited on the tool in the desired orientations according to a programmed routine. As the tape is laid down, the head removes the backing paper and applies a compaction force onto the prepreg. The head can also apply moderate heat to the prepreg to improve tackiness and formability. The head is programmed to follow the exact contour of the tool at a speed of about 50 m min^{-1} for the rapid deposition of prepreg (4–45 kg h^{-1}). When the tape-laying head reaches the location where the ply terminates then the tape is automatically cut by blades within the head, the head changes direction, and the tape laying process continues. The head can lay any number of prepreg plies on top of each other in a series of numerically controlled steps with a high degree of accuracy, thereby assuring consistent shape, thickness and quality for the part. After the automated tape lay-up is complete, the prepreg is consolidated and cured. The ATL process is capable of producing composite parts with a flat or slightly curved profile; it is not suited for highly contoured parts which are better made using the automated fibre placement process.
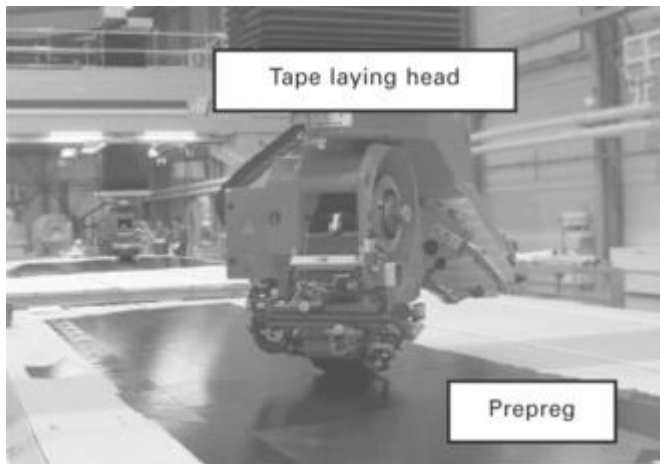
14.20 ATL process in the manufacture of aircraft panels.

14.5.3 AUTOMATED FIBRE PLACEMENT

Automated fibre placement (AFP) is used in the automated production of large aircraft structures from prepreg (Fig. 14.21). The process involves the lay-up of individual prepreg tows onto a mandrel using a numerically controlled fibre-placement machine. In the AFP process, prepreg tows or narrow strips of prepreg tape are pulled off holding spools and fed into the fibre placement head. Within the head, the tows,

which contain about 12 000 fibres and are approximately 3 mm wide, are collimated into bundles of 12, 24 or 32 tows to produce a narrow band of prepreg material that is deposited onto the mandrel which has the shape of the final component. The placement head is computer controlled via a gantry system suspended above the mandrel. During fibre placement, the mandrel is rotated so the prepreg is wound into the shape of the component. The head moves along the rotating mandrel to steer the fibres so they follow the applied stresses acting on the finished component in service. The head is able to stop, cut the prepreg, change direction and then re-start the lay-down of prepreg tows until the material is built up to the required thickness. Each tow is dispensed from the head at a controlled speed to allow it conform to the mandrel surface, thereby allowing highly curved components to be produced, not possible with ATL. After the lay-up process is complete, the prepreg is cured in the same way as composites manufactured by manual lay-up or ATL.
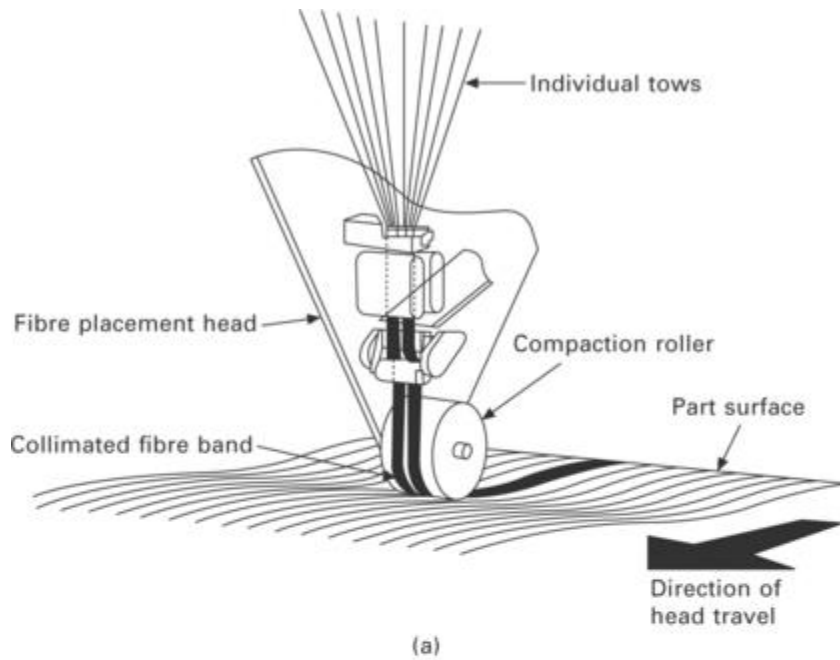
14.21 (a) Schematic of the automated fibre placement process. (b) ATL process in the construction of fuselage barrels for the B787 aircraft. Photograph by B. Nettles, Charleston Post and Courier.

The AFP process is used by the aerospace industry to fabricate large-circumference and highly contoured structures such as fuselage barrels, ducts, cowls, nozzle cones, spars and pressure tanks. The process is used in the construction of carbon–epoxy fuselage sections to the B787 *Dreamliner,* V-22 *Osprey,* and the *Premier* 1 and Hawker *Horizon* business jets. For the *Premier* 1, the AFP process is used to construct one-piece carbon–epoxy fuselage barrels measuring 4.5 m long and 2 m at the widest point. AFP is used to fabricate inlet ducts, side skins and covers to the F-18 E/F *Superhornet.*

14.6 Composites manufacturing by resin infusion

The aerospace industry is increasingly using manufacturing processes that do not rely on prepreg to produce composite components. Composites made using prepreg are high-quality materials with excellent mechanical properties owing to their high fibre content. However, prepreg is expensive, must be stored in a freezer, has limited shelf-life (usually 1–2 years), and must be cured in an autoclave which is slow and expensive. The aerospace industry is also keen to use 'out of autoclave' processes because of the faster manufacturing times and lower cost.

The industry is producing composite components using dry fabric which is infused with liquid resin and then immediately consolidated and cured. The types of fabrics used include the plain, twill, satin, knitted and non-crimped materials. These fabrics are infused with resin using one of several manufacturing processes, including resin transfer moulding, vacuum bag resin infusion, resin film infusion, filament winding and pultrusion. Many aerostructure companies also use their own proprietary manufacturing process that is developed in-house. Not all of the many processes are described here; instead just a few are outlined to illustrate the diversity of the processes.

14.6.1 RESIN TRANSFER MOULDING (RTM)

Resin transfer moulding (RTM) is used to fabricate composite components of moderate size (typically under 3 m), such as the fan blades of F135 engines and the spars and ribs for the mid-section fuselage and empennage of the F-35 *Lightning II* fighter. RTM is a closed-mould process that is illustrated in Fig. 14.22. Fabric is placed inside the cavity between two matched moulds with their inner surfaces having the shape of the final component. Fabric plies are stacked to the required orientation and thickness inside the mould, which is then sealed and clamped. Liquid resin is injected into the mould by means of a pump. The resin flows through the open spaces of the fabric until the mould is completely filled. The resin viscosity must be low enough for easy flow through the tiny gaps between the fibres and tows of the fabric. Aerospace-grade resins with low viscosity have been specifically developed for the RTM process. After injection, the mould is heated in order to gel and cure the polymer matrix to form a solid composite part. After curing, the mould is opened and the part removed for edge trimming and final finishing.
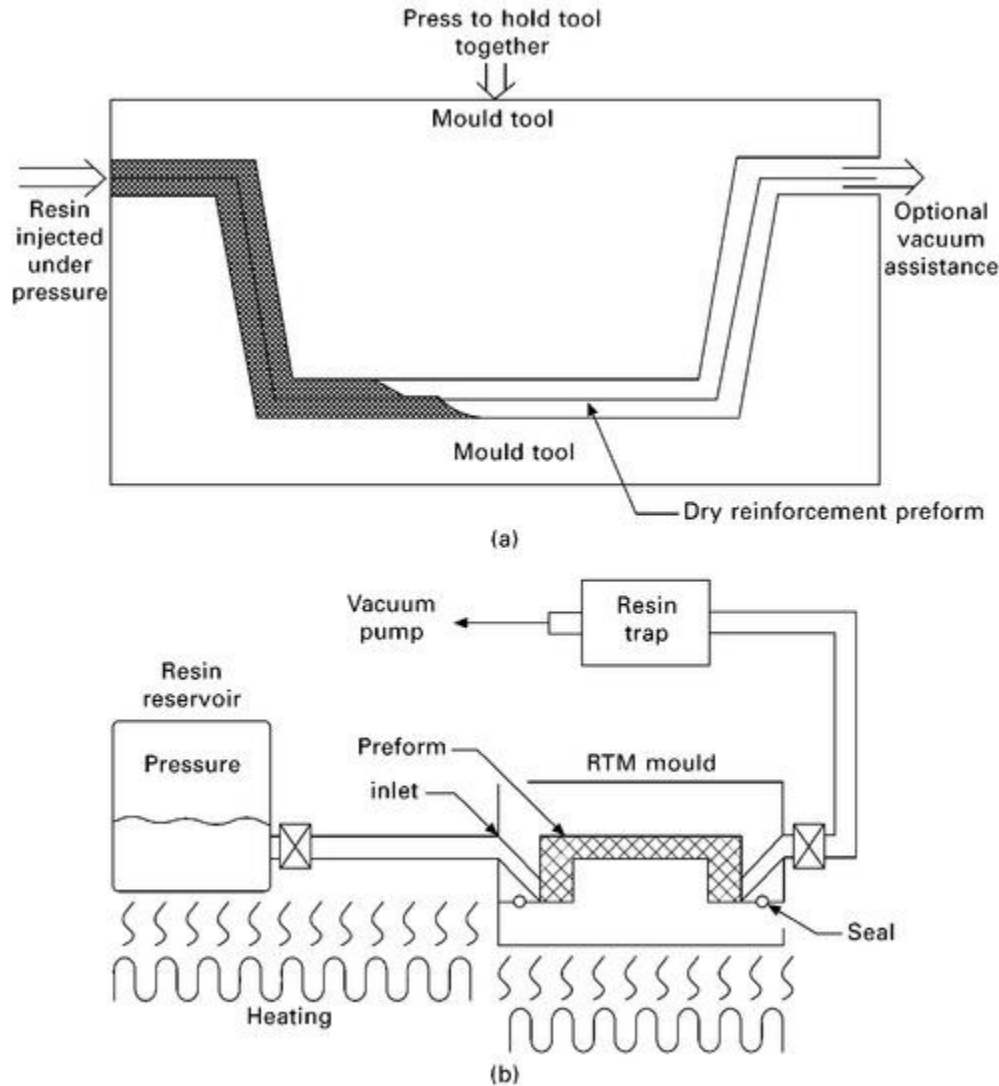
14.22 Schematics of the (a) resin transfer moulding and (b) vacuum assisted resin transfer moulding processes.

The RTM process can produce composites with high fibre volume content (up to 65%), making them suitable for primary aircraft structures that require high stiffness, strength and fatigue performance. However, it can be difficult to completely infuse some types of fabric with resin which leaves dry spots or voids in the cured composite. Furthermore, the fibre architecture can be disturbed by the high flow pressures needed to force the resin through some fabrics. To minimise these problems, a variant of the RTM process called vacuum-assisted resin transfer moulding (VARTM) is used.

The VARTM process is shown in Fig. 14.22b, and is different to conventional RTM in that a vacuum-pump system is used to evacuate air from the mould and draw resin through the fabric. After the mould containing the fabric is closed and sealed, a vacuum pump is used to extract air from the cavity placing it in a state of low pressure. Rather than resin being injected into the mould cavity under pressure as in conventional RTM, with VARTM the resin is drawn into the mould under the pressure differential created by the vacuum. Resin percolates between the fibres and tows of the fabric until the mould is filled, at which stage the infusion process stops and the part is cured at elevated temperature.

14.6.2 VACUUM BAG RESIN INFUSION (VBRI)

The vacuum bag resin infusion (VBRI) process and similar processes are used to fabricate various types of carbon–epoxy structural components. Figure 14.23 illustrates the basic configuration of the VBRI process, which uses an open mould rather than the two-piece closed mould of the RTM and VARTM processes. This results in VBRI having lower tooling costs, which can be a large capital cost. Fabric plies are stacked on the tool with the top layer being a resin distribution fabric. The fabric stack is enclosed and sealed within a flexible plastic bag that is connected at one point to a liquid resin source and at another point to a vacuum-pump system. Air is removed by the vacuum pump which causes the bag to squeeze the fabric layers to the shape of the mould surface. This part of the process is similar to the vacuum bagging of prepreg before autoclave curing. In the VBRI process, liquid resin flows into the bag under the pressure differential created by the vacuum pump. Resin is drawn through the tightly consolidated fabric as well as along the top resin distribution fabric, from where it seeps downwards into the fabric. After the fabric is completely infused with resin, the material is cured at high temperature within an oven.
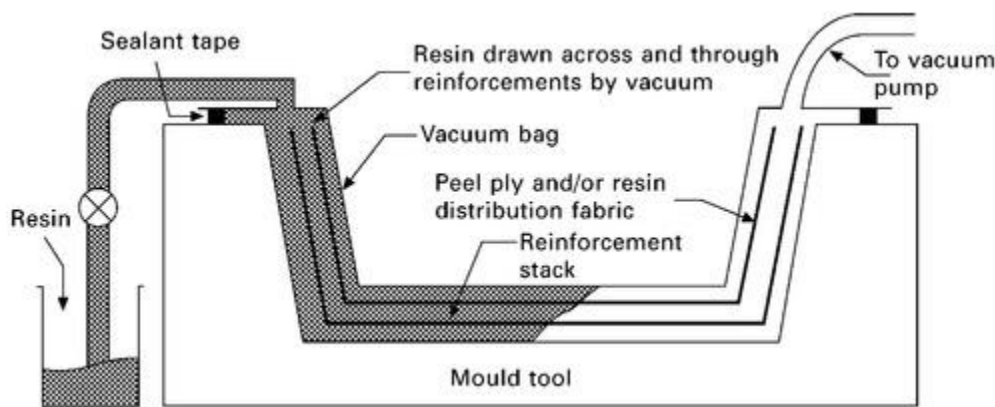
14.23 Schematic of the vacuum bag resin infusion process.

14.6.3 RESIN FILM INFUSION (RFI)

The resin film infusion (RFI) process is suited for making relatively large structures such as stiffened skins and rib-type structures (Fig. 14.24). The process uses an open mould upon which layers of dry fabric and solid resin film are stacked. The film is a B-stage cured resin similar to the cure condition of the resin matrix in prepreg. Film is placed at the bottom, top or between the layers of fabric. The materials are sealed within a vacuum bag and then air is removed using a vacuum pump. The entire assembly is placed into an autoclave and subjected to pressure and heat. The temperature is increased to reduce the resin viscosity to a level when it is fluid enough to flow into the fabric layers under the applied pressure. Once the infusion is complete the pressure and temperature are raised to consolidate and fully cure the component.
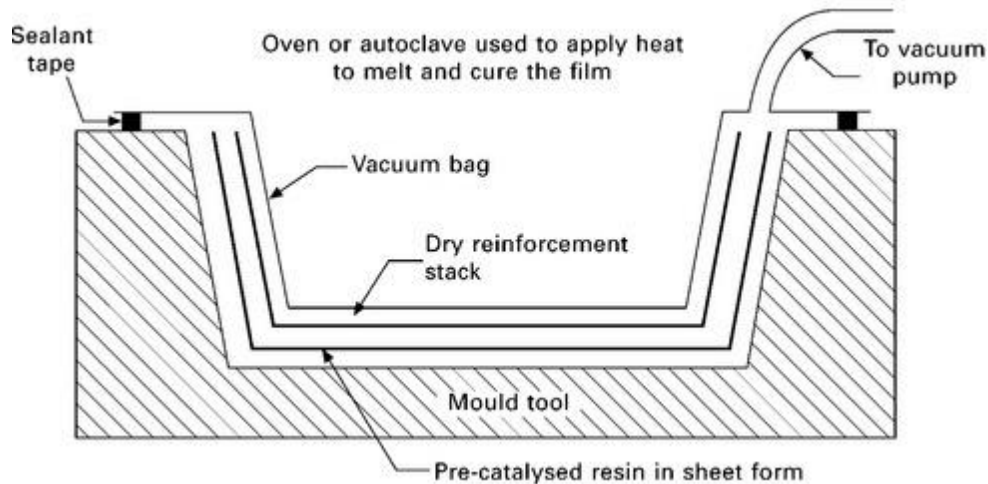
14.24 Schematic of the resin film infusion process.

14.6.4 FILAMENT WINDING

Filament winding is a manufacturing process where cylindrical components are made by winding continuous fibre tows over a rotating or stationary mandrel, as shown in Fig. 14.25. There are two types of filament winding process: wet winding and prepreg winding. Wet winding involves passing continuous tows through a resin bath before reaching a feed head which deposits them onto a cylindrical mandrel. Prepreg winding involves depositing thin strips of prepreg onto the mandrel in a similar manner to the ATP process. The feed head is rotated around the stationary mandrel or, more often, the mandrel is rotated while the feed head passes backwards and forwards along its length. Successive layers of tows are laid down at a constant or varying angle until the desired thickness is reached. Winding angles can range between 25° and 80°, although most winding processes are performed around 45° to provide the part with high hoop stiffness and strength. After winding is complete, the composite is cured at room temperature or at elevated temperature inside an oven or autoclave. The mandrel is then pulled away from the cured composite.

Angle of fibre warp controlled by ratio of carriage speed to rotation speed

Rotating mandrel

Nip rollers

Resin bath

Moving carriage

Fibres

(a)

(b)
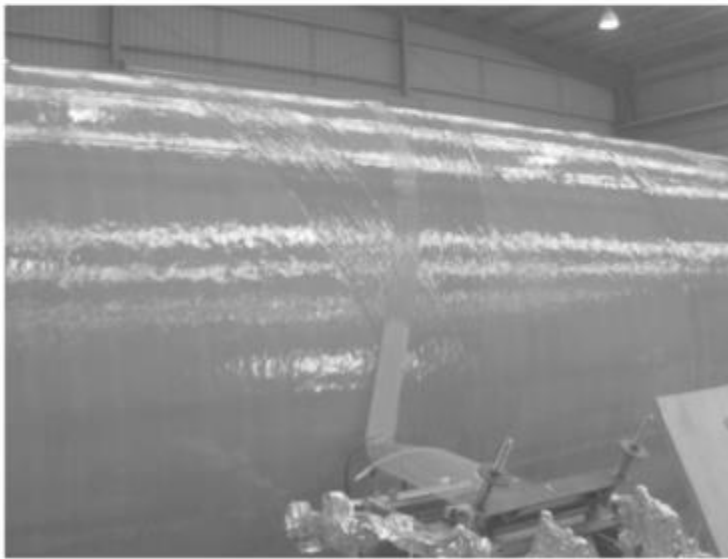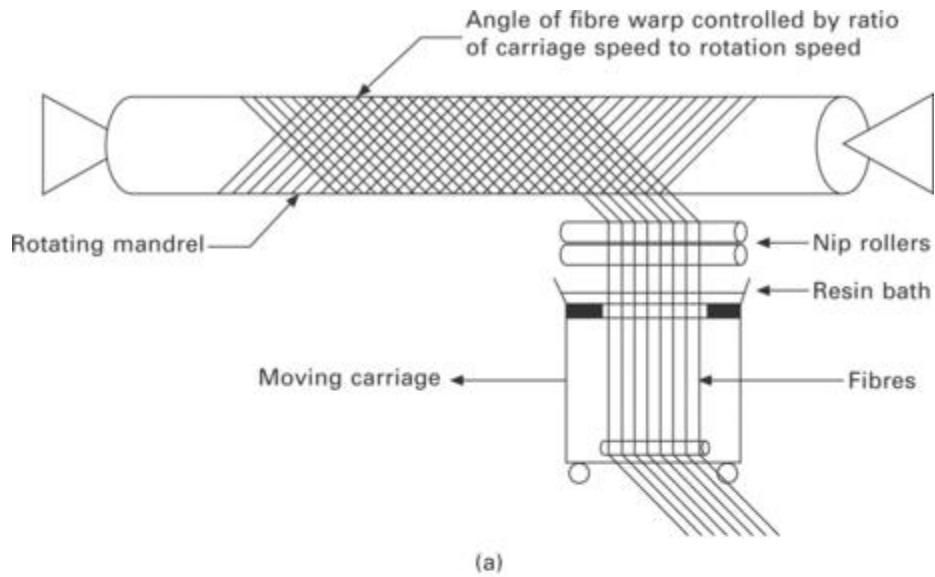
14.25 (a) Schematic and (b) photograph of the filament winding process.

The filament-winding process is used to produce cylindrical composite components. Examples of aerospace components produced using this process include motor cases for Titan IV, Atlas and Delta rockets, pressure vessels, missile launch tubes and drive shafts. Some of these components, such as rocket motor cases, are very large (exceeding 4 m in diameter).

14.6.5 PULTRUSION

Pultrusion is an automated, continuous process used to manufacture composite components with constant cross-section profiles. Figure 14.26 illustrates the pultrusion process which is a linear operation starting from the right-hand side of the diagram. Continuous fibres (tows) are pulled off storage spools and drawn through a liquid resin bath. The resin-impregnated fibres exit the bath and are pulled through a series of wipers that remove excess polymer. After this, the fibre-resin bundles pass through a collimator before entering a heated die which has the shape of the final component. As the material passes through the die it

is formed to shape while the resin is cured. Heated dies are often about 1 m long, and it is essential that, as the material travels through the die, there is sufficient time to fully cure the resin. When the pull-through speed is too fast the composite exits the die in a partially cured condition and when the speed is too slow then the production rate of the process is too slow. The pulling speed for epoxy-based composites is in the range of 10 to 200 cm min^{-1}. The cured composite leaves the die and is cut by a flying saw to a fixed length. Unlike most other manufacturing processes, pultrusion is a continuous process with the material being pulled through the die by a set of mechanically or hydraulically driven grippers.

(a)

(b)
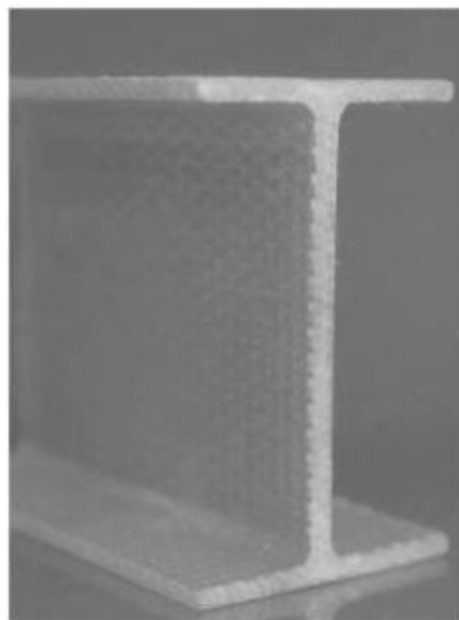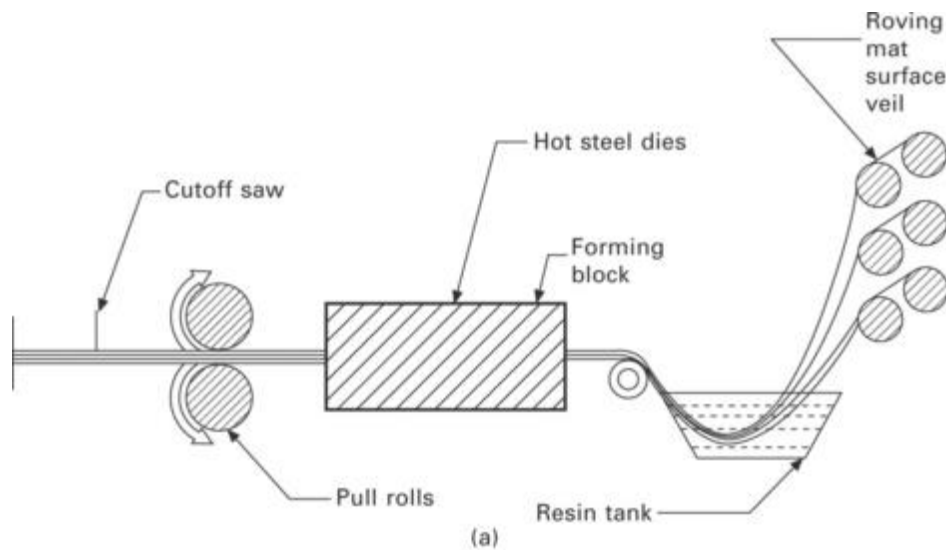
14.26 (a) Schematic of the pultrusion process and (b) I-beam demonstrator for aircraft produced by pultrusion photograph courtesy of the Cooperative Research Centre for Advanced Composite Structures.

There are few examples of pultruded composite components used in aircraft or helicopters. In part, this is because the process produces components having a constant cross-sectional shape with no bends or tapers.

Few aerospace components are flat with a constant cross-section. Another problem is that the process is designed for large production runs whereas the production runs for aircraft are usually measured in the hundreds spread over several years. Nevertheless, the pultrusion process has potential for the production of high-strength floor beams and other selected parts for aircraft.

14.7 Machining of composites

The majority of processes used to manufacture composites produce components to the near-net shape. This is one of the advantages of manufacturing with composites rather than metals, which often require extensive milling and machining to remove large amounts of material to produce the final component. Most machining operations for composites simply involve trimming to remove excess material from the edges and hole drilling for fasteners. Trimming can be performed using high-speed saws and routers, although care is required to avoid edge splitting (delamination damage). The preferred method of trimming carbon–epoxy composites is water jet cutting because of high cut accuracy with little edge damage. Water jet cutting is a process involving the use of a high-pressure stream of water containing hard, tiny particles that cut through the material by erosion. Most water jet systems used by the aerospace industry are high-pressure units that use garnet or aluminium oxide particles as the abrasive.

Hole drilling of composites requires the use of specialist drill bits, several of which are shown in Figure 14.27. The aerospace industry often uses flat two-flute and four-flute dagger drills for carbon–epoxy. Drilling must be performed using a sharp bit at the correct force and feed-rate otherwise the material surrounding the hole is damaged. The application of excessive force causes push-down damage involving delamination cracking ahead of the drill bit (Fig. 14.28). Drilling at a high feed rate can also generate high friction temperatures at the hole, thereby overheating the polymer matrix. Aramid fibre composites are particularly difficult to drill without the correct bit because the fibres have a tendency of fuzz and fray. The aramid drill contains a 'C' type cutting edge that grips the fibres on the outside of the hole and keeps them in tension during the cutting process, thereby avoiding fraying.
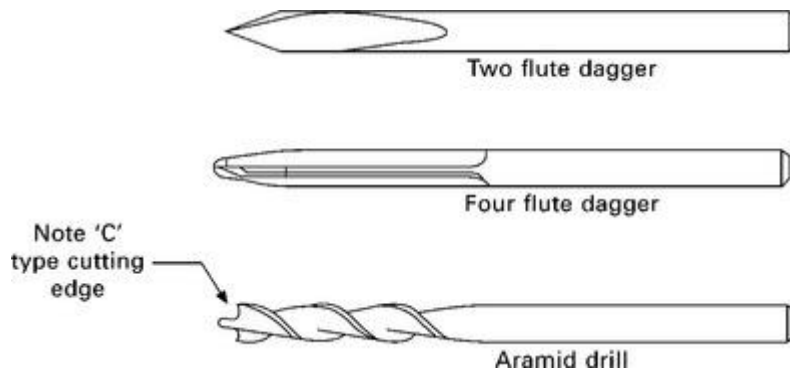
14.27 Drill bits used for carbon–epoxy (two and four flutes daggers) and aramid fibre composites reproduced from F. C. Campbell, *Manufacturing Technology for Aerospace Structural Materials,* Elsevier Science & Technology, 2006.
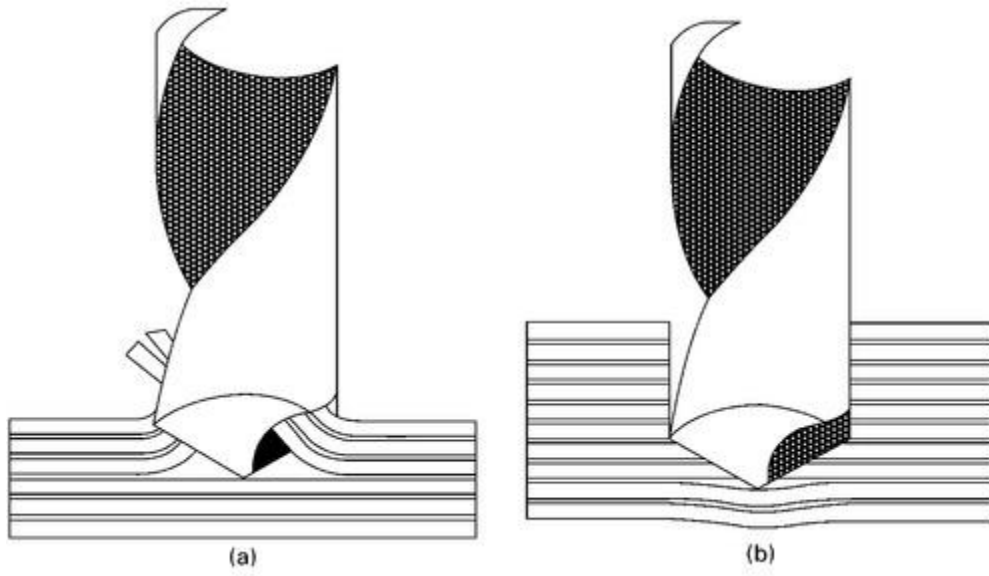
14.28 (a) Peel-up and (b) push down damage to composite materials caused by incorrect drilling.

Fibre–polymer composites for aerospace structures and engines

15.1 Introduction

Composites are an important group of materials made from a mixture of metals, ceramics and/or polymers to give a combination of properties that cannot otherwise be achieved by each on their own. Composites are usually made by combining a stiff, strong but brittle material with a ductile material to create a two-phase material characterised by high stiffness, strength and ductility. Composites consist of a reinforcement phase and a matrix phase and, usually, the reinforcement is the stiffer, stronger material which is embedded in the more ductile matrix material.

The main purpose of combining materials to create a composite is to gain a synergistic effect from the properties of both the reinforcement and matrix. For example, carbon–epoxy composite used in aircraft structures is a mixture of carbon fibres (the reinforcement phase) embedded in epoxy resin (the matrix phase). The carbon fibre reinforcement provides the composite with high stiffness and strength while the epoxy matrix gives ductility. Used on their own, carbon fibres and epoxy are unsuitable as aircraft structural materials, the fibres being too brittle and the epoxy too weak, but when combined as a composite they create a high-performance material with many excellent properties.

This chapter examines fibre-reinforced polymer matrix composites used in aircraft. In chapter 14, the manufacture of composite materials, including the production of the fibre reinforcement and core materials, was described. This chapter examines the applications and properties of the manufactured composites. The application of fibre–polymer composites in aircraft and jet engines is described, including the benefits and problems with using these materials. The mechanical properties of composites are discussed, including the mechanics-based theories used to calculate the elastic and strength properties. Control of the mechanical properties of composites by the type, volume fraction and orientation of the fibre reinforcement as well as by the selection of the polymer matrix is explained. Other properties of polymer matrix composites are dealt with in following chapters, including their fracture properties (chapters 18 and 19), fatigue properties (chapter 20), creep properties (chapter 22) and methods for their recycling and disposal (chapter 24).

15.2 Types of composite materials

Composites are usually classified according to the material used for the matrix: metal matrix, ceramic matrix or polymer matrix. There is also a special type of composite called fibre–metal laminate that does not really fit into any of these three classes. The composites used in aircraft are almost exclusively polymer matrix materials, with the polymer often being a thermoset resin (e.g. epoxy, bismaleimide) and occasionally a high-performance thermoplastic (e.g. PEEK). Metal matrix composites, ceramic matrix composites and fibre–metal laminates are used in much smaller amounts, as described in chapter 16.

The matrix phase of composite material has several important functions, including binding the discrete reinforcement particles into a solid material; transmitting force applied to the composite to the stiff, strong fibres, which carry most of the stress; and protecting the fibres from environmental effects such as moisture and abrasion.

Composites can also be classified based on the shape and length of the reinforcing phase. The three main categories are particle-reinforced, whisker-reinforced and fibre-reinforced composites (Fig. 15.1). The reinforcement, regardless of its shape and size, is always dispersed within the continuous-matrix phase. The main functions of the reinforcement are to provide high stiffness, strength, fatigue resistance, creep performance and other mechanical properties. In some instances, the reinforcement may be used to alter the electrical conductivity, thermal conductivity or other nonmechanical properties of the composite. The stiffening and strengthening attained from the reinforcement is dependent on its shape, and increases in the order: particle, whisker and fibre. For this reason, the composite materials used in aircraft structures contain

long, continuous fibres. Composites containing particles or whiskers are rarely used in structural components.

Particle-reinforced composite   Whisker-reinforced composite   Fire-reinforced composite
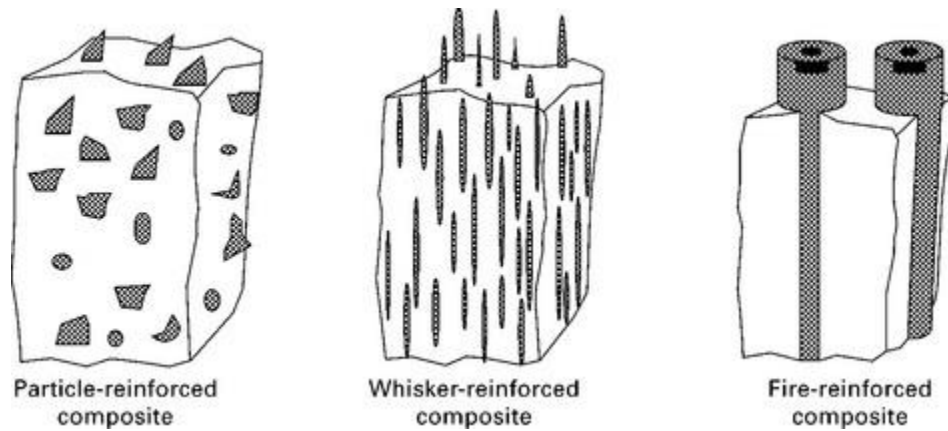
15.1 Different types of composites based on the shape of the reinforcement.

The size of the reinforcement used in composites can range from ultrafine particles in the nanometre size range to large particles up to 1 mm or more. The reinforcement used in aircraft composite materials is mostly in the micrometre size range, typically 5–15 μm, in diameter or slightly larger, as shown in Fig. 15.2. The composites used in aircraft structures are reinforced with continuous fibres rather than whiskers or particles. The mechanical properties in the fibre direction increase with the fibre length, as shown in Fig. 15.3. Therefore using continuous fibres that can extend the entire length of the structure maximises the structural efficiency.
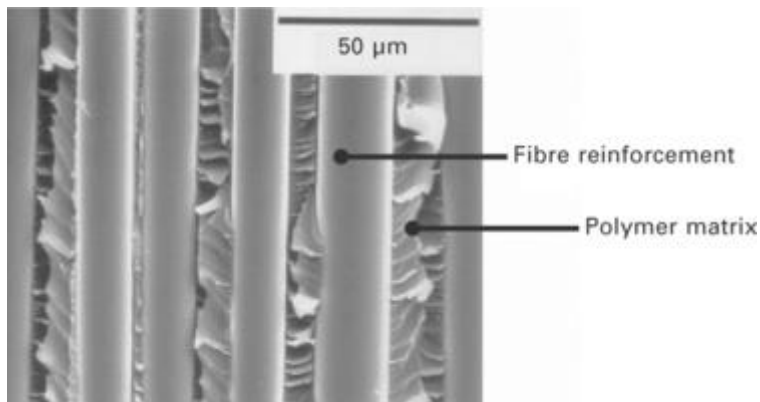
15.2 Microstructure of an aircraft-grade composite material containing continuous-fibre reinforcement having a diameter in the micrometre size range.
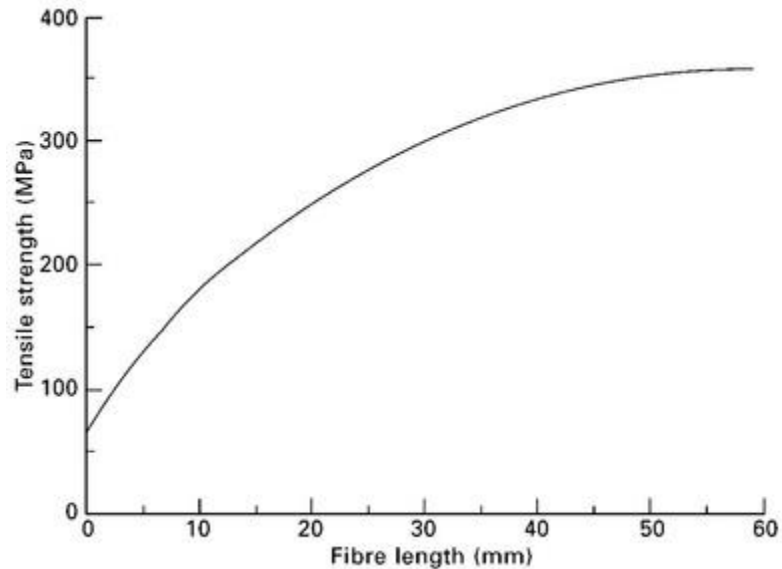
15.3 Effect of fibre length on the tensile strength of the carbon-reinforced polymer composite.

There is growing interest in nanoparticle composites, such as polymers reinforced with carbon nanotubes, for use in aircraft structures due to their exceptional mechanical properties (see chapter 14). In some cases, hybrid composites consisting of two or more types of reinforcing fibres (e.g. carbon and glass or carbon and aramid) are used together to optimise the material properties. For example, aramid fibres used in combination with carbon fibres increase the ballistic resistance of carbon-fibre composite materials. Hybrid composites containing both glass and carbon fibres are used in helicopter rotor blades.

It is worthwhile at this point to distinguish between composites and metal alloys, which are also created by combining two or more materials. The constituent materials in a composite, which are the reinforcement and matrix, are combined but there is no dissolution of one phase into the other phase. In other words, the reinforcement and matrix remain physically discrete phases when combined into the composite. In contrast, in metal alloys the solute material (i.e. alloying elements) dissolves into the solvent (i.e. base metal) and, therefore, the solute does not retain its original physical condition. Only materials which retain the physical properties of the constituents are considered composites.

Fibre–polymer composites alongside aluminium alloys are the most used materials in aircraft structures. The use of composites in civil aircraft, military fighters and helicopters has increased rapidly since the 1990s, and it is now competing head-to-head with aluminium as the material of choice in many airframe structures (as described in chapter 2). The use of composites in gas turbine engines for both civil and military aircraft is also growing. The main reasons for using composites are to reduce weight, increase specific stiffness and strength, extend fatigue life, and minimise problems with corrosion.

Composites used in aircraft structures are in the form of laminates or sandwich materials. Laminates consist of continuous fibres in a polymer matrix, and the most common type used in aircraft is carbon fibre–epoxy. The fibres are stacked in layers, called plies or laminae, often in different orientations to support multidirectional loads. Laminates made of glass fibre–epoxy, carbon fibre–bismaleimide and carbon fibre–thermoplastic may also be used in aircraft, although in smaller amounts than carbon–epoxy. Laminates are used in the most heavily-loaded composite structures and are often supported by ribs, spars and frames. The thickness of the laminate can range from a few millimetres to around 25 mm, depending on the design load. Sandwich composites are used in lightweight secondary structures requiring high buckling resistance and flexural rigidity, and are often constructed with thin carbon–epoxy face skins covering a lightweight core of polymer foam, Nomex or (in older aircraft types) aluminium honeycomb.

15.3 Aerospace applications of fibre–polymer composites

15.3.1 COMPOSITES IN MILITARY AIRCRAFT

The use of composites in aircraft has been led by the military, particularly with fighter aircraft and helicopters. Carbon fibre–epoxy composites have been used in the primary structures of fighter aircraft for many years, including the wings and fuselage, to minimise weight and maximise structural efficiency. The amount of composite varies between different types of fighter aircraft, and the usage has increased greatly since the 1970s (see Fig. 2.12). Composite material used in fighter aircraft ranges from a small amount, as in the F-14 *Tomcat* (4% of the structural mass) and F-16 *Fighting Falcon* (5%), to greater amounts as in the F/A-18 E/F *SuperHornet* (20%), AV8B *Harrier II* (22%), *Dassualt Rafale B/C* (25%) and F-22 *Raptor* (25%). Composites are the most used structural material in late-generation fighters such as *Eurofighter* (40%) and F-35 *Lightning II* (35%). The structural applications of composites, mostly carbon fibre–epoxy and carbon fibre–bismaleimide, in the F-35 are shown in Fig. 15.4.

Mid fuselage:
- Skins: composite and titanium
- Bulkheads and frames: titanium, aluminium and composite
- Fuel floors: composite
- Weapons bay doors: composite

Aft fuselage:
- Aft fuselage: titanium
- Core: aluminium
- Keel web: composite
- Upper skins: titanium and composite

Forward fuselage
- Skins: composite
- Bulkhead frame: composite and aluminium
- Fuel tank walls: composite
- Avionics and side array doors: composite

Wings:
- Skins: composite
- Forward spars: titanium
- Intermediate and rear spars: composite and titanium

Empennage:
- Skins: composite
- Core: aluminium
- Spars and ribs: composite

15.4 Application of composites in the F-35 *Lightning II*.

15.3.2 COMPOSITES IN PASSENGER AIRCRAFT

Composites have been used in single- and twin-aisle passenger aircraft since the late-1960s, with the first applications being in non-safety critical components such as fairings and undercarriage doors. The use of composites in the primary structures of passenger airliners has lagged behind fighter aircraft. The first primary composite structure was the carbon fibre–epoxy horizontal stabilizer for the Boeing 737, which was certified in 1982. The uses of composites in airframe structures developed gradually during the 1990s, and typical applications are shown in Fig. 15.5.
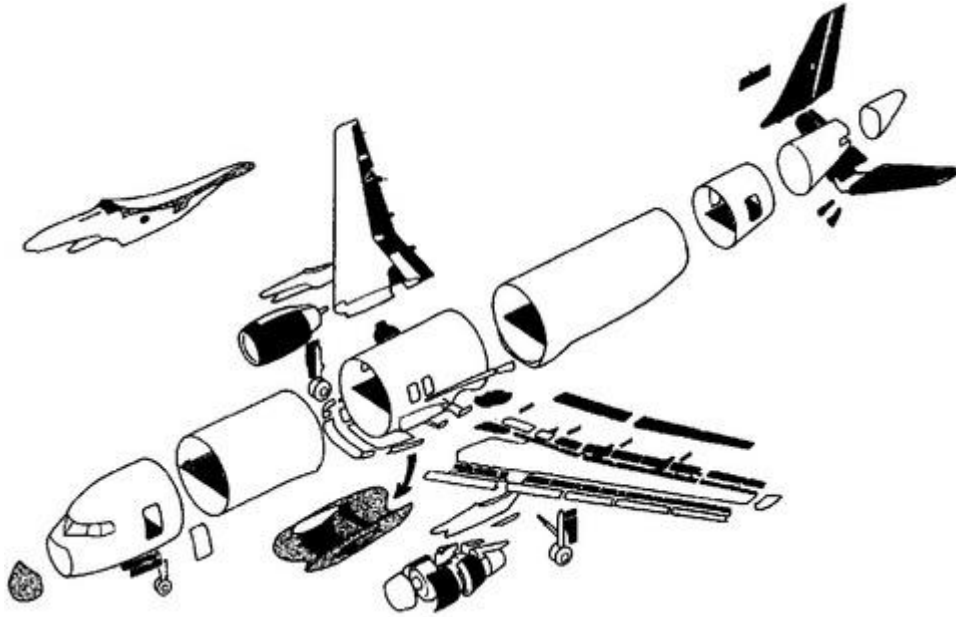
15.5 Composite structures on the Airbus A320 (shaded black). This illustrates typical structures made of composite material before the introduction of the Airbus 380 and Boeing 787.

A major expansion in the use of composites occurred with the Airbus 380, which is a 280 tonne airliner (typical operating empty weight) built from 25% composite materials. Carbon-fibre composites are used in many major structural components including the vertical and horizontal tail planes, tail cone, centre wing box, and wing ribs (see Fig. 15.6). The aircraft is also constructed of fibre–metal laminate, which is another type of composite material and is discussed in the next chapter. The Boeing 787 represents the latest in composite applications to large airliners, with 50% of the structural mass consisting of carbon fibre–epoxy composite material. The Airbus A350 is constructed using a similar amount of composite material (about 50% of the structural mass). Table 15.1 gives a summary of the structural components in Airbus and Boeing aircraft made using composite material. Although the use of composites is now widespread in commercial aircraft, it is unusual for the entire airframe to be built with these materials. Apart from a limited number of Beech Starship aircraft, no all-composite commercial airliner has yet gone into production. Aluminium alloy and other metals remain important structural materials to be used in combination with composites for the foreseeable future.

Table 15.1

Composite components on Airbus and Boeing airliners

Composite component	Airbus	Boeing
Fuselage and nose components		
Fuselage	A380	B787
Belly fairing	A380	
Rear pressure bulkhead	A340-600	
	A380	
Floor beams	A350	B787
	A400M	
Keel beam	A340-600	
	A380	
Nose cone	A340-600	B787
	A380	
Wing and empennage components		
Wingbox	A380	B787
	A400M	
Wing beams	A350	B787
	A380	
Wing skins	A350	B787
	A380	
Horizontal stabiliser	A340	B737
	A350	B777
		B787
Vertical tailplane	A380	B777
Engine components		
Nacelles	A340	B787
	A380	
Reversers	A340	B787
	A380	
	A350	
Reverser details	A320 (Reverser doors)	
	A380 (Gutter fairing	
	A340 (Reverser doors)	
	A380 (Reverser doors)	
Fan blades		B787
Cone spinners		B787
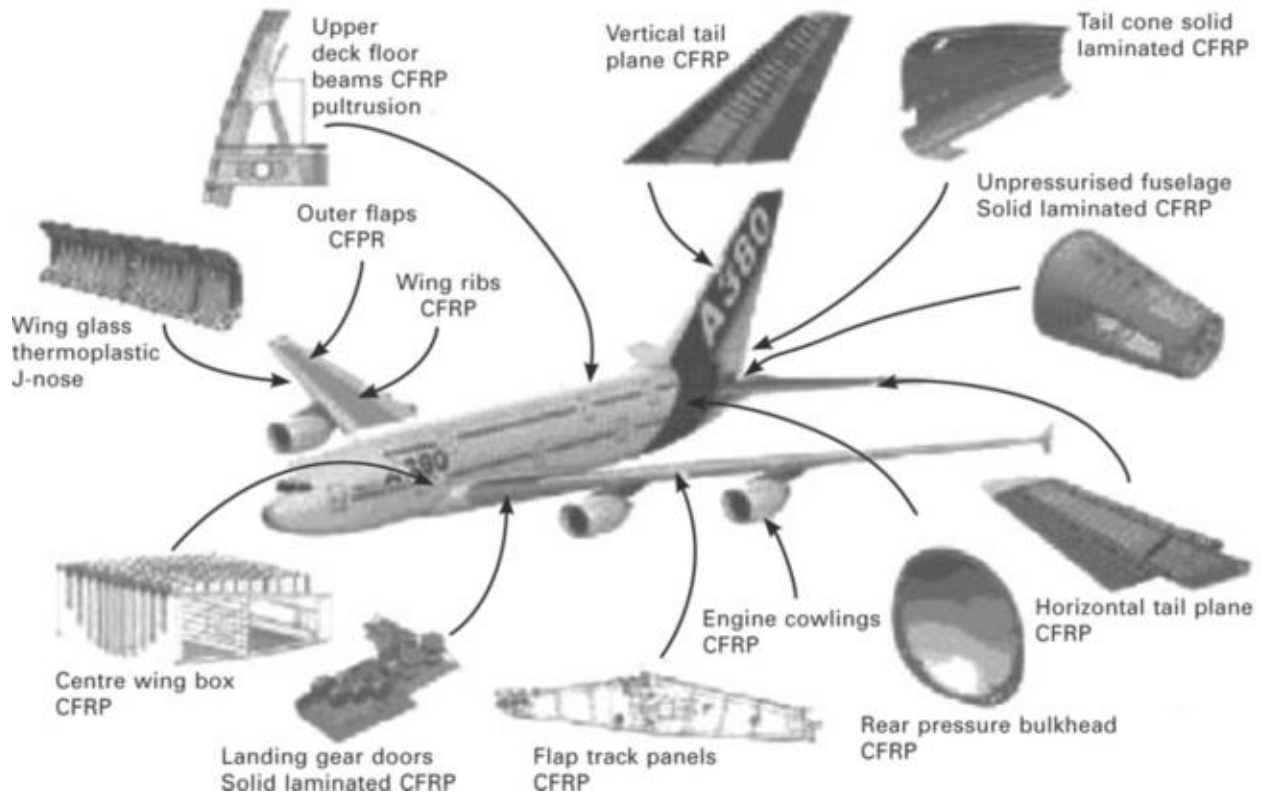
15.6 Application of composites in the Airbus 380 CFRP, carbon-fibre reinforced polymer. (image courtesy of Airbus).

15.3.3 COMPOSITES IN HELICOPTERS

Composites are often used in the fuselage and rotor blades of helicopters. Carbon, glass and aramid fibre composites are regularly used in the main body and tail boom of many commercial and military helicopters to reduce weight, vibration and corrosion as well as to increase structural performance. Composites are being used increasingly to replace aluminium in the main rotor blades to prolong the operating life by improving resistance against fatigue. Most metal blades must be replaced after between 2000 and 5000 h of service to ensure fatigue-induced failure does not occur, and the operating life can be extended to 20 000 h or more with a composite blade. Figure 15.7 presents a cross-section view of a composite rotor blade, which is a sandwich construction containing both carbon and glass fibres in the face skins.
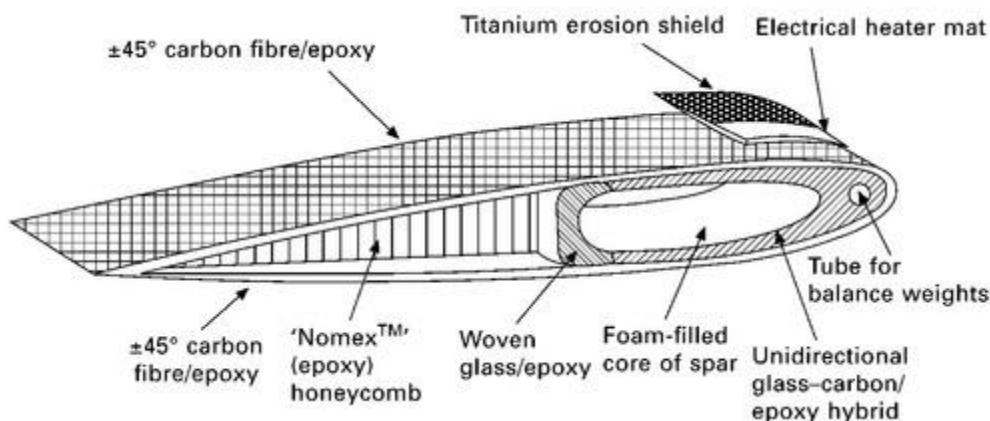
15.7 Helicopter rotor blade constructed of sandwich composite material (image courtesy of Westland Helicopters).

15.3.4 COMPOSITES IN GAS TURBINE ENGINES

Composites are used in gas turbine engine components including the fan blades, front fan case, nacelle, outlet guide vanes, bypass ducts, nose cone spinner and cowling (Fig. 15.8). The replacement of incumbent metal components with composites provides a saving in the vicinity of 20–30% of the total engine lifetime operation cost. The use of composites is restricted to engine parts required to operate at temperatures below about 150 °C to avoid softening and heat distortion. Carbon-fibre laminates with a high-temperature polymer matrix (such as bismaleimide) is often the composite material of choice for jet engines.

(a)   (b)

(c)

15.8 (a) Fan blade and (b) casing made of composite material for the GEnx gas turbine engine. (c) Composite nacelle and cowling of a gas turbine engine.

The three major reasons for the use of composites in engines are lower weight, improved structural performance and reduced operating/maintenance cost. The trend in gas turbine engines is towards larger (and consequently heavier) fan sections. The addition of 1 kg to the fan blade assembly needs a compensatory increase in the weight of the fan blade containment case of 1 kg. This 2 kg increase requires a compensatory weight increase of about 0.5 kg to the rotor as well as incremental increases to the weights of the wings and fuselage. Any weight savings gained by using light materials in the fan blade translates to significant savings in the weight of other components. For example, the use of carbon-fibre composite in the two GEnx engines on the Boeing 787 provides an overall weight saving of about 350 kg, which translates directly into fuel burn saving and greater aircraft range. The other benefit of using lightweight composite fan blades is reduced centrifugal force (owing to their light mass) thus increasing the fatigue life.

15.3.5 COMPOSITES IN SPACECRAFT

Polymer matrix composites have been used for many years in space structures, including truss elements, antennas, and parabolic reflectors. The main truss of the Hubble space telescope, for example, is made of carbon fibre–epoxy composite for lightness, high stiffness and low coefficient of thermal expansion. As another example, the main cargo doors of the space shuttle orbiter are made of sandwich composite material and the arm of the remote manipulator system is made of carbon-fibre composite (Fig. 15.9).
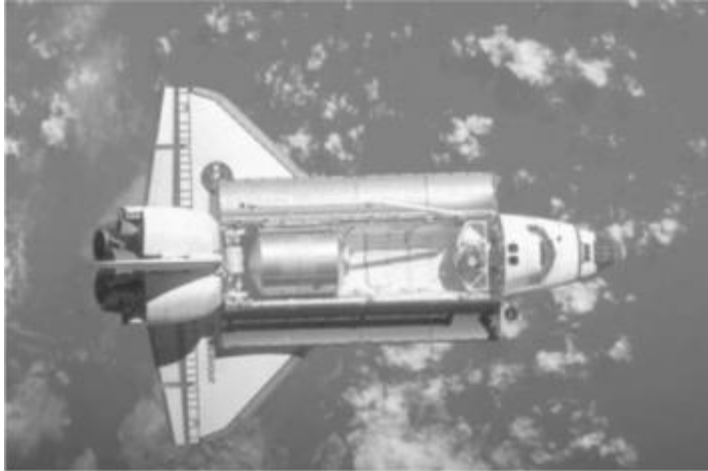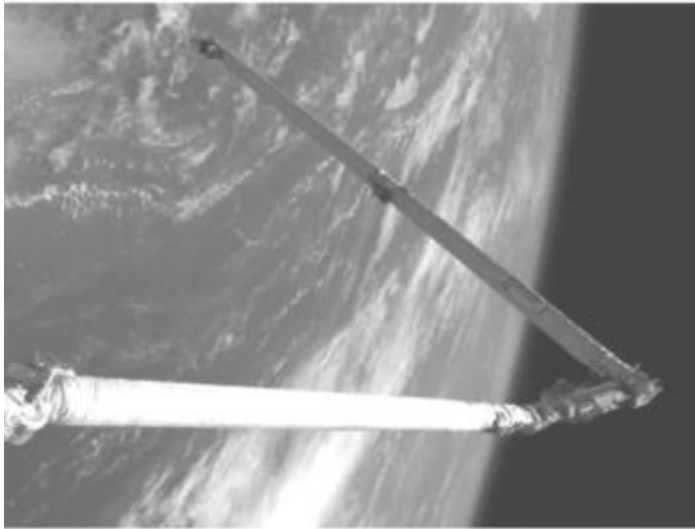
15.9 (a) Cargo bay doors and (b) remote arm of the space shuttle orbiter are made of composite materials.

15.4 Advantages and disadvantages of using fibre-polymer composites

15.4.1 ADVANTAGES OF USING FIBRE–POLYMER COMPOSITES

There are many benefits to be gained from using carbon–epoxy and other types of fibre–polymer composite materials instead of aluminium alloy in aircraft. The main advantages are summarised here and a comparison between carbon–epoxy composite and an aircraft-grade aluminium alloy is given in Table 15.2.

Table 15.2

Comparison of properties of carbon–epoxy laminate (quasi-isotropic) and aluminium alloy (2024 Al)

Property	Carbon–epoxy	Aluminium alloy
Density (g cm^{-3})	1.6	2.7
Structural efficiency		
Specific modulus, E/ρ (MPa m^3 kg^{-1})	71	26
Specific strength, σ/ρ (MPa m^3 kg^{-1})	0.4	0.2
Fatigue resistance (endurance stress limit after one million load cycles)	70–80% of the ultimate strength	20–35% of the ultimate strength
Corrosion resistance	Excellent	Fair
Thermal conductivity (W m^{-1} K^{-1})	20	250
Coefficient of thermal expansion (K^{-1})	2×10^{-6}	22×10^{-6}

Weight

The lower density and superior mechanical properties of carbon-fibre composite compared with aluminium results in significant weight saving. With careful design, it is possible to a achieve weight savings of 10–20% using carbon fibre–epoxy composite. For instance, the Boeing 787 is about 20% lighter than an equivalent aircraft made entirely of aluminium which, together with other factors, translates to a fuel saving of about 20% and reduced seat-mile costs by around 10%.

Integrated manufacture

Composite manufacturing processes are better suited than metal forming processes to produce one-piece integrated structures with fewer parts. Typically, assembly accounts for about 50% of the production cost of the airframe, and the possibility of producing integrated structures offers the opportunity to reduce the labour, part count, and number of fasteners. For example, one mid-sized aircraft fuselage barrel made using aluminium requires about 1500 sheets held together with nearly 50 000 fasteners. An equivalent barrel made of composite material only requires about 3000 fasteners because of the fewer number of parts. The F-35 Lightening II has just one-half the number of parts of the F-18 *SuperHornet*, one of the aircraft it may replace.

Structural efficiency

The mechanical properties of composites can be tailored by aligning the fibre reinforcement in the load direction, thereby providing high stiffness and strength where it is needed. As a result, the specific stiffness and strength properties of carbon-fibre composites are superior to aluminium alloy. Furthermore, the choice of high-stiffness or high-strength carbon fibres provides the aircraft engineer with greater flexibility in the design of structurally efficient components.

Fatigue resistance

Composites have high fatigue resistance under cyclic stress loading, thereby reducing the maintenance cost and extending the operating life. The superior fatigue resistance of carbon-fibre composite compared with aluminium is a major reason for its use in aircraft structures, helicopter rotor blades, and fan blades for gas turbine engines.

Corrosion resistance

Carbon-fibre composites are immune to corrosion, which is a major problem with aluminium. The high cost of inspecting and repairing metal structures damaged by corrosion is minimised with the use of composites. The corrosion resistance of composite material allows for a higher humidity level inside the cabin, which creates a more comfortable environment for crew and passengers. The humidity for an

aluminium fuselage must be kept at a very low level (around 5%) to avoid corrosion, and this can be increased in a composite fuselage (15–20%) for greater comfort.

Radar absorption properties

Using specialist designs, materials and manufacturing processes, composites can be made with high radar absorption properties. When radar absorbing composite material is used in stealth military aircraft they are difficult to detect using radar.

Heat insulation

The thermal conductivity of composites is much lower than metals, which makes them a good heat insulator. This property is used in fighter aircraft to reduce heat conduction from the engines through the fuselage, thereby making the aircraft harder to detect using infrared devices.

Low coefficient of thermal expansion

Carbon-fibre composites have a very low coefficient of thermal expansion, which means they experience little or no expansion or contraction when heated or cooled. This property is utilised in structures that need high dimensional stability with changes in temperature. For example, the truss supporting the antenna and deep-space observation devices in the Hubble space telescope is made of composite material. When the temperature of the telescope changes the truss does not change shape, thereby providing a stable platform for the antenna and devices.

15.4.2 DISADVANTAGES OF USING FIBRE–POLYMER COMPOSITES

Composites, like any material, are not without their drawbacks and limitations. The major issues are discussed in this section.

Cost

The cost of producing aircraft components from composite material is often more expensive than using aluminium. The higher cost of composite is caused by several factors, including the high cost of carbon fibres, the labour-intensive nature of many of the manufacturing processes, and high tooling costs.

Slow manufacture

The production of aircraft components using composites can be slower than with aluminium owing to the long time needed to lay-up the fabric or prepreg ply layers and the curing time of the polymer matrix. The use of automated lay-up processes and multilayer non-crimp fabrics reduce production time, although most manufacturing processes are not well suited to the rapid production of a large number of thermoset matrix parts.

Anisotropic properties

Designing aircraft components made of composite materials is more challenging than for metal alloys owing to their anisotropic properties. Careful design and manufacture is required to ensure the fibres are aligned in the load direction, otherwise the composite may have inferior mechanical performance.

Low through-thickness mechanical properties

The stiffness, strength, damage tolerance and other mechanical properties of composites are low in the through-thickness direction owing to the absence of reinforcing fibres. Figure 15.10 shows typical values for the in-plane and through-thickness mechanical properties of carbon fibre–epoxy composite. The through-thickness property values are just a small fraction of the inplane values, and the application of through-thickness loads on to composites must be avoided.

Fibre direction:
Young's modulus = 80–200 GPa
Tensile strength = 500–1500 MPa
Fracture toughness = 30–45 MPa m$^{-1/2}$

Antifibre direction:
Young's modulus = 5–8 GPa
Tensile strength = 20–50 MPa
Fracture toughness = 0.02–0.1 MPa m$^{-1/2}$
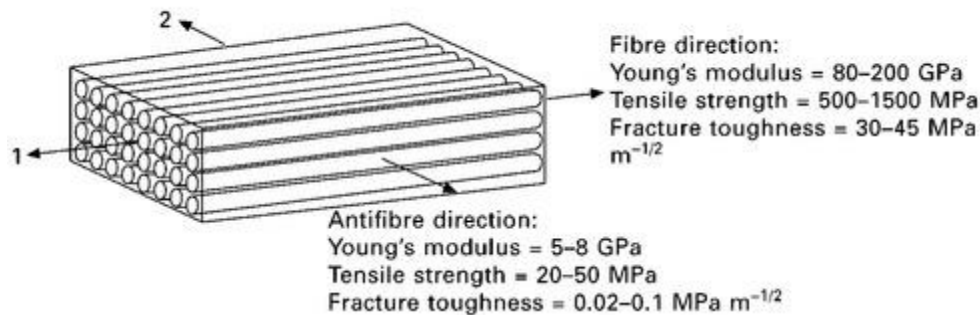
15.10 Elastic modulus, strength and fracture toughness properties of a carbon–epoxy composite in the fibre and antifibre (through-thickness) directions. The properties vary over a range of values depending on the fibre type, fibre volume content, and matrix material.

Impact damage resistance

Composites are susceptible to delamination cracking when impacted at low energies because of their low through-thickness strength and fracture toughness. Impact events such as bird strike, large hail stone impacts, and tools which are accidentally dropped during maintenance can damage composites more severely than occurs with a metal alloy. A related problem is impact damage, which can reduce the compressive strength and other mechanical properties of the composite.

Damage tolerance

The growth of damage (e.g. delamination cracks) in composite materials is difficult to control and predict. A large amount of damage growth can occur rapidly with little or no warning. For this reason, primary composite aircraft structures must be designed according to the so-called ' no growth' damage tolerance philosophy, which means that pre-existing damage must not grow over a specified period of time of aircraft service (usually two or more inspection intervals). As a result, composite structures must be over-designed to ensure adequate damage tolerance, thus increasing their weight and cost.

Notch sensitivity

The reduction in the failure strength of composites owing to notches (e.g. bolt holes, windows) can be greater than the loss suffered by metal alloys. Composite materials with highly anisotropic properties (i.e. a large percentage of fibres aligned in one direction) experience a high concentration of stress near notches when under load, resulting in a large knock-down in strength.

Temperature operating limit

Composites soften and distort at lower temperatures than aluminium owing to the glassy-to-rubbery transformation of the polymer matrix. The maximum operating temperature of epoxy matrix composites is typically in the range 100–150 °C, which limits their use for high-temperature applications.

Flammability

Composite materials are flammable, and burn, produce smoke and release heat when exposed to a high-temperature fire, as may occur in a post-crash accident.

Low electrical conductivity

Composite materials are much poorer conductors of electricity than the metals used on aircraft. An electrically conductive material (such as copper mesh) must be incorporated into composite materials used on the external surface of aircraft to dissipate electricity in the event of lightning strike.

15.5 Mechanics of continuous-fibre composites

15.5.1 PRINCIPLES OF COMPOSITE MECHANICS

Understanding the mechanical behaviour of continuous-fibre–polymer composites is different to understanding the mechanical properties of metals and their alloys, which has been a major focus of this book. The properties of metals are controlled by vacancies, dislocations, grain boundaries, precipitates, solute (alloying and impurity) elements, and other microstructural features. These features have no role to play in the mechanical properties of composite materials. Instead, understanding the mechanical properties is based on the key concept of load sharing between the fibre reinforcement (which is stiff and strong) and the polymer matrix (which is compliant and weak). The properties of composites are determined by the fibre properties, matrix properties, interfacial properties between the fibre and matrix, and how effectively the load is shared between the fibres and matrix.

When an external load is applied to a composite, a certain proportion of that load is carried by the fibre reinforcement and the remainder by the polymer matrix. At the simplest level, the applied load is shared between the fibres and matrix based on their relative volume fractions. This is expressed mathematically as:

$$P = P_f V_f + P_m V_m \quad \text{[15.1]}$$

where P is the total applied load, $P_f V_f$ is the proportion of load on the fibres, and $P_m V_m$ is the proportion of the load on the matrix. P_f and P_m are the loads carried by the fibres and matrix, and V_f and V_m are the volume fractions of the fibres and matrix, respectively.

Provided the response of the composite to the applied load is elastic, then the distribution of load-sharing between the fibres and matrix is independent of the stress level. In other words, the relative distribution of load between the fibres and matrix remains the same for any stress up to the elastic stress limit of the composite, which quite often is the ultimate failure stress. Because the fibre reinforcement is much stiffer and stronger than the polymer matrix, it is important that as high a proportion of the applied load as possible is borne by the fibres. For this reason, the fibre content of aircraft composites is as high as practically possible. The fibre volume content is typically in the range of 55–65%, the maximum values that can be achieved using the manufacturing processes described in chapter 14. The relative proportions of the load borne by the fibres and the matrix is dependent not only on their relative volume fractions, but also on the shape and orientation of the fibres together with the elastic properties of the fibres and matrix.

The concept of load-sharing between the fibres and matrix is the basis for the theoretical understanding of the mechanical properties of composites as well as the practical aspects in the design and manufacture of composites with maximum mechanical performance. The concept of load-sharing is applied to the micromechanics of composites, which is the mathematical analysis of the mechanical properties based on the properties and interactions of the fibres and matrix. Analytical and finite element models are used to simulate the microstructure of composites, and from this the mechanical properties (such as elastic modulus or strength) are calculated in terms of the properties and volume fractions of the fibres and matrix. Figure 15.11 illustrates the basic premise of micromechanics, where the properties of the fibre reinforcement are combined with the properties of the polymer matrix to calculate the 'average' properties of the composite material based on volume-averagis of the two constituents.
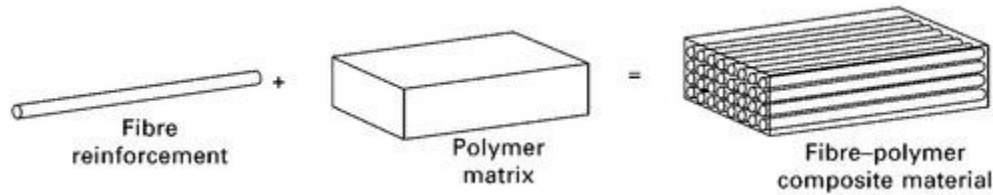
15.11 Representation of the averaging approach used in micromechanics.

The averaging approach to micromechanical analysis assumes that the fibres are arranged in a regular pattern. In actual composite materials, the fibres are randomly distributed throughout the matrix phase, with regions of higher than average volume content of fibres and other regions with lower than average fibre content. Micromechanical analysis assumes that the fibres are packed in a regular pattern. For example, Fig. 15.12 shows two regular fibre packing patterns: the square array and the hexagonal array. Either array can be viewed as a repetition of a single unit cell of the composite which contains the fibre and matrix. The unit cell represents the basic building block of the composite material, and is the simplest geometry for analysing using the volume averaging approach to micromechanics.
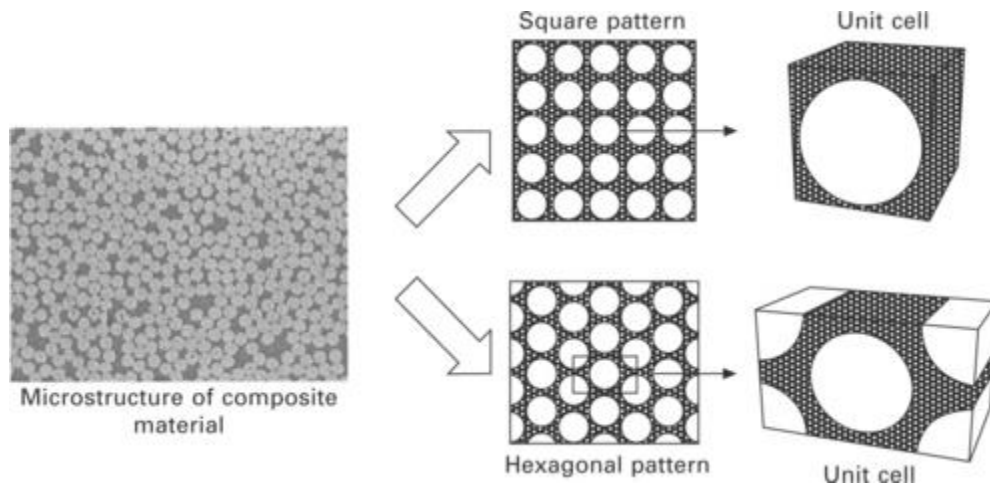
15.12 Unit cell model for the micromechanical analysis of composites.

The simplest approach to micromechanical analysis of composite materials involves treating the fibre and resin separately within a unit cell, and assuming that there is no interaction between the two constituents. The property averaging concept is called 'rule-of-mixtures', and it is applied to derive simple-to-use equations for mechanical and other properties including:
○ density,
○ in-plane and transverse elastic properties,
○ in-plane and transverse tensile strength,
○ in-plane compressive strength, and
○ in-plane and transverse thermal conductivity.

Once the properties of the unit cell have been calculated using micromechanics, it is then possible to calculate the properties of composite structures using a hierarchical approach to modelling as shown in Fig. 15.13. Micromechanical modelling of the unit cell is the foundation for higher levels of modelling which follow the sequence of single-ply modelling, laminate (or ply-by-ply) modelling, and finally structural modelling. Single-ply modelling calculates the properties of one ply layer within a composite, in which the fibres and matrix are treated separately (as depicted in Fig. 15.11). All of the fibres within the

single ply are assumed to be aligned in the same direction (i.e. unidirectional fibre laminate). Taking the properties calculated for a single ply, the next level of modelling involves analysing multiple-ply layers with different fibre angles to calculate the properties of a multidirectional composite. Laminate modelling treats each ply layer separately and the fibres and matrix within each ply are treated as a continuum. Structural (also called macroscopic) modelling analyses the composite as a single orthotropic material with the geometric features of the final component. Structural modelling is used to predict the stiffness, strength and other properties of the final composite structure, and this is performed using finite element and other numerical methods.
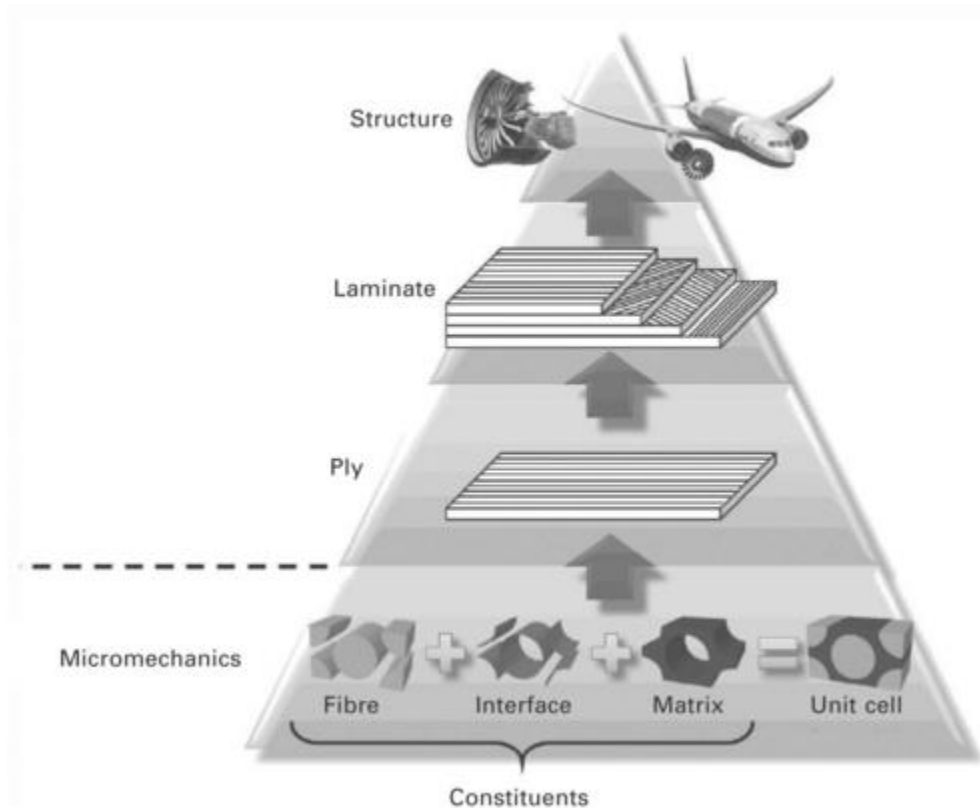
15.13 Hierarchy of micromechanics-based analysis for composite structures.

15.5.2 ELASTIC PROPERTIES OF COMPOSITE MATERIALS

Longitudinal Young's modulus of composites

One of the main reasons for using continuous-fibre composites in aircraft structures is their high specific stiffness compared with many metal alloys. The elastic modulus properties of carbon-fibre composites are superior to aluminium, which is an important reason for the increasing use of composites and the corresponding decline in the application of aluminium in aircraft structures.

The elastic modulus of a unidirectional composite reinforced with straight, continuous fibres when loaded in the fibre direction can be calculated using rule-of-mixtures modelling. The unidirectional composite shown in Fig. 15.10 is loaded in tension along the fibre direction (which is also called the 1– or longitudinal direction). In this load state, the fibre and matrix are assumed to act in parallel and both constituents experience the same elastic strain (ε_1). This iso-strain condition is true even though the elastic moduli of the fibres and matrix are different. The iso-strain condition is expressed as:

$$\varepsilon_1 = \varepsilon_f = \frac{\sigma_f}{E_f} = \varepsilon_m = \frac{\sigma_m}{E_m} \quad \textbf{[15.2]}$$

where ε_f and ε_m are the strain values of the fibre and matrix; σ_f and σ_m are the stresses carried by the fibre and matrix, and E_f and E_m are the Young's modulus of the fibres and matrix, respectively.

Based on the iso-strain condition, the longitudinal Young's modulus can be calculated using:

$$E_1 = E_f V_f + E_m V_m \quad \textbf{[15.3]}$$

where $V_f + V_m = 1$ when no voids are present.

Because the elastic modulus of the matrix is much lower than the fibre reinforcement, the fibres contribute between 95 and 99% of the in-plane stiffness of a unidirectional composite containing carbon at the typical volume contents used in aerospace materials ($V_f \sim 0.55$–0.65). The type of polymer matrix (e.g. epoxy, bismaleimide, PEEK) does not have much effect, and the matrix is chosen for reasons other than longitudinal stiffness, such as cost, maximum operating temperature or durability.

Rule-of-mixtures analysis is remarkably accurate in the calculation of the longitudinal Young's modulus of unidirectional composites. For instance, Fig. 15.14 compares the measured and calculated Young's modulus values for a unidirectional composite over a range of fibre contents, and the excellent agreement demonstrates that the in-plane stiffness can be accurately predicted using this simple analysis. Rule-of-mixtures modelling can be used to determine the longitudinal modulus for various types of composite materials to identify which provides the highest stiffness, as shown in Fig. 15.15. Rule-of-mixtures is only accurate over the fibre volume content between about 0.2 and 0.7, which is within the range used in aerospace composites.
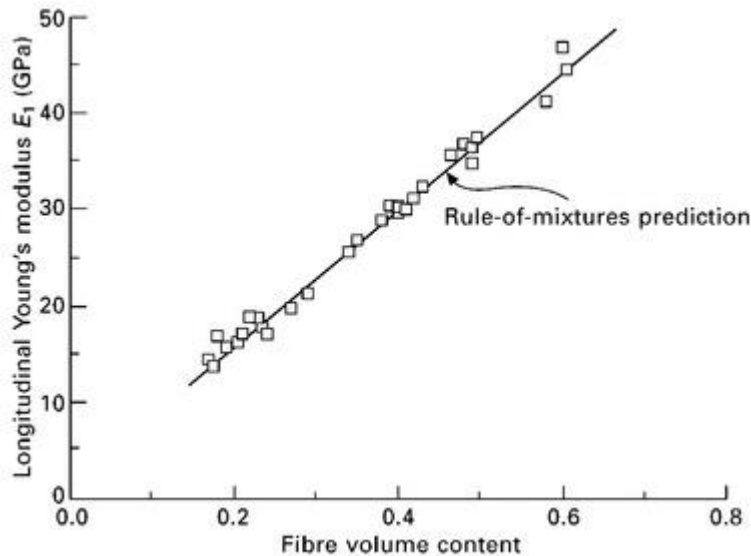
15.14 Measured (data points) and calculated (line) Young's modulus for unidirectional fibreglass composite with increasing fibre content.
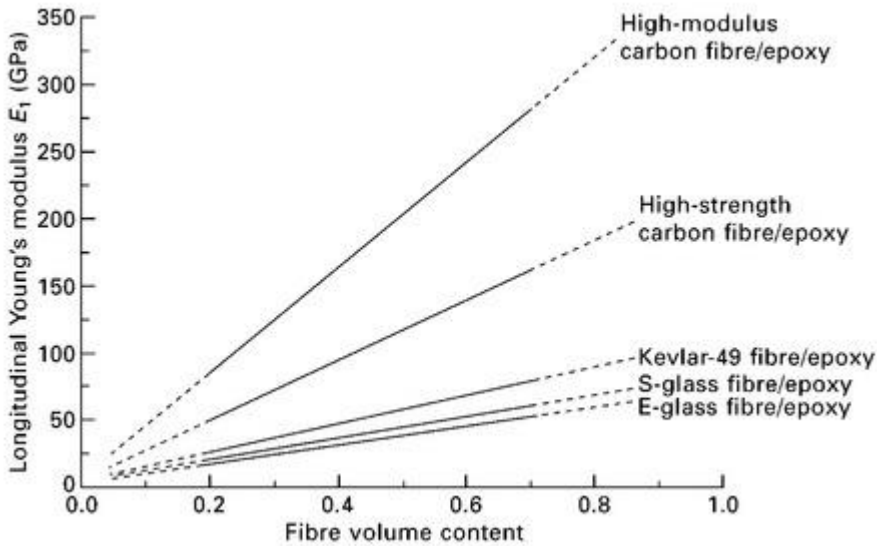
15.15 Effect of fibre type and fibre volume content on the Young's modulus of different types of unidirectional composite materials. The solid line indicates the approximate range of fibre contents over which rule-of-mixtures analysis is valid.

Transverse Young's modulus of composites

Composite materials must be designed to ensure that the external load is applied parallel to the fibres. The load should never be applied in the antifibre direction because of the low transverse stiffness and strength of the composite. The simplest model to calculate the transverse modulus assumes that the fibres and matrix act in series under an external load, and is expressed as:

$$E_2 = \left[\frac{V_f}{E_f} + \left(\frac{V_m}{E_m} \right) \right]^{-1} \quad \textbf{[15.4]}$$

Figure 15.16 shows the effects of fibre type and fibre volume content on the transverse Young's modulus of different types of unidirectional composites. The fibre reinforcement has a much smaller effect on the transverse Young's modulus compared with the longitudinal modulus, with virtually identical stiffness properties for composites containing fibres with vastly different modulus values.
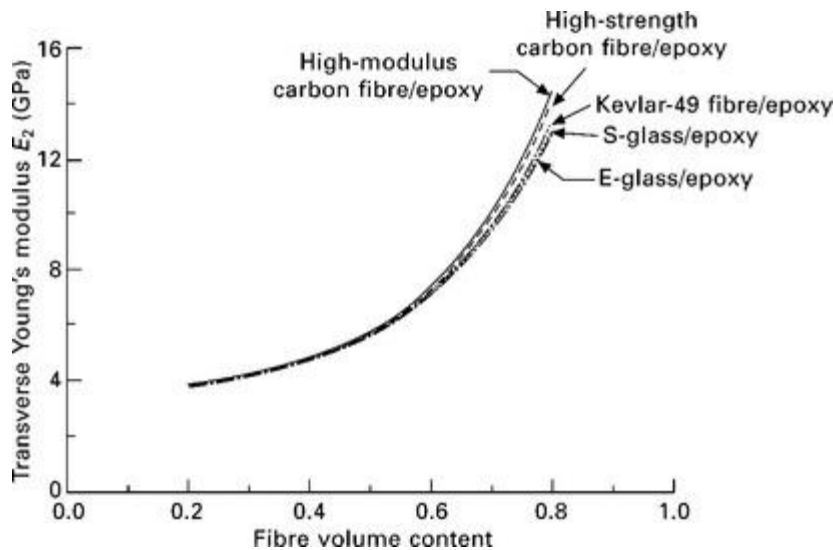
15.16 Effect of fibre type and fibre volume content on the transverse modulus of different types of unidirectional composite materials.

The transverse modulus is not always accurately calculated using <u>equation [15.4]</u> because the strain is not uniform when a composite is loaded in the antifibre direction. Owing to the large difference between the elastic modulus of the fibres and matrix, the strain is distributed unevenly in the matrix under a transverse load. <u>Figure 15.17</u> shows the heterogeneous strain field in a composite loaded in transverse tension, where the darkest fringe lines (located above and below the fibres) indicate regions where the matrix is highly strained. The heterogeneous strain affects the accuracy of the micromechanical analysis given in <u>equation [15.4]</u>, with the model underpredicting the transverse modulus.
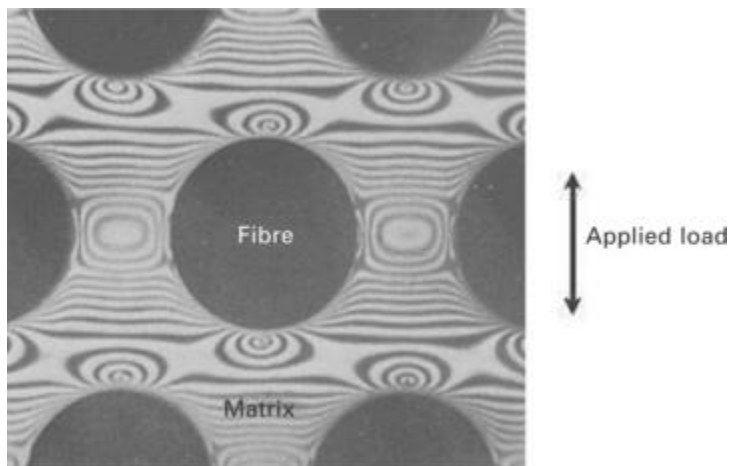
15.17 Photoelastic image of a composite-type material loaded normal to the fibre direction showing the heterogeneous strain distribution indicated by the fringe lines (from A. Puck, Zur Beanspruchen und Verformung von GFK-Mehrschichtenverbund-Bauelmenten, *Kunststoffe*, 57 (1967), 965–673.

Other models have been developed to account for the heterogeneous strain distribution through the polymer matrix. One such model is the Halpin–Tsai model, which states that the transverse modulus is calculated using:

$$E_2 = \frac{E_m\left(1 + \xi\eta V_f\right)}{\left(1 - \eta V_f\right)}$$ **[15.5]**

where the interaction ratio is:

$$\eta = \frac{\left(\dfrac{E_{2f}}{E_m} - 1\right)}{\left(\dfrac{E_{2f}}{E_m} + \xi\right)}$$

and ξ is an adjustable factor.

Other elastic properties as well as the thermal properties of composites can be calculated using rule-of-mixtures analysis. Table 15.3 gives equations to predict the shear modulus, Poisson's ratio, thermal conductivity, and specific heat capacity of unidirectional composites.

Table 15.3

Rule-of-mixtures equations for unidirectional composites

Property	Equation
In-plane shear modulus	$G_{12} = \left[\dfrac{V_f}{G_f} + \dfrac{V_m}{G_m}\right]^{-1}$
	G_f: shear modulus of fibre
	G_m: shear modulus of matrix
In-plane Poisson's ratio	$v_{12} = v_f V_f + v_m V_m$
	v_f: Poisson's ratio of fibre
	v_m: Poisson's ratio of matrix
Transverse Poisson's ratio	$v_{21} = (v_f V_f + v_m V_m)\dfrac{E_2}{E_1}$
In-plane thermal conductivity	$k_1 = k_f V_f + k_m V_m$
	k_f: thermal conductivity of fibre
	k_m: thermal conductivity of matrix
Transverse thermal conductivity	$k_2 = k_m \dfrac{k_f(1 + V_f) + k_m V_m}{k_f V_m + k_m (1 + V_f)}$
In-plane specific heat capacity	$C = \dfrac{1}{\rho}[C_f \rho_f V_f + C_m \rho_m V_m]$
	C_f: specific heat capacity of fibre
	C_m: specific heat capacity of matrix

Effect of fibre orientation on Young's modulus of composites

The Young's modulus of a unidirectional composite is much higher when loaded in the longitudinal direction than in the transverse direction owing to the high stiffness provided by the fibres. For example,

the longitudinal modulus for a high modulus carbon fibre–epoxy composite is more than 200 times higher than the transverse modulus. The longitudinal (or 0°) and transverse (90°) directions are the two extremes for loading of a unidirectional composite: parallel and perpendicular to the fibre direction. Between these two extremes the Young's modulus changes continuously with the fibre angle. For instance, Fig. 15.18 shows the effect of fibre angle on the elastic modulus properties of a unidirectional carbon–epoxy composite. The Young's modulus decreases with increasing fibre angle, particularly from 0° to 30° when the stiffness falls sharply by nearly 80%. The high sensitivity of the Young's modulus to fibre angle occurs for any type of unidirectional composite material, and their fibres must be closely aligned to the load direction to achieve high stiffness.
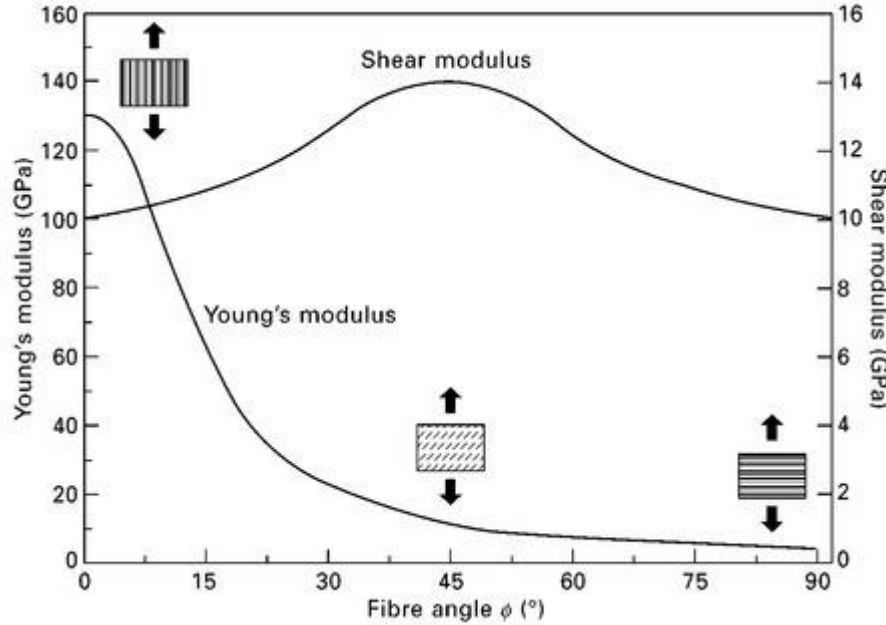
15.18 Effect of load angle on the Young's modulus (*E*) and shear modulus (*G*) of a unidirectional carbon–epoxy composite.

The Young's modulus of a unidirectional composite loaded at any fibre angle (ϕ) between 0° and 90° can be calculated using:

$$E(\phi) = \left[\frac{\cos^4 \phi}{E_1} + \frac{\sin^4 \phi}{E_2} + \left(\frac{1}{G_{12}} - \frac{2\nu_{12}}{E_1} \right) \sin^2 \phi \cos^2 \phi \right]^{-1} \quad \text{[15.6]}$$

The other elastic properties of unidirectional composites are also dependent on the fibre angle. Figure 15.17 also shows the variation in the shear modulus of carbon/epoxy with fibre angle, and this property is highest at 45° and lowest when the load is applied in the fibre (0°) and anti-fibre directions (90°). The change in the shear modulus with fibre angle can be determined using:

$$G(\phi) = 2 \left(\frac{2}{E_1} + \frac{2}{E_2} + \frac{4\nu_{12}}{E_1} - \frac{1}{G_{12}} \right) \sin^2 \phi \cos^2 \phi + \frac{1}{G_{12}} \left(\sin^4 \phi \cos^4 \phi \right) \quad \text{[15.7]}$$

The highly orthotropic nature of the elastic properties of unidirectional composites means they should not be used in aircraft and other engineering structural applications. The loads applied to aircraft structures are rarely unidirectional. The majority of aircraft structures are subject to multidirectional loads which cannot be effectively carried using a composite material in which all the fibres are aligned in the same direction. The composites used in aircraft structures are designed with the fibres aligned in two or more directions to support multidirectional loads. The two most common fibre patterns are cross-ply [0/90] where 50% of the fibres are aligned in the 0° direction and 50% in the 90° direction and quasi-isotropic [0/± 45/90] where 25% of the fibres are aligned in each of the 0°, + 45°, -45° and 90° directions. The quasi-isotropic fibre pattern is shown in Fig.14.18. The 0° and 90° fibres in the quasi-isotropic pattern is used to carry in-plane tension, compression and bending loads whereas the + 45° and -45° fibres carry in-plane shear loads. The cross-ply pattern is used when shear loads are absent. The effect of load angle on the Young's modulus of quasi-isotropic and cross-ply composites is shown in Fig. 15.19, and the variation in stiffness with angle is much less extreme than the unidirectional condition. The Young's modulus of a quasi-isotropic composite is relatively insensitive to the angle, and its in-plane elastic behaviour is approaching that of a fully isotropic material. The elastic properties of composite laminates with multidirectional fibre patterns can be calculated using laminate analysis.
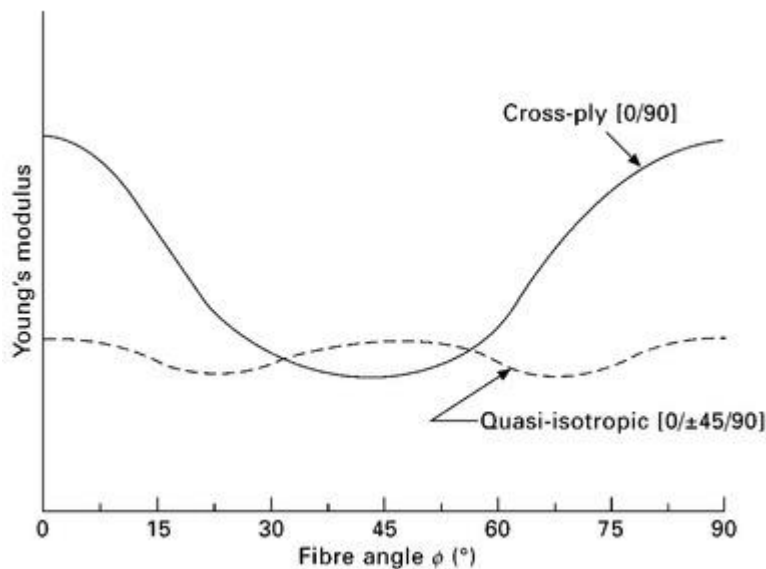
15.19 Effect of load angle on the Young's modulus of quasi-isotropic and cross-ply composites.

Other fibre patterns are used occasionally in composite aircraft structures, although the most common is the quasi-isotropic pattern followed by the cross-ply pattern. An important consideration in the fibre arrangement of multidirectional composites is that the fibre pattern is symmetric about the mid-thickness point; that is, the fibre pattern in the upper half of the composite is a mirror image of the fibre pattern in the lower half. As mentioned in the previous chapter, symmetric fibre arrangement is essential to avoid warping and distortion of the composite component.

15.5.3 STRENGTH PROPERTIES OF COMPOSITE MATERIALS

Tensile strength properties of composites

The longitudinal tensile strength of composite materials is determined mostly by the strength and volume content of the fibre reinforcement. The breaking strength of the fibres is much greater than the strength of the polymer matrix, and therefore the fibres determine the ultimate strength of the composite. Table 15.4 lists the tensile strength and failure strain values for several types of fibres and

polymers used in aircraft composites. The fibre strengths are typically 50 to 100 times higher than the matrix and, consequently, the strength of the matrix has little influence on the in-plane tensile strength of composite materials.

Table 15.4

Tensile properties for several types of fibres and polymers used in aircraft composite materials

Material	Tensile strength (MPa)	Failure strain (%)
High-modulus carbon fibre	3500–5500	0.1–1.0
High-strength carbon fibre	3500–4800	1.5–2.0
S-glass fibre	3500	4.5
E-glass fibre	4600	5.0
Kevlar-49 fibre	3000	2.8
Epoxy	90	3
Bismaleimide	50	3
Polyetheretherketone (PEEK)	96	50

The fibres used in aircraft composites have high stiffness and strength, but they have little or no ductility and as a result fail at low strain. Figure 15.20 shows tensile stress–strain curves for various types of fibres used in aircraft composite materials. Carbon fibres are brittle materials that sustain no plastic deformation before breaking at low strain (less than 0.5–2.0%). Similar behaviour occurs with glass fibres whereas aramid fibres experience a small amount of plastic flow before final failure. The brittle nature and low failure strain of carbon fibre has important consequences on the tensile behaviour of carbon-fibre composites used in aircraft structures and engines.
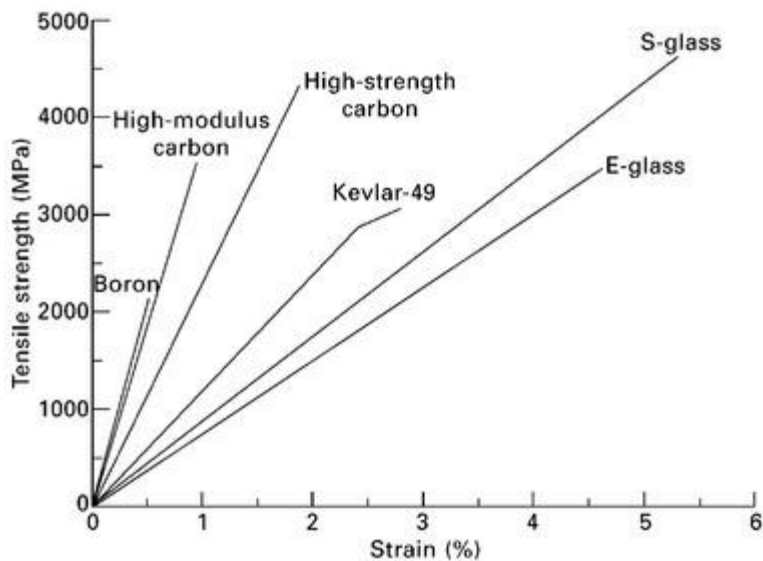
15.20 Tensile stress–strain curves for fibres used in aerospace composite materials.

Brittle materials such as carbon and glass do not have a well-defined tensile strength, unlike metals or polymers. For example, the aircraft-grade 7075-T76 aluminium alloy has a fixed tensile yield strength close to 470 MPa. Likewise, epoxy resin has a constant strength of about 100 MPa when fully cured. The strength

of carbon fibre, however, varies over a very wide range (1400 to 4800 MPa or more) despite being produced, like metals and polymers, under controlled conditions which should ensure a consistent strength value.

The strength of brittle fibres is extremely variable because the failure stress is highly sensitive to the presence of flaws and defects. Tiny cracks and voids are present in fibres, and these have a major influence on fibre strength. For example, a surface crack in carbon fibre as small as 0.3–0.4 μm reduces the breaking strength by more than 50%. Cracks are accidentally created at the fibre surface when the individual filaments are collimated into bundles after being produced. The fibres slide and rub against each other during winding and handling which introduces tiny scratches on the surface. Even when fibres are wound and handled with great care it is difficult to avoid surface damage. Lubricants within the size coating are applied to fibres to minimise sliding friction, but this does not completely eliminate surface damage. The small cracks and other surface damage caused to the fibres are not all the same size, but vary randomly along the fibre length as illustrated is Fig. 15.21. Fracture of the fibre always occurs at the largest flaw, which determines the tensile strength, and the other (smaller) flaws have no influence on fibre strength. Because the maximum flaw size can vary from the fibre to fibre, despite being manufactured and handled under the same conditions, the strength is different from fibre to fibre.
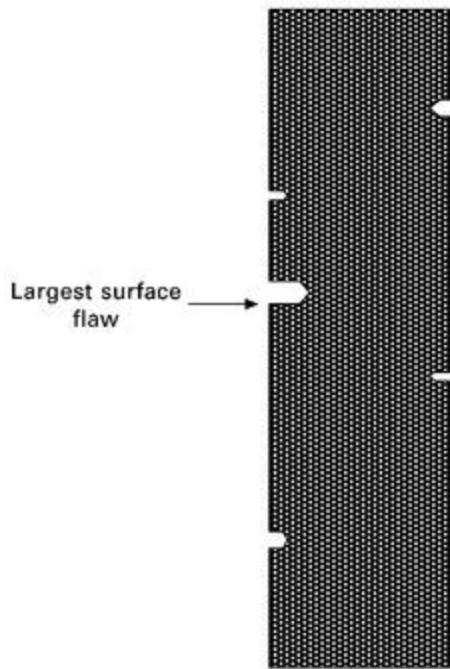
15.21 Schematic of surface flaws of different lengths that occur at random locations along the fibre. Failure occurs at the largest flaw.

The tensile strength of brittle fibres (σ_f) such as carbon is related to the largest crack length (c) according to:

$$c = \frac{\pi}{4}\left(\frac{K_c}{\sigma_f}\right)^2 \quad \text{[15.8]}$$

where K_c is the fracture toughness of the fibre material. (The concept of fracture toughness and the fracture properties of composites and other aerospace materials are described in (chapters 18 and 19). The fracture

toughness of carbon is very low (about 1 MPa m$^{1/2}$), which means its strength is very sensitive to crack size. Figure 15.22 shows the dependence of carbon fibre strength on the largest crack size, and the strength decreases rapidly with very small increases in the crack length. Owing to this high sensitivity of fibre strength to crack size, and the random nature of the maximum crack size between fibres, the tensile strength varies over a wide range. Figure 15.23 shows the strength distribution plot for carbon fibre and, unlike metals and polymers that have a single strength value, the fibre strength varies over a wide range.
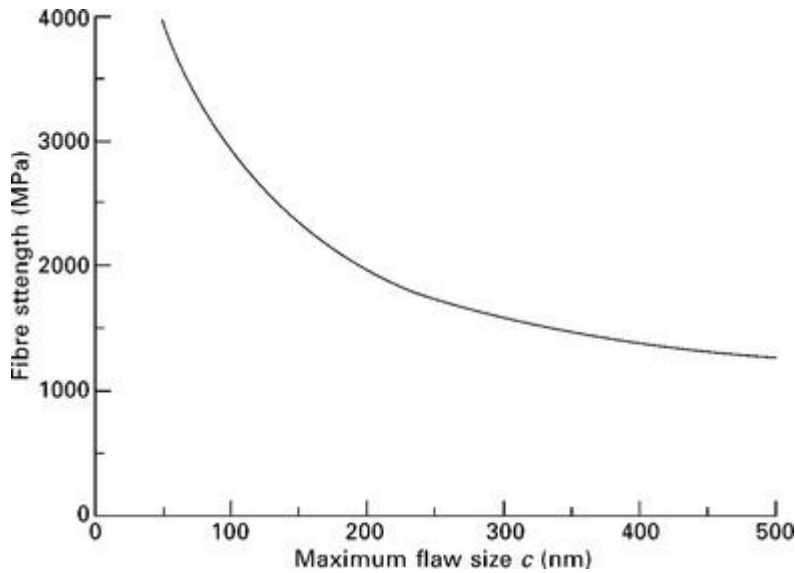
15.22 Effect of maximum surface flaw size on the tensile strength of carbon fibre.
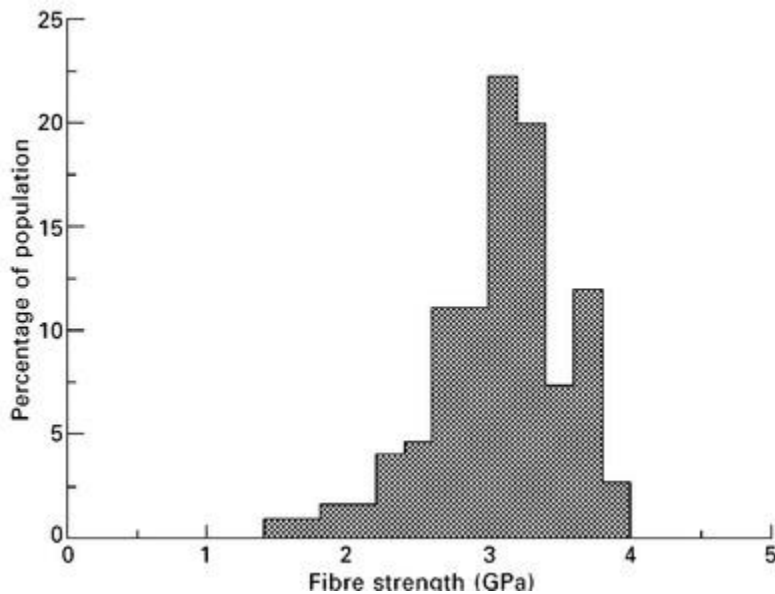
15.23 Strength distribution plot for carbon fibre.

Longitudinal tensile strength of unidirectional composites

The tensile strength of unidirectional composite materials such as carbon fibre–epoxy is much higher than many aerospace alloys, including the aluminium alloys used in aircraft structures. For

example, Table 15.2 shows that the specific tensile strength of carbon fibre–epoxy is about twice that of 2024 aluminium alloy. Owing to the failure stress of the fibres used in aerospace composites being much higher than the polymer matrix, the longitudinal tensile strength is strongly influenced by the tensile strength and volume fraction of the fibres. For example, the fibres typically account for 95–98% of the tensile strength of a unidirectional carbon–epoxy composite at the volume contents used in aircraft structures ($V_f \sim 0.55$–0.65). The contribution of the polymer matrix to the strengthening of unidirectional composites is very small.

Unlike the calculation of the elastic properties, micromechanical modelling is usually not accurate in the calculation of the tensile strength of composite materials. The accurate determination of the strength properties requires tensile testing of the material. Modelling based on weighted averaging can be used to approximate the longitudinal strength, but should never be used as an accurate value without being validated by tensile testing.

The simplest micromechanical model for longitudinal tensile strength assumes two cases: (i) the fibre failure strain is lower than the matrix failure strain or (ii) the fibres fail at a higher strain than the matrix. The first case is represented by the stress–strain condition shown in Fig. 15.24, and it applies to carbon fibre–epoxy and most other composite materials used in aircraft.
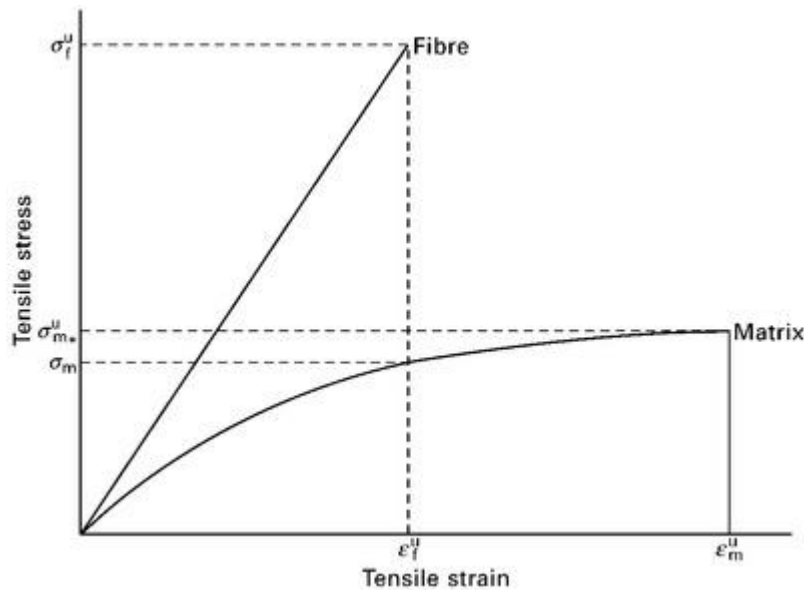
15.24 Tensile stress–strain curves for the fibre reinforcement and polymer matrix where the ultimate failure strain of the fibre (ε_f^u) is lower than the matrix $\left(\varepsilon_m^u \right)$.

When the failure strain of the fibres is lower than the matrix, then the longitudinal tensile strength (X_T) of a unidirectional composite is given by:

$$X_T = \sigma_f^u V_f + \sigma_m^* V_m \quad \textbf{[15.9]}$$

where σ_m^* is the matrix strength at the fibre failure strain.

As mentioned, the failure strength of brittle fibres is determined by the size of the largest flaw, which varies from fibre to fibre. As a result, fibres break over a range of stress values when a composite is loaded in tension. Those fibres with the lowest strength (because they contain the largest flaw) are the first to fail within the material. As the tension stress applied to the composite increases the fibres containing smaller

flaws break until all the fibres are broken, and this event defines the ultimate tensile strength of the composite material. For example, Fig. 15.25 shows the effect of increasing tensile stress on the number of broken fibres within a unidirectional carbon-epoxy composite. The fibres begin to break at a threshold stress level, above which the total number of broken fibres rises at an increasing rate until the final failure stress. The design load limit for composite materials used in aircraft structures is well below this threshold limit to ensure that no fibres are broken during routine flight operations.
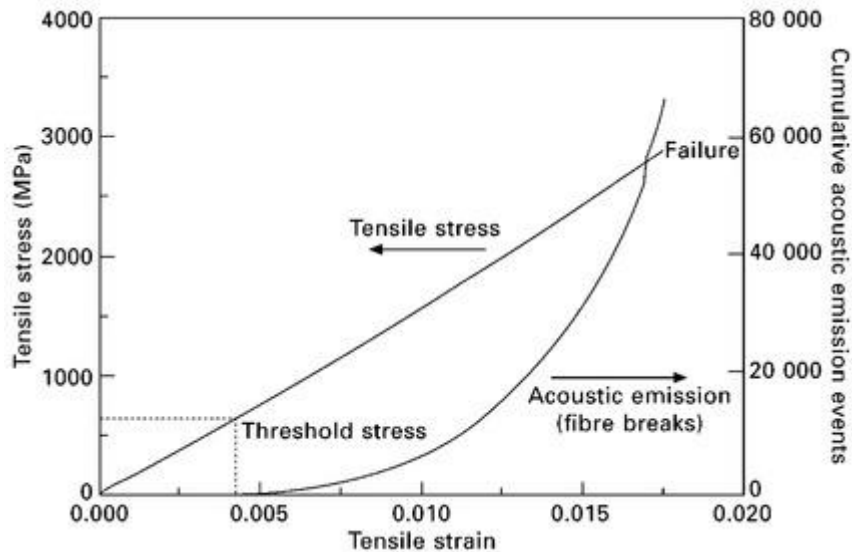
15.25 Effect of increasing tensile stress on the number of fibres broken (as measured by the cumulative number of acoustic emission events) within a unidirectional carbon–epoxy composite.

An important process in the tensile failure of fibres is shear lag, which is illustrated in Fig. 15.26. When a fibre breaks, its capacity to carry the applied tensile stress does not immediately drop to zero. The broken fibre can continue to carry load by transferring the stress across the break by shear lag. This is a process whereby tensile stress is transferred between the two ends of a broken fibre by shear flow of the surrounding polymer matrix. The efficacy of the shear lag process to transfer stress across a broken fibre decreases with increasing tensile strain because the two fibre ends become further apart. Therefore, the tensile load capacity of broken fibres decreases with increasing strain, and this has the result of more stress being exerted on the unbroken fibres. These fibres then become overstressed which causes them to break. As more fibres break the number of remaining intact fibres becomes fewer until eventually the composite fails. Without this shear lag process, the longitudinal tensile strength of composite materials would be lower than it actually is.
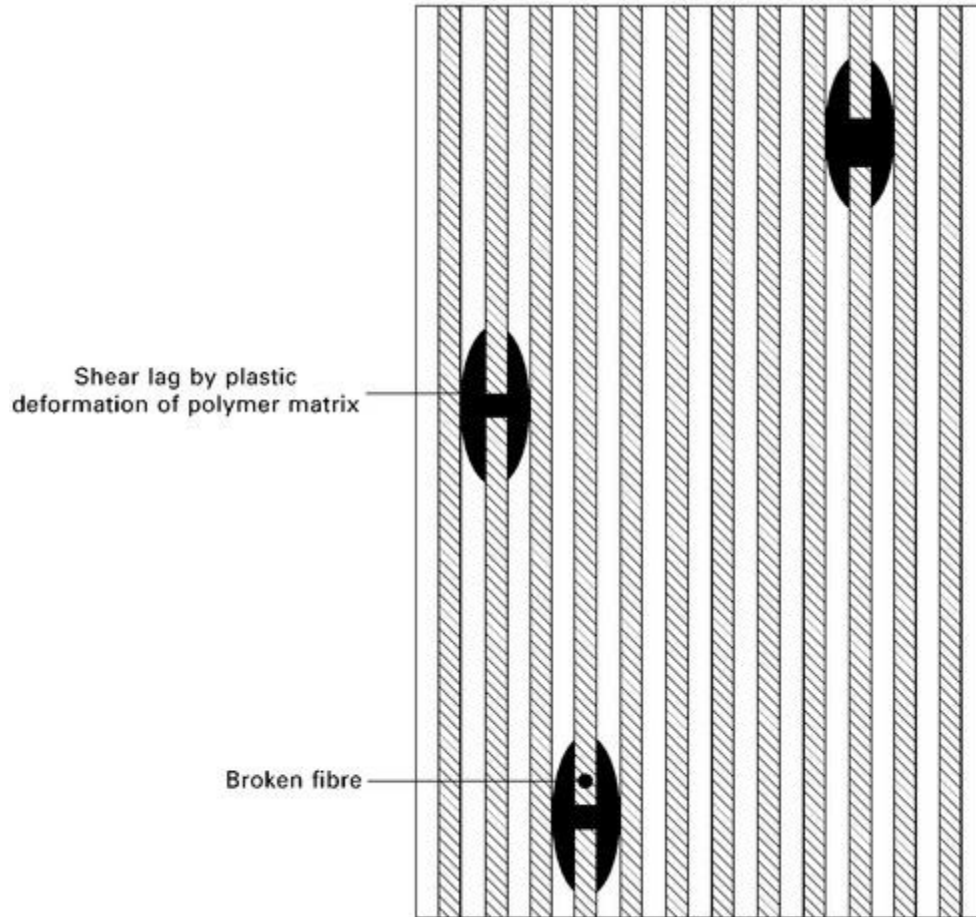
15.26 Schematic of the shear lag process whereby the applied tensile stress is carried across the broken ends of fibres by shear deformation of the matrix.

Transverse tensile strength of composites

The transverse tensile strength of composite materials is much lower than their longitudinal strength owing to the absence of fibres aligned in the transverse direction. Figure 15.27 compares the longitudinal and transverse tensile strengths of a carbon–epoxy composite over a range of fibre contents, and the failure strength in the transverse direction is just a small fraction (typically less than 5–10%) of the longitudinal strength. This is one reason for the poor impact damage resistance of composite structures, with impact events such as bird strike causing significant damage owing to the low transverse strength. (The impact damage resistance of composites is described in chapter 19).
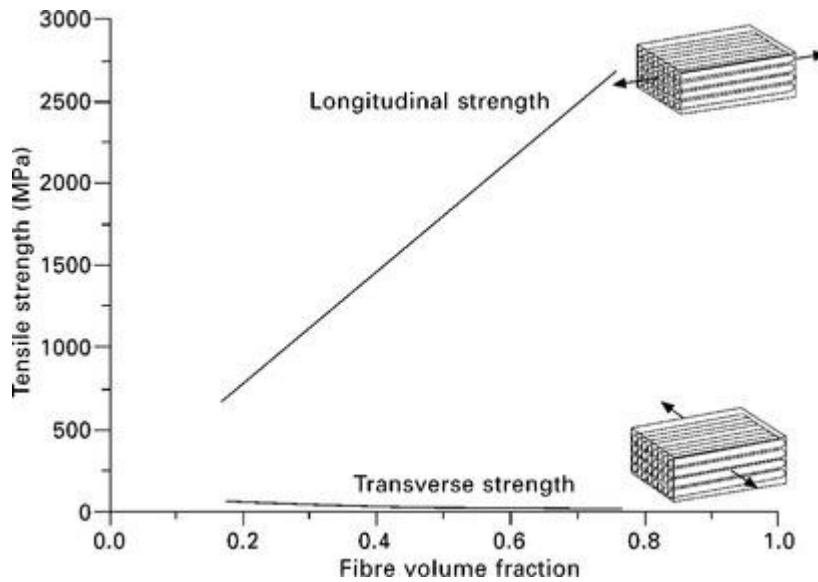
15.27 Effect of fibre content on the longitudinal and transverse tensile strengths of a unidirectional carbon–epoxy composite.

The transverse strength is controlled by the failure strength of the interface between the fibres and matrix. Failure under transverse tensile loading usually occurs by cracking along the fibre–matrix interface, as shown in Fig. 15.28. The use of sizing compounds on the fibre surface to promote strong adhesion bonding with the polymer matrix is one of the common ways to increase the transverse tensile strength. Like the transverse Young's modulus, the transverse tensile strength is not influenced significantly by the type or properties of the fibres and, therefore, different types of composite materials have similar failure strengths (usually in the range of 30–80 MPa).
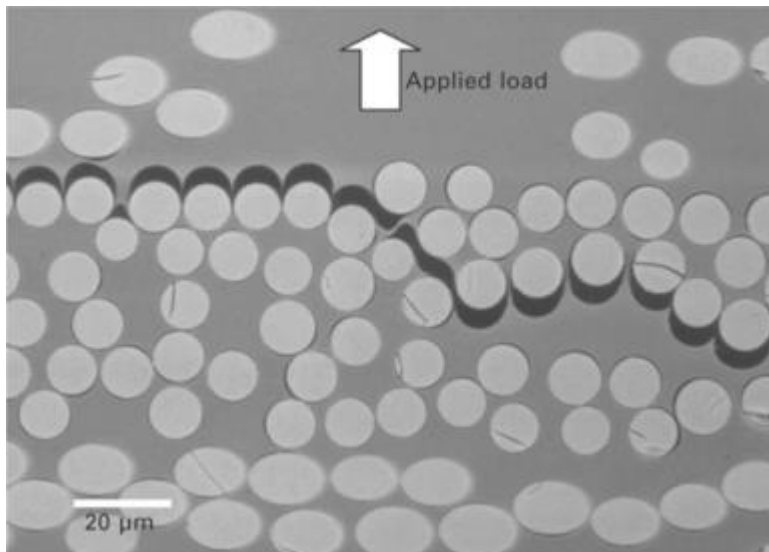
15.28 Cracking between the fibres and matrix in a composite material under transverse tensile loading.

Analytical models have been developed to calculate the transverse tensile strength of composite materials. The simplest model treats the fibres as cylindrical holes in the polymer matrix that have no strength, as

illustrated in Fig. 15.29. The transverse strength (Y_T) is then calculated by considering the reduction in the effective load-bearing area owing to the holes created by the fibres, which can be expressed as:
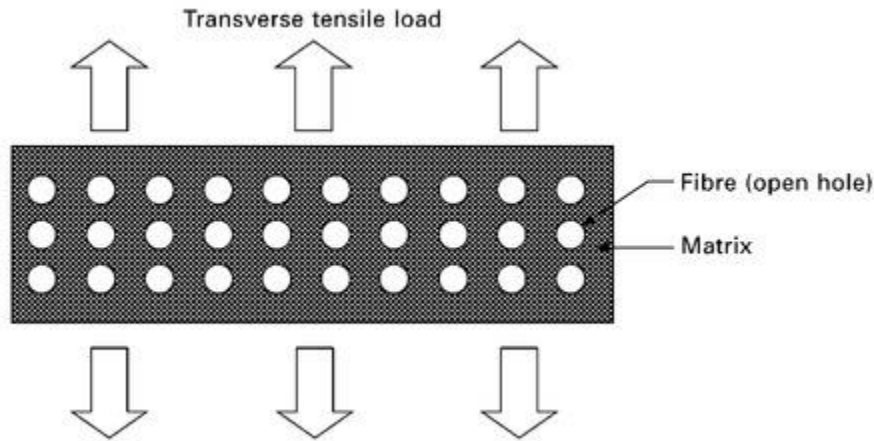
15.29 Representation of a composite material with a square pattern of fibres subjected to transverse tensile loading.

$$Y_T = \sigma_m \left[1 - 2\left(\frac{V_f}{\pi}\right)^{1/2} \right]$$ **[15.10]**

when the fibres are arranged in a square grid pattern. σ_m is the tensile strength of the polymer used for the matrix. Equation [15.10] gives an approximate estimate of the transverse tensile strength of composite materials, but like the longitudinal strength the most accurate method for determining the strength is by tensile testing.

Effect of fibre orientation on tensile strength

The tensile strength of a unidirectional composite is dependent on the fibre angle in a similar way to the Young's modulus. Figure 15.30 shows the effect of fibre angle on the tensile strengths of unidirectional carbon–epoxy and glass–epoxy materials. The strength drops rapidly with increasing angle owing to the loss in load-bearing capacity of the fibres, which are only highly effective when aligned close to the load direction (within 3–5°). This behaviour, along with the highly orthotopic modulus properties, is the reason why unidirectional composites should not be used in aircraft structures.
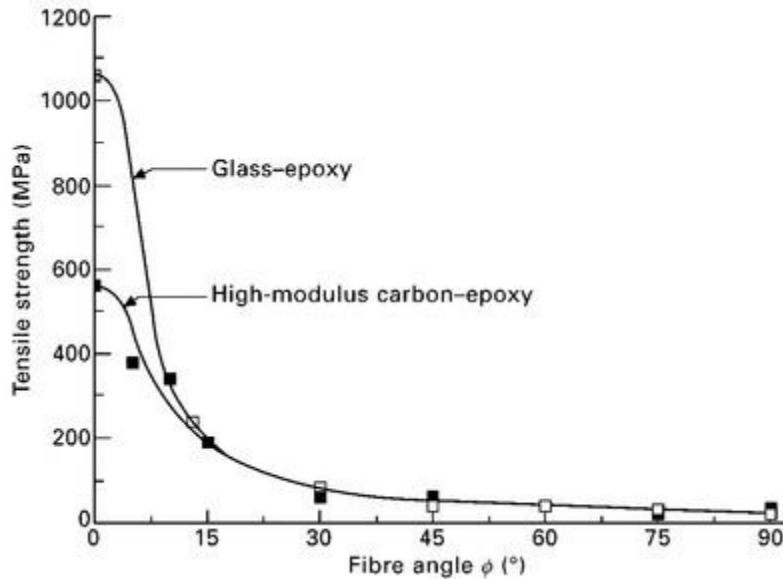
15.30 Effect of fibre angle on the tensile strength of unidirectional carbon–epoxy and glass–epoxy composites.

The effect of fibre angle on the tensile strength of a unidirectional composite can be calculated in several ways, although the easiest method is to treat the failure process using three arbitrary stress states. Failure is assumed to occur in one of three modes:

○ Mode I: failure occurs by tensile rupture of fibres at small angles (typically $\phi < 5°$).
○ Mode II: failure occurs by shear of the matrix or fibre/matrix interface between small and intermediate angles ($5° < \phi < 45–60°$).
○ Mode III: failure occurs by transverse tensile fracture at high angles ($\phi > 45–60°$).

Failure of a unidirectional composite under off-axis tensile loading can be estimated using the maximum stress criterion. This criterion assumes that the stresses for the three mode conditions are related to the fibre angle as follows:

○ Mode I: axial tensile stress: $\sigma = X_T/\cos^2 \phi$
○ Mode II: shear stress: $\sigma = 2S_{12}/\sin 2\phi$
○ Mode III: transverse tensile stress: $\sigma = Y_T/\sin^2 \phi$

where X_T, S_{12} and X_Y represent the failure strengths of the composite in axial tension ($\phi = 0°$), in-plane shear ($\phi = 45°$) and transverse tension ($\phi = 90°$), respectively. These three equations are solved over the range of fibre angles between 0° and 90°, as shown in Fig. 15.31. The curve which has the lowest strength value over the range of fibre angles is then used to define the failure strength. It is shown in Fig. 15.31 that this approach provides a good estimation of the reduction to the tensile strength of a unidirectional composite with increasing fibre angle.
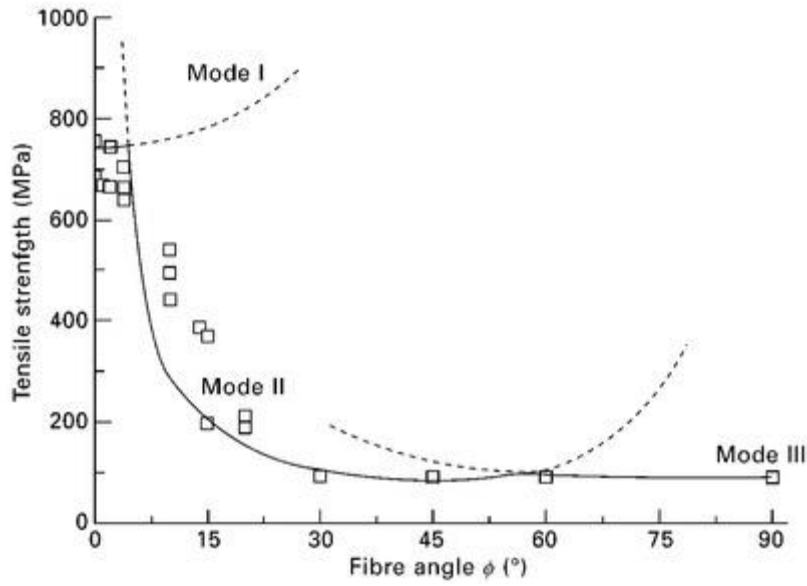
15.31 Calculation of the effect of fibre angle on the tensile strength of a unidirectional carbon–epoxy composite using the maximum stress criterion. The data points are experimental strength values. The full curves indicate the range of fibre angles when the equations for the maximum stress criterion are valid.

Longitudinal compressive strength of composites

The failure strength of composite materials under compression loading is usually different than under tension owing to the different failure behaviour. The most common failure modes of composites under in-plane compression are microbuckling or kinking of the load-bearing fibres. Microbuckling involves the lateral (out-of-plane) buckling of fibres over a small region, as shown schematically in Fig. 15.32. Kinking involves the localised out-of-plane rotation and fracture of the fibres, as shown in Fig. 15.33, and occurs more often in carbon fibre–epoxy composites than microbuckling.
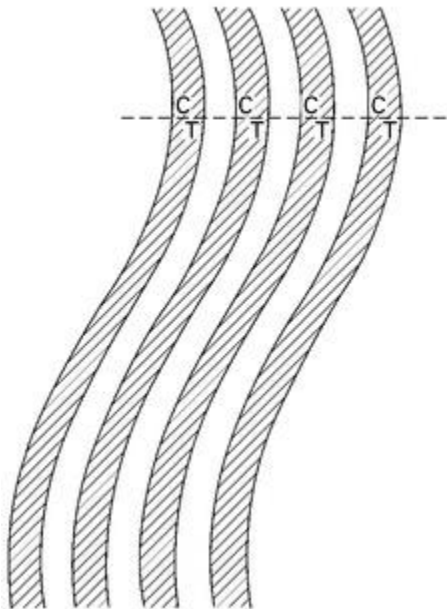
15.32 Schematic of microbuckling of a unidirectional composite under compression loading. 'C' represents compression and 'T' represents tension loading on the fibre surface during microbuckling.
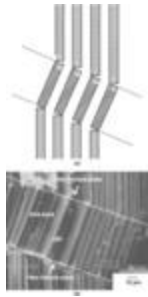
15.33 (a) Schematic of kinking and (b) a kink band within a composite material.

Kinking occurs from a local buckling instability, which develops in the load-bearing fibres. The instability arises from a defect (e.g. void, resin-rich region) or free edge which does not provide sufficient lateral restraint to the fibre under compression loading. The instability allows the fibre to rotate in a very small region towards the defect or free edge, with the amount of fibre rotation increasing with the compressive strain. As the small region of fibres is rotated, the surrounding polymer matrix is plastically deformed by shear stress generated by the rotation process. Eventually, the fibres rotate over a sufficiently large angle that they break over a small length (usually 100–200 μm long), which is called a kink band. Once the first fibres fail by kinking, the other fibres are overloaded and they also then fail by kinking. A kink band propagates rapidly through the composite material causing compressive failure. Although the kink band is short in length, once it has propagated through the load-bearing section of the composite the material can no longer support an applied compression load.

Brittle fibre composites, such as carbon or glass-reinforced materials, fracture along a well-defined kink plane when loaded to the compressive failure stress. The compressive strength of a unidirectional composite that fails by kinking is calculated using:

$$X_C = \frac{\tau_y}{\gamma_y + \phi}$$ [15.11]

where τ_y and γ_y are the shear yield stress and shear yield strain, respectively, of the polymer matrix, and ϕ is the fibre misalignment angle. This equation shows that the kinking stress is dependent on the fibre angle, and maximum compressive strength is attained when the fibres are aligned with the direction of compression loading. The kinking stress decreases rapidly with increasing fibre angle in a manner similar to the tensile strength (Fig. 15.30). The kinking stress is also dependent on the shear properties of the polymer matrix, and one of the most effective ways of increasing the compressive strength of composites is to have a polymer matrix with high shear resistance. For example, Fig. 15.34 shows the large improvement to the compressive kinking stress that can be attained by increasing the matrix shear strength.
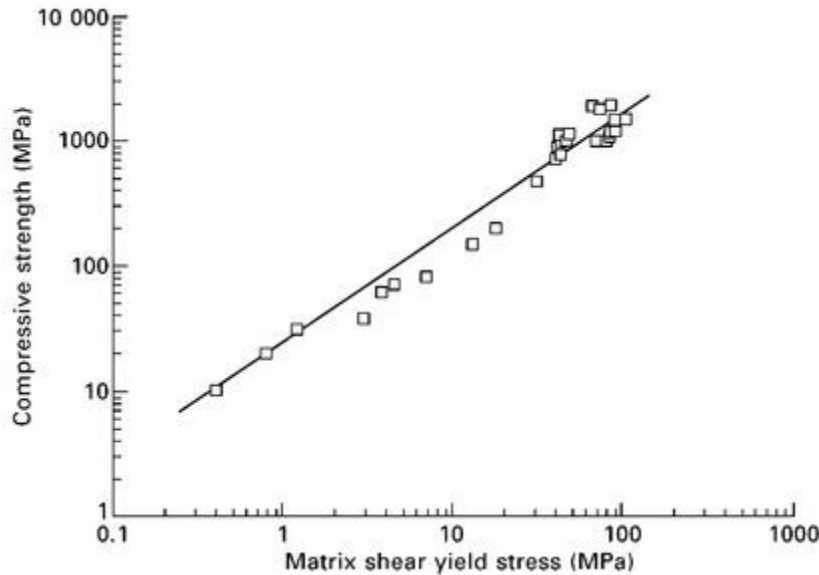
15.34 Effect of matrix shear yield strength on the compressive strength of unidirectional composite materials (adapted from P. M. Jelf and N. A. Fleck, 'Compressive failure mechanisms in unidirectional composites', *Journal of Composite Materials*, 26 (1992), 2706–2726).

Strength properties of multidirectional composites

As mentioned, unidirectional composites are not used in aircraft structures owing to their highly orthotropic properties. These materials are only structurally efficient when the load is applied parallel with the fibre, which is difficult to ensure for aircraft structures. Instead, quasi-isotropic and cross-ply composite materials are commonly used, and the effect of load angle on their tensile and compressive strength properties are similar to that shown in Fig. 15.19 for the Young's modulus. The strength properties are reasonably constant at the different load angles in the quasi-isotropic composite owing to the presence of an equal proportion of 0°, +45°, −45° and 90° fibres. The tensile and compressive strengths of the cross-ply composite are highest in the 0° and 90° directions and lowest at 45°.

15.5.4 EFFECT OF MICROSTRUCTURAL DEFECTS ON MECHANICAL PROPERTIES

The mechanical properties of composite materials can be adversely affected by defects which are inadvertently created using manufacture. Manufacturing defects include voids, dry spots, resin-rich regions, irregular fibre distribution, micro-cracks, shrinkage, and misaligned fibres. Controlled manufacturing conditions and stringent quality control checks are applied to ensure that the composites produced for aircraft structures have a defect content which is below an acceptable level. Composites having high defect content must be repaired (if economically feasible) or scrapped.

Of the many types of defects, the most common are voids which are created by air being trapped within the material during ply lay-up or by gas created as a by-product of the cure reaction of the polymer matrix. The processes used to manufacture aerospace composites, such as autoclave curing, resin transfer moulding and vacuum bag resin infusion, result in low void contents (typically under 1% by volume). In addition, the epoxy and other thermoset resins used as the matrix material are formulated to yield little or no gaseous volatiles during curing and, therefore, void formation is minimised. Despite these measures, voids can still occur, thus reducing the mechanical properties. Voids are more detrimental to the mechanical properties influenced by the matrix, the so-called matrix-dominated properties, than the fibre-dominated properties. Matrix-dominated properties include interlaminar shear strength, impact resistance and delamination

fracture toughness. Fibre-dominated properties include the tensile modulus and strength, and these are not affected significantly by voids unless present at a high volume content.

Figure 15.35 shows the effect of volume content of voids in an aircraft-grade carbon–epoxy composite on the interlaminar shear strength (matrix-dominated property) and tensile strength (fibre-dominated property). The interlaminar shear strength decreases rapidly with increasing void content above about 1%, and this behaviour is typical for matrix-dominated properties, whereas the tensile strength is largely unaffected. For this reason, the volume content of voids (and other defect types) in aircraft composite materials must be kept to very low levels (under 0.5–1.0%) to avoid any significant loss in mechanical performance.
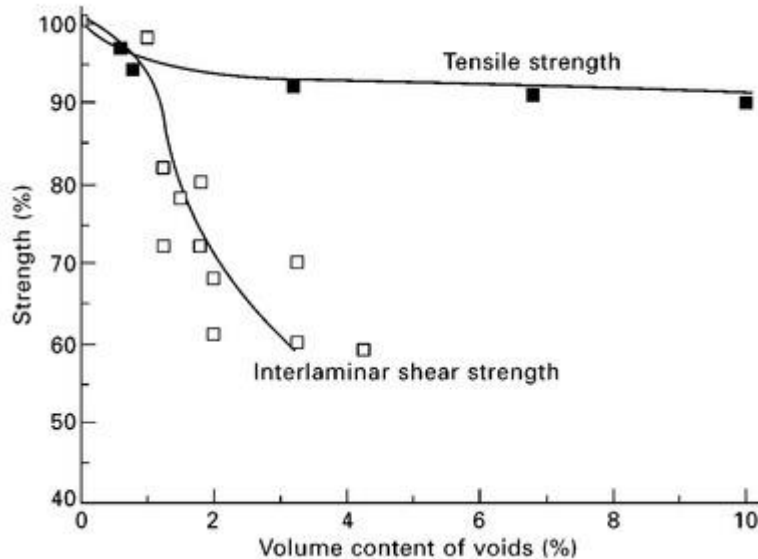
15.35 Effect of void content on the percentage tensile and interlaminar shear strengths of a carbon fibre–epoxy composite.

15.6 Sandwich composites

Sandwich composite materials consist of thin face skins bonded to a thick low-density core material. By the correct choice of materials for the skins and core, sandwich composites provide higher ratios of stiffness-to-weight and strength-to-weight than many metals and fibre–polymer laminates. In most cases, the main reason sandwich construction is used is to reduce weight, but it also provides other advantages including improved acoustic damping (noise reduction), thermal insulation, and impact absorption.

Sandwich composites are used almost exclusively in secondary aircraft structures such as the control surfaces (e.g. ailerons, flaps, spoilers, slats), engine nacelles, radomes, floor panels, and the vertical tailplane (Fig. 15.36). Rarely, if ever, are sandwich materials used in primary structures of conventional civil or military aircraft. An exception is the sandwich fuselage of the Beech Starship, which is an all composite aircraft (Fig. 15.37). Sandwich composites are also used in the fuselage and wings of sailplanes and other ultralight aircraft.
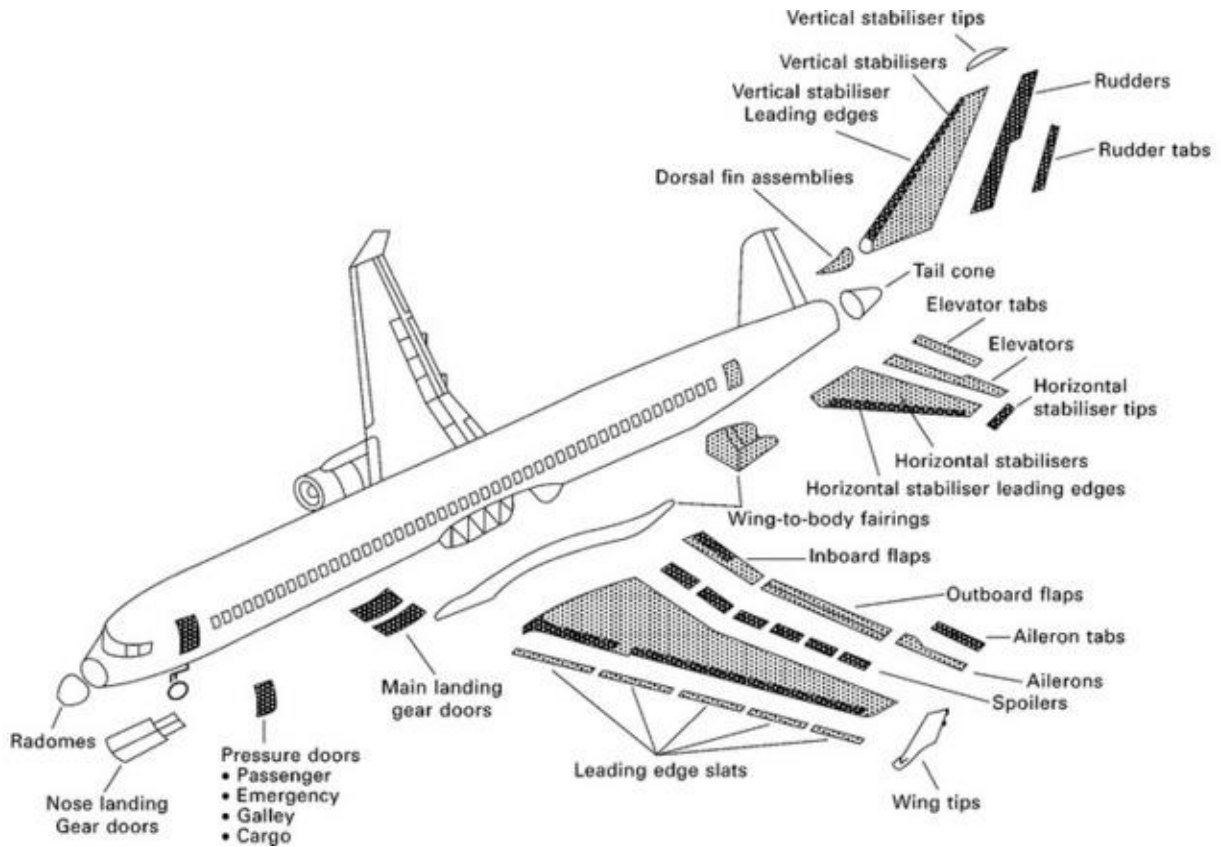
15.36 Aerospace applications of sandwich composites.

15.37 Beech Starship has a sandwich composite fuselage construction.

Sandwich construction is used most often for aircraft structures subjected to bending loads. The separation of the face skins, which are stiff and strong, using the lightweight core offers the possibility of making the resulting stresses act far from the neutral axis of the structure. Moving the skins away from the neutral axis greatly increases the bending stiffness and thereby makes sandwich structures resistant to buckling. The skins carry most of the in-plane tension, compression and bending loads applied to the sandwich structure.

The function of the core is to carry shear stresses resulting from transverse loads, to support the face skins, and to maintain a separation distance between the skins. To fulfil these functions the core material must have sufficient shear stiffness. Table 15.5 compares the structural efficiency of a monolithic material (in this case a 0.8 mm sheet of aluminium) against two sandwich composite materials with different thickness. When loaded in bending, the stiffness and strength increases with the thickness of the sandwich material. At the highest thickness, the strength is increased over 9 times and the stiffness by 37 times, but with only a 6% increase in weight.

Table 15.5

Structural efficiency of sandwich composite panels. Note that the overall material thickness doubles but the skin material thickness remains the same for cases B and C
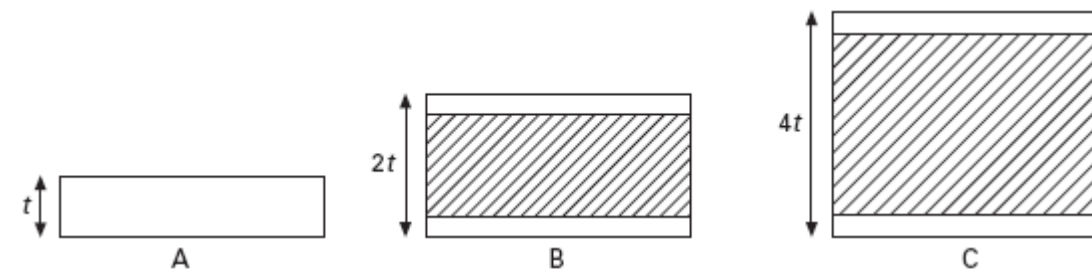
Property	A	B	C
Relative stiffness	100	700	3700
Relative strength	100	350	925
Relative weight	100	103	106

The face skins are made of a thin sheet of fibre–polymer laminate such as carbon–epoxy, although in earlier sandwich constructions aluminium alloy was used. There are four main groups of low-density core materials: honeycomb cores, corrugated cores, foam cores, and monolithic cores of homogeneous material. The first three types are used in aircraft sandwich composites, whereas the monolithic core materials (of which the most common is balsa wood) are rarely used.

Honeycomb core consists of very thin sheets attached in such a way that connected cells are formed. The cell structure closely resembles the honeycomb found in a beehive. The two most common honeycomb configurations are shown in Fig. 15.38: hexagonal and rectangular. Various types of material are used for the honeycomb, with aluminium alloy (usually 5052-H39, 5056-H39 or 2024-T3) and Nomex being the most common in aircraft sandwich components. Nomex is the tradename for a honeycomb material based on aramid fibre paper in a phenolic resin matrix. Aluminium and Nomex core materials have a lightweight cellular honeycomb structure which provides high shear stiffness.
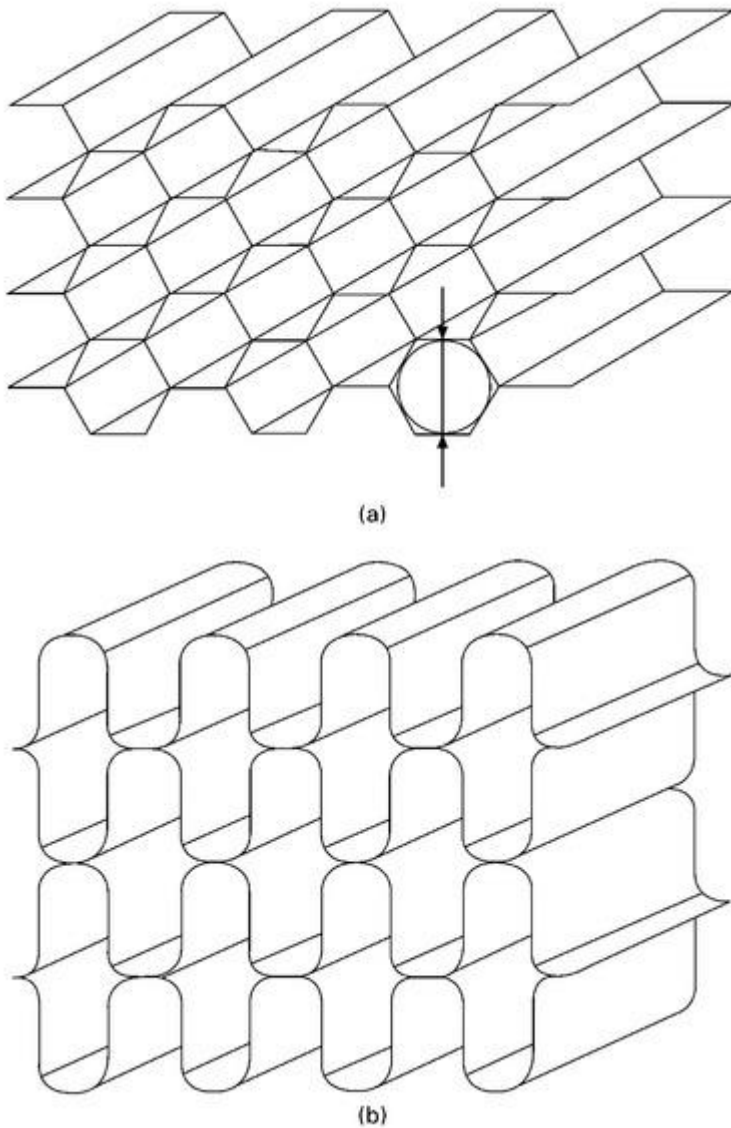
15.38 Honeycomb core types: (a) hexagonal core and (b) rectangular core.

The aerospace industry is increasingly using polymer foams instead of aluminium honeycomb and Nomex because of their superior durability and resistance to water absorption. The foams used are often closed cell, which means the cell voids are completely surrounded by a thin membrane of the solid polymer. Some types of polymer foams have an open cell structure where the cells are interconnected, although these are used rarely in aircraft in preference to closed-cell foams. Examples of closed cell foams are polyetherimide (PEI) and polymethacrylimide (PMI), and these materials have a low-density cellular structure which has high specific stiffness and strength (Fig. 15.39). New types of foam metals are emerging, such as aluminium foams, although these are not currently used in aircraft sandwich materials.
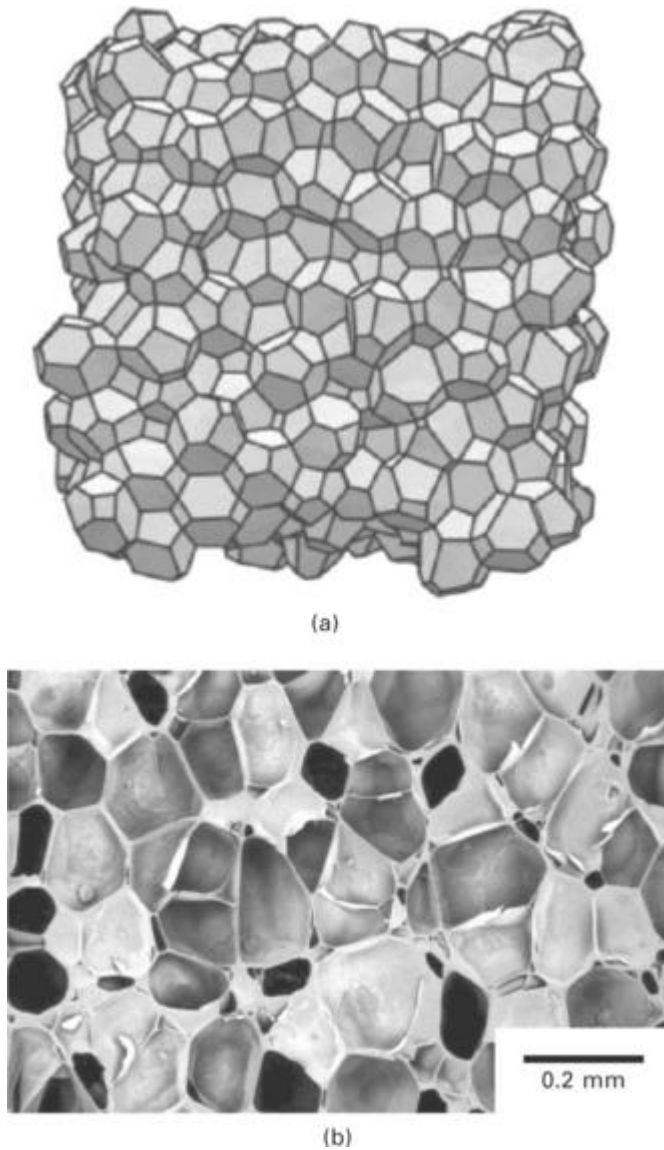
15.39 (a) Schematic and (b) photograph of the closed cell structure of polymer foams.

The mechanical properties of the face skins and core must be balanced to achieve high structural efficiency. The core must have sufficient shear and compressive strength to ensure effective support of the skins. If the core is too weak in shear, the skins bend independently and the bending stiffness of the sandwich material is low. The stiffness and strength properties of core materials increase linearly with their density, as shown in Fig. 15.40, and therefore increased mechanical performance comes with a weight penalty. The core materials used in aircraft structures commonly have density values in the range of 75 to 250 kg m^{-3}, which provides a good balance between mechanical performance and light weight. The stiffness and strength of the skins must be sufficient to provide high tensile and compressive properties to the sandwich composite.
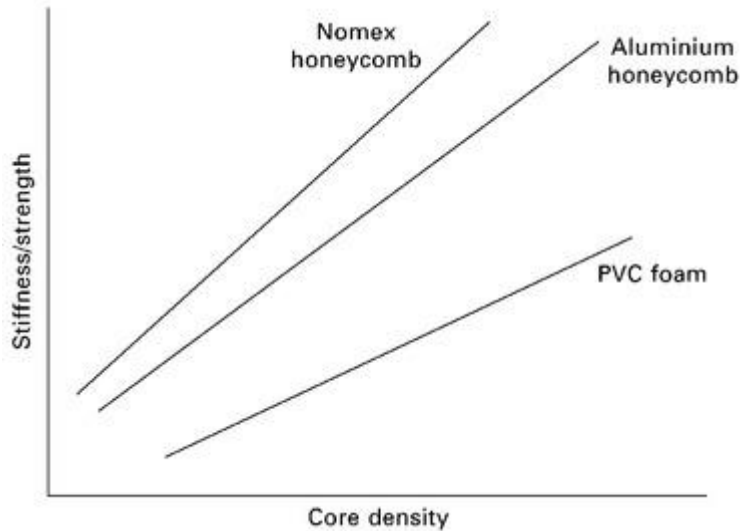
15.40 Effect of the core density on the stiffness and strength of core materials. The PVC foam is shown for comparison, but is not used in aircraft sandwich composite materials.

15.7 Environmental durability of composites

15.7.1 MOISTURE ABSORPTION OF COMPOSITES

The properties of laminates and sandwich composite materials may be affected by the environmental operating conditions of the aircraft. Composites absorb moisture from the atmosphere and this can degrade the physical, chemical and mechanical properties over time so that measures have to be taken to minimise any deterioration by the environment. The combination of high humidity and warm temperature found in the tropics has the synergistic effect of increasing the rate of moisture absorption and accelerating the deterioration of the material. This effect is called hygrothermal (hot/wet) ageing, and it is the most common environmental condition for degrading the properties of composite materials. Aircraft components may also be affected by various fluids used on aircraft, including fuels, fuel additives and hydraulic fluids, as well as by ultraviolet radiation. The long-term durability of composite materials in the aviation environment is essential to maintain structural integrity and safety whilst also minimising maintenance costs and aircraft downtime for inspection and repair.

The absorption of moisture occurs mostly via the diffusion of water molecules through the polymer matrix. Moisture is also absorbed along the fibre–matrix interfacial region, which in some materials can provide a pathway for the rapid ingress of water. Carbon and glass fibres do not absorb moisture and therefore do not assist in the diffusion process. Organic-based fibres, on the other hand, can absorb significant amounts of moisture; for example, aramid fibres can absorb up to 6% of their own weight in water. Because most of the moisture is absorbed by the polymer matrix, the type of resin used in a composite has a large effect on environmental durability. Moisture absorption and its effect on properties can vary by an order of magnitude between different types of polymers. For example, some thermoplastics such as PEEK absorb less than 1% of their own weight in water whereas some thermosets (such as phenolics) can absorb more than 10%. Epoxy resins absorb between about 1% and 4% in water (depending on the type of epoxy), and the epoxies used in external aircraft structures exposed directly to the atmosphere are often selected for their low moisture absorption.

15.7.2 FICKIAN DIFFUSION OF MOISTURE IN COMPOSITES

Exposure of composite materials to humid air and water (rain) allows moisture to diffuse through the outer plies of the composite towards the centre. Water molecules diffuse through the matrix via the ' free space' between the polymer chains under a concentration gradient where the moisture content is highest at the

surface and decreases towards the centre. After a period of time at constant humidity, an even distribution of moisture occurs through the material and this is the saturation limit of the polymer matrix.

The diffusion of moisture into aircraft composite materials can usually be described by Fickian diffusion behaviour. Fickian diffusion is characterised by a progressive increase in weight of the material owing to the uptake of water until an asymptotic value is reached at full saturation, as shown in Fig. 15.41. The rate of moisture absorption increases with the temperature, but is not strongly influenced by the relative humidity of the environment. In other words, the moisture uptake by a composite material occurs faster in warm than in cool conditions, but is not affected significantly by whether it is dry or moist air. The saturation limit, defined by the maximum, steady-state weight gain of the composite, increases with the humidity level of the atmosphere. The absorption of moisture by composites which exhibit Fickian diffusion behaviour is often reversible, and when the material is exposed to a dry environment the water can diffuse out into the atmosphere. Therefore, composite structures used in aircraft that operate in different environmental conditions may undergo cyclic absorption and loss of moisture.
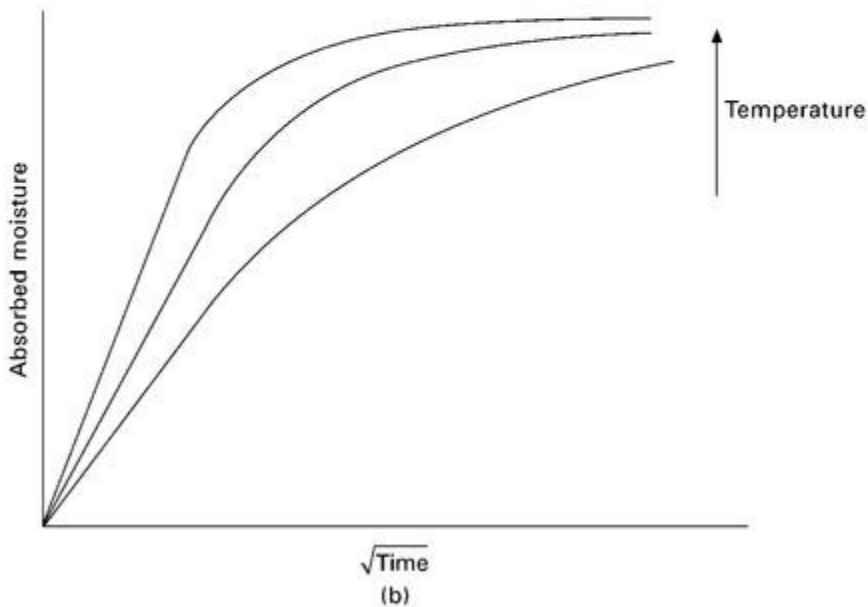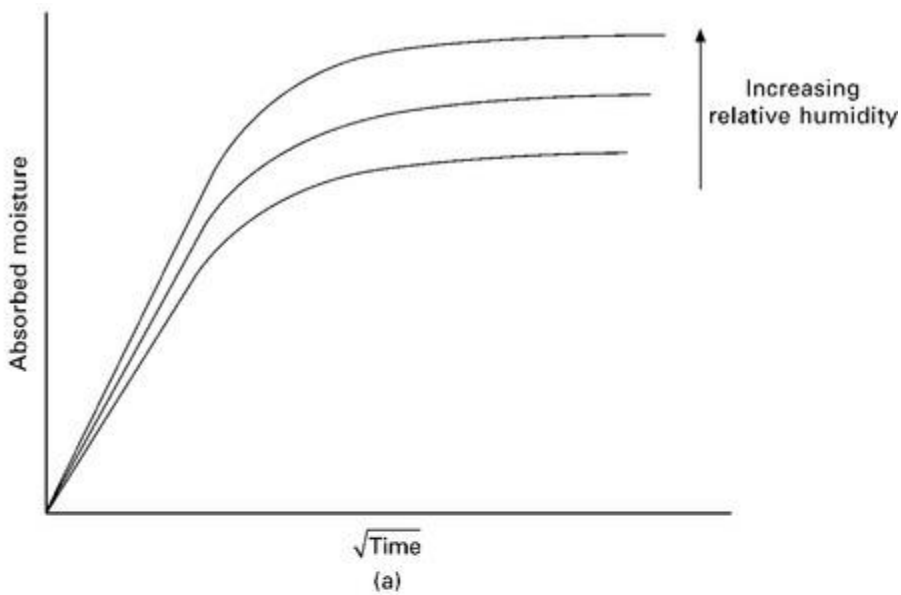
15.41 Weight gain owing to moisture absorption against time ($\sqrt{t}$) for composite materials exhibiting Fickian diffusion behaviour: (a) effect of humidity level; and (b) effect of temperature.

The absorption of moisture into a composite material can be calculated using Fickian diffusion kinetics, which allows the time to saturation to be determined. Fickian behaviour assumes that the moisture concentration gradient through-the-thickness of a material can be expressed as a function of time:

$$\frac{\partial c}{\partial t} = \frac{\mathrm{d}}{\mathrm{d}x}\left(D\frac{\partial c}{\partial x}\right)$$ [15.12]

where c is the moisture concentration, t is time, x is the distance below the material surface, and D is the diffusion coefficient of moisture through the material. The diffusion coefficient is calculated using an Arrhenius equation:

$$D = D_{o}\exp\left(-\frac{E}{RT}\right)$$ [15.13]

where D_o is the diffusion coefficient at a known temperature (T), E is the activation energy for diffusion, and R is the universal gas constant. The diffusion coefficient is related exponentially to temperature, and therefore the rate of moisture absorption increases rapidly with temperature. Figure 15.42 shows the relationship between the diffusion coefficient for water in a carbon fibre–epoxy composite with temperature. An increase in temperature of 10 ° C typically doubles the diffusion rate.
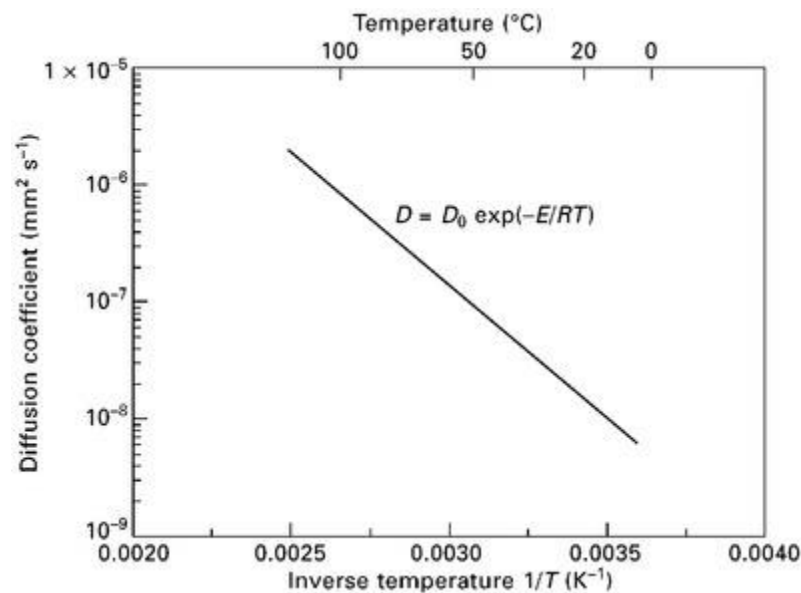
15.42 Relationship between the temperature and the diffusion coefficient for a carbon fibre–epoxy composite.

The weight gain of a composite with increasing time is calculated using:

$$M_t = \left\{ 1 - \frac{8}{\pi^2} \sum_{n=0}^{\infty} \frac{1}{(2n+1)^2} \exp\left[-D(2n+1)^2 \pi^2 t / h^2\right] \right\} M_\infty$$

[15.14]

where t is the time, M_∞ is the mass change at saturation, and h is the thickness of the composite material. This expression can be used to predict the weight gain with time for any fixed environment condition (constant humidity and temperature) where the diffusion coefficient is known.

The diffusion coefficient for anisotropic materials such as a unidirectional composite depends on the fibre orientation, as shown in Fig. 15.43. The diffusion coefficient when moisture ingress is perpendicular to the fibres, which is the case for most composite materials exposed to a humid environment, is calculated using:
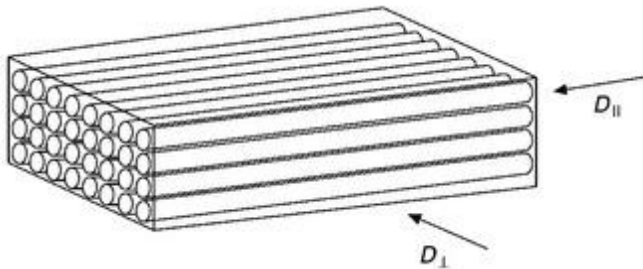
15.43 Moisture absorption in composite materials is anisotropic with the diffusion rate parallel to the fibres ($D_\parallel$) being higher than normal to the fibres ($D\perp$).

$$D_\perp = \left[1 - 2(V_f / \pi)^{1/2}\right] D_m$$

[15.15]

where D_m is the diffusion coefficient for the matrix phase at the known temperature. When moisture ingress occurs parallel to the fibres then:

$$D_\parallel = (1 - V_f) D_m$$

[15.16]

where it is assumed that the fibres are arranged in a regular square pattern. Diffusivity of water in the fibre direction in a carbon–epoxy composite can be up to 10 times higher than that perpendicular to the fibres. However, most composite structures are designed with the fibres parallel to the surface, and therefore only moisture ingress perpendicular to the fibres is considered.

15.7.3 EFFECT OF MOISTURE ON PHYSICAL AND MECHANICAL PROPERTIES OF COMPOSITES

Environmental degradation of the polymer matrix can occur in different ways, depending on the type of resin. Plasticisation, which is characterised by a loss in stiffness and strength, occurs with epoxy and other thermoset resins used in aircraft composites. For example, Fig. 15.44 shows the reduction in the open-hole compressive strength with increasing temperature for a carbon fibre–epoxy composite in a dry or saturated condition. The reduction in strength becomes more extreme in the saturated composite with increasing temperature owing to plasticisation of the matrix phase. Matrix-dominated properties are more sensitive to plasticisation than fibre-dominated properties. As a general rule, for a carbon fibre–epoxy composite cured at 180 °C, moisture reduces the matrix-dominated mechanical properties by up to 10% for subsonic aircraft and 25% for supersonic aircraft (owing to their higher skin temperatures). The absorption of water can also

reduce the glass transition temperature and consequently the maximum operating temperature of the composite. Reductions in the glass transition temperature of 30 °C or more can be experienced, as discussed in chapter 13. Plasticisation is a reversible process, and the properties recover when moisture is driven out of the composite by drying.
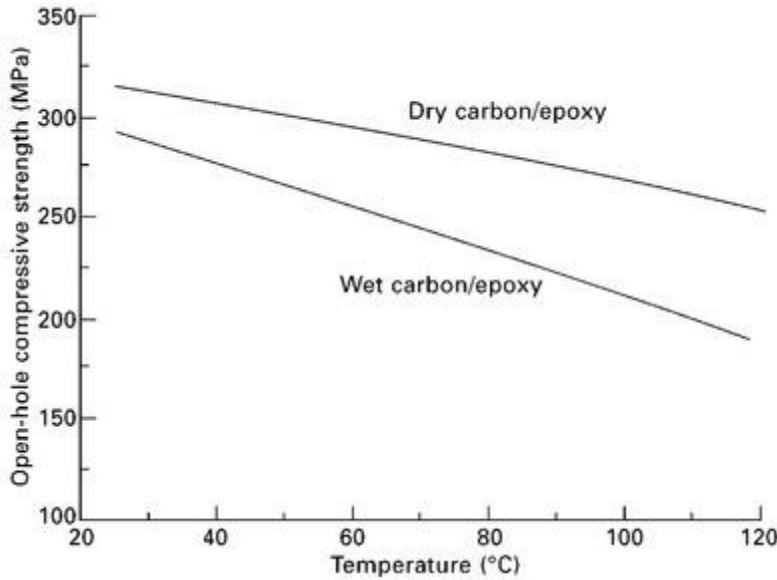
15.44 Effect of moisture absorption on the open-hole compressive strength of carbon fibre–epoxy composite.

More severe forms of degradation of the matrix include chemical changes by hydrolysis or chain scission reactions between the polymer and water. The polymer chains can be broken down by chemical reactions with the water. These changes are irreversible, and epoxies and other aerospace resins are formulated to avoid this type of damage. Swelling and volumetric stresses can occur when a large amount of moisture is absorbed, which causes warping and cracking of the composite.

Moisture absorption is a problem for sandwich composites with an open-cell core material, such as Nomex or aluminium honeycomb. Moisture diffuses through the laminate face skin and forms water droplets within the core, as shown in Fig. 15.45. Often after long-term exposure the water builds up at the bottom of the cells where it can soften Nomex and corrode aluminium honeycomb. This problem can be avoided by the use of closed cell polymer foam.
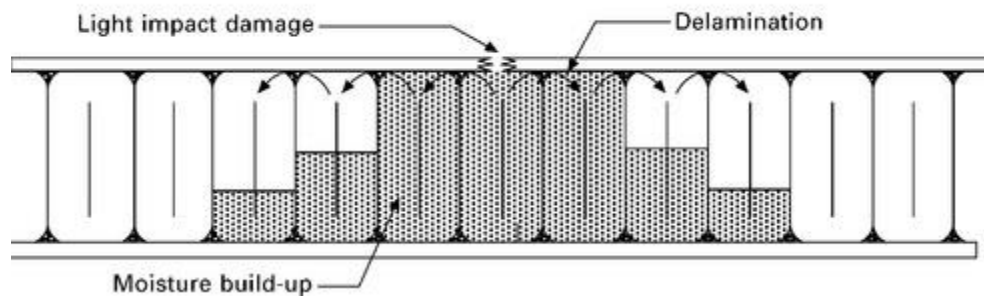
15.45 Moisture absorption into open-cell cores within sandwich composites owing to skin damage (reproduced from G. Kress, 'Design Criteria', in: *ASM Handbook Volume 21: Composites*, ASM International, Materials Park, OH, 2001).

Water trapped within composites can seriously affect the properties when it freezes. Water that collects within voids and cracks in composites and within the cells of core materials freezes when exposed to cold conditions at high altitude. Water expands when it freezes and has a higher bulk modulus than epoxy resin. Therefore, when water freezes it exerts tensile pressure on the surrounding composite material that can cause permanent damage, such as delamination cracking. The water freezes and melts each time the aircraft ascends or descends from high altitude, which causes cyclic stressing of the composite in a process called freeze/thaw.

15.7.4 EFFECT OF ULTRAVIOLET RADIATION ON COMPOSITES

The surface of composite materials can be degraded by ultraviolet (UV) radiation which breaks down the polymer matrix and, if present, organic fibres such as aramid. UV radiation destroys the chemical bonds in epoxy resins and many other types of polymers, and the degraded material is then removed from the surface by wind and rain. UV damage is often confined to the topmost layers of the material, and the bulk properties are unlikely to be affected owing to the slow rate of degradation. It is possible to dope polymers with UV-absorbing compounds to minimise the damage or, alternatively the composite surface can be protected using UV absorbent paint.

15.8 Summary

Composites consist of a reinforcement phase and a matrix phase. The reinforcement can be particles, whiskers or continuous fibres. Aerospace composites are reinforced with continuous fibres which provide higher stiffness and strength than particles or whiskers. The matrix phase can be metallic, ceramic or polymeric, although the matrix for most aerospace composites is a thermoset resin (e.g. epoxy, bismaleimide) or high-performance thermoplastic (e.g. PEEK). The functions of the polymer matrix are to bind the reinforcement fibres into a solid material; transmit force applied to the composite on to the fibres; and to protect the fibres from environmental damage.

There are many advantages as well as several problems with using carbon-fibre composites rather than aluminium in aircraft. The advantages include reduced weight, capability to manufacture integrated structures from fewer parts, higher structural efficiency (e.g. stiffness/weight and strength/weight), better resistance against fatigue and corrosion, radar absorption properties, good thermal insulation, and lower coefficient of thermal expansion. The disadvantages of composites include higher cost, slower manufacturing processes, anisotropic properties making design more difficult, low through-thickness mechanical properties and impact damage resistance, higher sensitivity to geometric stress raisers such as notches, lower temperature operating limit, and lower electrical conductivity.

The mechanical properties of composite aircraft structures are determined using a hierarchical approach to modelling that begins with micromechanical analysis of the unit cell followed by ply analysis then laminate analysis and, finally, structural analysis.

The elastic modulus and strength properties of unidirectional composites are anisotropic, with the mechanical properties decreasing rapidly with fibre angle from the longitudinal (0°) to the transverse (90°) direction. The longitudinal tensile properties are controlled mostly by the properties and volume content of the fibre reinforcement. The transverse properties are more dependent on the matrix properties. The anisotropic properties of composites is minimised by using cross-ply [0/90] or, in particular, quasi-isotropic [0/± 45/90] fibre patterns.

The carbon and glass fibres used in composite materials are brittle and fail at low strain. The fibre strength is determined by the largest flaw, which varies from fibre to fibre. As a result, the tensile strength of fibres varies over a wide range, and does not have a single strength value.

Failure of composites under compression loading occurs by microbuckling or, more often, kinking. Kinking involves the localised out-of-plane rotation and fracture of load-bearing fibres caused by a buckling instability. The compressive strength is determined by the applied stress required to cause kinking, which increases with the shear properties of the polymer matrix and the closer the fibres are aligned to the load direction.

Microstructural defects such as voids, microcracks, resin-rich regions and wavy fibres can reduce the Young's modulus and, in particular, the strength properties of composite materials. Matrix-dominated properties (e.g. interlaminar shear strength, impact resistance) are affected more by defects than fibre-dominated properties (e.g. tensile strength).

Sandwich composites are used in aircraft structures that require high bending stiffness and buckling resistance. The core material must have sufficiently high shear stiffness to transfer load to the face skins. Different types of core materials are used, including honeycombs and closed-cell polymer foams.

Composites can absorb moisture and other fluids (e.g. fuel, hydraulic oil) which can adversely affect their physical and mechanical properties. The most common environmental durability issue for aerospace composites is moisture absorption from the atmosphere, particularly under hot/wet conditions. Thermoset resins generally absorb more moisture than highperformance thermoplastics, and epoxies can gain 1–4% of their original weight owing to water absorption. The composite materials used in aircraft structures often exhibit Fickian behaviour which is characterised by a steady uptake of water until the saturation limit is reached. The absorption rate increases rapidly with temperature whereas the maximum amount of moisture absorbed at the saturation limit is determined by the relative humidity of the environment. The absorption of moisture by epoxy matrix composites causes plasticisation, which is reversible when the material is dried. The absorption of moisture reduces the glass transition temperature and mechanical properties (particularly the matrix-dominated properties). Composites are also susceptible to environmental degradation by freeze/thaw and UV radiation.

Metal matrix, fibre–metal and ceramic matrix composites for aerospace applications

16.1 Metal matrix composites

16.1.1 INTRODUCTION TO METAL MATRIX COMPOSITES

Metal matrix composites (MMCs) are lightweight structural materials used in a small number of aircraft, helicopters and spacecraft. MMC materials consist of hard reinforcing particles embedded within a metal matrix phase. The matrix of MMCs is usually a low density metal alloy (e.g. aluminium, magnesium or titanium). The metal alloys used in aircraft structures, such as 2024 Al, 7075 Al and Ti–6Al–4 V, are popular matrix materials for many MMCs. Nickel superalloys may be used as the matrix phase in MMCs for high-temperature applications.

The metal matrix phase is strengthened using ceramic or metal oxide in the form of continuous fibres, whiskers or particles. Boron (or borsic, a SiC-coated boron), carbon and silicon carbide (SiC) are often used as continuous fibre reinforcement, and these are distributed through the matrix phase. Silicon carbide, alumina (Al_2O_3) and boron carbide (B_4C) are popular particle reinforcements. The maximum volume content of reinforcement in MMCs is usually below 30%, which is lower than the fibre content of aerospace carbon–epoxy composites (55–65% by volume). Reinforcement contents above about 30% are not often used because of the difficulty in processing, forming and machining of the MMC owing to high hardness and low ductility.

16.1.2 PROPERTIES OF METAL MATRIX COMPOSITES

MMCs offer a number of advantages compared with their base metal, including higher elastic modulus and strength, lower coefficient of thermal expansion, and superior elevated temperature properties such as improved creep resistance and rupture strength. Some MMCs also have better fatigue performance and wear resistance than the base metal.

Lower density is an attractive property of MMCs made using a metal matrix having a higher specific gravity than the ceramic reinforcement. The density of most ceramic materials is moderately low (generally under 3 g cm^{-3}) and, when used in combination with a denser metal, there is an overall reduction in weight. Titanium, steel and nickel matrix composites, for example, have lower densities than their base metal which translates into a weight saving. However, aluminium and magnesium alloys, which have a lower or similar density to the ceramic reinforcement, may incur a weight penalty. Figure 16.1 shows the percentage density change of several aerospace alloys with increasing volume content of silicon carbide reinforcement. The weight saving is an incentive for heavy metals such as nickel-based superalloys, provided this is done without degrading important structural properties such as toughness and creep resistance.
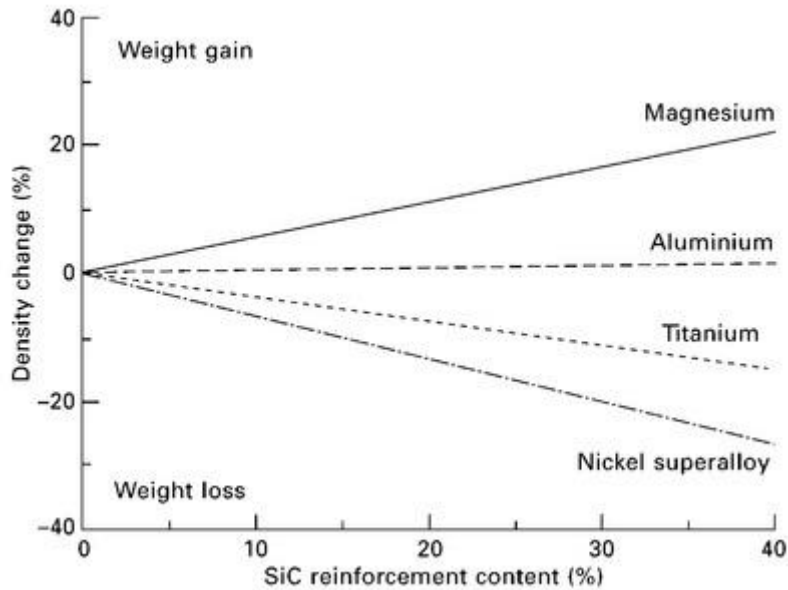
16.1 Percentage change in density of aerospace alloys owing to SiC reinforcement.

MMCs are characterised by high stiffness, strength and (in most materials) fatigue resistance. The improvement in these properties is controlled by the stiffness, strength, volume content and shape of the reinforcement. This control allows the properties of MMCs to be tailored to an application requiring a combination of high properties. The properties of MMC reinforced with continuous fibres are anisotropic, with their mechanical properties such as stiffness and strength being highest in the fibre direction. The modulus is isotropic in MMCs containing whiskers that are randomly aligned or particles that are evenly dispersed through the metal matrix phase. Figure 16.2 shows the effect of increasing volume content of continuous fibres of alumina on the elastic modulus and yield strength of an aluminium–lithium alloy in the parallel and transverse (anti-fibre) directions. The longitudinal and transverse properties increase linearly with the fibre content, and it is possible to increase the stiffness and strength by 50–100% compared with the base metal. The greatest improvement in longitudinal stiffness and strength is achieved using continuous fibres, followed by whiskers and then particles. The fatigue performance of metals can also be improved by ceramic reinforcement. For example, Fig. 16.3 shows a large increase in the fatigue life of an aluminium alloy when reinforced with silicon carbide particles. Improvements in fatigue are generally the result of higher modulus and work-hardening rates of the composite compared with the base material. However, there are occasions when the fatigue life is degraded by ceramic reinforcement.
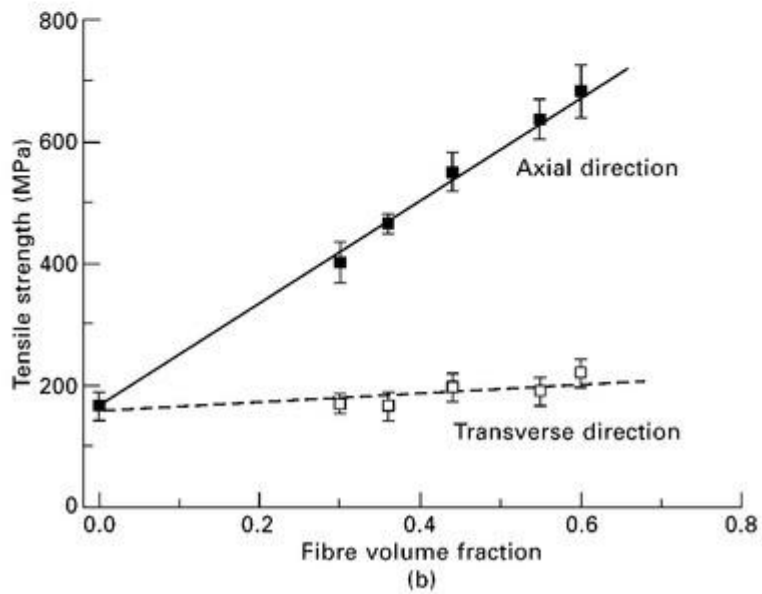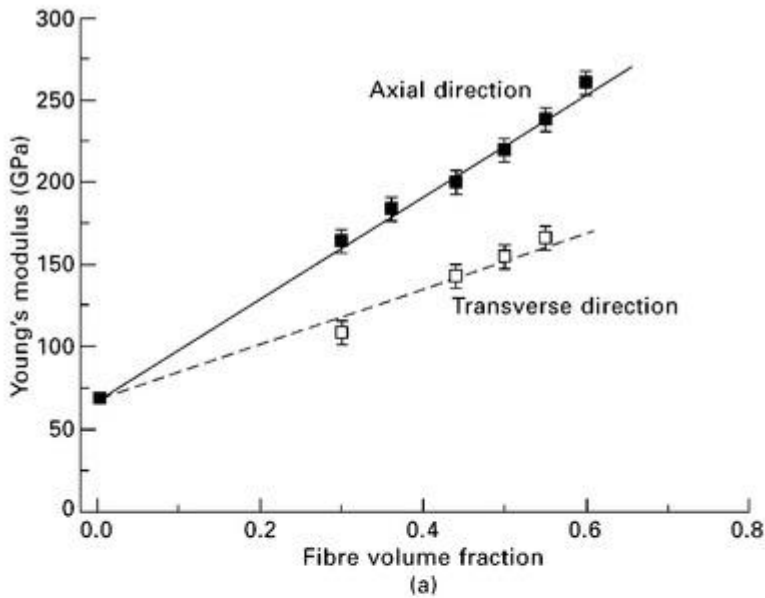
16.2 Effect of increasing Al₂O₃ reinforcement content on the (a) Young's modulus and (b) tensile strength of an aluminium–lithium alloy.
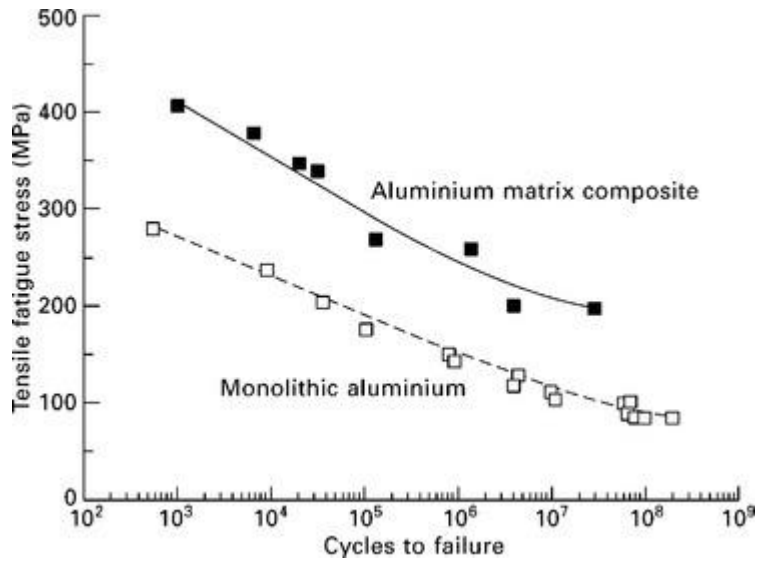
16.3 Fatigue life graphs for an aluminium alloy with and without ceramic particle reinforcement.

MMCs are characterised by low fracture toughness and ductility, which are problems when used in damage-tolerant structures. The toughness and ductility of MMCs depends on several factors: composition and microstructure of the matrix alloy; type, size and orientation of the reinforcement; and the processing conditions. Figure 16.4 shows reductions to the fracture toughness and ductility of aluminium when the reinforcement content is increased to 30–40%, which are typical concentrations used for high-strength applications. Reductions in toughness of over 30% and ductility to under 2–3% are common with many MMC materials.
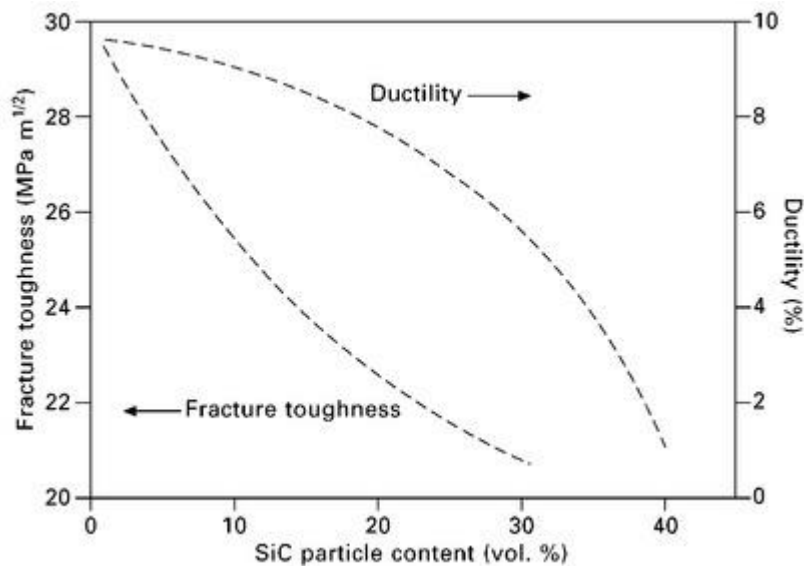
16.4 Typical effect of increasing reinforcement content on the fracture toughness and ductility of metal matrix composites.

16.1.3 AEROSPACE APPLICATIONS OF METAL MATRIX COMPOSITES

Aerospace applications of MMCs are few, and their use is not expected to grow significantly in the foreseeable future owing to problems with high manufacturing costs and low toughness. The current applications are confined to structural components where the design and certification issues are straightforward and there is low risk of failure. MMCs are currently not used on civil airliners and only rarely in military aircraft. One notable application is the two ventral fins on the F-16 *Fighting Falcon*, which are located on the fuselage just behind the wings (Fig. 16.5). The original ventral fins were made of 2024-T4 aluminium. The fins are subjected to turbulent aerodynamic buffeting which causes fatigue cracking in the aluminium alloy. Replacement ventral fins made using a ceramic particle-reinforced aluminium matrix composite (6092Al–17.5% SiC) are fitted to the F-16 to alleviate the fatigue problem. This MMC increased the specific stiffness of the fins by 40% over the baseline design, which reduced the tip deflections by 50% and lowered the torsion loads induced by buffeting. The use of MMC is expected to extend the service life of the fins by about 400%; with the reduced maintenance, downtime and inspections costs saving the USAF an estimated $26 million over the aircraft life. The 6092Al–17.5% SiC particle composite is also used in fuel access door covers on F-16 aircraft. Similar to the ventral fins, the higher stiffness, strength and fatigue life of the MMC eliminated cracking problems experienced with the original aluminium alloy used in door covers.

16.5 Al–SiC composites are used in the ventral fins (circled) and fuel access doors of the F-16 *Fighting Falcon*.

MMCs are used in the main rotor blade sleeve of the Eurocopter EC120 and N4 helicopters. The sleeve is a critical rotating component because failure results in total loss of the main rotor blade. Sleeve materials require an infinite fatigue life under the operating stresses of the rotor blades, together with high specific stiffness and good fracture toughness. Titanium alloy is normally used for the sleeve, but to reduce cost and weight while maintaining high fatigue performance, strength and toughness, the sleeves for the EC120 and N4 are fabricated using a particle-reinforced aluminium composite (2009Al–15% SiC).

The first successful application of MMCs reinforced using continuous fibres was in the space shuttle orbiter. Struts used to stiffen the mid-fuselage (payload) section of the orbiter are made using aluminium alloy reinforced with 60% boron fibres. This composite is also used in the landing gear drag line of the orbiter. The continuous boron fibres are aligned along the axis of the tubular struts and drag line to provide high longitudinal specific stiffness. About 300 MMC struts are used as frame and rib truss members to form the load-bearing skeleton of the orbiter cargo bay, which provides a 45% weight saving over conventional aluminium construction.

Another space application of continuous-fibre MMCs is the high gain antenna boom for the Hubble space telescope (Fig. 16.6). The boom, which is 3.6 m long, is a lightweight structure requiring high axial stiffness and low coefficient of thermal expansion to maintain the position of the antenna during space manoeuvres. The boom also provides a wave guide function and therefore needs good electrical conductivity to transmit signals between the spacecraft and antenna dish. The boom is made using 6061 aluminium reinforced with continuous carbon fibres. The material provides a 30% weight saving compared with previous designs based on monolithic aluminium or carbon–epoxy composite.
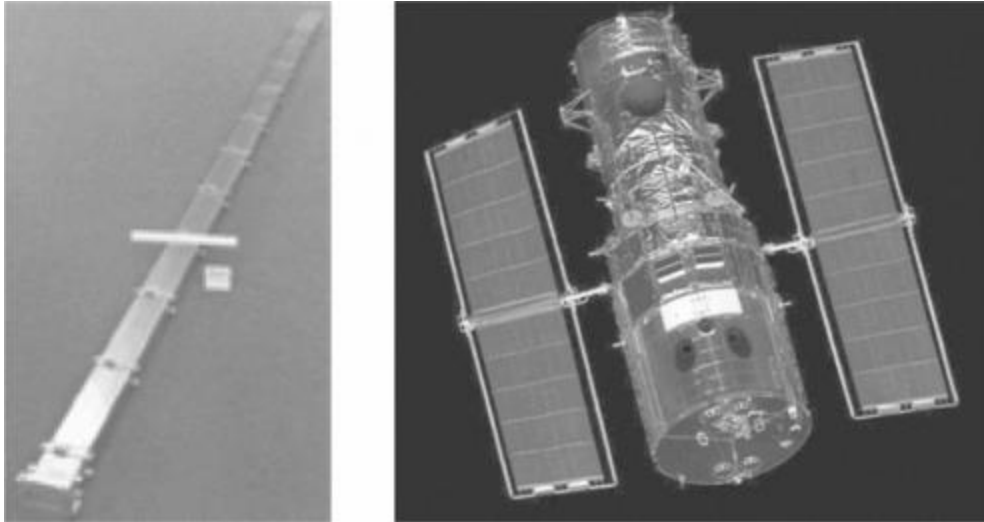
16.6 MMC boom for the Hubble space telescope.

There are many potential applications for MMCs in aircraft gas turbine engines and scram jet engines owing to their low weight, high-temperature stability and excellent creep resistance. Titanium matrix composites may replace heavier nickel-based superalloys in high-pressure turbine blades and compressor discs for jet engines, although much more development work is needed before this is achieved.

The engine and structural applications for MMCs is limited owing to a number of technological problems that are difficult to resolve. MMCs are expensive materials to process into finished components because of high costs in manufacturing, shaping and machining. MMCs are difficult to plastically form using conventional plastic forming processes such as rolling or extrusion owing to their low ductility and high hardening rate. Relatively low levels of plastic forming can cause micro-cracking in the forged MMC component. MMCs are also difficult to machine by milling, routing, drilling and other material removal processes because of their high hardness, which causes rapid tool wear.

MMCs also have poor ductility and low toughness, which is a major concern for the aerospace applications where damage tolerance is a key design consideration for many structural and engine components. Lastly, aerospace engineers are not familiar with MMCs and the large database of technical information required for aircraft certification is lacking. Until the technical issues are resolved, the technology reaches maturity, and aircraft designers become familiar and confident with MMCs, it is likely that the applications for these materials will remain limited despite their high specific stiffness and strength.

16.2 Fibre–metal laminates

16.2.1 INTRODUCTION TO FIBRE–METAL LAMINATES

Fibre–metal laminates (FMLs) are lightweight structural materials consisting of alternating thin layers of metal and fibre–polymer composite (Fig. 16.7). FML is made using thin sheets (0.2–0.4 mm) of lightweight metal, such as aluminium or titanium, bonded to thin layers of prepreg composite, with the outer surfaces

being metal. The most common FML used in aerospace structures is GLARE® (glass-reinforced fibre–metal laminate). GLARE® consists of thin sheets of aluminium alloy bonded to thin layers of high strength glass–epoxy prepreg composite. GLARE® is used in the upper fuselage and leading edges of the vertical fin and horizontal stabilisers of the Airbus 380 aircraft. GLARE® is also used in the cargo doors of the C-17 Globemaster III. Another FML is ARALL® (aramid aluminium laminate) that is made of alternating sheets of aluminium alloy and aramid–epoxy. ARALL® has exceptional impact resistance and damage tolerance, but its use in aerospace structures is limited because of moisture ingress problems into the aramid–epoxy layers, which reduces material integrity.
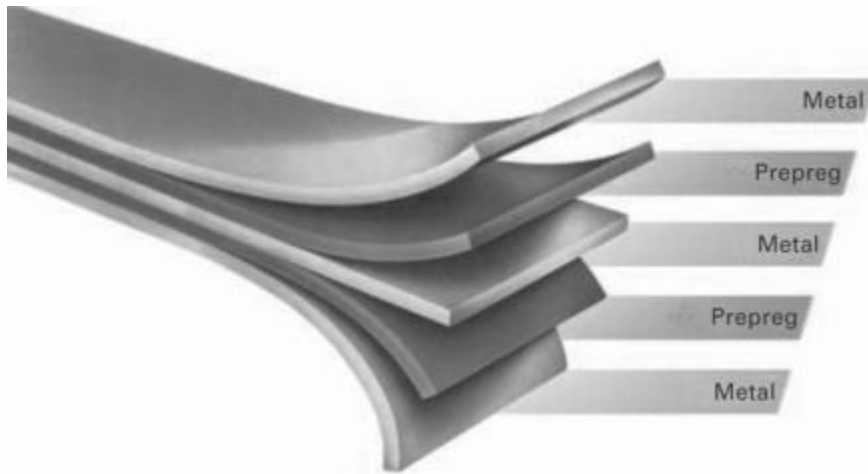
16.7 Fibre–metal laminate.

16.2.2 PROPERTIES OF FIBRE–METAL LAMINATES

FMLs have physical and mechanical properties that make them suitable for aerospace structural applications. These properties include:

• Low weight. FMLs are lighter than the equivalent monolithic metal owing to the lower density layers of prepreg composite. For example, GLARE® has a lower density (~ 2.0 g cm^{-3}) than monolithic aluminium alloy (2.7 g cm^{-3}), which results in a significant weight saving in the A380.

• Mechanical properties. FMLs have higher tensile strength, damage tolerance, impact strength and fatigue resistance than the monolithic metal. These are key reasons for the use of GLARE® in the A380 fuselage. Under flight-loading conditions, the rate of fatigue crack growth in GLARE® is 10–100 times slower than monolithic aluminium alloy because the cracks are stopped or deflected at the metal–composite interfaces.

• Tailored properties. It is possible to tailor the structural properties of FMLs by adjusting the number, type and alignment of the prepreg layers to suit local stresses and shapes through the aircraft.

• Corrosion resistance. Through-the-thickness corrosion is prevented in FML owing to the barrier role played by the composite layers. This limits corrosion damage to the surface metal layer and the internal metal sheets are protected by the composite. Therefore, the incidence of corrosion damage such as pitting and stress corrosion cracking, which are major problems for monolithic aluminium aircraft structures (see chapter 21), is reduced with GLARE®.

• Fire. FML has high fire resistance owing to its low thermal conductivity. GLARE® has lower through-thickness thermal conductivity than monolithic aluminium which results in slower heat flow through the fuselage structure in the event of post-crash fire. FML has better resistance to burn-through in the event of fire and can potentially substitute for titanium in firewalls.

Despite the many benefits derived from using FMLs such as GLARE®, the future of these materials in aircraft structures is uncertain because of their high cost. FMLs are typically 7–10 times more expensive than the monolithic metal, and the high cost is a major impediment to their use in aircraft.

16.3 Ceramic matrix composites

16.3.1 INTRODUCTION TO CERAMIC MATRIX COMPOSITES

Ceramics are used mainly in aerospace for their outstanding thermal stability; which includes high melting temperature, low thermal conductivity, and high modulus, compressive strength and creep resistant properties at high temperature. There are many types of ceramics, with the most important for aerospace being polycrystalline materials and glass–ceramics. A characteristic of ceramic materials is high strength under compression loading, but low strength and toughness under tension. The compressive strength of most polycrystalline ceramics is in the range 4000–10 000 MPa, whereas the tensile strength is only 50–200 MPa. The fracture toughness of most ceramics is 10–50 times lower than high-strength aluminium alloy. Ceramics have low tolerance to tiny voids and cracks that occur during fabrication or in service, and these defects cause brittle fracture under low tensile loads. For this reason, the strength, ductility and toughness properties are too low for ceramics to be used in aerospace structures.

Ceramic matrix composites (CMCs) are used to increase the tensile strength and toughness of conventional ceramic material while retaining such properties as lightness, high stiffness, corrosion resistance, wear resistance and thermal stability. CMCs consist of a ceramic matrix phase reinforced with ceramic fibres or whiskers. The reinforcing fibres and whiskers greatly increase the breaking strength and toughness of ceramics, as shown in Table 16.1. Improvements in the strength and toughness of over 100% are gained when ceramics are reinforced with continuous fibres. Although the mechanical properties are improved by the reinforcement, the strength and toughness are still too low for their use in primary aerospace structures. However, the properties are sufficient for the use of CMCs in lightly loaded aerospace components requiring thermal stability.

Table 16.1

Effect of SiC reinforcement fibres on the bending strength and fracture toughness of selected ceramic materials

Material	Flexural strength (MPa)	Fracture toughness (MPa m$^{-1/2}$)
SiC	500	3
SiC/SiC	760	18
Al_2O_3	550	4
Al_2O_3/SiC	790	8

Si$_3$N$_4$	470	3
Si$_3$N$_4$/SiC	790	41
Glass	60	1
Glass/SiC	830	14

CMCs also have high resistance against thermal shock, which is the resistance to cracking and failure when rapidly heated and cooled (often in the presence of high pressure). Rapid cooling of the surface of a hot material is accompanied by surface tensile stresses. The surface contracts more than the interior, which is still relatively hot. As a result, the surface 'pushes' the interior into compression and is itself 'pulled' into tension. Surface tensile stress creates the potential for brittle fracture. The high thermal shock resistance of CMCs is the result of their high strength at high temperature combined with their low coefficient of thermal expansion. The excellent thermal shock resistance and thermal stability allows CMCs to be used at temperatures many hundreds of degrees higher than the melting point of metal alloys. Current metals-based technology can produce alloys stable to about 1000 °C, and nickel superalloys can be used at slightly higher temperatures when insulated with a thermal barrier coating and when cooling systems are included. CMCs can survive for long periods of time at temperatures well above the melting point of superalloys. CMCs retain their stiffness, strength and toughness properties to temperatures close to their melting temperature, which can exceed 3000 °C.

The CMC materials most often used in aerospace are silicon carbide-silicon carbide (SiC–SiC) composite, glass–ceramic composite, and carbon–carbon composite. All three types are used in aerospace thermal protection systems. SiC–SiC composites are only used in a few niche applications, such as convergent–divergent engine nozzles to fighter aircraft where the temperatures reach ~ 1400 °C. Several types of glass–ceramic composites are used in heat shields for re-entry spacecraft such as the space shuttle orbiter. The most important ceramic matrix composite is carbon–carbon, which is used in heat shields, rocket engines and aircraft brake pads.

16.3.2 PROPERTIES OF CARBON–CARBON COMPOSITE

Carbon–carbon composites consist of carbon fibres embedded in a carbon matrix. Continuous carbon fibres (rather than short whiskers) are used as the reinforcement to maximise strength and toughness. Similarly to polymer matrix laminates, the tailored arrangement of carbon fibres in selected orientations within a continuous carbon matrix is used to achieved the desired properties. The fibre architectures include unidirectional, bidirectional, three-dimensional orthogonal weaves, or multidirectional weaves and braids. Carbon–carbon composites are expensive to fabricate and costly to machine into the final product shape. A major drawback of these materials is their high cost which makes them prohibitively expensive for many aerospace applications where otherwise they are well suited. The manufacturing process involves impregnating fibrous carbon fabric with an organic resin such as phenolic. The material is pyrolysed (i.e. heated in the absence of oxygen) at high temperature to convert the resin matrix to carbon. The material,

which is soft and porous, is impregnated with more resin and pyrolysed several more times until it forms a compact, stiff and strong composite.

Carbon–carbon composites have many thermal and mechanical properties required by aerospace materials that must operate at high temperature. These properties include stable mechanical properties to temperatures approaching 3000 °C; high ratios of stiffness-to-weight and strength-to-weight; low thermal expansion; and good resistance to thermal shock, corrosion and creep. The material properties of carbon–carbon composites, as for fibre–polymer composites, are anisotropic. The stiffness, strength and thermal conductivity is highest along the fibre axis and lowest normal to the fibre direction. The properties also depend on the fibre fraction, type of carbon fibre, fibre architecture and processing cycle.

Table 16.2 shows the improvement in properties achieved by reinforcing polycrystalline carbon with continuous carbon fibres. The carbon fibres improve the properties of monolithic carbon by ten times or more, with no increase in weight. A unique feature of carbon–carbon composite is that its strength can increase with temperature. Figure 16.8 shows the strength properties of several carbon–carbon composites and other aerospace materials over a wide temperature range. The strength of advanced types of carbon–carbon increase with the temperature up to at least 2000 °C, which is an obvious benefit when used at high temperature. The improvement in strength is caused by the closing of microcracks in the interface between the carbon matrix and the fibre matrix when the temperature is raised.

Table 16.2

Mechanical properties of monolithic carbon (polycrystalline) and reinforced carbon–carbon composite

Property	Polycrystalline (monolithic) carbon	Reinforced carbon–carbon composite
Elastic modulus (GPa)	10–15	40–100
Tensile strength (MPa)	40–60	200–350
Compressive strength (MPa)	110–200	150–200
Fracture toughness (MPa m$^{-1/2}$)	0.07–0.09	5–10
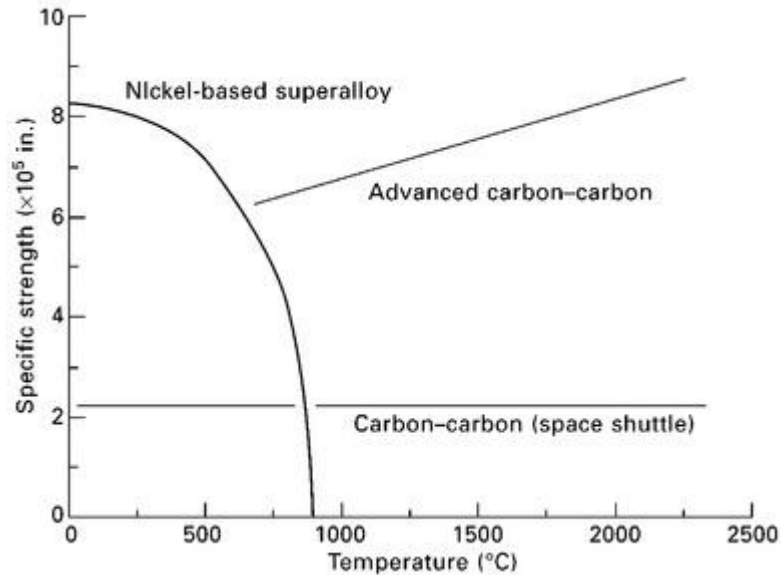
16.8 Dependence of specific strength on temperature for carbon–carbon composites and nickel superalloy. (adapted from D. R. Askeland, *The science and engineering of materials*, Stanley Thornes (Publishers) Ltd., 1996)

Carbon–carbon composite suffers severe high-temperature oxidation which causes rapid degradation and erosion. Carbon becomes susceptible to oxidation when heated above 350 °C and the oxidation rate rises rapidly with temperature. As a result, there is carbon–carbon breakdown in the presence of air. It is necessary to protect carbon–carbon composites using an oxidation-resistant surface coating. The carbon–carbon tiles on the space shuttle orbiter, for example, are coated with silicon carbide to provide oxidation protection to about 1200 °C.

16.3.3 AEROSPACE APPLICATIONS OF CARBON–CARBON COMPOSITES

Heat shields of re-entry space vehicles such as the space shuttle orbiter are made using carbon–carbon composite. This material is used in the nose cone and leading edges of the orbiter where the temperature reaches 1600 °C during re-entry. These materials are also used in the nose cones of intercontinental ballistic missiles. Carbon–carbon is also used in rocket engines and nozzles for its high thermal stability and thermal shock resistance. During blast-off, the thrusters generate temperatures ranging from 1500–3500 °C at heating rates of 1000–5000 °C s^{-1} and produce combustion pressures approaching 300 atmospheres. This generates extreme thermal shock, a rapid rise in temperature and pressure, which shatters most materials. The excellent thermal shock resistance of carbon–carbon composite ensures their survival in these harsh conditions.

Another space application for carbon–carbon composites is in thermal doublers, which are used to remove heat from a spacecraft (usually generated by internal electronics equipment) and then radiate that heat into space. These composites have the thermal properties and low weight required for thermal doublers on satellites. It is also possible to use carbon–carbon composite in aircraft heat exchangers, which are used to cool hot gases and liquids such as hydraulic and engine fluids. Heat exchangers require materials with high thermal conductivity, corrosion resistance, stiffness, strength, low permeability and high temperature stability; carbon–carbon composite is one of the few materials with this unique combination of properties. Carbon–carbon composite is used in aircraft brake pads because of its low weight, high wear resistance and high-temperature properties. The friction between aircraft brake discs can generate average temperatures of around 1500 °C, with transient hot-spot temperatures of up to 3000 °C. The disc material must therefore have high temperature strength, thermal shock resistance and high thermal conductivity to rapidly remove

heat from the contact zone between the disc surfaces. Carbon–carbon is one of the few materials with this combination of properties required for brakes discs. The weight of aircraft brakes is also significant. A large civil airliner usually has eight sets of brakes with a combined weight of over 1000 kg when made using heat-resistant steel. An equivalent set of brakes made of carbon–carbon weigh less than 700 kg. Carbon–carbon brakes are used in most fighter aircraft and increasingly in civil airliners. The Boeing 767 and 777 airliners and several Airbus aircraft are equipped with carbon–carbon brake discs.

Although not currently used, CMCs such as carbon-carbon have potential applications in jet engines because of their ability to operate uncooled at temperatures beyond the reach of metals. Cycle efficiency improvements, from reducing cooling air to turbine aerofoils and seals, lead to significant fuel consumption benefits. For example, it has been estimated that the replacement of metal seals by advanced CMCs technology would yield a saving of $250 000 on the Boeing 777 over 15 years.

.

Ablative cooling

With ablative cooling, combustion gas-side wall material is sacrificed by melting, vaporization and chemical changes to dissipate heat. As a result, relatively cool gases flow over the wall surface, thus lowering the boundary-layer temperature and assisting the cooling process.
sink cooling uses a combination of endothermic reactions The common method of ablative cooling or heat sink cooling uses a combination of breakdown or distillation of matrix material into endothermic reactions 'smaller compounds and gases), pyrolysis of organic materials counter-current heat flow and coolant gas mass flow, charring and localized melting. An ablative material usually
consists of a series of strong, oriented fibers (such as glass, Kevlar, or an organic material (such as carbon fibers) engulfed by a matrix of plastics, epoxy resins or phenolic resins). As shown in Fig. 14-11, the gases seep out of the matrix and form a protective film cooling layer on the matrix form a the inner wall surfaces. The fibers and the residues of hard char or porous coke-like material that preserves the wall contour shapes.

Ablative Materials.

These are not only commonly used in the nozzles of rocket motors, but also in some insulation materials. They are usually a composite material of high-temperature organic or inorganic high strength fibers, namely high silica glass, aramids (Kevlar), or carbon fibers impregnated with organic plastic materials such as phenolic or epoxy resin. The fibers may be individual strands or bands (applied in a geometric pattern on a winding machine), or come as a woven cloth or ribbon, all impregnated with resin. The ablation process is a combination of surface melting, sublimation, charring evaporation, decomposition in depth, and film progressive layers of the ablative   cooling. As shown in Fig material undergo an endothermic degradation, that is, physical and some of the ablative material chemical changes that absorb heat. While evaporates (and some types also have a viscous liquid phase), enough charred and porous solid material remains on the surface
to preserve the basic geometry and surface integrity. Upon rocket start the ablative material acts like any thermal heat sink, but the poor conductivity causes the surface temperature to rise rapidly. At 650 to 800 K some of the resins start to decompose endothermically into a porous carbonaceous char and pyrolysis gases. As the char depth increases, these gases undergo an endothermic cracking process as they percolate through the char in a counterflow direction to the heat flux. These gases then form an

protective, relatively cool, but flimsy boundary layer 'artificial fuel-rich over the char.

Since char is almost all carbon and can withstand 3500 K or 6000 R, the porous char layer allows the original surface to be maintained (but with a rough surface texture) and provides geometric integrity. Char is a weak material and can be damaged or abraded by direct impingement of solid particles in the gas. Ablative material construction is used for part or all of the chambers.
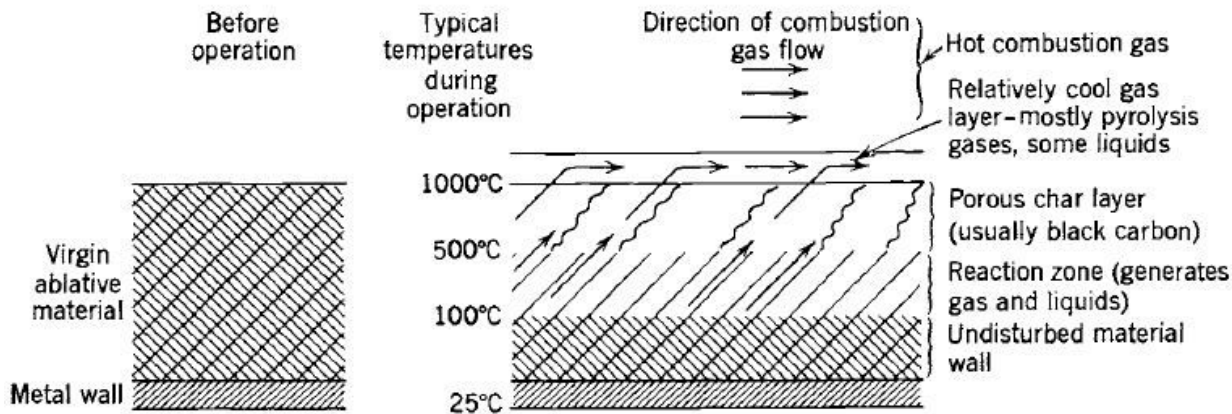
FIGURE 14–11. Zones in an ablative material during rocket operation with fibers at 45° to the flow.

Transpiration

Transpiration cooling provides coolant (either gaseous or liquid propellant) through a porous chamber wall at a rate sufficient to maintain the chamber hot gas wall to the desired temperature. The technique is really aspecial case of film cooling.

Radiation cooling

With *radiation cooling*, heat is radiated from the outer surface of the combustion chamber or nozzle extension wall. Radiation cooling is typically used for small thrust chambers with a high-temperature wall material (refractory) and in low-heat flux regions, such as a nozzle extension.

Film cooling

Film cooling provides protection from excessive heat by introducing a thin film of coolant or propellant through orifices around the injector periphery or through manifolded orifices in the chamber wall near the injector or chamber throat region. This method is typically used in high heat flux regions and in combination with regenerative cooling.

Film Cooling

This is an auxiliary method applied to chambers and/or nozzles, augmenting either a marginal steady-state or a transient cooling method. It can be applied to a complete thrust chamber or just to the nozzle, where heat transfer is the highest. Film cooling is a method of cooling whereby a relatively cool thin fluid film covers and protects exposed wall surfaces from excessive heat transfer. Fig. 8-11 shows film-cooled chambers. The film is introduced by injecting small quantities of fuel or an inet fluid at very low velocity through a large number of orifices along the exposed surfaces in such a manner that a protective relatively cool gas film is formed. A coolant with a high heat of vaporization and a high boiling point is particularly desirable. In liquid propellant rocket engines extra fuel can also be admitted through extra injection holes at the outer layers of the injector; thus a propellant mixture is achieved (at the periphery of the chamber), which has a much lower combustion temperature. This differs from film cooling or transpiration cooling because there does not have to be a chamber.
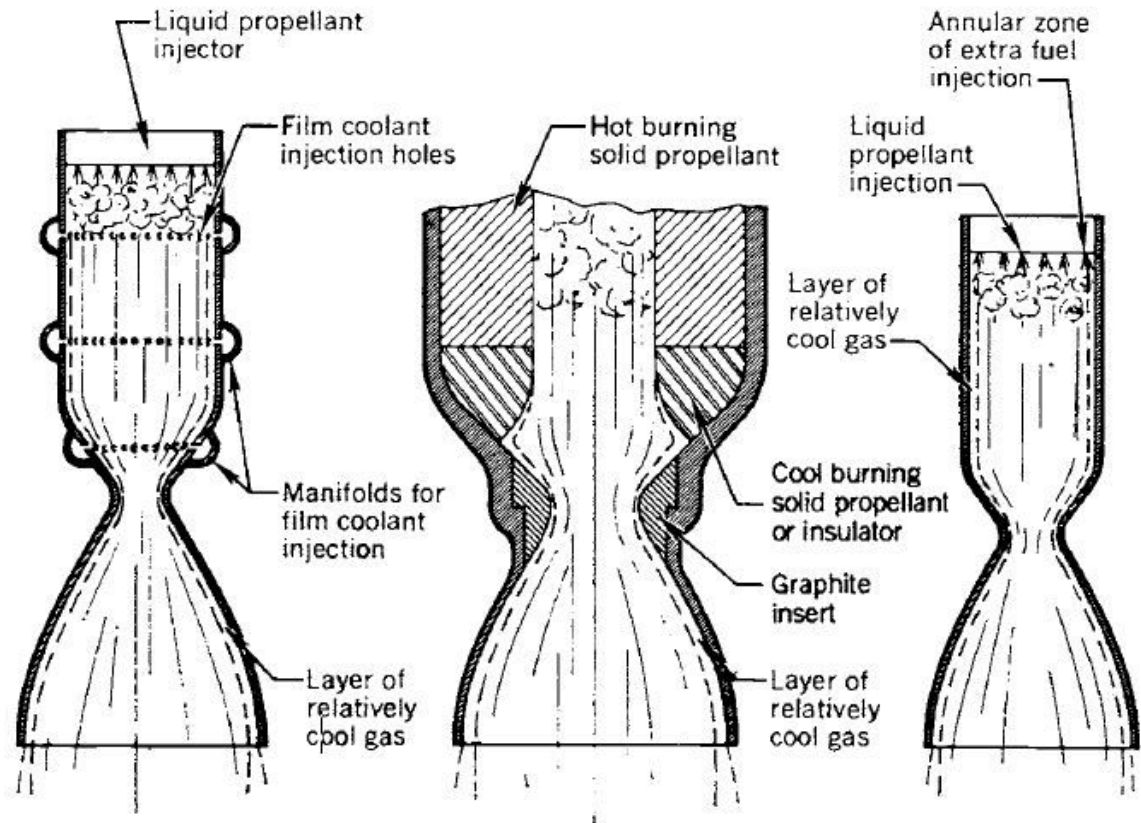
FIGURE 8-11. Simplified diagrams of three different methods of forming a cool boundary layer.

Propellant Burning Rate.

It is possible to approximate the burning rates as a function of chamber pressure, at least over a limited range of chamber pressures. For most production-type propellants, this empirical equation is used,

rb = a (Pc)^n   Regression Law –St. Robert's Law

Regression rate proportional to pressure to some index n.

Also, **Log(rb) = a n Log(Pc)**

a is an empirical constant influenced by ambient grain temperature. Also a is known as the temperature coefficient and it is not dimensionless.
  ➢ The burning rate exponent n, sometimes called the combustion index. It is independent of the initial grain temperature and describes the influence of chamber pressure on the burning rate.

Note: n has to be ≤ 1 for stability
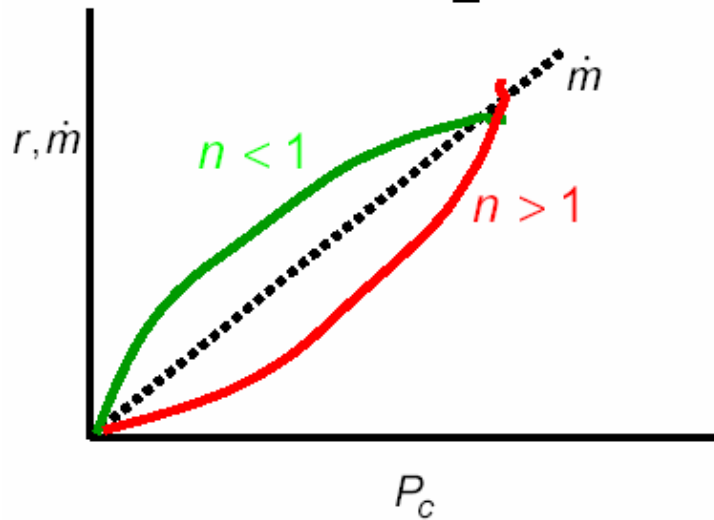
The burning rate is very sensitive to the exponent n. For stable operation, n has values greater than 0 and less than 1.0. High values of n give a rapid change of burning rate with pressure. This implies that even a small change in chamber pressure produces substantial changes in the amount of hot gas produced. Most production propellants have a pressure exponent n ranging between 0.2 and 0.6.

- In practice, as n approaches 1, burning rate and chamber pressure become very sensitive to one another and disastrous rises in chamber pressure can occur in a few milliseconds.
- When the n value is low and comes closer to zero, burning can become unstable and may even extinguish itself. Some propellants display a negative n which is important for "restartable" motors or gas generators.
- A propellant having a pressure exponent of zero displays essentially zero change in burning rate over a wide pressure range. Plateau propellants are those that exhibit a nearly constant burning rate over a limited pressure range.

Ablation

Introduction

In aerospace design, ablation is used to both cool and protect mechanical parts that would otherwise be damaged by extremely high temperatures. Examples are heat shields for spacecraft, satellites, and missiles entering a planetary atmosphere from space and cooling of rocket engine nozzles. Basically, ablative material is designed to slowly burn away in a controlled manner, so that heat can be removed from the spacecraft by the gases generated by ablation, whereas the remaining solid material insulates the spacecraft from superheated gases. There has been an entire branch of spaceflight research involving the search for new fireproof materials to achieve the best ablative performance. Such a function is critical to protect the spacecraft occupants from otherwise excessive heat loading. The physical phenomena associated with ablation heat transfer depend on the application, but most involve in-depth material pyrolysis (charring) and thermochemical surface ablation. In numerical modeling, it is required to solve an energy equation, including effects of pyrolysis on a domain that changes as the surface ablates. Fig. 2.1 gives a general view of the ablation process and the involved mechanisms. As the material is heated, one or more components of the original composite material pyrolyze and yield a pyrolysis gas and a porous residue. The pyrolysis gas percolates away from the pyrolysis zone. The residue is often a carbonaceous char. The solution procedure is in principle a transient heat conduction calculation coupled to a pyrolysis rate calculation and subject to boundary conditions from the flow field.
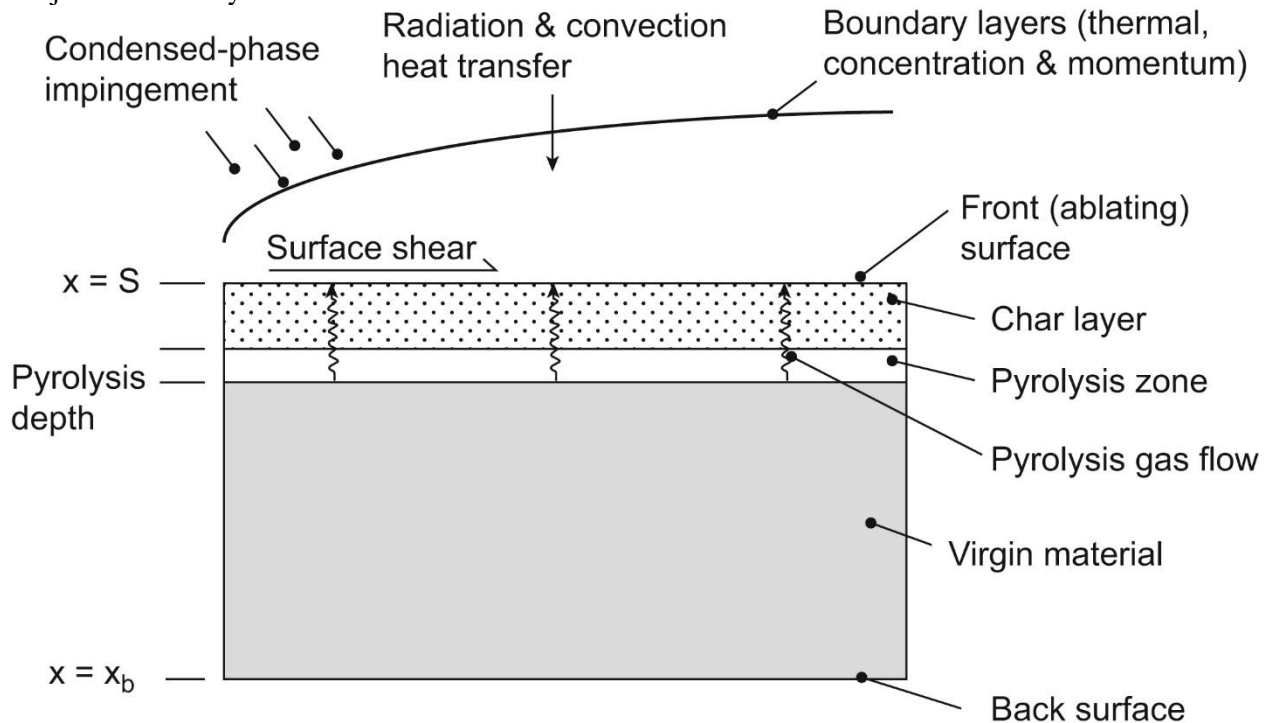
FIGURE 2.1 Ablation process.

In terms of heat transfer, the following mechanisms are involved: (a) convection in the boundary layer, which gives rise to the main thermal load; (b) radiation; and (c) conduction in the virgin material. In addition, resin decomposition and fiber decomposition may occur. In the boundary layer, shocks may appear, and in some cases, there may be combustion.

Ablation is affected by the freestream conditions, the geometry of the reentry body, and the surface material. The vehicles range from blunt configurations, such as spacecraft, to slender sphere-cone projectiles. At low heating values, ablators of Teflon are used, whereas at high heat loads, graphites and carbon-based materials

are used. The most common ablative materials are composites, i.e., materials consisting of a high-melting-point matrix and an organic binder. The matrix might be glass, asbestos, carbon, or polymer fibers braided in various ways. A honeycomb structure filled with a mixture of organic and inorganic substances and with high insulating characteristics can be used. Advances in chemistry and materials technology extend the possibilities of selecting improved ablative materials.

Also surface movement occurs by, e.g., material spallation. Various methods exist to solve the moving boundary problems, commonly referred to as the Stefan problems. Basically two methods are considered: the front-tracking methods and the front-fixing methods. With the front-tracking methods, the ablating surface (the front) is tracked as it moves into the material.

2.2. An Illustrative Example of Ablation

In this section a simplified model of ablation is presented. Basically a transient heat conduction analysis is presented. The transient thermal response of the material exposed to a high-energy environment is important knowledge in the design of heat shields for reentry vehicles. The surface of a semi-infinite solid is heated by applying a constant heat flux q_0 (caused by frictional or aerodynamic heating) as shown in Fig. 2.2.
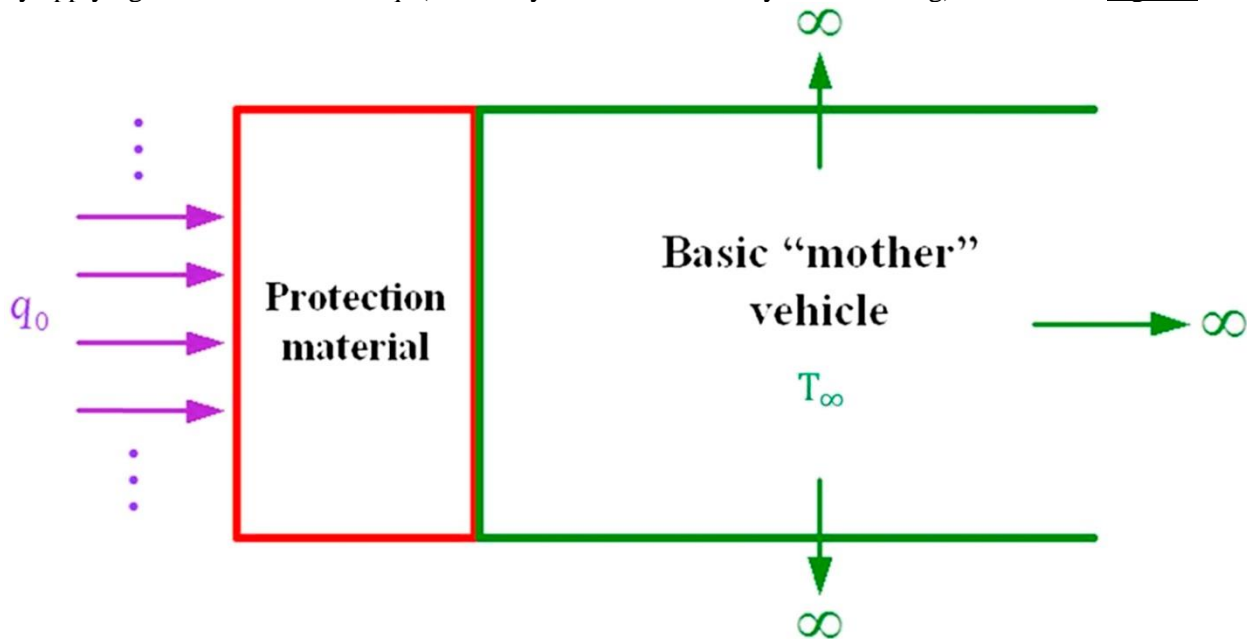
FIGURE 2.2 Simple illustration of an ablation process.

At time $\tau = 0$ the surface temperature has risen to the melting temperature T_p and phase change is initiated. The melted material (liquid) formed is completely removed by the aerodynamic forces. In this case the surface recedes with time but the surface temperature remains constant at the phase change temperature. A temperature distribution exists only in the remaining solid as conjectured in Fig. 2.3.

At a certain time the solid surface is located at $x = X(\tau)$. The temperature variation in the solid material penetrates to a depth $x = \delta(\tau)$. The temperature of the solid at far distances, $x > \delta(\tau)$, from the surface is kept at the constant initial temperature T_∞.

Introduce $\theta(x, \tau) = T - T_\infty$, which implies that $\theta(X, \tau) = T_p - T_\infty = \theta_P$.

The one-dimensional unsteady heat conduction is then governed by

$$\frac{\partial \theta}{\partial \tau} = \alpha \frac{\partial^2 \theta}{\partial X^2} \quad \textbf{(2.1)}$$
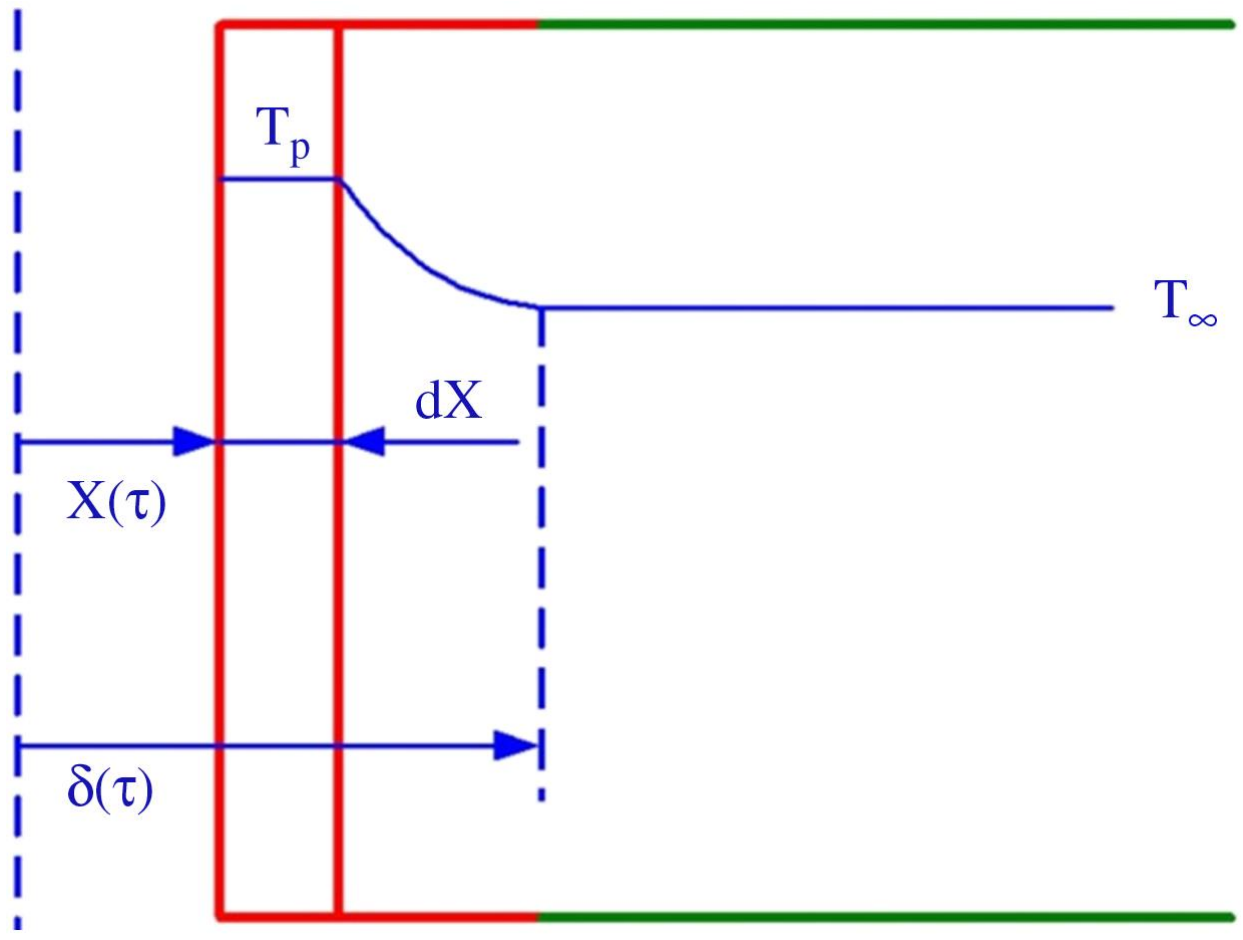
FIGURE 2.3 Temperature distribution in the simplified ablation process.
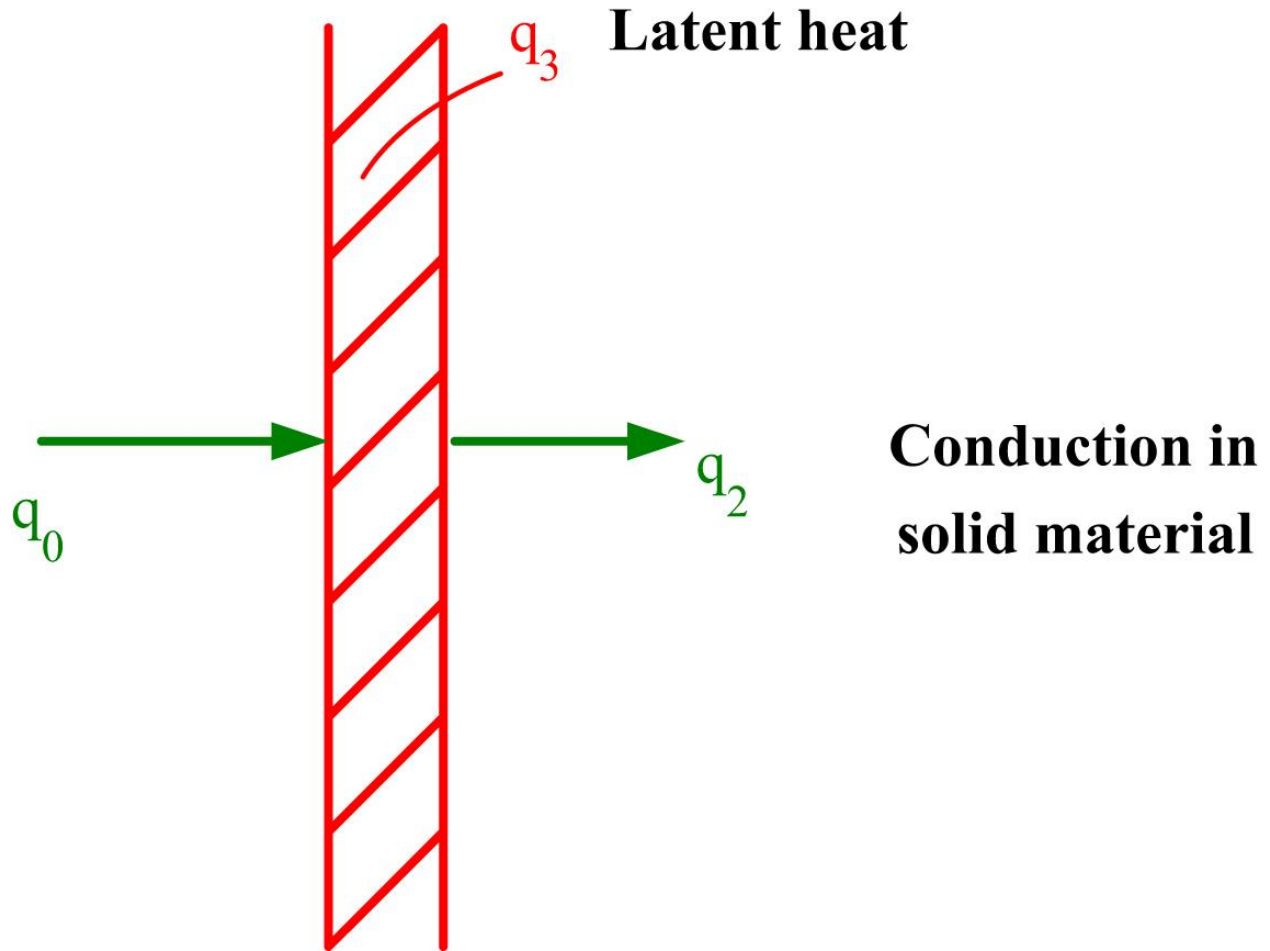
FIGURE 2.4 Heat balance at the liquid–solid interface.
In Fig. 2.4 the heat balance at the interface is presented.
The thermal balance at the interface can be expressed as below:

$$q_0 - q_2 = q_3 \quad \text{(2.2a)}$$

$$q_0 + k\frac{\partial \theta}{\partial X} = \rho Q_L \frac{dX}{d\tau} \quad \text{(2.2b)}$$

The solution of Eq. (2.1) can be found by some standard procedures but here the integrated form is used. Details are given below.
The integrated form of Eq. (2.1) can be written as

$$\frac{d}{d\tau}\left[\int_X^\delta \theta(x,\tau)dx - \theta(\delta,\tau)\cdot X\delta(\tau) + \theta(X,\tau)X(\tau)\right] = \alpha\left[\frac{\partial \theta}{\partial x}(\delta,\tau) - \frac{\partial \theta}{\partial x}(X,\tau)\right] \quad \text{(2.3)}$$

A second-order polynomial temperature profile is assumed as

$$\frac{\theta(x,\tau)}{\theta_P} = \left[1 - 2\frac{x - X}{\delta - X} + \left(\frac{x - X}{(\delta - X)}\right)^2\right]_{(2.4)}$$

With the conditions $\theta(\delta,\tau) = 0$ and $\theta(X,\tau) = \theta_P$.

By combining the interface heat balance Eq. (2.2) with Eq. (2.3) and the assumed temperature profile Eq. (2.4), one obtains

$$\frac{d}{d\tau}\left[\frac{1}{3}(\delta - X)\right] + \left(1 + \frac{Q_L}{c\theta_P}\right)\frac{dX}{d\tau} = \frac{q_0}{\rho c\theta_P}_{(2.5)}$$

Further combination of the equations gives

$$\rho Q_L \frac{dX}{d\tau} = q_0 \frac{2k\theta_P}{-\delta - X}_{(2.6)}$$

Eqs. (2.5) and (2.6) are simultaneous equations, making the solutions of $X(\tau)$ and $\delta - X$ possible. The initial condition for X is $X(0) = 0$. The initial condition for $\delta(\tau)$, the specification for δ when the surface reaches the melting temperature T_P, can be obtained from solutions of a semi-infinite solid exposed to a time varying surface heat flux by the equations (see, e.g., Ref. [1])

$$\delta(\tau) = \sqrt{6\alpha\tau}$$

which gives the value of $\delta(\tau)$ if a parabolic temperature profile is assumed, and

$$\delta(\tau) = \sqrt{1.5\alpha}$$

which gives the specification for the surface temperature as a result of a constant heat flux input q_0.

Using the above equations the value of $\delta(\tau_P)$ when the surface temperature reaches θ_P may be calculated as

$$\delta(\tau_P) = 2\frac{k\theta_P}{q_0}_{(2.7)}$$

which is the remaining required initial condition.

Eqs. (2.5) and (2.6) have a steady-state solution if $dX/d\tau = A$ is a constant. Thus from Eq. (2.6), the value of δ—X must be constant, and then Eq. (2.5) gives

$$\frac{dX}{d\tau} = A = \frac{q_0}{\rho(Q_L + c\theta_P)}_{(2.8)}$$

Goodman [2] has solved Eqs. (2.5) and (2.6) by eliminating $dX/d\tau$ between them to obtain finally

$$\Omega = -\frac{1}{3}\left[\zeta - 2 + 2(1 + v)\ln\frac{2(1 + v) - \zeta}{2v}\right]_{(2.9)}$$

where

$$\Omega = \frac{\tau q_0^2}{\rho k \theta_P Q_L}, \quad v = \frac{Q_L}{c \theta_P}, \quad \zeta = \frac{(\delta - X)q_0}{k \theta_P}$$

Substituting Eq. (2.9) into Eq. (2.6) yields

$$\lambda = -\frac{1}{3}\left[\zeta - 2 + 2v\ln\frac{2(1 + v) - \zeta}{2v}\right] \quad \text{(2.10)}$$

where $\lambda = \dfrac{Xq_0}{k\theta_P}$.

The results above are depicted in Fig. 2.5. It presents, in dimensionless form, the melt-line location versus time, and the parametric influence of the variable v introduced as $v = Q_L/(c \cdot \theta_P)$ is also clearly depicted.

2.3. Additional Information

Other simplified analyses have been presented by Han [3] and Holman [4]. In the analyses, it was assumed that a steady-state situation is attained and that the surface ablates at a constant rate.

Problems related to a melting solid for a variety of other boundary conditions have been presented in the literature. For instance, vaporization at the surface and aerodynamic heating by thermal radiation have been considered. Murray and Russell [5] presented a method for coupled aeroheating and ablation for missile configurations. Surface temperature and transient heat conduction calculations were carried out. The heat transfer coefficient was assumed to follow a known time function. The calculation method was verified against the flight test data.
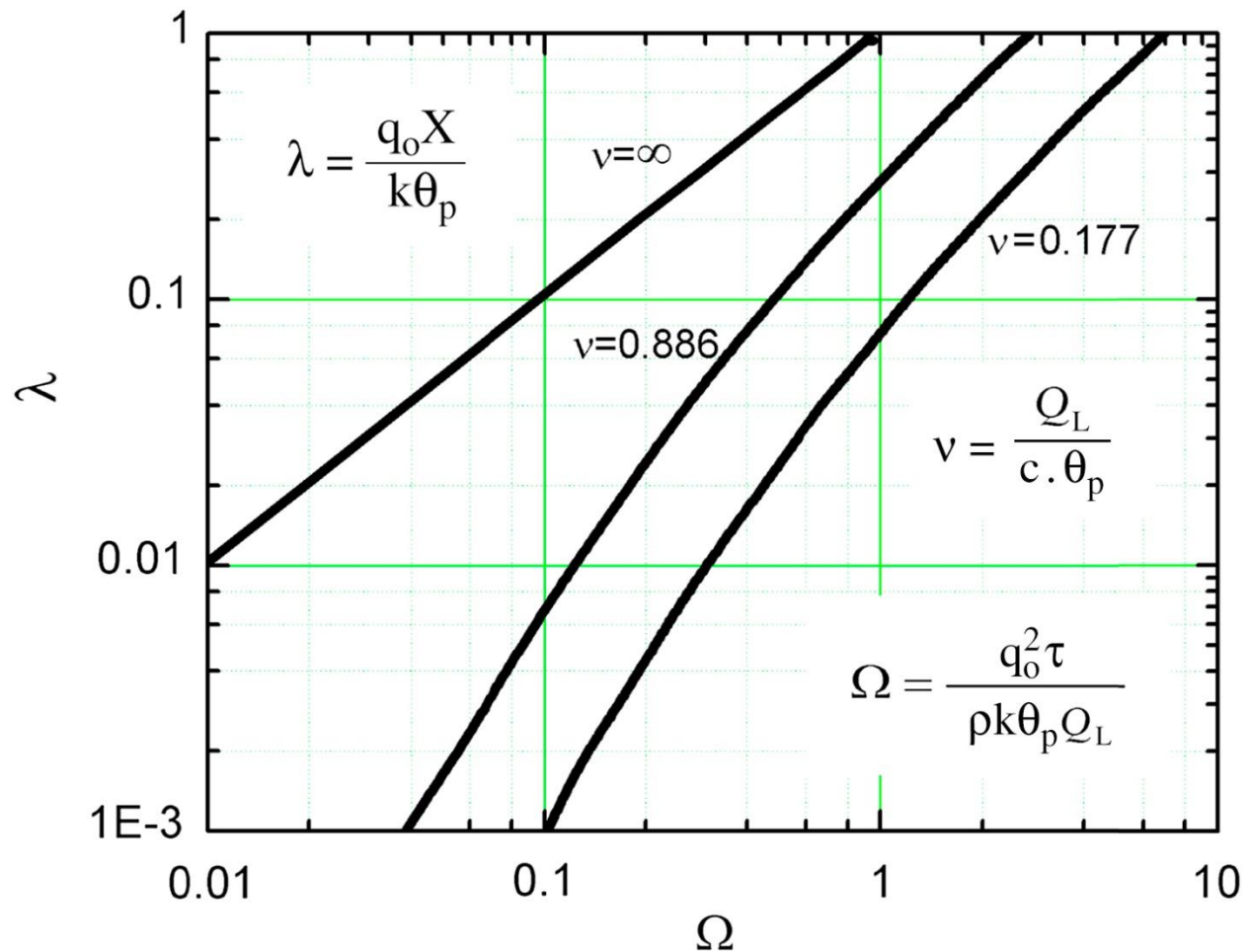
FIGURE 2.5 The melt-line location versus time in dimensionless form. Redrawn from Goodman Goodman R, The heat balance integral and its application to problems involving a change of phase. Trans. ASME 1958;80(2):335–345.

In Ref. [6], a method of thermal protection for transatmospheric vehicles exposed to high heating rates was introduced. The method involved combined radiation, ablation, and transpiration cooling. By placing an ablative material behind an outer shield that is of fixed shape and is porous, the effectiveness of the transpiration cooling was maintained, while retaining the simplicity of a passive mechanism. In the analysis, a simpfied one-dimensional approach was used to derive the governing equations, which were reduced to a nondimensional form. In doing so, two parameters appeared to control the thermal protection effectiveness and ablation. The parameters are related to the thermal properties of the ablative and shield materials. The ablative material was also required to absorb a sufficient amount of thermal energy (related to the heat of ablation or vaporization) to keep the outer shield temperature below a specified value. A low vaporization temperature was found favorable to allow for the release of gaseous products and take advantage of the transpiration mechanism completely. Four ablative materials were considered and it was found that one material with thermal properties similar to those of Teflon behaved very well.

A relatively old report [7] presented a qualitative review of fundamental relationships involved in engineering and aerodynamic heating. The report included aerodynamic heating, boundary layer mass transfer, general thermal protection, ablative materials, and the structural aspects of ablation. In particular the general properties of charring ablators were discussed.

A comprehensive study of thermal protection systems was presented in a doctoral thesis [8], in which most mechanisms of the ablation phenomenon were treated in detail but mainly by computational fluid dynamics (CFD)-based methods.

A simplified analysis, similar to the one presented in this chapter, of ablation in cylindrical bodies was presented in Ref. [9]. The so-called general integral transform technique (GITT) was used to analyze the unsteady heat conduction, but with a transient surface heat flux.

References

[1] Eckert E.R.G, Drake Jr. R.M. *Analysis of heat and mass transfer*. McGraw-Hill, Kogakusha; 1972.

[2] Goodman T.R. The heat balance integral and its application to problems involving a change of phase. *Trans ASME*. 1958;80(2):335–345.

[3] Han J.C. *Analytical heat transfer*. New York: CRC Press; 2012.

[4] Holman J.P. *Heat transfer*. 10th ed. New York: McGraw-Hill; 2009.

[5] Murray A, Russell G. Coupled aeroheating/ablation analysis for missile Neumann configurations. *J Spacecr Rockets*. 2002;39(34):501–508.

[6] Camberos J.A, Roberts L. *Analysis of internal ablation for the thermal control of aerospace vehicles, Joint Institute for Aeronautics and Acoustics, JIAA TR-94*. Stanford University; 1989.

[7] Achard R.T. *Fundamental relationships for ablation and hyperthermal heat transfer, AADL-TR-66–25*. 1966.

[8] Bianchi D. *Modeling of ablation phenomena in space applications* PhD thesis. Universita degli Studi di Roma "La Sapienza"; 2007.

[9] Aparecido Gomes F.A, Campos Silva J.B, Diniz J.A. Heat transfer with ablation in cylindrical bodies. In: *24th International Congress of the Aeronautical Sciences*. ICAS; 2004.

Wood in small aircraft construction

17.1 Introduction

The first structural material used in powered aircraft was wood. The mainframe of *Kitty Hawk* flown by the Wright brothers in 1903 was made from timber covered with fabric. Wood was the material of choice in early aircraft because of its good strength-to-weight ratio. Also, wood can be easily crafted and shaped into spars and beams for the fuselage, wings and other structures. Wood was the most used structural material in aircraft until the introduction of high-strength aluminium and steel in the 1920s. The use of wood in large modern aircraft is now nonexistent, although it remains a useful material in the construction of small aircraft; notably guilders, ultralights, aerobatic aircraft and certain types of piston-driven aircraft (Fig. 17.1). Wood is used in spars, ribs, longerons and stringers of the mainframe of several types of small aircraft.

17.1 Application of wood in aircraft: glider made of spruce and ply. (photograph supplied courtesy of C. White)

In this chapter, we examine the properties of wood that are important to its use in small aircraft. The structure, composition and properties of wood are studied. Important factors concerning the structural performance and durability of wood are also examined; including mechanical anisotropy, moisture absorption, and its effect on mechanical performance and durability in the aviation environment.

17.2 Advantages and disadvantages of wood

The properties of wood that appeal to the designers and builders of small aircraft are lightness, stiffness, strength and toughness. Table 17.1 gives the properties of two woods used in aircraft, Sitka spruce and Douglas fir, and of several aerospace grade metal alloys and carbon fibre–epoxy composite. The density of wood is very low (typically under 0.5 g cm^{-3}) compared with the other types of aerospace materials, although the Young's modulus, tensile strength and fracture toughness are also lower. Because of the low density, the specific mechanical properties of wood are similar to 2024 aluminium alloy and most magnesium alloys. However, the specific properties of wood are inferior to the other types of aerospace materials.

Table 17.1

Comparison of mechanical properties of Sitka spruce and Douglas fir with other aerospace structural materials

Materials	Specific gravity* (g cm^{-3})	Young's modulus* (GPa)	Specific modulus* x10^6 (N m kg^{-1})	Yield strength* (MPa)	Specific strength* x10^3 (N m kg^{-1})	Fracture toughness[†] (MPa m$^{0.5}$)	Specific fracture toughness[†] x10^3 (N m$^{1.5}$ kg^{-1})
Sitka spruce*	0.4	9	22.5	55	138	4	10.0
Douglas fir*	0.5	12	24.0	70	140	6	12.4
Ti alloy (Ti-6Al-4V)	4.6	108	23.5	1003	217	100	21.7
Al alloy (2024 Al-T6)	2.7	70	25.9	385	142	37	13.7
Al alloy (7075 Al-T76)	2.7	70	25.9	470	174	29	10.7
Mg alloy (WE46-T6)	1.7	45	26.5	200	117	20	11.8
Carbon/epoxy composite[‡]	1.7	50	29.4	760	450	38	22.4

*Wood properties for 15% moisture content measured parallel to grain.

[†]Wood properties for 15% moisture content measured transverse to grain.

[‡][0/± 45/90] carbon/epoxy; fibre volume content = 60%.

There are many properties of wood that make it inferior to metals and composites as an aircraft structural material. As mentioned, the stiffness, strength and toughness of wood are lower. Other drawbacks of wood are:

• Lack of uniformitty in properties such as density and strength. The properties of timber pieces taken from the same species of tree may differ by 100% or more. It is therefore necessary to apply high design safety factors to wooden structures, which diminishes the potential weight savings otherwise gained by using such a low density material.

• Mechanical properties of wood are highly anisotropic. Large differences occur in the stiffness, strength and toughness in the longitudinal and transverse directions of cut timber.

• Defects in wood, such as knots and pitch pockets, reduce the strength properties.

• Wood is hygroscopic; it shrinks, swells and undergoes changes to the mechanical properties depending on the atmospheric humidity.

• Wood is prone to attack from insects, fungus and other microorganisms when used without effective chemical treatment and surface protection.

17.3 Hardwoods and softwoods

Timber is classified as hardwood or softwood depending on whether it is harvested from a deciduous or evergreen tree. Hardwoods are deciduous trees such as oak, elm and birch, whereas softwoods are evergreens such as spruce, pine and fir. As their name implies, hardwoods are generally harder and stronger than softwoods. For example, the bending strength of most hardwoods is within the range 45–80 MPa whereas softwoods are usually within 30–60 MPa. Hardwoods are generally heavier than softwoods, with their density in the range 0.5–0.8 g cm^{-3} whereas the density of most softwoods is within 0.30–0.6 g cm^{-3}. Certain softwoods have a good combination of density and strength to be suitable for aircraft construction, the most common are Sitka spruce and Douglas fir.

17.4 Structure and composition of wood

The properties of wood that make it a useful aircraft material (i.e. lightness, strength and toughness), are controlled by its structure and composition. For this reason, it is useful to understand the structure and composition of wood at several levels: the macro level (above ~ 1 cm in size), microstructural level (~ 0.1 to 1 cm) and cellular level (below ~ 0.1 cm).

17.4.1 MACROSTRUCTURE OF WOOD

The macrostructure of wood consists of several distinct zones that occur across a tree trunk, as shown in Fig. 17.2. The outer layer, or bark, provides some protection for the inside of a tree against birds, insects, fungi and other organisms. Just beneath the bark is a zone called the cambium that contains new growing cells for both the bark and inner region of the tree. During the warmer months of each year, the cambium grows new wood cells on its inner surface and new bark cells on its outer surface. The sapwood is a region adjoining the cambium that contains cells where nutrients are stored and sap (containing water and

minerals) is transported along the trunk and into the branches and twigs. The inner core of the tree is called the heartwood, and is composed entirely of dead cells. The heartwood is denser and stronger than the cambium and sapwood, and provides most of the mechanical support for a tree. Only wood taken from the heartwood of a mature, fully grown tree is used for aircraft construction. Even then, not all the heartwood is suitable because of knots and other defects. Usually less than 5% of timber taken from the heartwood is suitable for aircraft construction. This is another problem with using wood: the large amount of waste material generated for a small amount of quality timber.
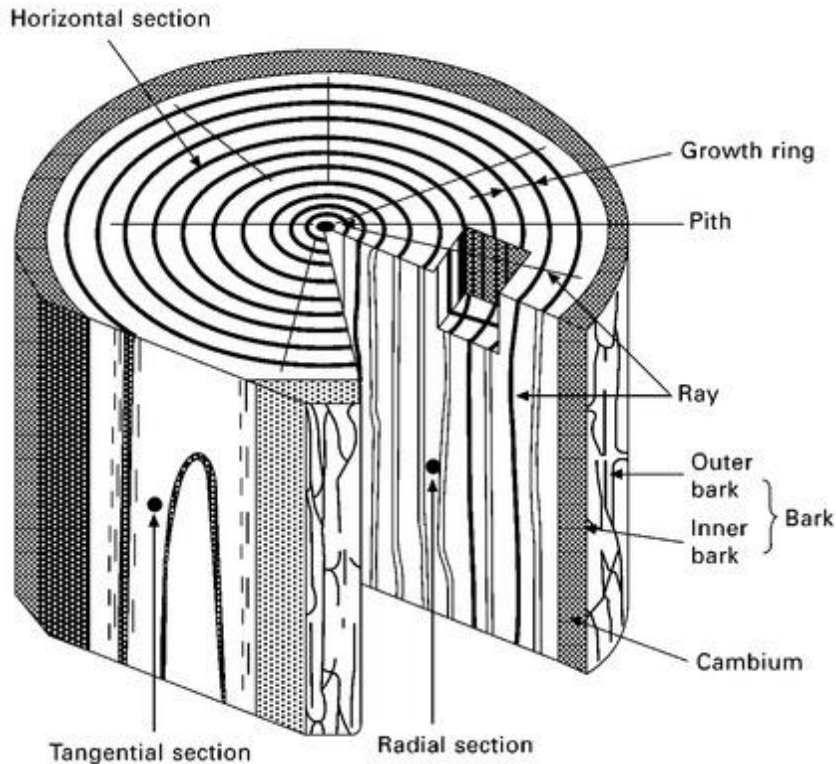
17.2 Cross-section of a tree showing the different regions across the trunk.

Wood is a highly anisotropic material. Three axes are used to describe the directionality of cut timber, as shown in Fig. 17.3. The axes are mutually perpendicular to each other. The longitudinal axis (L) is parallel with the axis of the trunk, and is also known as the fibre or grain direction. The radial axis (R) is across the diameter of the trunk and the tangential axis (T) is normal to the radial direction. The mechanical properties are different along each axis, and therefore it is important that timber used in aircraft construction is cut in the direction that maximises structural performance. For example, stiffness and strength are highest when timber is loaded parallel with the longitudinal axis and lowest in the radial direction for reasons that are explained in 17.5.2. Wood is toughest when cracking occurs in the radial direction and is more susceptible to splitting in the other directions. Care is needed when constructing structures to ensure the wood grain is aligned with the major loads acting on the aircraft.
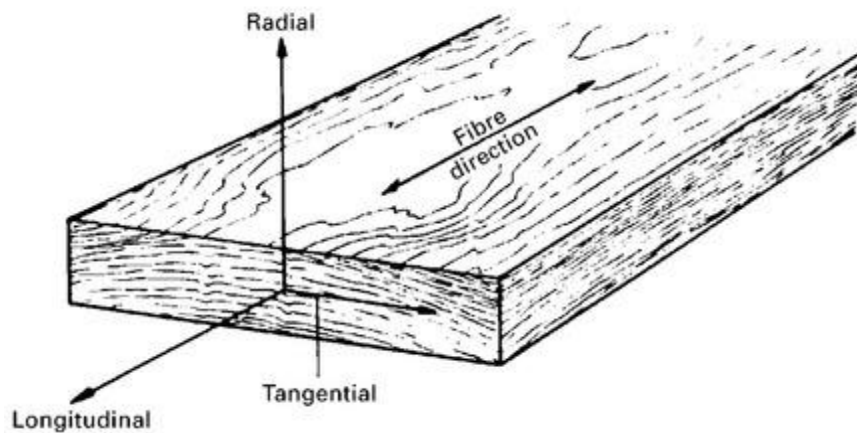
17.3 Axes used to specify directions in cut timber. (reproduced with permission from the US Department of Agriculture, Handbook No. 72)

17.4.2 MICROSTRUCTURE OF WOOD

The microstructure of heartwood consists of long and thin hollow cells that are extended in the longitudinal direction. Figure 17.4 shows the microstructure of Douglas fir viewed under a microscope at the magnification of 300 times. The microstructure consists of long, hollow cells squeezed together like drinking straws. These cells are called fibres or fibrils because of their very high aspect ratio (length-to-width) of 100 or more. Fibre cells are less than 0.01 mm wide and roughly 1 mm long in hardwoods and 5 mm long in softwoods. The fibres provide wood with most of its stiffness, strength and toughness.
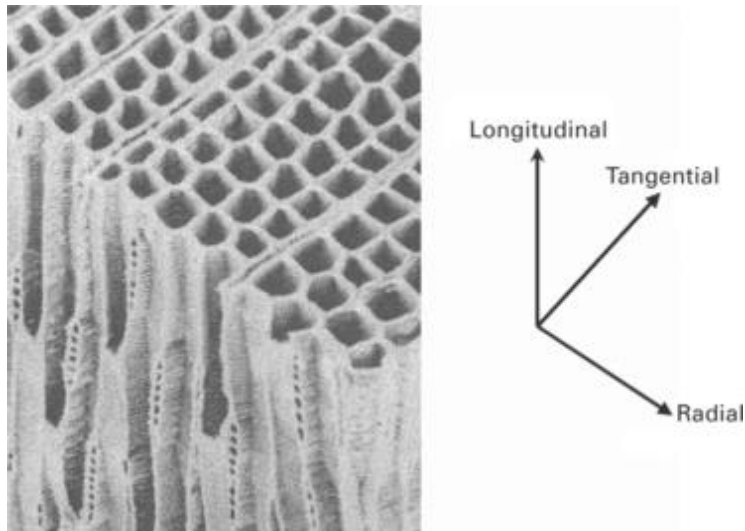
17.4 Wood microstucture showing the cellular network. (photograph supplied courtesy of US Forest Products Laboratory, Madison, Wisconsin)

The microstructure of wood is often considered in the materials engineering context as a unidirectional fibre–polymer composite. Wood consists of long fibre cells aligned in the same direction, which is analogous to the fibres in a composite, which are bonded together in an organic matrix. Most of the wood fibres are roughly parallel with the longitudinal axis, and this is called the grain direction. The term grain

describes both the cell direction and the wood texture; the grain direction has a major influence on the mechanical properties of wood.

17.4.3 CELL STRUCTURE OF WOOD

The structure and composition of cells in the heartwood are similar for most hardwoods and softwoods. Figure 17.5 shows a typical cell that consists of a hollow core and multilayer wall structure. The wall consists of several layers of microfibrils, which are crystalline cellulose $(C_6H_{10}O_5)_n$ molecules clumped together into long strands. Each molecular chain consists of long segments of linear, crystalline cellulose separated by shorter segments of amorphous cellulose. Cellulose is a linear molecule with no cumbersome sidegroups, and so it crystallises easily into strands of great stiffness and strength. The crystalline cellulose strands are encased in a layer of hemicellulose. This is a semicrystalline polymer of glucose that acts as a binding agent to the cellulose strands. The hemicellulose is covered with lignin, which is an amorphous polymer (phenol–propane) that also acts as a binder. A microfibril then consists of a bundle of crystalline cellulose chains that are encased with hemicellulose and lignin. This structure is somewhat anagolous to a fibre–polymer composite, where the cellulose strands act as the fibres and the hemicellulose and lignin are the matrix binding phase.
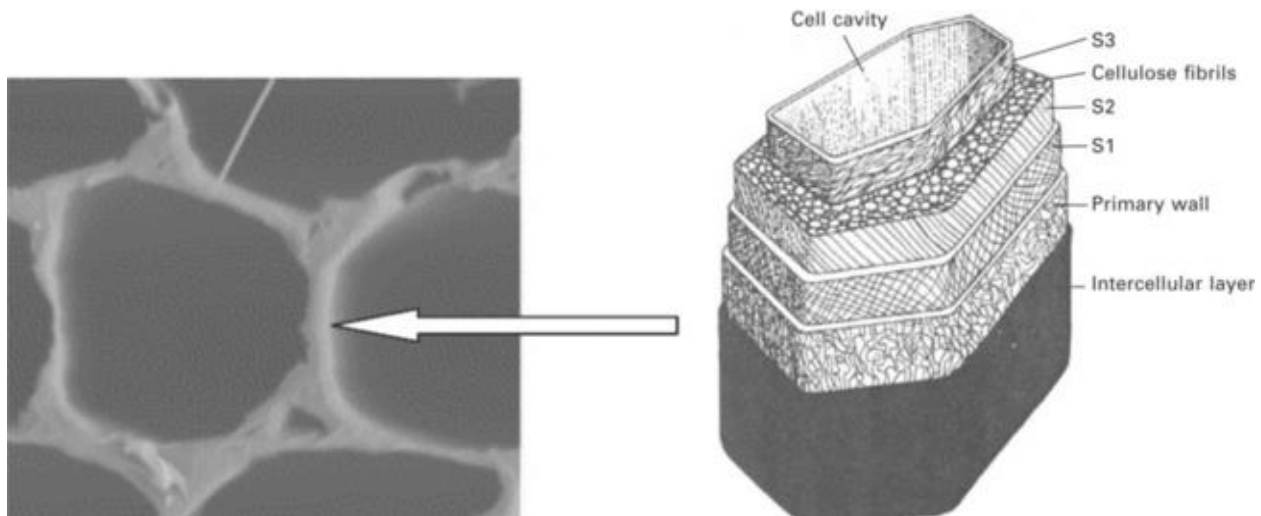
17.5 Typical cross-sectional structure of a wood cell. (reproduced with permission from the US Department of Agriculture, Forest Products Laboratory, Madison, Wisconsin)

Crystalline cellulose accounts for 40–50% by weight of the cell wall and the hemicellulose and lignin together account for another 40%. The wall also contains extractives, which are organic chemicals and oils that are not chemically bonded into the microfibril structure. Extractives give colour to the wood and act as preservatives against the environment and insects. As much as 10% of the wood may be extractives.

Cell walls are composed of two substructures: the outer primary wall and inner secondary wall. In the primary wall, the microfibrils are in a loose, disordered network. They are not aligned in any particular direction, but are random. The secondary wall consists of three layers: S1 which is a crisscross network of microfibrils, S2 is an array of microfibrils in a parallel, spiral-type network, and S3 is another disordered network of microfibrils. S2 makes up 70–90% of the cell wall and is responsible for most of the stiffness and strength in the longitudinal direction. Strength in the radial and tangential directions is dependent mostly on the strength properties of the hemicellulose and lignin that binds the wall layers, and these are much weaker than for the crystalline cellulose. For this reason, the strength is much higher in the longitudinal direction, and aircraft wooden structures must be designed with the loads acting in this direction.

Section 17.9 at the end of the chapter presents a case study of the *Spruce Goose*, a Hughes H-4 Hercules made almost entirely of wood.

17.5 Engineering properties of wood

17.5.1 DENSITY

The density of woods vary over a wide range from ultralight (e.g. balsa at ~ 0.1 g cm^{-3}) to heavy (e.g. oak at ~ 0.7 g cm^{-3}). Most softwoods have a density between 0.30 and 0.50 g cm^{-3}, and are lighter than hardwoods that are mostly between 0.45 and 0.80 g cm^{-3}. The density of wood is dependent on two parameters: the cell density and the moisture content. The cell density is determined by the volume of the inner cell cavity compared with the volume of the cell wall. Lightweight woods such as balsa have a high cavity-to-wall volume ratio whereas heavy woods such as oak have a smaller ratio.

The density is also controlled by the moisture content. Water is present in the cell cavities and cell walls. Green wood (freshly cut timber) can contain up to 50% water and is not suitable for aircraft because it is too heavy, soft and prone to attack from fungi and parasites. Wood must be dried by seasoning, which takes anywhere between 2 and 10 years at room temperature. More often wood is seasoned by kiln drying at elevated temperature, which takes a few days. When wood dries, the density is reduced because moisture is driven out by evaporation from the cell cavities and, to a lesser extent, cell walls. The drying of wood increases the longitudinal stiffness and strength because the cellulose fibrils in the cell walls pack more closely together into space that was occupied by water molecules.

The target moisture content when drying wood for use in aircraft is about 12%, at which point the density, mechanical properties, durability and dimensional stability have reached a near optimum level. However, the actual moisture content may be anywhere between 10 and 15% depending on the temperature and humidity of the environment.

The density of seasoned timber is usually classified (at 12% moisture content) as being:
• Very light, under 0.3 g cm^{-3}.
• Light, 0.3 to 0.45 g cm^{-3}
• Medium, 0.45 to 0.65 g cm^{-3}
• Heavy, 0.65 to 0.80 g cm^{-3}
• Very heavy, 0.80 g cm^{-3} and above.

The requirement for aircraft materials to have low density combined with high strength means that most woods are at the lower band of the medium density classification. This includes the softwoods used in aircraft, such as Sitka spruce (average density of 0.4 g cm^{-3}) and Douglas fir (0.5 g cm^{-3}). The exception is wood used in aircraft propellers which is often heavier because of the requirement for higher stiffness and strength than the airframe.

A single density value for a particular type of wood is often quoted in research studies and aircraft design manuals, although there is much scatter in the density for the same species of tree. For example, Fig. 17.6 shows the variation in density for Sitka spruce used in aircraft. The density varies because it is influenced by the maturity, environment and growth conditions of the tree as well as the part of the trunk from which the timber is cut. For this reason, the density of individual timber pieces should be measured before they are built into an aircraft to ensure the total structural weight is within the design limit.
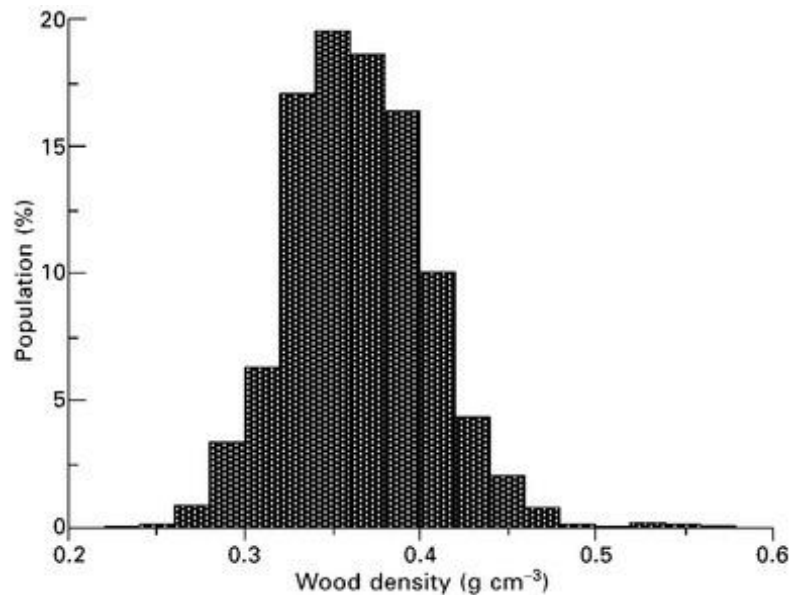
17.6 Histogram plot of density values for Sitka spruce.

17.5.2 MECHANICAL PROPERTIES

The mechanical properties of wood are highly anisotropic, and therefore care is needed when constructing timber aircraft structures. The longitudinal modulus and yield strength are much higher because the applied load acts parallel to the microfibrils in the cell wall. The crystalline cellulose chains in the microfibrils are stiff and strong and therefore able to carry a relatively high load. The cell walls collapse by microbuckling and kinking in much the same way as fibre–polymer composites fail in compression. The transverse properties are determined mainly by the hemicellulose and lignin that binds the microfibrils, which are much weaker than crystalline cellulose. The properties are also lower because of the voids and lack of continuity to the cell structure in the transverse direction.

Table 17.2 gives elastic modulus, compressive strength and fracture toughness for a variety of woods measured in the longitudinal and radial directions. The longitudinal modulus is typically 10–20 times higher than the transverse modulus. The longitudinal strength properties are 5–10 times higher than in the radial direction. The fracture toughness is much higher when crack growth occurs in the radial direction. The fracture toughness is anywhere between 5 and 25 times higher across the grain than along it. This is because of two important toughening mechanisms. Firstly, when a crack grows across the grains it is forced to spread, at right angles to the break, along the fibril interfaces, leading to a large fracture surface. After cracking along the interfaces, the fibrils are then pulled out, which requires a high force and strain. Toughness in the grain direction is lower because the crack grows through the brittle lignin phase at cell interfaces without significant branching or fibril pull-out. It is for this reason that wood is easier to split along the trunk than cut across it using an axe.

Table 17.2

Engineering properties of woods

Wood	Density (g cm^{-3})	Young's modulus (GPa)*		Compression strength (MPa)†		Fracture toughness (MPa m$^{0.5}$)‡	
		Long.	Radial	Long.	Radial	Long.	Radial
Balsa	0.20	4	0.2	12	0.5	0.05	1.2
Mahogany	0.53	13.5	0.8	34	12.1	0.25	6.3
Douglas fir	0.55	16.4	1.1	39	9.0	0.34	6.2
Pine	0.55	16.3	0.8	36	7.4	0.35	6.1
Birch	0.62	16.3	0.9	39	8.3	0.56	–
Ash	0.67	15.8	1.1	38	11.0	0.61	9.0
Oak	0.69	16.6	1.0	39	15.0	0.51	4.0
Beech	0.75	16.7	1.5	39	12.5	0.95	8.9

*Dynamic moduli; moduli in static tests are about two-thirds. Data from M.F. Ashby & D.R.H. Jones, *Engineering Materials 2*, Elsevier, Oxford 2006.

†Data from L.J. Markwardt, 'Aircraft woods: Their properties, selection and characteristics', *U.S. Forest Products Laboratory Report*, No. 354.

‡Data from M.F. Ashby & D.R.H. Jones, *Engineering materials 2*, Elsevier, Oxford 2006.

Timber used in aircraft must be cut with their grains parallel to the surface to ensure maximum mechanical performance. Large reductions in the properties are experienced when the grain angle is more than a few degrees from the load direction. Figure 17.7 shows the effect of grain angle on the percentage reduction in the elastic modulus of Sitka spruce and white ash. The modulus decreases rapidly with increasing grain angle, and similar losses are experienced with strength. For this reason, the grains along the longitudinal axis of timber used in aircraft must be reasonably straight. It is recommended that the maximum grain slope should not deviate from the longitudinal axis by more than 1:16, which is equivalent to a grain angle of 3°. The strength properties of wood are seriously degraded by defects which disrupt the grain structure, such as knots and pitch pockets. Only high quality timber that is free of defects should be used in aircraft construction. It is for this reason that only a small amount (usually under 5%) of the timber taken from a tree trunk is suitable for use in aircraft.
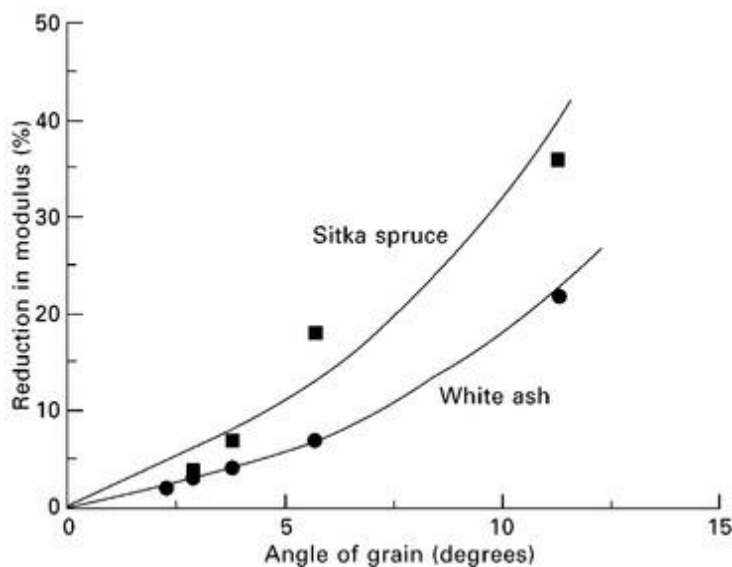
17.7 Effect of grain angle relative to longitudinal axis on the percentage reduction in elastic modulus of Sitka spruce and white ash.

In addition to grain direction, many of the key engineering properties considered in the selection of wood for airframes are dependent on the density. Properties such as elastic modulus, strength, fracture toughness and impact resistance increase with the density. For example, Fig. 17.8 shows that the compressive strength of woods measured in the longitudinal and radial directions increase with density. The longitudinal modulus E_L and strength σ_L increase rectilinearly with their density; i.e. $E_L \propto \rho$ and $\sigma_L \propto \rho$. However, the transverse modulus increases as a cubic function of density ($E_T \propto \rho^3$) and the transverse strength rises as a squared function of density ($\sigma_T \propto \rho^2$). Therefore, using denser wood in an aircraft structure is more beneficial to the longitudinal properties than the radial and tangential properties.
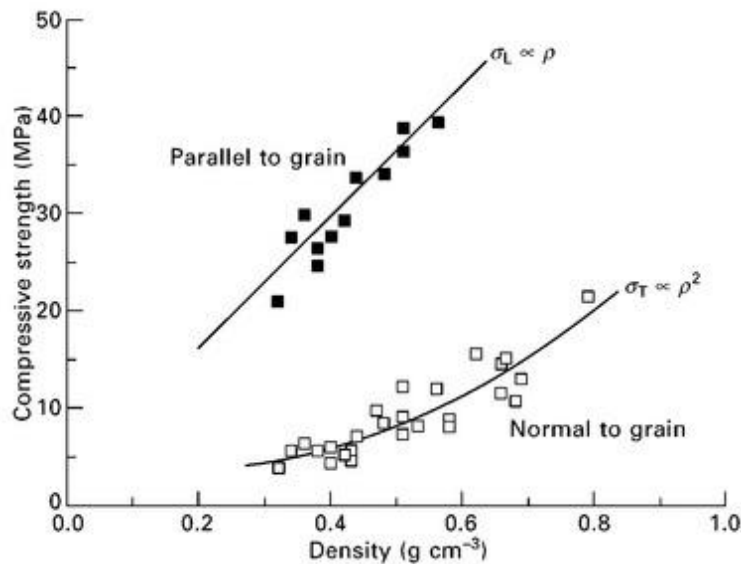
17.8 Comparison of the compressive strengths of woods with different densities measured in the longitudinal and transverse directions.

17.5.3 LAMINATED PLYWOOD

Wood in aircraft is often used as a laminated plywood construction to avoid the problems of mechanical anisotropy. Plywood is produced by bonding thin sheets (0.5–1.0 mm thick) of timber together so that the grains of each sheet run perpendicular to the adjacent sheets. In this way the material is nearly isotropic along the plane of a timber structure. Plywood is also more resistant to splitting, cracking and warping than regular wood. Aircraft plywood has traditionally been made from spruce, birch, mahogany or gabbon. High-strength and durable adhesives must be used for bonding the timber sheets; with epoxy, casein and resorcinol formaldehyde being used for aircraft plywood construction.

17.5.4 ENVIRONMENTAL PROBLEMS WITH WOOD

The mechanical properties of wood are susceptible to the operating environment of the aircraft. Firstly and most importantly, wood is hygroscopic causing the moisture content to change with the humidity of the atmosphere. This means the density and mechanical properties change with the humidity level. In dry conditions, the water content of seasoned timber can drop to as low as 8%. In hot and wet tropical environments, the moisture content can reach 18–20%, causing density to rise and mechanical performance to fall. Timber also swells and shrinks with changes in moisture content, which can lead to loosening of bolted connections, particularly propeller flange bolts, and warping of the airframe under extreme

conditions. Excessive moisture absorption can reduce the mechanical properties, in some cases by more than 20%. Figure 17.9 shows the effect of water content on the longitudinal bending modulus and strength of Sitka spruce. The properties drop rapidly with rising moisture content until it rises above 25% where they remain low and constant. Similar behaviour is observed for the longitudinal tensile and compressive properties. Therefore every effort should be used to seal and protect timber aircraft against water and humidity.
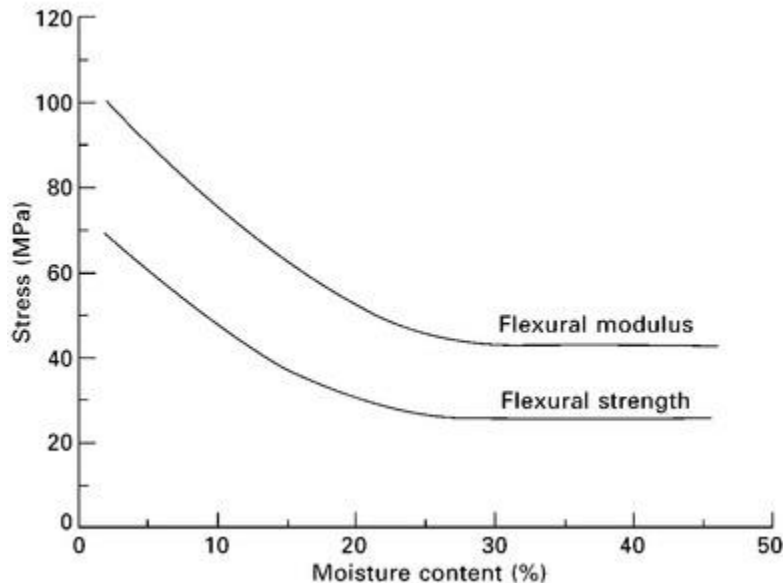
17.9 Effect of moisture content on the modulus and strength of Sitka spruce.

Another problem is that the strength of wood is inversely proportional to the temperature. Figure 17.10 shows the percentage reduction in the compressive strength of balsa with increasing temperature. Although wooden aircraft do not experience extremely high temperatures, they are heated above 50 °C when operating in hot environments. Surface temperatures as high as 70 °C have been measured on aircraft based at airports in hot, arid regions. Softening of the hemicellulose in the microfibrils begins at about 50 °C, weakening wooden structures. The aircraft industry uses a rule-of-thumb for estimating softening caused by hot weather: the tensile stiffness and strength decrease by about 1% for every 1 °C increase in the wood temperature.
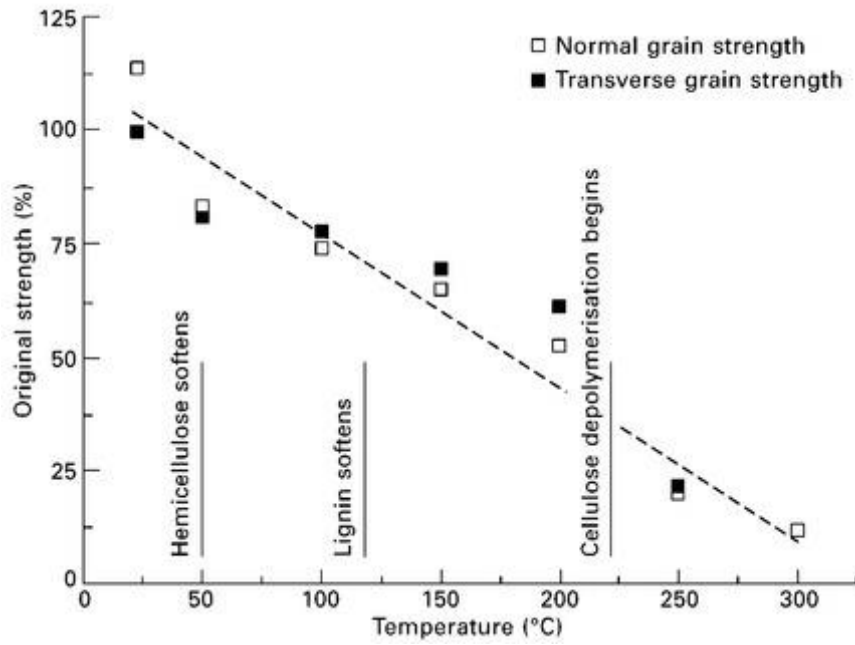
17.10 Effect of temperature on the percentage reduction in the compressive strength of balsa in the longitudinal and transverse directions.

Notes on high temperature super conductors

SUMMARY

The successful development of high-temperature superconductors (HTS) could have a major impact on future aeronautical propulsion and aeronautical flight vehicle systems. A preliminary examination of the potential application of HTS for aeronautics indicates that significant benefits may be realized through the development and implementation of these newly discovered materials. Applications of high-temperature superconductors (currently substantiated at 95 K) have been envisioned for several classes of aeronautical systems, including subsonic and supersonic transports, hypersonic aircraft, V/STOL aircraft, rotorcraft, and solar, microwave and laser powered aircraft.

In this paper, we shall introduce and describe particular applications and potential benefits of high-temperature superconductors as related to aeronautics and/or aeronautical systems.

INTRODUCTION

The recent discovery of high-temperature superconductors (HTS) has created a stir of excitement in the scientific community. The potential benefits which may be provided through application of these newly discovered superconducting materials (ceramic perovskite structures) are now being explored by investigators. Studies have been initiated to assess the potential advantage of HTS in a number of areas, including: electrical power transmission and storage, communications, computer systems, medical diagnostic equipment, and ground transportation systems (magnetically levitated high-speed trains).

Despite the acclaims and projections made for these newly discovered superconducting materials, it is generally agreed that a significant effort will be required before these materials can be developed to a state where they can be successfully used in practical applications. For example, problems associated with the physical and chemical stability of these materials must be addressed and solved. Also, methods must be developed for fabricating these materials into relatively strong, useful shapes (wires, films, etc.) for specific uses and/or applications. Nevertheless, the feeling of many researchers seems to be that most or all of the currently recognized problems with HTS can be resolved through applied research efforts (ref. 1). Based on this premise, HTS likely, in time, will find a way into a number of specific

applications. In this paper, we shall look into the potential application of high-temperature superconductors in relation to aeronautics and/or aeronautical systems.

HTS RESEARCH AND DEVELOPMENT

Critical Temperature

In general, it appears that the successful development of HTS technology could have far-reaching benefits in the field of aeronautics. The real benefits, however, will depend on several factors-some of which are not well known at this time. For example, the critical temperature (T_c) of high-temperature superconductors most certainly will influence the projected benefits which may be realized-particularly for some proposed applications related to aeronautics. (Critical temperature, T_c, is defined as the upper temperature limit at which a material exhibits superconducting properties.) At the present time, critical temperatures of, or near, 95 K (171 °R) have been well substantiated. And several researchers[2] have reported (in a popular technical magazine) evidence of superconductivity at temperatures near 300 K (540 °R).

Obviously, the higher the critical temperature, the smaller the cooling requirement will be. And this is especially important in aircraft systems because coolant for maintaining the T_c must be carried on board. There are, however, applications in aeronautics where the need to carry coolant on board may not be an overriding concern. In supersonic and/or hypersonic aircraft, where the fuel may be cryogenic (liquid methane or liquid hydrogen), the fuel may be used as a heat sink to maintain the superconducting materials at or below the critical temperature. Likewise, for aircraft flight missions which are short duration, the coolant requirements may be relatively small and of a lesser significance. Then, too, in aero applications where superconducting motors and generators are proposed, the predicted high efficiencies of these components could reduce the cooling requirements to a more reasonable and manageable level.

Materials

Before high-temperature superconductors can be successfully used in practical applications, specific processes and techniques will need to be developed for fabricating these materials into useful shapes. The inherently brittle nature of these ceramic based materials poses a problem which will need to be addressed.

Superconducting wires and ribbons which exhibit both strength and flexibility will be required for fabrication of superconducting components, such as electrical power transmission lines, motors, and generators. For aero applications, in particular, these components must be lightweight and must offer advantages over conventional electrical components.

Motors/Generators

Preliminary estimates indicate that HTS motors and generators could have a significant weight advantage over conventional electric motors and generators. This estimated weight advantage may be realized in practice, however, only if the HTS materials have the strength necessary to withstand the loads generated. The possible need for large supporting structures to withstand the high torques could also diminish the estimated weight advantage of HTS motors and generators.

The efficiencies of large HTS electric motors (induction-type) and generators have been estimated to be extremely high, i.e., in the neighborhood of 99.9 percent. Essentially all of the energy resulting from inefficiencies shows up as heat generation. Thus, with a 99.9 percent motor efficiency rating, 0.1 percent of the power input to the motor is transformed into heat. This heat generation rate, although only a small part of the motor power, results in a significant cooling requirement. The penalty imposed by the cooling requirement will depend largely on the critical temperature (T_c) of the superconducting material. If the critical temperature is relatively high, say 300 K (540 °R), then ambient temperature air (or slightly precooled air) may be used for cooling. The penalty associated with using ambient air as a coolant is estimated to be small. However, if the critical temperature is near 95 K (171 °R), some other cooling scheme, such as use of liquid nitrogen, may be required. And this could impose a more significant penalty. For example, it can be shown that the amount of liquid nitrogen coolant that must be vaporized to cool a 100 HP HTS motor (of 99.9 percent efficiency) is about 3.0 lb/hr.

AERO APPLICATIONS OF HTS

Mag-Lev Aircraft Launch Systems

The principles of electromagnetic (EM) propulsion and levitation, enhanced through the use of the new high-T_c superconducting (HTS) materials, can provide the foundation for airports of the future. The technology for EM Airports is a blend of that used in magnetically levitated (MAGLEV) trains and in certain EM mass driver concepts.

Aircraft launching can be accomplished through magnetic levitation and low "g" acceleration by means of either linear synchronous (d-c field windings) or linear induction (a-c) motors. Since superconducting magnets are only able to tolerate d-c currents without energy loss, linear synchronous motors (similar to those developed for MAGLEV trains) offer significant advantages. The most straightforward approach for aircraft launch is to attach the aircraft (via quick-disconnect cables) to an EM shuttle vehicle that rides on linear stator tracks. One configuration, for example, uses the operating principle of a squirrel-cage-motor, except that instead of the stator being in circular form with the rotor revolving within it, the stator is unrolled and laid out flat with the moving shuttle vehicle becoming a linear rotor. For aircraft launching, the linear EM propulsion track is located below the airfield surface, with only the top portion of the accelerating shuttle car and its aircraft cable connections protruding slightly above the surface level.

An alternative to the EM catapult system described above is the application of EM fields directly to the underbody of the aircraft itself and omitting the track shuttle vehicle. This approach would be more analogous to the levitation/propulsion systems under development for MAGLEV trains. However, the EM shuttle/catapult approach offers several advantages which include: the magnetic fields can be applied over a larger surface area than would be available on the airplane itself, location of the EM field (rotor) windings in the shuttle vehicle results in reduced aircraft weight, and the airplane passengers could be more easily shielded from effects of the magnetic fields.

In all likelihood, the most probable near-term application of aircraft EM launch will be aboard naval carriers. Figure 1 depicts a mag-lev aircraft launch system operating from a naval carrier. A mag-lev launch system such as shown here could be a welcomed replacement for the noisy steam catapult launchers on present-day carriers.

HTS Electric Motors For Propulsion

The proposed use of electric motors for powered flight has been studied by a number of investigators (refs. 3 and 4, for example). For the most part, these studies indicated that electric motors did not offer a distinct advantage over conventional aircraft engines (recips. and/or turboshafts). Electric motor weight and the inefficiency associated with conversion of mechanical shaft power to electrical power were considered to be major drawbacks.

Whereas conventional electric motors typically have power-to-weight ratios that are relatively low (0.5 to 1.0 hp/lb), estimates for HTS motors indicate that much higher power-to-weight ratios are possible, e.g., 15 hp/lb. Likewise, the projected efficiencies of HTS motors are expected to be far better than conventional electric motors. These projected improvements, taken together, may significantly improve the attractiveness of electric motors for aircraft propulsion and/or particular powered flight applications.

Figure 2 shows the progression of specific shaft power as a function of time for both electric motors and gas turbine engines. The values shown for the gas turbine with transmission are indicative of systems used for rotor-craft, where the transmission represents a significant part (~40 percent) of the overall propulsion system weight. As indicated in figure 2, present-day gas turbine engines of this type have about twice the specific shaft power of conventional electric motors. Future projections for these systems are shown on the far right side of figure 2. With advanced technology, the specific shaft power of the gas turbine system could increase in the future to a value near 2.5 hp/lb. And the specific shaft power of electric motors, with HTS technology (currently with T_c of 95 °R), may reach a value of about 15 hp/lb. An improvement of this magnitude, i.e., a fifteen-fold change in specific shaft power, could revolutionize the thinking regarding electric motors for aero propulsion and aero applications.

Lightweight HTS motors and generators may, in some cases, offer advantages over conventional aero propulsion systems. In the paragraphs which follow, HTS electric motors and generators are considered as a means of supplying propulsive power for specific types of aircraft. The types of aircraft to be considered here are: helicopters, subsonic transports, supersonic/hypersonic and solar powered aircraft.

Helicopters. – Most commonly, the propulsion system for conventional helicopters consists of a turboshaft engine and a shaft speed reduction system (transmission). Because of the large reduction in shaft speed required between the turboshaft engine and the rotor system, the transmissions for rotorcraft are normally large, heavy and generate considerable noise. Typically, the weight of the transmission system for helicopters represents approximately 40 percent of the total weight of the gas generator and transmission system. A conventional rotorcraft propulsion system with onboard fuel is depicted in figure 3(a).

A conceptual propulsion system for rotorcraft which uses a HTS generator/motor is shown in figure 3(b). In this conceptual system, the turboshaft engine drives a HTS generator which, in turn, supplies electrical power to a HTS motor. The HTS motor, in turn, drives the helicopter rotor. The HTS generator/motor system just described is currently being studied by Pratt and Whitney under a NASA-Lewis sponsored contract.

The potential advantage of this conceptual system (fig. 3(b)) is that the heavyweight gearbox is eliminated from the propulsion system. But, as indicated in fig. 3(b), a HTS generator/motor system is added in place of the heavy gearbox. Nevertheless, a net weight advantage may be realized by this exchange if the specific shaft power of the generator/motor system is relatively high. For example, if we assume the specific shaft power of the conventional rotorcraft propulsion system to be 1.25 hp/lb, and also assume the transmission weight to be 40 percent of the total propulsion system weight, we can then estimate the potential improvement which may result. By using a specific shaft power of 15 hp/lb for the HTS generator/motor system, it can be shown that the total weight of a rotorcraft propulsion system can be reduced by nearly 25 percent. That is, the weight of the total propulsion system shown in figure 3(b) is nearly 25 percent less than the conventional system shown in figure 3(a). This is obviously a substantial improvement. Other more subtle advantages of the system shown in figure 3(b) are elimination of gearbox noise and vibration and a possible improvement in the rotorcraft weight distribution.

Figure 3(c) depicts a more advanced conceptual propulsion system for rotorcraft which uses HTS technology. In this conceptual system, microwave power is beamed to a rectenna (a rectifying antenna) on board the rotorcraft. The rectenna, in turn, converts microwave energy directly to electrical energy which then powers an HTS electric motor. The HTS motor, in turn, drives the helicopter rotor. High temperature superconductors are projected to offer significant weight reductions for both the electric motor and the rectenna.

The advantages of the system shown in figure 3(c) are rather apparent. This conceptual system carries no onboard fuel and the propulsion system consists only of a rectenna and an HTS electric motor. A rotorcraft powered by the conceptual system shown in figure 3(c) could be a valuable resource for long duration surveillance activities, such as for specific naval operations at sea.

Subsonic transports. – HTS motors and generators may be used to advance and improve the propulsion systems of subsonic transport aircraft. A conceptual application of HTS motors and generators to a subsonic transport propulsion system is shown in figure 4. A collection of several separate applications of HTS is included here. In this system, gas turbine engines mounted below the aircraft wings are used to drive HTS electric generators.

The generators, in turn, supply electric power to systems and subsystems on board the aircraft. In effect, the aircraft shown in figure 4 is an all-electric powered aircraft. In this aircraft, a major portion of the electric power generated is used by HTS motors located at the rear of the fuselage. These HTS motors drive propulsors (propellers or fans) which provides thrust to the aircraft. A minor portion of the electric power is used for other sub-systems. These include: winglet propellers or "proplets" (powered by small HTS motors) to counter the drag produced by wing-tip vorticies, and suction devices (driven by HTS motors) to promote a laminar boundary layer and thereby reduce drag on the wing surfaces.

The major advantage of the conceptual propulsion system shown in figure 4 is that the turboshaft engines and propulsors need not be colocated on the aircraft. By locating the propulsors at the rear of the fuselage, aircraft cabin noise can be reduced. This arrangement may also improve the aircraft balance and/or weight distribution. And, finally, the total drag of the air-craft may be significantly reduced through use of "proplets" and laminar boundary layer control.

Again, the critical temperature of the HTS materials needed in this application is of major importance. Mostly likely, an all-electric propulsion system such as shown in figure 4 would be advantageous only if superconductors with relatively high critical temperatures (>95 K) were available.

Supersonic/hypersonic aircraft. - High-speed supersonic and hypersonic aircraft are again being strongly advocated for some civil and military mis-sions. In the high-speed flight regime (Mach 3 and above) cryogenic fuels (liquid methane and liquid hydrogen) appear to be especially attractive because of their heat sink capacity. Cryo fuels may be used to cool high-temperature components on both the vehicle and propulsion system. Specific examples are: the leading edge of wings, the leading fuselage structure and the engine inlet cowl/lip structures.

Most of the proposed propulsion systems for high-speed flight, say to Mach 6 or so, are "composite" engine systems. These systems consist, usually, of a low by-pass turbofan engine for flight speeds up to about Mach 3 and a ramjet engine for speeds above Mach 3. A conceptual turbofan engine which uses HTS technology and which may offer superior performance for flight speeds up to Mach 3 is shown in figure 5. The key feature of this engine is the all-electric, tip-powered fan. The engine fan is effectively the rotor of an electric motor and the fan shroud contains the stator windings which surround the fan and/or rotor.

It appears that high-temperature superconductors may be the enhancing or enabling technology for this type of conceptual all-electric tip powered turbo-fan system. And cryogenic hydrogen may provide the cooling needed to maintain the HTS materials at or below their critical temperature, even for T_c values of or near 95 K.

Solar powered aircraft. - A solar powered civil aircraft is illustrated in figure 6. A manned aircraft of this type has already been flown across the English Channel. The basic performance of the aircraft shown in figure 6 may be improved by use of a superconducting electric motor and generator, and energy storage coils. The storage coils would be used to supply power for

nighttime operation and would be recharged during the day. This type of air-
plane could be used for weather observations and predictions, and for communi-
cation. The airplane may fly for months at a time and hence the critical
temperature of the HTS is extremely important.

A solar powered airplane can fly using existing technology for electric
drive motors and storage batteries. A future system based on room-temperature
HTS would be enhancing and may provide a low-cost means of surveilance for
civil needs.

The same airplane system described above may also be applicable for mili-
tary missions as illustrated in figure 7. Such an aircraft may be advantageous
for long duration survey/reconnaissance activities such as those connected
with naval operations at sea.

Aircraft secondary electric power systems. Current subsonic transport
aircraft use three different types of secondary power; namely, hydraulic,
pneumatic and electric. As indicated in figure 8, secondary power is used to
activate control surfaces and other systems (flaps, spoilers, slats, landing
gear, etc.) on the aircraft.

It has already been shown in reference 5 that an all-electric secondary
power system (which uses conventional conductors) can provide significant bene-
fits over the currently used multiple power system. Reference 5 indicates,
for example, that a conventional (copper-wire) all-electric secondary power
system could produce nearly a 10 percent reduction in the mission fuel require-
ment of a subsonic transport aircraft. The benefit cited in reference 5 may
be improved further if an all-electric HTS secondary system is used. Indica-
tions are that mission fuel could be cut an additional three percentage points
with an all-electric HTS secondary power system. This additional reduction in
mission fuel is the result of lighter weight and higher efficiency HTS motors.

In this particular application, however, critical temperature of the HTS
material is especially important. If cooling of the superconducting materials
is required, the potential benefits of HTS for secondary all-electric power
could be reduced or lost. Thus, for this application, a room temperature
superconductor may be both desirable and necessary to achieve the gains just
cited.

Magnetic Bearings

Significant benefits may be realized through the use of magnetic bearings
in aero propulsion systems. Preliminary estimates by Pratt and Whitney indi-
cate that the exclusive use of conventional-type magnetic bearings in turbofan
engines could provide as much as a 6 percent reduction in engine weight and a
3 percent improvement in thrust specific fuel consumption (TSFC) for a subsonic
high BPR turbofan. These estimated improvements come about from: (1) the
ability to operate a turbofan engine at higher rotor speeds, (2) reduced rotor
tip clearance resulting from tighter bearing clearance, (3) significantly lower
friction and heat generation, and (4) reduced engine nacelle size resulting
from smaller bearing compartments.

Magnetic bearings made of HTS materials should be significantly smaller and lighter than conventional mag bearings. As depicted in figure 9, the HTS magnetic bearings have smaller coils, contain no iron and are stiffer than conventional mag bearings. Estimates indicate that these bearings could provide an additional improvement in fan performance over that projected for conventional mag bearings.

Magnetic Braking

The high-conductivity plasma created upon entry of a hypersonic aircraft (or spacecraft) into the atmosphere can potentially be used as the working plasma of a MHD braking system. A vehicle flying at high speed through the atmosphere may raise the local stagnation temperature high enough that the air becomes ionized and hence an electrical conductor. In principle, a strong magnetic field generated by HTS could be used to deflect the plasma formed and thereby decelerate the vehicle through an imposed reaction force.

Magnetic braking could minimize the need for heat shields of the type used on the shuttle spacecraft. Magnetic braking may also permit the deceleration of a spacecraft to begin at a more distant point in the trajectory, thereby reducing the peak reaction forces on the spacecraft. Figure 10 depicts a spacecraft entering the atmosphere and being decelerated by aerodynamic drag forces (upper left) and magnetic braking forces (lower right).

CONCLUDING REMARKS

The successful development of high-temperature superconductors could have a major impact on future aero propulsion and aero flight vehicle systems. A number of conceptual aero applications of HTS have been identified and described herein. The next step in the study of HTS applications for aeronautics is to quantify the potential advantages in terms of performance, weight and cost. In general, it is believed that aero applications of HTS will be more sensitive to critical temperature than most other applications. This is because the cooling system weight must be carried on-board the aircraft and, as such, may compromise the payload and/or range of the aircraft.

Finally, the technologies that must be developed for the most attractive applications of HTS need to be identified and the appropriate research should be initiated.

TYPES OF PROPELLANTS

Propellants, the working substances of rocket engines, constitute the fluid that undergoes chemical and thermodynamic changes. The term *liquid propellant* embraces all the various propellants stored as liquids and may be one of the following

1. Oxidizer (liquid oxygen, nitric acid, nitrogen tetroxide, etc.).

2. Fuel (kerosene, alcohol, liquid hydrogen, etc.).
3. Chemical compound (or mixtures of oxidizer and fuel ingredients) capable of self-decomposition, such as hydrazine.

4. Any of the above, but with a gelling agent (these have yet to be approved for production).

A *bipropellant* consists of two separate liquid propellants, an oxidizer and a fuel. They are the most common type. They are stored separately and are mixed inside the combustion chamber (see definition of the mixture ratio below). A *hypergolic* bipropellant combination *self-ignites* upon contact between the oxidizer and the liquid fuel. A *nonhypergolic* bipropellant combination needs energy to start combusting (e.g., heat from an electric discharge) and such engines need an ignition system.

A *monopropellant* may contain an oxidizing agent and combustible matter in a single liquid substance. It may be a stored mixture of several compounds or it may be a homogeneous material, such as hydrogen peroxide or hydrazine. Monopropellants are stable at ambient storage conditions but decompose and yield hot combustion gases when heated or catalyzed in a chamber.

A *cold gas propellant* (e.g., helium, argon, or gaseous nitrogen) is stored at ambient temperatures but at relatively high pressures; it gives a comparatively low performance but allows a simple system, and is usually very reliable. They have been used for roll control and attitude control.

A *cryogenic propellant* is a liquefied gas at lower than ambient temperatures, such as liquid oxygen (−183 °C) or liquid hydrogen (−253 °C). Provisions for venting the storage tank and minimizing vaporization losses are necessary with this type.

Storable propellants (e.g., nitric acid or gasoline) are liquid at ambient temperatures and at modest pressures and can be stored for long periods in sealed tanks. *Space-storable propellants* remain liquid in the space environment; their storability depends on the specific tank design, thermal conditions, and tank pressures. An example is ammonia.

A *gelled propellant* is a thixotropic liquid with a gelling additive. It behaves in storage as a jelly or thick paint (it will not spill or leak readily) but can flow under pressure and will burn, thus being safer in some respects. Gelled propellants have been used in a few experimental rocket engines but, to date, gelled propellants have not been in production (see Eighth edition of this book).

Hybrid propellants usually have a liquid oxidizer and a solid fuel.

For bipropellants, the propellant *mixture ratio* represents the ratio at which the oxidizer and fuel flows are mixed and react in the chamber to give the hot flow of gases. The mixture ratio r is defined as the ratio of the oxidizer mass flow rate $\dot{m}_o$ to the fuel mass flow rate $\dot{m}_f$ or

$$6\text{–}1 \quad r = \dot{m}_o / \dot{m}_f$$

this mixture ratio affects the composition and temperature of the combustion products. It is usually chosen to give a maximum value of specific impulse (or the ratio $T_1/\mathfrak{M}$, where T_1 is the absolute combustion temperature and $\mathfrak{M}$ is the average molecular mass of the reaction gases, see Eq. 3–16 and Fig.). For a given thrust F and a given effective exhaust velocity c, the total propellant flow rate $\dot{m}$ is given by Eq. 2–6; namely, $\dot{m} = F/c$. Actual relationships between $\dot{m}, \dot{m}_o, \dot{m}_f$, and r are as follows:

$$6\text{–}2 \quad \dot{m} = \dot{m}_o + \dot{m}_f$$
$$6\text{–}3 \quad \dot{m}_o = r\dot{m}/(r+1)$$
$$6\text{–}4 \quad \dot{m}_f = \dot{m}/(r+1)$$

The above four equations are often valid when w and $\dot{w}$ (weight and weight flow rate) are substituted for m and $\dot{m}$.

LIQUID PROPELLANTS

In this chapter, we discuss properties, performance, hazards, and other characteristics of commonly used propellants that are stored as liquids (and a few as gases). These characteristics influence engine and vehicle design, test facilities, and propellant storage and handling. At the present time, we ordinarily use three liquid bipropellant combinations: (1) the cryogenic *oxygen–hydrogen propellant system*, used in upper stages and sometimes booster stages of space launch vehicles, giving the highest specific impulse nontoxic propellant combination and one that is best for high vehicle velocity missions; (2) the *liquid oxygen–hydrocarbon propellant combination*, used for booster stages (and a few second stages) of space launch vehicles — having a higher average density allows more compact booster stages with less inert mass when compared to the previous combination (historically, it was developed first and was originally used with ballistic missiles); (3) not a single bipropellant combination but several ambient temperature *storable propellant combinations* used in large rocket engines for first and second stages of ballistic missiles and in almost all bipropellant low-thrust, auxiliary or reaction control rocket engines (this term is defined below); these allow for long-term storage and almost instant readiness (starting without the delays and the precautions that come with cryogenic propellants). Each of these propellant systems is further described in this chapter. Presently, Russia and China favor nitrogen tetroxide as the oxidizer and unsymmetrical dimethylhydrazine, or UDMH, as the fuel for ballistic missiles and for auxiliary engines. The U.S. has used nitrogen tetroxide and a fuel mixture of 50% UDMH with 50% hydrazine in the Titan II and III missiles' large engines. For auxiliary engines in many satellites and upper stages, the United States uses a nitrogen-tetroxide/monomethylhydrazine bipropellant. A subcategory of item (3) above is the *storable monopropellant* such as hydrogen peroxide or hydrazine. The International Space Station and many U.S. satellites use monopropellant hydrazine for low-thrust auxiliary engines.

No truly new liquid propellant has been adopted for operational rocket flight vehicles in the past 30 years. Some new propellants (such as hydroxyl ammonium nitrate) were synthesized, manufactured, and ground tested in thrust chambers and flown in experimental vehicles in the past two decades, but they have not found their way into operational rocket engine applications. Between 1942 and 1975, a number of other propellants were successfully flown; these included ammonia (X-15 Research test aircraft), ethyl alcohol (German V-2 or U.S. Redstone missile), and aniline (WAC Corporal). They each had some disadvantages and are no longer used in operational flights today. Liquid fluorine and fluorine containing chemicals (such as chlorine pentafluoride and oxygen difluoride) give excellent performance and have been investigated and experimentally evaluated but, because of their extreme toxicity, they are no longer being considered.

A comparative listing of various performance quantities for a number of propellant combinations is given in Table 5–5 and in Ref. 7–1. Some important physical properties of selected common liquid propellants are shown in Table 7–1 (water is also listed for comparison). Specific gravities and vapor pressures are shown in Figs. 7–1 and 7–2. The *specific gravity* is defined to represent the ratio of the density of any given liquid to that of water at standard conditions (273 K and 1.0 atm) and thus carries no dimensions.

Table 7–1 Physical Properties of Liquid Propellants

Propellant	Liquid Oxygen	Nitrous oxide	Nitrogen Tetroxide	Nitric Acid_a_ (99% pure)	Rocket Fuel RP-1, RP-2
Chemical formula	O_2	N_2O	N_2O_4	HNO_3	Hydrocarbon $CH_{1.97}$
Molecular mass	31.988	44.013	92.016	63.016	~175

Propellant	Liquid Oxygen	Nitrous oxide	Nitrogen Tetroxide	Nitric Acid[a] (99% pure)	Rocket Fuel RP-1, RP-2
Melting or freezing point (K)	54.8	182.29	261.95	231.6	225
Boiling point (K)	90.2	184.67	294.3	355.7	460–540
Heat of vaporization (kJ/kg)	213	374.3 (at 1 atm)	413[2]	480	246[b]
Specific heat	0.4	0.209	0.374	0.042	0.48+
(kcal/kg-K)	(65 K)		(290 K)	(311 K)	(298 K)
			0.447	0.163	
			(360 K)	(373 K)	
Specific gravity[c]	1.14	1.23[b]	1.38	1.549	0.58
	(90.4 K)		(293 K)	(273.15 K)	(422 K)
	1.23		1.447	1.476	0.807
	(77.6 K)		(322 K)	(313.15 K)	(289 K)
Viscosity	0.87	0.0146 (gas at 300 K)	0.47	1.45	0.75
(centipoises)	(53.7 K)		(293 K)	(273 K)	(289 K)
	0.19		0.33		0.21
	(90.4 K)		(315 K)		(366 K)
Vapor pressure	0.0052	5.025	0.1014	0.0027	0.002
(MPa)	(88.7 K)	(293 K)	(293 K)	(273.15 K)	(344 K)
			0.2013	0.605	0.023
			(328 K)	(343 K)	(422 K)

Propellant	Liquid Oxygen	Nitrous oxide	Nitrogen Tetroxide	Nitric Acid[a] (99% pure)	Rocket Fuel RP-1, RP-2
para–H_2	CH_4	$CH_3 NHNH_2$	$N_2 H_4$	$(CH_3)_2 NNH_2$	H_2O
2.016	16.04	46.072	32.045	60.099	18.02
14.0	90.67	220.7	275.16	216	273.15
20.27	111.7	360.8	387.46	335.5	373.15
446	510[b]	808	1219[b]	543	2253[2]
2.34[b]	0.835[b]	0.700	0.736	0.704	1.008
(20.27 K)		(298 K)	(293 K)	(298 K)	(273.15 K)
—	—	0.735	0.758	0.715	
		(393 K)	(338 K)	(340 K)	
0.071	0.424	0.8702	1.0037	0.7861	1.002
(20.4 K)	(111.5 K)	(298 K)	(298 K)	(298 K)	(373.15 K)
0.076	—	0.857	0.952	0.784	1.00
(14 K)		(311 K)	(350 K)	(244 K)	(293.4 K)
0.024	0.12	0.775	0.97	0.492	0.284
(14.3 K)	(111.6 K)	(298 K)	(298 K)	(298 K)	(373.15 K)
0.013	0.22	0.40	0.913	0.48	1.000
(20.4 K)	(90.5 K)	(344 K)	(330 K)	(300 K)	(277 K)
0.2026	0.033	0.0066	0.0019	0.0223	0.00689
(23 K)	(100 K)	(298 K)	(298 K)	(298 K)	(312 K)

Propellant	Liquid Oxygen	Nitrous oxide	Nitrogen Tetroxide	Nitric Acid[a] (99% pure)	Rocket Fuel RP-1, RP-2
0.87	0.101	0.638	0.016	0.1093	0.03447
(30 K)	(111.7 K)	(428 K)	(340 K)	(339 K)	(345 K)

[a] Red fuming nitric acid (RFNA) has 5 to 20% dissolved NO_2 with an average molecular mass of about 60, and a density and vapor pressure somewhat higher than those of pure nitric acid.
[b] At boiling point.
[c] Reference for specific gravity ratio: 10^3 kg/m^3 or 62.42 lbm/ft^3.
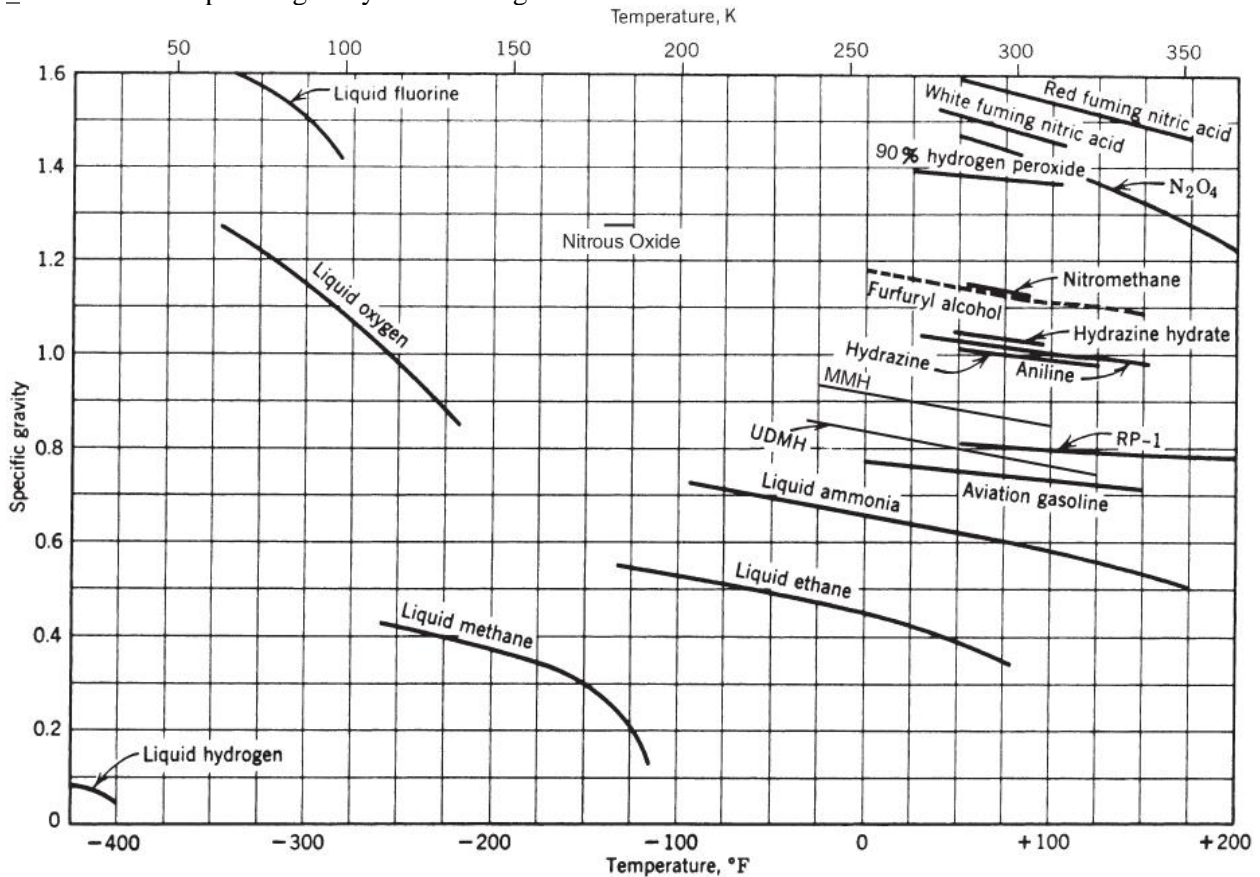
Figure 7–1 Specific gravities of several liquid propellants as a function of temperature.
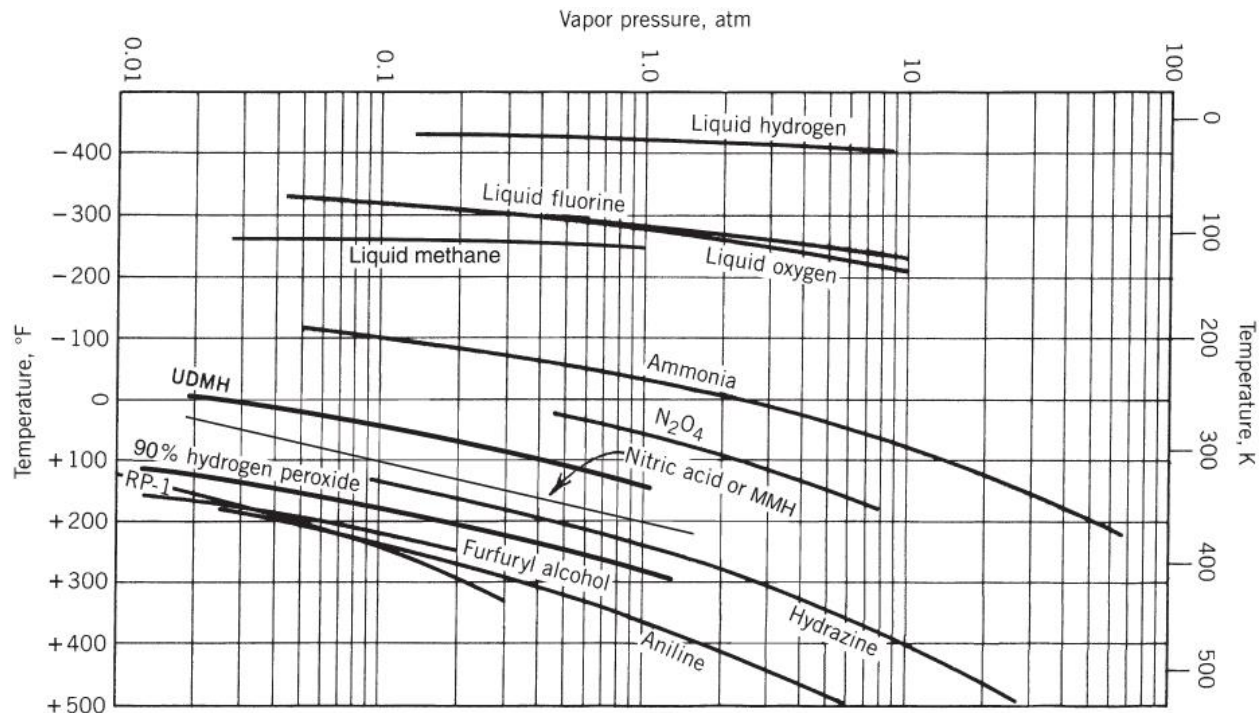
Figure 7–2 Vapor pressures of several liquid propellants as a function of temperature.

Green propellants (Ref. 7–2), a recently minted term, represent those liquid propellants and their exhaust gases that are "environmentally friendly" and can be used without causing damage to people, equipment, or the surroundings. An excellent example is the liquid oxygen–liquid hydrogen propellant combination—they are not toxic, not corrosive, not hypergolic and will not decompose or explode. Some authors use a more restricted interpretation for the green propellant category, namely, one that can replace a toxic and/or potentially explosive propellant with a chemical substance that is harmless.

7.1 PROPELLANT PROPERTIES

It is important to distinguish between characteristics and properties of *liquid propellants* (i.e., fuel and oxidizer liquids in their unreacted condition) and those of the *hot gas mixture* resulting from their reaction in the combustion chamber. The chemical nature of liquid propellants and their mixture ratio determine the properties and characteristics of both storage and reaction products. Because none of the known practical propellants encompass all properties deemed desirable, the selection of propellant combinations is usually a compromise between various economic factors, such as those listed below.

ECONOMIC FACTORS

Availability in quantity and a *low cost* are very important considerations in propellant selection. In military applications, consideration has to be given to the *logistics* of production, supply, storage, along with other factors. The production process should require only ordinarily available chemical equipment and available raw materials. It is more expensive to use toxic or cryogenic propellants than storable, nontoxic ones, because the former require additional steps in their operation, more safety provisions, additional design features, longer check-out procedures prior to launch, and often better trained personnel.

PERFORMANCE OF PROPELLANTS

The performance rocket engines may be compared on the basis of their *specific impulse*, *exhaust velocity*, *characteristic velocity*, and/or other engine parameters. The specific impulse and exhaust velocity are functions of pressure ratio, specific heat ratio, combustion temperature, mixture ratio, and molecular mass. Equilibrium values of performance parameters for various propellant combinations can be calculated

with a high degree of accuracy and several are listed in Table 5–5. Very often, performance is also expressed in terms of *flight performance parameters* for specific rocket applications, as explained in Chapter 4. Here, average propellant density, total impulse, and engine mass ratio usually enter into the various flight relation descriptions.

For high performance, *high chemical energy content* per unit of propellant mixture is desirable because this yields high chamber temperatures. A *low molecular mass* for the combustion products gases is also desirable. This can be accomplished by using fuels rich in hydrogen obtained when a significant portion of the hydrogen gas injected or produced remains uncombined. In general, therefore, the best mixture ratio for many bipropellants is not stoichiometric (which results in complete oxidation and yields the highest flame temperature) but fuel-rich, containing a large amounts of low-molecular-mass reaction products

When relatively small metallic fuel particles (such as beryllium or aluminum) are suspended in the liquid fuel, it is theoretically possible to increase the specific impulse by between 9 and 18%. A particular chemical propellant combination having the highest ideal specific impulse known (approximately 480 sec at 1000 psia chamber pressure and expansion to sea-level atmosphere, and 565 sec in a vacuum with a nozzle area ratio of 50) uses a toxic liquid fluorine oxidizer with hydrogen fuel plus suspended toxic solid particles of beryllium; as yet, acceptably safe and practical means for storing such seeded propellants and their practical rocket engine use remain undeveloped.

Gelled propellants are materials that have additives that make them thixotropic. They have the consistency of thick paint or jelly when at rest, but do liquefy and flow through pipes, valves, pumps and/or injectors when an adequate pressure or shear stress is applied. In spite of extensive research and development work and demonstrations of better safety and certain "green" qualities, to date they have not been adopted for any production rocket engine. Gelled propellants have been described in the Sixth, Seventh, and Eighth editions of this book.

COMMON PHYSICAL HAZARDS

Although several hazard categories are described below, they do not all apply to each propellant or to every bipropellant combination. Hazards can be different for each specific propellant and must be carefully understood before working with it. The consequences of unsafe operation or unsafe design are usually also unique to each propellant.

Corrosion

Several propellants, such as nitrogen tetroxide, nitric acid, nitric oxide and/or hydrogen peroxide, can only be handled in containers and pipelines made from special materials. When any propellant gets contaminated with corrosion products, its physical and chemical properties may sufficiently change to make it unsuitable for its intended operation. Corrosion caused by expelled gaseous reaction products is most critical in applications where the reaction products are likely to damage launch or ground test structures and parts of the vehicle, and/or affect communities and housing near a test facility or launch site.

Explosion Hazard

Over time some propellants (e.g., hydrogen peroxide or nitromethane) can become unstable in their storage tanks and may even detonate under certain conditions, depending on local impurities, temperatures, and shock magnitudes. When liquid oxidizers (e.g., liquid oxygen) and fuels get unintentionally mixed together, detonation may sometimes result. Unusual flight vehicle launch mishaps or transport accidents have caused such mixing and subsequent explosions to occur

Fire Hazard

Many oxidizers will react with a large variety of organic compounds. Nitric acid, nitrogen tetroxide, fluorine, and/or hydrogen peroxide react spontaneously when in contact with many organic substances resulting in fires. Most of rocket fuels exposed to air are readily ignitable when heated. Also some

household dusts, certain paints, or smoke particles can oxidize. Oxygen by itself will not usually start a fire with organic materials but it will greatly enhance an existing fire.

Accidental Spills

Unforeseen mishaps during engine operation or traffic accidents on highways or railroads while transporting hazardous materials, including many propellants, have on occasion caused spills which expose people to intense fires and/or potential health hazards. The U.S. Department of Transportation has strict rules for marking and containing hazardous materials during transport and also guidelines for emergency actions

Health Hazards

Exposure to many commonly used propellants represents a health hazard. Toxic unburned chemicals or poisonous exhaust species affect the human body in a variety of ways and the resulting health disorders are propellant specific. Nitric acid causes severe skin burns and tissue disintegration. Skin contact with aniline or hydrazine may cause nausea and other adverse health effects. Hydrazine, monomethylhydrazine, unsymmetrical dimethylhydrazine, or hydrazine hydrate are known animal and suspected human carcinogens. Many propellant vapors cause eye irritation, even in small concentrations. Inadvertent ingestion of many propellants may result severe health degradation.

Inhalation of toxic exhaust gases or gaseous or vaporized liquid propellants is perhaps the most common health hazard. It can cause severe damage if the exposure is long or in concentrations that exceed established maximum threshold values. In the United States, the Occupational Safety and Health Administration (OSHA) has established limits or thresholds on the allowable exposure and concentration for most propellant chemicals.

Toxic Propellants

These require special safety provisions, strict rules, and specific procedures for handling, transferring to other containers, road transport, inspection, and for working on rocket engines that contain them (such as the removal of residuals after testing or after return from a space mission). Instruments are available to detect toxic vapors or toxic contents in liquids or water. For personnel protection, face shields and gas masks (some with an oxygen supply), special gloves and boots, sealed communications equipment, medical supplies and periodic medical examinations need to be available. For accidental toxic spills or leaks there should be equipment for diluting with water or other suitable chemical, and for safe disposal of the contaminants from a test stand or launch platform. Chemicals for neutralization and detoxification should always be on hand. In case of mishaps instructions and procedures for notifying management, certain government offices and relevant others should be available and not overlooked. When compared to nontoxics, operations with toxic-propellants require two to four times as many trained workers. Only subsets of the precautions listed above apply to any one operation

Materials Compatibility

For several liquid propellants there are only a limited number of truly compatible materials, both metals and nonmetals, particularly for making gaskets or O-rings. There have been many failures (causing fires, leakage, corrosion, or other malfunctions) when improper or incompatible hardware materials have been used in rocket engines. Depending on the specific component and loading conditions, structural materials have to withstand high stresses, stress corrosion, and in some applications high temperatures and/or abrasion. Several specific material limitations are mentioned in the next section. Certain storage materials may act to catalyze the self-decomposition of hydrogen peroxide into water and oxygen making long-term storage difficult and causing any closed containers to explode. Many structural materials, when exposed to cold (cryogenic) propellants become unacceptably brittle.

DESIRABLE PHYSICAL PROPERTIES

Low Freezing Point

This permits operation of rockets in cold environments. The addition of small amounts of freezing point depressants has been found to help lower the freezing point in some liquid propellants that might otherwise solidify at environmental storage conditions.

High Specific Gravity

Denser propellants provide a larger propellant mass for a given vehicle tank volume. Alternatively, for a given mass, they permit smaller tank volumes and, consequently, lower structural vehicle mass and lower aerodynamic drag. The specific gravity of a propellant, therefore, has an important effect on the maximum flight velocity and range of any rocket-powered vehicle or missile flying within the Earth's atmosphere as explained in Chapter 4. Specific gravities for various propellants are plotted in Fig. 7–1. Variations of ambient temperature in stored propellants cause changes of the liquid level in their storage tanks.

For a given bipropellant mixture ratio r, the *average specific gravity* of any propellant combination δ_{av} can be determined from the specific gravities of the fuel δ_f and of the oxidizer δ_o. This average specific gravity δ_{av} is defined below. Here r is the mixture ratio; it represents the oxidizer mass flow rate divided by the fuel mass flow rate (see Eq. 6–1):

$$\delta_{av} = \frac{\delta_o \delta_f (1 + r)}{r\delta_f + \delta_o}$$
7–1

Values of δ_{av} for various propellant combinations are listed in Table 5–5. The value of δ_{av} can be increased by adding high density materials to the propellants, either by solution or colloidal suspension. An identical equation can be written for the average density ρ_{av} in terms of the fuel and oxidizer densities:

$$\rho_{av} = \frac{\rho_o \rho_f (1 + r)}{\rho_f r + \rho_o}$$
7–2

Though the specific gravity is unitless, in the SI system it has the same numerical value as the density expressed in units of grams per cubic centimeter or kg/liter. In some performance comparisons the parameter *density specific impulse I_d* is used. It is defined as the product of the average specific gravity δ_{av} and the specific impulse I_s:

7–3 $I_d = \delta_{av} I_s$

A *propellant density increase* will allow increases in mass flow and total propellant mass when all other system parameters remain the same. For example, Fig. 7–1 shows that lowering the temperature of liquid oxygen from –250 to –280 °F raises its specific gravity by approximately 8%. Therefore, the system's mass flow rate and the total mass will increase by approximately the same amount. These changes will enable increases in chamber pressure, total impulse, and thrust; changes of less than 1% in specific impulse may also be noticed. So there is some benefit to vehicle performance in operating with the liquid propellants at their lowest practical temperature. In ground-based systems, cooling of liquid oxygen may be achieved with a (colder) liquid nitrogen heat exchanger just before launch. The percent increase in performance with propellants other than oxygen is usually much smaller.

Stability

Proper *chemical stability* means no decomposition of the liquid propellant during operation or storage, even at elevated temperatures. With many propellants, insignificant amounts of *deterioration* and/or *decomposition* during long-term (over 15 years) storage and minimal *reaction with the atmosphere* have been attained. A desirable liquid propellant should also experience no *chemical deterioration* when in contact with tubing, pipes, tank walls, valve seats, and gasket materials even at relatively high ambient temperatures. No appreciable *absorption of moisture* and no adverse effects of small amounts of *impurities* are also desirable properties. There should also be no appreciable chemical

deterioration when liquids flow through hot cooling jacket passages of a regeneratively cooled thrust chamber. When carbon-containing coolants decompose and form (carbonaceous) deposits on hot inside surfaces of cooling passages, such deposits may harden, reducing the heat flow, increasing metal temperatures locally, and thus may cause the unit to weaken and eventually fail. Unavoidably, even in well-insulated tanks, between 1 and 20% of a cryogenic propellant may evaporate daily when stored in the flight vehicle.

Heat Transfer Properties

High specific heat, high thermal conductivity, *low freezing temperature*, and *high boiling or decomposition temperature* are all desirable properties for propellants used for thrust chamber cooling

Pumping Properties

Low *vapor pressures* permit not only easier handling of propellants, but also more effective pump designs in applications where propellants must be pumped. Low vapor pressures also reduce the potential for pump cavitation. When the propellant *viscosity* is too high, then pumping and engine-system calibrations become difficult. Propellants with high vapor pressures (such as LOX, liquid hydrogen, and other liquefied gases) require special design provisions, unusual handling techniques, and special low-temperature materials.

Temperature Variation of Physical Properties

Temperature variations in the physical properties of any liquid propellant should be small and should be very similar for the fuel and oxidizer. For example, wide temperature variations in vapor pressure and density or unduly high changes in viscosity with temperature make it difficult to accurately calibrate rocket engine flow systems and/or to predict their performance over any reasonable range of operating temperatures. While stored in a flight vehicle, if one of the propellants experiences a larger temperature change than the other, this may cause a noticeable change in mixture ratio and in specific impulse, and possibly a significant increase in unusable or undesirable propellant residue.

IGNITION, COMBUSTION, AND FLAME PROPERTIES

When a propellant combination is *spontaneously ignitable* burning is initiated as soon as the oxidizer and the fuel come in contact with each other. Spontaneously or self-ignitable propellant combinations are called *hypergolic* propellants. Although ignition systems are not necessarily objectionable, their elimination simplifies the propulsion system. In order to reduce potential explosion hazards during starting, all rocket propellants should be readily ignitable and exhibit acceptably short ignition time delays in order to eliminate potential explosion hazards.

Nonspontaneously ignitable propellants must be energized by external means for ignition to begin. Igniters are devices that accomplish a localized initial chamber pressurization and initial heating of the propellant mixture to a state where steady flow combustion can be self-sustained. The amount of energy needed from the igniter to activate the propellants should be small so that low-power, light-weight ignition systems may be used. The energy required for satisfactory ignition usually diminishes with increasing propellant storage temperature. At low ambient temperatures ignition can become relatively slow (0.05 to 0.02 sec).

Certain propellant combinations burn very smoothly, without vibration (i.e., gas pressure oscillations). Other propellant combinations do not exhibit such *combustion stability* and, therefore, become less desirable.

Smoke formation is objectionable in many applications because it may deposit on the surrounding equipment and parts. *Smoke* and brilliantly *luminous exhaust flames* are objectionable for certain military applications since they can be easily detected. In some applications, the condensed species from gaseous exhausts can cause *surface contamination* on spacecraft windows or optical lenses, and the presence of free electrons in a flame may cause undesirable *interference* or *attenuation of communications radio signals*.

PROPERTY VARIATIONS AND SPECIFICATIONS

Propellant properties and quality must not vary from delivered batch to batch because this can affect engine performance and combustion from changes in physical and/or chemical properties. The same propellant must have consistent composition and storage properties; rocket operating characteristics should not change even when propellants are manufactured at different times or made by different manufacturers. For these reasons propellants are purchased to conform to strict specifications which define ingredients, maximum allowable impurities, packaging methods and/or compatible materials, allowable tolerances on physical properties (such as density, boiling point, freezing point, viscosity, or vapor pressure), quality control requirements, container cleaning procedures, documents of inspections, laboratory analyses, and/or test results. A careful chemical analysis of composition and impurities is always necessary. Reference 7–7 describes some of these methods of analysis.

ADDITIVES

Altering and tailoring propellant properties may be achieved with additives. For example, a reactive ingredient is added to make a nonhypergolic fuel become hypergolic (readily ignitable). To desensitize concentrated hydrogen peroxide and reduce self-decomposition, it is diluted with 3 to 15% of pure water. To increase the density or to alleviate certain combustion instabilities, a fine powder of a heavy solid material (such as aluminum) is suspended in the fuel. The use of additives to lower the freezing-point temperature of nitrogen tetroxide is treated later.

7.2 LIQUID OXIDIZERS

The most energetic known oxidizer producing the highest specific impulse and having the highest density is liquid fluorine. It has been tested in several complete experimental rocket engines but abandoned because of its extreme hazards. Many different types of new storable and cryogenic liquid oxidizer propellants have been synthesized, tested in small thrust chambers, or proposed; these included mixtures of liquid oxygen and liquid fluorine, oxygen difluoride (OF_2), chlorine trifluoride (ClF_3), and chlorine pentafluoride (ClF_5). None of these are used today because they are highly toxic and very corrosive.

7.5 GASEOUS PROPELLANTS

Propellants that store as a gas at ambient temperatures or *cold gas propellants* have been used successfully in reaction control systems (RCSs) for more than 70 years. The phrase "cold gas" distinguishes them from "warm gas," those expanded after being heated. The applicable engine system components are relatively simple, consisting of one or more high-pressure gas tanks, multiple simple nozzles (often aluminum or plastic) each with an electrical control valve, a pressure regulator, and provisions for filling and venting the gas. Tank sizes are smaller when the storage pressures are high. Because these pressures can typically be between 300 and 1000 MPa (about 300 to 10,000 psi), strong (often thick-walled and massive) gas tanks are needed.

Typical cold gas propellants and some relevant properties and characteristics are listed in Table 7–3. Nitrogen, argon, dry air, and helium have been employed for spacecraft RCS. With high-pressure hydrogen or helium as the cold gas, the specific impulse is much higher, but because their densities are lower they require much larger gas storage volumes and/or more massive high-pressure tanks; in most applications any extra inert mass outweighs the advantages of better performance. In a few applications the gas (and sometimes also its storage tank) may be heated electrically or chemically. This improves the specific impulse and allows for smaller tanks, but it also introduces complexity

Table 7–3 Properties of Gaseous Propellants Used for Auxiliary Propulsion

Propellant	Molecular Mass	Density[a] (lbm/ft³)	Specific Heat Ratio k	Theoretical Specific Impulse[b] (sec)
Hydrogen	2.0	1.77	1.40	284
Helium	4.0	3.54	1.67	179
Methane	16.0	14.1	1.30	114
Nitrogen	28.0	24.7	1.40	76
Air	28.9	25.5	1.40	74
Argon	39.9	35.3	1.67	57
Krypton	83.8	74.1	1.63	50

[a] At 5000 psia and 20 °C.
[b] In vacuum with nozzle area ratio of 50:1 and initial temperature of 20 °C.

Selection of propellant gas, storage tanks, and RCS design depend on many factors, such as volume and mass of the storage tanks, maximum thrust and total impulse, gas density, required maneuvers, duty cycle, and flight duration. Cold gas systems have been used for producing total impulses of up to 22,200 N-sec or 5000 lbf-sec; higher values usually require liquid mono- or bipropellants.

During short operations (most of the gas utilized in a few minutes while the main engine is running), gas expansions will be close to adiabatic (no heat absorption by gas) which are often analyzed as isentropic expansions. The gas temperature in high-pressure storage tanks, the (unregulated) pressures, and the specific impulse will drop as the gas is being utilized. For intermittent low-duty-cycle operations (months or years in space) heat from the spacecraft may transfer to the gas and tank temperatures stay essentially constant; then expansions will be nearly isothermal.

Advantages and disadvantages of cold gas thrusters and systems are further described in Section 8.3 in the discussion of low thrust.

7.6 SAFETY AND ENVIRONMENTAL CONCERNS

To minimize any hazards and potential damages inherent in reactive propellant materials, it is necessary to be very conscientious of all likely risks and hazards (see Refs. 7–5, 7–17, and 7–18). These relate to toxicity, explosiveness, fires and/or spill dangers, and others mentioned in Section 7.1. Before an operator, assembler, maintenance mechanic, supervisor, or engineer is allowed to transfer or use any particular propellant, he or she should receive safety training in that particular propellant, its characteristics, its safe handling or transfer, potential damage to equipment or the environment, and in countermeasures for limiting the consequences in case of accidents. Staff must also be aware of potential hazards to personnel health, first aid remedies in case of contact exposure of the skin, ingestion, or inhaling, and of how to use safety equipment. Examples of safety equipment are protective clothing, face shields, detectors for toxic vapors, remote controls, warning signals, and/or emergency water deluges. Personnel working with or close to highly toxic materials usually must undergo periodic health monitoring. Also, rocket engines need to be designed for safety to minimize the occurrence of leaks, accidental spills, unexpected fires, and/or other potentially unsafe conditions. Most organizations have one or more safety specialists who review the safety of test plans, manufacturing operations, designs, procedures, and/or safety equipment. With proper training, equipment, precautions, and design safety features, all propellants can be handled safely.

When safety violation occur or if an operation, design, procedure, or practice is found to be (or appears to be) unsafe, then a thorough investigation of the particular item or issue should be undertaken, the cause of the lack of safety should be investigated and identified, and an appropriate remedial action should be selected and initiated as soon as possible.

The discharge of toxic exhaust gases to the environment and their wind dispersion may cause exposure to operating personnel as well as the general public in nearby areas, and result in damage to plants and animals. This is discussed in Section 20.2. The dumping or spilling of toxic liquids contaminates subterranean aquifers and surface waters, and their vapors pollute the air. Today the type and amount of gaseous and liquid discharges are regulated and monitored by government authorities. These discharge quantities must be controlled or penalties will be assessed against violators. Obtaining a permit to discharge can be a lengthy and involved procedure.

One way to enhance safety against accidents (explosions, fires, spills, bullet impacts, etc.) is to use *gelled propellants*. They have additives to make them thixotropic materials, with the consistency of very thick paint when at rest; they readily flow through valves or injectors when under a pressure gradient or shear stress. Different gelling agents have been extensively investigated with several common propellants and the reader should consult the literature for details (e.g., Ref. 7–19 or Section 7.5 of the Eighth edition of this book). As far as the authors know, there is as yet no production engine using gelled propellants.

SOLID PROPELLANTS

This is the second of four chapters dealing with solid propellant rocket motors. Here we describe several common solid rocket propellants, their principal categories, ingredients, hazards, manufacturing processes, and quality control. We also discuss liners and insulators, propellants for igniters, propellant tailoring, and propellants for gas generators.

Thermochemical analyses are needed to characterize the performance of any given propellant and specific methods are described in Chapter 5. Such analyses provide values for the effective average molecular mass, combustion temperature, average specific heat ratio, and characteristic velocity—these are all functions of propellant composition and chamber pressure. Specific impulses can also be computed for given nozzle configurations and exhaust conditions.

The term *solid propellant* has several connotations, including: (1) the rubbery or plastic-like mixture of oxidizer, fuel, and other ingredients that have been processed (including curing) and constitute the finished grain; (2) the processed but uncured product; (3) a single ingredient, such as the fuel or the oxidizer. In this field, acronyms and chemical symbols are used indiscriminately as abbreviations for propellant and ingredient names; only some of these will be shown in this chapter.

13.1 CLASSIFICATION

Historically, the early rocket motor propellants used to be grouped into two classes: *double-base* (DB)[1] propellants were the first production propellants and subsequently the development of polymers as binders made the *composite* propellants feasible. Processed modern propellants are more finely classified as described below. Such classifications are helpful but they are neither rigorous nor complete. Sometimes the same propellant will fit into two or more classifications.

1. Propellants are often tailored to and classified by *specific applications*, such as space launch booster propellants or tactical missile propellants, each having specific chemical ingredients, different burning rates, different physical properties, and different performance. Table 12–1 shows four *rocket motor applications* (each with somewhat different propellants), plus several *gas generator applications* and an *artillery shell* application. Propellants for rocket motors produce hot (over 2400 K) gases and are used for thrust, but gas generator propellants operate with lower-temperature combustion gases (800 to 1200 K in order to use uncooled hardware) and are used to produce power, not thrust.

2. *Double-base* (DB)[1] propellants form a *homogeneous* propellant grain, usually a nitrocellulose (NC)[1]—a solid ingredient that absorbs liquid nitroglycerine (NG), plus minor percentages of additives. The major ingredients are highly energetic materials and they contain both fuel and oxidizer. Both *extruded double-base* (EDB) and *cast double-base* (CDB) propellants have found extensive applications, mostly in small tactical missiles of older design. By adding crystalline nitramines (HMX or RDX)[1] both performance and density can be improved; these are sometimes called *cast-modified double-base* propellants. Adding an elastomeric binder (rubber-like, such as crosslinked polybutadiene) further improves the physical properties and allows more nitramine and thus increasing performance slightly. The resulting propellant is called *elastomeric-modified cast double-base* (EMCDB). These four classes of double-base propellants have nearly smokeless exhausts. Adding some solid ammonium perchlorate (AP) and aluminum (Al) increases the density and the specific impulse slightly, but exhaust gases becomes smoky—such propellant is called *composite-modified double-base propellant* or CMDB.

   Two operational systems produced by ATK that use double-based propellants are the AGM-114 Hellfire (which uses XLDB, a minimum smoke crosslinked propellant) and the Hydra 70 rocket (with a plateau burning propellant, see Fig. 12–6).

3. *Composite propellants* form a *heterogeneous* propellant grain between oxidizer crystals and powdered fuel (usually aluminum) held together in a matrix of synthetic rubber (or plastic) binder, such as polybutadiene (HTPB).[1] Composite propellants are cast from a mix of solid (AP crystals, Al powder) and liquid (HTPB, PPG)[1] ingredients. The propellant is hardened by crosslinking or curing the liquid binder polymer with a small amount of curing agent, and curing it in an oven, where it becomes solid. In the past four decades composites have been the most commonly used class of propellant. Composites can be further subdivided:
    1. Conventional *composite propellants*, which usually contain between 60 and 72% AP as crystalline oxidizer, up to 22% Al powder as a metal fuel, and 8 to 16% of elastomeric binder (organic polymer) including its plasticizer.
    2. Modified composite propellant where an *energetic nitramine* (HMX or RDX) is added for obtaining some added performance and also a somewhat higher density.
    3. Modified composite propellant where an *energetic plasticizer* such as nitroglycerine (used in double-base propellants) is added to give increased performance. Sometimes HMX is also added.
    4. *High-energy composite solid propellant* (with added aluminum), where the organic elastomeric binder and the plasticizer are largely replaced by highly energetic materials and where some of the AP is replaced by HMX and RDX. Hexanitrohexaazaiso-wurtzitane or CL-20 is a recent propellant ingredient being used; it is produced outside of the United States (see Section 13–4 and Ref. 13–1). Some propellants are called elastomer-modified cast double-base propellants (EMCDB). Most are experimental propellants. Their theoretical specific impulse can be between 250 and 275 sec at standard conditions as explained below.
    5. *Lower-energy composite propellant*, where *ammonium nitrate* (AN) is the crystalline oxidizer (not AP). These are used for gas generator propellants. When large amounts of HMX are added, they become minimum smoke propellants with fair performance.
4. Propellants may also be classified by the smoke density in the exhaust plume as *smoky, reduced smoke*, or *minimum smoke* (essentially smokeless). Aluminum powder, a desirable fuel ingredient for performance, is oxidized to aluminum oxide during burning, which yields visible, small, solid smoky particles in the exhaust gas. Most composite propellants (e.g., AP) are also smoky. By replacing AP with HMX and RDX and by using energetic binders and plasticizers to compensate for eliminating aluminum, the amount of smoke may be considerably reduced in composite propellants. Carbon (soot) particles and metal oxides, such as zirconium oxide or iron oxide, are also visible in high enough concentrations. This is further discussed in Chapter 20.
5. *Safety ratings* for detonation can distinguish propellants as a potentially *detonable* material (class 1.1) or as a *nondetonable* material (class 1.3), as described in Section 13.3. Examples of class 1.1 propellant are double-base propellants and composite propellants containing a significant portion of a solid explosive (e.g., HMX or RDX), together with certain other ingredients.
6. Propellants can be classified by some of the principal manufacturing processes used. A *cast propellant* is made by mechanically mixing solid and liquid ingredients, followed by casting and curing; it is the most common process for composite propellants. *Curing* of many cast propellants takes place through a chemical reaction between binder and curing agent at above ambient temperatures (45 to 150°C); however, there are some that can be cured at ambient temperatures (20 to 25°C) or hardened by nonchemical processes such as crystallization. Propellants can also be made by a *solvation* process (dissolving a plasticizer in a solid pelletized matrix, whose volume is expanded). *Extruded propellants* are made by mechanical mixing (rolling into sheets) followed by extrusion (pushing through a die at high pressure). Solvation and extrusion processes are applied primarily to double-base propellants.
7. Propellants have also been classified by their *principal ingredient*, such as the *principal oxidizer (ammonium perchlorate propellants, ammonium nitrate propellants*, or *azide-type propellants*) or their *principal binder* or *fuel ingredient*, such as *polybutadiene propellants* or *aluminized*

propellants. This classification of propellants by ingredients is further described later in Section 13.4 and Table 13–8.

8. Propellants with *toxic* and *nontoxic* exhaust gases are discussed in more detail in Section 13.3.
9. *Experimental* and/or *production propellants*. Such propellants are selected after extensive testing (preflight test, qualification tests) and demonstrated safety, life, and other essential properties. The culmination of any successful research and development (R&D) program is to have a propellant selected for production in a flight vehicle application.

Figures 13–1 and 13–2 show general regions for the specific impulse, burning rate, and density for the more common classes of propellants. The ordinate in these figures is an actual or estimated specific impulse at standard conditions (1000 psi chamber pressure and expansion to sea-level pressure). These results do not reflect pressure drops in the chamber, nozzle erosion, or combustion losses and scaling assumptions. Composite propellants are shown to have a wide range of burning rates and densities; most of them have specific gravities between 1.75 and 1.81 and burning rates between 7 and 20 mm/sec. Composite propellants give higher densities, specific impulse, and a wider range of burning rates than others. Table 13–1 lists performance characteristics for several propellants. DB propellants and AN propellants have lower performance and density. Most composite propellants display similar performance and density but with a wider range of burning rates. The highest performance indicated is for a CMDB propellant whose ingredients are identified as DB/AP-HMX/Al, though it is only 4% higher than the next.
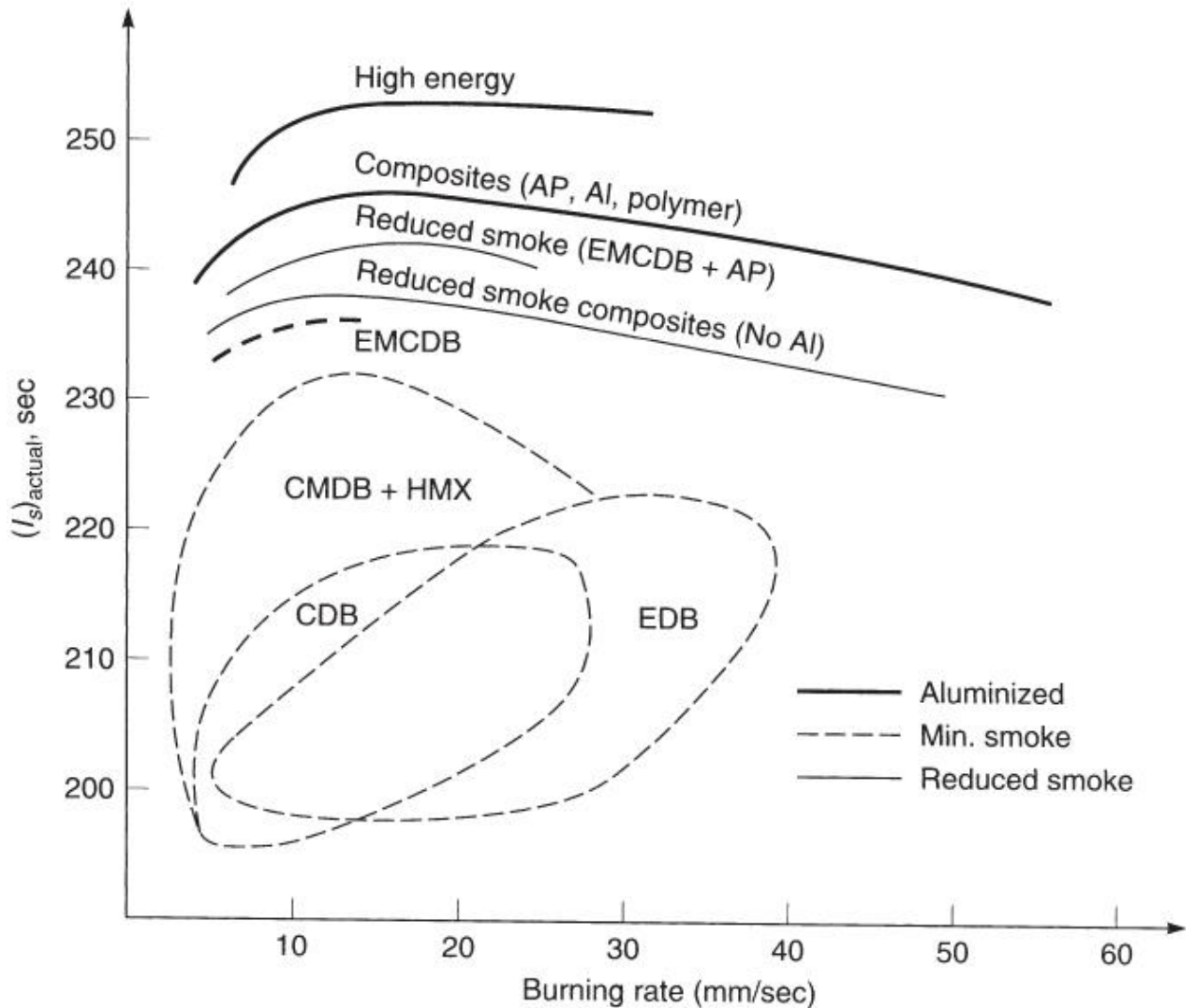
Figure 13–1 Typical delivered specific impulse and burning rate for several solid propellant categories. Adapted and reproduced from Ref. 13–2 with permission of the AIAA.
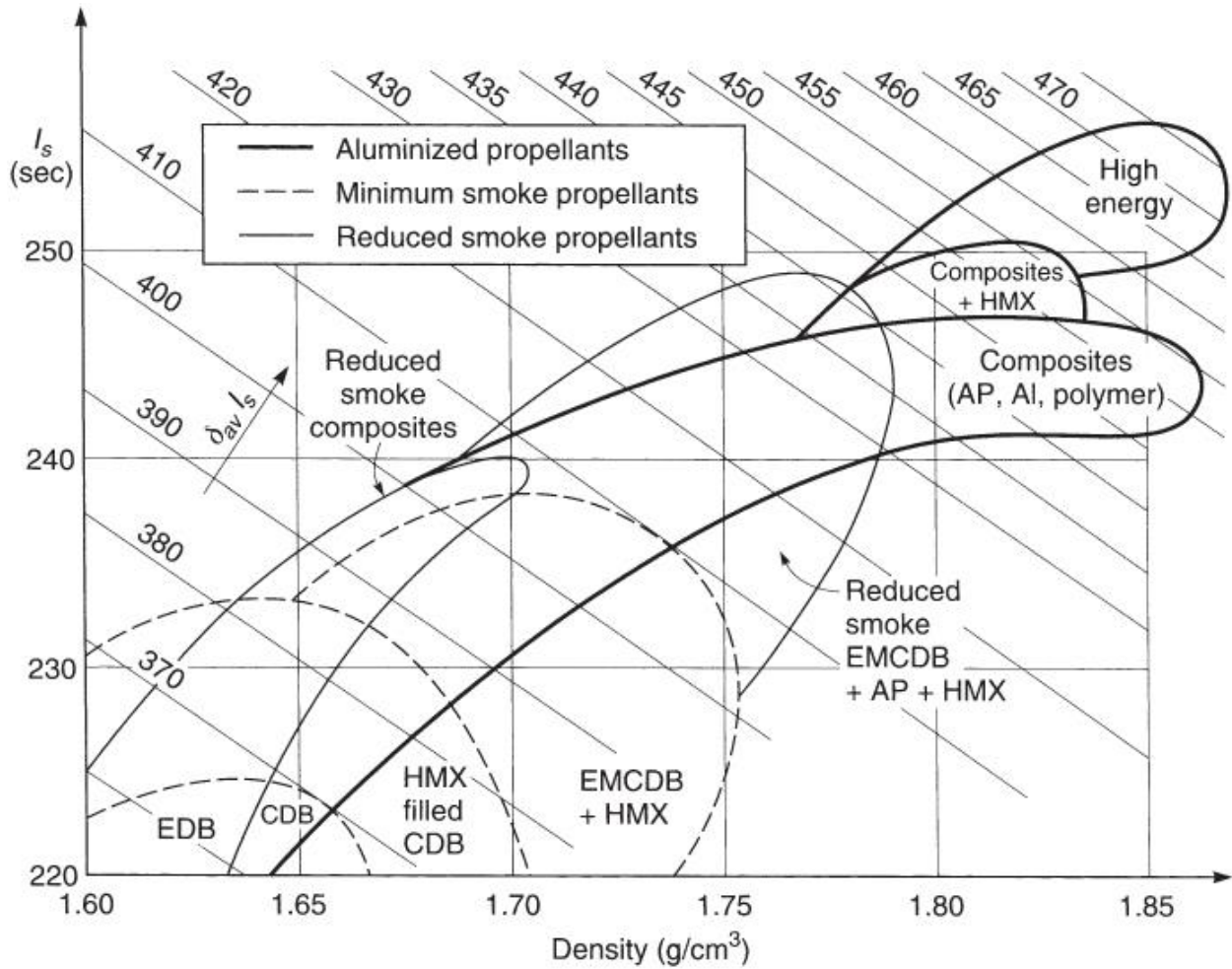
Figure 13–2 Typical delivered specific impulse and density-specific impulse for several solid propellant categories with an expansion of 7 to 0.1 MPa.

Adapted and reproduced from Ref. 13–2 with permission of the AIAA.

Table 13–1 Characteristics of Some Operational Solid Propellants

Propellant Type[a]	I_S Range (sec)[b]	Flame Temperature[e]		Density or Spec. Gravity[e]		Metal Content (mass %)	Burning Rate[c][e] (in./sec)	Pressure Exponent[e] n	Hazard Classification[d]	Stress (psi)/Strain (%)		Typical Processing Method
		(°F)	(K)	(lbm/in³)	(SG)					−60°F	+150°F	
DB	220–230	4100	2550	0.058	1.61	0	0.05–1.2	0.30	1.1	4600/2	490/60	Extruded
DB/AP/Al	260–265	6500	3880	0.065	1.80	20–21	0.2–1.0	0.40	1.3	2750/5	120/50	Extruded
DB/AP–HMX/Al	265–270	6700	4000	0.065	1.80	20	0.2–1.2	0.49	1.1	2375/3	50/33	Solvent cast
PVC/AP/Al	260–265	5600	3380	0.064	1.78	21	0.3–0.9	0.35	1.3	369/150	38/220	Cast or extruded
PU/AP/Al	260–265	5700	3440	0.064	1.78	16–20	0.2–0.9	0.15	1.3	1170/6	75/33	Cast
PBAN/AP/Al	260–263	5800	3500	0.064	1.78	16	0.25–1.0	0.33	1.3	520/16	71/28	Cast
										(at −10 °F)		

Propellant Type[a]	I_S Range (sec)[b]	Flame Temperature[e] (°F)	(K)	Density or Spec. Gravity[e] (lbm/in³)	(SG)	Metal Content (mass %)	Burning Rate[c][e] (in./sec)	Pressure Exponent[e] n	Hazard Classification[d]	Stress (psi)/Strain (%) −60°F	+150°F	Typical Processing Method
CTPB/AP/Al	260–265	5700	3440	0.064	1.78	15–17	0.25–2.0	0.40	1.3	325/26	88/75	Cast
HTPB/AP/Al	260–265	5700	3440	0.067	1.86	4–17	0.25–3.0	0.40	1.3	910/50	90/33	Cast
HTPE[7]/AP/Al	248–269	5909	3538	0.07	1.70		0.4–0.7	0.50	1.3	174/44	(77°F)	Cast
PBAA/AP/Al	260–265	5700	3440	0.064	1.78	14	0.25–1.3	0.35	1.3	500/13	41/31	Cast
AN/Polymer	180–190	2300	1550	0.053	1.47	0	0.06–0.5	0.60	1.3	200/5	NA	Cast

[a] Al, aluminum; AN, ammonium nitrate; AP, ammonium perchlorate; CTPB, carboxy-terminated polybutadiene; DB, double-base; HMX, cyclotetramethylene tetranitramine; HTPB, hydroxyl-terminated polybutadiene; HTPE hydroxyl terminated polyether; PBAA, polybutadiene-acrylic acid polymer; PBAN, polybutadiene–acrylic acid–acrylonitrile terpolymer; PU, polyurethane; PVC, polyvinyl chloride.
[b] At 1000 psia expanding to 14.7 psia, ideal or theoretical value at reference conditions.
[c] At 1000 psia.
[d] See hazard classification section.
[e] I_s, flame temperature, density, burn rate, and pressure exponent will vary slightly with specific composition.

Data from Ref. 13–3, CPIAC, and Orbital ATK.

Several of the above listed classifications tend to be confusing. The term composite-modified double-base propellant (CMDB) has been used for a DB propellant, where some AP, Al, and binder are added;

alternatively, the same propellant could be classified as a composite propellant to which some double-base ingredients have been added.

A large variety of *chemical ingredients* and propellant formulations have been synthesized, analyzed, and tested in experimental rocket motors. A typical solid propellant has between 4 and 12 different ingredients and this chapter discusses about a dozen basic propellant types, but many other types are still being investigated. Table 13–2 presents some advantages and disadvantages of selected propellant classes. Representative formulations for three types of propellant are given in Table 13–3. In actual practice, each propellant manufacturer uses its own formulation and processing procedures. The exact percentages of ingredients, even for a given propellant such as PBAN, can not only vary among manufacturers but often vary from one rocket motor application to another. The practice of adjusting mass percentages together with adding or deleting one or more of the minor ingredients (additives) is known as *propellant tailoring*. Tailoring is the practice of taking an established propellant and changing it slightly to fit a new application, different processing equipment, altered motor ballistics, storage life, temperature limits, and/or even a change in ingredient source.

Table 13–2 Characteristics of Selected Propellants

Propellant Type	Advantages	Disadvantages
Double base (extruded)	Modest cost; nontoxic clean exhaust, smokeless; good burn rate control; wide range of burn rates; simple well-known process; good mechanical properties; low-temperature coefficient; very low pressure exponent; plateau burning is possible	Freestanding grain requires structural support; low performance, low density; high to intermediate hazard in manufacture; can have storage problems with NG bleeding out; diameter limited by available extrusion presses; class 1.1*a*
Double base (castable)	Wide range of burn rates; nontoxic smokeless exhaust; relatively safe to handle; simple, well-known process; modest cost; good mechanical properties; good burn rate control; low-temperature coefficient; plateau burning can be achieved	NG may bleed out or migrate; high to intermediate manufacture hazard; low performance; low density; higher cost than extruded DB; class 1.1*a*
Composite modified double base or CMDB with some AP and Al	Higher performance; good mechanical properties; high density; less likely to have combustion stability problems; intermediate cost; good background experience	Complex facilities; some smoke in exhaust; high flame temperature; moisture sensitive; moderately toxic exhaust; hazards in manufacture; modest ambient temperature range; the value of n is high (0.8–0.9); moderately high temperature coefficient

Propellant Type	Advantages	Disadvantages
Composite AP, Al, and PBAN or PU or CTPB binder	Reliable; high density; long experience background; modest cost; good aging; long cure time; good performance; usually stable combustion; low to medium cost; wide temperature range; low to moderate temperature sensitivity; good burn rate control; usually good physical properties; class 1.3	Modest ambient temperature range; high viscosity limits at maximum solid loading; high flame temperature; toxic, smoky exhaust; some are moisture sensitive; some burn-rate modifiers (e.g., aziridines) are carcinogens
Composite AP, Al, and HTPB binder; most common composite propellant	Slightly better solids loading % and performance than PBAN or CTPB; wide ambient temperature limits; good burn-rate control; usually stable combustion; medium cost; good storage stability; wide range of burn rates; good physical properties; good experience; class 1.3	Complex facilities; moisture sensitive; fairly high flame temperature; toxic, smoky exhaust
Modified composite AP, Al, PB binder plus some HMX or RDX	Higher performance; good burn-rate control; usually stable combustion; high density; moderate temperature sensitivity; can have good mechanical properties	Expensive, complex facilities; hazardous processing; harder-to-control burn rate; high flame temperature; toxic, smoky exhaust; can be impact sensitive; can be class 1.1,[a] high cost; pressure exponent 0.5–0.7
Composite with energetic binder and plasticizer such as NG, and with AP, HMX	Highest performance; high density; narrow range of burn rates	Expensive; limited experience; impact sensitive; high-pressure exponent; class 1.1[a]
Modified double-base with HMX	Higher performance; high density; stable combustion; narrow range of burn rates	Same as CMDB above; limited experience; most are class 1.1[a]; high cost
Modified AN propellant with HMX or RDX added	Fair performance; relatively clean; smokeless; nontoxic exhaust	Relatively little experience; can be hazardous to manufacture; need to stabilize AN to limit grain growth; low burn rates; impact sensitive; medium density; class 1.1 or 1.3[a]

Propellant Type	Advantages	Disadvantages
Ammonium nitrate plus polymer binder (gas generator)	Clean exhaust; little smoke; essentially nontoxic exhaust; low-temperature gas; usually stable combustion; modest cost; low-pressure exponent	Low performance; low density; need to stabilize AN to limitgrain growth and avoid phase transformations; moisture sensitive; low burn rates

a Class 1.1 and 1.3—see Section 13.3 on Hazard Classification.

Table 13–3 Representative Propellant Formulations

Source: Courtesy of Air Force Phillips Laboratory, Edwards, California.

Double Base (JPN Propellant)		Composite (PBAN Propellant)		Composite Double Base (CMDB Propellant)	
Ingredient	Mass %	Ingredient	Mass %	Ingredient	Mass %
Nitrocellulose	51.5	Ammonium perchlorate	70.0	Ammonium perchlorate	20.4
Nitroglycerine	43.0	Aluminum powder	16.0	Aluminum powder	21.1
Diethyl phthalate	3.2	Polybutadiene–acrylic acid–acrylonitrile	11.78	Nitrocellulose	21.9
Ethyl centralite	1.0	Epoxy curative	2.22	Nitroglycerine	29.0
Potassium sulfate	1.2			Triacetin	5.1
Carbon black	<1%			Stabilizers	2.5
Candelilla wax	<1%				

New propellant formulations are typically developed using laboratory-size mixers, curing ovens, and related equipment with the propellant mixers (1 to 5 liters), and operated by remote control for safety reasons. Process studies usually accompany the development of new propellant formulations to evaluate the "processability" and to guide the design of any special production equipment needed in preparing ingredients, mixing, casting, or curing it.

Historically, black or gun powder (a pressed mixture of potassium nitrate, sulfur, and an organic fuel such as ground peach stones) was the very first propellant to be used. Many other types of propellants ingredients have been used in experimental motors, including fluorine compounds, propellants containing powdered beryllium, boron, hydrides of boron, lithium, or beryllium, or new synthetic organic plasticizer and binder

materials with azide or nitrate groups. Most of these have not yet been considered satisfactory or practical for production in rocket motors.

13.2 PROPELLANT CHARACTERISTICS

Propellant selection is critical to rocket motor design. *Desirable propellant characteristics* are listed below and further discussed in other parts of this book. Many requirements for particular solid propellant rocket motors will influence priorities for choosing these characteristics:

1. High performance or *high specific impulse*; this implies a high gas temperature and/or low exhaust gas molecular mass.
2. Predictable, reproducible, and initially adjustable *burning rate* to fit grain-design needs and thrust-time requirements.
3. For minimum variations in thrust or chamber pressure during burning, both the *pressure* or *burning rate exponent* and the *temperature coefficient* should be small.
4. Adequate *physical properties* (including bond strengths) over the intended operating temperature range with allowance for some degradation due to cumulative damage.
5. High *density* (resulting in a small-volume rocket motor).

6. Predictable, reproducible ignition qualities (such as acceptable ignition overpressures).
7. Desirable *aging characteristics* and *long life*. Aging and life predictions depend on the propellant's chemical and physical properties, cumulative damage criteria with load cycling (see Section 12.4) and thermal cycling, and from actual tests on propellant samples and test data from failed motors.
8. Low *moisture* absorption, because moisture often causes chemical deterioration.
9. Simple, reproducible, safe, low-cost, controllable, and low-hazard *manufacturing*.
10. Guaranteed availability of all *raw materials* and *purchased components* over the production and operating life of the propellant, and acceptable control over undesirable impurities.
11. *Low technical risk*, such as a favorable history of prior applications.
12. Relative *insensitivity* to certain external energy stimuli as described Section 13.3, the hazards section.
13. *Nontoxic* and *noncorrosive exhaust* gases, also called *green exhausts*.
14. Not prone to *combustion instability* (see Chapter 14).
15. Equivalent composition, performance and properties with every new propellant batch.

16. No slow or long-term chemical reactions or migrations between propellant ingredients or between propellant and insulator/liner.

Some of these desirable characteristics will also apply to all materials and purchased components used in solid rocket motors, such as the igniter, insulator, case, or safe-and-arm device but several of these characteristics can sometimes be in conflict with each other. For example, increasing the physical strength (more binder and or more crosslinker) will reduce propellant performance and density. So a modification of the propellant for one of these characteristics may cause changes in a few others.

Several illustrations will now be given on how characteristics of a propellant change when the concentration of one of its major ingredients is changed. Figure 13–3 shows calculated variations in combustion or flame temperature, average product gas molecular mass, and specific impulse as a function of oxidizer concentration for composite propellants that use a polymer binder [hydroxyl-terminated polybutadiene (HTPB)] and various crystalline oxidizers; these results are taken from Ref. 13–4, based on a thermochemical analysis as explained in Chapter 5. The maximum values of I_s and T_1 occur at approximately the same concentration of oxidizer. For practical reasons, this optimum percentage for AP (about 90 to 93%) and AN (about 93%) cannot be implemented because concentrations greater than about 90% total solids (including the aluminum and solid catalysts) cannot be processed in a mixer—a castable slurry that will flow into a mold requires more than 10 to 15% liquid content.

Specific impulse, sec

RDX
HMX

AP

AN

KP

KN

Oxidizer concentration, %

Flame temperature, K

RDX
HMX

KP   AP

KN

AN

Oxidizer concentration, %

Molecular mass, kg/kg-mol

KN

KP

AP

AN

RDX
HMX

Oxidizer concentration, %
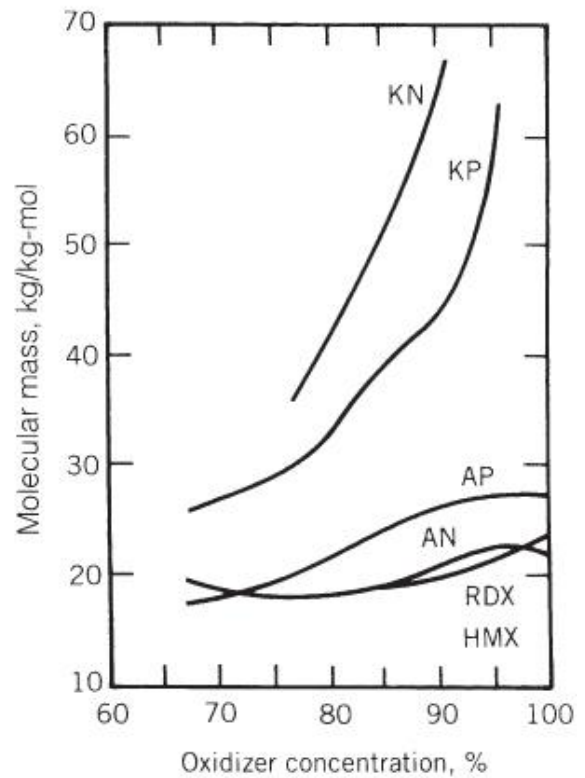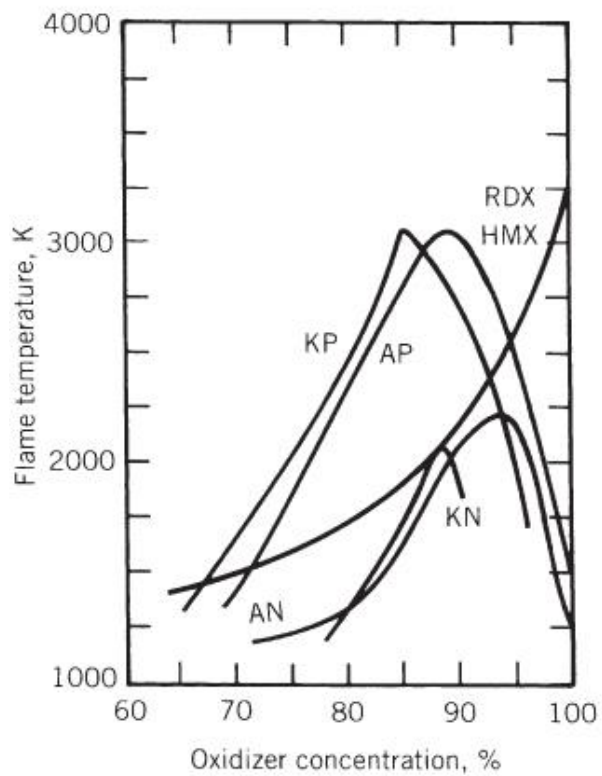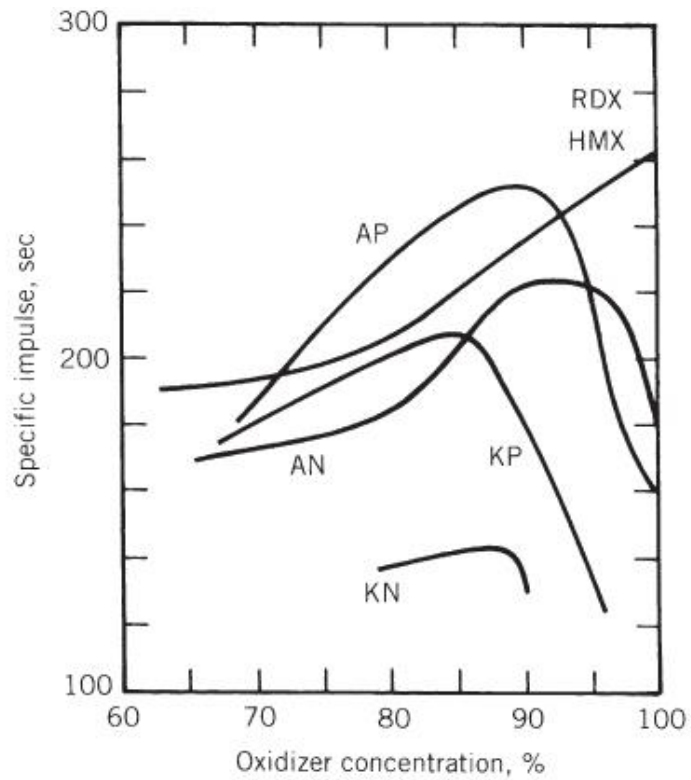
Figure 13–3 Variation of combustion temperature, average molecular mass of combustion gases, and theoretical specific impulse (at frozen equilibrium) as a function of oxidizer concentration for HTPB-based composite propellants. Data are for a chamber pressure of 68 atm and nozzle exit pressure of 1.0 atm.

Reproduced from Ref. 13–4 with permission of the AIAA.

A typical composition diagram for a composite propellant is depicted in Fig. 13–4. It shows how the specific impulse varies with changes in the composition of the three principal ingredients: the solid AP, solid Al, and viscoelastic polymer binder.
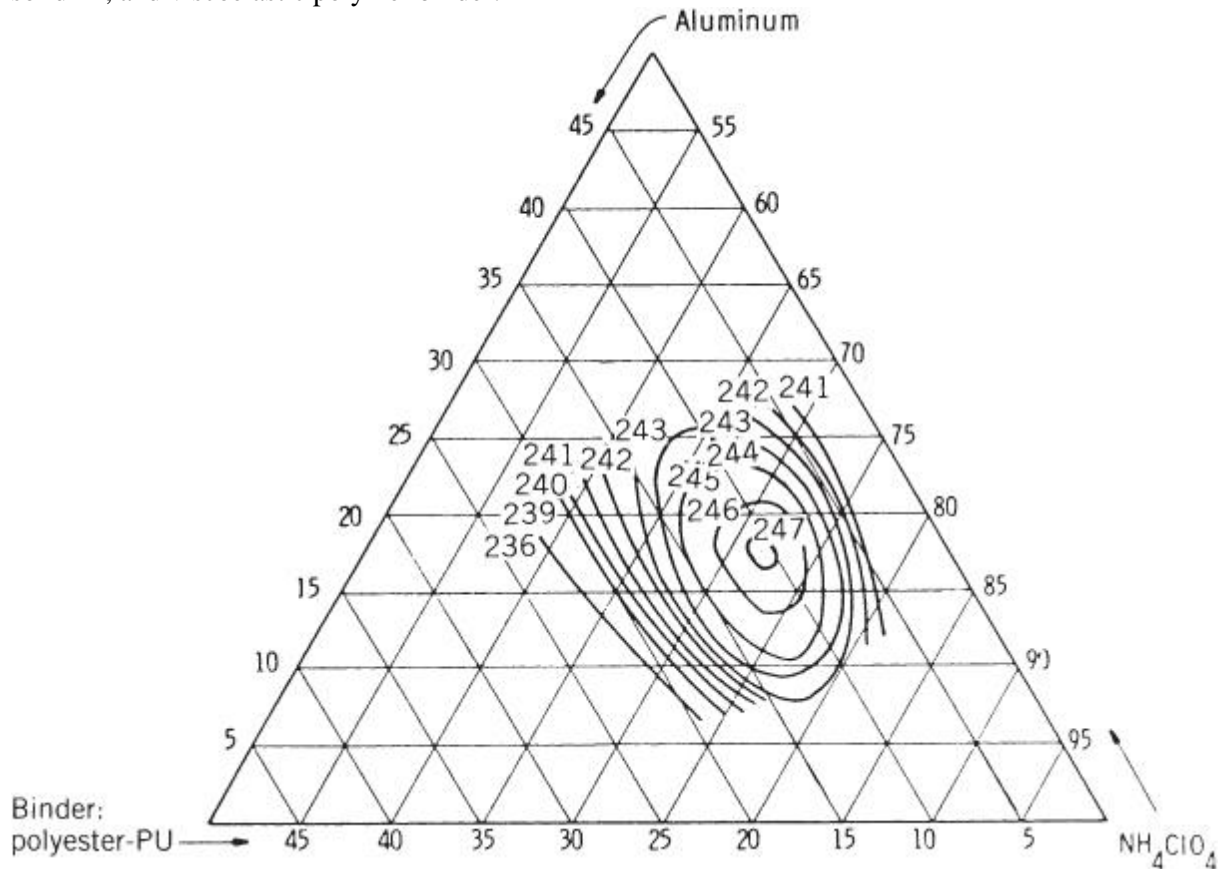
Figure 13–4 Composition diagram of calculated specific impulse for an ammonium perchlorate–aluminum–polyurethane propellant (PU is a polyester binder) at standard conditions (1000 psi and expansion to 14.7 psi). The maximum value of specific impulse occurs at about 11% PU, 72% AP, and 17% Al.

Reproduced from Ref. 13–5 with permission of the American Chemical Society.

For DB propellants variations of I_s and T_1 are shown in Fig. 13–5 as a function of nitroglycerine (NG) concentration. The theoretical maximum specific impulse occurs at about 80% NG. In practice, NG, which is a liquid, is seldom found in concentrations over 60% because its physical properties are poor at the higher concentrations. Other major solid or soluble ingredients are also needed to make a usable DB propellant.
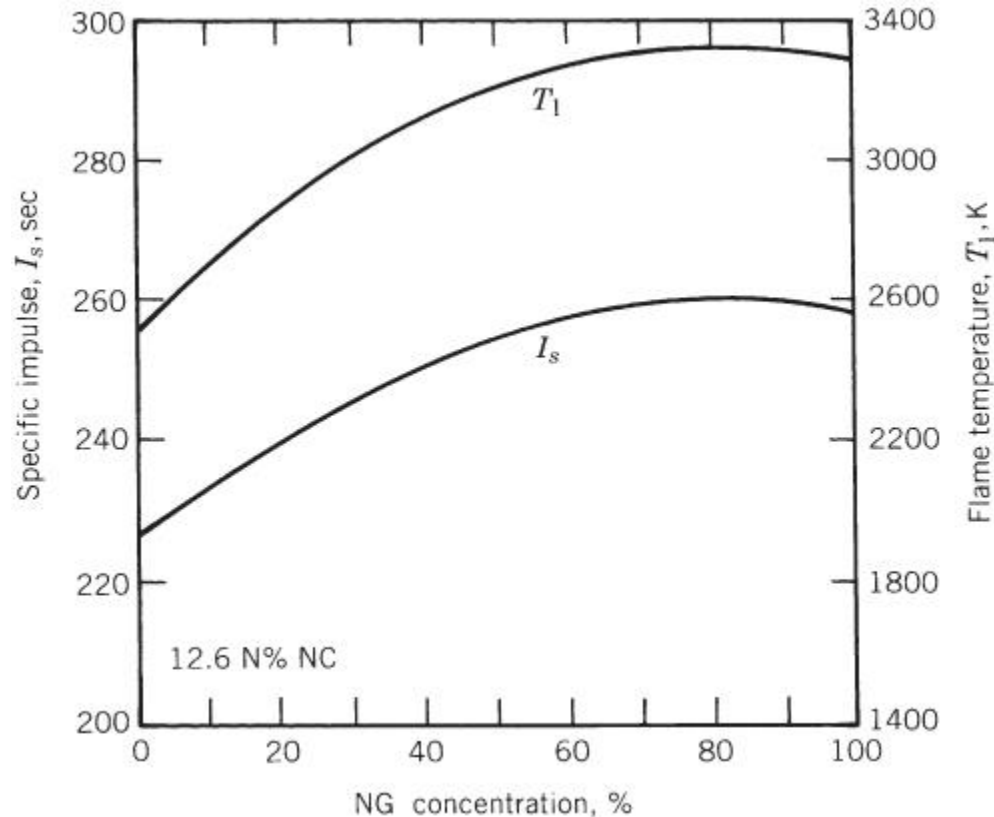
Figure 13–5 Specific impulse and flame temperature versus nitroglycerine (NG) concentration of double-base propellants.

Reproduced from Ref. 13–4 with permission of the AIAA.

For CMDB propellants the addition of either AP or a reactive nitramine such as RDX allows for higher I_s than with ordinary DB (where AP or RDX percent is zero), as shown in Fig. 13–6. Both AP and RDX greatly increase the flame temperature and thus make the effects of heat transfer more critical. The maximum values of I_s occur at about 50% AP and at 100% RDX (an impractical propellant concentration because it cannot be manufactured and will not have reasonable physical properties). At high concentrations of AP or RDX, the exhaust gases contain considerable H_2O and O_2 (as shown in Fig. 13–7); these enhance erosion rates in carbon-containing insulators or nozzle materials. In Fig. 13–7, the toxic HCl gas is present in concentrations between 10 and 20%, but in practical propellants it can seldom exceed 14%.
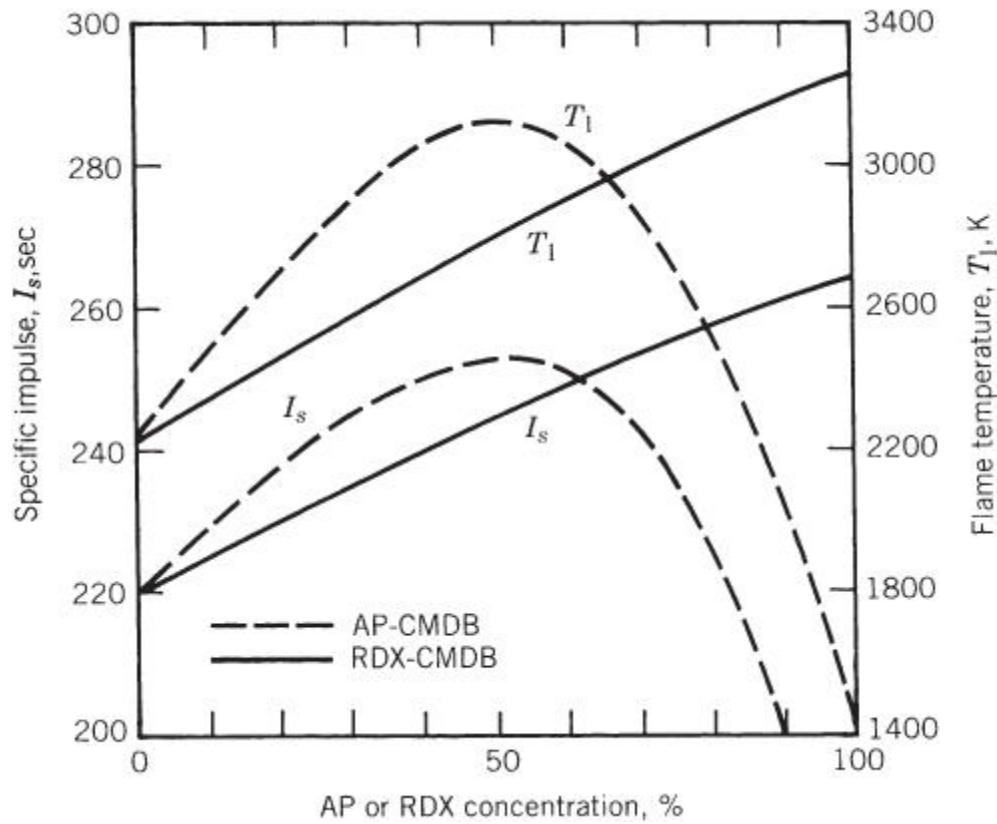
Figure 13–6 Specific impulse and flame temperature versus AP or RDX concentration of AP–CMDB propellants.

Reproduced from Ref. 13–4 with permission of the AIAA.
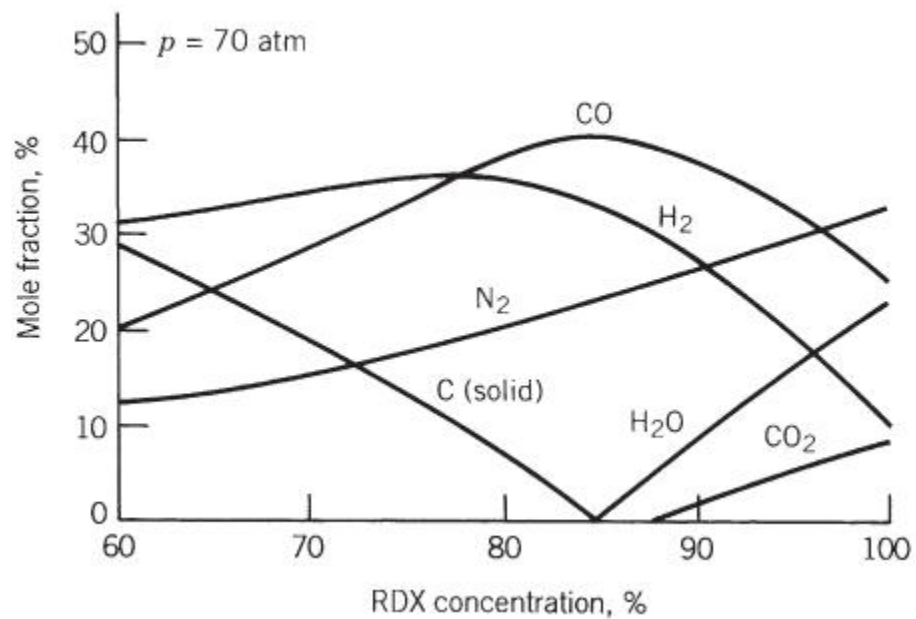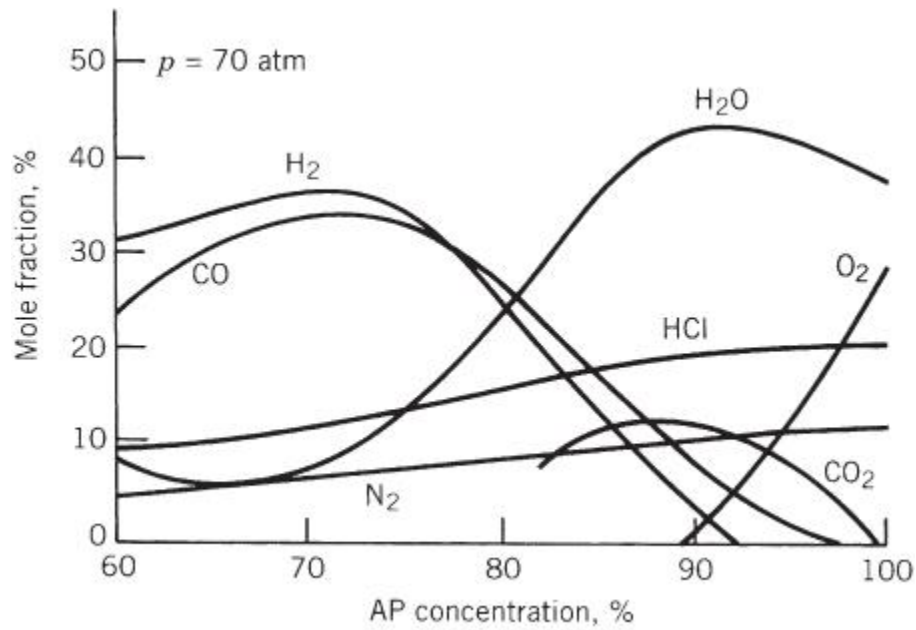
Figure 13–7 Calculated combustion products of composite propellant with varying amounts of AP or RDX. Adapted from permission of the AIAA.

Nitramines such as RDX or HMX contain relatively few oxidizing radicals and the binder surrounding the nitramine crystals cannot be fully oxidized. As the binder decomposes at the combustion temperature, it releases gases rich in hydrogen and carbon monoxide (which reduce the molecular mass), cooling the gas mixture to lower combustion temperatures. The exhaust gases of AP-based and RDX-based CMDB propellant are shown in Fig. 13–7 where it can be seen that solid carbon particles disappear when the RDX content is above 85%.

13.3 HAZARDS

With proper precautions, training and equipment, all common propellants can be manufactured, handled, and fired safely. It is necessary and imperative to fully understand all hazards and methods for preventing dangerous situations from arising. Each material has its own set of hazards; some of the more common ones are described briefly below and also in Refs. 13–6 and 13–7. Not all apply to every propellant.

INADVERTENT IGNITION

If a rocket motor is unexpectedly ignited and starts combustion, the very hot exhaust gases may cause burns and local fires, or ignition of adjacent rocket motors. Unless the motor is constrained or fastened down, its thrust will accelerate it to unanticipated high velocities or erratic flight paths that can cause much severe damage. Its exhaust cloud can be toxic and corrosive. Inadvertent ignitions may be caused by the following effects:

- Stray or induced currents that activate the igniter.
- Electrostatic charging causing unintended sparks or arc discharges.
- Fires excessively heating rocket motor exteriors, raising the solid propellant temperature above its ignition point.
- Impacts (bullet penetration or dropping the rocket motor onto a hard surface).
- Energy absorption from prolonged mechanical vibrations that overheat the propellant (e.g., transport over rough roads).
- Radiation from nuclear explosions.

An electromechanical system called *safe and arm system* is usually included to prevent stray currents from activating the igniter. It averts ignition induced by currents in other wires of the vehicle, radar- or radio-frequency-induced currents, electromagnetic surges, or pulses from a nuclear bomb explosion. It prevents any electric currents from reaching the igniter circuit during its "unarmed" condition. When in the "arm" position, it accepts and transmits a start signal to the igniter.

Electrostatic discharges (ESD) may be caused by lightning, friction in insulating materials, or by the moving separation of two insulators. The buildup of high electrostatic potentials (thousands of volts) may, upon discharge, allow rapid increases in electric current, which in turn may lead to arcing or exothermic reactions along the current's path. For this reason all propellants, liners, or insulators need to have sufficient electric conductivity to prevent any buildup of such an electrostatic charge. The well-known inadvertent ignition of a Pershing ground-to-ground missile is believed to have been caused by an electrostatic discharge while in the transporter-erector vehicle. ESD capabilities depend on materials, their surface and volume resistivities, dielectric constants, and the breakdown voltages.

Viscoelastic propellants are excellent absorbers of *vibration energy* and can become locally hot when oscillating for extensive periods at particular frequencies. This can happen in designs where a segment of the grain is not well supported and is free to vibrate at its natural frequencies. Because propellants can be accidentally ignited by extraneous means (such as mechanical friction or bullet impacts, or accidentally dropping a rocket motor) standard tests have been developed to measure the propellant's resistance to such energy inputs. Considerable effort is spent in developing new propellants resistant to these energy inputs.

AGING AND USEFUL LIFE

This topic is briefly discussed in the section on Structural Design in the previous chapter. The *aging* of a propellant can be measured with test motors and propellant sample tests when the loading history during the life of the motor can be correctly anticipated. It has then been possible to estimate and predict the useful *shelf or storage life* of a rocket motor (see Refs. 13–7 and 13–8). When changes in physical properties, caused by estimated thermal or mechanical load cycles (cumulative damage), reduce the safety margin on stresses and/or strains to a danger point, the rocket motor is no longer considered to be safe to be ignited or operated. Once this age limit or its predicted, weakened condition is reached, the rocket motor

has a high probability of failure and should be removed from any ready inventory and the aged propellant removed and replaced.

The *life* of a particular motor depends on its propellant composition, the frequency and magnitude of imposed loads or strains, and the design among other factors. Typical life values range from 5 to 25 years. Shelf life can usually be increased by increasing the physical strength of the propellants (e.g., by increasing the amount of binder), selecting chemically compatible, stable ingredients with minimal long-term degradation, and/or by minimizing the vibration loads, temperature limits, or number of cycles (i.e., controlling the storage and transport environments).

CASE OVERPRESSURE AND FAILURE

A rocket motor case will break and/or explode during operation when the chamber pressure exceeds the case's burst pressure. The release of high-pressure gases can cause explosions where motor pieces are thrown out into adjacent areas. Any sudden depressurization from chamber pressure to ambient pressure (which is usually below the deflagration limit) would normally stop the burning in a class 1.3 propellant (see Hazard Classification). Large pieces of unburned propellant are often found after violent case bursts. Case overpressure rocket motor failure may be caused by one of the following:

1. The grain is overaged, porous, or severely cracked and/or has major unbonded areas due to severe accumulated damage.

2. There have been a significant chemical changes in the propellant due to migration or slow, low-order chemical reactions; these can reduce the allowable physical properties, weakening the grain, so that it will crack or cause unfavorable increases in the burning rate. In some cases chemical reactions create gaseous products, which produce many small voids and raise the pressure in sealed stored rocket motors.

3. The rocket motor has not properly been manufactured. Obviously, careful fabrication and inspection are a must.

4. The motor has been damaged. For example, a nick or dent in the case caused by improper handling will reduce the case strength. This can be prevented by careful handling and repeated inspections.

5. An obstruction plugs the nozzle (e.g., a loose large piece of insulation) causing a rapid increase in chamber pressure.

6. In propellants that contain hygroscopic ingredients, moisture absorption can degrade strength and strain capabilities by factors of 3 to 10. Rocket motors are routinely sealed to prevent humid air access.

Detonation versus Deflagration

When the burning rocket motor propellant is overpressurized, it may either continue to deflagrate (burn) or detonate (explode violently), as described in Table 13–4. In a detonation, the chemical reaction energy of the entire grain is released in a very short time (microseconds), and in effect it becomes an exploding bomb. Detonations happen with some propellants that contain certain ingredients (e.g., nitroglycerine or HMX as described later in this chapter). Proper designs, correct manufacture, and safe handling and operating procedures are essential in order to minimize or totally avoid detonations.

Table 13–4 Comparison of Burning (Deflagration) and Detonation

Characteristic	Burning with Air	Deflagration within Rocket Motors	Detonation of Rocket Motor
Typical material	Coal dust and air	Propellant, no air	Rocket propellant or explosives
Common means of initiating reaction	Heat	Heat	Shock wave; sudden pressure rise plus heat
Linear reaction rate (m/sec)	10^{-6} (subsonic)	0.2 to 5×10^{-2} (subsonic)	2 to 9×10^{3} (supersonic)
Shock waves	No	No	Yes
Time for completing reaction (sec)	10^{-1}	10^{-2}–10^{-3}	10^{-6}
Maximum pressure [MPa (psi)]	0.07–0.14 (10–20)	0.7–100 (100–14,500)	7000–70,000 (10^{6}–10^{7})
Process limitation	By heat transfer at burning surface	Strength of case	By physical and chemical properties of material, (e.g., density, composition)
Increase in burning rate can result in:	Potential furnace failure	Overpressure and explosive failure of motor case	Motor case failure and violent rapid explosion of all the propellant
Remainder	Unburnt coal dust pockets may continue to burn	After case failure, unused propellant pieces will usually stop burning	No propellant remainder to burn
Classification	None	Class 1.3	Class 1.1

Any given propellant material may either burn or detonate depending on its chemical formulation, physical properties (such as density or porosity) the type and intensity of the initiation, the degree of confinement,

and the geometric characteristics of the rocket motor. It is also possible for certain burning propellants to change suddenly from an orderly deflagration to a detonation. A simplified explanation of this transition is as follows: normal burning starts at the rated chamber pressure; then hot gases penetrate some existing but unknown pores or small cracks in the unburned propellant, where gas confinement causes the pressure to become locally very high; the combustion front then attains shock wave speeds with a low-pressure differential and then it accelerates further to the strong, fast, high-pressure shock wave, characteristic of detonations. The degree and rigidity of the motor geometric confinement and some scale factor (e.g., larger-diameter grain) influence the severity and occurrence of detonations.

Hazard Classification

Propellants that may transition from deflagration to detonation are considered more hazardous and are usually designated as class 1.1-type propellants. Class 1.3 propellants will not detonate even if while burning the case bursts as the chamber pressure becomes too high. The required tests and rules for determining this hazard category are treated in Ref. 13–9. Propellant samples are subjected to various tests, including impact tests (dropped weight) and card gap tests (which determine the force needed to initiate a propellant detonation when a sample is subjected to a blast from a known booster explosive). Even when the case bursts violently with a class 1.3 propellant, much of the remaining unburnt propellant is ejected and then usually stops burning. With a class 1.1 propellant, a powerful detonation can sometimes ensue, which rapidly gasifies all the remaining propellant, and is much more powerful and destructive than the bursting of the case under high pressure. Unfortunately, the term *explosion* has been used to describe both case bursting with its remaining unburned propellant fragmentation, and also the higher rate of energy release in a detonation which leads to more rapid and much more energetic fragmentation of the rocket motor.

The Department of Defense (DOD) classification of 1.1 or 1.3 determines the method of labeling and the cost of shipping rocket propellants, loaded military missiles, explosives, or ammunitions; it also defines required limits on propellant amounts that may be stored or manufactured in any one site and the minimum separation distance of that site to the next building or site. The DOD system (Ref. 13–9) is the same as that which has been used by the United Nations.

INSENSITIVE MUNITIONS

Any accidental ignition or otherwise unplanned rocket or military missile operation or explosion may cause severe damage to equipment and injure or kill personnel. This may be avoided or minimized by making rocket motor designs and their propellants insensitive to a variety of energetic stimuli. The worst scenario is propellant detonation, releasing all the propellant's energy explosively, and this scenario must be avoided at all cost. Missiles and their rocket motors must undergo a series of prescribed tests to determine their resistance to inadvertent ignition using the most likely energy inputs during any possible battle situation. Table 13–5 describes a series of tests called out in military specifications,
. Other tests besides those listed in Table 13–5 are sometimes needed, such as friction tests and drop tests. A *threat hazard assessment* must be made prior to any such tests, to evaluate the logistic and operational threats during the missile's life cycle. This may result in modifications to the test setups, changes to acceptance criteria, and/or the skipping of some such tests.

Table 13–5 Typical Testing for Insensitivity of Rockets and Missiles

Test	Description	Criteria for Passing
Fast cook-off	Build a fire (of jet fuel or wood) underneath the missile or its rocket motor	No reaction more severe than burning propellant
Slow cook-off	Gradual heating (6°F/*hr*) to failure	Same as above
Bullet impact	One to three 50-caliber bullets fired at short intervals	Same as above
Fragment impact	Small high-speed steel fragment	Same as above
Sympathetic detonation	Detonation from an adjacent similar motor or a nearby specific munition	No detonation of test motor
Shaped explosive charge impact	Blast from specified shaped charge in specified location	No detonation
Spall impact	Several high-speed spalled fragments from a steel plate which is subjected to a shaped charge	Fire, but no explosion or detonation

In all prescribed tests, the missiles together with their rocket motors are destroyed. If the rocket motor should detonate (an unacceptable result), the motor must be redesigned and/or undergo a change in propellant. There are some newer propellants that are more resistant to external stimuli and are therefore preferred for tactical missile applications, even though there may be a penalty in propulsion performance. If explosions (not detonations) occur, it may be possible to redesign the rocket motor and mitigate the explosion effects (make it less violent). For example, motor cases can have a provision for venting prior to explosion. Changes to shipping containers can also mitigate some of these effects. If the result is a fire (a sometimes acceptable result), it should be confined to the particular grain or rocket motor. Under some circumstances a burst failure of the case may also be acceptable. In the past decade a new class of insensitive propellants has been developed with new types of binders. Their purpose remains to minimize any drastic consequences (e.g., detonations) when the rocket motor is exposed to various unexpected energetic stimuli, such as external fires, and impact or pressure waves (see Table 13–5). Recently, insensitive propellants have been selected for some military missions, reflecting an important milestone in their development. The leading example is a recent composite propellant with HTPE (hydroxyl-terminated polyether) as the binder, see Ref. 13–11. HTPE has been qualified and applied to the MK 134 rocket motor for the ship-launched Evolved Sea Sparrow Missile (ESSM). This motor is co-manufactured by ATK in the United States and NAMMO Raufoss in Norway for member nations of the NATO Sea Sparrow Consortium. A relatively insensitive propellant has also been developed in France, namely, a nonmigrating ferrocene-grafted HTPB binder called Butacene. It has been qualified for a few systems in the United States and other countries

When the pressure-rise rate and the absolute pressure become sufficiently high (as in some impact tests or in the high acceleration of a gun barrel), some propellants will detonate. For many propellants these pressures are above approximately 1500 MPa or 225,000 psi, but for others they can be lower (as low as 300 MPa or 45,000 psi). The values quoted represent defined *upper pressure limits* beyond which such a propellant should not operate.

Many solid propellants do not have any significant toxicity problem. A number of propellant ingredients (e.g., some crosslinking agents and burning rate catalysts) and a few of the plastics used in fiber-reinforced cases can be dermatological or respiratory toxins; a few are carcinogens or suspected carcinogens. They, and the mixed uncured propellant containing these materials, must be handled carefully to prevent operator exposure. This means using gloves, face shields, good ventilation, and, with some high-vapor-pressure ingredients, gas masks. Usually, the finished or cured grain or motor is not toxic.

Exhaust plume gases can be very toxic if they contain beryllium or beryllium oxide particles, chlorine gas, hydrochloric acid gas, hydrofluoric acid gas, or some other fluorine compounds. When an ammonium perchlorate oxidizer is used, the exhaust gas may contain up to about 14% hydrochloric acid, which is a toxic gas. For large rocket motors this can mean many tons of highly toxic gas. Test and launch facilities for rockets with toxic plumes require very special precautions and occasionally decontamination processes, as explained in Chapter 21.

Among the most effective ways to control hazards and prevent accidents are: (1) to acquaint personnel of the hazards of each propellant being handled by teaching them how to properly avoid hazardous conditions and to prevent accidents and how to recover from them; (2) to design the rocket motors, their fabrication as well as test facilities and equipment to be as safe as possible; and (3) to institute and enforce rigid safety rules during design, manufacture, and operation. There are many such rules. Examples include avoiding smoking (and matches) in areas where there are propellants or loaded motors, wearing spark-proof shoes and using spark-proof tools, shielding all electrical equipment, providing a water-deluge fire extinguishing system in test facilities to cool motors or extinguish burning, and/or proper grounding of all electrical equipment and items that could build up static electrical charges.

13.4 PROPELLANT INGREDIENTS

A number of relatively common propellant ingredients are listed in Table 13–6 for double-base propellants and for composite-type solid propellants in Table 13–7. They are categorized by major *function*, such as *oxidizer, fuel, binder, plasticizer, curing agent*, and so on, and each category is briefly described later in this section. However, several ingredients can have *more than one function*. These lists are not complete because over 200 other ingredients have been tried in experimental rocket motors. Most ingredients in Table 13–6 have a shelf life of over 30 years.
Table 13–8 shows a classification for modern propellants (including some new types that are still in the experimental phase) according to their binders, plasticizers, and solid ingredients; these solids may be an oxidizer, a solid fuel, or a combination or a compound of both.

Ingredient properties and impurities both may have a profound effect on propellant characteristics. A seemingly minor change in one ingredient can cause measurable changes in ballistic properties, physical properties, migration, aging, and/or ease of manufacture. When the propellant's performance or ballistic characteristics have tight tolerances, ingredient purity and properties must conform to equally tight

tolerances and careful handling (e.g., no exposure to moisture). In the remainder of this section, a number of the important ingredients, grouped by function, are briefly discussed.

INORGANIC OXIDIZERS

Some thermochemical properties of several oxidizers and radical-containing oxygen compounds are listed in Table 13–9. Listed values depend on the chemical nature of each ingredient.

Table 13–6 Typical Ingredients of Double-Base (DB) Propellants and Composite-Modified Double-Base (CMDB) Propellants

Type	Percent	Acronym	Typical Chemicals
Binder	30–50	NC	Nitrocellulose (solid), usually plasticized with 20–50% nitroglycerine
Reactive plasticizer (liquid explosive)	20–50	NG	Nitroglycerine
		DEGDN	Diethylene glycol dinitrate
		TEGDN	Triethylene glycol dinitrate
		PDN	Propanediol-dinitrate
		TMETN	Trimethylolethane trinitrate
Plasticizer (organic liquid fuel)	0–10	DEP	Diethyl phthalate
		TA	Triacetin
		DMP	Dimethyl phthalate
			Dioctyl phthalate
		EC	Ethyl centralite
		DBP	Dibutyl phthalate
Burn Rate Modifier	Up to 3	PbSa	Lead salicylate
		PbSt	Lead stearate
		CuSa	Copper salicylate
		CuSt	Copper stearate
Coolant		OXM	Oxamide
Opacifier		C	Carbon black (powder or graphite powder)
Stabilizer and or antioxidant.	>1	DED	Diethyl diphenyl
		EC	Ethyl centralite
		DPA	Diphenyl amine
Visible flame Suppressant	Up to 2	KNO_3	Potassium nitrate
		K_2SO_4	Potassium sulfate
Lubricant (for extruded propellant only)	> 0.3	C	Graphite
			Wax
Metal fuel[a]	0–15	Al	Aluminum, fine powder (solid)
Crystalline oxidizer[a]	0–15	AP	Ammonium perchlorate
		AN	Ammonium nitrate
Solid explosive crystals[a]	0–20	HMX	Cyclotetramethylenetetranitramine
		RDX	Cyclotrimethylenetrinitramine
		NQ	Nitroguanadine

[a]Several of these, but not all, are added to CMDB propellant.

Table 13–7 Typical Ingredients of Composite Solid Propellants

Type	Percent	Acronym	Typical Chemicals
Oxidizer (crystalline)	0–70	AP	Ammonium perchlorate
		AN	Ammonium nitrate
		KP	Potassium perchlorate
		KN	Potassium nitrate
		ADN	Ammonium dinitramine
Metal fuel (also acts as a combustion stabilizer)	0–30	Al	Aluminum
		Be	Beryllium (experimental propellant only)
		Zr	Zirconium (also acts as burn rate modier)
Fuel/binder, polybutadiene type	5–18	HTPB	Hydroxyl-terminated polybutadiene
		CTPB	Carboxyl-terminated polybutadiene
		PBAN	Polybutadiene acrylonitrile acrylic acid
		PBAA	Polybutadiene acrylic acid
Fuel/binder, polyether and polyester type	0–15	PEG	Polyethylene glycol
		PCP	Polycaprolactone polyol
		PGA	Polyglycol adipate
		PPG	Polypropylene glycol
		HTPE	Hydroxyl-terminated polyether
		PU	Polyurethane polyester or polyether
Curing agent or crosslinker, which reacts with polymer binder	0.2–3.5	MAPO	Methyl aziridinyl phosphine oxide
		IPDI	Isophorone diisocyanate
		TDI	Toluene-2,4-diisocyanate
		HMDI	Hexamethylene diisocyanide
		DDI	Dimeryl diisocyanate
		TMP	Trimethylol propane
		BITA	Trimesoyl-1(2-ethyl)-aziridine
Burn Rate Modifier	0.2–3	FeO	Ferric oxide
		nBF	*n*-Butyl ferrocene
			Oxides of Cu, Pb, Zr, Fe
			Alkaline earth carbonates
			Alkaline earth sulfates
			Metallo-organic compounds
Explosive filler (solid)	0–40	HMX	Cyclotetramethylenetetranitramine
		RDX	Cyclotrimethylenetrinitramine
		NQ	Nitroguanadine
		CL-20	Hexanitrohexaazaisowurtzitane
Plasticizer/pot life control (organic liquid)	0–7	DOP	Dioctyl phthalate
		DOA	Dioctyl adipate
		DOS	Dioctyl sebacate
		DMP	Dimethyl phthalate
		IDP	Isodecyl pelargonate
Energetic plasticizer (liquid)	0–14	GAP	Glycidyl azide polymer
		NG	Nitroglycerine
		DEGDN	Diethylene glycol dinitrate
		BTTN	Butanetriol trinitrate
		TEGDN	Triethylene glycol dinitrate
		TMETN	Trimethylolethane trinitrate
		PCP	Polycaprolactone polymer

Type	Percent	Acronym	Typical Chemicals
Energetic fuel/ binder	0–35	GAP	Glycidyl azide polymer
		PGN	Propylglycidyl nitrate
		BAMO/ AMMO	Bis-azidomethyloxetane/Azidomethyl-methyloxetane copolymer
		BAMO/ NMMO	Bis-azidomethyloxetane/3-Nitramethyl-3-methyloxetane copolymer
Bonding agent	> 0:1	MT-4	MAPO–tartaric acid–adipic acid condensate
(improves bond to solid particles)		HX-752	1,1'-Isophthaloyl-bis-(2-methylaziridine)
Stabilizer (reduces chemical deterioration)	> 0:5	DPA	Diphenylamine
		—	Phenylnaphthylamine
		NMA	N-methyl-p-nitroaniline
		—	Dinitrodiphenylanine
Processing aid	> 0:5	—	Lecithin
		—	Sodium lauryl sulfate

Table 13–8 Classification of Solid Rocket Propellants Used in Flying Vehicles According to Their Binders, Plasticizers, and Solid Ingredients

Designation	Binder	Plasticizer	Solid Oxidizer and/or Fuel	Propellant Application
Double base, DB	Plasticized NC	NG, TA, etc.	None	Minimum signature and smoke
CMDB[a]	Plasticized NC	NG, TMETN, TA, BTTN, etc.	Al, AP, KP	Booster, sustainer, and spacecraft
	Same	Same	HMX, RDX, AP	Reduced smoke
	Same	Same	HMX, RDX, azides	Minimum signature, gas generator

Designation	Binder	Plasticizer	Solid Oxidizer and/or Fuel	Propellant Application
EMCDB[a]	Plasticized NC + elastomeric polymer	Same	Like CMDB above, but generally superior mechanical properties with elastomer added as binder	
Polybutadiene	HTPB	DOA, IDP, DOP, DOA, etc.	Al, AP, KP	Booster, sustainer, or spacecraft; used extensively in many applications
	HTPB	DOA, IDP, DOP, DOA, etc.	AN, HMX, RDX, some AP	Reduced smoke, gas generator
	CTPB, PBAN, PBAA	All like HTPB above, but somewhat lower performance due to higher processing viscosity and consequent lower solids content. Still used in applications with older designs.		
Polybutadyene with HMX or RDX	HTPB	DOA, IDP, DOP, DOA, etc.	AP, Al, HMX, or RDX	High energy vehicles
Polyether and polyesters	PEG, PPG, PCP, PGA, HTPE,[b] and mixtures	DOA, IDP, TMETN, DEGDN, etc.	Al, AP, KP, HMX, BiO_3	Booster, sustainer, or spacecraft
Energetic binder (other than NC)	GAP, PGN, BAMO/ NMMO, BAMO/AMMO	TMETN, BTTN, etc. GAP-azide, GAP-nitrate, NG	Like polyether/polyester propellants above, but with slightly higher performance. Experimental propellant.	

a CMDB, composite-modified double-base; EMCDB, elastomer-modified cast double-base. For definition of acronyms and abbreviations of propellant ingredients see Tables 13–2 and 13–3.
b HTPE, hydroxyl-terminated polyether, binder for propellant developed for Insensitive Munitions by Orbital ATK.

Table 13–9 Comparison of Crystalline Oxidizers

Oxidizer	Chemical Symbol	Molecular Mass (kg/kg-mol)	Density (kg/m^3)	Total Oxygen Content (mass%)	Available Oxygen Content (mass%)	Remarks
Ammonium perchlorate	NH$_4$ClO$_4$	117.49	1949	54.5	34.0	Low n, low cost, readily available, high performance
Potassium perchlorate	KClO$_4$	138.55	2519	46.2	40.4	Low burning rate, medium performance
Sodium perchlorate	NaClO$_4$	122.44	2018	52.3		Hygroscopic, high performance, bright flame
Ammonium nitrate	NH$_4$NO$_3$	80.0	1730	60.0	20.0	Smokeless, medium performance, low cost

Ammonium perchlorate (NH$_4$ClO$_4$) is the most widely used crystalline oxidizer in solid propellants. It dominates the solid oxidizer field because of its desirable characteristics that include compatibility with other propellant materials, good performance, satisfactory quality and uniformity, low impact and friction sensitivities, and good availability. Other solid oxidizers, particularly ammonium nitrate and potassium perchlorate, have occasionally been used in production rockets but are now replaced by more modern propellants containing ammonium perchlorate. None of the many other oxidizer compounds that were investigated during the 1970s have reached production status.

The oxidizing potential of the perchlorates is generally high, which makes this material suited for high-specific-impulse propellants. Both ammonium and potassium perchlorate are only slightly soluble in water, a favorable propellant trait. All the perchlorate oxidizers generate gaseous hydrogen chloride (HCl) and other toxic and corrosive chlorine compounds in their reaction with fuels. In the firing of rockets, care is required, particularly for very large rockets, to safeguard operating personnel and/or communities in the path of exhaust gas clouds. Ammonium perchlorate (AP) is supplied in the form of small white crystals. Particle size and shape influences their manufacturing process and propellant burning rate. Therefore, close control of crystal sizes and size distributions present in a given quantity or batch is required. AP crystals are rounded (to nearly ball shape) to make for easier mixing than with sharp, fractured crystals. From the factory, they come in sizes ranging from about 600 µm (1 µm = 10^{-6} m) diameter to about 80 µm. Diameters below about 40 µm are considered more hazardous (e.g., can easily be ignited and sometimes detonate) and are not shipped; instead, propellant manufacturers take the larger crystals and grind them (at a motor factory) to smaller sizes (down to 2 µm) just before they are incorporated into a propellant.

Inorganic nitrates are relatively low-performance oxidizers compared with perchlorates. However, *ammonium nitrate* (AN) is used in some applications because of its very low cost as well as its smokeless and relatively nontoxic exhaust. Its principal use is in low-burning-rate, low-performance rocket and gas generator applications. Ammonium nitrate changes its crystal structure at several phase transformation temperatures. These changes cause slight changes in volume. One phase transformation at

32°C causes about a 3.4% change in volume. Repeated temperature cycling through this transition temperature creates tiny voids in the propellant, resulting in growth in the grain and a change in physical and/or ballistic properties. The addition of a small amount of stabilizer such as nickel oxide (NiO) or potassium nitrate (KNO_3) appears to change this transition temperature to above 60°C, a high enough value so that normal ambient temperature cycling will no longer cause recrystallization (Refs. 13–12 and 13–13). With such an additive, AN is known as *phase-stabilized ammonium nitrate* (PSAN). Moreover, AN is hygroscopic and any moisture absorption will degrade and destabilize propellants containing AN.

FUELS

This section discusses solid fuels of which *powdered spherical aluminum* is the most common. It consists of small spherical particles (5 to 60 µm diameter) and is used with a wide variety of composite and composite-modified double-base propellant formulations, usually constituting 14 to 20% of the propellant by weight. Small aluminum particles can burn in air and aluminum powder is mildly toxic if inhaled. During rocket combustion this fuel is oxidized to aluminum oxide. Such oxide particles tend to agglomerate and form larger particles. Aluminum increases the heat of combustion, the propellant density, the combustion temperature, and thus the specific impulse. The oxide starts in liquid droplet form during combustion but solidifies in the nozzle as the gas temperature drops. When in the liquid state, the oxide can form a molten slag, which can accumulate in pockets (e.g., around an improperly designed submerged nozzle), thus adversely affecting the vehicle's mass ratio. It also can deposit on walls inside the combustion chamber, as described in Refs. 13–14 and 13–15. Reference 13–16 addresses important issues related to adding aluminum as fuel to solid propellants,

Boron is a high-energy fuel that is lighter than aluminum and has a high melting point (2304°C). It is difficult to burn with high efficiency in combustion chambers of practical lengths. However, it can be efficiently oxidized if the boron particle size is sufficiently small. Boron has been used advantageously as a propellant in a rocket combined with an air-burning engine, where there is adequate combustion volume and atmospheric oxygen.

Beryllium burns much more easily than boron, improving the specific impulse of a solid propellant motor by about 15 sec, but both beryllium and its highly toxic oxide powders are absorbed by animals and humans when inhaled. The technology with composite propellants using powdered beryllium fuel has been experimentally proven, but its severe toxicity makes any earth-bound application unlikely.

BINDERS

In composite propellants, binders provide the structural matrix or glue with which the solid granular ingredients are held together. In raw form, these materials are liquid prepolymers or monomers. Polyethers, polyesters, and poly-butadienes have been used (see Tables 13–6 and 13–7). After they are mixed with their solid ingredients, cast and cured, they form a hard rubber-like material that constitutes the grain. Polyvinylchloride (PVC) and polyurethane (PU) (Table 13–1) were used 50 years ago and are still used in a few rocket motors, mostly of old design. Binder materials also act as fuels for solid propellant rockets and are oxidized in the combustion process. The binding ingredient, typically a polymer of one type or another, has a primary effect on motor reliability and its mechanical properties, propellant processing complexity, storability, aging, and costs. Some polymers undergo complex chemical reactions, crosslinking, and branch chaining during curing of the propellant. HTPB has been a favorite binder in recent years, because it allows somewhat higher solids fraction (88 to 90% of AP and Al), a small performance improvement, and relatively good physical properties at the temperature limits. Several common binders are listed in Tables 13–6 , and 13–7. Elastomeric binders can be added to plasticized double-base-type nitrocellulose to improve its physical properties. Polymerization occurs when the binder monomer and its crosslinking agent react (beginning in the mixing process) to form long chains and complex three-dimensional polymers. Other types of binders, such as PVC, cure or plasticize without molecular reactions (see Refs. 13–4, 13–5, and 13–15). Often called *plastisol-type binders*, these form very viscous dispersions of powdered polymerized resins in nonvolatile liquids; they polymerize slowly.

BURNING-RATE MODIFIERS

A burning-rate *catalyst* or burning-rate *modifier* helps to accelerate or decelerate combustion at the burning surface and thus increases or decreases the propellant burning rate. It permits tailoring of the burning rate to fit a specific grain design and thrust–time curve. Several are listed in Tables 13–6 and 13–7. Some, like iron oxide or lead stearate, increase the burning rate; however, others, like lithium fluoride, will reduce the burning rate of some composite propellants. Inorganic catalysts do not contribute to the combustion energy, but consume energy by being heated to combustion temperatures. These modifiers are effective because they can change combustion mechanisms, these are mentioned in Chapter 14 (examples of modifiers that change the burning rate of composite propellants are given in Chapter 2 of Ref. 13–4).

Burning rate is defined in Section 12.1; it is a strong function of the propellant composition. For composite propellants it may be increased by changing the propellant characteristics as follows:

1. Introduce a burning rate *catalyst*, or burning rate *modifier* (0.1 to 3.0% of propellant) or increase percentage of existing catalyst.
2. *Decrease* the *oxidizer particle size*.
3. *Increase oxidizer percentage*.
4. Increase the *heat of combustion* of the binder and/or the plasticizer.
5. Imbed high-conductivity *wires* or *metal staples* in the propellant.

PLASTICIZERS

A plasticizer is usually a relatively low-viscosity, liquid organic ingredient, which also acts as fuel. It is added to improve the elongation of the propellant at low temperatures and to improve its processing properties, such as lower viscosity for casting or longer pot life of the mixed but uncured propellants. The plasticizers listed in Tables 13–6, 13–7 and 13–8 represent several examples.

CURING AGENTS OR CROSSLINKERS

A curing agent or crosslinker causes prepolymers to form longer chains of larger molecular mass and interlocks between chains. Even though these curing agents are present in small amounts (0.2 to 3%), a minor change in their percentage can have a major effect on the propellant physical properties, manufacturability, and aging. They are used primarily with composite propellants and cause the binder to solidify and become hard. Several curing agents are listed in Table 13–7.

ENERGETIC BINDERS AND PLASTICIZERS

Energetic binders and/or plasticizers are used in lieu of the conventional organic materials. They contain oxidizing species (such as azides or organic nitrates) as well as other organic species. They add some energy to the propellant causing a modest increase in performance. They serve also as binders to hold other ingredients, or as energetic plasticizers liquid. They can self-react exothermally and burn without a separate oxidizer. Glycidyl azide polymer (GAP) is an example of an energetic, thermally stable, hydroxyl-terminated prepolymer that can be polymerized. It has been used in experimental propellants. Other energetic binder or plasticizer materials are listed in Tables 13–6, 13–7, and 13–8.

ORGANIC OXIDIZERS OR EXPLOSIVES

Organic oxidizers are highly energetic compounds with $-NO_2$ radicals or other oxidizing fractions incorporated into their molecular structure. References 13–4 and 13–15 describe their properties, manufacture, and applications. They are used with high-energy propellants and/or with smokeless propellants. They can be crystalline solids, such as the *nitramines* HMX or RDX, fibrous solids such as NC, or energetic plasticizer liquids such as DEGDN or NG. These materials can react or burn by themselves when initiated with enough activating energy and all may detonate under certain conditions. Both HMX and RDX are stoichiometrically balanced materials and their addition into either fuel or oxidizer reduces

the values of T_1 and I_s. Therefore, when binder fuels are added to hold the HMX or RDX crystals in a viscoelastic matrix, it is also necessary to add an oxidizer such as AP or AN.

RDX and HMX are quite similar in structure and properties. Both are white crystalline solids that can be made in different sizes. For safety, they are shipped in a desensitizing liquid, which is removed prior to propellant processing. HMX has a higher density, a higher detonation rate, yields more energy per unit volume, and has a higher melting point than RDX. Also extensively used in military and commercial explosives are NG, NC, HMX, and RDX. To achieve higher performance or other desirable characteristics, HMX or RDX can be included in DB, CMDB, or composite propellants. The amount added can range up to 60% of the propellant. Processing propellant with these or similar ingredients can be hazardous and the necessary extra safety precautions make the processing more expensive.

Liquid *nitroglycerine* (NG) by itself is very sensitive to shock, impact, or friction. It is an excellent plasticizer for propellants when desensitized by the addition of other liquids (like triacetin or dibutyl phthalate) or by compounding it with nitrocellulose. It readily dissolves in many organic solvents, and in turn it acts as a solvent for NC and other solid ingredients (Ref. 13–15).

Nitrocellulose (NC) is a key ingredient in DB and CMDB propellants. It is made by the acid nitration of natural cellulose fibers from wood or cotton and is a mixture of several organic nitrates. Although crystalline, it retains the fiber structure of the original cellulose (see Ref. 13–15). The nitrogen content is important in defining the significant properties of nitrocellulose, which can range from 8 to 14%, but the grades used for propellant are usually between 12.2 and 13.1%. Since it is impossible to make NC from natural products with an exact nitrogen content, the required properties are achieved by careful blending. Since the solid-fiber-like NC material is difficult to make into a grain, it is usually mixed with NG, DEGDN, or other plasticizers to gelatinize or solvate it when used with DB and CMDB propellants.

A newly identified organic oxidizer, hexanitrohexaazaiso-wurtzitane (also known as HNIW or CL-20), is being extensively investigated for its potential as a practical propellant, see Refs. 13–1 and 13–17. It may yield the highest specific impulse to date, slightly higher than currently modified solid propellants with HMX, and can act as a most powerful explosive (20% more power than HMX). To date (in 2015), it has only been produced in small laboratory quantities. Two major factors have restrained the full implementation of Cl-20, namely, its high cost (up to \$ 570/pound in 2013) and its high sensitivity—impact and friction tests indicate that CL-20 is less stable than HMX. CL-20's density is somewhat higher than any other explosive ingredients (2.04 g/cm^3). Investigations on its potential uses are continuing.

ADDITIVES

Additives perform many functions, including accelerating or lengthening *curing times*, improving *rheological properties* (easier casting of viscous raw mixed propellant), improving some *physical properties*, adding *opaqueness* to a transparent propellant to prevent radiation heating at places other than the burning surface, limiting *migration of chemical species* from the propellant to the binder or vice versa, minimizing any slow oxidations or *chemical deterioration* during storage, and improving *aging* characteristics or moisture resistance. *Bonding agents* are additives that enhance adhesion between the solid ingredients (AP or Al) and the binder. *Stabilizers* are intended to minimize slow chemical or physical reactions that may occur in propellants. *Catalysts* are sometimes added to crosslinker or curing agents to slow down curing rates. Lubricants are an aid the extrusion process. Desensitizing agents help to make propellants more resistant to inadvertent energy stimuli. Such additives are usually included in very small quantities.

PARTICLE-SIZE PARAMETERS

The size, shape, and size distribution of solid particles like AP, Al, or HMX within the propellant can have a major influence on composite propellant characteristics. These particles are made spherical in shape to allow for easier mixing and to attain higher solid percentages in the propellant than shapes of sharp-edged

natural crystals. Normally, ground AP oxidizer crystals are rated according to particle size ranges as follows:

Coarse	400 to 600 µm (1 µm = 10^{-6} m)
Medium	50 to 200 µm
Fine	5 to 15 µm
Ultrafine	sub micrometer to 5 µm

Coarse and medium-grade AP crystals are handled as class 1.3 materials, whereas the fine and ultrafine grades are considered as class 1.1 high explosives and are usually manufactured on-site from medium or coarse grades, (see Section 13.3 for a definition of these explosive hazard classifications). Most propellants use a multimodal blend of oxidizer particle sizes to maximize the amount of oxidizer per unit volume of propellant, with the small particles filling part of the voids between the larger particles. A *monomodal* propellant has one size of solid oxidizer particles, a bimodal has two sizes (say, 20 and 200 µm), and a trimodal propellant has three sizes; multiple modes allow a larger mass of solids to be placed into a given volume. Problem 13–1 has a sketch depicting how voids between the largest particles are filled with smaller particles.

Figure 13–8 shows the influence of varying the ratio of coarse to fine oxidizer particle sizes on propellant burning rate together with the influence of a burning rate additive. Figure 13–9 shows that the effect of particle size of aluminum fuels on propellant burning rate is much less pronounced than that of oxidizer particle size (Fig. 13–8 also shows an effect of particle size). Particle size, range, and shape for both the oxidizer (usually ammonium perchlorate AP]) and solid fuel (usually aluminum) have significant effects on solid packing fractions and on rheological properties (associated with the flowing or pouring of viscous liquids) of uncured composite propellants. By definition, *packing fraction* is the volume fraction of all solids when packed to minimum volume (a theoretical condition). High packing fractions make mixing, casting, and handling during propellant fabrication more difficult. Figure 13–10 shows a resulting distribution of AP particle size using a blend of sizes; the shape of this curve can be altered drastically by controlling size ranges and ratios. Also, solid particle size, range and shape affect the *solids loading ratio*, which is the mass ratio of solid to total ingredients in the uncured propellants. Computer-optimizing methods exist for adjusting particle-size distributions to improve the loading of solids, which can be as high as 90% in some composite propellants. Even though high solids loadings are desirable for high performance, they often introduce complexity and higher costs into the processing of propellant. Trade-offs among ballistic (performance) requirements, processability, mechanical strength, rejection rates, and facility costs are an ever-present concern with many high-specific-impulse composite propellants. References 13–4 and 13–15 report on the influence of particle size on motor performance.
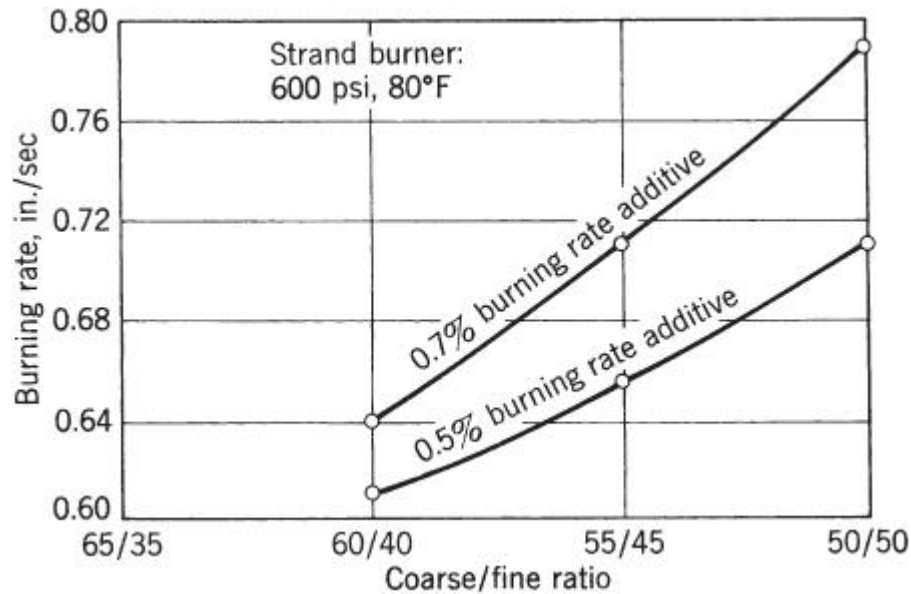
Figure 13–8 Typical effect of oxidizer (ammonium perchlorate) particle size mixture and burning rate additive on the burning rate of a composite propellant.

From NASA report: 260-SL-3 Motor program, Volume 2, 260-SL-3 motor propellant development, NASA-CR-72262, AGC-7096, Jul 1967, 110 pp. Accession Number: N68-16051. http://ntrs.nasa.gov/archive/nasa/casi.ntrs.nasa.gov/19680006582_1968006582.pdf.
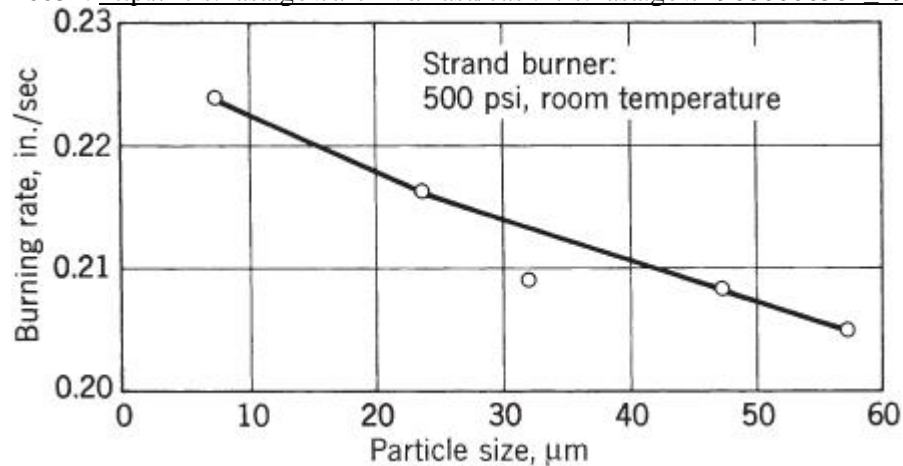
Figure 13–9 Typical effect of aluminum particle size on propellant burning rate for a composite propellant. From NASA report: Solid propellant processing factor in rocket motor design, NASA-SP-8075, 82 pp. (Oct 1972); N72-31767. http://hdl.handle.net/2060/19720024117; NTRS Document ID: 19720024117.
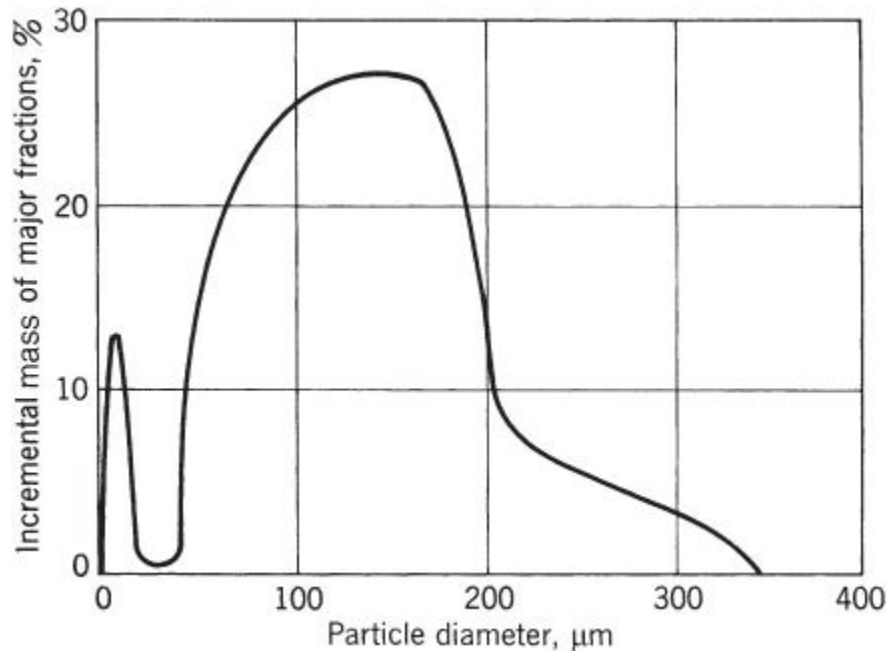
Figure 13–10 The oxidizer (AP) particle size distribution is a blend of two or more different particle sizes; this particular composite propellant consists of a narrow cut at about 10 µm and a broad region from 50 to 200 µm.

13.5 OTHER PROPELLANT CATEGORIES

GAS GENERATOR PROPELLANTS

Gas generator propellants are used to produce hot gases, not thrust. They generally have a low combustion temperature (800 to 1600 K), and most do not require internal insulators when used with metal cases. Typical applications of gas generators are listed in Table 12–1. Of the large variety of propellants utilized to for gas generators only a few will be mentioned.

Stabilized AN-*based propellants* have been used for many years with various binder ingredients. They give a clean, essentially smokeless exhaust and operate at a low combustion temperature. Because of their low burning rate they are useful for long-duration gas generator applications, say 30 to 300 sec. Typical compositions are given in Ref. 13–13 and Table 13–10 describes a propellant representative of early gas generators. It is often of interest to add some fuel to AN that acts as a coolant.

Table 13–10 Typical Gas Generator Propellant Using Ammonium Nitrate Oxidizer

Ballistic Properties	
Calculated flame temperature (K)	1370
Burning rate at 6.89 MPa and 20°C (mm/sec)	2.1
Pressure exponent *n* (dimensionless)	0.37

Temperature sensitivity σ_P (%/K)	0.22
Theoretical characteristic velocity, c^* (m/sec)	1205
Ratio of specific heats	1.28
Molecular mass of exhaust gas	19
Composition (Mass Fraction)	
Ammonium nitrate (%)	78
Polymer binder plus curing agent (%)	17
Additives (processing aid, stabilizer, antioxidant) (%)	5
Oxidizer particle size, (μm)	150
Exhaust Gas Composition (Molar %)	
Water (steam)	26
Carbon monoxide	19
Carbon dioxide	7
Nitrogen	21
Hydrogen	27
Methane	Trace
Physical Properties at 25°C *or* 298 K	

Tensile strength (MPa)	1.24
Elongation (%)	5.4
Modulus of elasticity in tension (N/m^2)	34.5
Specific gravity	1.48

One method of reducing flame temperatures is to burn conventional AP propellants hot and then to add water to bring combustion gas temperatures down to where uncooled metals can contain them. This is used on the MX missile launcher tube gas generator (Ref. 13–18). Another formulation uses HMX or RDX with an excess of polyether- or polyester-type polyurethane.

For the inflation of automobile collision safety bags the combusted gas must be nontoxic, smoke free, have a low temperature (so as not to burn people), be quickly initiated; the propellant must be storable for rather long times without degrading and reliably available. One solution is to use alkali metal azides (e.g., NaN_3 or KN_3) with an oxide and an oxidizer. The resulting nitrates or oxides are solid materials that are removed by filtering, and the gas is clean largely composed of moderately hot nitrogen. In one model, air can be aspirated into the air bag by the hot, high-pressure gas (see Ref. 13–19). One particular composition uses 65 to 75% NaN_3, 10 to 28% Fe_2O_3, and 5 to 16% $NaNO_3$ as an oxidizer, a burn rate modifier, and a small amount of SiO_2 for moisture absorption. The resultant solid nitride slag is caught in a filter.

The ideal power P delivered by a gas generator can be expressed as (see Chapters 3 and 5)

$$13\text{--}1 \quad P = \dot{m}(h_1 - h_2) = [\dot{m}T_1 Rk/(k-1)][1 - (p_2/p_1)^{(k-1)/k}]$$

where $\dot{m}$ is the mass flow rate, h_1 and h_2 are the enthalpies per unit mass respectively (at the gas generator chamber and exhaust pressure conditions), T_1 is the flame temperature in the gas generator chamber, R is the gas constant, p_2/p_1 is the reciprocal of the pressure ratio through which these gases are expanded, and k the specific heat ratio. Because flame temperatures are relatively low, there is no appreciable dissociation and frozen equilibrium calculations are usually adequate.

SMOKELESS OR LOW-SMOKE PROPELLANT

Several types of DB propellant, DB modified with HMX, nitramine (HMX or RDX) based composites, AN composites, and/or combinations of these have very few or no solid particles in their exhaust gases. They do not contain aluminum or AP (generally resulting in lower specific impulses than comparable propellants with AP) and have very little primary smoke, but they may produce secondary smoke in unfavorable weather. Several of these propellants have been used in tactical missiles. For certain military applications smokeless propellants are needed as discussed in Chapter 20.

It is difficult to make a solid propellant that produces truly smokeless exhaust gases. A distinction must be made, therefore, between *low-smoke* also called *minimum-smoke* (almost smokeless) and *reduced-smoke propellants,* which have a faintly visible plume. Visible smoke trails typically originate from solid metal oxide particles in the plume, such as aluminum oxide. With enough of these, the exhaust plume will scatter and/or absorb light and become as visible as *primary smoke* sources. Exhaust particles can also act as nuclei for moisture condensation, which occurs in saturated air or under high-humidity and low-temperature

conditions. Moreover, vaporized plume molecules such as water or hydrochloric acid may condense in cold air to form droplets and thus a cloud trail. These processes create a *vapor trail* or *secondary smoke*.

As stated, *minimum-smoke propellants* are not a special class with a peculiar formulation but a variation of one of the classes mentioned previously. Propellants containing Al, Zr, Fe_2O_3 (a burn rate modifier), and/or other metallic species will form visible and often undesirable clouds in the exhaust. *Reduced-smoke propellants* are usually composite propellants with low concentrations of aluminum (1 to 6%) that results in having low percentages of aluminum oxide in their exhaust plume; they are faintly visible as primary smoke but may precipitate heavy secondary smoke in unfavorable weather. Their specific impulse is much better than that of minimum-smoke propellants, as seen in Fig. 13–1.

IGNITER PROPELLANTS

The process of propellant ignition is discussed in Section 14.2, and several types of igniter hardware are discussed in Section 15.3. Propellants for igniters, a specialized field of propellant technology, are briefly described here. Requirements for igniter propellants include the following:

- Fast high heat release and high gas evolution per unit propellant mass to allow rapid filling of grain cavity with hot gas and to partially pressurize the chamber.
- Stable initiation and operation over a wide range of pressures (from subatmospheric to the high chamber pressures) and smooth burning at low pressures with no ignition overpressure surges.
- Rapid initiation of igniter propellant burning and low ignition time delays.
- Low sensitivity of burn rate to ambient temperature changes and low burning rate pressure exponent.
- Proper start, operation and storage over the required ambient temperature ranges.
- Safe and easy to manufacture, and safe to ship and handle.
- Satisfactory aging characteristics and long life.
- Minimal moisture absorption or degradation with time.
- Low cost of ingredients and fabrication.
- Low or no toxicity and low corrosive effects.

Some igniters not only generate hot combustion gases but also can produce hot solid particles or hot liquid droplets, which radiate heat and impinge on the propellant surface in the chamber where they embed themselves and assist in propellant burning on the exposed grain surface.

There is a wide variety of igniter propellants and their development has been largely empirical. Black powder, which was used in early rocket motors, is no longer favored because its properties are difficult to duplicate. Extruded double-base propellants are now frequently utilized, usually in the form of a large number of small cylindrical pellets. In some instances, rocket propellants used in the main grain are also used for the igniter grain, sometimes slightly modified. They are made in the form of a small rocket motor within the larger motor that is to be ignited. A common igniter formulation uses 20 to 35% boron and 65 to 80% potassium nitrate with 1 to 5% binder. Binders typically include epoxy resins, graphite, nitrocellulose, vegetable oils, polyisobutylene, and other binders listed in Table 13–7. Another formulation contains magnesium with a fluorocarbon (Teflon); this gives hot particles and hot gases (Refs. 13–20 and 13–21). Other igniter propellants are listed in Ref. 13–11.

13.6 LINERS, INSULATORS, AND INHIBITORS

Liners, insulators, and inhibitors represent three layer types that reside at grain interfaces and are defined in Section 12.3. Their materials do not contain any oxidizing ingredients but they may ablate, cook, char, vaporize, or disintegrate in the presence of hot gases. Many will actually burn if the hot combustion gases contain even small amounts of oxidizing species, but they will not usually burn by themselves. Liners, internal insulators, or inhibitors must be *chemically compatible* with the propellant and with each other to

avoid migration (described below) and/or changes in material composition; they must have *good adhesive strength* so that they stay bonded to the propellant, or to each other. The *temperatures* at which they experience damage or large *surface regressions* should be adequately high. They should all have low densities in order to reduce inert mass. Typical materials are neoprene (specific gravity 1.23), butyl rubber (0.93), a synthetic rubber called ethylene propylene diene or EPDM (0.86), or a propellant binder such as polybutadiene (0.9 to 1.0); these values are low relative to propellant specific gravities of 1.6 to 1.8. For low-smoke propellant these three rubber-like materials should only give off some gases but few, if any, solid particles (see Ref. 13–22).

The *liners* principal purpose is to provide a proper bond between the grain and the case, or between the case and any internal thermal insulation. In addition to the desired characteristics listed in the previous paragraph, the *liner* should be a soft stretchable rubber-type thin material (typically 0.02 to 0.04 in. thick with 200 to 450% elongation) to allow relative movement along the bond line between the grain and the case. This differential expansion is needed because the thermal coefficient of expansion of the grain is typically an order of magnitude higher than that of the case. A liner will also seal fiber-wound cases (particularly thin cases), which are often porous, so that high-pressure hot gases cannot escape. Typical liners for tactical guided missiles have been made from polypropylene glycol (about 57%) with a titanium oxide filler (about 20%), a di-isocyanate crosslinker (about 20%), and minor ingredients such as an antioxidant. Rocket motor cases have to be preheated to about 82°C prior to liner application. Often used as polymer for liners is ethylene propylene diene monomer (EPDM) linked into ethylene propylene diene terpolymer to form a synthetic rubber; it adheres and elongates nicely.

In some present-day motors, *internal insulators* not only provide for thermal protection of the case (from the hot combustion gases) but also often serve as a *liner* providing good bonding between propellant and insulator or insulator and case. Most motors today still have a separate liner and an insulating layer. Internal thermal insulation should also fulfill these additional requirements:

1. It must be erosion resistant, particularly at the motor aft-end or blast tube. This may be achieved in part by using tough elastomeric materials, such as neoprenes or butyl rubbers that are chemically resistant to the hot gases and to the impact of particulates. Such surface integrity is also achieved when a porous black-carbon layer formed on a heated surface (called a porous char layer) remains after some interstitial materials have been decomposed and vaporized.

2. It must provide good thermal resistance and have low thermal conductivity to limit heat transfer to the case and thus keep the case below its maximum allowable temperature, which is usually between 160 and 350°C for the plastic in composite material cases and about 550 and 950°C for most steel cases. These are accomplished by filling the insulator either with silicon oxide, graphite, Kevlar, or ceramic particles. Asbestos, an excellent filler material, is no longer used because of health hazards.

3. It should allow large-deformations or strains to accommodate grain deflections upon pressurization or temperature cycling, and should transfer loads between the grain and the case.

4. Surface regression should be minimal so as to retain much of its original geometric surface contour and allow for thin insulation.

A simple relationship for the internal insulation thickness d at any location in the rocket motor depends on the exposure time t_e, the erosion rate r_e (obtained from erosion tests at the likely gas velocity and temperature), and the safety factor f which can range from 1.2 to 2.0:

13–2
$$d = t_e r_e f$$

For small test rocket motors, some designers use the rule that the insulation depth should be twice the charred depth of the insulation.

Usually, the thickness of insulators cannot be uniform, varying by factors up to 20. It has to be thicker at locations near the nozzle where it is exposed to longer intervals and higher scrubbing velocities than at insulator locations protected by bonded propellant. Before making any material selection, it is necessary to

evaluate the burned-propellant flow field and thermal environment (combustion temperature, gas composition, pressure, exposure duration, and internal ballistics) in order to carry out proper thermal analyses (erosion predictions and estimated thickness of insulator). Evaluation of loads and deflections under loads at different motor locations are also needed to estimate shear and compression stresses. When high stresses or relief flaps are involved, structural analyses are also needed. Various software codes, such as those mentioned in Refs. 13–23 and 13–24, have been used.

Inhibitors are usually made of the same materials as internal insulators. They are applied (bonded, molded, glued, or sprayed) to grain surfaces that should not burn. In a segmented rocket motor, for example (see Fig. 15–2), where burning is allowed only on the internal port area, the faces of the cylindrical grain sections may be inhibited.

Migration describes the transfer of mobile (liquid) chemical species from the solid propellant to the liner, insulator, or inhibitor, and vice versa. Liquid plasticizers such as NG or DEGDN or unreacted monomers or liquid catalysts are known to migrate. This migratory transfer occurs very slowly but may cause dramatic changes in physical properties (e.g., the propellant next to the liner becomes brittle or weak), and there are several instances where nitroglycerine that migrated into an insulator made it flammable. Migration can be prevented or inhibited by using (1) propellants without plasticizers, (2) insulators or binders with plasticizers identical to those used in propellants, (3) a thin layer of an impervious material or a migration barrier (such as PU or a thin metal film), and (4) an insulator material that will not allow migration (e.g., PU) (see Ref. 13–25).

The graphite–epoxy case of the launch-assist rocket motors used to boost the Delta launch vehicle utilizes a three-layer *liner:* EPDM (ethylene propylene diene terpolymer) as a thin primer to enhance bond strength, a polyurethane barrier to prevent migration of the plasticizer into the EPDM liner, and a plasticized HTPB-rich liner to prevent burning next to the case–bond interface. Composite AP–Al propellants also use the same HTPB binder.

Liners, insulators, and/or inhibitors may be applied to the grain in several ways: by painting, coating, dipping, spraying, or by gluing sheets or strips to the case or the grain. Often automated, robotic machines are used to achieve uniform thicknesses and high quality. Reference 13–22 describes the manufacture of particular insulators.

External insulation is often added to the outside of the motor case when it is part of the vehicle's structure, particularly in tactical missiles or high-acceleration launch boosters. Such insulation reduces the heat flow from any hot boundary layers outside the vehicle surface (aerodynamic heating) to the case, and then to the propellant. It may thus prevent fiber-reinforced plastic cases from becoming weak or propellants from becoming soft or, in extreme situations, from being ignited. Such insulator must withstand oxidation from hot air flows, have good adhesion, have structural integrity to loads imposed by the flight or launch, and must have reasonable cure temperatures. Materials ordinarily used as internal insulators are unsatisfactory because they burn in the atmosphere generating additional heat. The best is a nonpyrolyzing, low-thermal-conductivity refractory material (Ref. 13–26) such as certain high-temperature paints. Any internal and external insulation also helps to reduce grain temperature fluctuations and thus thermal stresses imposed by thermal cycling, such as day–night variations or high- and low-altitude temperature variations for airborne missiles.

13.7 PROPELLANT PROCESSING AND MANUFACTURE

The manufacture of solid propellant involves many complex physical and chemical processes. In the past, propellants have been produced by several different processes such as compaction or pressing of powder charges, extrusion of propellant through dies under pressure using heavy presses, and mixing with a solvent which is later evaporated. Even for the same type of propellant (e.g., double-base, composite, or composite double-base), fabrication processes are usually not identical for different manufacturers, motor types, sizes, or propellant formulation, and no single simple generalized process flowsheet or fabrication technique

prevails. Most rocket motors in production today use composite-type propellants and therefore more emphasis on this process is given here.

Figure 13–11 is a representative flowsheet for the manufacture of a complete solid rocket motor with a composite propellant made by batch processes. Processes marked with an asterisk are potentially hazardous, are usually operated or controlled remotely, and are usually performed in buildings designed to withstand potential fires or explosions. Mixing and casting processes are the most complex, being more critical than other processes in determining quality, performance, burn rate, and physical properties of the resulting propellant.

Chemical ingredients receiving, storage, inspection, weighing, and preparation

| Igniter chemicals * | Oxidizer crystals | Aluminum powder | Binder (monomer) | Additives | Curing agent |

Classify ↔ Grind *

Weigh

Store ← Premix

Weigh, blend, mix and cure *

Dry, blend

Mixing * → Clean mixer *

Cure case → Clean & apply insulator & liner → Inspect, assemble & test → Casting into case * ← Clean & repair tooling * ← Fabricate tooling

Fabricate and assemble case ← Fabricate/ mold aft & fwd. domes, insulators & flaps

Curing *

Remove mandrel & tooling *

Fabricate nozzle → Inspect & clean

Safe and arm device → Electrical test & inspect

Machine off excess propellant *

Fabricate TVC → TVC tests & inspect

X-ray inspect

Final assembly

Fabricate igniter hardware → Igniter assembly & check-out *
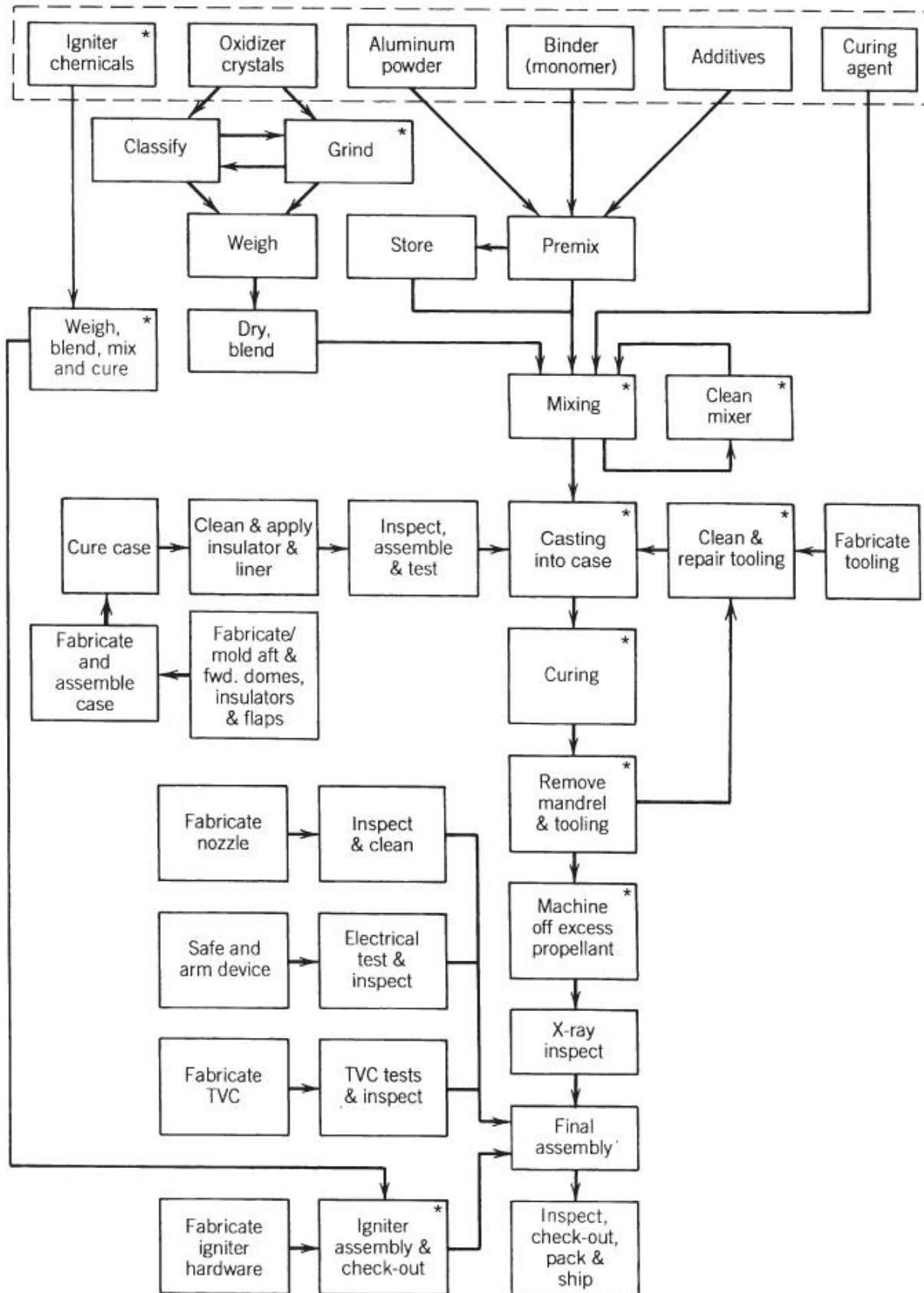
Inspect, check-out, pack & ship

Figure 13–11 Simplified manufacturing process flow diagram for a rocket motor and its composite solid propellant. An asterisk means it is a more hazardous operation.

The rheological properties of uncured propellants (e.g., their flow properties in terms of shear rate, stress, and time) are all-important to their processability and these properties usually change substantially throughout the path of the processing line. Batch-type processing of propellants, including the casting (pouring) of propellants into motors that serve as their own molds, is the most common method. For very large motors several days are needed for casting up to perhaps 40 batches into a single case to form a single grain. Vacuum is almost always imposed on the propellant during the mixing and casting operations to remove air and other dispersed gases and to avoid air bubbles in the grain. Viscosity measurements of the mixed propellant (in the range of 10,000 to 20,000 poise) are made for quality control. Vacuum, temperature, vibration, energy input to the mixer, and time are some factors affecting the viscosity of the uncured propellant. Time is important in terms of *pot life*, that is, that period of time the uncured propellant remains reasonably fluid after mixing before it cures and hardens. Short pot lives (a few hours) require fast operations in emptying mixers, measuring for quality control, transporting, and casting into motors. Some binder systems, such as those using PVC, present a very long pot life and avoid the urgency or haste in the processing line. References 13–15, 13–11, and 13–27 give details on propellant processing techniques and equipment.

Double-base propellants and modified double-base propellants are manufactured by a different set of processes. The key goal here is the diffusion of liquid nitroglycerine into the fibrous solid matrix of nitrocellulose, thus forming, by means of solvation, a fairly homogeneous, well-dispersed, relatively strong solid material. Several processes for making double-base rocket propellant are in use today, including extrusion and slurry casting. In the slurry casting process the case (or the mold) is filled with solid casting powder (a series of small solid pellets of nitrocellulose with a small amount of nitroglycerine) and the case is then flooded with liquid nitroglycerine, which then solvates the pellets. Figure 13–12 shows a simplified diagram of a typical setup for a slurry cast process. Double-base propellant manufacturing details are shown in Refs. 13–5 and 13–15.
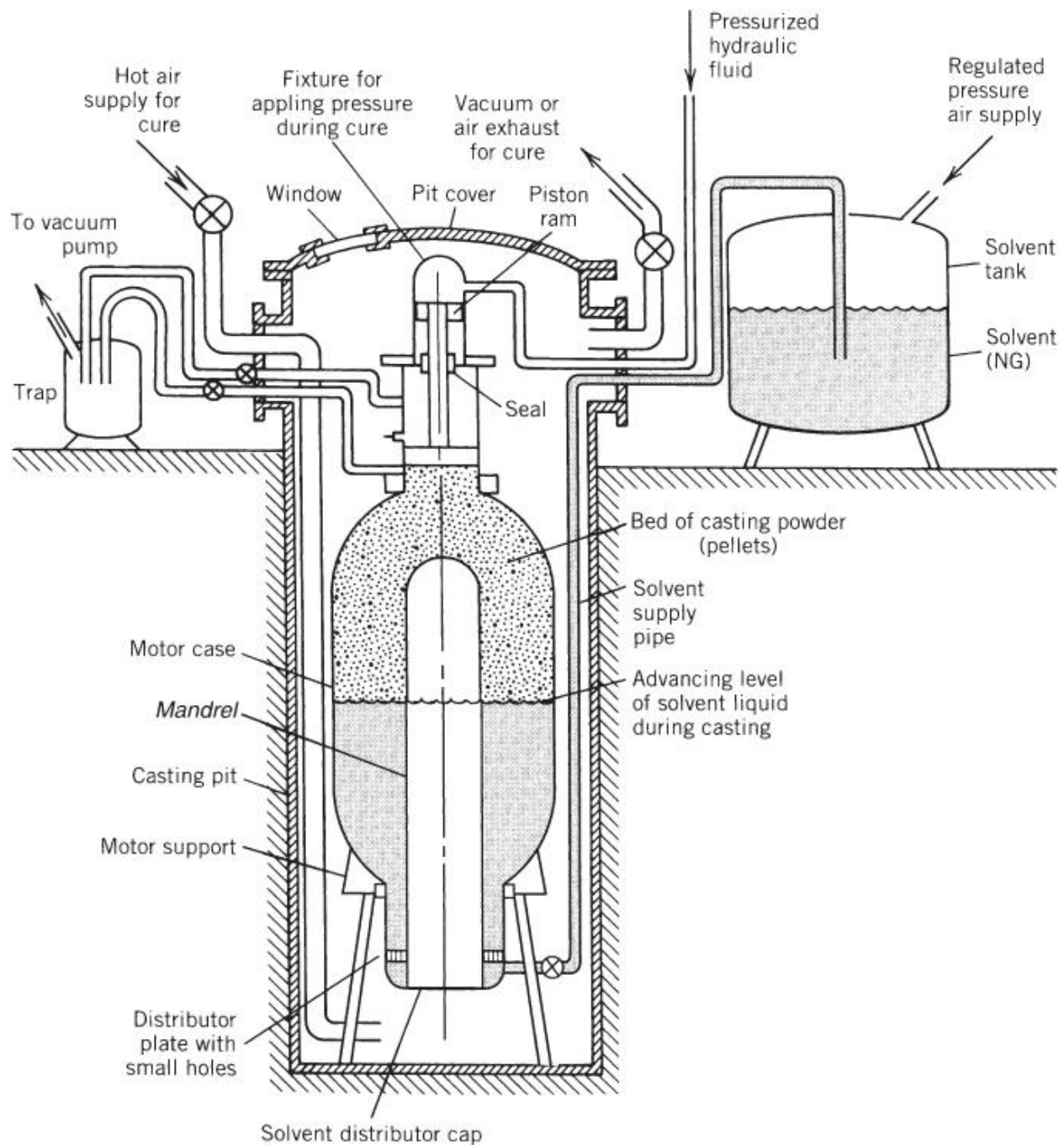
Figure 13–12 Basic diagram of one system for slurry casting and initial curing of a double-base solid propellant.

Mandrels are used during casting and curing to assure the proper internal cavity or perforation pattern. They are made of metal in the shape of the internal bore (e.g., star or dogbone) and are often slightly tapered and coated with a nonbonding material, such as Teflon, to facilitate the withdrawal of the mandrel after curing without tearing the grain. For complicated internal passages, such as a conocyl, complex built-up mandrels, which can be withdrawn through the nozzle flange opening in smaller pieces or which can be collapsed are necessary. Some manufacturers have had success in making permanent mandrels (that are not withdrawn but stay with the motor) out of a lightweight foamed propellant that burn very quickly once ignited.

An important objective in processing is to produce a propellant grain free of cracks, low-density areas, voids, or other flaws. In general, voids and other flaws degrade the ballistic and mechanical properties of the propellant grain. Many small dispersed gas bubbles in a propellant grain may result in an abnormally high burning rate, one so high as to cause excessive pressure and catastrophic case failure.

The finished grain (or rocket motor) is usually inspected for defects (cracks, voids, and debonds) using X-rays, ultrasonics, heat conductivity probes, and/or other nondestructive inspection techniques. Propellant samples are taken from each batch, tested for rheological properties, and cast into physical property specimens and/or small rocket motors, which are then cured and subsequently tested. Any determination of the sensitivity of rocket motor performance, including possible failure, to propellant voids and other flaws often requires the test firing of motors with known defects. Data from such tests are important in establishing inspection criteria for accepting and rejecting production rocket motors.

Special processing equipment is required in the manufacture of propellants. For composite propellants this includes mechanical mixers (usually with two or three blades rotating on vertical shafts agitating propellant ingredients in a mixer bowl under vacuum), casting equipment, curing ovens, and/or machines for automatically applying the liner or insulation to the case, see Ref. 13–11. Double-base processing requires equipment for mechanically working the propellant (rollers, presses) or special tooling for allowing a slurry cast process. Computer-aided filament winding machines are used for laying the fibers of fiber-reinforced plastic cases and nozzles.

Casting of propellant into large boosters and strap-ons very near the launch site and the vertical keeping of rocket motors has the potential to decrease problems associated with handling and transportation, as well as with propellant slump. This decreases the time from manufacturing to launch but is not recommended for long storage times in any vertical position.

Cryogenics

Abstract

In this chapter, a general introduction to thermal phenomena at cryogenic temperature is presented. Typical applications are discussed and then pressurization and thermal stratification in liquid hydrogen tanks are analyzed numerically. The tanks are exposed to heat-in-leaks from the environment.

KEYWORDS

Kapitza number; Kapitza resistance; Liquid hydrogen tank; Pressurization; Superconductivity; Thermal stratification

5.1. Introduction

This chapter presents applied heat transfer principles in the range of extremely low temperatures. The specific features of heat transfer at cryogenic temperatures, such as variable properties, near-critical convection, and the Kapitza resistance, are described. The chapter will include some examples to illustrate specific phenomena.

The cryogenic temperature range is commonly defined as from −150°C to absolute zero (i.e., −273°C or 0K). At 0K the molecular motion comes as close as theoretically possible to ceasing completely. Cryogenic temperatures are considerably lower than those encountered in ordinary physical processes. At these extreme conditions the thermal conductivity, ductility, strength of materials, and electric resistance are altered, which is of great importance. As heat is considered to be created by the random motion of molecules, this implies that substances at cryogenic temperatures are very close to a static and highly ordered state. The development of cryogenics has been connected to the development of refrigeration systems. As the ability of many supercooled metals to lose resistance to electricity was discovered, the phenomenon of superconductivity was introduced. Temperatures below 3K are primarily used in laboratories, particularly in the research of the properties of helium. Helium is liquefied at 4.2K and this liquid is called helium I. At 2.17K, it is abruptly transferred to helium II. This liquid has such a low viscosity that it can crawl up the side of a glass and flow through microscopic holes too small to permit the passage of ordinary liquids, including helium I. This property is called superfluidicity.

A very important commercial application of cryogenic liquefaction methods is storage and transportation of liquefied natural gas (LNG). Natural gas is liquefied at 110K and becomes very compact and accordingly suitable for efficient transport in specially insulated tankers or containers. For preservation of food, very low temperatures are also used. The food products are placed in well-sealed tanks and liquid nitrogen (LN$_2$, liquefied at 77K) is sprayed over them. The nitrogen vaporizes immediately and absorbs the heat content of the products.

In the so-called cryosurgery, scalpels or probes are cooled by LN$_2$ and then used to freeze unhealthy tissue. Then the dead cells are removed by normal processes. An advantage of cryosurgery is that freezing the tissue results in less bleeding when compared to cutting methods.

For space vehicles, cryogens such as liquid hydrogen (LH$_2$) and liquid oxygen (LOX) are used as propellants. The major disadvantage of using hydrogen as fuel in aerospace vehicles is its need for a large storage volume. At standard pressure and temperature, hydrogen has a density of about 0.09 kg/m^3, whereas gasoline and kerosene have about 800 kg/m^3. This is the main reason why hydrogen is stored under cryogenic conditions (20.46K) in liquid phase. At a given amount of energy the volume of hydrogen would

be four times larger than that of kerosene. LH_2 is also proposed to have a dominant role in clean and fossil-free energy systems in transportation.

The superconductivity of materials being cooled to an extremely low temperature has a significant application in the construction of superconducting electromagnets for particle accelerators. Such large research facilities require very powerful electromagnetic fields.

In big cities, it is difficult to transmit electric power by overhead cables and hence, underground cables are used extensively nowadays. However, the underground cables become heated and the resistance of the wires increases, leading to waste of power. Superconductors are frequently used to increase the power throughput, which requires cryogenic liquids such as nitrogen and helium to cool special alloy-containing cables to increase the power transmission.

Cryocoolers (heat exchangers operating at very low temperatures) are required on many satellites to cool infrared and microwave detectors, and thus, sharper images can be received.

5.2. Kapitza Resistance

The Kapitza resistance is a thermal resistance to heat transfer across the interface between liquid helium and a solid. In liquid helium and solids (e.g., copper), heat is carried by phonons, which are thermal equilibrium sound waves with frequencies in the gigahertz and terahertz region. The acoustic impedance of helium and solids can differ up to 1000 times, which implies that the phonons mostly reflect at the boundary, like an echo from a cliff face. This property, together with the fact that the number of phonons decreases very rapidly at low temperatures, means that at about 1K, there are few phonons to carry heat and even fewer to get across the interface. The prediction is that the Kapitza resistance at the interface is comparable to the thermal resistance of a10-m-long copper material with the same cross section.

Significant interest has been shown in the thermal properties of amorphous polymers at low temperatures. Such polymers, such as Kapton, exhibit good mechanical, chemical, and electrical properties. Therefore, they are used in many cryogenic applications such as in thermal and electrical insulation for superconducting magnet winding, as key components for cryogenic target or space applications, and in low-temperature heat exchangers. For all these cryogenics applications an accurate design is required, and thus the knowledge of the thermal properties of such materials, such as thermal conductivity and thermal resistance, dominated by the Kapitza resistance, at the solid–He II interface is essential. For pressurized helium II the reciprocal Kapitza resistance, i.e., conductance is about 0.6 W/cm^2K. However, it has been found that the impedance mismatch between a solid and a cryogen is dominant at very low temperatures and small above approximately 4K, and accordingly, it is important only for helium systems.

5.2.1. KAPITZA NUMBER

The Kapitza number (Ka) is a dimensionless number expressing the ratio of the surface tension force to inertial force. Physically it indicates the hydrodynamic wave regime in falling liquid films. In evaporators, heat exchangers, microreactors, absorbers, electronic and microprocessor cooling, and air-conditioning, liquid films are important. The Kapitza number is a material property and is defined as

$$Ka = \frac{\sigma}{\rho(g \sin \beta)^{1/3} v^{4/3}}$$

where σ is the surface tension (N/m); g, the gravitational acceleration (m/s^2); ρ, the density (kg/m^3); β, the inclination angle (radian); and v, the kinematic viscosity (m/s^2).

5.3. Cryogenic Tanks

Cryogens, in particular, LH_2 and LOX, are important as both power supply and life support fluids in space explorations because of their high-efficient thrust and nonpolluting waste [1,2]. During rocket launch, cryogenic propellant tanks are exposed to severe aerodynamic heating and different space radiations. As the liquid propellants have a low boiling point, they are highly sensitive to heat leaks from the external thermal environment [3]. Complex heat and mass transfer exchanges are involved in the pressurization and thermal stratification process in cryogenic tanks. The heat will be carried to the liquid–vapor interface by conduction and natural convection causing vaporization, which in a closed tank results in pressurization. Thus it is essential to understand and be able to control the pressurization and thermal stratification processes in cryogenic tanks, and this will be important for successful drainage and safe storage of cryogenic propellant for a long time, as well as for successful operation of space emissions.

Several experimental and numerical investigations have been performed on the ground under normal gravity and some under microgravity. For instance, experimental investigations of LH_2 stratification have been conducted. Effects of side-wall heating and bottom-wall heating have been studied. Various theoretic studies have been conducted but the more recent ones are based on computational fluid dynamics (CFD). Reviews can be found in Refs. [4–7]. In aerospace applications, cryogenic tanks will experience orbital transfer, slow rotation, and altitude adjustment during the coast period, and accordingly, fluid thermal stratification during such conditions has been considered in Ref. [8].

5.4. Analysis of Pressurization and Thermal Stratification in an LH_2 Tank

This section presents an analysis of self-pressurization and thermal stratification in a closed LH_2 tank by employing the so-called volume of fluid (VOF) model and phase change effect. The phenomena are investigated in a partially filled LH_2 tank for different fill levels and in-leak heat fluxes. A full tank and a partially filled tank are investigated.

5.4.1. MATHEMATICAL MODEL

An axisymmetric cylindrical tank partially filled with LH_2 is shown in Fig. 5.1. Only hydrogen vapor is considered to be present in the vapor space.

The VOF method [9], which is a kind of Eulerian method, has been widely used in predicting various two-phase fluid flows and is adopted in this analysis. The VOF formulation relies on the fact that two or more fluids do not interpenetrate each other. For each phase considered in the model a variable is introduced as the volume fraction of the phase in the computational cell. In each of the control volumes, the volume fractions of all phases sum up to unity. Because the temperature changes slightly, all the fluid properties, except density, are considered constant.
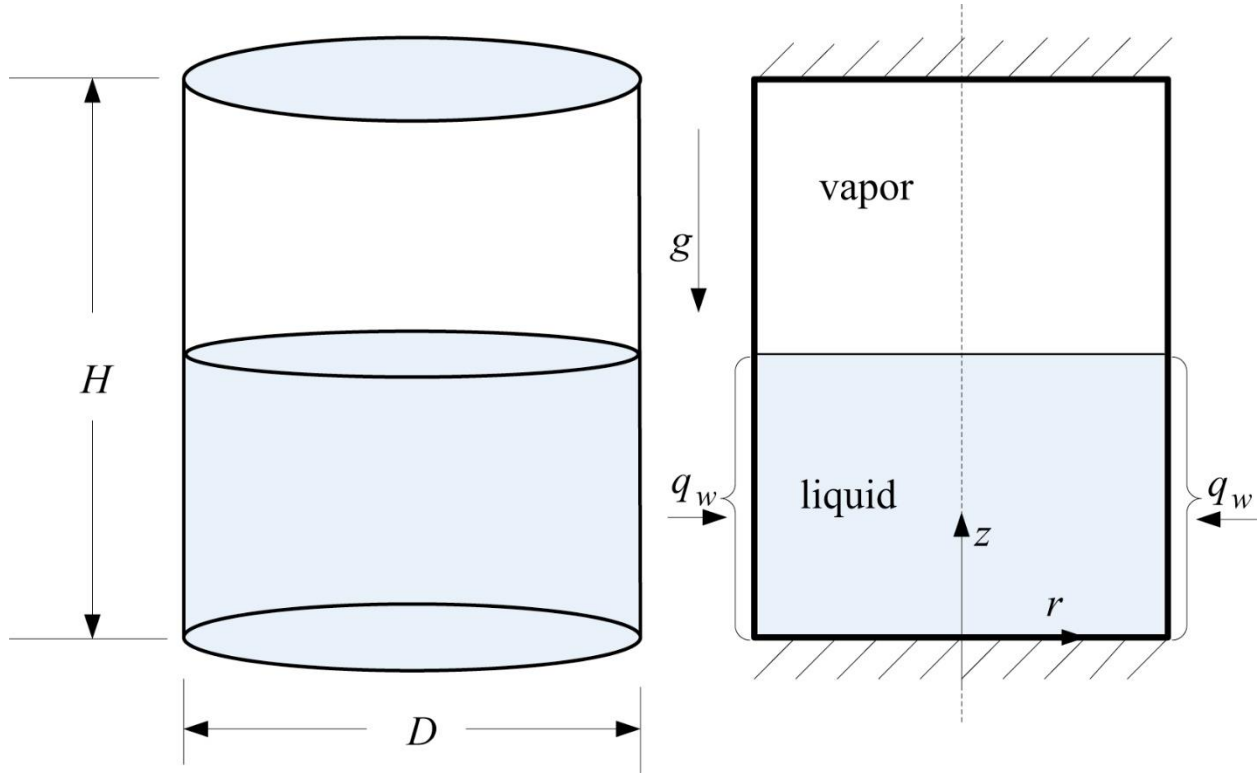
FIGURE 5.1 Cylindrical cryogenic tank under consideration.

The density variation versus temperature is described by the Boussinesq approximation for evaluation of the buoyancy force. In the solution procedure the governing equations for conservation of mass, momentum, and energy are given by

$$\frac{\partial \rho}{\partial \tau} + \nabla \cdot \left(\rho \vec{V} \right) = 0 \tag{5.1}$$

$$\frac{\partial \left(\rho \vec{V} \right)}{\partial \tau} + \nabla \cdot \left(\rho \vec{V} \vec{V} \right) = - \nabla p - \rho \beta \vec{g} \left(T - T_0 \right)$$

$$+ \nabla \cdot \left[\mu_{\text{eff}} \left(\nabla \vec{V} + \nabla \vec{V^T} \right) \right] + \vec{F} \tag{5.2}$$

$$\frac{\partial \rho E}{\partial \tau} + \nabla \cdot \left(\vec{V} (\rho E + p) \right) = \nabla \cdot \left(k_{\text{eff}} \nabla T \right) + S_h \tag{5.3}$$

where $\vec{F}$ is the body force resulting from surface tension at the interface and S_h is the energy source related to the phase change. A formulation of the continuum surface force (CSF) model is used, and the surface tension can finally be written in terms of the pressure jump across the interface surface. The force at the surface can be expressed as a volume force F_{vol}, using the divergence theorem [10]. The volume force acts as the source term in the momentum equation and has the following form:

$$F_{vol} = \sigma_{lv} \frac{\alpha_l \rho_l \kappa_v \nabla \alpha_v + \alpha_v \rho_v \kappa_l \nabla \alpha_l}{0.5(\rho_l + \rho_v)} \quad (5.4)$$

where σ_{lv} is the interfacial surface tension between the liquid and the vapor. The curvatures of the liquid and vapor are defined as

$$\kappa_l = \frac{\nabla \alpha_l}{|\nabla \alpha_l|}, \kappa_l = \frac{\nabla \alpha_v}{|\nabla \alpha_v|} \quad (5.5)$$

The tracking of the interface between the phases is accomplished by solving the continuity equation for the volume fraction of the second phase. This equation reads

$$\frac{\partial}{\partial \tau}(\alpha_v \rho_v) + \nabla \cdot (\alpha_v \rho_v \vec{V}) = \dot{m} \quad (5.6)$$

where $\dot{m}$ is the phase change flow rate caused by evaporation or condensation at the interface, positive or negative, respectively. It is regarded as a source term in the continuity equation. The Lee phase change model [11] is applied to consider this mass transfer and is described as

$$\dot{m} = r_l \alpha_l \rho_l (T_l - T_{sat}) \quad \text{if } T_l \geq T_{sat} \quad (5.7a)$$

$$\dot{m} = r_v \alpha_v \rho_v (T_v - T_{sat}) \quad \text{if } T_v \leq T_{sat} \quad (5.7b)$$

The saturation temperature, T_{sat}, changes according to the pressure in the tank by the Clausius–Clapeyron equation. The coefficient, r, is determined by the trial and error procedure described in Ref. [12]. Thus the energy source term S_h will be

$$S_h = L_H \dot{m} \quad (5.8)$$

where L_H is the latent heat of hydrogen.

The properties appearing in the transport equations are determined by the presence of the component phases in each control volume. For instance, thermal conductivity, density, dynamic viscosity, and specific heat can be determined by the following respective expressions:

$$k = \alpha_l k_l + (1 - \alpha_l) k_v \quad (5.9)$$

$$\rho = \alpha_l \rho_l + (1 - \alpha_l) \rho_v \quad (5.10)$$

$$\mu = \alpha_l \mu_l + (1 - \alpha_l) \mu_v \quad (5.11)$$

$$c_p = \frac{1}{\rho} [\alpha_l \rho_l c_{pl} + (1 - \alpha_l)] \rho_v c_{pv} \quad (5.12)$$

5.4.2. THERMAL ENVIRONMENT

The cryogenic tank is exposed to serious aerodynamic heating and various heat leaks, and all the environmental physical properties change with height. Aerodynamic heating is maximum in the atmosphere, but in space the cryogenic tank is subjected to various space heat leakages. Solar incident radiation, earth albedo radiation, infrared radiation, and deep-space infrared radiation are the main heat sources. The method to estimate these four kinds of space radiation can be found in Ref. [3]. In the analysis in this chapter the heat flux is given certain values and presents effective mean values to enable parametric analysis.

The boundary conditions are as follows, see Fig. 5.1. The top and bottom surfaces of the tank are assumed to be flat and perfectly insulated, respectively. Heat-in-leak takes place only at the cylindrical wet walls and different rates of the heat-in-leak q_w are specified. The heating of LH_2 at the walls induces free convection currents, with the warmer LH_2 in the near-wall region being transferred to the upper regions of the liquid column.

Quiescent saturation conditions are assumed to prevail before the heat flux q_w is imposed at the cylindrical walls. The initial conditions at $\tau = 0$ are

$$u(r, z) = u_r = u_z \quad (5.13)$$

The initial pressure is set to 1 atm (101.32 kPa) and the initial temperature corresponds to the H_2 saturation temperature at that pressure (20.268 K). The initial temperature is assumed to be the same throughout the liquid and vapor. The pressure in the liquid is taken as a function of the height and density. No slip boundary conditions are imposed on the sidewalls.

The top and bottom surfaces are assumed to be insulated and an adiabatic boundary condition is thus valid:

$$\frac{\partial T}{\partial n} = 0 \quad (5.14)$$

whereas on the sidewalls the Neumann boundary condition is formulated as

$$-k\frac{\partial T}{\partial n} = q_w \quad (5.15)$$

5.4.3. NUMERICAL SOLUTION PROCEDURE

The tank has a diameter of 0.5 m and its height is 1 m. Because of the cylindrical geometry, imposed boundary conditions, and the physics of the problem, symmetry conditions can be applied. Thus the flow and temperature fields are treated as axisymmetric. The influence of the fill level on the pressurization and thermal stratification is analyzed for three fill levels of 30%, 50%, and 80%. Various values of the incident heat flux are, respectively, considered: 50, 150, and 250 W/m^2. For the lowest wall heat flux the influence of the fill level is presented. If gravity is present, an important parameter for determining the flow regime is the dimensionless Rayleigh number. It is defined as

$$Ra^* = \frac{g\beta\rho^2 c_p q_w L^4}{\mu k^2} \quad \text{(5.16)}$$

For a heat flux of 50 W/m^2 the Ra is $1.13 \cdot 10^{13}$.

Sometimes the so-called Bond number, Bo, is introduced to reveal the ratio of buoyancy forces to surface tension. It is defined as

$$Bo = g(\rho_l - \rho_v)L^2/\sigma \quad \text{(5.17)}$$

For zero gravity, Bo = 0 and the surface tension becomes very important, whereas for normal gravity, the Bo is quite high and the surface tension is less important.

The commercial CFD code ANSYS FLUENT was used as a solver for the conservation equations. The interfacial mass and heat transfer model was implemented via the so-called user-defined functions.

The SIMPLEC (semi-implicit method for pressure linked equations consistent) procedure was chosen as the pressure–velocity coupling algorithm. For the pressure interpolation required to solve the momentum equation, the body-force-weighted scheme was applied because it is effective in numerically solving the buoyant natural convection problems. A second-order upwind scheme was chosen for the convection terms in the conservation equations. For turbulent cases, the k–ε turbulence model was selected based on some initial tests. The enhanced wall function approach is used for handling the near-wall region. The y$^+$ values closest to the solid walls were within the recommended range for this turbulence model. The maximum y$^+$ value was 30. Turbulent flow prevailed only under normal gravity. As the Rayleigh number is high, no particular model for handling the transition from laminar to turbulent flow was adopted.

The geometric reconstruction scheme using the piecewise linear approximation is applied for the volume fraction equation to capture the interface.

Sensitivity tests were carried out to reveal the importance of the number of control volumes of the computational grid. A grid with a total of 20,000 quadrilateral elements was used for the axisymmetric simulations, with successively increasing number of control volumes toward the walls and interface. As the computations concerned transient heat transfer and fluid flow in the domain, the time step had to be chosen in such a way that the Courant number is less than 0.1.

It should be noted that with the VOF method, it is possible to identify the various regions being occupied by the vapor and liquid, but the detailed mechanisms of the phase change process cannot be detected.

In visualization and interpretation of the flow field, the stream function is a convenient property to consider. It is generally formulated as a relation between the streamlines and the statement of conservation of mass. A streamline is a line that is tangent to the velocity vector of the flowing fluid.

In this case, as an axisymmetric flow is considered, the stream function is defined as

$$\rho u_r = \frac{1}{r}\frac{\partial \psi}{\partial z}, \rho u_z = -\frac{1}{r}\frac{\partial \psi}{\partial r} \quad \text{(5.18)}$$

where u$_r$ and u$_z$ are the radial and axial velocities, respectively.

Further details are available in Ref. [13].

5.4.4. RESULTS

In this section, simulations of self-pressurization and thermal stratification in a partially filled LH_2 tank are presented. When the influence of the imposed heat flux is investigated, the comparison is carried out at a fixed fill level. Similarly, the imposed heat flux is fixed as the fill level effect is studied. The influence of gravity, surface tension, and wettability will be presented in Chapter 9.

Fig. 5.2 shows the pressure rise versus time in the LH_2 tank for various values of the sidewall heat flux. The pressure starts to rise after a certain time. During this period, there is only marginal evaporation. This can be attributed to a coupling between the buoyancy force and convective cooling. Warm liquid created by the sidewall heat flux needs some time to flow and reach the interface, and there is also increase in the enthalpy. At the onset of evaporation the pressure rises gradually and the rise rate tends to gradually approach a constant value. The mass of the LH_2 left in the tank decreases as the evaporation process progresses. A similar phenomenon was also found by Kumar et al. [14] by using a homogeneous two-phase flow model. As the heat flux increases, the elapsed time becomes shorter before the evaporation is initiated. This is because the buoyancy force is essentially proportional to the difference between the temperatures of the warm liquid and the interface. The timescale for the liquid enthalpy increase and the liquid motion to the interface becomes shorter. However, as the heat flux is increased, more liquid is initially evaporated and a longer initial transient period is observed. This was also found in the experiments by Seo and Jeong [15]. After the initial evaporation phase, the liquid approaches a stable configuration, even though the average temperature is still increasing. A certain temperature stratification appears in the liquid. A part of the thermal energy entering through the tank wall is used to raise the average liquid temperature and the remaining is transferred to the vapor region. Both parts resume constant values as a stable configuration is reached. Eventually, the rate of the pressure rise becomes constant. As the heat flux increases, the pressure and pressure rise rate increase.
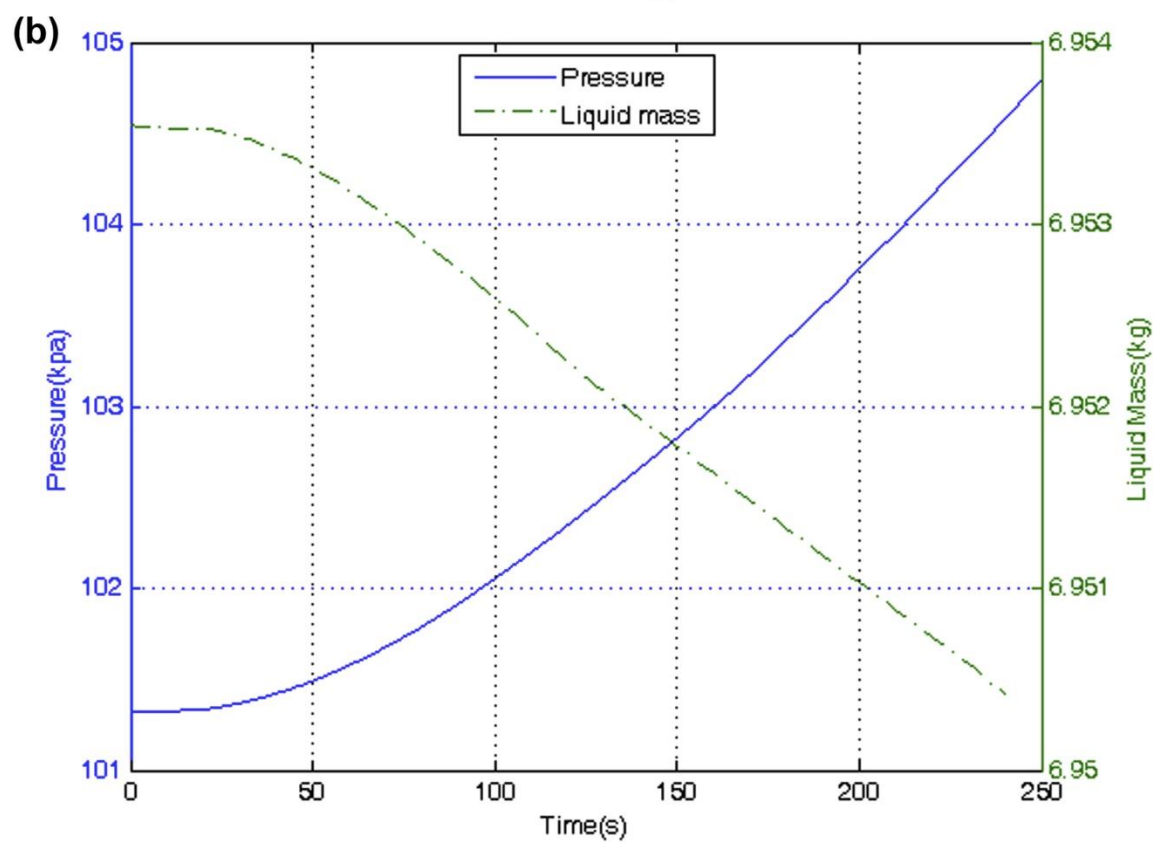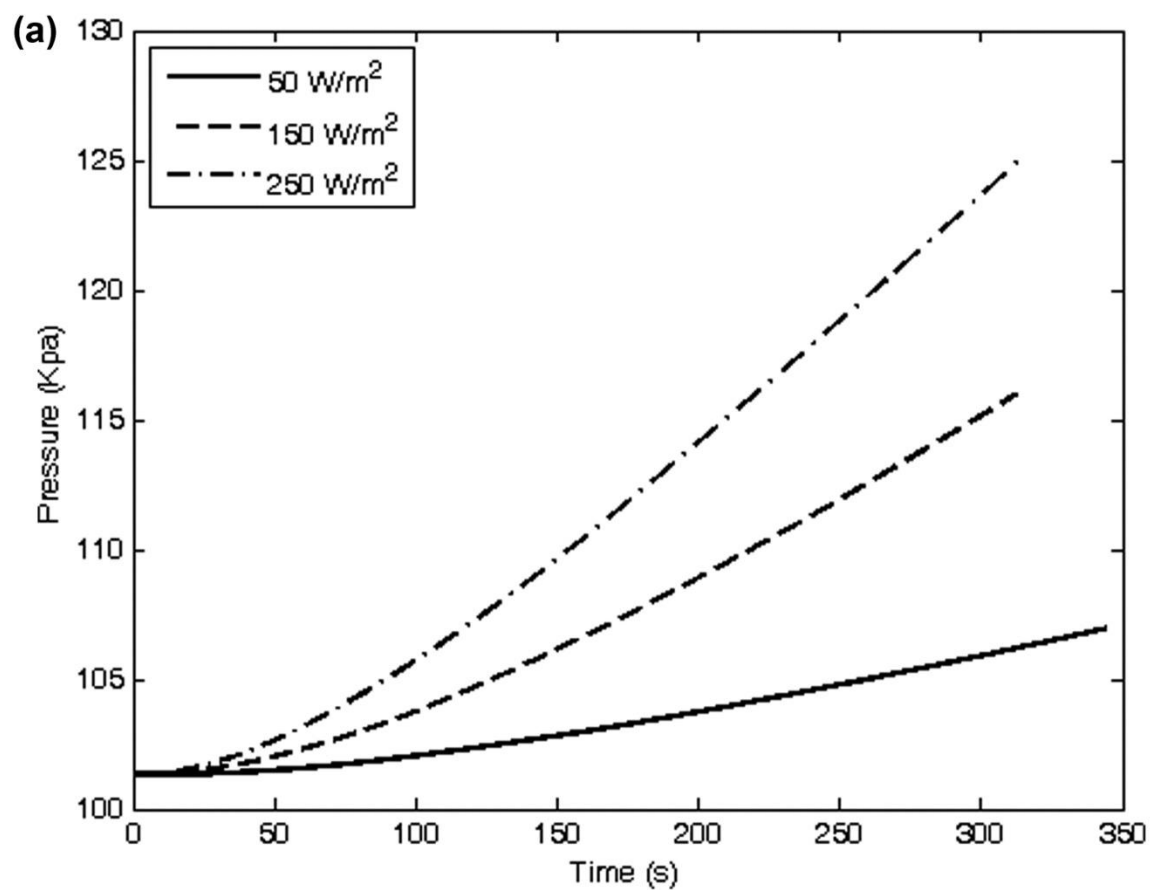
FIGURE 5.2 (a) Variation of vapor pressure for different heat fluxes. (b) Variation of vapor pressure and liquid mass with time. The heat flux is 50 W/m^2.

Fig. 5.3 presents temperature distributions in the LH$_2$ tank after 100 s of heating. It can be observed that temperature stratification appears in the liquid zone. The stratification is more intensive for larger heat fluxes. At the sidewall where the heat load is imposed, steep temperature gradients occur. This also happens at the interface (Fig. 5.3a and b). The temperature at the interface is higher than the given temperature range for the heat flux 250 W/m^2, so it is not shown in Fig. 5.3c. As the sidewall heat flux is increased, not only does the free surface temperature increase but also evaporation commences before a stratified layer is built up. In the vapor part, temperature stratification occurs mainly in the radial direction with a steep gradient at the centerline. This can be explained by the fluid flow, as shown in Fig. 5.4.
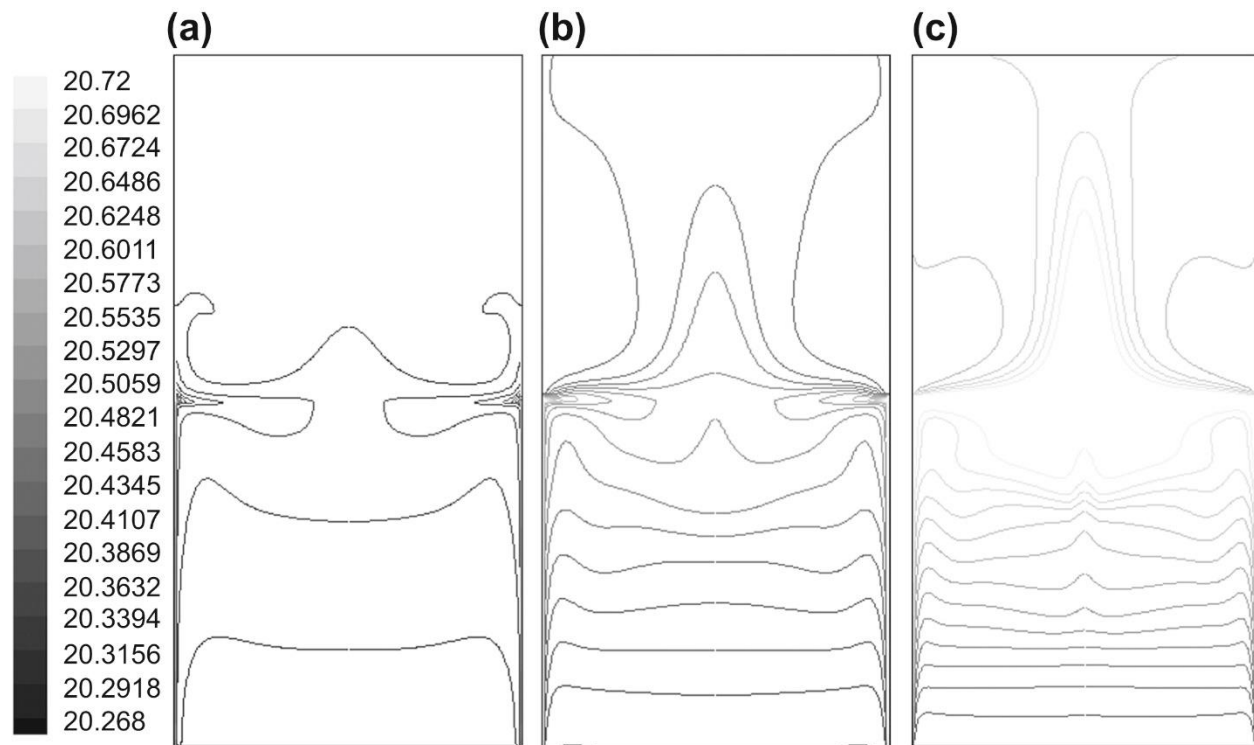
FIGURE 5.3 Temperature contours for three different heat fluxes after 100 s: (a) 50, (b) 150, and (c) 250 W/m^2.

Fig. 5.4 shows that the liquid near the heated wall moves up because of buoyancy forces. After reaching the top surface, it turns toward the central part. Because of the symmetry at the centerline, it then turns toward the bottom. Circulating flow patterns are formed in the liquid. The downward movement near the wall indicates that the circulating fluid temperature is higher than that of the layer adjacent to the boundary layer along the wall. This is because in case of a uniform wall heat flux, the wall temperature increases with height [16], and the circulating fluid is hottest when it reaches the top of the cavity. Although the fluid loses some heat while executing its first loop, its temperature may still be higher than that of the boundary layer adjacent to the wall. A secondary loop is also observed. Below this circulating zone, there is a bulk fluid movement toward the bottom to compensate the upward flow near the heated walls. This kind of fluid flow was also observed in experiments carried out by Das et al. [17]. The vapor part seems to be heated from the

bottom by the evaporation process. The hottest liquid parts meet at the center of the interface. Part of the liquid enters the flow loops in the liquid region for cooling, whereas another part becomes vapor by evaporation, and the latent heat of the phase change is absorbed. The heated vapor in the central part reaches the top of the tank because of the buoyancy forces. After the hot vapor has reached the top, it turns toward the cool side vapor wall. For the smaller heat flux, more time is needed to develop the vapor flow. At the same time, the larger the heat flux, the bigger the developed flow region. As time elapses, the pressure rise rate becomes constant and the liquid region represents a thermally stable and stratified region (Fig. 5.5). The contour plots are combined into a single image with the isotherms to the left and the streamlines to the right in each of Fig. 5.5(a)–(c). The average temperature of the liquid becomes high and the liquid remaining for cooling is not sufficient, so the hot liquid flow intensively induces many small loops just below the interface.
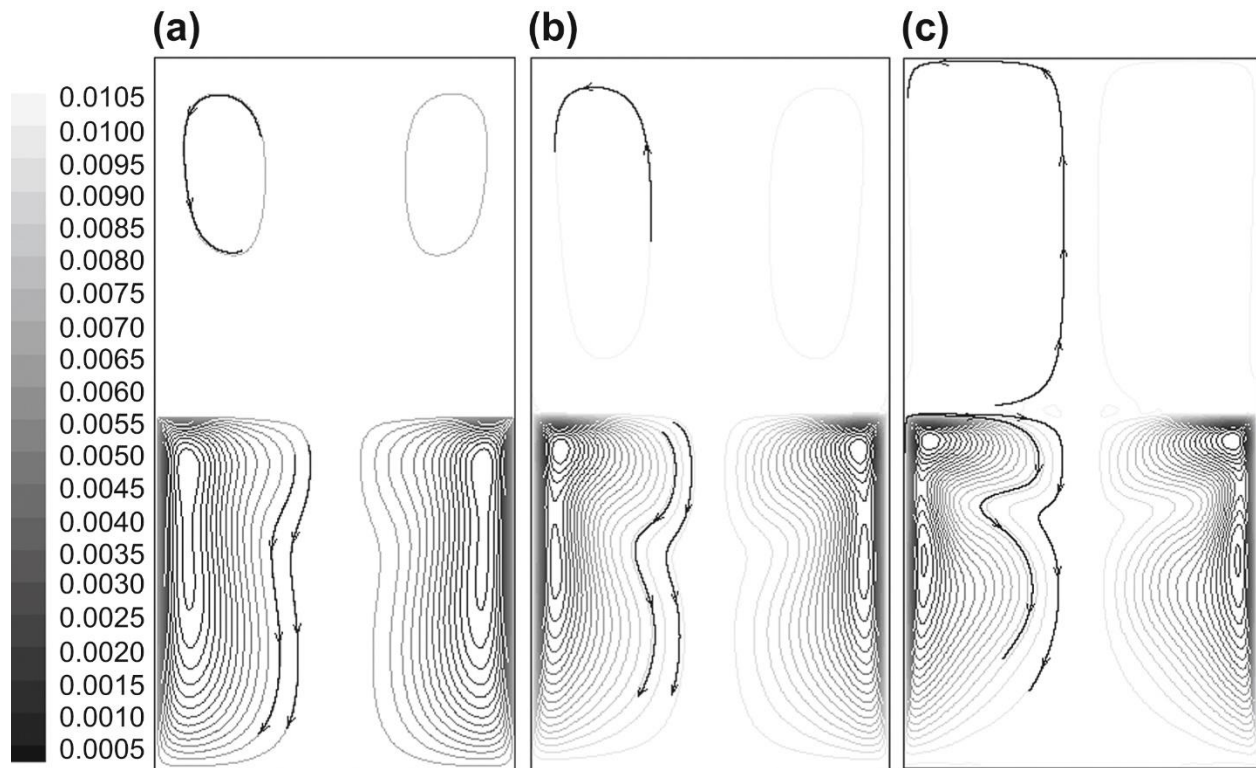
FIGURE 5.4 Streamlines for three different heat fluxes at 100 s: (a) 50, (b) 150, and (c) 250 W/m².

In Fig. 5.6 the tank pressurization behavior is depicted for different fill levels. The pressure variations for the fill levels 30%, 50%, and 80% at a heat flux of 50 W/m² are shown. Again the pressure rise begins after a certain period of sidewall heating. The liquid is heated and this forces the enthalpy to exceed the saturation value corresponding to the vapor hydrogen pressure. Evaporation is then assumed to occur. The superheated period decreases as the fill level increases. A longer time is required before the pressure rise rate becomes constant for higher fill levels. The larger the liquid fraction, the larger the pressure rise caused by the expansion of the initial liquid volume. The thermal stratification degree in the liquid is similar, so about the same amount of heat is transferred to the vapor. The vapor volume is smaller for high fill levels and accordingly the pressures are higher than those for low fill levels.

FIGURE 5.5 Isocontours of temperature and stream function of self-pressurization for three different heat fluxes: (a) 50, (b) 150, and (c) 250 W/m^2.
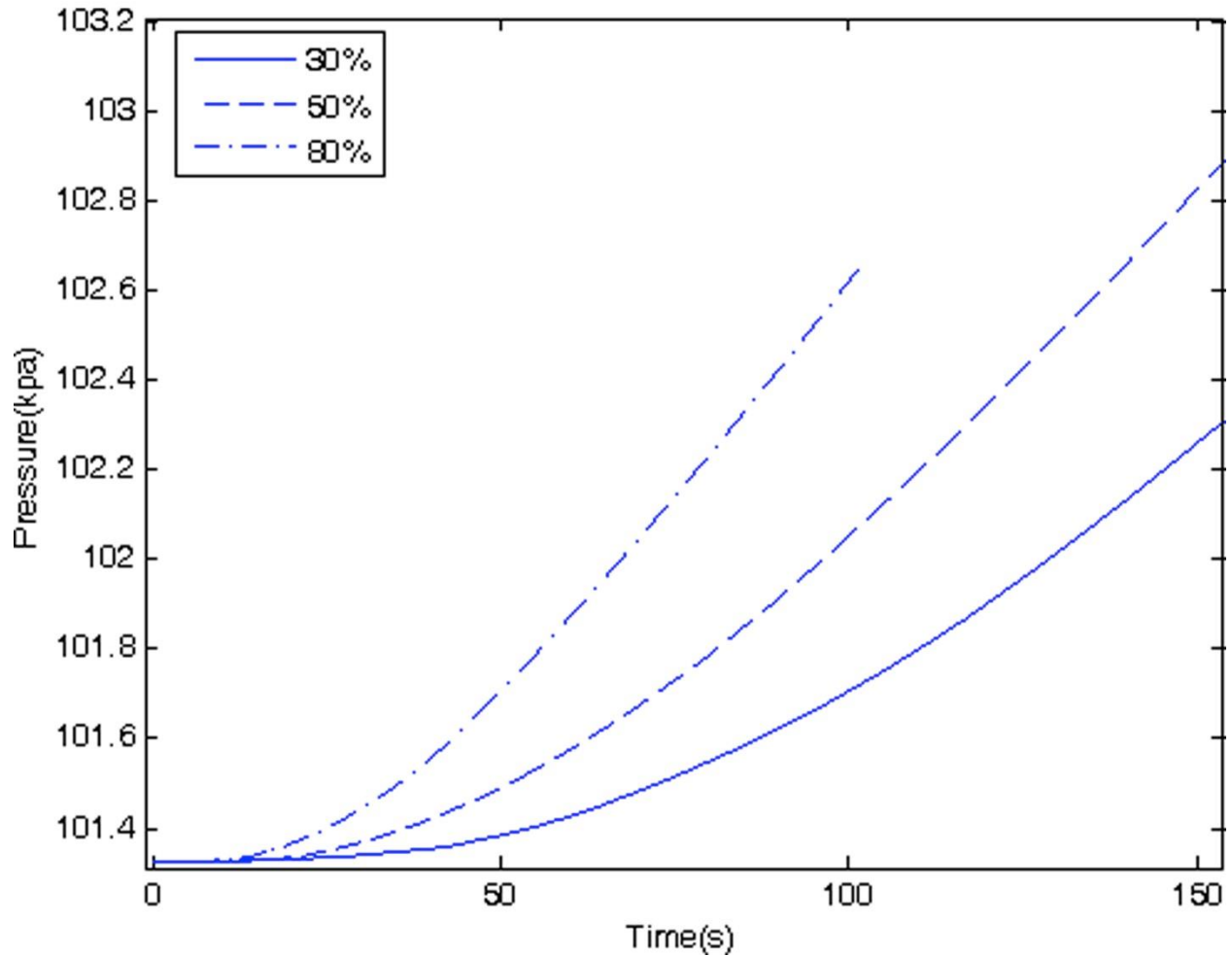
FIGURE 5.6 Variation of vapor pressure for different fill levels.

The temperature variation and stream function for three fill levels are illustrated in <ins>Fig. 5.7</ins>. It is observed that the stratification degree is similar, and the stream function is also similar. This is because when the fill level increases, the amount of heat transferred to the tank also increases as the heat flux on the LH_2 side is kept uniform at 50 W/m^2.

5.5. Cryogenic Heat Transfer Characteristics

Generally the heat transfer processes with cryogens are very similar to those at higher temperature ranges. The superfluid helium might, however, show some differences. Also many investigations have been carried out on helium, whereas other cryogens such as LH_2 are much less investigated. The strong variation of the thermophysical properties of fluids and materials at low temperature has some impacts. The relative and absolute magnitude of the various heat transfer processes may be very different from those at room temperature and the equations become nonlinear. This has to be taken into account in the cryogenic thermal design of, e.g., thermal insulation of cryostats and transfer lines. In this section the process of heat transfer between a solid material and an adjacent cryogenic fluid is considered. The processes of interest are internal forced flow in single phase, free convection in single phase, internal two-phase flow, and pool boiling two-phase flow. The current understanding is primarily from empirical correlations based on

dimensionless numbers. The issue is relevant to the design of heat exchangers, cryogenic fluid storage, superconducting magnets, and low-temperature instrumentation.

(a)
20.72
20.6962
20.6724
20.6486
20.6248
20.6011
20.5773
20.5535
20.5297
20.5059
20.4821
20.4583
20.4345
20.4107
20.3869
20.3632
20.3394
20.3156
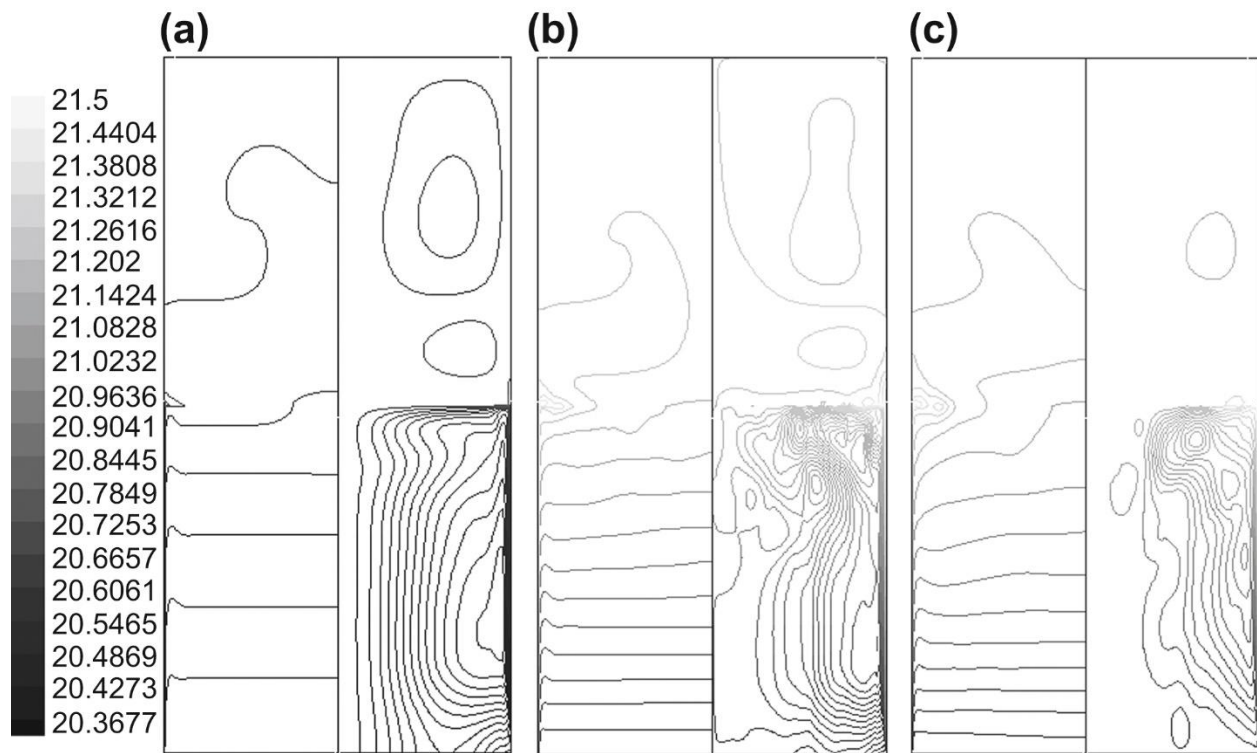20.2918
20.268

(b)

(c)
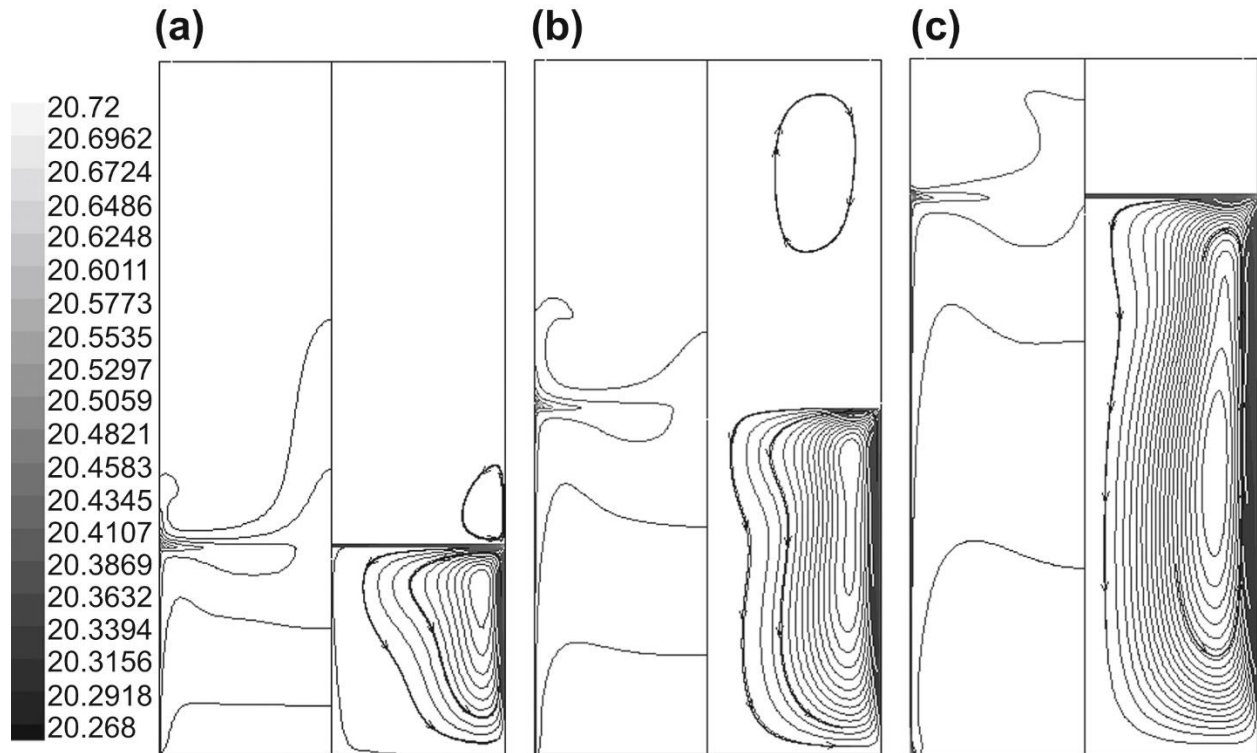
FIGURE 5.7 Isocontours of temperature and stream function of self-pressurization for three different fill levels at 100 s: (a) 30%, (b) 50%, and (c) 80%.

For single-phase internal flow heat transfer, commonly, the classical correlations [18] are used. This means if entrance effects are not considered, the Nusselt number is 3.656 or 4.364 depending on the boundary conditions for laminar flow, whereas for turbulent flow the Dittus–Boelter correlation is applied. For forced convection heat transfer experiments in supercritical helium, it has been found that the heat transfer coefficients are somewhat higher than those predicted by the Dittus–Boelter correlation. A slightly modified correlation has been suggested by Giarratano et al. [19,20], as it provided the best representation of many data. The correlation reads as

$$\mathrm{Nu} = 0.0259 \cdot \mathrm{Re}^{0.8} \cdot \mathrm{Pr}^{0.4} \cdot \left(\frac{T_w}{T_b}\right)^{-0.716}$$

(5.19)

Here, in comparison to the Dittus–Boelter correlation, the constant in front of the Reynolds number is increased from 0.023 and a temperature correction factor is introduced to take care of the temperature dependence of the thermophysical properties. T_w is the wall temperature and T_b is the fluid bulk temperature.

Heat exchangers in cryogenic systems might be of forced single-phase fluid–fluid counterflow type like a refrigerator or liquefier. LN_2 can be used for precooling of helium in a coil placed in a pool of cryogenic LN_2. Static boiling liquid–liquid might be used as a liquid subcooler in a magnet system.

For free or natural convection in low-temperature helium, correlations for the laminar and turbulent regimes have been suggested as

$$\text{Ra} < 10^9; \; \text{Nu} = 0.615 \cdot (\text{Gr} \cdot \text{Pr})^{0.258} \tag{5.20}$$

$$\text{Ra} > 10^9; \; \text{Nu} = 0.0176 \cdot (\text{Gr} \cdot \text{Pr})^{0.38} \tag{5.21}$$

where Gr is the Grashof number and Gr·Pr is the Rayleigh number, Ra. The constants and exponents in Eqs. (5.20) and (5.21) differ slightly from formulas for higher temperatures and other media [18]. In helium cryostats, strong natural convection processes with the Grashof number up to 10^{12} have been reported.

An investigation [21] on liquid and supercritical hydrogen in pool boiling has shown that the nucleate boiling heat transfer coefficient is higher at higher pressure. The critical heat flux is highest close to 0.4 MPa but is lower than the value predicted by the Kutateladze correlation for higher pressure. The reason is that the transition to film boiling is dominated not by the heat flux due to hydrodynamic instability but by the surface temperature. Another study [22] focused on pool boiling of hydrogen for normal gravity and low-gravity situations. A validated and proposed gravity scaling analysis was presented, and this might be helpful in the design process of hydrogen heat transfer systems.

General conclusions from heat transfer studies of cryogenics reveal the following:

a. Single-phase heat transfer correlations (free and forced convection) for common fluids are also applicable for cryogenic fluids, but as stated earlier, constants and exponents may differ somewhat.

b. Two-phase heat transfer in cryogenic fluids can be based on correlations for common fluids. This holds for nucleate boiling, the critical heat flux, and film boiling.

c. Transient heat transfer is governed by diffusive process for ΔT and onset of film boiling.

5.6. Hydrogen in Aerospace Applications

A review of the scenario for using hydrogen as a fuel with a potential for zero emission was presented by Cecere et al. [23]. The history of hydrogen as propellant was summarized. The hydrogen fuel engines in low-and high-Mach-number flights were reviewed. It was concluded that hydrogen might be the fuel of the future as environmental issues and supply sources are taken into consideration. A drawback is that if hydrogen is burnt in air, NO_x is created and this might be a concern for ground transportation. For long-range aircraft transportation, use of hydrogen is believed to have some potential and the LH_2 might be stored in the fuselage to minimize the surface-to-volume ratio and prevent heat losses. Hydrogen is used in space propulsion, and it is foreseen that it will be used in future hypersonic commercial aircraft using supersonic ram jets (scramjet) because of its high energy content.

Introduction

- Storage of a cryogen (say, **LN2**) is difficult, as there is a continuous boil off due to heat in leaks.

- These vessels cannot be sealed as boil off generates huge volumes of vapour, resulting in large pressure rise. This may lead to bursting.

- For example, vapor to liquid volume ratio for a general cryogen is 175 (1600 for water).

- To avoid the pressure rise, the need of insulation is vital. Insulation or a combination of insulations, minimize all these modes of heat transfer.

Heat Transfer

- Consider a **LN2** container as shown in the figure.

- The inner vessel is housed inside an outer vessel and these vessels are separated by some form of insulation.

- Also, the inner vessel is supported using lateral beams as shown.

- The liquid boils off continuously due to the various modes of heat transfer.
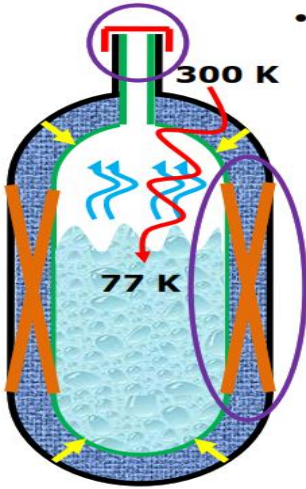
Heat Transfer

- Different modes of heat transfer are
  - **Conduction**: The heat is conducted through lateral beams, neck and residual gas conduction.

  - **Convection**: The air between inner and outer vessels convect heat into the liquid.

  - **Radiation**: The radiation heat transfer from 300 K outer vessel to 77 K inner vessel.

Types of Insulation

```
                    Insulation
                        |
        +---------------+---------------+
        |               |               |
      Mass          Reflective        Vacuum
        |                               
   +----+----+                          
   |    |    |                          
Cellular Granular Fibrous              
                  |                     
            +-----+-----+               
            |           |               
         Metal      Multi Layer         
         Foils      Insulation          
```
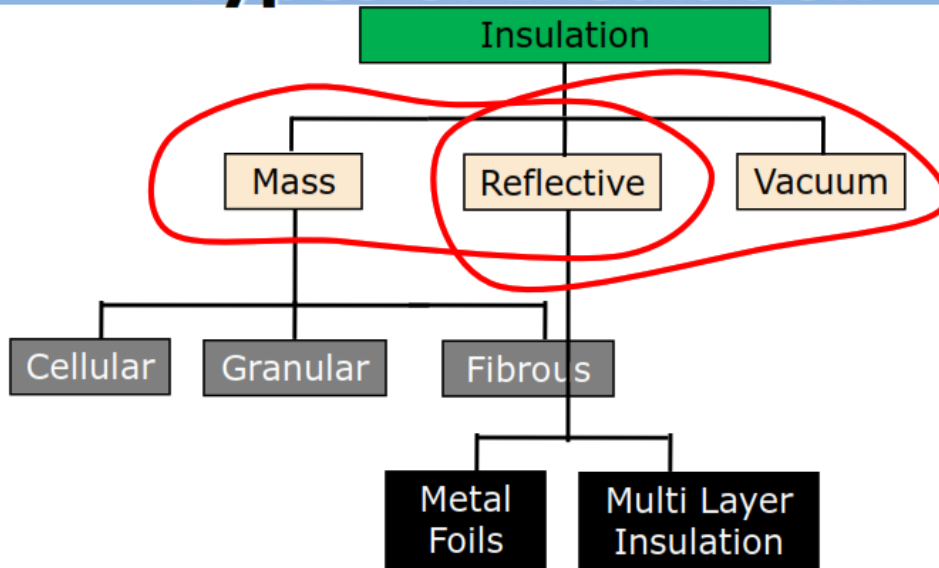
Types of Insulation

- Expanded Foam – Mass

- Gas Filled Powders & Fibrous Materials – Mass

- Vacuum alone – Vacuum

- Evacuated Powders – Mass + Vacuum

- Opacified Powders – Mass + Vacuum + Reflective

- Multilayer Insulation – Vacuum + Reflective

Types of Insulation

- The choice of insulation for a particular application is a compromise between the following factors.

  - Thermal Conductivity
  - Temperature
  - Effectiveness of Insulation
  - Cost
  - Ease of application
  - Weight and reliability

- A combination of insulations is used to prevent different modes of heat transfer.

Apparent Thermal Conductivity

- As seen earlier, the different modes of heat transfer are Gas and Solid Conductions, Convection and Radiation.

- Consider an element of insulation, separated by two temperatures ($T_1 > T_2$) as shown below.

$T_1 \xrightarrow{\quad Q \quad} T_2$
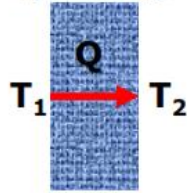
- Let **Q** be net heat transferred across this element by all possible modes of heat transfer mentioned above.

Apparent Thermal Conductivity

$T_1 \xrightarrow{\quad Q \quad} T_2$

A

L
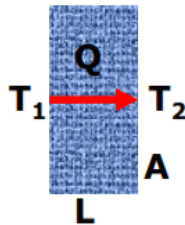
- If **A** and **L** be the area of the cross section and length of the element respectively, the apparent thermal conductivity (k_A) is defined as

$$k_A = \frac{QL}{A(T_1 - T_2)}$$

- In other words, this apparent thermal conductivity is calculated based on all possible modes of heat transfer.

Expanded Foams

- Expanded foam is a low density, cellular structure which is formed by evolving gases during the manufacturing process.

- Gases that are generally used are CO_2 and Freon.

- In other words, it is a solid – gas matrix with void spaces. The solid connections together with gas trapped in cellular spaces form a continuous path.

- The heat is transferred only by conduction (solid conduction). The contribution by convection and radiation are negligible.

Expanded Foams

- Examples are polyurethane foam, polystyrene foam, rubber, silica glass foam.

- k_A and density are as shown below. The operating temperature is between **77 K** to **300 K**.

Foam	ρ (kg/m³)	k (mW/mK)
Polyurethane	11	33
Polystyrene	39	33
	46	26
Rubber	80	36
Silica	160	55
Glass	140	35

Expanded Foams

Thermal Conductivity – mW/m-K

Mean Cell Diameter - µm
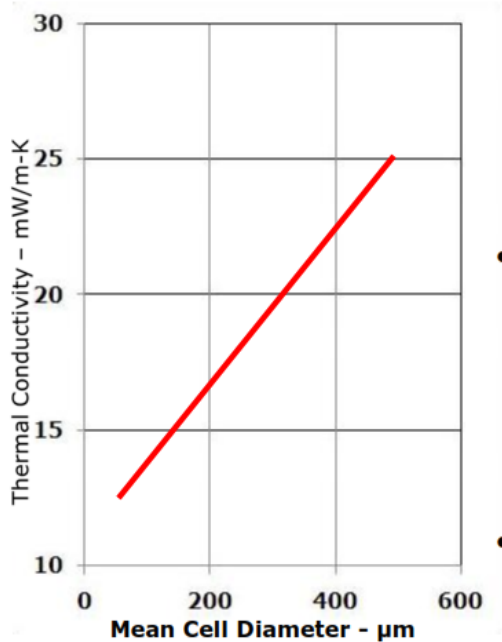
- The k_A of the foam depends on the type of gas used and also the temperature of the insulation.

- For a given gas, the performance of the foam is improved by varying the void size and bulk density.

- The adjacent figure shows the variation of k_A with the mean cell diameter.

Expanded Foams

Thermal Conductivity – mW/m-K

Mean Cell Diameter - µm
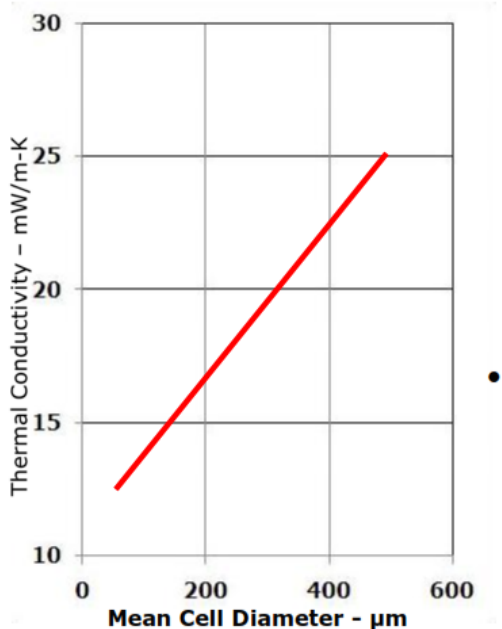
- With the decrease in the mean cell diameter, the solid conduction path increases in the foam insulation.

$$k_A = \frac{QL}{A(T_1 - T_2)}$$

- From the above equation, the **Q** decreases and hence the k_A decreases.

Expanded Foams
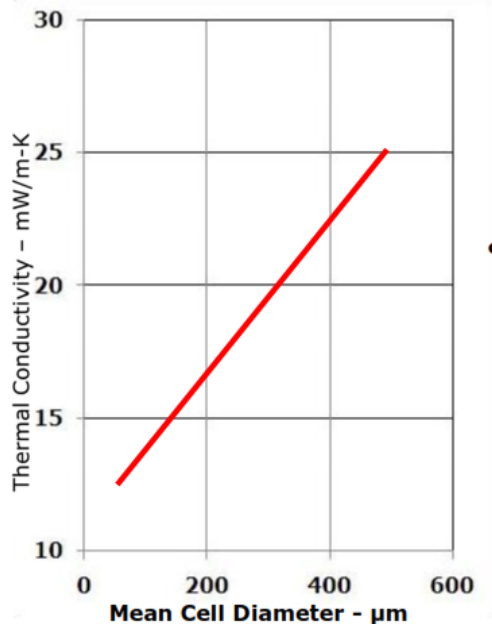
- At the same time, with the decrease in the mean cell diameter, the bulk density of the foam increases.

- Therefore, k_A is also a function of bulk density and it increases with the increase in bulk density.

Expanded Foams

- The major advantage of an expanded foam is that it offers an ease of fabrication.

- The foam is directly blown onto the surface of the vessel to be insulated. It forms a self supporting structure.

- The cost of this insulation is also low as compared to other types of insulations.

Expanded Foams

- Exposure of a CO_2 expanded foam to **LN2** temperatures, increases the thermal conductivity.

- At **LN2** temperature, the vapor pressure of CO_2 is less. As a result, most of CO_2 is condensed within the insulation and caters for the heat transfer.

- Also over a period of time, air, hydrogen or helium diffuse into foam from external atmosphere.

- The k_A of the foam increases due to increase in the gas conduction at room temperature.

Expanded Foams

- Expanded foams have large thermal contractions, which pose a major disadvantage.

- A rigid foam has a large thermal contraction between -30°C to +30°C.

- For example, coefficients of linear expansion are
  - $\alpha_{\text{Polystyrene Foam}}$: 7.20×10^{-5}/°C
  - $\alpha_{\text{Carbon Steel}}$: 1.15×10^{-5}/°C

- The foam when closely fitted around a **LN2** vessel, crack due to difference in shrinkages.

Gas Filled Powder & Fibrous Insulations

- A gas filled powder or a fibrous insulation reduces or eliminates the gas convection due to the small size of voids within the material.

- This is because, the distance between the powder particles within the insulation is much smaller than the gas mean free path.

- As a result, the gaseous conduction mechanism shifts from continuum to free molecular conduction decreasing the apparent thermal conductivity, k_A.

Gas Filled Powder & Fibrous Insulations

- The commonly used insulations of this type are Fiber Glass, Perlite (Silica Powder), Santocel, Rockwool, Vermichlitine.

- k_A and density are as shown below. The operating temperatures are between **77 K** to **300 K**.

Insulation	ρ (kg/m³)	k (mW/mK)
Perlite	50	26
Silica Aerogel	80	19
Fiber glass	10	25
Rockwool	160	35

Gas Filled Powder & Fibrous Insulations

- The advantages of a gas filled powder are low thermal conductivity, low density and low particle distribution to minimize the vibration effects.

- The insulation can either be evacuated or non – evacuated. Heat transfer by residual gas is further minimized by low vapor pressure of the gas.

- Finely divided particulate materials make solid conduction paths disjointed and discontinuous.

Gas Filled Powder & Fibrous Insulations

- The disadvantage is that moisture and air diffuse through the material to the cold surface unless a vapor barrier is used. N_2 purging is used.

- Fill – gas should be unreactive and compatible with powder material.

- Powder tends to settle and packs due to vibrations, thermal contraction and expansion.

- The disadvantage is that moisture and air diffuse through the material to the cold surface unless a vapor barrier is used. N_2 purging is used.

- Fill – gas should be unreactive and compatible with powder material.

- Powder tends to settle and packs due to vibrations, thermal contraction and expansion.

- This creates increased solid conduction.

Gas Filled Powder & Fibrous Insulations

- Nusselt & Bayer developed the following expression for k_A for a gas filled powder.

$$k_A = \left[\frac{V_r}{k_s} + \left[\frac{k_g}{(1-V_r)} + \frac{4\sigma T^3 d}{V_r} \right]^{-1} \right]^{-1}$$

- V_r – Ratio of solid particulate to total volume.
- k_s & k_g – Thermal conductivity of Solid and Gas.
- T – Mean temperature.
- d – Mean diameter of fiber or powder.

Gas Filled Powder & Fibrous Insulations

$$k_A = \left[\frac{V_r}{k_s} + \left[\frac{k_g}{(1-V_r)} + \frac{4\sigma T^3 d}{V_r} \right]^{-1} \right]^{-1}$$

- At cryogenic temperatures, two assumptions are made
  - T^3 term is very small relative to k_g term.
  - $k_s \gg k_g$

- Therefore, the equation is $\quad k_A = \dfrac{k_g}{(1-V_r)}$

Gas Filled Powder & Fibrous Insulations

$$k_A = \frac{k_g}{(1-V_r)}$$

- Therefore, as V_r tends to zero, k_A approaches k_g.

- This is the lowest possible thermal conductivity of this insulation.

Radiation – Fundamentals

- Consider two flat surfaces maintained at different temperatures ($T_1 > T_2$) as shown in the figure.
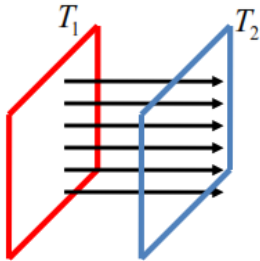
- There is continuous heat transfer between the two plates due to the radiation.

- This mode of heat transfer does not require any medium and is given by the following equation.

$$Q = F_e F_{1 \to 2} \sigma A_1 \left(T_2^4 - T_1^4 \right)$$

Radiation – Fundamentals

$$Q = F_e F_{1 \to 2} \sigma A_1 \left(T_2^4 - T_1^4 \right)$$
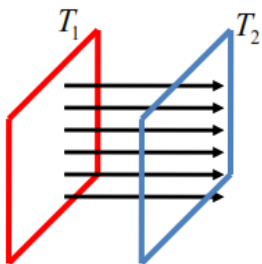
- In the above equation, it is clear that for a given A_1, T_1, T_2, $F_{1 \to 2}$, **Q** is directly proportional to the emissivity factor F_e.

- The F_e is reduced by introducing the radiation shields in the path of radiation heat transfer as shown.

- The effect of these shields is as explained in the next slide.

Radiation Shields

- The effective emissivity factor **F$_N$** after introduction of **N** shields is as given below.

$$\frac{1}{F_N} = \left(\frac{1}{e_1} + \frac{1}{e_s} - 1\right) + (N-1)\left(\frac{2}{e_s} - 1\right) + \left(\frac{1}{e_2} + \frac{1}{e_s} - 1\right)$$

- For the sake of understanding, let the values of **e$_1$**, **e$_2$**, and **e$_s$** be 0.8, 0.8, 0.05 respectively.

- Students are advised to calculate and compare **F$_N$** for following cases.
    - Case 1: N=0
    - Case 2: N=10

Radiation Shields

- Case 1 : N=0 – $F_N = 0.667$

- Case 2 : N=10 – $F_N = 0.00255$

- It is clear that the **F$_N$** decreases drastically with the introduction of radiation shields.

- These shields are aluminum foils with a very high reflectivity.

Summary

- Cryogenic vessels need insulation to minimize all modes of heat transfer.

- The apparent thermal conductivity is calculated based on all possible modes of heat transfer.

- Expanded foam is a low density, cellular structure. The heat is transferred only by solid conduction.

- With the decrease in the mean cell diameter, the k_A decreases. With the increase in the bulk density, the k_A also increases.

- A gas filled powder or a fibrous insulation reduces gas convection due to the small size of voids. The heat is transferred by free molecular conduction.

- Fill – gas should be unreactive and compatible with powder material.

- Radiation heat transfer does not require any medium. It is reduced by introduction of radiation shields.

- These shields are aluminum foils with a very high reflectivity.

Chapter 3
Aircraft Fabric Covering

General History

Fabric-covered aircraft play an important role in the history of aviation. The famous Wright Flyer utilized a fabric-covered wood frame in its design, and fabric covering continued to be used by many aircraft designers and builders during the early decades of production aircraft. The use of fabric covering on an aircraft offers one primary advantage: light weight. In contrast, fabric coverings have two disadvantages: flammability and lack of durability.

Finely woven organic fabrics, such as Irish linen and cotton, were the original fabrics used for covering airframes, but their tendency to sag left the aircraft structure exposed to the elements. To counter this problem, builders began coating the fabrics with oils and varnishes. In 1916, a mixture of cellulose dissolved in nitric acid, called nitrate dope, came into use as an aircraft fabric coating. Nitrate dope protected the fabric, adhered to it well, and tautened it over the airframe. It also gave the fabric a smooth, durable finish when dried. The major drawback to nitrate dope was its extreme flammability.

To address the flammability issue, aircraft designers tried a preparation of cellulose dissolved in butyric acid called butyrate dope. This mixture protected the fabric from dirt and moisture, but it did not adhere as well to the fabric as nitrate dope. Eventually, a system combining the two dope coatings was developed. First, the fabric was coated with nitrate dope for its adhesion and protective qualities. Then, subsequent coats of butyrate dope were added. Since the butyrate dope coatings reduced the overall flammability of the fabric covering, this system became the standard fabric treatment system.

The second problem, lack of durability, stems from the eventual deterioration of fabric from exposure to the elements that results in a limited service life. Although the mixture of nitrate dope and butyrate dope kept out dirt and water, solving some of the degradation issue, it did not address deterioration caused by ultraviolet (UV) radiation from the sun. Ultraviolet radiation passed through the dope and degraded not only the fabric, but also the aircraft structure underneath. Attempts to paint the coated fabric proved unsuccessful, because paint does not adhere well to nitrate dope. Eventually, aluminum solids were added to the butyrate coatings. This mixture reflected the sun's rays, prevented harmful UV rays from penetrating the dope, and protected the fabric, as well as the aircraft structure.

Regardless of treatments, organic fabrics have a limited lifespan; cotton or linen covering on an actively flown aircraft lasts only about 5–10 years. Furthermore, aircraft cotton has not been available for over 25 years. As the aviation industry developed more powerful engines and more aerodynamic aircraft structures, aluminum became the material of choice. Its use in engines, aircraft frames, and coverings revolutionized aviation. As a covering, aluminum protected the aircraft structure from the elements, was durable, and was not flammable.

Although aluminum and composite aircraft dominate modern aviation, advances in fabric coverings continue to be made because gliders, home-built, and light sport aircraft, as well as some standard and utility certificated aircraft, are still

Figure 3-1. *Examples of aircraft produced using fabric skin.*

produced with fabric coverings. *[Figure 3-1]* The nitrate/butyrate dope process works well, but does not mitigate the short lifespan of organic fabrics. It was not until the introduction of polyester fabric as an aircraft covering in the 1950s that the problem of the limited lifespan of fabric covering was solved. The transition to polyester fabric had some problems because the nitrate and butyrate dope coating process is not as suitable for polyester as it is for organic fabrics. Upon initial application of the dopes to polyester, good adhesion and protection occurred; as the dopes dried, they would eventually separate from the fabric. In other words, the fabric outlasted the coating.

Eventually, dope additives were developed that minimized the separation problem. For example, plasticizers keep the dried dope flexible and nontautening dope formulas eliminate separation of the coatings from the fabric. Properly protected and coated, polyester lasts indefinitely and is stronger than cotton or linen. Today, polyester fabric coverings are the standard and use of cotton and linen on United States certificated aircraft has ceased. In fact, the long staple cotton from which grade-A cotton aircraft fabric is made is no longer produced in this country.

Re-covering existing fabric aircraft is an accepted maintenance procedure. Not all aircraft covering systems include the use of dope coating processes. Modern aircraft covering systems that include the use of nondope fabric treatments show no signs of deterioration even after decades of service. In this

chapter, various fabrics and treatment systems are discussed, as well as basic covering techniques.

Fabric Terms

To facilitate the discussion of fabric coverings for aircraft, the following definitions are presented. *Figure 3-2* illustrates some of these items.
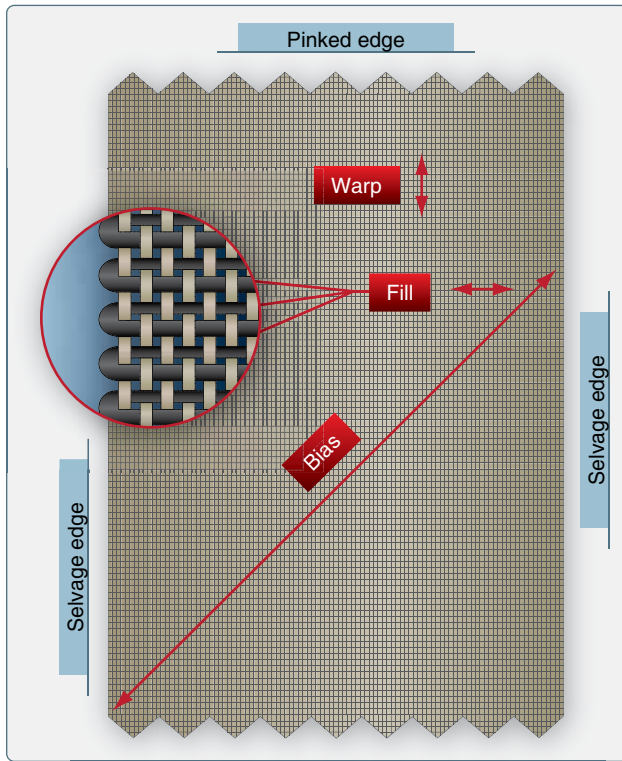
Figure 3-2. *Aircraft fabric nomenclature.*

- Warp—the direction along the length of fabric.
- Fill or weave—the direction across the width of the fabric.

- Count—the number of threads per inch in warp or filling.
- Ply—the number of yarns making up a thread.
- Bias—a cut, fold, or seam made diagonally to the warp or fill threads.
- Pinked edge—an edge which has been cut by machine or special pinking shears in a continuous series of Vs to prevent raveling.
- Selvage edge—the edge of cloth, tape, or webbing woven to prevent raveling.
- Greige—condition of polyester fabric upon completion of the production process before being heat shrunk.
- Cross coat—brushing or spraying where the second coat is applied 90° to the direction the first coat was applied. The two coats together make a single cross coat. *[Figure 3-3]*

Legal Aspects of Fabric Covering

When a fabric-covered aircraft is certificated, the aircraft manufacturer uses materials and techniques to cover the aircraft that are approved under the type certificate issued for that aircraft. The same materials and techniques must be used by maintenance personnel when replacing the aircraft fabric. Descriptions of these materials and techniques are in the manufacturer's service manual. For example, aircraft originally manufactured with cotton fabric can only be re-covered with cotton fabric unless the Federal Aviation Administration (FAA) approves an exception. Approved exceptions for alternate fabric-covering materials and procedures are common. Since polyester fabric coverings deliver performance advantages, such as lighter weight, longer life, additional strength, and lower cost, many older aircraft originally manufactured with cotton fabric have received approved alteration authority and have been re-covered with polyester fabric.
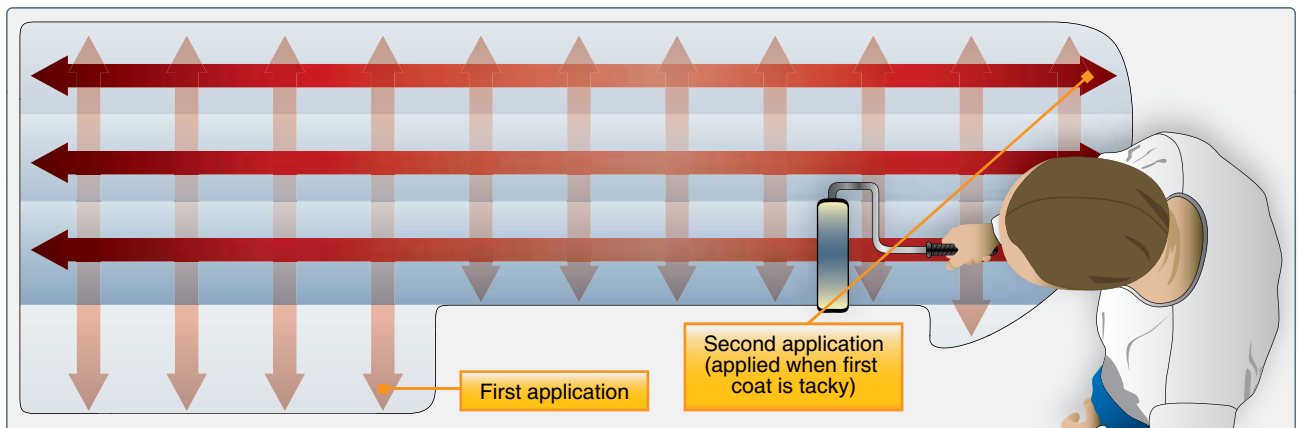
Figure 3-3. *A single cross coat is made up of two coats of paint applied 90° to each other.*

There are three ways to gain FAA approval to re-cover an aircraft with materials and processes other than those with which it was originally certificated. One is to do the work in accordance with an approved supplemental type certificate (STC). The STC must specify that it is for the particular aircraft model in question. It states in detail exactly what alternate materials must be used and what procedure(s) must be followed. Deviation from the STC data in any way renders the aircraft unairworthy. The holder of the STC typically sells the materials and the use of the STC to the person wishing to re-cover the aircraft.

The second way to gain approval to re-cover an aircraft with different materials and processes is with a field approval. A field approval is a one-time approval issued by the FAA Flight Standards District Office (FSDO) permitting the materials and procedures requested to replace those of the original manufacturer. A field approval request is made on FAA Form 337. A thorough description of the materials and processes must be submitted with proof that, when the alteration is completed, the aircraft meets or exceeds the performance parameters set forth by the original type certificate.

The third way is for a manufacturer to secure approval through the Type Certificate Data Sheet (TCDS) for a new process. For example, Piper Aircraft Co. originally covered their PA-18s in cotton. Later, they secured approval to recover their aircraft with Dacon fabric. Recovering an older PA-18 with Dacron in accordance with the TCDS would be a major repair, but not an alteration as the TCDS holder has current approval for the fabric.

Advisory Circular (AC) 43.13.1, Acceptable Methods, Techniques, and Practices—Aircraft Inspection and Repair, contains acceptable practices for covering aircraft with fabric. It is a valuable source of general and specific information on fabric and fabric repair that can be used on Form 337 to justify procedures requested for a field approval. Submitting an FAA Form 337 does not guarantee a requested field approval. The FSDO inspector considers all aspects of the procedures and their effect(s) on the aircraft for which the request is being filed. Additional data may be required for approval.

Title 14 of the Code of Federal Regulations (14 CFR) part 43, Appendix A, states which maintenance actions are considered major repairs and which actions are considered major alterations. Fabric re-covering is considered a major repair and FAA Form 337 is executed whenever an aircraft is re-covered with fabric. Appendix A also states that changing parts of an aircraft wing, tail surface, or fuselage when not listed in the aircraft specifications issued by the FAA is a major alteration. This means that replacing cotton fabric with polyester fabric is a major alteration. A properly executed FAA Form 337 also needs to be approved in order for this alteration to be legal.

FAA Form 337, which satisfies the documentation requirements for major fabric repairs and alterations, requires participation of an FAA-certificated Airframe and Powerplant (A&P) mechanic with an Inspection Authorization (IA) in the re-covering process. Often the work involved in re-covering a fabric aircraft is performed by someone else, but under the supervision of the IA (IA certification requires A&P certification). This typically means the IA inspects the aircraft structure and the re-cover job at various stages to be sure STC or field approval specifications are being followed. The signatures of the IA and the FSDO inspector are required on the approved FAA Form 337. The aircraft logbook also must be signed by the FAA-certificated A&P mechanic. It is important to contact the local FSDO before making any major repair or alteration.

Approved Materials

There are a variety of approved materials used in aircraft fabric covering and repair processes. In order for the items to legally be used, the FAA must approve the fabric, tapes, threads, cords, glues, dopes, sealants, coatings, thinners, additives, fungicides, rejuvenators, and paints for the manufacturer, the holder of an STC, or a field approval.

Fabric

A Technical Standard Order (TSO) is a minimum performance standard issued by the FAA for specified materials, parts, processes, and appliances used on civil aircraft. For example, TSO-15d, Aircraft Fabric, Grade A, prescribes the minimum performance standards that approved aircraft fabric must meet. Fabric that meets or exceeds the TSO can be used as a covering. Fabric approved to replace Grade-A cotton, such as polyester, must meet the same criteria. TSO-15d also refers to another document, Society of Automotive Engineers (SAE) Aerospace Material Specification (AMS) 3806D, which details properties a fabric must contain to be an approved fabric for airplane cloth. Lighter weight fabrics typically adhere to the specifications in TSO-C14b, which refers to SAE AMS 3804C.

When a company is approved to manufacture or sell an approved aviation fabric, it applies for and receives a Parts Manufacturing Approval (PMA). Currently, only a few approved fabrics are used for aircraft coverings, such as the polyester fabrics Ceconite™, Stits/Polyfiber™, and Superflite™. These fabrics and some of their characteristics are shown in *Figure 3-4*. The holders of the PMA for these fabrics have also developed and gained approval for the various tapes, chords, threads, and liquids that are used in the covering process. These approved materials, along with the procedures for using them, constitute the STCs for each particular fabric covering process. Only the approved materials can be used. Substitution of other materials is forbidden and results in the aircraft being unairworthy.

Approved Aircraft Fabrics					
Fabric Name or Type	Weight (oz/sq yd)	Count (warp x fill)	New Breaking Strength (lb) (warp, fill)	Minimum Deteriorated Breaking Strength	TSO
Ceconite™ 101	3.5	69 x 63	125,116	70% of original specified fabric	C-15d
Ceconite™ 102	3.16	60 x 60	106,113	70% of original specified fabric	C-15d
Polyfiber™ Heavy Duty-3	3.5	69 x 63	125,116	70% of original specified fabric	C-15d
Polyfiber™ Medium-3	3.16	60 x 60	106,113	70% of original specified fabric	C-15d
Polyfiber™ Uncertified Light	1.87	90 x 76	66,72	uncertified	
Superflight™ SF 101	3.7	70 x 51	80,130	70% of original specified fabric	C-15d
Superflight™ SF 102	2.7	72 x 64	90,90	70% of original specified fabric	C-15d
Superflight™ SF 104	1.8	94 x 91	75,55	uncertified	
Grade A Cotton	4.5	80 x 84	80,80	56 lb/in (70% of New)	C-15d

Figure 3-4. *Approved fabrics for covering aircraft.*

Other Fabric Covering Materials

The following is an introduction to the supplemental materials used to complete a fabric covering job per manufacturer's instruction or a STC.

Anti-Chafe Tape

Anti-chafe tape is used on sharp protrusions, rib caps, metal seams, and other areas to provide a smoother surface to keep the fabric from being torn. It is usually self-adhesive cloth tape and is applied after the aircraft is cleaned, inspected, and primed, but before the fabric is installed.

Reinforcing Tape

Reinforcing tape is most commonly used on rib caps after the fabric covering is installed to protect and strengthen the area for attaching the fabric to the ribs.

Rib Bracing

Rib bracing tape is used on wing ribs before the fabric is installed. It is applied spanwise and alternately wrapped around a top rib cap and then a bottom rib cap progressing from rib to rib until all are braced. *[Figure 3-5]* Lacing the ribs in this manner holds them in the proper place and alignment during the covering process.

Surface Tape

Surface tape, made of polyester material and often pre-shrunk, is obtained from the STC holder. This tape, also known as finishing tape, is applied after the fabric is installed.
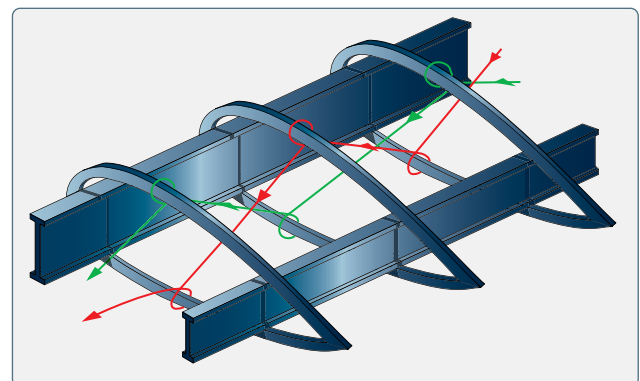
Figure 3-5. *Inter-rib bracing holds the ribs in place during the covering process.*

It is used over seams, ribs, patches, and edges. Surface tape can have straight or pinked edges and comes in various widths. For curved surfaces, bias cut tape is available, which allows the tape to be shaped around a radius.

Rib Lacing Cord

Rib lacing cord is used to lace the fabric to the wing ribs. It must be strong and applied as directed to safely transfer in-flight loads from the fabric to the ribs. Rib lacing cord is available in a round or flat cross-section. The round cord is easier to use than the flat lacing, but if installed properly, the flat lacing results in a smoother finish over the ribs.

Sewing Thread

Sewing of polyester fabric is rare and mostly limited to the creation of prefitted envelopes used in the envelope method covering process. When a fabric seam must be made with no structure underneath it, a sewn seam could be used. Polyester threads of various specifications are used on polyester fabric. Different thread is specified for hand sewing versus machine sewing. For hand sewing, the thread is typically a three-ply, uncoated polyester thread with a 15-pound tensile strength. Machine thread is typically four-ply polyester with a 10-pound tensile strength.

Special Fabric Fasteners

Each fabric covering job involves a method of attaching the fabric to wing and empennage ribs. The original manufacturer's method of fastening should be used. In addition to lacing the fabric to the ribs with approved rib lacing cord, special clips, screws, and rivets are employed on some aircraft. *[Figure 3-6]* The first step in using any of these fasteners is to inspect the holes into which they fit. Worn holes may have to be enlarged or re-drilled according to the manufacturer's instructions. Use of approved fasteners is mandatory. Use of unapproved fasteners can render the covering job unairworthy if substituted. Screws and rivets often incorporate the use of a plastic or aluminum washer. All fasteners and rib lacing are covered with finishing tape once installed to provide a smooth finish and airflow.

Grommets

Grommets are used to create reinforced drain holes in the aircraft fabric. Usually made of aluminum or plastic, they are glued or doped into place on the fabric surface. Once secured, a hole is created in the fabric through the center of the grommet. Often, this is done with a hot soldering pencil that also heat seals the fabric edge to prevent raveling. Seaplane grommets have a shield over the drain hole to prevent splashed water from entering the interior of the covered structure and to assist in siphoning out any water from within. *[Figure 3-7]* Drain holes using these grommets must be made before the grommets are put in place. Note that some drain holes do not require grommets if they are made through two layers of fabric.

Inspection Rings

The structure underneath an aircraft covering must be inspected periodically. To facilitate this in fabric-covered aircraft, inspection rings are glued or doped to the fabric. They provide a stable rim around an area of fabric that can be cut to allow viewing of the structure underneath. The fabric remains uncut until an inspection is desired. The rings are typically plastic or aluminum with an approximately three-inch inside diameter. Spring clip metal panel covers can be
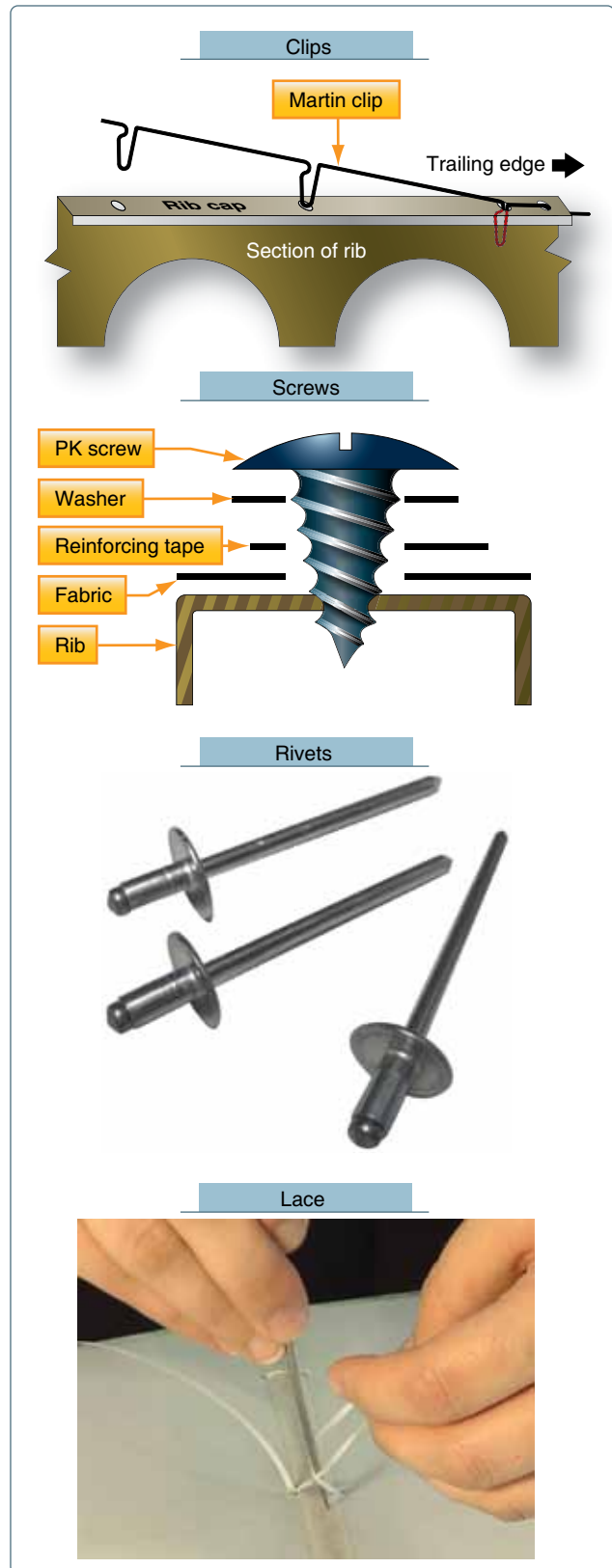
Figure 3-6. *Clips, screws, rivets, or lace are used to attach the fabric to wing and empennage ribs.*
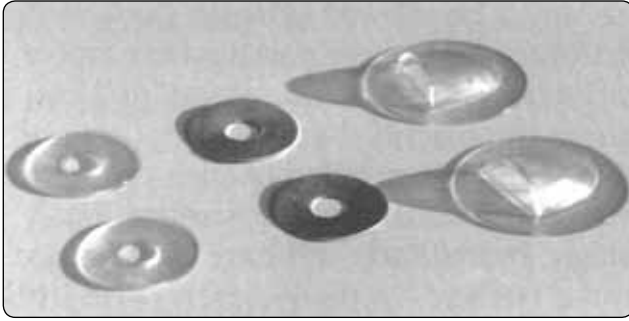
Figure 3-7. *Plastic, aluminum, and seaplane grommets are used to reinforce drain holes in the fabric covering.*

Figure 3-8. *Inspection rings and an inspection cover.*

fitted to close the area once the fabric inside the inspection ring has been cut for access. *[Figure 3-8]* The location of the inspection rings are specified by the manufacturer. Additional rings are sometimes added to permit access to important areas that may not have been fitted originally with inspection access.

Primer

The airframe structure of a fabric covered aircraft must be cleaned, inspected, and prepared before the fabric covering process begins. The final preparation procedure involves priming the structure with a treatment that works with the adhesive and first coats of fabric sealant that are to be utilized. Each STC specifies which primers, or if a wood structure, which varnishes are suitable. Most often, two-part epoxy primers are used on metal structure and two-part epoxy varnishes are used on wood structure. Utilize the primer specified by the manufacturer's or STC's instructions.

Fabric Cement

Modern fabric covering systems utilize special fabric cement to attach the fabric to the airframe. There are various types of cement. *[Figure 3-9]* In addition to good adhesion qualities, flexibility, and long life, fabric cements must be compatible

Aircraft Covering Systems							
APPROVED PROPRIETARY PRODUCT NAME							
Covering System	STC #	Allowable Fabrics	Base	Cement	Filler	UV Block	Topcoats
Air-Tech	SA7965SW	Ceconite™ Poly-Fiber™ Superflite™	Urethane	UA-55	PFU 1020 PFU 1030	PFU 1020 PFU 1030	CHSM Color Coat
			Water		PFUW 1050	PFUW 1050	
Ceconite™/ Randolph System	SA4503NM	Ceconite™	Dope	New Super Seam	Nitrate Dope	Rand-O-Fill	Colored Butyrate Dope Ranthane Polyurethane
Stits/Poly-Fiber™	SA1008WE	Poly-Fiber™	Vinyl	Poly-tak	Poly-brush	Poly-spray	Vinyl Poly-tone, Aero-Thane, or Ranthane Polyurethane
Stewart System	SA01734SE	Ceconite™ Poly-Fiber™	Water-borne	EkoBond	EkoFill	EkoFlll	EkoPoly
Superflite™ • System1 • System VI	SA00478CH and others	Superflite™ 101,102	Dope	U-500	Dacproofer	SrayFil	Tinted Butyrate Dope
		Superflite™ 101,102	Urethane	U-500	SF6500	SF6500	Superflite™ CAB

Figure 3-9. *Current FAA-approved fabric covering processes.*

with the primer and the fabric sealer that are applied before and after the cement.

Fabric Sealer

Fabric sealer surrounds the fibers in the fabric with a protective coating to provide adhesion and keep out dirt and moisture. The sealer is the first coat applied to the polyester fabric after it is attached to the airframe and heat shrunk to fit snugly. Dope-based fabric coating systems utilize non-tautening nitrate dope as the primary fabric sealant. The application of tautening dope may cause the fabric to become too taut resulting in excess stress on the airframe that could damage it. Nondope coating systems use proprietary sealers that are also nontautening. *[Figure 3-9]*

Fillers

After the fabric sealer is applied, a filler is used. It is sprayed on in a number of cross coats as required by the manufacturer or the fabric covering process STC. The filler contains solids or chemicals that are included to block UV light from reaching the fabric. Proper fill coating is critical because UV light is the single most destructive element that causes polyester fabric to deteriorate. Dope-based processes use butyrate dope fillers while other processes have their own proprietary formulas. When fillers and sealers are combined, they are known as fabric primers. Aluminum pastes and powders, formerly added to butyrate dope to provide the UV protection, have been replaced by premixed formulas.

Topcoats

Once the aircraft fabric has been installed, sealed, and fill-coat protected, finishing or topcoats are applied to give the aircraft its final appearance. Colored butyrate dope is common in dope-based processes, but various polyurethane topcoats are also available. It is important to use the topcoat products and procedures specified in the applicable STC to complete an airworthy fabric re-covering job.

The use of various additives is common at different stages when utilizing the above products. The following is a short list of additional products that facilitate the proper application of the fabric coatings. Note again that only products approved under a particular STC can be used. Substitution of similar products, even though they perform the same basic function, is not allowed.

- A catalysts accelerates a chemical reaction. Catalysts are specifically designed for each product with which they are mixed. They are commonly used with epoxies and polyurethanes.

- A thinner is a solvent or mixture of solvents added to a product to give it the proper consistency for application, such as when spraying or brushing.

- A retarder is added to a product to slow drying time. Used mostly in dope processes and topcoats, a retarder allow more time for a sprayed coating to flow and level, resulting in a deeper, glossier finish. It is used when the working temperature is elevated slightly above the ideal temperature for a product. It also can be used to prevent blushing of a dope finish when high humidity conditions exist.

- An accelerators contains solvents that speed up the drying time of the product with which it is mixed. It is typically used when the application working temperature is below that of the ideal working temperature. It can also be used for faster drying when airborne contaminants threaten a coating finish.

- Rejuvenator, used on dope finishes only, contains solvents that soften coatings and allow them to flow slightly. Rejuvenator also contains fresh plasticizers that mix into the original coatings. This increases the overall flexibility and life of the coatings.

- Fungicide and mildewicide additives are important for organic fabric covered aircraft because fabrics, such as cotton and linen, are hosts for fungus and mildew. Since fungus and mildew are not concerns when using polyester fabric, these additives are not required. Modern coating formulas contain premixed anti-fungal agents, providing sufficient insurance against the problem of fungus or mildew.

Available Covering Processes

The covering processes that utilize polyester fabric are the primary focus of this chapter. The FAA-approved aircraft covering processes are listed in *Figure 3-9*. The processes can be distinguished by the chemical nature of the glue and coatings that are used. A dope-based covering process has been refined out of the cotton fabric era, with excellent results on polyester fabric. In particular, plasticizers added to the nitrate dope and butyrate dopes minimize the shrinking and tautening effects of the dope, establish flexibility, and allow esthetically pleasing tinted butyrate dope finishes that last indefinitely. Durable polyurethane-based processes integrate well with durable polyurethane topcoat finishes. Vinyl is the key ingredient in the popular Poly-Fiber covering system. Air Tech uses an acetone thinned polyurethane compatible system.

The most recent entry into the covering systems market is the Stewart Finishing System that uses waterborne technology to apply polyurethane coatings to the fabric. The glue used in the system is water-based and nonvolatile. The Stewart Finishing System is Environmental Protection Agency (EPA) compliant and STC approved. Both the Stewart and Air Tech systems operate with any of the approved polyester fabrics as stated in their covering system STCs.

All the modern fabric covering systems listed in *Figure 3-9* result in a polyester fabric covered aircraft with an indefinite service life. Individual preferences exist for working with the different approved processes. A description of basic covering procedures and techniques common to most of these systems follows later in this chapter.

Ceconite™, Polyfiber™, and Superflight™ are STC approved fabrics with processes used to install polyester fabric coverings. Two companies that do not manufacturer their own fabric have gained STC approval for covering accessories and procedures to be used with these approved fabrics. The STCs specify the fabrics and the proprietary materials that are required to legally complete the re-covering job.

The aircraft fabric covering process is a three-step process. First, select an approved fabric. Second, follow the applicable STC steps to attach the fabric to the airframe and to protect it from the elements. Third, apply the approved topcoat to give the aircraft its color scheme and final appearance.

Although Grade-A cotton can be used on all aircraft originally certificated to be covered with this material, approved aircraft cotton fabric is no longer available. Additionally, due to the shortcomings of cotton fabric coverings, most of these aircraft have been re-covered with polyester fabric. In the rare instance the technician encounters a cotton fabric covered aircraft that is still airworthy, inspection and repair procedures specified in AC 43.13-1, Chapter 2, Fabric Covering, should be followed.

Determining Fabric Condition—Repair or Recover?

Re-covering an aircraft with fabric is a major repair and should only be undertaken when necessary. Often a repair to the present fabric is sufficient to keep the aircraft airworthy. The original manufacturer's recommendations or the covering process STC should be consulted for the type of repair required for the damage incurred by the fabric covering. AC 43.13-1 also gives guidelines and acceptable practices for repairing cotton fabric, specifically when stitching is concerned.

Often a large area that needs repair is judged in reference to the overall remaining lifespan of the fabric on the aircraft. For example, if the fabric has reached the limit of its durability, it is better to re-cover the entire aircraft than to replace a large damaged area when the remainder of the aircraft would soon need to be re-covered.

On aircraft with dope-based covering systems, continued shrinkage of the dope can cause the fabric to become too tight. Overly tight fabric may require the aircraft to be re-covered

rather than repaired because excess tension on fabric can cause airframe structural damage. Loose fabric flaps in the wind during flight, affecting weight distribution and unduly stressing the airframe. It may also need to be replaced because of damage to the airframe.

Another reason to re-cover rather than repair occurs when dope coatings on fabric develop cracks. These cracks could expose the fabric beneath to the elements that can weaken it. Close observation and field testing must be used to determine if the fabrics are airworthy. If not, the aircraft must be re-covered. If the fabric is airworthy and no other problems exist, a rejuvenator can be used per manufacturer's instructions. This product is usually sprayed on and softens the coatings with very powerful solvents. Plasticizers in the rejuvenator become part of the film that fills in the cracks. After the rejuvenator dries, additional coats of aluminum-pigmented dope must be added and then final topcoats applied to finish the job. While laborious, rejuvenating a dope finish over strong fabric can save a great deal of time and money. Polyurethane-based finishes cannot be rejuvenated.

Fabric Strength

Deterioration of the strength of the present fabric covering is the most common reason to re-cover an aircraft. The strength of fabric coverings must be determined at every 100-hour and annual inspection. Minimum fabric breaking strength is used to determine if an aircraft requires re-covering.

Fabric strength is a major factor in the airworthiness of an aircraft. Fabric is considered to be airworthy until it deteriorates to a breaking strength less than 70 percent of the strength of the new fabric required for the aircraft. For example, if an aircraft was certificated with Grade-A cotton fabric that has a new breaking strength of 80 pounds, it becomes unairworthy when the fabric strength falls to 56 pounds, which is 70 percent of 80 pounds. If polyester fabric, which has a higher new breaking strength, is used to re-cover this same aircraft, it would also need to exceed 56 pounds breaking strength to remain airworthy.

In general, an aircraft is certified with a certain fabric based on its wing loading and its never exceed speed (V_{NE}). The higher the wing loading and V_{NE}, the stronger the fabric must be. On aircraft with wing loading of 9 pounds per square foot and over, or a V_{NE} of 160 miles per hour (mph) or higher, fabric equaling or exceeding the strength of Grade A cotton is required. This means the new fabric breaking strength must be at least 80 pounds and the minimum fabric breaking strength at which the aircraft becomes unairworthy is 56 pounds.

On aircraft with wing loading of 9 pounds per square foot or less, or a V_{NE} of 160 mph or less, fabric equaling or exceeding

the strength of intermediate grade cotton is required. This means the new fabric breaking strength must be at least 65 pounds and the minimum fabric breaking strength at which the aircraft becomes unairworthy is 46 pounds.

Lighter weight fabric may be found to have been certified on gliders or sailplanes and may be used on many uncertificated aircraft or aircraft in the Light Sport Aircraft (LSA) category. For aircraft with wing loading less than 8 pounds per square foot or less, or V_{NE} of 135 mph or less, the fabric is considered unairworthy when the breaking strength has deteriorated to below 35 pounds (new minimum strength of 50 pounds). *Figure 3-10* summarizes these parameters.

How Fabric Breaking Strength is Determined

Manufacturer's instructions should always be consulted first for fabric strength inspection methodology. These instructions are approved data and may not require removal of a test strip to determine airworthiness of the fabric. In some cases, the manufacturer's information does not include any fabric inspection methods. It may refer the IA to AC 43.13-1, Chapter 2, Fabric Covering, which contains the approved FAA test strip method for breaking strength.

The test strip method for the breaking strength of aircraft covering fabrics uses standards published by the American Society for Testing and Materials (ASTM) for the testing of various materials. Breaking strength is determined by cutting a 1¼ inch by 4–6 inch strip of fabric from the aircraft covering. This sample should be taken from an area that is exposed to the elements—usually an upper surface. It is also wise to take the sample from an area that has a dark colored finish since this has absorbed more of the sun's UV rays and degraded faster. All coatings are then removed and the edges raveled to leave a 1-inch width. One end of the strip is clamped into a secured clamp and the other end is clamped such that a suitable container may be suspended from it. Weight is added to the container until the fabric breaks. The breaking strength of the fabric is equal to the weight of the lower clamp, the container, and the weight added to it. If the breaking strength is still in question, a sample should be sent to a qualified testing laboratory and breaking strength tests made in accordance with ASTM publication D5035.

Note that the fabric test strip must have all coatings removed from it for the test. Soaking and cleaning the test strip in methyl ethyl ketone (MEK) usually removes all the coatings.

Properly installed and maintained polyester fabric should give years of service before appreciable fabric strength degradation occurs. Aircraft owners often prefer not to have test strips cut out of the fabric, especially when the aircraft or the fabric covering is relatively new, because removal of a test strip damages the integrity of an airworthy component if the fabric passes. The test strip area then must be repaired, costing time and money. To avoid cutting a strip out of airworthy fabric, the IA makes a decision based on knowledge, experience, and available nondestructive techniques as to whether removal of a test strip is warranted to ensure that the aircraft can be returned to service.

An aircraft made airworthy under an STC is subject to the instructions for continued airworthiness in that STC. Most STCs refer to AC 43.13-1 for inspection methodology. Poly-Fiber™ and Ceconite™ re-covering process STCs contain their own instructions and techniques for determining fabric strength and airworthiness. Therefore, an aircraft covered under those STCs may be inspected in accordance with this information. In most cases, the aircraft can be approved for return to service without cutting a strip from the fabric covering.

The procedures in the Poly-Fiber™ and Ceconite™ STCs outlined in the following paragraphs are useful when inspecting any fabric covered aircraft as they add to the information gathered by the IA to determine the condition of the fabric. However, following these procedures alone on aircraft not re-covered under these STCs does not make the aircraft airworthy. The IA must add his or her own knowledge, experience, and judgment to make a final determination of the strength of the fabric and whether it is airworthy.

Fabric Performance Criteria				
IF YOUR PERFORMANCE IS. . .		FABRIC STRENGTH MUST BE. . .		
Loading	V_{NE} Speed	Type	New Breaking Strength	Minimum Breaking Strength
> 9 lb/sq ft	> 160 mph	≥ Grade A	> 80 lb	> 56
< 9 lb/sq ft	< 160 mph	≥ Intermediate	> 65 lb	> 46
< 8 lb/sq ft	< 135 mph	≥ Lightweight	> 50 lb	> 35

Figure 3-10. *Aircraft performance affects fabric selection.*

Exposure to UV radiation appreciably reduces the strength of polyester fabric and forms the basis of the Poly-Fiber™ and Ceconite™ fabric evaluation process. All approved covering systems utilize fill coats applied to the fabric to protect it from UV. If installed according to the STC, these coatings should be sufficient to protect the fabric from the sun and should last indefinitely. Therefore, most of the evaluation of the strength of the fabric is actually an evaluation of the condition of its protective coating(s).

Upon a close visual inspection, the fabric coating(s) should be consistent, contain no cracks, and be flexible, not brittle. Pushing hard against the fabric with a knuckle should not damage the coating(s). It is recommended the inspector check in several areas, especially those most exposed to the sun. Coatings that pass this test can move to a simple test that determines whether or not UV light is passing through the coatings.

This test is based on the assumption that if visible light passes through the fabric coatings, then UV light can also. To verify whether or not visible light passes through the fabric coating, remove an inspection panel from the wing, fuselage, or empennage. Have someone hold an illuminated 60-watt lamp one foot away from the exterior of the fabric. No light should be visible through the fabric. If no light is visible, the fabric has not been weakened by UV rays and can be assumed to be airworthy. There is no need to perform the fabric strip strength test. If light is visible through the coatings, further investigation is required.

Fabric Testing Devices

Mechanical devices used to test fabric by pressing against or piercing the finished fabric are not FAA approved and are used at the discretion of the FAA-certificated mechanic to form an opinion on the general fabric condition. Punch test accuracy depends on the individual device calibration, total coating thickness, brittleness, and types of coatings and fabric. If the fabric tests in the lower breaking strength range with the mechanical punch tester or if the overall fabric cover conditions are poor, then more accurate field tests may be made.

The test should be performed on exposed fabric where there is a crack or chip in the coatings. If there is no crack or chip, coatings should be removed to expose the fabric wherever the test is to be done.

The Maule punch tester, a spring-loaded device with its scale calibrated in breaking strength, tests fabric strength by pressing against it while the fabric is still on the aircraft. It roughly equates strength in pounds per square inch (psi) of resistance to breaking strength. The tester is pushed squarely against the fabric until the scale reads the amount

of maximum allowable degradation. If the tester does not puncture the fabric, it may be considered airworthy. Punctures near the breaking strength should be followed with further testing, specifically the strip breaking strength test described above. Usually, a puncture indicates the fabric is in need of replacement.

A second type of punch tester, the Seyboth, is not as popular as the Maule because it punctures a small hole in the fabric when the mechanic pushes the shoulder of the testing unit against the fabric. A pin with a color-coded calibrated scale protrudes from the top of the tester and the mechanic reads this scale to determine fabric strength. Since this device requires a repair regardless of the strength of the fabric indicated, it is not widely used.

Seyboth and Maule fabric strength testers designed for cotton- and linen-covered aircraft, not to be used on modern Dacron fabrics. Mechanical devices, combined with other information and experience, help the FAA-certificated mechanic judge the strength of the fabric. *[Figure 3-11]*
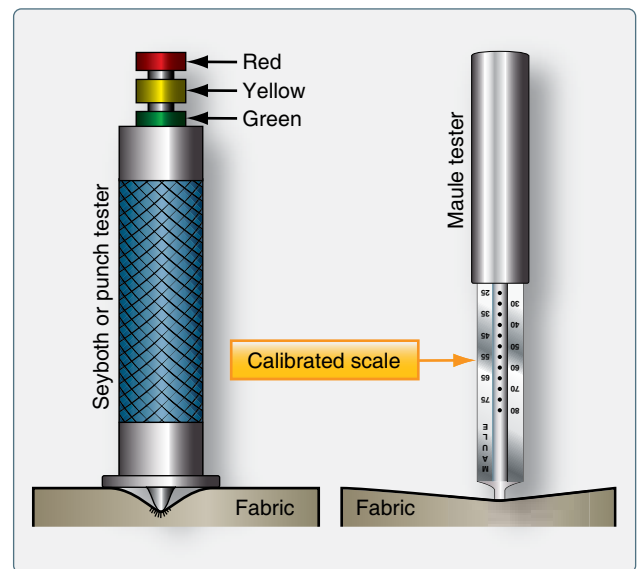
Figure 3-11. *Seyboth and Maule fabric strength testers.*

General Fabric Covering Process

It is required to have an IA involved in the process of re-covering a fabric aircraft because re-covering is a major repair or major alteration. Signatures are required on FAA Form 337 and in the aircraft logbook. To ensure work progresses as required, the IA should be involved from the beginning, as well as at various stages throughout the process.

This section describes steps common to various STC and manufacturer covering processes, as well as the differences of some processes. To aid in proper performance of fabric

covering and repair procedures, STC holders produce illustrated, step-by-step instructional manuals and videos that demonstrate the correct covering procedures. These training aids are invaluable to the inexperienced technician.

Since modern fabric coverings last indefinitely, a rare opportunity to inspect the aircraft exists during the re-covering process. Inspectors and owner-operators should use this opportunity to perform a thorough inspection of the aircraft before new fabric is installed.

The method of fabric attachment should be identical, as far as strength and reliability are concerned, to the method used by the manufacturer of the aircraft being recovered or repaired. Carefully remove the old fabric from the airframe, noting the location of inspection covers, drain grommets, and method of attachment. Either the envelope method or blanket method of fabric covering is acceptable, but a choice must be made prior to beginning the re-covering process.

Blanket Method vs. Envelope Method

In the blanket method of re-covering, multiple flat sections of fabric are trimmed and attached to the airframe. Certified greige polyester fabric for covering an aircraft can be up to 70 inches in width and used as it comes off the bolt. Each aircraft must be considered individually to determine the size and layout of blankets needed to cover it. A single blanket cut for each small surface (i.e., stabilizers and control surfaces) is common. Wings may require two blankets that overlap. Fuselages are covered with multiple blankets that span between major structural members, often with a single blanket for the bottom. Very large wings may require more than two blankets of fabric to cover the entire top and bottom surfaces. In all cases, the fabric is adhered to the airframe using the approved adhesives, following specific rules for the covering process being employed. *[Figure 3-12]*

Figure 3-12. *Laying out fabric during a blanket method re-covering job.*

An alternative method of re-covering, the envelope method, saves time by using precut and pre-sewn envelopes of fabric to cover the aircraft. The envelopes must be sewn with approved machine sewing thread, edge distance, fabric fold, etc., such as those specified in AC 43.13-1 or an STC. Patterns are made and fabric is cut and stitched so that each major surface, including the fuselage and wings, can be covered with a single, close-fitting envelope. Since envelopes are cut to fit, they are slid into position, oriented with the seams in the proper place, and attached with adhesive to the airframe. Envelope seams are usually located over airframe structure in inconspicuous places, such as the trailing edge structures and the very top and bottom of the fuselage, depending on airframe construction. Follow the manufacturer's or STC's instructions for proper location of the sewn seams of the envelope when using this method. *[Figure 3-13]*

Figure 3-13. *A custom-fit presewn fabric envelope is slid into position over a fuselage for the envelope method of fabric covering. Other than fitting, most steps in the covering process are the same as with the blanket covering method.*

Preparation for Fabric Covering Work

Proper preparation for re-covering a fabric aircraft is essential. First, assemble the materials and tools required to complete the job. The holder of the STC usually supplies a materials and tools list either separately or in the STC manual. Control of temperature, humidity, and ventilation is needed in the work environment. If ideal environmental conditions cannot be met, additives are available that compensate for this for most re-covering products.

Rotating work stands for the fuselage and wings provide easy, alternating access to the upper and lower surfaces while the job is in progress. *[Figure 3-14]* They can be used with sawhorses or sawhorses can be used alone to support the aircraft structure while working. A workbench or table, as well as a rolling cart and storage cabinet, are also recommended. *Figure 3-15* shows a well conceived fabric covering workshop. A paint spray booth for sprayed-on coatings and space to store components awaiting work is also recommended.
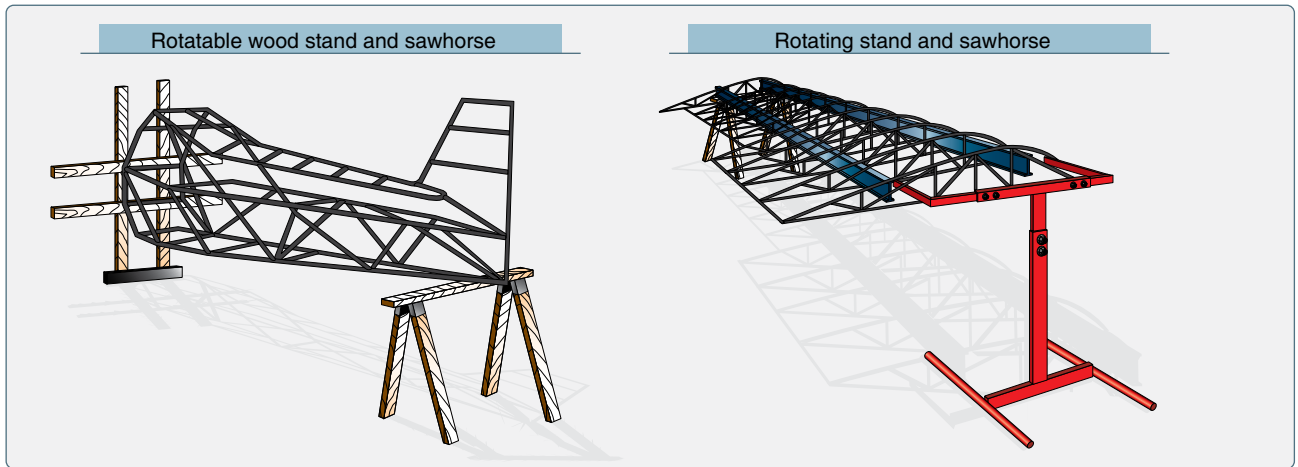
Figure 3-14. *Rotating stands and sawhorses facilitate easy access to top and bottom surfaces during the fabric covering process.*
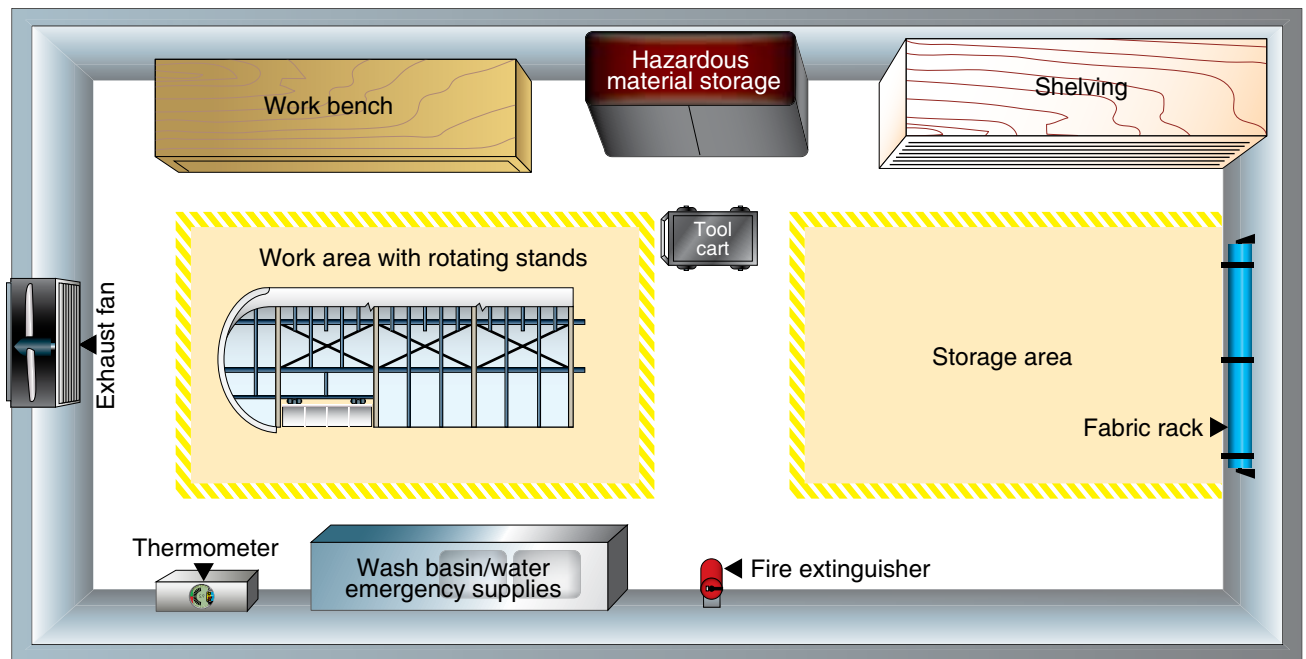
Figure 3-15. *Some components of a work area for covering an aircraft with fabric.*

Many of the substances used in most re-covering processes are highly toxic. Proper protection must be used to avoid serious short and long term adverse health effects. Eye protection, a proper respirator, and skin protection are vital. As mentioned in the beginning of this chapter, nitrate dope is very flammable. Proper ventilation and a rated fire extinguisher should be on hand when working with this and other covering process materials. Grounding of work to prevent static electricity build-up may be required. All fabric re-covering processes also involve multiple coats of various products that are sprayed onto the fabric surface. Use of a high-volume, low-pressure (HVLP) sprayer is recommended. Good ventilation is needed for all of the processes.

Removal of Old Fabric Coverings

Removal of the old covering is the first step in replacing an aircraft fabric covering. Cut away the old fabric from the airframe with razor blades or utility knife. Care should be taken to ensure that no damage is done to the airframe. *[Figure 3-16]* To use the old covering for templates in transferring the location of inspection panels, cable guides, and other features to the new covering, the old covering should be removed in large sections. NOTE: any rib stitching fasteners, if used to attach the fabric to the structure, should be removed before the fabric is pulled free of the airframe. If fasteners are left in place, damage to the structure may occur during fabric removal.

Carefully cut away the fabric.

Gently roll the fabric back as the cut is made.
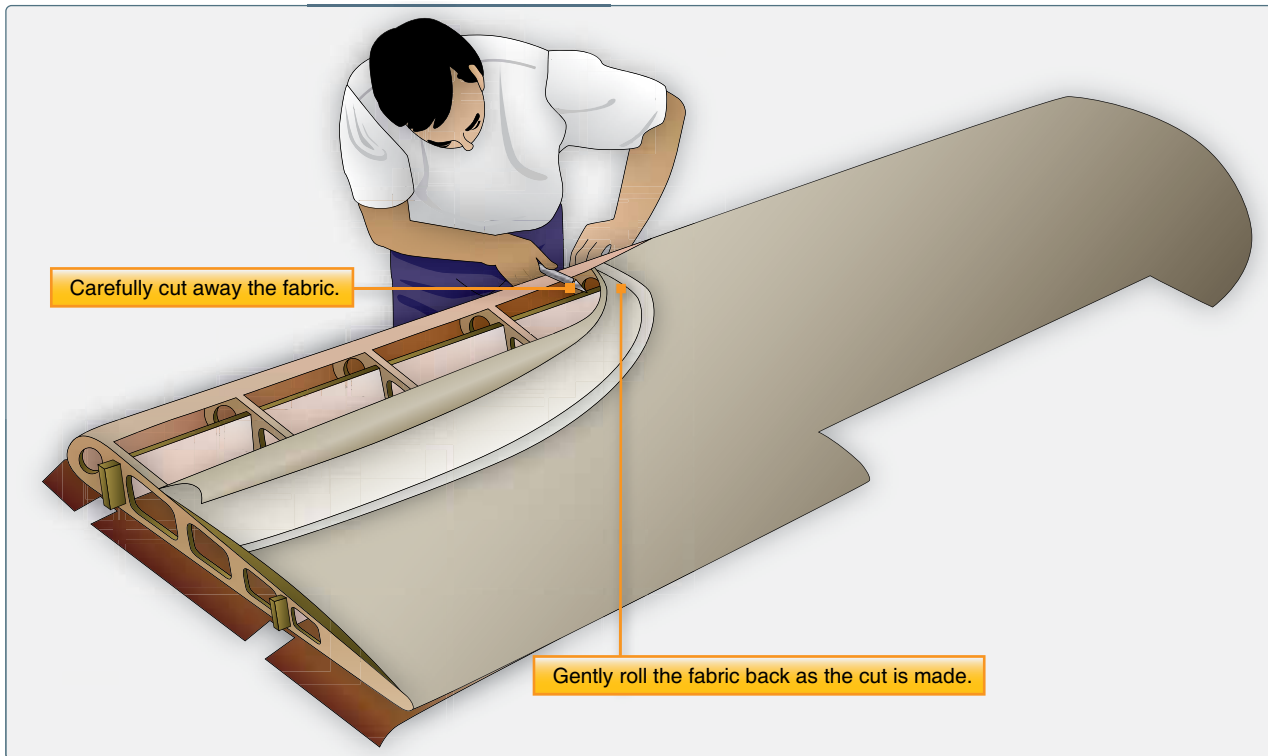
Figure 3-16. *Old fabric coverings are cut off in large pieces to preserve them as templates for locating various airframe features. Sharp blades and care must be used to avoid damaging the structure.*

Preparation of the Airframe Before Covering

Once the old fabric has been removed, the exposed airframe structure must be thoroughly cleaned and inspected. The IA collaborating on the job should be involved in this step of the process. Details of the inspection should follow the manufacturer's guidelines, the STC, or AC 43.13-1. All of the old adhesive must be completely removed from the airframe with solvent, such as MEK. A thorough inspection must be done and various components may be selected to be removed for cleaning, inspection, and testing. Any repairs that are required, including the removal and treatment of all corrosion, must be done at this time. If the airframe is steel tubing, many technicians take the opportunity to grit blast the entire airframe at this stage.

The leading edge of a wing is a critical area where airflow diverges and begins its laminar flow over the wing's surfaces, which results in the generation of lift. It is beneficial to have a smooth, regular surface in this area. Plywood leading edges must be sanded until smooth, bare wood is exposed. If oil or grease spots exist, they must be cleaned with naphtha or other specified cleaners. If there are any chips, indentations, or irregularities, approved filler may be spread into these areas and sanded smooth. The entire leading edge should be cleaned before beginning the fabric covering process.

To obtain a smooth finish on fabric-covered leading edges of aluminum wings, a sheet of felt or polyester padding may be applied before the fabric is installed. This should only be done with the material specified in the STC under which the technician is working. The approved padding ensures compatibility with the adhesives and first coatings of the covering process. When a leading edge pad is used, check the STC process instructions for permission to make a cemented fabric seam over the padding. *[Figure 3-17]*

When completely cleaned, inspected, and repaired, an approved primer, or varnish if it is a wood structure, should be applied to the airframe. This step is sometimes referred to as dope proofing. Exposed aluminum must first be acid etched. Use the product(s) specified by the manufacturer or in the STC to prepare the metal before priming. Two part epoxy primers and varnishes, which are not affected by the fabric adhesive and subsequent coatings, are usually specified. One part primers, such as zinc chromate and spar varnish, are typically not acceptable. The chemicals in the adhesives dissolve the primers, and adhesion of the fabric to the airframe is lost.

Sharp edges, metal seams, the heads of rivets, and any other feature on the aircraft structure that might cut or wear through the fabric should be covered with anti-chafe tape. As

Figure 3-17. *The use of specified felt or padding over the wing leading edges before the fabric is installed results in a smooth regular surface.*

Figure 3-18. *Anti-chafe tape is applied to all features that might cut or wear through the fabric.*

described above, this cloth sticky-back tape is approved and should not be substituted with masking or any other kind of tape. Sometimes, rib cap strips need to have anti-chafe tape applied when the edges are not rounded over. *[Figure 3-18]*

Inter-rib bracing must also be accomplished before the fabric is installed. It normally does not have an adhesive attached to it and is wrapped only once around each rib. The single wrap around each rib is enough to hold the ribs in place during the covering process but allows small movements during the fabric shrinking process. *[Figure 3-19]*

Attaching Polyester Fabric to the Airframe

Inexperienced technicians are encouraged to construct a test panel upon which they can practice with the fabric and various substances and techniques to be used on the aircraft. It is often suggested to cover smaller surfaces first, such as the empennage and control surfaces. Mistakes on these can be corrected and are less costly if they occur. The techniques employed for all surfaces, including the wings and fuselage, are basically the same. Once dexterity has been established, the order in which one proceeds is often a personal choice.

When the airframe is primed and ready for fabric installation, it must receive a final inspection by an A&P with IA.

Figure 3-19. *Inter-rib bracing holds the ribs in place during the re-covering process.*

When approved, attachment of the fabric may begin. The manufacturer's or STC's instructions must be followed without deviation for the job to be airworthy. The following are the general steps taken. Each approved process has its own nuances.

Seams

During installation, the fabric is overlapped and seamed together. Primary concerns for fabric seams are strength, elasticity, durability, and good appearance. Whether using the blanket method or envelope method, position all fabric seams over airframe structure to which the fabric is to be adhered during the covering process, whenever possible. Unlike the blanket method, fabric seam overlap is predetermined in the envelope method. Seams sewn to the specifications in AC 43.13-1, the STC under which the work is being performed, or the manufacturer's instructions should perform adequately.

Most covering procedures for polyester fabric rely on doped or glued seams as opposed to sewn seams. They are simple and easy to make and provide excellent strength, elasticity, durability, and appearance. When using the blanket method, seam overlap is specified in the covering instructions and the FAA-certificated A&P mechanic must adhere to these specifications. Typically, a minimum of two to four inches of fabric overlap seam is required where ends of fabric are joined in areas of critical airflow, such as the leading edge of a wing. One to two inches of overlap is often the minimum in other areas.

When using the blanket method, options exist for deciding where to overlap the fabric for coverage. Function and the final appearance of the covering job should be considered. For example, fabric seams made on the wing's top surface of a high wing aircraft are not visible when approaching the aircraft. Seams on low wing aircraft and many horizontal stabilizers are usually made on the bottom of the wing for the same reason. *[Figure 3-20]*

Fabric Cement

A polyester fabric covering is cemented or glued to the airframe structure at all points where it makes contact. Special formula adhesives have replaced nitrate dope for adhesion in most covering processes. The adhesive (as well as all subsequent coating materials) should be mixed for optimum characteristics at the temperature at which the work is being performed. Follow the manufacturer's or STC's guidance when mixing.

To attach the fabric to the airframe, first pre-apply two coats of adhesive to the structure at all points the fabric is to contact it. (It is important to follow the manufacturer's or STC's guidance as all systems are different.) Allow these to dry. The fabric is then spread over the surface and clamped into position. It should not be pulled tighter than the relaxed but not wrinkled condition it assumes when lying on the structure. Clamps or clothespins are used to attach the fabric completely around the perimeter. The Stewart System STC does not need clamps because the glue assumes a tacky condition when precoated and dried. There is sufficient adhesion in the precoat to position the fabric.

The fabric should be positioned in all areas before undertaking final adhesion. Final adhesion often involves lifting the fabric,
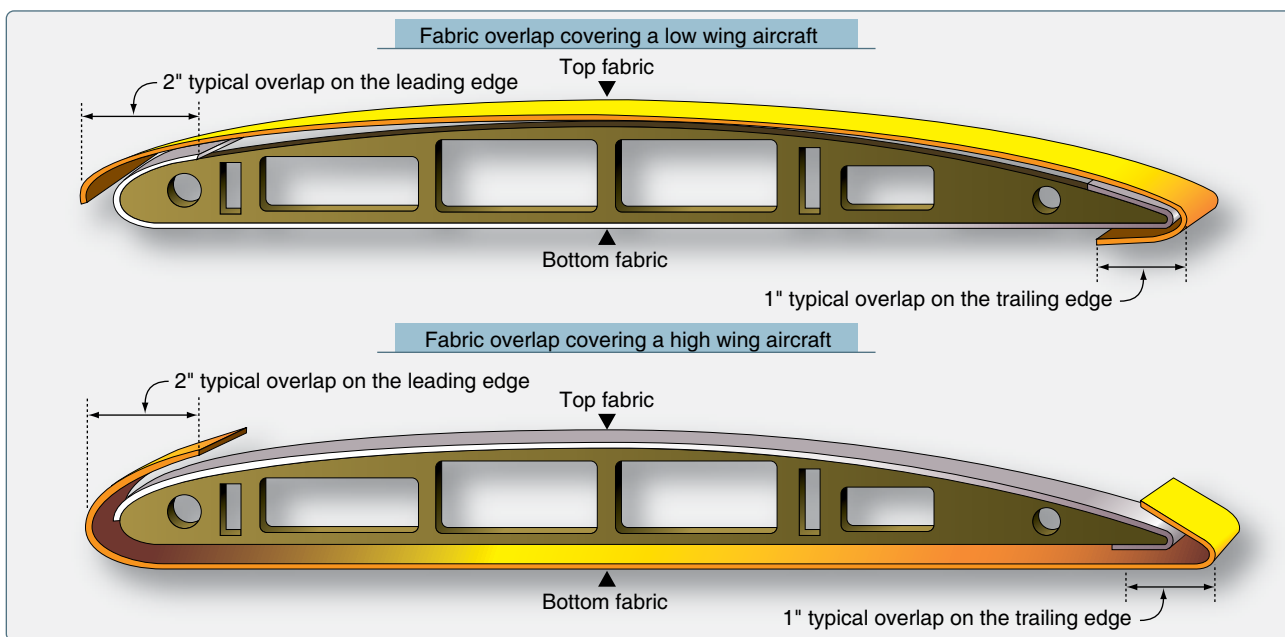

Figure 3-20. *For appearance, fabric can be overlapped differently on high wing and low wing aircraft.*

applying a wet bed of cement, and pressing the fabric into the bed. An additional coat of cement over the top of the fabric is common. Depending on the process, wrinkles and excess cement are smoothed out with a squeegee or are ironed out. The Stewart System calls for heat activation of the cement precoats through the fabric with an iron while the fabric is in place. Follow the approved instructions for the covering method being used.

Fabric Heat Shrinking

Once the fabric has been glued to the structure, it can be made taut by heat shrinking. This process is done with an ordinary household iron that the technician calibrates before use. A smaller iron is also used to iron in small or tight places. *[Figure 3-21]* The iron is run over the entire surface of the fabric. Follow the instructions for the work being performed. Some processes avoid ironing seams while other processes begin ironing over structure and move to spanned fabric or visa-versa. It is important to shrink the fabric evenly. Starting on one end of a structure and progressing sequentially to the other end is not recommended. Skipping from one end to the other, and then to the middle, is more likely to evenly draw the fabric tight. *[Figure 3-22]*

The amount polyester fabric shrinks is directly related to the temperature applied. Polyester fabric can shrink nearly 5 percent at 250 °F and 10 percent at 350 °F. It is customary to shrink the fabric in stages, using a lower temperature first, before finishing with the final temperature setting. The first shrinking is used to remove wrinkles and excess fabric. The final shrinking gives the finished tautness desired. Each

Figure 3-21. *Irons used during the fabric covering process.*

process has its own temperature regime for the stages of tautening. Typically ranging from 225 °F to 350 °F, it is imperative to follow the process instructions. Not all fabric covering processes use the same temperature range and maximum temperature. Ensure irons are calibrated to prevent damage at high temperature settings.
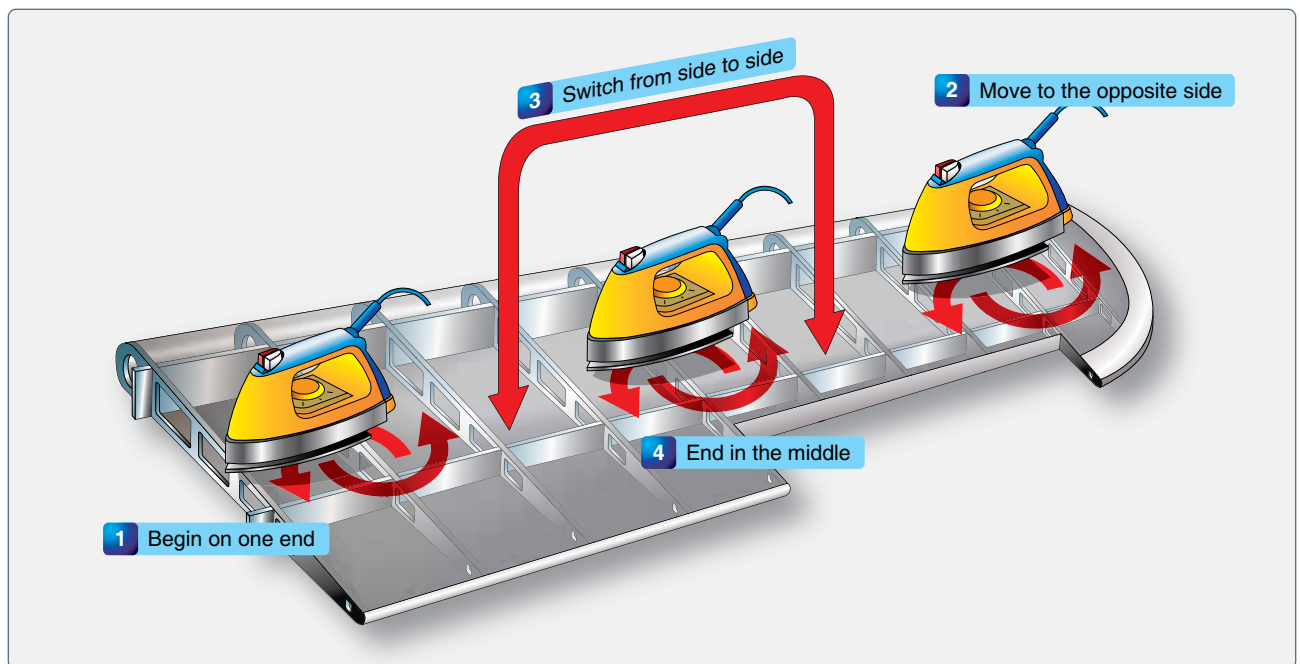

Figure 3-22. *An example of a wing fabric ironing procedure designed to evenly taughten the fabric.*

Attaching Fabric to the Wing Ribs

Once the fabric has been tautened, covering processes vary. Some require a sealing coat be applied to the fabric at this point. It is usually put on by brush to ensure the fibers are saturated. Other processes seal the fabric later. Whatever the process, the fabric on wings must be secured to the wing ribs with more than just cement. The forces caused by the airflow over the wings are too great for cement alone to hold the fabric in place. As described in the materials section, screws, rivets, clips and lacing hold the fabric in place on manufactured aircraft. Use the same attach method as used by the original aircraft manufacturer. Deviation requires a field approval. Note that fuselage and empennage attachments may be used on some aircraft. Follow the methodology for wing rib lacing described below and the manufacturer's instructions for attach point locations and any possible variations to what is presented here.

Care must always be taken to identify and eliminate any sharp edges that might wear through the fabric. Reinforcing tape of the exact same width as the rib cap is installed before any of the fasteners. This approved sticky-back tape helps prevent the fabric from tearing. *[Figure 3-23]* Then, screws, rivets, and clips simply attach into the predrilled holes in the rib caps to hold the fabric to the caps. Rib lacing is a more involved process whereby the fabric is attached to the ribs with cord.
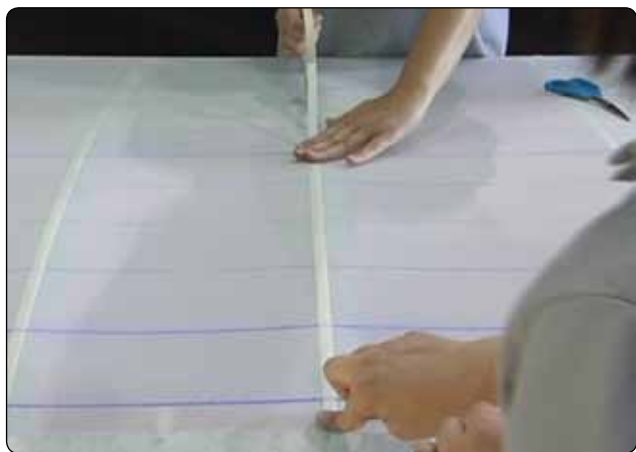

Figure 3-23. *Reinforcing tape the same width as the wing ribs is applied over all wing ribs.*

Rib Lacing

There are two kinds of rib lacing cord. One has a round cross-section and the other flat. Which to use is a matter of preference based on ease of use and final appearance. Only approved rib lacing cord can be used. Unless a rib is unusually deep from top to bottom, rib lacing uses a single length of cord that passes completely through the wing from the upper surface to the lower surface thereby attaching the top and bottom skin to the rib simultaneously.

Holes are laid out and pre-punched through the skin as close to the rib caps as possible to accept the lacing cord. *[Figure 3-24]* This minimizes leverage the fabric could develop while trying to pull away from the structure and prevents tearing. The location of the holes is not arbitrary. The spacing between lacing holes and knots must adhere to manufacturer's instructions, if available. STC lacing guidance refers to manufacturer's instructions or to that shown on the chart in *Figure 3-25* which is taken from AC 43.13-1. Notice that because of greater turbulence in the area of the propeller wash, closer spacing between the lacing is required there. This slipstream is considered to be the width of the propeller plus one additional rib. Ribs are normally laced from the leading edge to the trailing edge of the wing. Rib lacing is done with a long curved needle to guide the cord in and out of holes and through the depth of the rib. The knots are designed not to slip under the forces applied and can be made in a series out of a single strand of lacing. Stitching can begin at the leading edge or trailing edge. A square knot with a half hitch on each side is typically used for the first knot when lacing a rib. *[Figure 3-26]* This is followed by a series of modified seine knots until the final knot is made and secured with a half hitch. *[Figure 3-27]* Hidden modified seine knots are also used. These knots are placed below the fabric surface so only a single strand of lacing is visible across the rib cap. *[Figure 3-28]*

Figure 3-24. *A premarked location for a lacing hole, which is punched through the fabric with a pencil.*

Structure and accessories within the wing may prevent a continuous lacing. Ending the lacing and beginning again can avoid these obstacles. Lacing that is not long enough to complete the rib may be ended and a new starting knot can be initiated at the next set of holes. The lacing can also be extended by joining it with another piece of lacing using the splice knot shown in *Figure 3-29*.
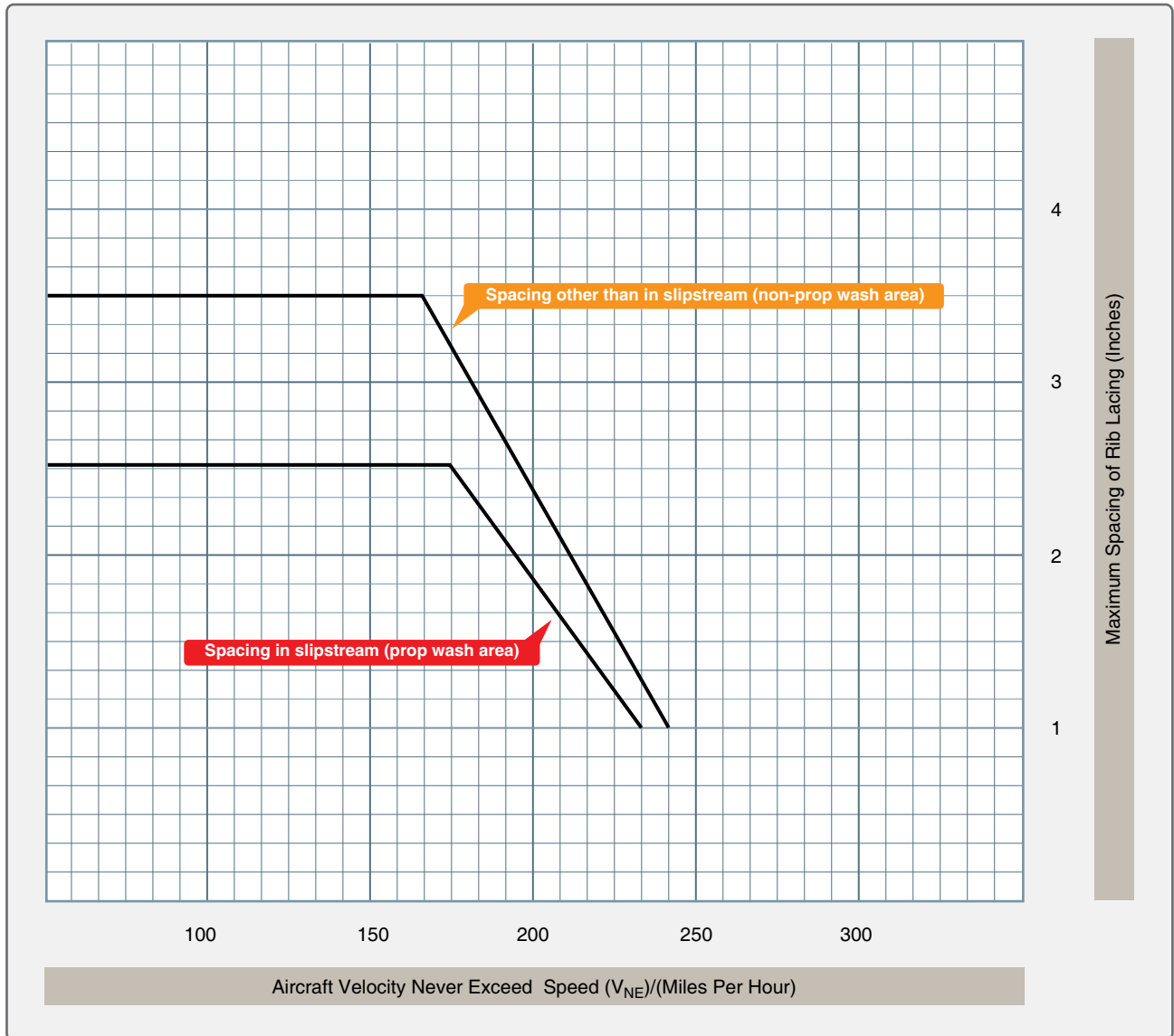
Figure 3-25. *A rib lacing spacing chart. Unless manufacturer data specifies otherwise, use the spacing indicated.*

Occasionally, lacing to just the rib cap is employed without lacing entirely through the wing and incorporating the cap on the opposite side. This is done where ribs are exceptionally deep or where through lacing is not possible, such as in an area where a fuel tank is installed. Changing to a needle with a tighter radius facilitates threading the lacing cord in these areas. Knotting procedures remain unchanged.

Technicians inexperienced at rib lacing should seek assistance to ensure the correct knots are being tied. STC holder videos are invaluable in this area. They present repeated close-up visual instruction and guidance to ensure airworthy lacing. AC 43.13-1, Chapter 2, Fabric Covering, also has in-depth instructions and diagrams as do some manufacturer's manuals and STC's instructions.
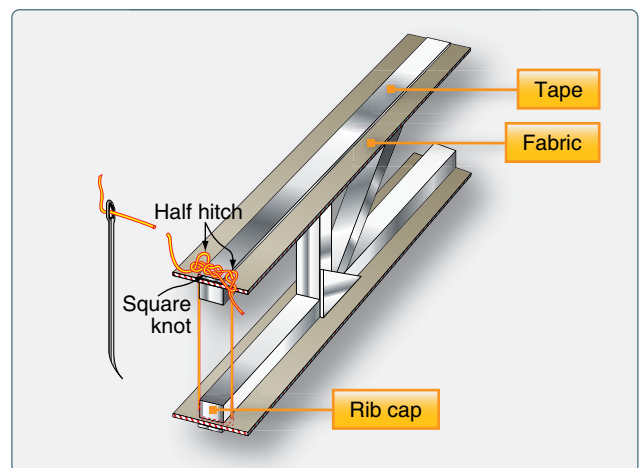
Figure 3-26. *A starter knot for rib lacing can be a square knot with a half hitch on each side.*

3-19
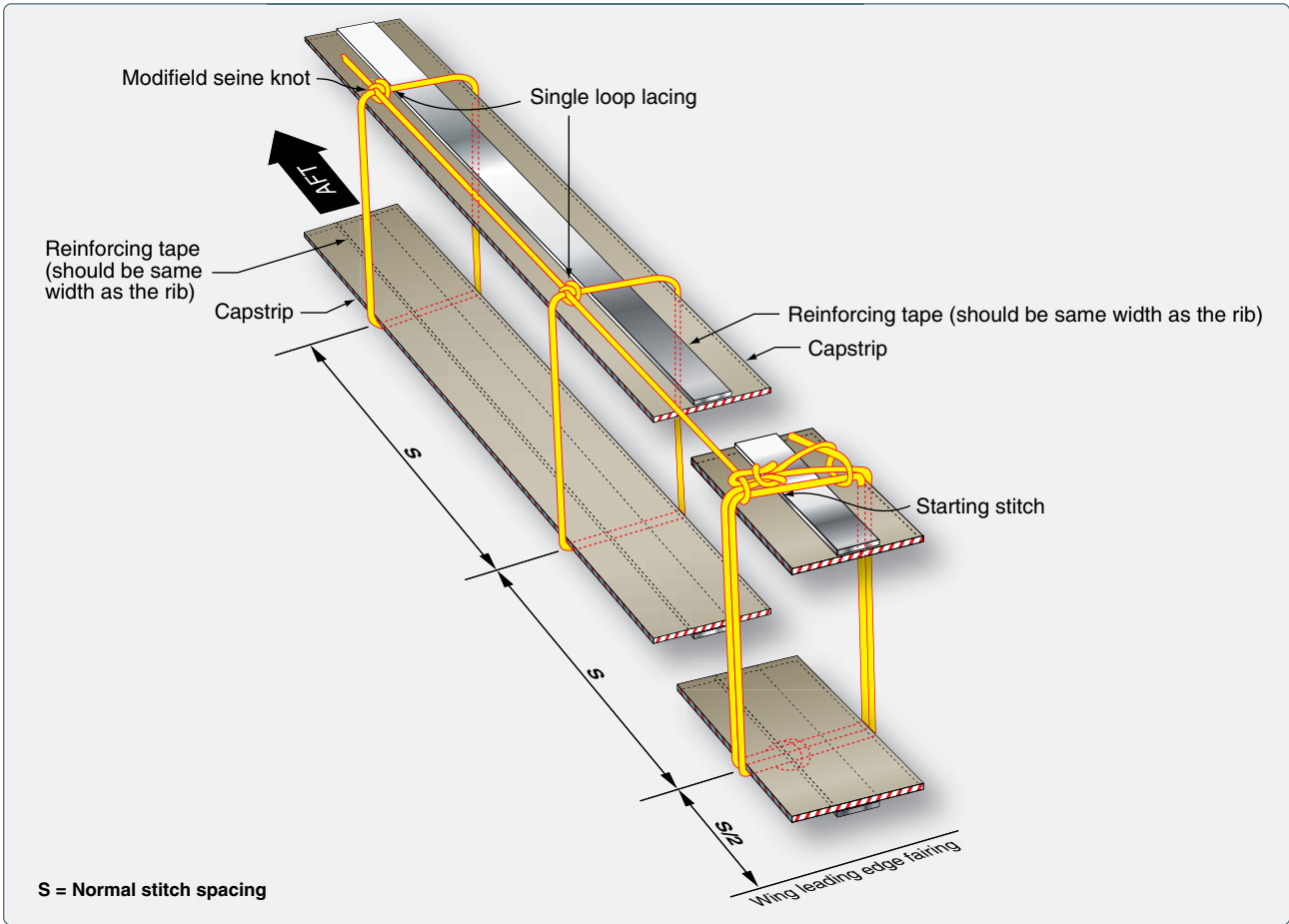
Figure 3-27. *In this example of rib lacing, modified seine knots are used and shown above the fabric surface. Hidden modified seine knots are common. They are made so that the knots are pushed or pulled below the fabric surface.*
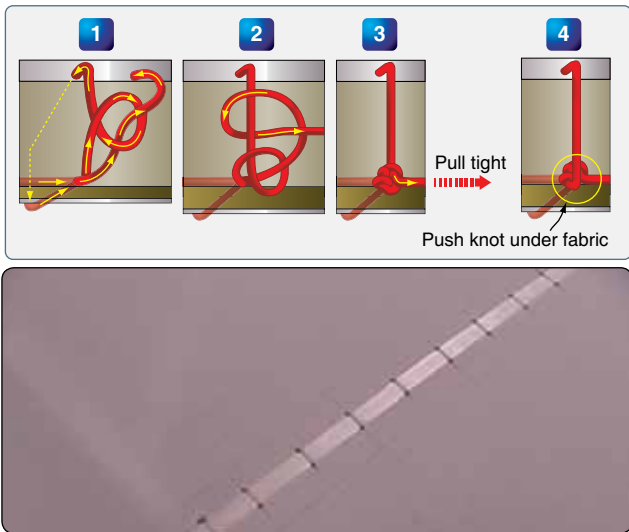
Figure 3-28. *Hiding rib lacing knots below the fabric surface results in a smooth surface.*
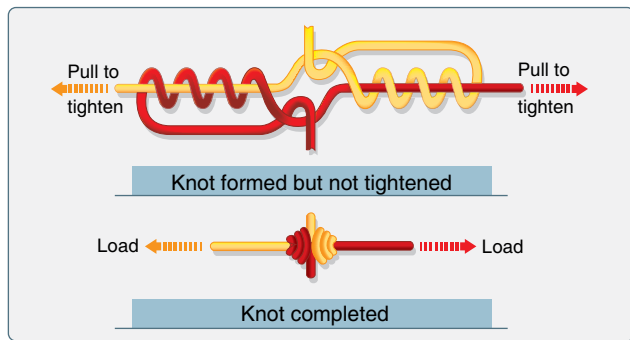
Figure 3-29. *The splice knot can be used to join two pieces of rib lacing cord.*

Rings, Grommets, and Gussets

When the ribs are laced and the fabric covering completely attached, the various inspection rings, drain grommets, reinforcing patches, and finishing tapes are applied. Inspection rings aid access to critical areas of the structure (pulleys, bell cranks, drag/anti-drag wires, etc.) once the fabric skin is in place. They are plastic or aluminum and normally cemented to the fabric using the approved cement and procedures. The area inside the ring is left intact. It is removed only when inspection or maintenance requires access through that ring. Once removed, preformed inspection panels are used to close the opening. The rings should be positioned as specified by the manufacturer. Lacking that information, they should be positioned as they were on the previous covering fabric. Additional rings should be installed by the technician if it is determined a certain area would benefit from access in the future. *[Figure 3-30]*

Figure 3-30. *This inspection ring was cemented into place on the fabric covering. The approved technique specifies the use of a fabric overlay that is cemented over the ring and to the fabric.*

Water from rain and condensation can collect under the fabric covering and needs a way to escape. Drain grommets serve this purpose. There are a few different types as described in the materials section above. All are cemented into position in accordance with the approved process under which the work is being performed. Locations for the drain grommets should be ascertained from manufacturer's data. If not specified, AC 43.13-1 has acceptable location information. Each fabric covering STC may also give recommendations. Typically, drain grommets are located at the lowest part of each area of the structure (e.g., bottom of the fuselage, wings, empennage). *[Figure 3-31]* Each rib bay of the wings is usually drained with one or two grommets on the bottom of the trailing edge. Note that drain holes without grommets are sometimes approved in reinforced fabric.

It is possible that additional inspection rings and drain grommets have been specified after the manufacture of the
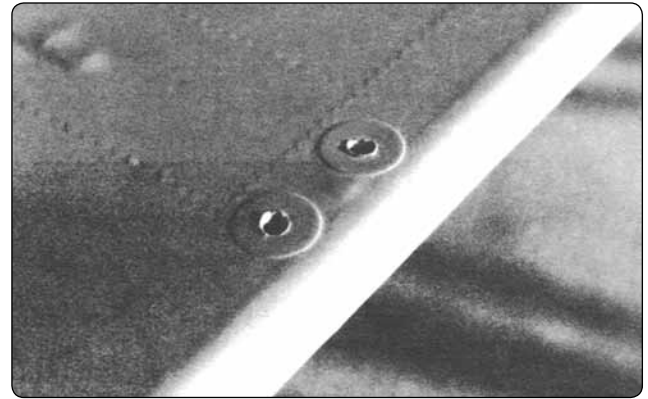
Figure 3-31. *Drain grommets cemented into place on the bottom side of a control surface.*

aircraft. Check the Airworthiness Directives (ADs) and Service Bulletins for the aircraft being re-covered to ensure required rings and grommets have been installed.

Cable guide openings, strut-attach fitting areas, and similar features, as well as any protrusions in the fabric covering, are reinforced with fabric gussets. These are installed as patches in the desired location. They should be cut to fit exactly around the feature they reinforce to support the original opening made in the covering fabric. *[Figure 3-32]* Gussets made to keep protrusions from coming through the fabric should overlap the area they protect. Most processes call for the gusset material to be preshrunk and cemented into place using the approved covering process cementing procedures.

Finishing Tapes

Finishing tapes are applied to all seams, edges, and over the ribs once all of the procedures above have been completed. They are used to protect these areas by providing smooth aerodynamic resistance to abrasion. The tapes are made from the same polyester material as the covering fabric. Use of lighter weight tapes is approved in some STCs. Preshrunk tapes are preferred because they react to exposure to the environment in the same way the as the fabric covering. This minimizes stress on the adhesive joint between the two. Straight edged and pinked tapes are available. The pinking provides greater surface area for adhesion of the edges and a smoother transition into the fabric covering. Only tapes approved in the STC under which work is being accomplished may be used to be considered airworthy.

Finishing tapes from one to six inches in width are used. Typically, two inch tapes cover the rib lacing and fuselage seams. Wing leading edges usually receive the widest tape with four inches being common. *[Figure 3-33]* Bias cut tapes are often used to wrap around the curved surfaces of the airframe, such as the wing tips and empennage surface edges. They lay flat around the curves and do not require notching.

Figure 3-32. *A strut fitting and cable guide with reinforcing fabric gussets cemented in place.*

Figure 3-33. *Cement is brushed through a four-inch tape during installation over the fabric seam on a wing leading edge. Two-inch tapes cover the wing ribs and rib lacing.*

Finishing tapes are attached with the process adhesive or the nitrate dope sealer when using a dope-based process. Generally, all chordwise tapes are applied first followed by the span-wise tapes at the leading and trailing edges. Follow the manufacturer's STC or AC 43.13-1 instructions.

Coating the Fabric

The sealer coat in most fabric covering processes is applied after all finishing tapes have been installed unless it was applied prior to rib lacing as in a dope-based finishing process. This coat saturates and completely surrounds the

fibers in the polyester fabric, forming a barrier that keeps water and contaminants from reaching the fabric during its life. It is also used to provide adhesion of subsequent coatings. Usually brushed on in a cross coat application for thorough penetration, two coats of sealer are commonly used but processes vary on how many coats and whether spray coating is permitted.

With the sealer coats installed and dried, the next step provides protection from UV light, the only significant cause of deterioration of polyester fabric. Designed to prevent UV light from reaching the fabric and extend the life of the fabric indefinitely, these coating products, or fill coats, contain aluminum solids premixed into them that block the UV rays. They are sprayed on in the number of cross coats as specified in the manufacturer's STC or AC 43.13-1 instructions under which work is done. Two to four cross coats is common. Note that some processes may require coats of clear butyrate before the blocking formula is applied.

Fabric primer is a coating used in some approved covering processes that combines the sealer and fill coatings into one. Applied to fabric after the finishing tapes are installed, these fabric primers surround and seal the fabric fibers, provide good adhesion for all of the following coatings, and contain UV blocking agents. One modern primer contains carbon solids and others use chemicals that work similarly to sun block for human skin. Typically, two to four coats of fabric primer are sufficient before the top coatings of the final finish are applied. *[Figure 3-34]*

Figure 3-34. *Applying a primer with UV blocking by spraying cross coats.*

The FAA-certificated mechanic must strictly adhere to all instructions for thinning, drying times, sanding, and cleaning. Small differences in the various processes exist and what

works in one process may not be acceptable and could ruin the finish of another process. STCs are issued on the basis of the holder having successfully proven the effectiveness of both the materials and the techniques involved.

When the fill coats have been applied, the final appearance of the fabric covering job is crafted with the application of various topcoats. Due to the chemical nature of the fill coating upon which topcoats are sprayed, only specified materials can be used for top coating to ensure compatibility. Colored butyrate dope and polyurethane paint finishes are most common. They are sprayed on according to instructions.

Once the topcoats are dry, the trim (N numbers, stripes, etc.) can be added. Strict observation of drying times and instructions for buffing and waxing are critical to the quality of the final finish. Also, note that STC instructions may include insight on finishing the nonfabric portions of the airframe to best match the fabric covering finish.

Polyester Fabric Repairs

Applicable Instructions

Repairs to aircraft fabric coverings are inevitable. Always inspect a damaged area to ensure the damage is confined to the fabric and does not involve the structure below. A technician who needs to make a fabric repair must first identify which approved data was used to install the covering that needs to be repaired. Consult the logbook where an entry and reference to manufacturer data, an STC, or a field approval possibly utilizing practices from AC 43.13-1 should be recorded. The source of approved data for the covering job is the same source of approved data used for a repair.

This section discusses general information concerning repairs to polyester fabric. Thorough instructions for repairs made to cotton covered aircraft can be found in AC 43.13-1. It is the responsibility of the holder of an STC to provide maintenance instructions for the STC alteration in addition to materials specifications required to do the job.

Repair Considerations

The type of repair performed depends on the extent of the damage and the process under which the fabric was installed. The size of the damaged area is often a reference for whether a patch is sufficient to do the repair or whether a new panel should be installed. Repair size may also dictate the amount of fabric-to-fabric overlap required when patching and whether finishing tapes are required over the patch. Many STC repair procedures do not require finishing tapes. Some repairs in AC 43.13-1 require the use of tape up to six inches wide.

While many cotton fabric repairs involve sewing, nearly all repairs of polyester fabric are made without sewing. It is possible to apply the sewing repair techniques outlined in AC 43.13-1 to polyester fabric, but they were developed primarily for cotton and linen fabrics. STC instructions for repairs to polyester fabric are for cemented repairs which most technicians prefer as they are generally considered easier than sewn repairs. There is no compromise to the strength of the fabric with either method.

Patching or replacing a section of the covering requires prepping the fabric area around the damage where new fabric is to be attached. Procedures vary widely. Dope-based covering systems tend toward stripping off all coatings to cement raw fabric to raw fabric when patching or seaming in a new panel. From this point, the coatings are reapplied and finished as in the original covering process. Some polyurethane-based coating processes require only a scuffing of the topcoat with sandpaper before adhering small patches that are then refinished. *[Figure 3-35]* Still, other processes may remove the topcoats and cement a patch into the sealer or UV blocking coating. In some repair processes, preshrunk fabric is used and in others, the fabric is shrunk after it is in place. Varying techniques and temperatures for shrinking and gluing the fabric into a repair also exist.

These deviations in procedures underscore the critical nature of identifying and strictly adhering to the correct instructions from the approved data for the fabric covering in need of repair. A patch or panel replacement technique for one covering system could easily create an unairworthy repair if used on fabric installed with a different covering process.

Large section panel repairs use the same proprietary adhesives and techniques and are only found in the instructions for the process used to install the fabric covering. A common technique for replacing any large damaged area is to replace all of the fabric between two adjacent structural members (e.g., two ribs, two longerons, between the forward and rear spars). Note that this is a major repair and carries with it the requirement to file an FAA Form 337.

Cotton-Covered Aircraft

You may encounter a cotton fabric-covered aircraft. In addition to other airworthiness criterion, the condition of the fabric under the finished surface is paramount as the cotton can deteriorate even while the aircraft is stored in a hanger. Inspection, in accordance with the manufacturer maintenance manual or AC 43.13-1, should be diligent. If the cotton covering is found to be airworthy, repairs to the fabric can be made under those specifications. This includes sewn-in and doped-in patches, as well as sewn-in and doped-in panel repairs. Due to the very limited number of airworthy aircraft that may still be covered with cotton, this handbook does not cover specific information on re-covering with cotton or
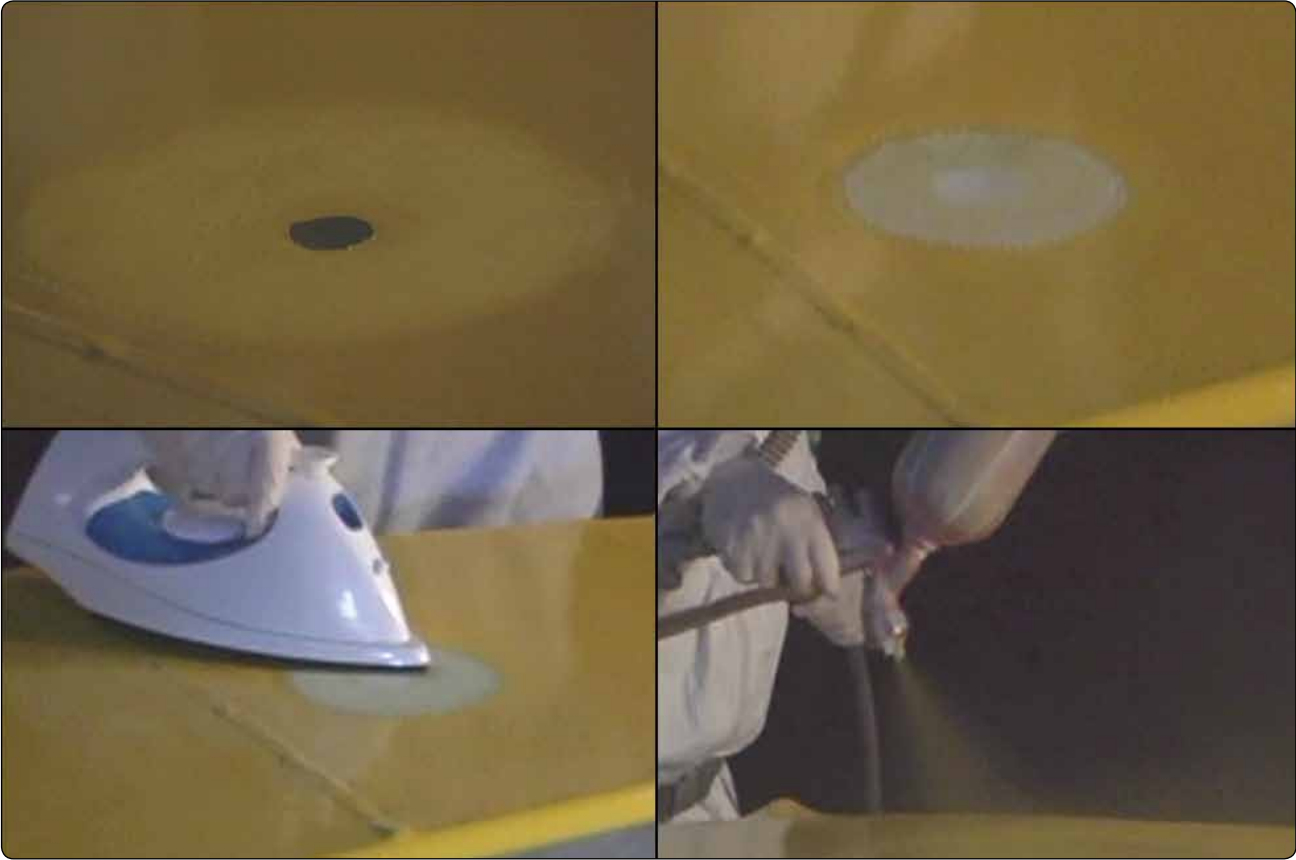
Figure 3-35. *A patch over this small hole on a polyurethane top coat is repaired in accordance with the repair instructions in the STC under which the aircraft was re-covered. It requires only a two-inch fabric overlap and scuffing into the top coat before cementing and refinishing. Other STC repair instructions may not allow this repair.*

cotton fabric maintenance and repair procedures. Refer to AC 43.13-1, Chapter 2, Fabric Covering, which thoroughly addresses these issues.

Fiberglass Coverings

References to fiberglass surfaces in aircraft covering STCs, AC 43.13-1, and other maintenance literature address techniques for finishing and maintaining this kind of surface. However, this is typically limited to fiberglass ray domes and fiberglass reinforced plywood surfaces and parts that are still in service. Use of dope-based processes on fiberglass is well established. Repair and apply coatings and finishes on fiberglass in accordance with manufacturer data, STC instructions, or AC 43.13-1 acceptable practices.

Chapter 8
Aircraft Painting and Finishing

Introduction

Paint, or more specifically its overall color and application, is usually the first impression that is transmitted to someone when they look at an aircraft for the first time. Paint makes a statement about the aircraft and the person who owns or operates it. The paint scheme may reflect the owner's ideas and color preferences for an amateur-built aircraft project, or it may be colors and identification for the recognition of a corporate or air carrier aircraft.

DO NOT ARC STROKE

	Hitrate	Nitrate dope	Butyrate dope	Nitro-cellulose lacquer	Poly-tone Poly-brush Poly-spray	Synthetic enamel	Acrylic lacquer	Acrylic enamel	Ure ena
Methanol		S	IS	IS	IS	PS	IS	PS	IS
Toluol (Toluene)		IS	IS	IS	S	IS	S	ISW	IS
MEK (Methyl ethyl ketone)		S	S	S	S	ISW	S	ISW	IS
Isopropanol		IS	IS	IS	S	S	S	IS	IS
Methylene chloride		SS	VS	S	VS	IS	S	IS	IS
					ISW		ISW	ISW	

Dial

Locking bolt

Spreader adjustment valve

Fluid needle valve

Air valve

Gun body

Dial at 0

Dial at 2

Dial at 4

Dial at 6

Di

Paint is more than aesthetics; it affects the weight of the aircraft and protects the integrity of the airframe. The topcoat finish is applied to protect the exposed surfaces from corrosion and deterioration. Also, a properly painted aircraft is easier to clean and maintain because the exposed surfaces are more resistant to corrosion and dirt, and oil does not adhere as readily to the surface.

A wide variety of materials and finishes are used to protect and provide the desired appearance of the aircraft. The term "paint" is used in a general sense and includes primers, enamels, lacquers, and the various multipart finishing formulas. Paint has three components: resin as coating material, pigment for color, and solvents to reduce the mix to a workable viscosity.

Internal structure and unexposed components are finished to protect them from corrosion and deterioration. All exposed surfaces and components are finished to provide protection and to present a pleasing appearance. Decorative finishing includes trim striping, the addition of company logos and emblems, and the application of decals, identification numbers, and letters.

Finishing Materials

A wide variety of materials are used in aircraft finishing. Some of the more common materials and their uses are described in the following paragraphs.

Acetone

Acetone is a fast-evaporating colorless solvent. It is used as an ingredient in paint, nail polish, and varnish removers. It is a strong solvent for most plastics and is ideal for thinning fiberglass resin, polyester resins, vinyl, and adhesives. It is also used as a superglue remover. Acetone is a heavy-duty degreaser suitable for metal preparation and removing grease from fabric covering prior to doping. It should not be used as a thinner in dope because of its rapid evaporation, which causes the doped area to cool and collect moisture. This absorbed moisture prevents uniform drying and results in blushing of the dope and a flat no-gloss finish.

Alcohol

Butanol, or butyl alcohol, is a slow-drying solvent that can be mixed with aircraft dope to retard drying of the dope film on humid days, thus preventing blushing. A mixture of dope solvent containing 5 to 10 percent of butyl alcohol is usually sufficient for this purpose. Butanol and ethanol alcohol are mixed together in ratios ranging from 1:1 to 1:3 to use to dilute wash coat primer for spray applications because the butyl alcohol retards the evaporation rate.

Ethanol or denatured alcohol is used to thin shellac for spraying and as a constituent of paint and varnish remover. It can also be used as a cleaner and degreaser prior to painting.

Isopropyl, or rubbing alcohol, can be used as a disinfectant. It is used in the formulation of oxygen system cleaning solutions. It can be used to remove grease pencil and permanent marker from smooth surfaces, or to wipe hand or fingerprint oil from a surface before painting.

Benzene

Benzene is a highly flammable, colorless liquid with a sweet odor. It is a product used in some paint and varnish removers. It is an industrial solvent that is regulated by the Environmental Protection Agency (EPA) because it is an extremely toxic chemical compound when inhaled or absorbed through the skin. It has been identified as a Class A carcinogen known to cause various forms of cancer. It should be avoided for use as a common cleaning solvent for paint equipment and spray guns.

Methyl Ethyl Ketone (MEK)

Methyl ethyl ketone (MEK), also referred to as 2-Butanone, is a highly flammable, liquid solvent used in paint and varnish removers, paint and primer thinners, in surface coatings, adhesives, printing inks, as a catalyst for polyester resin hardening, and as an extraction medium for fats, oils, waxes, and resins. Because of its effectiveness as a quickly evaporating solvent, MEK is used in formulating high solids coatings that help to reduce emissions from coating operations. Persons using MEK should use protective gloves and have adequate ventilation to avoid the possible irritation effects of skin contact and breathing of the vapors.

Methylene Chloride

Methylene Chloride is a colorless, volatile liquid completely miscible with a variety of other solvents. It is widely used in paint strippers and as a cleaning agent/degreaser for metal parts. It has no flash point under normal use conditions and can be used to reduce the flammability of other substances.

Toluene

Referred to as toluol or methylbenzene, toluene is a clear, water-insoluble liquid with a distinct odor similar to that of benzene. It is a common solvent used in paints, paint thinners, lacquers, and adhesives. It has been used as a paint remover in softening fluorescent-finish, clear-topcoat sealing materials. It is also an acceptable thinner for zinc chromate primer. It has been used as an antiknocking additive in gasoline. Prolonged exposure to toluene vapors should be avoided because it may be linked to brain damage.

Turpentine

Turpentine is obtained by distillation of wood from certain pine trees. It is a flammable, water-insoluble liquid solvent used as a thinner and quick-drier for varnishes, enamels, and other oil-based paints. Turpentine can be used to clean paint equipment and paint brushes used with oil-based paints.

Mineral Spirits

Sometimes referred to as white spirit, Stoddard solvent, or petroleum spirits, mineral spirits is a petroleum distillate used as a paint thinner and mild solvent. The reference to the name Stoddard came from a dry cleaner who helped to develop it in the 1920s as a less volatile dry cleaning solvent and as an alternative to the more volatile petroleum solvents that were being used for cleaning clothes. It is the most widely used solvent in the paint industry, used in aerosols, paints, wood preservatives, lacquers, and varnishes. It is also commonly used to clean paint brushes and paint equipment. Mineral spirits are used in industry for cleaning and degreasing machine tools and parts because it is very effective in removing oils and greases from metal. It has low odor, is less flammable, and less toxic than turpentine.

Naphtha

Naphtha is one of a wide variety of volatile hydrocarbon mixtures that is sometimes processed from coal tar but more often derived from petroleum. Naphtha is used as a solvent for various organic substances, such as fats and rubber, and in the making of varnish. It is used as a cleaning fluid and is incorporated into some laundry soaps. Naphtha has a low flashpoint and is used as a fuel in portable stoves and lanterns. It is sold under different names around the world and is known as white gas, or Coleman fuel, in North America.

Linseed Oil

Linseed oil is the most commonly used carrier in oil paint. It makes the paint more fluid, transparent, and glossy. It is used to reduce semipaste oil colors, such as dull black stenciling paint and insignia colors, to a brushing consistency. Linseed oil is also used as a protective coating on the interior of metal tubing. Linseed oil is derived from pressing the dried ripe flax seeds of the flax plant to obtain the oil and then using a process called solvent extraction. Oil obtained without the solvent extraction process is marketed as flaxseed oil. The term "boiled linseed oil" indicates that it was processed with additives to shorten its drying time.

A note of caution is usually added to packaging of linseed oil with the statement, "Risk of Fire from Spontaneous Combustion Exists with this Product." Linseed oil generates heat as it dries. Oily materials and rags must be properly disposed after use to eliminate the possible cause of spontaneous ignition and fire.

Thinners

Thinners include a plethora of solvents used to reduce the viscosity of any one of the numerous types of primers, subcoats, and topcoats. The types of thinner used with the various coatings is addressed in other sections of this chapter.

Varnish

Varnish is a transparent protective finish primarily used for finishing wood. It is available in interior and exterior grades. The exterior grade does not dry as hard as the interior grade, allowing it to expand and contract with the temperature changes of the material being finished. Varnish is traditionally a combination of a drying oil, a resin, and a thinner or solvent. It has little or no color, is transparent, and has no added pigment. Varnish dries slower than most other finishes. Resin varnishes dry and harden when the solvents in them evaporate. Polyurethane and epoxy varnishes remain liquid after the evaporation of the solvent but quickly begin to cure through chemical reactions of the varnish components.

Primers

The importance of primers in finishing and protection is generally misunderstood and underestimated because it is invisible after the topcoat finish is applied. A primer is the foundation of the finish. Its role is to bond to the surface, inhibit corrosion of metal, and provide an anchor point for the finish coats. It is important that the primer pigments be either anodic to the metal surface or passivate the surface should moisture be present. The binder must be compatible with the finish coats. Primers on nonmetallic surfaces do not require sacrificial or passivating pigments. Some of the various primer types are discussed below.

Wash Primers

Wash primers are water-thin coatings of phosphoric acid in solutions of vinyl butyral resin, alcohol, and other ingredients. They are very low in solids with almost no filling qualities. Their functions are to passivate the surface, temporarily provide corrosion resistance, and provide an adhesive base for the next coating, such as a urethane or epoxy primer. Wash primers do not require sanding and have high corrosion protection qualities. Some have a very small recoat time frame that must be considered when painting larger aircraft. The manufacturers' instructions must be followed for satisfactory results.

Red Iron Oxide

Red oxide primer is an alkyd resin-based coating that was developed for use over iron and steel located in mild environmental conditions. It can be applied over rust that is free of loose particles, oil, and grease. It has limited use in the aviation industry.

Gray Enamel Undercoat

This is a single component, nonsanding primer compatible with a wide variety of topcoats. It fills minor imperfections, dries fast without shrinkage, and has high corrosion resistance. It is a good primer for composite substrates.

Urethane

This is a term that is misused or interchanged by painters and manufacturers alike. It is typically a two-part product that uses a chemical activator to cure by linking molecules together to form a whole new compound. Polyurethane is commonly used when referring to urethane, but not when the product being referred to is acrylic urethane.

Urethane primer, like the urethane paint, is also a two-part product that uses a chemical activator to cure. It is easy to sand and fills well. The proper film thickness must be observed, because it can shrink when applied too heavily. It is typically applied over a wash primer for best results. Special precautions must be taken by persons spraying because the activators contain isocyanates (discussed further in the Protective Equipment section at the end of this chapter).

Epoxy

Epoxy is a synthetic, thermosetting resin that produces tough, hard, chemical-resistant coatings and adhesives. It uses a catalyst to chemically activate the product, but it is not classified as hazardous because it contains no isocyanates. Epoxy can be used as a nonsanding primer/sealer over bare metal and it is softer than urethane, so it has good chip resistance. It is recommended for use on steel tube frame aircraft prior to installing fabric covering.

Zinc Chromate

Zinc chromate is a corrosion-resistant pigment that can be added to primers made of different resin types, such as epoxy, polyurethane, and alkyd. Older type zinc chromate is distinguishable by its bright yellow color when compared to the light green color of some of the current brand primers. Moisture in the air causes the zinc chromate to react with the metal surface, and it forms a passive layer that prevents corrosion. Zinc chromate primer was, at one time, the standard primer for aircraft painting. Environmental concerns and new formula primers have all but replaced it.

Identification of Paints

Dope

When fabric-covered aircraft ruled the sky, dope was the standard finish used to protect and color the fabric. The dope imparted additional qualities of increased tensile strength, airtightness, weather-proofing, ultraviolet (UV) protection, and tautness to the fabric cover. Aircraft dope is essentially a colloidal solution of cellulose acetate or nitrate combined with plasticizers to produce a smooth, flexible, homogeneous film.

Dope is still used on fabric covered aircraft as part of a covering process. However, the type of fabric being used to cover the aircraft has changed. Grade A cotton or linen was the standard covering used for years, and it still may be used if it meets the requirements of the Federal Aviation Administration (FAA), Technical Standard Order (TSO) C-15d/AMS 3806c.

Polyester fabric coverings now dominate in the aviation industry. These new fabrics have been specifically developed for aircraft and are far superior to cotton and linen. The protective coating and topcoat finishes used with the Ceconite® polyester fabric covering materials are part of a Supplemental Type Certificate (STC) and must be used as specified when covering any aircraft with a Standard Airworthiness Certificate. The Ceconite® covering procedures use specific brand name, nontautening nitrate and butyrate dope as part of the STC.

The Poly-Fiber® system also uses a special polyester fabric covering as part of its STC, but it does not use dope. All the liquid products in the Poly-Fiber® system are made from vinyl, not from cellulose dope. The vinyl coatings have several real advantages over dope: they remain flexible, they do not shrink, they do not support combustion, and they are easily removed from the fabric with MEK, which simplifies most repairs.

Synthetic Enamel

Synthetic enamel is an oil-based single-stage paint (no clear coat) that provides durability and protection. It can be mixed with a hardener to increase the durability and shine while decreasing the drying time. It is one of the more economical types of finish.

Lacquers

The origin of lacquer dates back thousands of years to a resin obtained from trees indigenous to China. In the early 1920s, nitrocellulose lacquer was developed from a process using cotton and wood pulp.

Nitrocellulose lacquers produce a hard, semiflexible finish that can be polished to a high sheen. The clear variety yellows as it ages, and it can shrink over time to a point that the surface crazes. It is easy to spot repair because each new coat of lacquer softens and blends into the previous coat. This was one of the first coatings used by the automotive industry in mass production, because it reduced finishing times from almost two weeks to two days.

Acrylic lacquers were developed to eliminate the yellowing problems and crazing of the nitrocellulose lacquers. General Motors started using acrylic lacquer in the mid-1950s, and they used it into the 1960s on some of their premium model cars. Acrylics have the same working properties but dry to a less brittle and more flexible film than nitrocellulose lacquer.

Lacquer is one of the easiest paints to spray, because it dries quickly and can be applied in thin coats. However, lacquer is not very durable; bird droppings, acid rain, and gasoline spills actually eat down into the paint. It still has limited use on collector and show automobiles because they are usually kept in a garage, protected from the environment.

The current use of lacquer for an exterior coating on an aircraft is almost nonexistent because of durability and environmental concerns. Upwards of 85 percent of the volatile organic compounds (VOCs) in the spray gun ends up in the atmosphere, and some states have banned its use.

There are some newly developed lacquers that use a catalyst, but they are used mostly in the woodworking and furniture industry. They have the ease of application of nitrocellulose lacquer with much better water, chemical, and abrasion resistance. Additionally, catalyzed lacquers cure chemically, not solely through the evaporation of solvents, so there is a reduction of VOCs released into the atmosphere. It is activated when the catalyst is added to the base mixture.

Polyurethane
Polyurethane is at the top of the list when compared to other coatings for abrasion-, stain-, and chemical-resistant properties. Polyurethane was the coating that introduced the wet look. It has a high degree of natural resistance to the damaging effects of UV rays from the sun. Polyurethane is usually the first choice for coating and finishing the corporate and commercial aircraft in today's aviation environment.

Urethane Coating
The term urethane applies to certain types of binders used for paints and clear coatings. (A binder is the component that holds the pigment together in a tough, continuous film and provides film integrity and adhesion.) Typically, urethane is a two-part coating that consists of a base and catalyst that, when mixed, produces a durable, high-gloss finish that is abrasion and chemical resistant.

Acrylic Urethanes
Acrylic simply means plastic. It dries to a harder surface but is not as resistant to harsh chemicals as polyurethane. Most acrylic urethanes need additional UV inhibitors added when subject to the UV rays of the sun.

Methods of Applying Finish
There are several methods of applying aircraft finish. Among the most common are dipping, brushing, and spraying.

Dipping
The application of finishes by dipping is generally confined to factories or large repair stations. The process consists of dipping the part to be finished in a tank filled with the finishing material. Primer coats are frequently applied in this manner.

Brushing
Brushing has long been a satisfactory method of applying finishes to all types of surfaces. Brushing is generally used for small repair work and on surfaces where it is not practicable to spray paint.

The material to be applied should be thinned to the proper consistency for brushing. A material that is too thick has a tendency to pull or rope under the brush. If the materials are too thin, they are likely to run or not cover the surface adequately. Proper thinning and substrate temperature allows the finish to flow-out and eliminates the brush marks.

Spraying
Spraying is the preferred method for a quality finish. Spraying is used to cover large surfaces with a uniform layer of material, which results in the most cost effective method of application. All spray systems have several basic similarities. There must be an adequate source of compressed air, a reservoir or feed tank to hold a supply of the finishing material, and a device for controlling the combination of the air and finishing material ejected in an atomized cloud or spray against the surface to be coated.

A self-contained, pressurized spray can of paint meets the above requirements and satisfactory results can be obtained painting components and small areas of touchup. However, the aviation coating materials available in cans is limited, and this chapter addresses the application of mixed components through a spray gun.

There are two main types of spray equipment. A spray gun with an integral paint container is adequate for use when painting small areas. When large areas are painted, pressure-feed equipment is more desirable since a large supply of finishing material can be applied without the interruption of having to stop and refill a paint container. An added bonus is the lighter overall weight of the spray gun and the flexibility of spraying in any direction with a constant pressure to the gun.

The air supply to the spray gun must be entirely free of water or oil in order to produce the optimum results in the finished product. Water traps, as well as suitable filters to remove any trace of oil, must be incorporated in the air pressure supply line. These filters and traps must be serviced on a regular basis.

Finishing Equipment

Paint Booth

A paint booth may be a small room in which components of an aircraft are painted, or it can be an aircraft hangar big enough to house the largest aircraft. Whichever it is, the location must be able to protect the components or aircraft from the elements. Ideally, it would have temperature and humidity controls; but, in all cases, the booth or hangar must have good lighting, proper ventilation, and be dust free.

A simple paint booth can be constructed for a small aircraft by making a frame out of wood or polyvinyl chloride (PVC) pipe. It needs to be large enough to allow room to walk around and maneuver the spray gun. The top and sides can be covered with plastic sheeting stapled or taped to the frame. An exhaust fan can be added to one end with a large air-conditioning filter placed on the opposite end to filter incoming air. Lights should be large enough to be set up outside of the spray booth and shine through the sheeting or plastic windows. The ideal amount of light would be enough to produce a glare off of all the surfaces to be sprayed. This type of temporary booth can be set up in a hangar, a garage, or outside on a ramp, if the weather and temperature are favorable.

Normally, Environmental Protection Agency (EPA) regulations do not apply to a person painting one airplane. However, anyone planning to paint an aircraft should be aware that local clean air regulations may be applicable to an airplane painting project. When planning to paint an aircraft at an airport, it would be a good idea to check with the local airport authority before starting.

Air Supply

The air supply for paint spraying using a conventional siphon feed spray gun should come from an air compressor with a storage tank big enough to provide an uninterrupted supply of air with at least 90 pounds per square inch (psi) providing 10 cubic feet per minute (CFM) of air to the spray gun.

The compressor needs to be equipped with a regulator, water trap, air hose, and an adequate filter system to ensure that clean, dry, oil-free air is delivered to the spray gun.

If using one of the newer high-volume low-pressure (HVLP) spray guns and using a conventional compressor, it is better to use a two stage compressor of at least a 5 horsepower (hp)

that operates at 90 psi and provides 20 CFM to the gun. The key to the operation of the newer HVLP spray guns is the air volume, not the pressure.

If purchasing a new complete HVLP system, the air supply is from a turbine compressor. An HVLP turbine has a series of fans, or stages, that move a lot of air at low pressure. The more stages provide greater air output (rated in CFM) that means better atomization of the coating being sprayed. The intake air is also the cooling air for the motor. This air is filtered from dirt and dust particles prior to entering the turbine. Some turbines also have a second filter for the air supply to the spray gun. The turbine does not produce oil or water to contaminate the air supply, but the air supply from the turbine heats up, causing the paint to dry faster, so you may need an additional length of hose to reduce the air temperature at the spray gun.

Spray Equipment

Air Compressors

Piston–type compressors are available with one-stage and multiple-stage compressors, various size motors, and various size supply tanks. The main requirement for painting is to ensure the spray gun has a continuous supplied volume of air. Piston-type compressors compress air and deliver it to a storage tank. Most compressors provide over 100 psi, but only the larger ones provide the volume of air needed for an uninterrupted supply to the gun. The multistage compressor is a good choice for a shop when a large volume of air is needed for pneumatic tools. When in doubt about the size of the compressor, compare the manufacturer's specifications and get the largest one possible. *[Figure 8-1]*

Figure 8-1. *Standard air compressor.*

Large Coating Containers

For large painting projects, such as spraying an entire aircraft, the quantity of mixed paint in a pressure tank provides many advantages. The setup allows a greater area to be covered without having to stop and fill the cup on a spray gun. The painter is able to keep a wet paint line, and more material is applied to the surface with less overspray. It provides the flexibility of maneuvering the spray gun in any position without the restriction and weight of an attached paint cup. Remote pressure tanks are available in sizes from 2 quarts to over 60 gallons. *[Figure 8-2]*

Figure 8-2. *Pressure paint tank.*

System Air Filters

The use of a piston-type air compressor for painting requires that the air supply lines include filters to remove water and oil. A typical filter assembly is shown in *Figure 8-3*.

Miscellaneous Painting Tools and Equipment

Some tools that are available to the painter include:

- Masking paper/tape dispenser that accommodates various widths of masking paper. It includes a masking tape dispenser that applies the tape to one edge of the paper as it is rolled off to facilitate one person applying the paper and tape in a single step.

- Electronic and magnetic paint thickness gauges to measure dry paint thickness.

- Wet film gauges to measure freshly applied wet paint.

- Infrared thermometers to measure coating and substrate surfaces to verify that they fall in the recommended temperature range prior to spraying.

Figure 8-3. *Air line filter assembly.*

Spray Guns

A top quality spray gun is a key component in producing a quality finish in any coating process. It is especially important when painting an aircraft because of the large area and varied surfaces that must be sprayed.

When spray painting, it is of utmost importance to follow the manufacturer's recommendations for correct sizing of the air cap, fluid tip, and needle combinations. The right combination provides the best coverage and the highest quality finish in the shortest amount of time.

All of the following examples of the various spray guns (except the airless) are of the air atomizing type. They are the most capable of providing the highest quality finish.

Siphon Feed Gun

The siphon feed gun is a conventional spray gun familiar to most people, with a one quart paint cup located below the gun. Regulated air passes through the gun and draws (siphons) the paint from the supply cup. This is an external mix gun, which means the air and fluid mix outside the air cap. This gun applies virtually any type coating and provides a high quality finish. *[Figure 8-4]*

Gravity-Feed Gun

A gravity-feed gun provides the same high-quality finish as a siphon-feed gun, but the paint supply is located in a cup on top of the gun and supplied by gravity. The operator can make fine adjustments between the atomizing pressure and fluid flow and utilize all material in the cup. This also is an external mix gun. *[Figure 8-5]*

The HVLP production spray gun is an internal mix gun. The air and fluid is mixed inside the air cap. Because of the low pressure used in the paint application, it transfers at least 65

Figure 8-4. *Siphon-feed spray gun.*

Figure 8-5. *Gravity-feed spray gun.*

Figure 8-6. *A High Volume Low Pressure (HVLP) spray gun.*

spray gun under high hydraulic pressure (500 to 4,500 psi) to atomize the fluid. The fluid is then released through an orifice in the spray nozzle. This system increases transfer efficiency and production speed with less overspray than conventional air atomized spray systems. It is used for production work but does not provide the fine finish of air atomized systems. *[Figure 8-7]*

Figure 8-7. *Airless spray gun.*

percent and upwards of 80 percent of the finish material to the surface. HVLP spray guns are available with a standard cup located underneath or in a gravity-feed model with the cup on top. The sample shown can be connected with hoses to a remote paint material container holding from 2 quarts to 60 gallons. *[Figure 8-6]*

Because of more restrictive EPA regulations, and the fact that more paint is being transferred to the surface with less waste from overspray, a large segment of the paint and coating industry is switching to HVLP spray equipment.

Airless spraying does not directly use compressed air to atomize the coating material. A pump delivers paint to the

Fresh Air Breathing Systems

Fresh air breathing systems should be used whenever coatings are being sprayed that contain isocyanides. This includes

all polyurethane coatings. The system incorporates a high-capacity electric air turbine that provides a constant source of fresh air to the mask. The use of fresh air breathing systems is also highly recommended when spraying chromate primers and chemical stripping aircraft. The system provides cool filtered breathing air with up to 200 feet of hose, which allows the air pump intake to be placed in an area of fresh air, well outside of the spraying area. *[Figure 8-8]*

Figure 8-8. *Breathe-Cool II® supplied air respirator system with Tyvek® hood.*

A charcoal-filtered respirator should be used for all other spraying and sanding operations to protect the lungs and respiratory tract. The respirator should be a double-cartridge, organic vapor type that provides a tight seal around the nose and mouth. The cartridges can be changed separately, and should be changed when detecting odor or experiencing nose or throat irritation. The outer prefilters should be changed if experiencing increased resistance to breathing. *[Figure 8-9]*

Figure 8-9. *Charcoal-filtered respirator.*

Viscosity Measuring Cup

This is a small cup with a long handle and a calibrated orifice in the bottom, that allows the liquid in the cup to drain out at a specific timed rate. Coating manufacturers recommend

spraying their product at a specific pressure and viscosity. That viscosity is determined by measuring the efflux (drain) time of the liquid coating through the cup orifice. The time (in seconds) is listed on most paint manufacturers' product/technical data pages. The measurement determines if the mixed coating meets the recommended viscosity for spraying.

There are different manufacturers of the viscosity measuring devices, but the most common one listed and used for spray painting is known as a Zahn cup. The orifice number must correspond to the one listed on the product/technical data sheet. For most primers and topcoats, the #2 or #3 Zahn cup is the one recommended. *[Figure 8-10]*
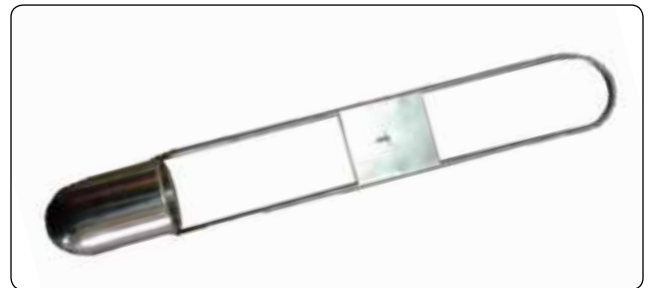
Figure 8-10. *A Zahncup viscosity measuring cup.*

To perform an accurate viscosity measurement, it is very important that the temperature of the sample material be within the recommended range of 73.5 °F ± 3.5 °F (23 ºC ± 2 ºC), and then proceed as follows:

1. Thoroughly mix the sample with minimum bubbles.

2. Dip the Zahn cup vertically into the sample being tested, totally immersing the cup below the surface.

3. With a stopwatch in one hand, briskly lift the cup out of the sample. As the top edge of the cup breaks the surface, start the stopwatch.

4. Stop the stopwatch when the first break in the flow of the liquid is observed at the orifice exit. The number in seconds is referred to as the efflux time.

5. Record the time on the stopwatch and compare it to the coating manufacturer's recommendation. Adjust the viscosity, if necessary, but be aware not to thin the coating below recommendations that could result in the release of VOCs into the atmosphere above the regulated limitations.

Mixing Equipment

Use a paint shaker for all coatings within 5 days of application to ensure the material is thoroughly mixed. Use a mechanical paint stirrer to mix larger quantities of material. If a mechanical stirrer is driven by a drill, the drill should be pneumatic, instead of electric. The sparks from an electric drill can cause an explosion from the paint vapors.

Preparation

Surfaces

The most important part of any painting project is the preparation of the substrate surface. It takes the most work and time, but with the surface properly prepared, the results are a long-lasting, corrosion-free finish. Repainting an older aircraft requires more preparation time than a new paint job because of the additional steps required to strip the old paint, and then clean the surface and crevices of paint remover. Paint stripping is discussed in another section of this chapter.

It is recommended that all the following procedures be performed using protective clothing, rubber gloves, and goggles, in a well-ventilated area, at temperatures between 68 °F and 100 °F.

Aluminum surfaces are the most common on a typical aircraft. The surface should be scrubbed with Scotch-Brite® pads using an alkaline aviation cleaner. The work area should be kept wet and rinsed with clean water until the surface is water break free. This means that there are no beads or breaks in the water surface as it flows over the aluminum surface.

The next step is to apply an acid etch solution to the surface. Following manufacturers' suggestions, this is applied like a wash using a new sponge and covering a small area while keeping it wet and allowing it to contact the surface for between 1 and 2 minutes. It is then rinsed with clean water without allowing the solution to dry on the surface. Continue this process until all the aluminum surfaces are washed and rinsed. Extra care must be taken to thoroughly rinse this solution from all the hidden areas that it may penetrate. It provides a source for corrosion to form if not completely removed.

When the surfaces are completely dry from the previous process, the next step is to apply Alodine® or another type of an aluminum conversion coating. This coating is also applied like a wash, allowing the coating to contact the surface and keeping it wet for 2 to 5 minutes without letting it dry. It then must be thoroughly rinsed with clean water to remove all chemical salts from the surface. Depending on the brand, the conversion coating may color the aluminum a light gold or green, but some brands are colorless. When the surface is thoroughly dry, the primer should be applied as soon as possible as recommended by the manufacturer.

The primer should be one that is compatible with the topcoat finish. Two-part epoxy primers provide excellent corrosion resistance and adhesion for most epoxy and urethane surfaces and polyurethane topcoats. Zinc chromate should not be used under polyurethane paints.

Composite surfaces that need to be primed may include the entire aircraft if it is constructed from those materials, or they may only be components of the aircraft, such as fairings, radomes, antennas, and the tips of the control surfaces.

Epoxy sanding primers have been developed that provide an excellent base over composites and can be finish sanded with 320 grit using a dual action orbital sander. They are compatible with two-part epoxy primers and polyurethane topcoats.

Topcoats must be applied over primers within the recommended time window, or the primer may have to be scuff sanded before the finish coat is applied. Always follow the recommendations of the coating manufacturer.

Primer and Paint

Purchase aircraft paint for the aviation painting project. Paint manufacturers use different formulas for aircraft and automobiles because of the environments they operate in. The aviation coatings are formulated to have more flexibility and chemical resistance than the automotive paint.

It is also highly recommended that compatible paints of the same brand are used for the entire project. The complete system (of a particular brand) from etching to primers and reducers to the finish topcoat are formulated to work together. Mixing brands is a risk that may ruin the entire project.

When purchasing the coatings for a project, always request a manufacturer's technical or material data and safety data sheets, for each component used. Before starting to spray, read the sheets. If the manufacturer's recommendations are not followed, a less than satisfactory finish or a hazard to personal safety or the environment may result. It cannot be emphasized enough to follow the manufacturer's recommendations. The finished result is well worth the effort.

Before primer or paint is used for any type application, it must be thoroughly mixed. This is done so that any pigment that may have settled to the bottom of the container is brought into suspension and distributed evenly throughout the paint. Coatings now have shelf lives listed in their specification sheets. If a previously opened container is found to have a skin or film formed over the primer or paint, the film must be completely removed before mixing. The material should not be used if it has exceeded its shelf life and/or has become thick or jelled.

Mechanical shaking is recommended for all coatings within 5 days of use. After opening, a test with a hand stirrer should be made to ensure that all the pigment has been brought into

suspension. Mechanical stirring is recommended for all two-part coatings. When mixing any two-part paint, the catalyst/activator should always be added to the base or pigmented component. The technical or material data sheet of the coating manufacturer should be followed for recommended times of induction (the time necessary for the catalyst to react with the base prior to application). Some coatings do not require any induction time after mixing, and others need 30 minutes of reaction time before being applied.

Thinning of the coating material should follow the recommendations of the manufacturer. The degree of thinning depends on the method of application. For spray application, the type of equipment, air pressure, and atmospheric conditions guide the selection and mixing ratios for the thinners. Because of the importance of accurate thinning to the finished product, use a viscosity measuring (flow) cup. Material thinned using this method is the correct viscosity for the best application results.

Thin all coating materials and mix in containers separate from the paint cup or pot. Then, filter the material through a paint strainer recommended for the type coating you are spraying as you pour it into the cup or supply pot.

Spray Gun Operation

Adjusting the Spray Pattern

To obtain the correct spray pattern, set the recommended air pressure on the gun, usually 40 to 50 psi for a conventional gun. Test the pattern of the gun by spraying a piece of masking paper taped to the wall. Hold the gun square to the wall approximately 8 to 10 inches from the surface. (With hand spread, it is the distance from the tip of the thumb to the tip of the little finger.)

All spray guns (regardless of brand name) have the same type of adjustments. The upper control knob proportions the air flow, adjusting the spray pattern of the gun. *[Figure 8-11]*

The lower knob adjusts the fluid passing the needle, which in turn controls the amount or volume of paint being delivered through the gun.

Pull the trigger lever fully back. Move the gun across the paper, and alternately adjust between the two knobs to obtain a spray fan of paint that is wet from top to bottom (somewhat like the pattern at dial 10.) Turning in (to the right) on the lower, or fluid knob, reduces the amount of paint going through the gun. Turning out increases the volume of paint. Turning out (to the left) on the upper, or pattern control knob, widens the spray pattern. Turning in reduces it to a cone shape (as shown with dial set at 0).

Once the pattern is set on the gun, the next step is to follow the correct spraying technique for applying the coating to the surface.

Applying the Finish

If the painter has never used a spray gun to apply a finish coat of paint, and the aircraft has been completely prepared, cleaned, primed, and ready for the topcoat, he or she may need to pause for some practice. Reading a book or an instruction manual is a good start as it provides the basic knowledge about the movement of the spray gun across the surface. Also, if available, the opportunity to observe an aircraft being painted is well worth the time.

At this point in the project, the aircraft has already received its primer coats. The difference between the primer and the finish topcoat is that the primer is flat (no gloss) and the finish coat has a glossy surface (some more than others, depending on the paint). The flat finish of the primer is obtained by paying attention to the basics of trigger control distance from the surface and consistent speed of movement of the spray gun across the surface.
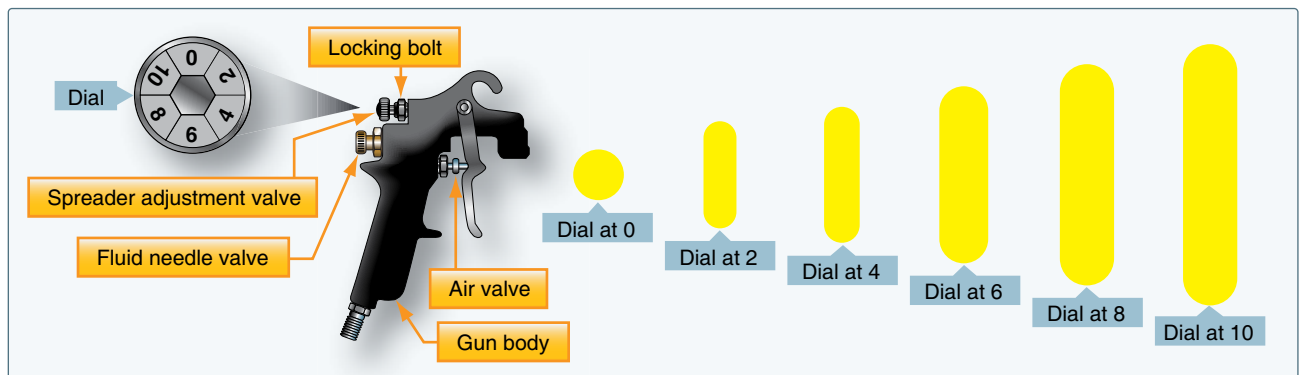

Figure 8-11. *Adjustable spray pattern.*

Primer is typically applied using a crosscoat spray pattern. A crosscoat is one pass of the gun from left to right, followed by another pass moving up and down. The starting direction does not matter as long as the spraying is accomplished in two perpendicular passes. The primer should be applied in light coats as cross-coating is the application of two coats of primer.

Primer does not tend to run because it is applied in light coats. The gloss finish requires a little more experience with the gun. A wetter application produces the gloss, but the movement of the gun, overlap of the spray pattern, and the distance from the surface all affect the final product. It is very easy to vary one or another, yielding runs or dry spots and a less than desirable finish. Practice not only provides some experience, but also provides the confidence needed to produce the desired finish.

Start the practice by spraying the finish coat material on a flat, horizontal panel. The spray pattern has been already adjusted by testing it on the masking paper taped to the wall. Hold the gun 8–10 inches away from and perpendicular to the surface. Pull the trigger enough for air to pass through the cap and start a pass with the gun moving across the panel. As it reaches the point to start painting, squeeze the trigger fully back and continue moving the gun about one foot per second across the panel until the end is reached. Then, release the trigger enough to stop the paint flow but not the air flow. *[Figure 8-12]*

The constant air flow through the gun maintains a constant pressure, rather than a buildup of pressure each time that the

trigger is released. This would cause a buildup of paint at the end of each pass, causing runs and sags in the finish. Repeat the sequence of the application, moving back in the opposite direction and overlapping the first pass by 50 percent. This is accomplished by aiming the center of the spray pattern at the outer edge of the first pass and continuing the overlap with each successive pass of the gun.

Once the painter has mastered spraying a flat horizontal panel, practice next on a panel that is positioned vertically against a wall. This is the panel that shows the value of applying a light tack coat before spraying on the second coat. The tack coat holds the second coat from sagging and runs. Practice spraying this test panel both horizontally with overlapping passes and then rotate the air cap 90° on the gun and practice spraying vertically with the same 50 percent overlapping passes.

Practice cross-coating the paint for an even application. Apply two light spray passes horizontally, overlapping each by 50 percent, and allowing it to tack. Then, spray vertically with overlapping passes, covering the horizontal sprayed area. When practice results in a smooth, glossy, no-run application on the vertical test panel, you are ready to try your skill on the actual project.

Common Spray Gun Problems

A quick check of the spray pattern can be verified before using the gun by spraying some thinner or reducer, compatible with the finish used, through the gun. It is not of the same viscosity as the coating, but it indicates if the gun is working properly before the project is started.
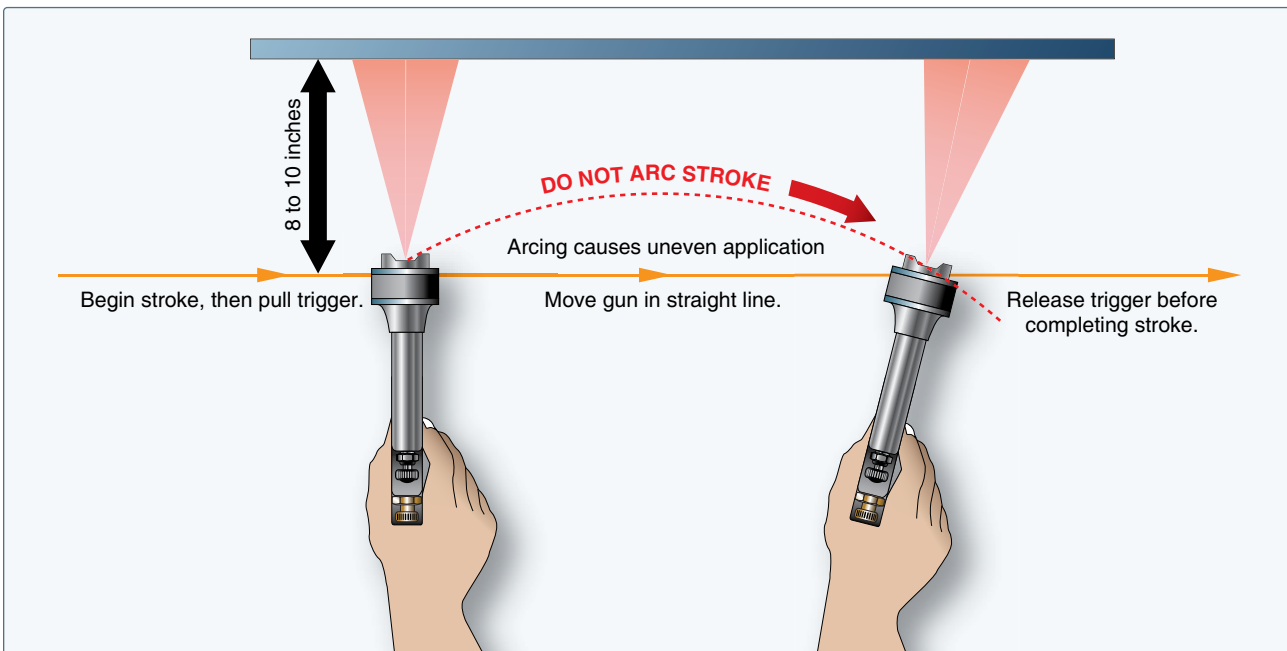

Figure 8-12. *Proper spray application.*

If the gun is not working properly, use the following information to troubleshoot the problem:

- A pulsating, or spitting, fan pattern may be caused by a loose nozzle, clogged vent hole on the supply cup, or the packing may be leaking around the needle.

- If the spray pattern is offset to one side or the other, the air ports in the air cap or the ports in the horns may be plugged.

- If the spray pattern is heavy on the top or the bottom, rotate the air cap 180°. If the pattern reverses, the air cap is the problem. If it stays the same, the fluid tip or needle may be damaged.

- Other spray pattern problems may be a result of improper air pressure, improper reducing of the material, or wrong size spray nozzle.

Sequence for Painting a Single-Engine or Light Twin Airplane

As a general practice on any surface being painted, spray each application of coating in a different direction to facilitate even and complete coverage. After you apply the primer, apply the tack coat and subsequent top coats in opposite directions, one coat vertically and the next horizontally, as appropriate.

Start by spraying all the corners and gaps between the control surfaces and fixed surfaces. Paint the leading and trailing edges of all surfaces. Spray the landing gear and wheel wells, if applicable, and paint the bottom of the fuselage up the sides to a horizontal break, such as a seam line. Paint the underside of the horizontal stabilizer. Paint the vertical stabilizer and the rudder, and then move to the top of the horizontal stabilizer. Spray the top and sides of the fuselage down to the point of the break from spraying the underside of the fuselage. Then, spray the underside of the wings. Complete the job by spraying the top of the wings.

The biggest challenge is to control the overspray and keep the paint line wet. The ideal scenario would be to have another experienced painter with a second spray gun help with the painting. It is much easier to keep the paint wet and the job is completed in half the time.

Common Paint Troubles

Common problems that may occur during the painting of almost any project but are particularly noticeable and troublesome on the surfaces of an aircraft include poor adhesion, blushing, pinholes, sags and/or runs, "orange peel," fisheyes, sanding scratches, wrinkling, and spray dust.

Poor Adhesion

- Improper cleaning and preparation of the surface to be finished.

- Application of the wrong primer.

- Incompatibility of the topcoat with the primer. *[Figure 8-13]*

- Improper thinning of the coating material or selection of the wrong grade reducer.

- Improper mixing of materials.

- Contamination of the spray equipment and/or air supply.

Figure 8-13. *Example of poor adhesion.*

Correction for poor adhesion requires a complete removal of the finish, a determination and correction of the cause, and a complete refinishing of the affected area.

Blushing

Blushing is the dull milky haze that appears in a paint finish. *[Figure 8-14]* It occurs when moisture is trapped in the paint. Blushing forms when the solvents quickly evaporate from the sprayed coating, causing a drop in temperature that is enough to condense the water in the air. It usually forms when the humidity is above 80 percent. Other causes include:

- Incorrect temperature (below 60 °F or above 95 °F).

- Incorrect reducer (fast drying) being used.

- Excessively high air pressure at the spray gun.

If blushing is noticed during painting, a slow-drying reducer can sometimes be added to the paint mixture, and then the area resprayed. If blushing is found after the finish has dried, the area must be sanded down and repainted.

Figure 8-14. *Example of blushing.*

Pinholes

Pinholes are tiny holes, or groups of holes, that appear in the surface of the finish as a result of trapped solvents, air, or moisture. *[Figure 8-15]* Examples include:

- Contaminants in the paint or air lines.

- Poor spraying techniques that allow excessively heavy or wet paint coats, which tend to trap moisture or solvent under the finish.

- Use of the wrong thinner or reducer, either too fast by quick drying the surface and trapping solvents or too slow and trapping solvents by subsequent topcoats.

Figure 8-15. *Example of pinholes.*

If pinholes occur during painting, the equipment and painting technique must be evaluated before continuing. When dry, sand the surface smooth and then repaint.

Sags and Runs

Sags and runs are usually caused by applying too much paint to an area, by holding the spray gun too close to the surface, or moving the gun too slowly across the surface. *[Figure 8-16]*

Figure 8-16. *Example of sags and runs.*

Other causes include:

- Too much reducer in the paint (too thin).

- Incorrect spray gun setting of air-paint mixture.

Sags and runs can be avoided by following the recommended thinning instructions for the coatings being applied and taking care to use the proper spray gun techniques, especially on vertical surfaces and projected edges. Dried sags and runs must be sanded out and the surface repainted.

Orange Peel

"Orange peel" refers to the appearance of a bumpy surface, much like the skin of an orange. *[Figure 8-17]* It can be the result of a number of factors with the first being the improper adjustment of the spray gun. Other causes include:

- Not enough reducer (too thick) or the wrong type reducer for the ambient temperature.

- Material not uniformly mixed.

- Forced drying method, either with fans or heat, is too quick.

Figure 8-17. *Example of orange peel.*

- Too little flash time between coats.
- Spray painting when the ambient or substrate temperature is either too hot or too cold.

Light orange peel can be wet sanded or buffed out with polishing compound. In extreme cases, it has to be sanded smooth and resprayed.

Fisheyes

Fisheyes appear as small holes in the coating as it is being applied, which allows the underlying surface to be seen. *[Figure 8-18]* Usually, it is due to the surface not being cleaned of all traces of silicone wax. If numerous fisheyes appear when spraying a surface, stop spraying and clean off all the wet paint. Then, thoroughly clean the surface to remove all traces of silicone with a silicone wax remover.

Figure 8-18. *Example of fisheyes.*

The most effective way to eliminate fisheyes is to ensure that the surface about to be painted is clean and free from any type of contamination. A simple and effective way to check this is referred to as a water break test. Using clean water, spray, pour, or gently hose down the surface to be painted. If the water beads up anywhere on the surface, it is not clean. The water should flatten out and cover the area with an unbroken film.

If the occasional fisheye appears when spraying, wait until the first coat sets up and then add a recommended amount of fisheye eliminator to the subsequent finish coats. Fisheyes may appear during touchup of a repair. A coat of sealer may help, but completed removal of the finish may be the only solution.

One last check before spraying is to ensure that the air compressor has been drained of water, the regulator cleaned, and the system filters are clean or have been replaced so that this source of contamination is eliminated.

Sanding Scratches

Sanding scratches appear in the finish paint when the surface has not been properly sanded and/or sealed prior to spraying the finish coats. *[Figure 8-19]* This usually shows up in nonmetal surfaces. Composite cowling, wood surfaces, and plastic fairings must be properly sanded and sealed before painting. The scratches may also appear if on overly rapid quick-drying thinner is used.

The only fix after the finish coat has set up is to sand down the affected areas using a finer grade of sandpaper, follow with a recommended sealer, and then repaint.

Figure 8-19. *Example of sanding scratches.*

Wrinkling

Wrinkling is usually caused by trapped solvents and unequal drying of the paint finish due to excessively thick or solvent-heavy paint coats. *[Figure 8-20]* Fast reducers can also contribute to wrinkling if the sprayed coat is not allowed to dry thoroughly. Thick coatings and quick-drying reducers allow the top surface of the coating to dry, trapping the
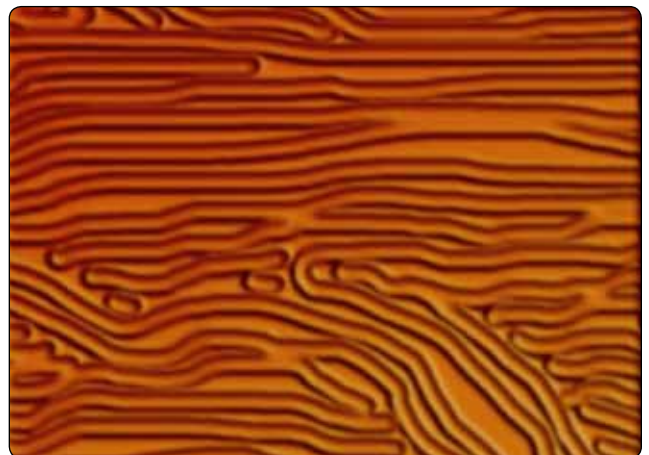

Figure 8-20. *Example of wrinkling.*

solvents underneath. If another heavy coat is applied before the first one dries, wrinkles may result. It may also have the effect of lifting the coating underneath, almost with the same result as a paint stripper.

Rapid changes in ambient temperatures while spraying may cause an uneven release of the solvents, causing the surface to dry, shrink, and wrinkle. Making the mistake of using an incompatible thinner, or reducer, when mixing the coating materials may cause not only wrinkles but other problems as well. Wrinkled paint must be completely removed and the surface refinished.

Spray Dust

Spray dust is caused by the atomized spray particles from the gun becoming dry before reaching the surface being painted, thus failing to flow into a continuous film. *[Figure 8-21]* This may be caused by:

- Incorrect spray gun setting of air pressure, paint flow, or spray pattern.

- Spray gun being held too far from the surface.

- Material being improperly thinned or the wrong reducers being used with the finish coats.

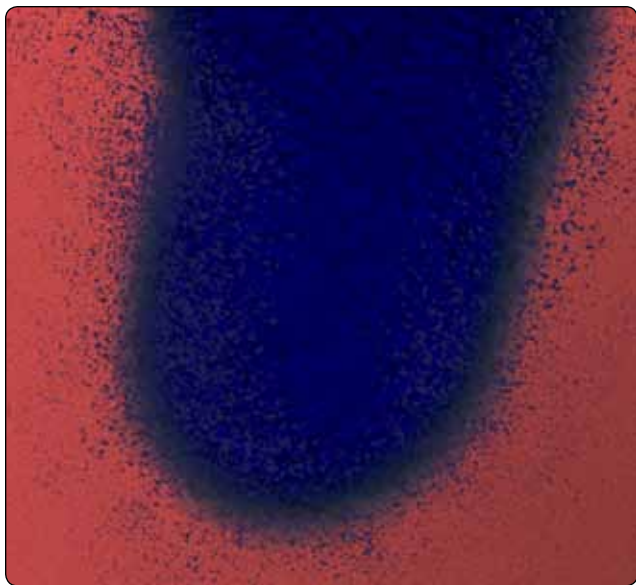The affected area needs to be sanded and recoated.

Figure 8-21. *Example of spray dust.*

Painting Trim and Identification Marks

Masking and Applying the Trim

At this point in the project, the entire aircraft has been painted with the base color and all the masking paper and tape carefully removed. Refer again to the coating manufacturer's technical data sheet for "dry and recoat" times for the

appropriate temperatures and "dry to tape" time that must elapse before safe application and removal of tape on new paint without it lifting.

Masking Materials

When masking for the trim lines, use 3M® Fine Line tape. It is solvent proof, available in widths of ⅛–1 inch and, when applied properly, produces a sharp edge paint line. A good quality masking tape should be used with masking paper to cover all areas not being trimmed to ensure the paper does not lift and allow overspray on the basecoat. Do not use newspaper to mask the work as paint penetrates newspaper. Using actual masking paper is more efficient, especially if with a masking paper/tape dispenser as part of the finishing equipment.

Masking for the Trim

After the base color has dried and cured for the recommended time shown in the manufacturer's technical data sheet, the next step is to mask for the trim. The trim design can be simple, with one or two color stripes running along the fuselage, or it can be an elaborate scheme covering the entire aircraft. Whichever is chosen, the basic masking steps are the same.

If unsure of a design, there are numerous websites that provide the information and software to do a professional job. If electing to design a personalized paint scheme, the proposed design should be portrayed on a silhouette drawing of the aircraft as close to scale as possible. It is much easier to change a drawing than to remask the aircraft.

Start by identifying a point on the aircraft from which to initiate the trim lines using the Fine Line tape. If the lines are straight and/or have large radius curves, use ¾-inch or one-inch tape and keep it pulled tight. The wider tape is much easier to control when masking a straight line. Smaller radius curves may require ½-inch or even ¼-inch tape. Try and use the widest tape that lays flat and allows for a smooth curve. Use a small roller (like those used for wallpaper seams) to go back over and roll the tape edges firmly onto the surface to ensure they are flat.

Finish masking the trim lines on one side of the aircraft, to include the fuselage, vertical fin and rudder, the engine nacelles and wing(s). Once complete, examine the lines. If adjustments are needed to the placement or design, now is the time to correct it. With one side of the aircraft complete, the entire design and placement can be transferred to the opposite side.

Different methods can be employed to transfer the placement of the trim lines from one side of the aircraft to the other. One method is to trace the design on paper and then apply it

to the other side, starting at the same point opposite the first starting point. Another method is to use the initial starting point and apply the trim tape using sheet metal or rivet lines as reference, along with measurements, to position the tape in the correct location.

When both sides are completed, a picture can be taken of each side and a comparison made to verify the tape lines on each side of the aircraft are identical.

With the Fine Line taping complete, some painters apply a sealing strip of ¾-inch or 1-inch masking tape covering half and extending over the outside edge of the Fine Line tape. This provides a wider area to apply the masking paper and adds an additional seal to the Fine Line tape. Now, apply the masking paper using 1-inch tape, placing half the width of the tape on the paper and half on the masked trim tape.

Use only masking paper made for painting and a comparable quality masking tape. With all the trim masking complete, cover the rest of the exposed areas of the aircraft to prevent overspray from landing on the base color. Tape the edges of the covering material to ensure the spray does not drift under it.

Now, scuff-sand all the area of trim to be painted to remove the gloss of the base paint. The use of 320-grit for the main area and a fine mesh Scotch-Brite pad next to the tape line should be sufficient. Then, blow all the dust and grit off the aircraft, and wipe down the newly sanded trim area with a degreaser and a tack cloth. Press or roll down the trim tape edges one more time before painting.

There are some various methods used by painters to ensure that a sharp defined tape line is attained upon removal of the tape. The basic step is to first use the 3M® Fine Line tape to mask the trim line. Some painters then spray a light coat of the base color or clear coat just prior to spraying the trim color. This will seal the tape edge line and ensure a clean sharp line when the tape is removed.

If multiple colors are used for the trim, cover the trim areas not to be sprayed with masking paper. When the first color is sprayed and dried, remove the masking paper from the next trim area to spray and cover the trim area that was first sprayed, taking care not to press the masking paper or tape into the freshly dried paint.

With all the trim completed, the masking paper should be removed as soon as the last trimmed area is dry to the touch. Carefully remove the Fine Line trim edge tape by slowly pulling it back onto itself at a sharp angle. Remove all trim and masking tape from the base coat as soon as possible to preclude damage to the paint.

As referenced previously, use compatible paint components from the same manufacturer when painting trim over the base color. This reduces the possibility of an adverse reaction between the base coat and the trim colors.

Display of Nationality and Registration Marks

The complete regulatory requirement for identification and marking of a U.S.-registered aircraft can be found in Title 14 of the Code of Federal Regulations (14 CFR), Part 45, Identification and Registration Marking.

In summary, the regulation states that the marks must:

- Be painted on the aircraft or affixed by other means to insure a similar degree of permanence;

- Have no ornamentation;

- Contrast in color with the background; and

- Be legible.

The letters and numbers may be taped off and applied at the same time and using the same methods as when the trim is applied, or they may be applied later as decals of the proper size and color.

Display of Marks

Each operator of an aircraft shall display on the aircraft marks consisting of the Roman capital letter "N" (denoting United States registration) followed by the registration number of the aircraft. Each suffix letter must also be a Roman capital letter.

Location and Placement of Marks

On fixed-wing aircraft, marks must be displayed on either the vertical tail surfaces or the sides of the fuselage. If displayed on the vertical tail surfaces, they shall be horizontal on both surfaces of a single vertical tail or on the outer surfaces of a multivertical tail. If displayed on the fuselage surfaces, then horizontally on both sides of the fuselage between the trailing edge of the wing and the leading edge of the horizontal stabilizer. Exceptions to the location and size requirement for certain aircraft can be found in 14 CFR part 45.

On rotorcraft, marks must be displayed horizontally on both surfaces of the cabin, fuselage, boom, or tail. On airships, balloons, powered parachutes, and weight-shift control aircraft, display marks as required by 14 CFR part 45.

Size Requirements for Different Aircraft

Almost universally for U.S.-registered, standard certificated, fixed-wing aircraft, the marks must be at least 12 inches high. A glider may display marks at least 3 inches high.

In all cases, the marks must be of equal height, two-thirds as wide as they are high, and the characters must be formed by solid lines one-sixth as wide as they are high. The letters "M" and "W" may be as wide as they are high.

The spacing between each character may not be less than one-fourth of the character width. The marks required by 14 CFR part 45 for fixed-wing aircraft must have the same height, width, thickness, and spacing on both sides of the aircraft.

The marks must be painted or, if decalcomanias (decals), be affixed in a permanent manner. Other exceptions to the size and location of the marks are applicable to aircraft with Special Airworthiness certificates and those penetrating ADIZ and DEWIZ airspace. The current 14 CFR part 45 should be consulted for a complete copy of the rules.

Decals

Markings are placed on aircraft surfaces to provide servicing instructions, fuel and oil specifications, tank capacities, and to identify lifting and leveling points, walkways, battery locations, or any areas that should be identified. These markings can be applied by stenciling or by using decals.

Decals are used instead of painted instructions because they are usually less expensive and easier to apply. Decals used on aircraft are usually of three types: paper, metal, or vinyl film. These decals are suitable for exterior and interior surface application.

To assure proper adhesion of decals, clean all surfaces thoroughly with aliphatic naphtha to remove grease, oil, wax, or foreign matter. Porous surfaces should be sealed and rough surfaces sanded, followed by cleaning to remove any residue.

The instructions to be followed for applying decals are usually printed on the reverse side of each decal. A general application procedure for each type of decal is presented in the following paragraphs to provide familiarization with the techniques involved.

Paper Decals

Immerse paper decals in clean water for 1 to 3 minutes. Allowing decals to soak longer than 3 minutes causes the backing to separate from the decal while immersed. If decals are allowed to soak less than 1 minute, the backing does not separate from the decal.

Place one edge of the decal on the prepared receiving surface and press lightly, then slide the paper backing from beneath the decal. Perform any minor alignment with the fingers. Remove water by gently blotting the decal and adjacent area with a soft, absorbent cloth. Remove air or water bubbles trapped under the decal by wiping carefully toward the nearest edge of the decal with a cloth. Allow the decal to dry.

Metal Decals with Cellophane Backing

Apply metal decals with cellophane backing adhesive as follows:

1. Immerse the decal in clean, warm water for 1 to 3 minutes.

2. Remove it from the water and dry carefully with a clean cloth.

3. Remove the cellophane backing, but do not touch adhesive.

4. Position one edge of the decal on the prepared receiving surface. On large foil decals, place the center on the receiving surface and work outward from the center to the edges.

5. Remove all air pockets by rolling firmly with a rubber roller, and press all edges tightly against the receiving surface to ensure good adhesion.

Metal Decals With Paper Backing

Metal decals with a paper backing are applied similarly to those having a cellophane backing. However, it is not necessary to immerse the decal in water to remove the backing. It may be peeled from the decal without moistening. Follow the manufacturer's recommendation for activation of the adhesive, if necessary, before application. The decal should be positioned and smoothed out following the procedures given for cellophane-backed decals.

Metal Decals with No Adhesive

Apply decals with no adhesive in the following manner:

1. Apply one coat of cement, Military Specification MIL-A-5092, to the decal and prepared receiving surface.

2. Allow cement to dry until both surfaces are tacky.

3. Apply the decal and smooth it down to remove air pockets.

4. Remove excess adhesive with a cloth dampened with aliphatic naphtha.

Vinyl Film Decals

To apply vinyl film decals, separate the paper backing from the plastic film. Remove any paper backing adhering to the adhesive by rubbing the area gently with a clean cloth

saturated with water. Remove small pieces of remaining paper with masking tape.

1. Place vinyl film, adhesive side up, on a clean porous surface, such as wood or blotter paper.

2. Apply recommended activator to the adhesive in firm, even strokes to the adhesive side of decal.

3. Position the decal in the proper location, while adhesive is still tacky, with only one edge contacting the prepared surface.

4. Work a roller across the decal with overlapping strokes until all air bubbles are removed.

Removal of Decals

Paper decals can be removed by rubbing the decal with a cloth dampened with lacquer thinner. If the decals are applied over painted or doped surfaces, use lacquer thinner sparingly to prevent removing the paint or dope.

Remove metal decals by moistening the edge of the foil with aliphatic naphtha and peeling the decal from the adhering surface. Work in a well-ventilated area.

Vinyl film decals are removed by placing a cloth saturated with MEK on the decal and scraping with a plastic scraper. Remove the remaining adhesive by wiping with a cloth dampened with a dry-cleaning solvent.

Paint System Compatibility

The use of several different types of paint, coupled with several proprietary coatings, makes repair of damaged and deteriorated areas particularly difficult. Paint finishes are not necessarily compatible with each other. The following general rules for coating compatibility are included for information and are not necessarily listed in order of importance:

1. Old type zinc chromate primer may be used directly for touchup of bare metal surfaces and for use on interior finishes. It may be overcoated with wash primers if it is in good condition. Acrylic lacquer finishes do not adhere to this material.

2. Modified zinc chromate primer does not adhere satisfactorily to bare metal. It must never be used over a dried film of acrylic nitrocellulose lacquer.

3. Nitrocellulose coatings adhere to acrylic finishes, but the reverse is not true. Acrylic nitrocellulose lacquers may not be used over old nitrocellulose finishes.

4. Acrylic nitrocellulose lacquers adhere poorly to bare metal and both nitrocellulose and epoxy finishes. For best results, the lacquers must be applied over fresh, successive coatings of wash primer and modified zinc

chromate. They also adhere to freshly applied epoxy coatings (dried less than 6 hours).

5. Epoxy topcoats adhere to any paint system that is in good condition, and may be used for general touchup, including touchup of defects in baked enamel coatings.

6. Old wash primer coats may be overcoated directly with epoxy finishes. A new second coat of wash primer must be applied if an acrylic finish is to be applied.

7. Old acrylic finishes may be refinished with new acrylic if the old coating is softened using acrylic nitrocellulose thinner before touchup.

8. Damage to epoxy finishes can best be repaired by using more epoxy, since neither of the lacquer finishes stick to the epoxy surface. In some instances, air-drying enamels may be used for touchup of epoxy coatings if edges of damaged areas are abraded with fine sandpaper.

Paint Touchup

Paint touchup may be required on an aircraft following repair to the surface substrate. Touchup may also be used to cover minor topcoat damage, such as scratches, abrasions, permanent stains, and fading of the trim colors. One of the first steps is to identify the paint that needs to be touched up.

Identification of Paint Finishes

Existing finishes on current aircraft may be any one of several types, a combination of two or more types, or combinations of general finishes with special proprietary coatings.

Any of the finishes may be present at any given time, and repairs may have been made using material from several different type coatings. Some detailed information for the identification of each finish is necessary to ensure the topcoat application does not react adversely with the undercoat. A simple test can be used to confirm the nature of the coatings present.

The following procedure aids in identification of the paint finish. Apply a coating of engine oil (MIL SPEC, MIL-PRF-7808, turbine oil, or equivalent) to a small area of the surface to be checked. Old nitrocellulose finishes soften within a period of a few minutes. Acrylic and epoxy finishes show no effects.

If still not identified, wipe a small area of the surface in question with a rag wet with MEK. The MEK picks up the pigment from an acrylic finish, but has no effect on an epoxy coating. Just wipe the surface, and do not rub. Heavy rubbing picks up even epoxy pigment from coatings that are not thoroughly cured. Do not use MEK on nitrocellulose

finishes. *Figure 8-22* provides a solvent test to identify the coating on an aircraft.

Surface Preparation for Touchup

In the case of a repair and touchup, once the aircraft paint coating has been identified, the surface preparation follows some basic rules.

The first rule, as with the start of any paint project, is to wash and wipe down the area with a degreaser and silicone wax remover, before starting to sand or abrade the area.

If a whole panel or section within a seam line can be refinished during a touchup, it eliminates having to match and blend the topcoat to an existing finish. The area of repair should be stripped to a seam line and the finish completely redone from wash primer to the topcoat, as applicable. The paint along the edge of the stripped area should be hand-sanded wet and feathered with a 320 grade paper.

For a spot repair that requires blending of the coating, an area about three times the area of the actual repair will need to be prepared for blending of the paint. If the damaged area is through the primer to the substrate, the repair area should be abraded with 320 aluminum oxide paper on a double-action (D/A) air sander. Then, the repair and the surrounding area should be wet sanded using the air sander fitted with 1500 wet paper. The area should then be wiped with a tack cloth prior to spraying.

Apply a crosscoat of epoxy primer to the bare metal area, following the material data sheet for drying and recoat times. Abrade the primer area lightly with 1500 wet or dry, and then abrade the unsanded area around the repair with cutting compound. Clean and wipe the area with a degreasing solvent, such as isopropyl alcohol, and then a tack cloth.

Mix the selected topcoat paint that is compatible for the repair. Apply two light coats over the sanded repair area, slightly extending the second coat beyond the first. Allow time for the first coat to flash before applying the second coat. Then, thin the topcoat by one-third to one-half with a compatible reducer and apply one more coat, extending beyond the first two coats. Allow to dry according to the material data sheet before buffing and polishing the blended area.

If the damage did not penetrate the primer, and only the topcoat is needed for the finish, complete the same steps that would follow a primer coat.

Paint touchup procedures generally are the same for almost any repair. The end result, however, is affected by numerous variables, which include the preparation, compatibility of the finishing materials, color match, selection of reducers and/or retarders based on temperature, and experience and expertise of the painter.

Stripping the Finish

The most experienced painter, the best finishing equipment, and newest coatings, do not produce the desired finish on an aircraft if the surface was not properly prepared prior to refinishing. Surface preparation for painting of an entire aircraft typically starts with the removal of the paint. This is done not only for the weight reduction that is gained by stripping the many gallons of topcoats and primers, but for the opportunity to inspect and repair corrosion or other defects uncovered by the removal of the paint.

Before any chemical stripping can be performed, all areas of the aircraft not being stripped must be protected. The stripper manufacturer can recommend protective material for this purpose. This normally includes all window material,

3–5 Minute Contact With Cotton Wad Saturated With Test Solvent

Hitrate	Nitrate dope	Butyrate dope	Nitro-cellulose lacquer	Poly-tone Poly-brush Poly-spray	Synthetic enamel	Acrylic lacquer	Acrylic enamel	Urethane enamel	Epoxy paint
Methanol	S	IS	IS	IS	PS	IS	PS	IS	IS
Toluol (Toluene)	IS	IS	IS	S	IS	S	ISW	IS	IS
MEK (Methyl ethyl ketone)	S	S	S	S	ISW	S	ISW	IS	IS
Isopropanol	IS	IS	IS	IS	IS	S	IS	IS	IS
Methylene chloride	SS	VS	S	VS	ISW	S	ISW	ISW	ISW

IS – Insoluble
ISW – Insoluble, film wrinkles
PS – Penetrate film, slight softening without wrinkling

S – Soluble
SS – Slightly Soluble
VS – Very Soluble

Figure 8-22. *Chart for solvent test of coating.*

vents and static ports, rubber seals and tires, and composite components that may be affected by the chemicals.

The removal of paint from an aircraft, even a small single-engine model, involves not only the labor but a concern for the environment. You should recognize the impact and regulatory requirements that are necessary to dispose of the water and coating materials removed from the aircraft.

Chemical Stripping

At one time, most chemical strippers contained methylene chloride, considered an environmentally acceptable chemical until 1990. It was very effective in removing multiple layers of paint. However, in 1990, it was listed as a toxic air contaminant that caused cancer and other medical problems and was declared a Hazardous Air Pollutant (HAP) by the EPA in the Clean Air Act Amendments of 1990.

Since then, other substitute chemical strippers were tested, from formic acid to benzyl alcohol. None of them were found to be particularly effective in removing multiple layers of paint. Most of them were not friendly to the environment.

One of the more recent entries into the chemical stripping business is an environmentally friendly product known as EFS-2500, which works by breaking the bond between the substrate and primer. This leads to a secondary action that causes the paint to lift both primer and top coat off the surface as a single film. Once the coating is lifted, it is easily removed with a squeegee or high-pressure water.

This product differs from conventional chemical strippers by not melting the coatings. Cleanup is easier, and the product complies with EPA rules on emissions. Additionally, it passed Boeing testing specifications related to sandwich corrosion, immersion corrosion, and hydrogen embrittlement. EFS-2500 has no chlorinated components, is non-acidic, nonflammable, nonhazardous, biodegradable, and has minimal to no air pollution potential.

The stripper can be applied using existing common methods, such as airless spraying, brushing, rolling, or immersion in a tank. It works on all metals, including aluminum, magnesium, cadmium plate, titanium, wood, fiberglass, ceramic, concrete, plaster, and stone.

Plastic Media Blasting (PMB)

Plastic media blasting (PMB) is one of the stripping methods that reduces and may eliminate a majority of environmental pollution problems that can be associated with the earlier formulations of some chemical stripping. PMB is a dry abrasive blasting process designed to replace chemical paint stripping operations. PMB is similar to conventional sand blasting except that soft, angular plastic particles are used as the blasting medium. The process has minimum effect on the surface under the paint because of the plastic medium and relatively low air pressure used in the process. The media, when processed through a reclamation system, can be reused up to 10 times before it becomes too small to effectively remove the paint.

PMB is most effective on metal surfaces, but it has been used successfully on composite surfaces after it was found to produce less visual damage than removing the paint by sanding.

New Stripping Methods

Various methods and materials for stripping paint and other coatings are under development and include:

- A laser stripping process used to remove coatings from composites.
- Carbon dioxide pellets (dry ice) used in conjunction with a pulsed flashlamp that rapidly heats a thin layer of paint, which is then blasted away by the ice pellets.

Safety in the Paint Shop

All paint booths and shops must have adequate ventilation systems installed that not only remove the toxic air but, when properly operating, reduce and/or eliminate overspray and dust from collecting on the finish. All electric motors used in the fans and exhaust system should be grounded and enclosed to eliminate sparks. The lighting systems and all bulbs should be covered and protected against breakage.

Proper respirators and fresh-air breathing systems must be available to all personnel involved in the stripping and painting process. When mixing any paint or two-part coatings, eye protection and respirators should be worn.

An appropriate number and size of the proper class fire extinguishers should be available in the shop or hangar during all spraying operations. They should be weighed and certified, as required, to ensure they work in the event they are needed. Fireproof containers should be available for the disposal of all paint and solvent soaked rags.

Storage of Finishing Materials

All chemical components that are used to paint an aircraft burn in their liquid state. They should be stored away from all sources of heat or flames. The ideal place would be in fireproof metal cabinets located in a well ventilated area.

Some of the finishing components have a shelf life listed in the material or technical data sheet supplied by the coating manufacturer. Those materials should be marked on the

container, with a date of purchase, in the event that they are not used immediately.

Protective Equipment for Personnel

The process of painting, stripping, or refinishing an aircraft requires the use of various coatings, chemicals, and procedures that may be hazardous if proper precautions are not utilized to protect personnel involved in their use.

The most significant hazards are airborne chemicals inhaled either from the vapors of opened paint containers or atomized mist resulting from spraying applications. There are two types of devices available to protect against airborne hazards: respirators and forced-air breathing systems.

A respirator is a device worn over the nose and mouth to filter particles and organic vapors from the air being inhaled. The most common type incorporate double charcoal-filtered cartridges with replaceable dust filters that fits to the face over the nose and mouth with a tight seal. When properly used, this type of respirator provides protection against the inhalation of organic vapors, dust, mists of paints, lacquers, and enamels. A respirator does not provide protection against paints and coatings containing isocyanates (polyurethane paint).

A respirator must be used in an area of adequate ventilation. If breathing becomes difficult, there is a smell or taste the contaminant(s), or an individual becomes dizzy or feel nauseous, they should leave the area and seek fresh air and assistance as necessary. Carefully read the warnings furnished with each respirator describing the limits and materials for which they provide protection.

A forced-air breathing system must be used when spraying any type of polyurethane or any coating that contains isocyanates. It is also recommended for all spraying and stripping of any type, whether chemical or media blasting. The system provides a constant source of fresh air for breathing, which is pumped into the mask through a hose from an electric turbine pump.

Protective clothing, such as Tyvek® coveralls, should be worn that not only protects personnel from the paint but also help keep dust off the painted surfaces. Rubber gloves must be worn when any stripper, etching solution, conversion coatings, and solvent is used.

When solvents are used for cleaning paint equipment and spray guns, the area must be free of any open flame or other heat source. Solvent should not be randomly sprayed into the atmosphere when cleaning the guns. Solvents should not be used to wash or clean paint and other coatings from bare hands and arms. Use protective gloves and clothing during all spraying operations.

In most states, there are Occupational Safety Hazard Administration (OSHA) regulations in effect that may require personnel to be protected from vapors and other hazards while on the job. In any hangar or shop, personnel must be vigilant and provide and use protection for safety.

High Energy Materials

A Brief History and Chemistry of Fireworks and Rocketry

Vedang Naik and K C Patil

Propellants used in rockets, pyrotechnics used in festivities, explosives used for military purposes, blasting chemicals used in construction activities, etc., are high energy materials. There is a lot of fascinating chemistry and interesting history behind them. This article gives an overview of these aspects, with somewhat more emphasis on propellants and working of rockets, and the chemistry of fireworks.

1. Introduction

High energy materials are compounds which store chemical energy. They are either single compounds like trinitrotoluene (TNT) containing both an oxidizing group, $-NO_2$ and a reducing group or a mixture of an oxidizer and fuel elements, e.g., gun powder ($KNO_3 + C + S$). Such materials, on stimulation by mechanical, thermal or electrical devices, undergo rapid decomposition giving out heat, light, sound and large volumes of gases. The amount of energy released varies with the properties of the material such as composition, structure, density, heat of formation and decomposition, etc. High energy materials are classified as explosives, propellants[1] and fireworks[2] depending upon their properties and applications. This article aims to understand the chemistry of these materials.

2. Explosives

2.1 *History*

Explosives have been around for a long time, the first one used being gunpowder. It was invented in China or India sometime around 1000 AD. In the 13th and 14th centuries, Roger Bacon and the Earl of Warwick introduced gunpowder to Europe. They used it for developing firearms and cannons. From then on until the 1800s, no major

(left) Vedang Naik is 14 years old and a student of 9th Standard at National Public School, Bengaluru. He is interested in chemistry, aerospace, as well as engineering.

(right) K C Patil was a Professor in the Inorganic and Physical Chemistry Department, Indian Institute of Science, Bengaluru and retired in 1997. He is currently Vice President of the Karnataka Association for Advancement of Science, Bengaluru, which organises programmes in schools and colleges to popularise science.

[1] These are chemical compounds or their mixtures that rapidly produce large volumes of hot gases when properly initiated.

developments took place in the field of explosives. But during the 19th century, many new materials such as nitric acid ester, nitrated paper (flash paper), nitrocotton (NC guncotton), smokeless nitrocellulose, wood powder, blasting gelatine, picric acid and trinitrotoluene (TNT, $C_7H_5N_3O_6$) were developed. The 20th century saw the development of many new and more powerful explosives, such as RDX ($C_3H_6N_6O_6$), HMX ($C_4H_8N_8O$), ADN ($NH_4N(NO_2)_2$), TNAZ ($C_3H_4N_3O_6$) and the latest and the most powerful explosive, HNIW ($C_6N_{12}H_6O_{12}$). *Table* 1 summarizes the history of explosives.

2.2 *Classification of Explosives*

Explosives are classified on the basis of chemical composition, properties and applications.

A. Composition

• Nitramines
• Nitric esters
• Derivatives of chloric and perchloric acid
• Azides: Heavy metal azides
• Others: Fulminates, styphnates, peroxides, ozonides, acetylides.

B. Properties

On the basis of intensity of explosion, explosives are classified as follows:

(i) primary or low explosives or initiators – these are normally employed as propellants. They burn rapidly at rates of up to 400 m/s, and

(ii) secondary or high explosives – these detonate[3] at 1000–8500 m/s. Primary explosives are very sensitive to heat, impact and friction, while secondary or high explosives are less sensitive and usually burn in small, unconfined space. However, there is no clear demarcation between primary and secondary explosives.

C. Applications: Civil and Military

Explosives are classified according to applications either for

Name	Inventor(s)	Country	Year
Gunpowder	Anonymous	China or India	~1000 AD
Gun powder (a mixture of 75% KNO_3, 15% charcoal and 10% sulphur by weight)	Roger Bacon	United Kingdom	13th century
Gun powder in cannon	Earl of Warwick	United Kingdom	14th century
Nitric acid ester of starch	Henri Braconnot	France	19th century
Nitrated paper	Theophile J Pelouze	France	19th century
Nitrocotton (NC) (guncotton)	Christian Schoenbein	Germany	19th century
Wood powder	Major E Schultze	Germany	19th century
Blasting gelatine	Alfred Nobel[1]	Sweden	19th century
Picric acid	Hermann Sprengel	Germany	19th century
Smokeless NC	Paul Vieille	France	19th century
TNT (Trinitrotoluene)	Julius Wilbrand	Germany	19th century
Pyrocellulose + diphenylamine	EI DuPont de Nemours	USA	20th century
RDX (Research Department Explosive or Royal Demolition Explosive)		United Kingdom	20th century
HMX (Her Majesty's or High Melting Exposive)		United Kingdom	20th century
ADN (Ammonium dinitramide)	Robert Schmitt and Jeffrey C Bottars	United Kingdom United Kingdom	20th century 20th century
TNAZ (Trinitroazetidine)	Kurt Bann and Tom Archibald		
HNIW (Hexanitrohexaza isowurtzitane)	Arnold Nielsen	United Kingdom	20th century

civilian use such as demolition of old buildings, construction of bridges, roads, tunnels and mining or for military purposes like bombs, landmines, etc.

Table 1. A brief history of explosives.

2.3 *Tests for Explosives*

In order to determine if a substance is an explosive or not, the following standard tests are conducted:

(i) Test for impact or friction sensitivity: A weight (100 g steel ball) is dropped upon the sample (few milligrams) from a height. If the substance explodes, it is sensitive to impact. Friction test is carried out by putting the sample between two steel plates along with sand and rotating the upper plate against the fixed lower plate.

(ii) Thermal stability: A 20 mg sample of the substance is kept in a constant temperature bath. If it explodes within 10 seconds, it is sensitive to heat.

[4] The velocity at which the shock wavefront travels through a detonated explosive is called the velocity of detonation.

[5] A counter chronograph is a timer device which measures the distance in metres/second for a shockwave to travel between two fixed points.

(iii) Velocity of detonation[4]: Direct flame photography, high speed photography and counter chronographs[5] are used to measure the velocity of detonation of an explosive.

(iv) Destruction power: It is carried out by the so-called lead block test. In this test, a 10 gram sample of the explosive is put into a hole drilled in the middle of the lead block (*Figure* 1). Sand is then poured over the explosive, sealing the explosive in the centre of the block. Then the explosive is detonated. The power of the explosive is determined by measuring the volume of hole in the lead block. The bigger the volume, the more powerful is the explosive.

Some properties of well-known explosives are listed in *Table* 2.

Figure 1. The lead block test.

Explosive/Density	Lead Block Volume cm^3/10 g	Velocity of Detonation (m/s)
TNT (1.65g/cm^3)	300	6700
Picric acid (1.76 g/cm^3)	315	4500
ANFO	316	3000
NC	373	7200–7300
Dynamite	412	
RDX (1.82 g/cm^3)	483	8200
PETN (1.77 g/cm^3)	520	8300
NG (1.6 g/cm^3)	530	
NC + NG	600	

3. Propellants

3.1 *History*

Table 2. Properties of some common explosives.

The first rockets were simple fireworks used by the Chinese to celebrate happy occasions and to frighten evil spirits. They later realised that rockets could be used as weapons to frighten and kill the enemy. In India, the Mysore rocket[6] using gun powder invented by Tipu Sultan was used in Srirangapattana war against British. Later, Sir William Congreve developed it in Europe in 1804. Robert Goddard in USA investigated liquid propellants and improved them in many ways. In World War II, Wernher von Braun designed the V-2 rockets which were the first inter-continental ballistic missiles (ICBMs). After the war, the Allied Powers captured German rocket scientists and made many developments in rocket technology, including the breaking of the sound barrier in a rocket-propelled plane called the Bell X-1. The Russians developed their versions of the V-2 rocket under the leadership of Sergei Korolev. Soon after, in 1981, followed the Space Shuttle, and after that, a wide range of advanced ICBMs, guided missiles and space launch vehicles. *Table* 3 summarizes the history of rocketry.

[6] Mysore rockets or Tipu rockets were the first iron-cased rockets stabilized by bamboo sticks. They consisted of an iron combustion chamber which was filled with compressed gunpowder. A pound of gunpowder could propel the rocket to almost 900 metres.

3.2 *Propellant Families*

There are several classes of propellants, e.g., monopropellants

Rocket invention/discovery	Inventor/discoverer	Year
First rockets used in artillery	Chinese	~1000 AD
The Mysore rocket	Tipu Sultan	1780s
Congreve rocket	Sir William Congreve	1804
Theory of interplanetary flight	Konstantin Tsiolkovsky	1903
First serious analysis of rockets	Robert Goddard	1912
V-2 rockets	Wernher von Braun	1920s-1930s
First ICBMs and SLBMs Germany	1942	
Bell X-1	USA	1948 (first test flight)
R-1, R-3. R-5 and R-7	Sergei Korolev (leader)	
First Moon landing	USA	1969
Space Shuttle	USA	1969 (idea), 1981 (first test flight)
Guided missiles, advanced IRBM, ICBM space rockets	Worldwide	Present day

Table 3. A brief history of rocketry.

[7] Slower explosive reactions propagated by thermal conduction and radiation are known as deflagration. The combustion (burning/reaction) is very rapid with VOD $\approx 10^{-2}$ to 10^2 ms^{-1}.

(N_2H_4, H_2O_2), solid propellants, liquid propellants and hybrid propellants. Here, we shall discuss the two common classes, namely the solid and the liquid propellants.

A. Solid Propellants

A solid propellant is made from low or diluted high explosives which are deflagrated[7] instead of detonated. They consist of a fuel, an oxidiser and a binder and are in the form of grains. The earliest rockets were solid-fuel-propelled. Solid propellants are easy to use and can be stored for a longer time, and are thus, mainly used by the military in missiles. However, their low performance does not allow them to be used in space rockets as they do not produce sufficient thrust. *Table* 4 gives the composition of some typical solid propellants.

B. Liquid Propellants

A liquid propellant, as the name indicates, is in liquid form. Liquids are favoured over solid fuels, because their high energy (I_{sp}) allows for smaller tanks. For the combustion to take place, the fuel and the oxidizer are mixed in a combustion chamber. Liquid propellant rockets can be monopropellant, bipropellant or tripropellant. Bipropellant rockets usually use a liquid fuel and a liquid oxidizer, such

Propellant name	General Information
Gun powder or black powder	One of the oldest solid propellants, this compound is easy to make and use. The fuel consists of a block which is made of finely compressed powder.
Double-based (DB) propellants	These contain two monopropellant fuels in which one acts as a high-energy unstable propellant and the other as a stabilizing agent. They are used where minimal smoke and medium power is needed. (NC + NG)
Composite propellants	These are made of a powdered fuel and an oxidizer held by a binder which also acts as a fuel. They are usually ammonium perchlorate (APCP) or ammonium nitrate (ANCP) based.
High-energy composites (HEC) or HMX in them.	They are composite propellants with a few crystals of RDX
Composite modified double-based propellants	These are propellants which are made by modifying a mixture of composite and double-based propellants. (NC + NG +Al powder)
Smokeless propellants	They have been developed using HNIW. This explosive has 14% more energy per mass and 20% more energy density than HMX. It is also very shock-insensitive and non-polluting.

as liquid hydrogen and liquid oxygen.

Solid propellants are stable and can be stored for use in warfare whereas liquid propellants are energetic and, being cryogenic, are mostly used in satellite launch vehicles.

Table 4. Composition of solid propellants.

A huge number of liquid fuel and liquid oxidizer combinations have been tried over the years. Some of them are:

• Liquid oxygen (LOX) and liquid hydrogen (LH$_2$)
• LOX and highly refined kerosene (commonly called RF-1)
• LOX and alcohol (C$_2$H$_5$OH)
• LOX and gasoline

3.3 *Rockets*

The working principle of rockets is briefly mentioned here. All rockets are based on Newton's Third Law: an action will always have an equal and opposite reaction. In a rocket, the thrust
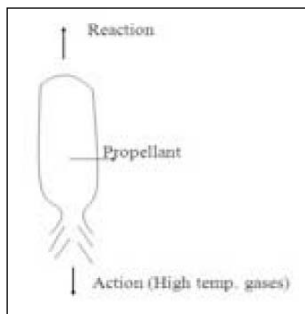
Figure 2. Schematic diagram of a rocket.

produced by the propellant is directed downward so that the rocket is pushed upwards. Fins or stabilizers on the sides of the rocket prevent it from turning suddenly in mid-air. To increase the thrust produced by the propellant, a de Laval nozzle is attached to the exhaust port. This nozzle forces the exiting hot gases into a small space, forcing them to increase their speed (*Figure* 2). This, in turn, increases the thrust. Guided missiles work in the same way, but have on-board computers to steer them in mid-air to their designated targets.

3.3 *Rocket Performance*

A. Oxygen Balance

All rockets and fireworks must have stochiometric amounts of fuel and oxidizer to work properly. When the oxidizer to fuel ratio is unity, the energy released is maximum; whereas, if it is greater or less than 1, the combustion is incomplete and various gases (CO, NOx, hydrocarbons), which cause environmental pollution, are formed.

Fuel-to-oxygen ration is the ratio of fuel elements to oxygen. Oxygen balance is the amount of oxygen required for complete combustion of all the carbon atoms to carbon dioxide and hydrogen atoms to water as shown in the equation. The formula for calculating oxygen balance[8] is

$$\text{Oxygen Balance} = \frac{1600}{\text{Molecular Weight of Fuel}} (Z - 2X - \frac{Y}{2}).$$

Here, X = number of carbon atoms, Y = number of hydrogen atoms, and Z = number of oxygen atoms.

B. Thrust and Specific Impulse

Thrust: Thrust is a force which is used to get a body from a stationary to a moving position. It is used to oppose drag and overcome the weight of a rocket.

Specific Impulse (I_{sp}): This is used to describe the efficiency of

[8] +ve oxygen balance: The amount of oxygen is more than enough for the reaction.
-ve oxygen balance: The amount of oxygen is not sufficient for the reaction.

a rocket. It represents force with respect to the amount of propellant used in a unit of time. The more the specific impulse of an engine or propulsion method, the less propellant it uses per unit time.

The specific impulse of a rocket can be calculated by the following formula:

$$\text{Specific Impulse} = \frac{\text{Thrust (Force in lbs)}}{\text{lbs of propellant used in 1 second}}.$$

Specific impulse is also calculated by the following formula:

$$I_{sp} = \sqrt{\frac{\text{Chamber Temperature}}{\text{Avg Mol Wt of Combustion Products}}}.$$

The values of specific impulse for some solid and liquid propellants are given in *Table* 5.

Oxidizer	Fuel	I_{sp} (sec)
Liquid oxygen	Liquid H_2	390
	RP-1	300
	UDMH	310
	(unsymmetrical	280
	dimethyl hydrazine)	
	Alcohol	
Liquid F_2	Liquid H_2	410
	RP-1	320
	UDMH	340
RFNA(Red fuming	RP-1	270
nitric acid)	UDMH	275
N_2O_4	UDMH	285
	N_2H_4	290
Black powder	–	40–80
NH_4ClO_4+Al+CTPB	–	240

Table 5. I_{sp} values of some solid and liquid propellants.

Figure 3. The fireworks square.

Table 6. A brief history of fireworks.
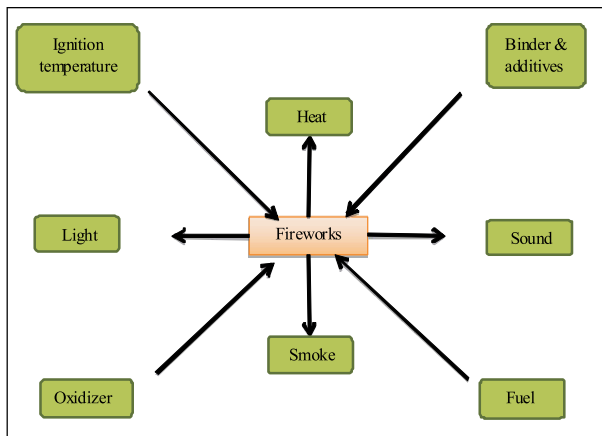
4. Pyrotechnics – The Art of Making Fireworks

Fireworks are a class of explosive pyrotechnic devices used for aesthetic, cultural, and religious purposes. The fireworks are designed to burn with flames and sparks of many hues and patterns. The square diagram of *Figure* 3 presents composition and outcome of fireworks ignition.

4.1 *History*

The first fireworks were invented by the Chinese sometime before 1000 AD. They later adapted them for military applications, and advanced the technology of making normal fireworks, including the invention of a crude version of the aerial fireworks we see today. Fireworks reached Italy during the Renaissance, where it was improved and evolved into an art. The development of the quick match[9], colours for use in rockets and flash powder took place in Italy from the 1700s to the 1850s. A brief history of fireworks is given in *Table* 6.

Firework/modification/event	Inventor/discoverer	Year
First fireworks	Chinese	Circa10th century AD
Fire arrows and fire lances	Chinese	10th century AD
Modification of gunpowder	Chinese	11th century AD
Aerial fireworks	Chinese civilian firework makers	Around 1200 AD
Firework shells, fountains and wheels	Italians	Renaissance Period
Quick match		Around 1730s
Fireworks in the new world	Settlers	1600s
New colours and the usage of potassium perchlorate	Southern Italy	1830s
Flash powder	Southern Italy	1830s

4.2 *How Fireworks Work*

Fireworks consist of a fuel, an oxidizer, a binder and additives for colours, (*Figure* 3). The most common oxidizer is potassium nitrate, and the fuel is usually charcoal or sulphur (gun powder). Gun powder is very sensitive to sparks and ignites instantly causing fire in fireworks factories and storehouses. Efforts to replace it with safer alternatives have not been successful so far! The binder can be sugar or starch, usually dextrin. When mixed, they form a kind of paste, which hardens around anything coated with it. A sparkler is made by dipping a wire of desired length into the slurry of this mixture. *Table* 7 lists various chemicals used in fireworks as fuels, oxidizers, binders, special effect initiators and their percentage weight in a standard skyrocket.

Rocket fireworks (or skyrockets) work much in the same way that space rockets do. A skyrocket consists of a cylinder packed

Table 7. Chemicals used in fireworks along with their function.

Fuels	Oxidizer	Binders
Aluminium,	Potassium nitrate	Dextrin
Charcoal,	/chlorate/perchlorate,	Red gum
Dextrin,	Barium nitrate/chlorate	Synthetic
Magnesium,	Ammonium perchlorate,	polymers
Red gum,	Strontium nitrate	
Sulphur,		
Titanium,		
Antimony sulphide,		
Polyvinyl chloride		

Chemicals for special effects

Red flame: strontium nitrate/chlorate, **Green flame:** barium nitrate/chlorate
Blue flame: copper chloride/sulphate/oxide, **Yellow flame:** sodium oxalate, cryolite (Na_3AlF_6)
White flame: magnesium and aluminium, **Gold sparks:** iron filings and charcoal
White sparks: aluminium, magnesium, aluminium-magnesium alloy and titanium
Whistle effect: potassium benzoate or sodium salicylate, **White smoke:** potassium nitrate or sulphur mix
Coloured smoke: potassium chlorate/sulphate/organic dye mixture

with gunpowder and additives for specific colour(s). On ignition they propel themselves into the sky and then burst into one or more colours and patterns.

4.3. *Classification of Fireworks*

A. Single-colour Skyrockets

A single-colour skyrocket consists of just a tube filled with gunpowder, the chemical(s) needed for that particular colour, a delay fuse and a long stick to stabilize it while taking off and flying. The propellant is at the bottom and the additives that burst into stars are packed at the upper part (*Figure* 4). When the fuse is lit, it burns, igniting the propellant first and then the additives burst into stars, creating a colourful display.

B. Multi-colour Rockets

Multi-colour rockets work in stages, just like the now outdated Saturn-V space rockets used to. In a multistage space rocket, each stage falls away as it finishes its load of fuel. Similarly, in a multi-colour rocket, each stage contains the chemicals for a different colour, which explode one after the other. Each segment
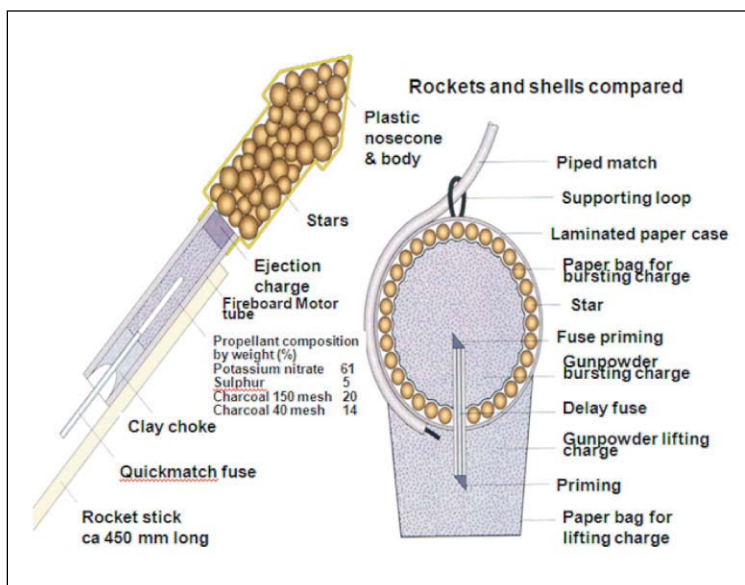

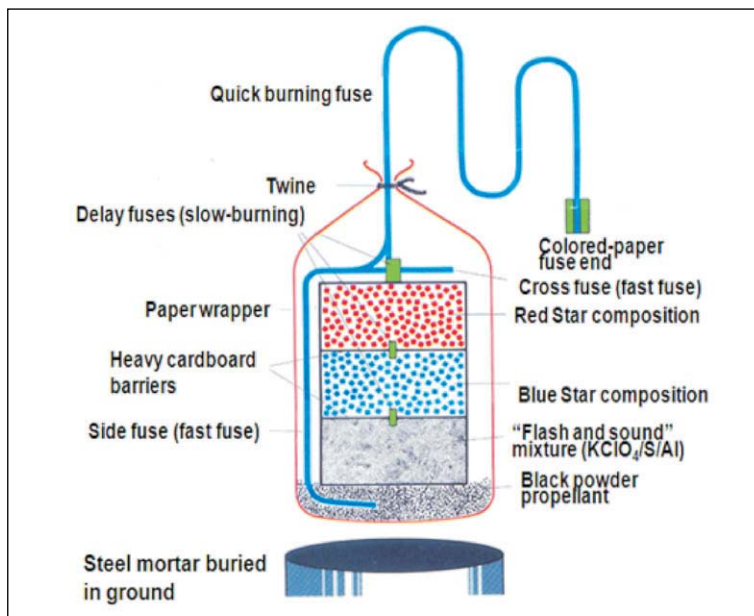**Figure 4.** Comparison of a single-colour skyrocket and shell [1].

of chemicals is separated from the next one by a sheet of cardboard, with the propellant being packed at the bottom of the rocket. There are many fuses in a multi-colour rocket. When the wick is lit, a fast-burning fuse ignites the propellant first, which subsequently propels the rocket high into the atmosphere. A slower, delay fuse then ignites the colour-stages in sequence, with the topmost one bursting first, followed by one or more colours exploding one after another in the sky (*Figure* 5). *Table* 8 gives a summary of some chemicals used for generating different colours in a multi-colour rocket.

Table 8. Chemicals used in a multi-colour rocket. Percentage of chemicals by weight in a standard sky rocket

Red Star	Blue Star	Cone Fountain	Green Fire
$KClO_3$ (64%)	$KClO_4$ (38%)	KNO_3 (53%)	NH_4ClO_4 (50%)
$SrCO_3$ (19%)	NH_4ClO_4 (29%)	Fe (32%)	$Ba(NO_3)_2$ (34%)
Red gum (13%)	$CuCO_3$ (14%)	S (8%)	Fine sawdust (8%)
Dextrin (4%)	Red gum (14%)	C (2%)	Shellac (8%)
Cone Foundatin	Dextrin (5%)	Al (4%) Stearic acid (1%)	

5. Conclusion

Scientists over many centuries have developed chemicals which are used as explosives in warfare, civilian application and fanciful fireworks display. Wicked and misguided people have been using them in mindless destruction of humans, which has marred the far more important application of these materials for constructive and recreational purposes. Alfred Nobel [3], who made explosives safe to handle for constructive use, repented his invention of dynamite when it was used for killing and destruction.

Acknowledgement

The authors are grateful to Dr S T Aruna, NAL Bengaluru for making the article suitable and ready for publication.

Address for Correspondence
Vedang Naik
K C Patil*
* Department of Inorganic and Physical Chemistry
Indian Institute of Science
Bengaluru 560 012
Email:
kcpatil37@yahoo.co.in

Suggested Reading

[1]   M Russel, Rocket fuel, *Chemistry in Britain*, p.26, Nov. 2002.

[2]   J A Conkling, Chemistry of Fireworks, *Chem. & Engg. News*, p.24, June 1981.

[3]   Gopalpur Nagendrappa, Alfred Bernhard Nobel, *Resonance*, Vol.18, No.6, pp.500–513, 2013.